A study of the African horse sickness virus using High Resolution Melt, multivariate and phylogenetic analyses for a potential serotyping assay

Shaun Reinder Groenink

BScHons, MScAgric

Submitted in fulfilment of the academic requirements for the degree of

Doctor of Philosophy (Biochemistry)

in the
School of Life Sciences
College of Agriculture, Engineering and Science
University of KwaZulu-Natal
Pietermaritzburg
August 2014

ABSTRACT

African horse sickness (AHS) is a viral disease that afflicts all equine species and has a 90% mortality rate in unvaccinated horses. The disease has a devastating effect on the national herd of South Africa each year and affects both the sport and racehorse industries, including the export of prized bloodstock, as well as the rural and subsistence economies that depend on animal traction. Transmitted by the *Culicoides* spp. of biting midge, the virus belongs to the *Orbivirus* genus of the *Reoviridae* family with nine known serotypes and ten genome segments. Segment 2 (which encodes VP2) is responsible for serotype determination while segment 10 (which encodes NS3) is merely serotype-divergent. Knowledge of the seroprevalence of the virus is poor. The increasing reluctance of horse owners to use the registered vaccine due to perceived inefficacy is of concern. As a means to increase knowledge output in this regard, and potentially provide a service to horse owners, a rapid serotyping assay is sought based on High Resolution Melt (HRM) analysis. HRM analysis is a powerful tool that is based on the release of a DNA intercalating dye from polymerase chain reaction products through gradual and controlled heating. The dye is released at a specific point that is dependent on the unique sequence of the amplicon. It can thus be used to distinguish, very sensitively, differences in divergent amplicons. Using a range of freely available bioinformatics software, such as Clustal X2, Primaclade, Treeview and BLAST analysis, primers were designed based on segment 2 that sought to differentiate the individual serotype from previously defined clades based on a pair of segment 10 primers. Reference and field isolates of the AHS virus were obtained from the National Institute of Communicable Disease and the Onderstepoort Veterinary Institute, South Africa, and were propagated on Vero cell monolayers. Total RNA was extracted using guanidine-thiocyanate and verified as containing AHSV genomic material using primers recognised by the World Organisation for Animal Health that target the genome segment encoding VP7. Variable amounts of total RNA did not influence the downstream analysis as individual serotypes were easily distinguished using HRM despite wide ranging template concentrations. Through testing the primers designed in the present study, various serotype anomalies were discovered with regard to the isolates obtained from the Onderstepoort Veterinary Institute. Serotype-specific primers and the segment 10 primers were used to interpret the serotype anomalies through High Resolution Melt analysis. Sequencing confirmed the anomalies: serotype 2 isolates were serotype 6 isolates and a serotype 5 isolate was serotype 8. A proposed protocol for a rapid serotyping assay was investigated. This involved an initial PCR to determine into which clade of segment 10 the sample fits. Following this, the serotype was

elucidated for each clade using segment 2 clade-specific primers. These reactions were performed in the Corbett Rotor-Gene™ 6000 and its in-built software was used. However, limitations of the software soon became apparent, as it was not able to completely distinguish the serotypes. Alternate methods were sought and included ScreenClust HRM® Software, principal component analysis (PCA) and discriminant analysis (DA). The use of normalised HRM fluorescence curves for PCA and DA was effective in standardising the template concentrations. These methods were successful in determining the serotype and rendered results with greater statistical confidence. Finally, a phylogenetic analysis was performed of all the available AHS virus sequences to determine the degree of possible genetic drift in the virus that may give rise to a new serotype. Minimal to no genetic drift could be found comparing sequences from the 1960s to sequences from the 2000s. This study presents the ability of HRM analysis to recognise and define AHS virus serotype anomalies, provide a new protocol for the serotyping of the virus with an extensive statistical analysis, the first for an orbivirus. Furthermore, the protocols described can be extrapolated to other orbiviruses.

Preface

The experimental work described in this thesis was carried out in Biochemistry, School of Life Sciences, University of KwaZulu-Natal, Pietermaritzburg, from January 2010 to December 2012, under the supervision of Prof. Theresa H. T. Coetzer and co-supervision of Dr. Marion B. Young and Dr. Gregory M. F. Watson.

These studies represent original work by the author and have not otherwise been submitted in any form for any degree or diploma to any University. Where use has been made of the work of others it is duly acknowledged in the text.

Shaun R. Groenink (candidate)

Prof. Theresa H.T. Coetzer (supervisor)

Dr. Marion Young (co-supervisor)

Dr. Gregory Watson (co-supervisor)

Candidate's Declaration

I, Shaun Reinder Groenink, declare that:

1. The research reported in this thesis is, except where otherwise indicated, my original research.
2. This thesis has not been submitted for any degree or examination at any other university
3. This thesis does not contain other persons' data, images, graphs or other information, unless specifically acknowledged as being sourced from other persons.
4. This thesis does not contain other persons' writing, unless specifically acknowledged as being sourced from other researchers. Where other written sources have been quoted, then:
    a. Their words have been re-written, but the general information attributed to them has been referenced.
    b. Where their exact words have been used, then their writing has been placed inside quotation marks and referenced.
5. This thesis does not contain text, graphics or tables copied and pasted from the internet, unless specifically acknowledged, and the source being detailed in the thesis and in the Reference sections.

Shaun R. Groenink

Table of Contents

ABSTRACT ..... **i**
Preface ..... **iii**
Candidate's Declaration ..... **iv**
Table of Contents ..... **v**
List of Figures ..... **x**
List of Tables ..... **xvi**
Acknowledgements ..... **xviii**
List of abbreviations ..... **xx**
CHAPTER 1: INTRODUCTION, LITERATURE REVIEW AND RESEARCH OBJECTIVES **1**
1.1. Introduction 1
1.1.1. Background 1
1.1.2. Research rationale 2
1.2. History of African horse sickness 4
1.3. Epidemiology 5
1.3.1. Epizootic events – beyond South Africa 5
1.3.2. Endemic events – South Africa 6
1.3.3. Simulation modelling 9
1.4. Range of AHSV hosts 10
1.4.1. Reservoirs 11
1.5. Vectors 12
1.5.1. Viral cycle in *Culicoides* species 15
1.6. Overwintering mechanisms 15
1.7. Pathogenesis 17
1.8. Differential diagnoses 19
1.9. Aetiology 20
1.9.1. AHSV taxonomy 20
1.9.2. AHSV properties 20
1.9.3. AHSV structure 21
1.9.4. AHSV replication 25

1.9.5. AHSV serotypes 25
1.9.6. AHSV stability 27
1.10. Control and prevention 28
1.10.1. Control 28
1.10.2. Vaccination 29
1.11. AHS in rural, subsistence communities 34
1.12. Overview of local and international policies to control AHS 35
1.12.1. South African controls to prevent the spread AHS 36
1.12.2. European controls to prevent an AHSV incursion 37
1.13. African horse sickness virus molecular diagnostics 37
1.13.1. Reverse transcription PCR (RT-PCR) 37
1.13.2. Using RT-PCR to detect AHS 38
1.14. High Resolution Melt analysis 42
1.14.1. Brief history and technique overview 42
1.14.2. High Resolution Melt and species/genotype differentiation 48
1.15. African horse sickness virus phylogenetics 52
1.15.1. Phylogenetic studies of the African horse sickness virus and other orbiviruses 52
1.16. Research objectives 60
CHAPTER 2: BIOINFORMATIC ANALYSIS OF AFRICAN HORSE VIRUS GENOME SEGMENTS 2 AND 10 FOR THE DESIGN OF PRIMERS TO SEROTYPE THE VIRUS USING HIGH RESOLUTION MELT ANALYSIS 62
2.1. Introduction 62
2.2. Materials and methods 66
2.2.1. Sequence retrieval 66
2.2.2. Multiple sequence alignment 66
2.2.3. Phylogenetic analysis and phylogeny visualisation 67
2.2.4. Primer design strategies 67
2.2.5. Primaclade 68
2.2.6. BLAST analysis 68
2.3. Results 69

2.3.1. Sequence retrieval....69
2.3.2. Bioinformatic analysis of segment 10 (NS3) 69
2.3.3. Bioinformatic analysis of segment 2 (VP2)....74
2.3.4. Bioinformatic analysis of segment 10 in combination with segment 2 76
2.3.5. BLAST analysis 77
2.4. Discussion 78
2.5. Conclusion....82
CHAPTER 3: AFRICAN HORSE SICKNESS VIRUS SEROTYPE IDENTIFICATION AND ANOMOLY RESOLUTION USING HIGH RESOLUTION MELT ANALYSIS....83
3.1. Introduction....83
3.2. Materials and methods....86
3.2.1. AHSV material....86
3.2.2. Vero cell culture....87
3.2.3. AHSV RNA extraction....88
3.2.4. RT-PCR of AHSV 89
3.3. Results....95
3.3.1. AHSV culture on Vero cell monolayers 95
3.3.2. Confirmation of the presence of AHSV RNA using OIE recognised primers 95
3.3.3. Optimisation of the clade-specific primers and segment 10 primers for RT-PCR .98
3.3.4. One-step vs. two-step RT-PCR protocol....103
3.3.5. Influence of RNA template concentration....105
3.3.6. Identification of anomalies 106
3.3.7. Serotype-specific primer analysis 108
3.3.8. Segment 10 analysis 111
3.3.9. Sequencing of the 10-190 bp region of segment 10 and the clade-specific and serotype-specific amplicons of segment 2 122
3.3.10. Serotype determination....126
3.4. Discussion 131
3.5. Conclusion....143

CHAPTER 4: SEROTYPING THE AFRICAN HORSE SICKNESS VIRUS USING MULTIVARIATE ANALYSIS POST-HIGH RESOLUTION MELT ANALYSIS.....144

4.1. Introduction.....144

4.2. Materials and methods.....146

4.2.1. AHSV material and data source.....146

4.2.2. ScreenClust HRM® Software.....147

4.2.3. GenStat® (14th edition).....147

4.3. Results.....149

4.3.1. Analysis of the melt curve data from the 10-190 bp region amplicon of segment 10 using the ScreenClust HRM® Software.....149

4.3.2. Analysis of the normalised HRM curve data from the 10-190 bp region of segment 10 using GenStat®.....155

4.3.3. Analysis of the melt curve and normalised HRM data from the 10-190 bp region of segment 10 using supervised analysis (ScreenClust HRM® Software) and multivariate discriminant analysis (GenStat®).....157

4.3.4. Analysis of the normalised HRM data from the clade-specific amplicons of segment 2 using multivariate discriminant analysis (GenStat®).....161

4.3.5. Influence of template concentration.....163

4.4. Discussion.....163

4.5. Conclusion.....166

CHAPTER 5: HISTORICAL PHYLOGENETIC ANALYSIS OF THE AFRICAN HORSE SICKNESS VIRUS.....168

5.1. Introduction.....168

5.2. Materials and methods.....170

5.2.1. Method outline.....170

5.2.2. Data retrieval.....170

5.2.3. Sequence alignment.....171

5.2.4. Tree construction.....172

5.2.5. Phylogenetic analysis.....172

5.3. Results.....172

5.4. Discussion.....187

5.5. Conclusion.....191

CHAPTER 6: GENERAL DISCUSSION AND CONCLUSION 192
REFERENCES.....204
Appendices.....227
Appendix A 227
Appendix B 228
Appendix C1 229
Appendix C2 232
Appendix D1 235
Appendix D2 237
Appendix E1 239
Appendix E2 244
Appendix E3 251

List of Figures

Figure 1.1: Confirmed outbreaks of African horse sickness in Southern Africa. 7

Figure 1.2: Bar graph showing the average number of cases per month for five recorded outbreaks of the AHSV in KwaZulu-Natal from 2007-2011..... 8

Figure 1.3: Images of *Culicoides* spp.....12

Figure 1.4: Different effects of ambient temperature on AHSV infection rates, virogenesis and midge survival rates. 14

Figure 1.5: The accepted mode of transmission for African horse sickness and possible overwintering mechanism. 16

Figure 1.6: Cardiac form and pulmonary form of the African horse sickness disease. 19

Figure 1.7: Electron micrographs of African horse sickness virus core particles stained with 2% uranyl acetate. 21

Figure 1.8: Schematic diagram of the structure of an orbivirus showing the organisation of the major and minor structural proteins.....23

Figure 1.9: African horse sickness virus serotype distribution between 2004 and 2006 per province as determined by the number of samples sent to the Equine Research Centre, Onderstepoort. 27

Figure 1.10: South African African horse sickness Controlled Area. 36

Figure 1.11: Simplified melt profile demonstrating the release of a fluorescent dye as the double-stranded DNA is denatured into single-stranded DNA.....43

Figure 1.12: Variations of the interpretations of fluorescence data post HRM analysis. 45

Figure 1.13: The basic steps involved in the analysis of HRM curves using the ScreenClust HRM® Software. 47

Figure 1.14: Comparison of Corbett Rotor-Gene™ 6000 Series Software and ScreenClust HRM® Software for single nucleotide polymorphism (SNP) analysis. 47

Figure 1.15: Using 3D scatter plots to utilise HRM profiles taken over time. 48

Figure 1.16: Melt curves obtained from *Naegleria* spp. using HRM analysis demonstrating unique positions and relative heights of peaks between the species. 49

Figure 1.17: Conventional melt curves of various wild-type and vaccine strains of IBV.....50

Figure 1.18: Relationships between serotypes 1, 3, 4, 8 and 9 of AHSV segment 10. 52

Figure 1.19: Phylogenetic analysis of segment 10 of various orbiviruses.....54

Figure 1.20: Unrooted phylogenetic analysis of AHSV segment 10 sequences isolated from southern African field samples between 2004 and 2006 using Bayesian inference and 1×10^6 iterations. 55

Figure 1.21: Phylogenetic analysis of segment 2 of five East African field strains of AHSV and reference strains from South Africa. 56

Figure 1.22: Phylogenetic analysis of equine encephalosis virus (EEV) segment 10 (NS3) isolated from horses in Israel in 2009. 57

Figure 1.23: Phylogenetic analysis of the genome encoding VP1 sequences from the *Reoviridae* family. 58

Figure 1.24: Phylogenetic analysis of a novel BTV serotype with the twenty-five reference strains of different BTV serotypes based on segment 6. 59

Figure 2.1: Schematic representation showing the ideal primer design across multiple sequences, such as that sought for all of the nine African horse sickness virus serotypes to develop a serotyping assay. 64

Figure 2.2: The phylogeny produced from the ClustalX2 alignment of the 10-190 bp region of segment 10 of the African horse sickness virus genome and viewed using TreeView. 64

Figure 2.3: HRM profiles of the product of the 10-190 bp region of AHSV segment 10 using the Corbett Rotor-Gene™ 6000 Series Software. 65

Figure 2.4: The phylogeny produced from the ClustalX2 alignment of the 10-190 bp region of segment 10 of the African horse sickness virus genome and viewed using TreeView. 68

Figure 2.5: The phylogeny produced from the ClustalX2 alignment of the 10-190 bp region of segment 10 of the African horse sickness virus genome and viewed using TreeView showing the identification of ether two or three clades. 70

Figure 2.6: The phylogeny produced from the ClustalX2 alignment of nucleotides 153-761 of AHSV segment 10 serotypes 1, 2, 3, 7 and 8 (Clade AB) and viewed using TreeView showing the separation of the region into two clades. 70

Figure 2.7: The phylogeny produced from the ClustalX2 alignment of nucleotides 153-712 of AHSV segment 10 serotypes 4, 5, 6 and 9 and viewed using TreeView showing the lack of clear clades for Clade C. 71

Figure 2.8: The phylogeny produced from the ClustalX2 alignment of nucleotides 153-358 of AHSV segment 10 serotypes 3 and 7 (Clade A) and viewed using TreeView to show the potential extent of the separation of the individual serotypes. 72

Figure 2.9: The phylogeny produced from the ClustalX2 alignment of nucleotides 153-284 of AHSV segment 10 serotypes 1, 2 and 8 (Clade B) and viewed using TreeView to show the potential extent of the separation of the individual serotypes. 72

Figure 2.10: Alignment of nucleotides 10-69 of segment 10 for full-length AHSV sequences using ClustalX2 to show the extent of the conservation over the potential probe region. 73

Figure 2.11: Boxshade version of the 33-62 bp position region of segment 10 for all nine available full-length AHSV sequences to investigate the separation of the serotypes into ‘unique’ probe sequence groups. 73

Figure 2.12: The phylogeny produced from the ClustalX2 alignment of the full-length sequences of AHSV segment 2 and viewed using TreeView to investigate potential clades for focused primer design. 74

Figure 2.13: Potential forward primer region (1-17 bp) of AHSV segment 2 based on Sailleau *et al.* (2000) for all nine serotypes. 75

Figure 2.14: Potential reverse primer region (207-228 bp) of AHSV segment 2 based on Sailleau *et al.* (2000) for serotypes 1, 2, 3, 7 and 9 using ClustalX2. 75

Figure 2.15: Potential reverse primer region (339-360 bp) of AHSV segment 2 based on Sailleau *et al.* (2000) for serotypes 4, 5, 6 and 8 using ClustalX2. 75

Figure 2.16: The phylogeny produced from the full-length ClustalX2 alignment of AHSV segment 2 serotypes 3 and 7 (Clade A) and viewed using TreeView to show the potential separation of the individual serotypes. 76

Figure 2.17: The phylogeny produced from the full-length ClustalX2 alignment of AHSV segment 2 serotypes 1, 2 and 8 (Clade B) and viewed using TreeView to show the potential separation of the individual serotypes. 77

Figure 2.18: The phylogeny produced from the full-length ClustalX2 alignment of AHSV segment 2 serotypes 4, 5, 6 and 9 (Clade C) and viewed using TreeView to show the potential separation of the individual serotypes. 77

Figure 2.19: Based on the primers in Table 2.1, phylogenies were drawn based on the theoretical amplicons to assess the ability of the amplicons to be distinguishable using HRM in downstream analysis of the RT-PCR 79

Figure 3.1: Analysis of RT-PCR products of AHSV RNA of OVIA serotypes 3, 7 and the negative control using VP7 OIE primers to amplify a 102 bp product of the genome segment encoding VP7. 96

Figure 3.2: Analysis of RT-PCR products of AHSV RNA of OVIA serotypes 1, 2, 8 and the negative control using VP7 OIE primers to amplify a 102 bp product of the genome segment encoding VP7. 97

Figure 3.3: Analysis of RT-PCR products of AHSV RNA of OVIA serotypes 4, 5, 6, 9 and the negative control using VP7 OIE primers to amplify a 102 bp product of the genome segment encoding VP7. 97

Figure 3.4: Analysis of RT-PCR products of AHSV OVIB serotypes 1-9 and the negative control using VP7 OIE primers to amplify a 102 bp product of the genome segment encoding VP7. 98

Figure 3.5: Analysis of RT-PCR products of AHSV NICD serotypes 1-9 and the negative control using VP7 OIE primers to amplify a 102 bp product of the genome segment encoding VP7. 98

Figure 3.6: Melt analysis of the amplification of AHSV serotype 7 of the OVIA set as an isolate representative of Clade A using its clade-specific primer pair, AF and AR. 99

Figure 3.7: Analysis of gradient RT-PCR products of AHSV serotype 7 of the OVIA set using primer pair AF and AR to amplify a 319 bp product. 100

Figure 3.8: Melt analysis of the amplification of AHSV serotype 8 of the OVIA set as an isolate representative of Clade B using its clade-specific primer pair, BF and BR. dF/dT (rate of change of fluorescence with respect to temperature) of melt curve. 100

Figure 3.9: Analysis of gradient RT-PCR products of AHSV serotype 8 of the OVIA set using primer pair BF and BR to amplify a 249 bp product. 101

Figure 3.10: Melt analysis of the amplification of AHSV serotype 9 of the OVIA set as an isolate representative of Clade C using its clade-specific primer pair, CF and CR. 101

Figure 3.11: Analysis of gradient RT-PCR products of AHSV serotype 9 of the OVIA set using primer pair CF and CR to amplify a 189 bp product. 102

Figure 3.12: Melt analysis of the amplification of AHSV serotype 1 of the OVIB set using primer pair 10F and 10R to determine optimum primer concentration. 102

Figure 3.13: Analysis of gradient RT-PCR products of AHSV serotype 1 of the OVIB set using primer pair 10F and 10R to determine optimum primer concentration and amplify a 181 bp product. 103

Figure 3.14: Amplification and High Resolution Melt of RNA of serotype 3 isolates of the OVIA, OVIB and NICD sets using clade A-specific primers AF/AR and a one-step protocol. 104

Figure 3.15: Amplification and High Resolution Melt of cDNA of serotype 3 isolates of the OVIA, OVIB and NICD sets using clade A-specific primers AF/AR and a two-step protocol. 105

Figure 3.16: High Resolution Melt of cDNA of from varying concentrations of template total RNA from OVIA2, OVIA5, OVIB1 and OVIB2 to assess the influence of starting RNA concentration on HRM analysis using segment 10 primers 10F/10R and a two-step protocol. 106

Figure 3.17: Rate of change of fluorescence with respect to temperature of the genome segment encoding VP2 of Clade C isolates using the CF/CR primer pair. 107

Figure 3.18: Analysis of RT-PCR products of Clade C isolates using the CF/CR primer pair. A 2.5% agarose gel was post-stained with ethidium bromide. ...108

Figure 3.19: Analysis of serotype 2 isolates of OVIA, OVIB and NICD sets using serotype 2 specific primers (2.2F_NM and 2.2R_NM). 109

Figure 3.20: Analysis of serotype 3 isolates of OVIA, OVIB and NICD sets using serotype 3-specific primers (2.3F_NM and 2.3R_NM). 110

Figure 3.21: Analysis of serotype 4 isolates of OVIA, OVIB and NICD sets using serotype 4-specific primers (2.4F_NM and 2.4R_NM). 110

Figure 3.22: Analysis of serotype 5 isolates of OVIA, OVIB and NICD sets using serotype 5-specific primers (2.5F_NM and 2.5R_NM). 111

Figure 3.23: Analysis of serotype 6 isolates of OVIA, OVIB and NICD sets using serotype 6-specific primers (2.6F_NM and 2.6R_NM). 111

Figure 3.24: Amplification and High Resolution Melt of serotypes 1-9 of the OVIA, OVIB and NICD sets using the 10F and 10R primer pairs.....112

Figure 3.25: Analysis of RT-PCR products of all nine serotypes of OVIA, OVIB and NICD sets using segment 10 primers 10F and 10R. 113

Figure 3.26: The High Resolution Melt analysis of the Clade A labelled isolates using the 10F and 10R primer pair. 114

Figure 3.27: The High Resolution Melt analysis of the Clade B labelled isolates using the 10F and 10R primer pair. 115

Figure 3.28: The High Resolution Melt analysis of the Clade C labelled isolates using the 10F and 10R primer pair. 115

Figure 3.29: Phylogeny of the sequenced 10-190 bp region of AHSV segment 10 from the OVIA, OVIB and NICD sets showing clades A, B and C. 116

Figure 3.30: Melt curve analysis comparison of the 10-190 bp region of segment 10 of the isolates labelled OVIA2, OVIB2, OVIA6 and NICDOD(2) using primers 10F and 10R. 117

Figure 3.31: Melt curve analysis comparison of the 10-190 bp region of segment 10 of the isolates labelled OVIA5, OVIA8, OVIB8 and NICDVH(5) using primers 10F and 10R. 117

Figure 3.32: Melt curve analysis comparison of the 10-190 bp region of segment 10 of the isolates labelled OVIB1 and NICD1 using primers 10F and 10R. 118

Figure 3.33: Melt curve analysis comparison of the 10-190 bp region of segment 10 of the isolates labelled OVIA4, OVIB4 and NICDV(4) using primers 10F and 10R. 118

Figure 3.34: Melt curve analysis comparison of the 10-190 bp region of segment 10 of the isolates labelled OVIA7, OVIB7 and NICDK(7) using primers 10F and 10R. 119

Figure 3.35: Melt curve analysis comparison of the 10-190 bp region of segment 10 of the isolates labelled OVIA8, OVIB8 and NICD18/60(8) using primers 10F and 10R. 119

Figure 3.36: Melt curve analysis comparison of the 10-190 bp region of segment 10 of the isolates labelled OVIA9, OVIB9 and NICD9 using primers 10F and 10R. 119

Figure 3.37: The High Resolution Melt analysis of the Clade A labelled isolates using the 10F and 10R primer pair. 125

Figure 3.38: Melt curve analysis of the 10-190 bp region of segment 10 of AHSV for the isolates labelled OVIB1 and NICD1 using primers 10F and 10R. 125

Figure 3.39: The High Resolution Melt analysis of the Clade C labelled and suspected isolates using the 10F and 10R primer pair. 125

Figure 3.40: Amplification and High Resolution Melt of cDNA of serotype 3 and 7 isolates of the OVIA, OVIB and NICD sets using clade A-specific primers AF/AR and a two-step protocol. 126

Figure 3.41: Amplification and High Resolution Melt of cDNA of serotypes 1, 2 and 8 of the OVIA, OVIB and NICD sets using clade B-specific primers BF/BR and a two-step protocol. 127

Figure 3.43: Amplification and High Resolution Melt of cDNA of serotype 4, 5, 6 and 9 of the OVIA, OVIB and NICD sets using clade C-specific primers CF/CR and a two-step protocol. 129

Figure 3.44: The phylogeny produced from the ClustalX2 alignment of the 10-190 bp region of segment 10 of the African horse sickness virus genome and viewed using TreeView. 140

Figure 3.45: Phylogeny of Clade B serotypes based on the segment 10 10-190 bp region. 141

Figure 3.46: Phylogeny of Clade B serotypes based on the segment 2 1302-1551 bp region. 142

Figure 4.1: Features of the melt curve included in the principal component analysis (PCA). 148

Figure 4.2: ScreenClust HRM® Software graphical output of the principal component scores for the 10-190 bp region of segment 10 of AHSV for the OVIA, OVIB and NICD sets. 151

Figure 4.3: The phylogeny produced from the ClustalX2 alignment of the 10-190 bp region of segment 10 of the African horse sickness virus genome and viewed using TreeView. 152

Figure 4.4: Cluster assignments for the segment 10 10-190 bp region for the OVIA isolates. 153

Figure 4.5: PCA of all AHSV isolated based on segment 10 HRM normalised data. 156
Figure 4.6: Discriminant analysis in GenStat® of OVIA, OVIB and NICD sets of AHSV using five attributes. 159
Figure 4.7: Discriminant analysis in GenStat® of OVIA, OVIB and NICD sets of AHSV using four attributes. 160
Figure 4.8: PCA biplot for the discriminant analysis using four attributes of the segment 10 HRM curve data. 161
Figure 4.9: Discriminant analysis of clade-specific amplicons of segment 2 using GenStat®. Clade A (serotypes 3 and 7), Clade B (serotypes 1, 2 and 8) and Clade C (serotypes 4, 5, 6 and 9). 162
Figure 4.10: Discriminant analysis of OVIB1, OVIA2, OVIB2 and OVIA5 using intial starting template concentrations ranging from 0.5 – 50 ng/µL using GenStat®. 163
Figure 5.1: AHSV segment 2 phylogenetic tree to identify the serotype of an isolate from the 2011 outbreak in the Western Province compared to segment 2 sequences from GenBank. 171
Figure 5.2: Phylogenetic tree of all available VP1 sequences of AHSV to identify potential serotype and/or isolate period relationships over time. 173
Figure 5.3: Phylogenetic tree of all available VP2 sequences of AHSV to identify potential serotype and/or isolate period relationships over time. 174
Figure 5.4: Phylogeny of all available VP3 sequences of AHSV to identify potential serotype and/or isolate period relationships over time. 175
Figure 5.5: Phylogeny of all available VP4 sequences of AHSV to identify potential serotype and/or isolate period relationships over time. 176
Figure 5.6: Phylogeny of all available VP5 sequences of AHSV to identify potential serotype and/or isolate period relationships over time. 177
Figure 5.7: Phylogeny of all available VP6 sequences of AHSV to identify potential serotype and/or isolate period relationships over time. 178
Figure 5.8: Phylogeny of all available VP7 sequences of AHSV to identify potential serotype and/or isolate period relationships over time. 179
Figure 5.9: Phylogeny of all available NS1 sequences of AHSV to identify potential serotype and/or isolate period relationships over time. 182
Figure 5.10: Phylogeny of all available NS2 sequences of AHSV to identify potential serotype and/or isolate period relationships over time. 183
Figure 5.11: Phylogeny of all available NS3 sequences of AHSV to identify potential serotype and/or isolate period relationships over time. Clade B and C branches have been collapsed. 185
Figure 5.12: Phylogeny of all available NS3 sequences of AHSV to identify potential serotype and/or isolate period relationships over time. 185
Figure 5.13: Phylogeny of all available NS3 sequences of AHSV to identify potential serotype and/or isolate period relationships over time. Clade A and B branches have been collapsed. 187

List of Tables

Table 1.1: Coding assignments of Grubman and Lewis (1992), Roy et al. (1994) and Mertens et al. (2006) for the ten genome segments of the African horse sickness virus. 22

Table 1.2: Data derived from a number of sources describing the accepted functions of the ten proteins common to all orbiviruses and their molecular weights. 24

Table 1.3: AHSV Serotypes and historical isolates/reference strains (Ozawa & Dardiri, 1970). 26

Table 1.4: Summary of recent RT-PCR assays for the African horse sickness virus. 40

Table 2.1: AHSV segment 2 primers to separate segment 10 clades into individual serotypes 78

Table 3.1: Details of the AHS virus reference strains from the NICD used in Vero cell culture for viral RNA isolation and subsequent RT-PCR and HRM analysis. 87

Table 3.2: Two sets of field isolated virus material supplied by OVI-ARC (designated OVIA and OVIB). 87

Table 3.3: List of primers used for the analysis of AHSV by HRM. 90

Table 3.4: Serotypes per clade as defined in Groenink (2009). 90

Table 3.5: Layout of gradient PCR for the determination of the optimum annealing temperature of the clade-specific primers (AF/AR, BF/BR, CF/CR). 91

Table 3.6: Layout of gradient PCR for the determination of the optimum primer concentration and annealing temperature for the segment 10 primers (10F/10R). 92

Table 3.7: Optimisation of RT-PCRs through gradient PCRs using AHSV clade-specific primers. 99

Table 3.8: Summary of AHSV serotype profiling following Rotor-Gene™ software genotype calling using the 10-190 bp region of segment 10 and clade-specific primers. 120

Table 3.9: Results of sequencing amplicons of both segments 2 and 10 for all isolates and allocation of the most likely serotype after BLASTn analysis of the edited sequences. 123

Table 3.10: Clade A HRM analysis genotyping for OVIA, OVIB and NICD using the Corbett Rotor-Gene™ 6000 Series Software 1.7™ 130

Table 3.11: Clade B HRM analysis genotyping for OVIA, OVIB and NICD using the Corbett Rotor-Gene™ 6000 Series Software 1.7™ 130

Table 3.12: Clade C HRM analysis genotyping for OVIA, OVIB and NICD using the Corbett Rotor-Gene™ 6000 Series Software 1.7™ 131

Table 3.13: Final allocation of serotypes, through sequencing, to the OVI and NICD isolates with anomalies highlighted. 138

Table 4.1: The cluster values of the nine AHS serotypes OVIA, OVIB and NICD. 150

Table 4.2: Cluster assignments of the 10-190 bp region of segment 10 for the OVIA set of AHSV using the ScreenClust HRM® Software. 153

Table 4.3: Cluster assignments of the 10-190 bp region of segment 10 for the OVIB set of AHSV using the ScreenClust HRM® Software. 154

Table 4.4: Cluster assignments of the 10-190 bp region of segment 10 for the NICD set of AHSV using the ScreenClust HRM® Software. 155

Table 4.5: Latent vectors of AHSV isolates in a principal component analysis in GenStat®....156

Table 4.6: Choice of isolates for references of each serotype for a supervised analysis in ScreenClust HRM® Software or a multivariate discriminant analysis in GenStat®. 157

Table 4.7: A supervised ScreenClust HRM® Software analysis of the three sets of AHSV isolates (OVIA, OVIB and NICD) using the selected representatives in Table 4.6....158

Table 5.1: AHSV sequences available on GenBank as at 15 May 2012. 172

Acknowledgements

Lord, You have carried me through this, in the good times and the not-so-good times and I pray that this dissertation does Your will.

I have had the privilege and honour to work under three fantastic supervisors:

Prof. Theresa Coetzer, thank you for taking this project on and allowing me to be a part of your research group. You opened up many doors for this project and I am greatly indebted to you for doing so and allowing me the freedom to follow my passion. Thank you also for your excellent and thorough review of this dissertation.

Dr. Marion Young, I think we have perfected the art of reciprocal management! Thank you for your friendship and shared passion for all things equine and how we can make the equine world a better one. Your never-ending faith in me and enthusiasm for the project never faltered. Thank you!

Dr. Gregory Watson, this project began when you planted the seed back in 2006. Thank you for introducing me to the world of HRM analysis and the enormous possibilities of it and all of the other techniques that I hope I have become proficient in, both in the lab and on computer. Thank you for always guiding me!

Dr. Sandy Bye, thank you for all of your support and encouragement over the final hurdles.

The National Research Foundation has been an invaluable part of this project and is duly acknowledged for personal financial support during the course of my post-graduate career.

The University of KwaZulu-Natal is gratefully acknowledged for their financial assistance towards this project through the Doctoral Scholarship Award.

The late Dr. Dave Mullins and the AHS Trust are duly acknowledged for financial support to attend and present at the Climate Change, Health and Ecology Conference in Uppsala, Sweden in September 2010.

To all of the members, past and present, of Prof. Coetzer's research group in Lab 44: it has been an honour to work with you and I am only sorry that I could not spend more time IN lab 44. Thank you for the friendship and support.

To all of the staff; academic, technical and administrative; in Biochemistry (and the old SBGM and new SLS) that took me in again, thank you for always being available, no matter how small a thing. Special mention must go the Ms. Charmaine Ahrens and Mrs. Robyn

Hillebrand for their tireless efforts to keep us post-grads in the lab, especially when the administrative protocols proved too much for us! Your work behind the scenes is an invaluable part in the lead up to this dissertation.

The Animal and Poultry Science discipline has been my ‘adopted’ home for the last five years and everyone there has made this journey so enjoyable. Thank you for the laughs, advice, support, encouragement and tea.

To my parents-in-law, Brian and Pauline, I am forever grateful for all of your support and prayers. Thank you.

Mom and Dad – I would be nothing without you and would never have been where I am today without your unwavering support and loyalty, through thick and thin. You have inspired me throughout this process. Thank you.

Robyn, my darling wife. There are no words to express what your support means to me. Your faith in me often exceeds my own. We have travelled an extraordinary path and I cannot wait to see what lies ahead for us. Thank you for allowing me to follow my dreams. God is forever faithful, I love you!

Do you give the horse its strength
or clothe its neck with a flowing mane?
Do you make it leap like a locust,
striking terror with its proud snorting?
It paws fiercely, rejoicing in its strength,
and charges into the fray.
It laughs at fear, afraid of nothing;
it does not shy away from the sword.
The quiver rattles against its side,
along with the flashing spear and lance.
In frenzied excitement it eats up the ground;
it cannot stand still when the trumpet sounds.
At the blast of the trumpet it snorts, ‘Aha!’
It catches the scent of battle from afar,
the shout of commanders and the battle cry.
Job 19:19-25

List of abbreviations

AHS	African horse sickness
AHSV	African horse sickness virus
bp	base pair(s)
BSL	bio-safety level
dF/dT	rate of change of fluorescence with respect to temperature
DNA	deoxyribonucleic acid
DEPC	diethylpyrocarbonate
DAFF	Department of Agriculture, Forestry and Fisheries
ds	double-stranded
EMEM	Eagle's minimum essential medium
FBS	foetal bovine serum
fg	femtogram(s)
HRM	High Resolution Melt
IPA	isopropyl alcohol
NCBI	National Centre for Biotechnology Information
NICD	National Institute of Communicable Diseases
NTC	no template control
OBP	Onderstepoort Biological Products
OIE	World Organisation for Animal Health
OVI	Onderstepoort Veterinary Institute
PC	principal component
PCA	principal component analysis
PCR	polymerase chain reaction
RNA	ribonucleic acid
RT-PCR	reverse transcriptase-polymerase chain reaction
Real-time PCR	real-time polymerase chain reaction
ss	single-stranded
$TCID_{50}$	50% tissue culture infective dose
TBE	tris-borate-EDTA buffer
VN	virus neutralisation

CHAPTER 1: INTRODUCTION, LITERATURE REVIEW AND RESEARCH OBJECTIVES

1.1. Introduction

1.1.1. Background

African horse sickness (AHS) is a devastating viral disease that afflicts members of the Equidae family. In South Africa, there are nearly 300,000 horses and approximately 160,000 donkeys that make up the national herd with over 30,000 zebra in protected areas around the country according to data from South African National Parks and KZN Wildlife (Gerdes, 2006). Horses are the most susceptible with a 90% mortality rate, while zebras remain subclinical for the virus and act as a reservoir of the virus (Coetzer & Erasmus, 1994).

The *African horse sickness virus* (AHSV) is a member of the *Orbivirus* genus that belongs to the *Reoviridae* family, with many similarities in epidemiology to the prototype virus, the *Bluetongue virus* (BTV). As an orbivirus, AHSV has a double-stranded RNA genome of ten segments (Oellermann *et al.*, 1970; Bremer, 1976; OIE, 2009). AHSV is a vectored arbovirus transmitted between equines via *Culicoides* spp. of midge. In South Africa, *Culicoides imicola* plays the largest role in the epidemiology of the virus although *C. bolitinos* has also been found to play a significant role in some areas (Meiswinkel & Braack, 1994; Meiswinkel & Paweska, 2003). AHSV competent *Culicoides* species have been found throughout the world from the Americas, Europe and Australasia (Boorman *et al.*, 1975; Mellor *et al.*, 1975; Mellor, 1994; Goffredo & Meiswinkel, 2004). In view of this, strict quarantine protocols are followed when horses are exported from sub-Saharan Africa. Previous incursions into Europe, the Middle East and Asia have been severe due to the serologically naïve status of equine species in these regions. The last major *ex situ* outbreak on the Iberian peninsula from 1987-1990 was caused by the candid importation of infected zebra from Namibia (Lubroth, 1988; Lord *et al.*, 1998b). The recent and widespread bluetongue outbreaks in Europe have prompted many countries to step up surveillance programmes and develop strategies to cope with a potential AHS outbreak (Mertens, 2007; Carpenter *et al.*, 2009; Maclachlan & Guthrie, 2010).

The necessary strict quarantine protocols in place for the export of equines from South Africa have a paralysing effect on the local equine industry. The international competitiveness of South African race and sport horses is seriously hampered, with costly and lengthy quarantine periods currently in place to export a horse from South Africa to the EU. Racing South Africa has, however, engaged with both the World Organisation for Animal Health

(OIE) and World Trade Organisation (WTO) to reduce this to just fourteen days, under ideal conditions. As part of the agreement, rapid, sensitive diagnostics are vital to effect this (RacingSA, 2012).

Furthermore, AHS has a significant effect on working equines. In much of the world, rural economies still rely on animal power, provided by donkeys, mules and horses (Simalenga & Joubert, 1997; El Idrissi & Lubroth, 2006). The socio-economic circumstances of the owners inevitably render knowledge of AHS to be very poor – both in identification of symptoms and control. One of the major problems in South Africa with regard to the AHS outbreaks is the large population of unvaccinated equids living in the rural parts of the country, away from the concentrated and controlled racing and sport horse communities (Gerdes, 2006). Despite the enormous role that these equines play in their communities, seemingly little attention is given to the health and welfare of these animals that may play an important epidemiological role in endemic and non-endemic outbreaks of AHS (El Idrissi & Lubroth, 2006).

Nine serotypes of AHSV have been isolated. The last was isolated in 1960, and, as such, AHSV is considered a relatively stable virus (Howell, 1962). Each genome consists of ten segments of dsRNA with two segments being responsible for serotype diversity – segment 2 (which encodes VP2) and segment 10 (which encodes NS3) (Grubman & Lewis, 1992). However, the role of serotypes in the epidemiology of the disease is poorly understood. This could be because only two or three serotypes may be prevalent in any one year and the state veterinarian's protocol that only requires the serotyping of one isolate per defined outbreak. OIE Reference Laboratories throughout the world do, however, maintain stock of recent isolates and reference strains. It is largely accepted that theses isolates are correctly serotyped when acquired for independent research.

1.1.2. Research rationale

An accurate and rapid diagnosis of equine infectious diseases is an important goal for researchers and veterinarians alike. Diagnosing the virus remains an integral part of disease management. Early detection of causative agents and identification of the serotype and/or strain has immediate benefits that include applying the correct treatment regime for the animal, notifying authorities in the case of notifiable diseases and implementing suitable control measures to prevent further spread of the disease. The development of rapid assay methods to identify AHS serotypes is imperative in the study of the disease, in order that control (including vaccination) might augment the conventional prophylactic strategies currently employed, hence the term point of care diagnostics. The ability to serotype the causative virus in an AHS outbreak rapidly, combined with the increasing development of monovalent vaccines makes a rapid serotyping assay even more important (Koekemoer *et*

al., 2000). As a result, the national equine population could be protected far more effectively against AHS. Furthermore, the serotyping and classification of the virus will assist greatly in a rapid classification of future outbreaks for taxonomic and epidemiological purposes. A rapid assay may also promote future exportation of South African equine athletes and improve the livelihood of rural people who depend on equines as working animals for subsistence.

Rapid point of care diagnostics are desirable, but should not come at the expense of specificity and/or sensitivity. In addition, serotyping the virus rapidly has important consequences for controlling the outbreak and protecting horses located within a certain radius of the initial outbreak. Monovalent vaccines, as stockpiled by the EU, would need to be rapidly deployed in the event of an outbreak in Europe (Anonymous, 2009). As such, the importance of identifying serotypes cannot be underestimated.

The objective of this research was to combine PCR with High Resolution Melt (HRM) analysis for detecting the AHS virus in the blood or other biological samples obtained from infected equids. Noteworthy advantages exist in using PCR and HRM analysis in clinical situations where conventional microbiology is inadequate, time-consuming or labour-intensive (e.g. cell culture), or difficult and hazardous (Abdalla *et al.*, 2002). The rapid nature of PCR also has important consequences for limiting the spread of highly contagious pathogens in an epidemic – results are typically available in less than 24 hours (Stone-Marschat *et al.*, 1994).

Non-PCR based serotyping techniques, such as virus neutralisation, take up to two weeks to achieve a result and it is imperative that the neutralising antibodies are specific (Aradaib *et al.*, 1995). This has further hindered the understanding of the seroprevalence of the virus and often leads to wild speculations by lay horse owners (author's observations). The development of an assay that can rapidly serotype the virus could potentially generate large amounts of data, if popularly accepted. This would facilitate an understanding of the interaction and relationships of the serotypes and the role each plays in the epidemiology of the virus and its course of disease in the equid.

In addition, the use of PCR and HRM analysis will make epidemiological studies into African horse sickness more thorough. Indeed, the modern nucleic-acid based assays have revolutionised the diagnosis of disease and its related epidemiological studies. These molecular systems have made the isolation of pathogens secondary. The characterisation of pathogens will follow this lead and other isolation steps may become obsolete (Eaton & White, 2004). This study represents the future in that regard. The cost and analysis time for serotyping will be drastically reduced. Blood from sub-clinical equids can provide differential

diagnoses for early-warning system strategies and interventions to be employed. These strategies and interventions include: early quarantining of viral 'hot spot' outbreaks, appropriate vaccination regimes to prevent the further spread of the outbreak (Guthrie *et al.*, 2009) and prophylactic measures that can be extrapolated to vector control and altered husbandry systems (Jenkins, 2008; Simpkin, 2008). Furthermore, the possibility of real-time simulation modelling on AHS becomes a very real possibility as the role that different serotypes play in the epidemiology of the disease could lead to a comprehensive modelling and surveillance strategy that will predict future outbreaks and so permit a more effective, monovalent vaccination programme.

In the last few years, phylogenetic studies have been increasingly used to characterise viruses and viral disease outbreaks and to confirm new serotypes in other orbiviruses. Molecular phylogenetics remains a powerful tool in this regard (Baldauf, 2003; Quan *et al.*, 2008).

The development of a rapid serotyping assay, with minimal cost, has huge advantages for South Africa, ranging from rural, subsistence equines, to the expedition of exporting high-value race and sport horses to the world. Internationally, this assay has the potential to greatly influence the response to a non-endemic outbreak.

1.2. History of African horse sickness

Although African horse sickness almost certainly originated from Africa, the first recorded epidemic of African horse sickness was in 1327 in the Yemen, (Moule, 1896; Henning, 1956). In Africa, a monk named Father Monclaro was the first to describe the disease from a 1569 account of journeys into central and east Africa, using horses imported from India (Theiler, 1921). In South Africa, the disease first appeared in horses when they were brought to the Cape of Good Hope in 1652 by the Dutch East India Company. Sixty years after the introduction of horses to the Cape the first major, officially recorded, outbreak occurred in 1719 when 1700 horses died. (Coetzer & Erasmus, 1994; Marlow, 2010) It was, however, already apparent that annual winter frost events appeared to retard the spread of the disease (Theiler, 1921). The most severe recorded outbreak of AHS was in 1854/55 when it was estimated that over 70,000 horses, or 40% of South Africa's horse population, died from AHS. By 1921, AHS outbreaks were reported in Northern Rhodesia (Zambia), South West Africa (Namibia), Angola, British East Africa (Kenya), German East Africa (Tanzania), Zanzibar, Uganda, Sudan/Southern Sudan, Abyssinia (Ethiopia) and Eritrea (Theiler, 1921; Huismans *et al.*, 1987).

In the early 1900s, pioneers of AHS research discovered that the disease was caused by a virus (Coetzer & Erasmus, 1994; de Sa *et al.*, 1994). At the same time it was becoming apparent to Theiler (1921) that immunologically distinct strains of the virus existed. This theory gained further credibility with the work of Alexander in the 1930s. Alexander also started research that would have important vaccine-related consequences when he showed that the virus was attenuated during passage in chicken egg embryos (Coetzer & Erasmus, 1994). In 1944, it was confirmed that the AHS virus was vectored by *Culicoides imicola* (du Toit, 1944). Nine serotypes have been described, the last being described in 1960, with no new publications suggesting otherwise (Howell, 1962). Major outbreaks of the disease occur approximately every 20-30 years. However, a decline in the zebra and horse population and the advent of the polyvalent vaccine produced by Onderstepoort Biological Products in the last century has largely prevented the massive outbreaks of the past, although outbreaks continue to have devastating consequences in certain, more localised areas (Mellor & Hamblin, 2004).

1.3. Epidemiology

1.3.1. Epizootic events – beyond South Africa

The distribution of AHS is limited to geographical regions that favour the biology of the *Culicoides* spp. midge (Mellor, 1993). AHS is endemic to sub-Saharan Africa, including both the tropical and sub-tropical regions and occurs from Senegal in the west to Sudan, Ethiopia and Somalia in the east and south to South Africa. The disease has been reported in North Africa, but it is generally constrained to the south of the Sahara due to the desert's large expanse that acts as a protective barrier. AHS has not been reported in Madagascar, nor any of the Indian Ocean islands (Abu Elzein *et al.*, 1989; Mellor, 1993; Guthrie, 2008; Bitew *et al.*, 2011; Gordon *et al.*, 2013; Haji Ende *et al.*, 2013).

Beyond the borders of Africa, AHS has occurred sporadically in the Middle East where it has been reported in 1930, 1944 and 1959-1961. In 1965 AHS occurred in the northern-most African countries and crossed into Spain in 1966, but was quickly suppressed through a mass vaccination and slaughter policy (Lord *et al.*, 1997b). The virus usually fails to persist outside Africa due to the climatic conditions experienced in winter (Mellor, 1993). The Iberian peninsula was again afflicted in 1987-1991 following the importation of AHSV serotype 4-infected zebra from Namibia (Lubroth, 1988). The disease initially disappeared with the arrival of winter. However, the same serotype surfaced again in 1988 and every year until 1991, spreading to Portugal and Morocco. The apparent ability of the virus to overwinter outside Africa caused widespread concern and led to a wave of AHS research in Europe, but

this has, sadly, subsequently decreased (Chuma *et al.*, 1992; Laviada *et al.*, 1992; Laviada *et al.*, 1993; Zientara *et al.*, 1993; Zientara *et al.*, 1994; Laviada *et al.*, 1995; Zientara *et al.*, 1995a; Zientara *et al.*, 1995b; Laviada *et al.*, 1997).

AHSV is only able to survive in the long-term through continuous and uninterrupted cycles of transmission between vertebrate and invertebrate hosts. Any 'vector-free' period cannot be longer than the duration of viraemia in a vertebrate host. In sub-Saharan Africa, no such 'vector-free' periods exist and the virus is able to survive from season to season and year to year. Generally, at higher and lower latitudes, the prevailing climatic conditions become less conducive to the survival of the vectors and the disease cycle is broken. This results in brief epizootics of the disease when specific environmental conditions are met, such as in the Iberian peninsula and Morocco (Mellor, 1994).

1.3.2. Endemic events – South Africa

1.3.2.1. Geographical distribution

In South Africa, AHS occurs every year, mainly east of the Karoo and Kalahari deserts (Figure 1.1) (AHS-Trust, 2008), but depends largely on the immune barrier (vaccinated population) and the timing within the season with regard to rainfall and ambient temperature (Gerdes, 2006). The disease historically and commonly appears to originate in the north-eastern parts of the country and move southward. Indeed, Lord *et al*. (2002) described the force of infection as being the strongest in the north-east, declining in a south-westerly direction. However, the 300,000 doses of vaccine that are sold by Onderstepoort Biological Products per year appear to have slowed this southward progression somewhat and formed what could be termed an 'immune barrier' (Guthrie, 2008). Theiler (1921) reported the absence of the disease from large parts of the Free State and Lesotho. This feature of AHS was also noted early on by the horse-breeding community, some from the early 1700s, on the high grounds of the Eastern Cape interior. AHS predominates in the warm coastal areas or low-lying, moist, inland areas. Theiler (1921) also reported that the disease occurs predominantly in and around lakes, pans, vleis and rivers of the south-eastern and eastern coastal belt. Heavy, early summer rainfall, followed by a drier period appears to favour the development of epidemics (Marlow, 2010).

Figure 1.1: Confirmed outbreaks of African horse sickness in Southern Africa. Left – 2011/2012 season; right – 2012/2013 season according to the African Horse Sickness Trust (AHS-Trust, 2012).

1.3.2.2. Seasonal distribution

Due to the disease's relationship with vector populations, it has a very seasonal nature (Figure 1.2). However, longer term studies have largely concluded its cyclical nature as well. It is seasonal as it peaks during the late summer/autumn months and cyclical as it has been proposed that the major outbreaks have occurred following El Niño warm-phase events, which occur approximately every 20 years (Theiler, 1921; Baylis *et al.*, 1999; Coetzee, 2000; OIE, 2008; Linthicum *et al.*, 2010). In general, AHS first emerges during December/January with a peak in cases during March/April. Following the first frosts in May/June, the disease appears to be arrested (Guthrie, 2008; Gordon *et al.*, 2013). Interestingly, in East Africa, the majority of cases are seen from September to December with a peak in October (Ayelet *et al.*, 2013). Generally, the severity of the annual outbreak is assumed to be largely due to a complex combination of El Niño patterns, especially in a water-scarce country such as South Africa (Baylis *et al.*, 1999; Gerdes, 2006). Early summer rains with high precipitation are generally followed by an AHS epizootic (Guthrie, 2008; Burne, 2011).

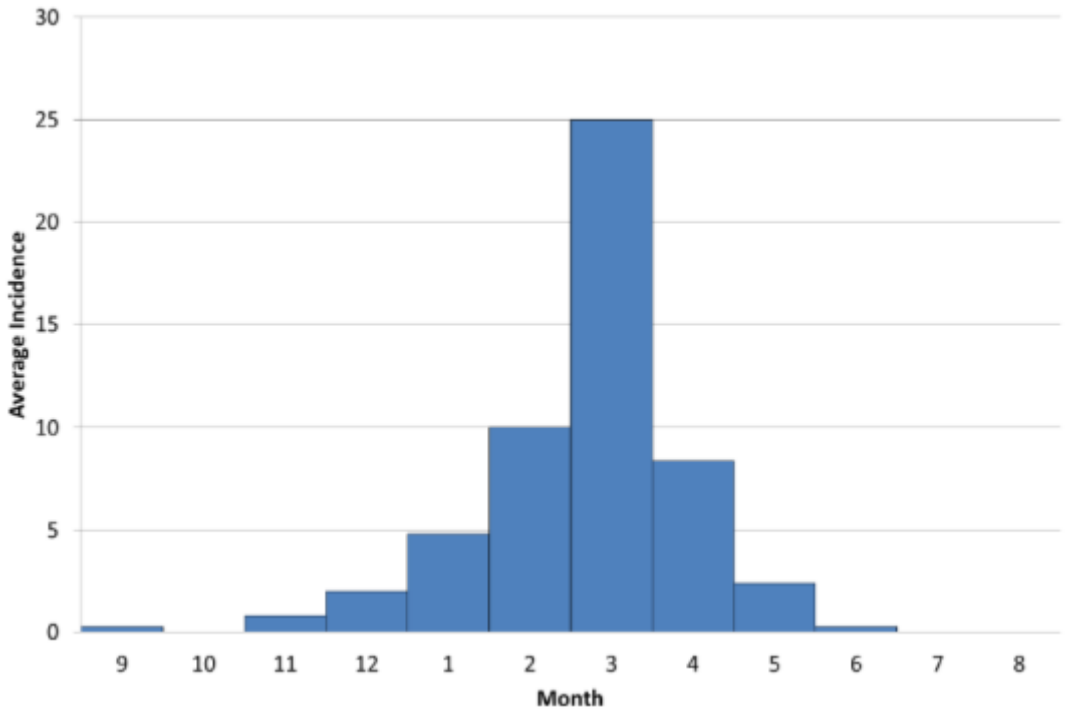

Figure 1.2: Bar graph showing the average number of cases per month for five recorded outbreaks of the AHSV in KwaZulu-Natal from 2007-2011. January (1) – December (12). This exhibits the seasonal pattern of AHS with a peak in March (3) and no recorded cases during the winter months (July-August/7-8) (Burne, 2011).

1.3.2.3. Serotype distribution

During an outbreak of AHS, one serotype will usually dominate, but it does not exclude other serotypes (Guthrie, 2008). Moreover, serotypes are seldom detected in the same area in successive years. Historically, serotypes 1-8 are mostly responsible for outbreaks in South Africa, while serotypes 4 and 9 have been recorded in outbreaks outside of Africa (Lubroth, 1988; Mellor *et al.*, 1990b), although this is becoming less clear (Aklilu *et al.*, 2012). Serotypes 1-8 were previously found to have a higher mortality (90-95%) than serotype 9 (70%) (Coetzer & Erasmus, 1994). All nine serotypes have been detected in eastern and southern Africa, with serotype 9 being more dominant in the north-west and north-east regions of sub-Saharan Africa (Guthrie, 2008; Ayelet *et al.*, 2013). In 2006, AHS serotype 2 was found to be responsible for an outbreak in Nigeria that subsequently spread to Senegal. This was the first isolation of serotype 2 in the Northern Hemisphere. The implied reasons for this incursion range from lax border controls in West Africa to the spread of the vector due to global warming (Fasina, 2008; Fasina *et al.*, 2008). However, broad scale and widespread studies are required to understand the relationship that virus serotypes play in AHS epidemiology more definitively.

1.3.3. Simulation modelling

Simulation modelling of epidemics can facilitate understanding of the factors involved in the cause and duration of epidemics, particularly when they occur in non-endemic regions. Lord *et al.* (1996b) suggested that midge population size, the recovery rate in horses and the time of year that the virus is introduced to an area, were found to be the most significant factors in contributing to the establishment of an epidemic. The size of the epidemic was found to be influenced by the inter-bloodmeal period of the midge, the mortality and recovery rates of the infected horses, midge population size and transmission rates.

A more sophisticated model was developed by Backer and Nodelijk (2011). Whilst also taking into account the time of introduction, temperature variability and vector season, horse density was also considered which directly affected vector-host ratios, which was considered the primary factor in the virus' ability to spread rapidly or not. One of the primary drawbacks in creating models that are more accurate is taking into account the complex relationship between environmental conditions and midge populations. By combining geographic information systems (GIS) and artificial neural networks (ANN) a reliably accurate model was developed (Eksteen *et al.*, 2011). However, it should be noted that models based on real data will also depend on the accuracy of reporting procedures that generated that data and how many cases are actually included in the model.

1.4. Range of AHSV hosts

The range of hosts for AHSV is confined primarily to equine species. The most susceptible are horses (70-95% mortality) followed by mules (50-70% mortality). African donkeys and zebras are the most resistant and seemingly remain subclinical for AHS (Theiler, 1921; Abu Elzein *et al.*, 1989; Bitew *et al.*, 2011; Teshome *et al.*, 2012). The high mortality of horses and mules indicates that they are most likely accidental hosts (Erasmus, 2004). Varying individual responses to the same virus have been recorded (Theiler, 1921). Native horse populations in AHS endemic/enzootic regions descended from herds from 2000 BC may have acquired resistance to AHS equal to that of a zebra or donkey (Coetzer & Erasmus, 1994). Recently, over a two year period, up to 8% of vaccinated horses were reported to be subclinically infected with AHSV. This has alarming implications in terms of surveillance programmes in South Africa and internationally (Weyer *et al.*, 2013). In the 2011 outbreak of AHSV in the Western Province, four equids were identified as being subclinical as well (Grewar *et al.*, 2013). Haji Ende *et al.* (2013) found that 46% of horses, 61% of mules and 36% of donkeys tested positive for AHSV antibodies.

Another host for AHS is the domestic dog (Salama *et al.*, 1981; el-Husseini *et al.*, 1986; van Sittert *et al.*, 2013). Historically, the dog only becomes viraemic after the ingestion of infected meat or experimental infection, but they are not considered to play any role in the transmission of AHS (Van Rensberg *et al.*, 1981; Braverman & Chizov-Ginzburg, 1996; Maclachlan & Guthrie, 2010). However, a recent case described the infection of a dog by AHSV without ingestion of infected meat which was kept in an accredited facility (van Sittert *et al.*, 2013). Other African carnivores that have been tested positive for AHS antibodies are the spotted hyena, lion, cheetah, African wild dog, jackal and genet (Alexander *et al.*, 1995). Anti-AHS antibodies have not been found in any wild or domestic ruminants save for the camel (Awad *et al.*, 1981a; Awad *et al.*, 1981b; Mellor & Hamblin, 2004). Moreover, the camel has been identified as a possible sentinel animal, or indicator host, for AHS in Morocco (Touil *et al.*, 2012) and is considered a possible means by which AHSV could be transported across the Sahara, introducing AHSV to Northern Africa, which is close to Europe (El-Harrak *et al.*, 2011). However, a serological survey undertaken in Algeria did not find antibodies to AHSV in the horses and donkeys tested (Madani *et al.*, 2011). Pigs, cats and monkeys are resistant to infection (Coetzer & Erasmus, 1994). The OIE reports that there is no evidence that humans could become infected with AHSV. However, it has been described previously that certain neurotropic vaccine strains may cause encephalitis and retinitis of the eyes in humans following aerosol infection during vaccine production (van der Meyden *et al.*, 1992).

1.4.1. Reservoirs

"The continued circulation of an insect-transmitted virus depends on the availability of susceptible hosts and competent vectors in sufficient numbers" (Barnard, 1993). Zebra (*Equus burchelli*) are considered to be the natural vertebrate host and reservoir for the disease and are instrumental in the persistence of the disease in Africa (Bigalke, 1994). Experimental infection of zebra, and the identification of anti-AHSV antibodies in free-living zebra is strongly suggestive of the reservoir role that zebras might fulfil in the persistence of AHSV (Barnard, 1993). Furthermore, the viraemic state in zebra may extend to up to 40 days (and remain subclinical), whereas in horses it is less than 7 days (Barnard *et al.*, 1994; Meiswinkel & Paweska, 2003; Maree & Paweska, 2005). Zebra are known to have existed on the highveld and southern savannah woodland in South Africa for perhaps millions of years and to have adapted to the infectious agents of the environment and so may act as carriers and maintenance hosts (Bigalke, 1994). The reservoir host theory has yet to be conclusively proven (Erasmus, 2004; OIE, 2009). The literature that exists concerning zebra and AHS makes this assumption without setting out to prove or disprove the assumption (Meyer, 2007). Although it is commonly accepted that viral transmission is halted in winter, it may continue at a lower rate in warmer, low-lying, tropical regions. In South Africa, this description would apply to the Kruger National Park. Coupled with the large numbers of zebras in the park, this may indeed constitute the reservoir host system needed for the virus to overwinter (Meiswinkel *et al.*, 1994). In a similar fashion, donkeys may perform the same role in other parts of the country where the population is high relative to the number of horses (Guthrie, 2008). The lack of zebra in areas outside Africa where outbreaks have occurred and not persisted is indicative of the fact that the horse is not a long-term reservoir for AHS. However, serotype 9 persists in areas of West Africa where zebra do not occur naturally (Mellor & Hamblin, 2004). It has been accepted that subclinically infected zebras imported into Spain were responsible for the Iberian outbreak in the late 1980s (Lubroth, 1988).

Since the beginning of the 20th Century, the number of outbreaks occurring throughout South Africa appears to have been declining. This pattern coincides with a reducing number of free ranging zebra across South Africa due to hunting. However, the proliferation of game parks (and restocking of zebra) in certain areas may result in a threshold population density being breached constituting a permanent host population that could become established in localised regions (Barnard, 1998; Mellor & Hamblin, 2004).

It is perhaps pertinent to note that since zebras remain subclinical for the virus and are largely unaffected, game farm/reserve owners have no need to invest, in partnership with horse owners, in reducing the impact of African horse sickness. This is a common conflict

worldwide between domestic animal owners and wildlife owners, where disease cycles are inherently joined, but the impacts are not (Bengis *et al.*, 2002).

1.5. Vectors

The vectors for AHSV are the crepuscular biting midges of the *Culicoides* genus (Figure 1.3), which transmit the virus by biological means (du Toit, 1944; Mellor, 1994; OIE, 2009). They are distributed virtually worldwide (Meiswinkel *et al.*, 1994). Generally, midges are only dispersed a few kilometres from their breeding sites, but it has been suggested that midges may be carried by wind for hundreds of kilometres (Mellor, 1994).

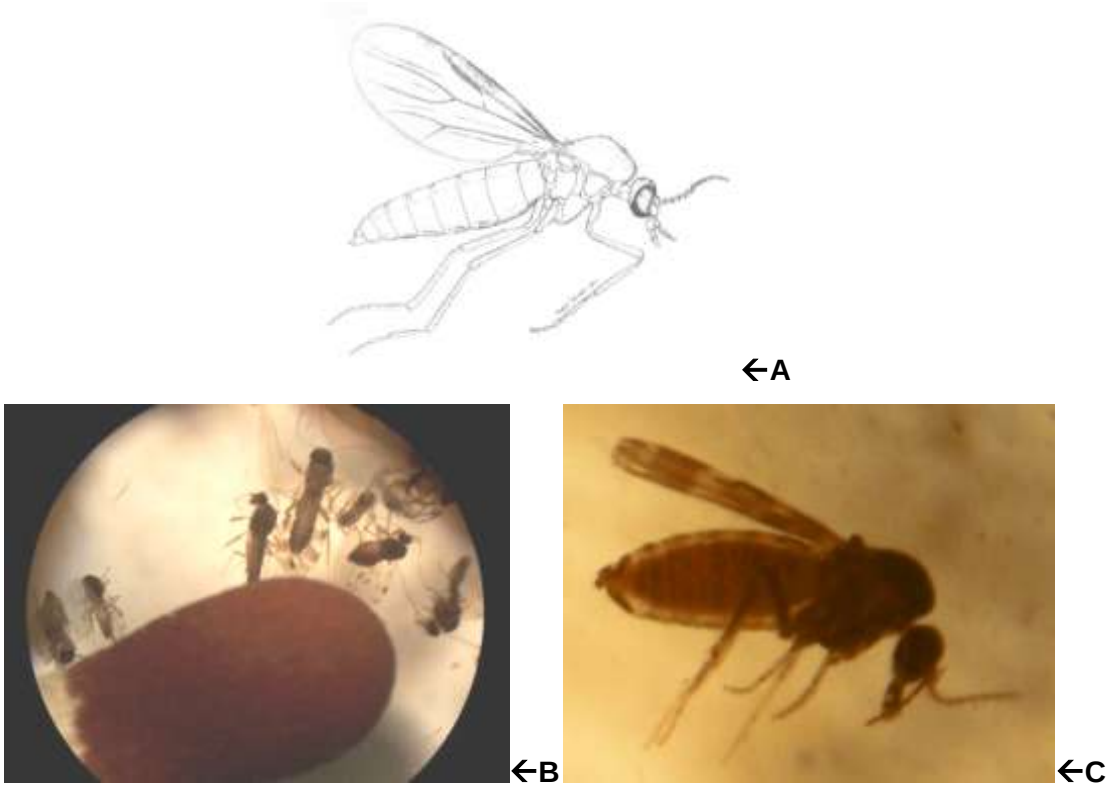

Figure 1.3: Images of *Culicoides* spp. A – *Culicoides* spp. lateral view (Meiswinkel *et al.*, 1994). B – comparative sizes of *Culicoides* spp. and a match head (Jenkins, 2008). C – an engorged female *Culicoides* spp. showing pigmentation of the abdomen with blood (Jenkins, 2008).

The similarities between malaria and 'Horsesickness' led Theiler (1921) to believe that the vector was a blood-sucking insect. Various arthropod vectors have been considered and studied, chief among them being mosquitoes, ticks and *Culicoides* spp. (Wetzel *et al.*, 1970; Mellor, 1994), but only *Culicoides* spp. have been found to play any significant role in the spread of AHS (Mellor, 1993). In 1944, it was shown that field collected *Culicoides* midges

were infected with AHSV (du Toit, 1944). This was later confirmed by Mellor *et al.* (1975) and Boorman *et al.* (1975) who showed that the transmission of the virus was possible after 7-10 days incubation at 26°C. The majority of experimental epizootiological evidence overwhelmingly suggests that the *Culicoides* species are the primary vectors of AHSV (Mellor, 1994). According to the OIE, certain mosquito and tick genera may constitute an occasional mode of transmission (OIE, 2009).

In sub-Saharan Africa, *Culicoides imicola* has been accepted as the primary vector of AHSV: *C. imicola* is found throughout sub-Saharan Africa, the Mediterranean Basin and South East Asia (Meiswinkel *et al.*, 1994; Venter *et al.*, 1996; Meiswinkel, 1998). In 1982, it was found in Spain and has since been indentified throughout the Mediterranean and southern Europe, even as far north as Switzerland (Goffredo & Meiswinkel, 2004). The occurrence of *C. imicola* across these regions may either be indicative of the improved and more intensive sampling strategies following the bluetongue epizootic (1998-2003), or that their range has moved further north due to climate change. Mellor and Hamblin (2004) suggest that it may be the latter. *Culicoides* samples taken in 1983 contained no *C. imicola.* Samples collected from 1999-2003 from similar locations revealed that *C. imicola* is 'widespread and abundant'. In 2005, 75.3% of the *Culicoides* spp. caught in Portugal were *C. imicola* (Ramilo *et al.*, 2012). Mellor and Hamblin (2004) further suggested that the presence of a viable vector for AHSV (as in the bluetongue outbreaks between 1998 and 2003) in these regions renders these areas particularly vulnerable to an AHS epizootic. Indeed, information on vector species plays a large role in determining the risk of AHSV incursion (Del Rio Lopez *et al.*, 2012).

However, the role of other *Culicoides* spp. as AHSV vectors continues to be established. As early as 1975, an American species, *C. sonorensis (= variipennis)* was shown to transmit AHSV (Boorman *et al.*, 1975; Mellor *et al.*, 1975). This also renders the north American continent susceptible to AHS outbreaks (Mellor, 2000). More recently, *C. bolitinos* was implicated in the transmission of AHS as a potential field vector. *C. bolitinos* is distributed widely in the cooler highland areas of South Africa where *C. imicola* is rarer (Venter *et al.*, 2000). Isolations from *C. obsoletus* and *C. pulicaris* collected during the Spanish outbreak of AHS indicated that they may also transmit AHSV (Mellor *et al.*, 1990a). Considering that *C. obsoletus* and *C. pulicaris* are the most common midge species across northern and western Europe, an AHS outbreak may not necessarily be confined to southern Europe. An additional *Culicoides* species that has been found to transmit the virus is *C. nubeculosus* that also exists across Europe (Mellor *et al.*, 1975). Interestingly, the proportion of minority *Culicoides* spp. appeared to differ depending on whether light traps or mechanical aspiration was performed to collect the insects (Scheffer *et al.*, 2012).

The distribution of *C. imicola*, geographically and seasonally, is dependent on a range of environmental factors. Temperature is probably the most influential extrinsic factor affecting the transmission, infectivity and virogenesis of AHSV in *Culicoides* vectors and the survival of the midges themselves (Mellor, 1994; Wellby *et al.*, 1996; Mellor, 2000; Carpenter *et al.*, 2011). The optimum temperature range for adult *Culicoides* spp. activity is 12.5 – 29°C. An increase in ambient temperature results in increased infection rates, faster virogenesis and earlier transmission. In a study, which examined the extrinsic incubation period of the bluetongue virus (BTV) in *C. sonorensis*, time to first transmissible infection occurred at three days post-infection at 30°C, four days at 25°C, five days at 20°C and 20 days at 15°C. No transmissible infection appeared possible at 12°C (Carpenter *et al.*, 2011). Survival rates of the midges, however, increase at lower ambient temperatures. On the other hand, as temperature increases, midge survival rates decrease (Mellor, 2000) (Figure 1.4). The effect of temperature on different AHSV serotypes is not known.

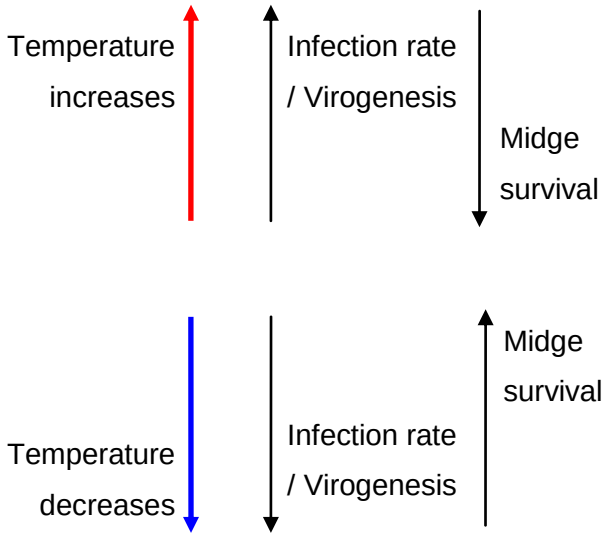

Figure 1.4: Different effects of ambient temperature on AHSV infection rates, virogenesis and midge survival rates (after Mellor, 2000; Mellor & Hamblin, 2004).

Although some reports state that the infection rate falls to zero when ambient temperatures fall below 15°C, Carpenter *et al.* (2011) elucidated that the threshold temperature for AHSV virogenesis in *C. sonorensis* was 11.4-13.3°C. It appears, however, that virions persist in the midge at low temperature and when temperatures rises again, virogenesis commences (Wellby *et al.*, 1996; Mellor, 2000). It has also been shown in other studies that midges may be active at temperatures as low as 3°C (Sellers & Mellor, 1993; Mellor, 2000). However, the virus cannot replicate at these temperatures. These findings suggest that even if there were

to be an incursion into northern Europe by AHSV, the midge populations would increasingly lose the ability to transmit the virus the further north it extends. Transmission would only be possible over the short summer months and be arrested in winter. A caveat exists, however, that at these low temperatures, midge survival increases dramatically, up to 90 days in some cases, in an inactive state. Should the local climate have a winter period (below 15°C average) of less than 90 days, it may be possible for the midge to carry over latent virus from the previous summer and begin a new cycle (Mellor, 2000).

Mellor & Hamblin (2004) viewed this phenomenon as a possible over-wintering mechanism where vertebrate reservoirs are not available. However, Rawlings (personal communication in Mellor, 1994) suggested that an 'accumulation of cold stress' might be a major contributor to *Culicoides* mortality, as opposed to a single cold event. This theory discredits the commonly accepted presumption that the first frost of the season totally arrests midge activity for the duration of the winter (Mellor, 1994). It would seem that a number of frost events over a short period would be more beneficial.

1.5.1. Viral cycle in *Culicoides* species

When a female *Culicoides* spp. takes a blood meal from a viraemic equine, the virus is deposited in the lumen of the mid-gut. The virus infects and replicates in these luminal cells from where the virus is released into the haemocoel and infects the secondary targets, such as the salivary glands. The virus continues to replicate in the salivary gland for the life of the midge. When the female takes another blood meal, the virus passes from the salivary glands into the blood stream of the animal (Mellor, 1993).

A study, in which midges were fed AHSV-infected blood, showed that 96% of them had ingested the virus immediately. After 10 days of incubation, 51% of the midges were still infected with AHSV, but the amount of virus had increased and was mostly confined to the abdomen (Scheffer *et al.*, 2011).

1.6. Overwintering mechanisms

A number of overwintering mechanisms have been proposed (Figure 1.5). Dependent on ambient temperatures during the winter, *Culicoides* spp. midges could remain infected with AHSV for the duration of the winter (Section 1.5, paragraph 6). Trans-ovarian transmission appears unlikely, but remains to be confirmed (Meiswinkel & Braack, 1994; Thompson *et al.*, 2012). Should the virus be able to overwinter through vertebrate hosts, it would most likely occur through animals that remain subclinical for AHS for extended periods, such as zebras and donkeys. Unknown hosts/vectors will always remain a possibility and should not be

ignored, especially as a possible ‘trigger’ mechanism for an outbreak, as opposed to an outbreak’s sustainability.

After the Iberian outbreak of 1987-1990, it was deduced that the virus was able to overwinter on the Iberian Peninsula as the winters were mild enough and a *Culicoides* spp. midge, a competent vector, is native to the region and active throughout the year (Bouayoune *et al.*, 1998; Capela *et al.*, 2003). However, with an increase in the international movement of horses, the possibility of an outbreak occurring in countries previously free of the disease has increased greatly (Archer, 1974; Anonymous, 2008). However, with climate change, the factors that have combined to prevent AHS over-wintering in Europe may now not be enough to prevent AHS from making a permanent and resident incursion (Wittmann & Baylis, 2000; Wittmann *et al.*, 2001). Indeed, Burne (2011) discovered that incidence is more correctly associated with the range of seasonal temperatures in a particular region and vaccine status in the host, which could suggest other overwintering mechanisms.

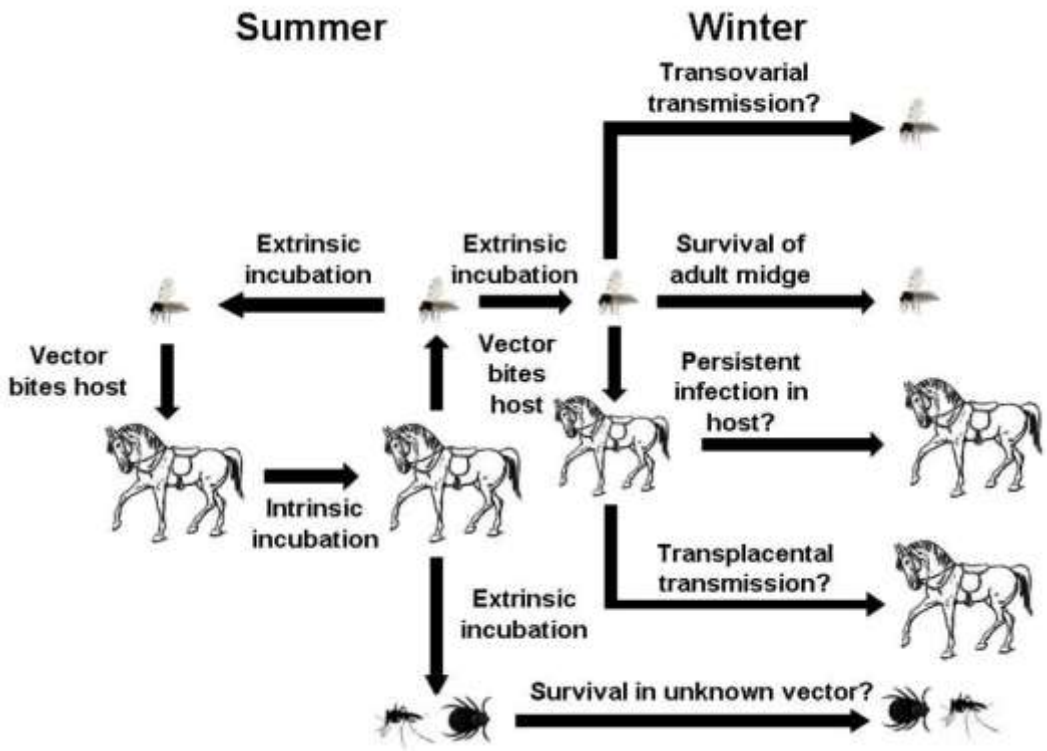

Figure 1.5: The accepted mode of transmission for African horse sickness (left) and possible overwintering mechanism (right) (Thompson *et al.*, 2012).

1.7. Pathogenesis

The severity of the disease depends largely on the virulence of the virus, the infective dose (related to the number of infected midges that bite the animal) and the susceptibility or immunological status of the animal. The factors that determine the virulence and pathogenesis characteristics of AHSV are not well known, although it is suspected that they involve the viral proteins VP2, VP5 and NS3 (Section 1.9.3) and are multifaceted (Huismans *et al.*, 2004). Clinical signs develop as a result of the damage to the endothelial cells in blood vessels and reduced function of the circulatory and respiratory systems (Mellor, 1993).

Initial viral multiplication occurs in the regional lymph nodes resulting in a 'primary viraemia' that disseminates the virus throughout the body via the blood and leads to the infection of target organs such as the heart, lungs, spleen and lymphoid tissues. The primary organs affected by all serotypes are heart and lung tissue followed by the spleen (Clift & Penrith, 2010). From the infected organs, a 'secondary viraemia' occurs, of varying titre and duration, depending on the host species (Coetzer & Erasmus, 1994). A hot spot for viral replication is microvascular endothelial cells and monocyte–macrophages (Clift & Penrith, 2010). In horses, the maximum titre is usually 10^5 $TCID_{50}$/mL with the viraemia lasting 4-8 days and paralleling the febrile reaction, although it may vary between 2-21 days (Erasmus, 2004). In donkeys and zebras, the viraemia is considerably lower and may last for up to 28 or 40 days depending on the study (Hamblin *et al.*, 1998; Erasmus, 2004; OIE, 2008). It has been found that in zebras, viraemia may co-exist with circulating antibodies (Coetzer & Erasmus, 1994). In experimental infections in horses, the incubation period lasts 5-7 days with a minimum of 2 days and a maximum of 10 days. This has been found to be dependent on the dose and virulence of the virus (Guthrie, 2008). The effect of infecting serotype has not been determined; however, in an attempt to monitor the viral life cycle in cell culture, a study found that there was a noticeable difference in the manner in which serotype 2 infected the cells versus serotype 3 and 4. Serotype 3 and 4, whilst producing far less dsRNA than serotype 2, appeared to be less infective (Cramer, 2010).

AHSV rapidly accumulates in the spleen, lungs, caecum, pharynx, choroids plexus and most lymph nodes. AHSV subsequently moves to other highly vascularised organs (Theiler, 1921; Wilson *et al.*, 2009; Clift & Penrith, 2010). Only trace amounts are found in secretions (Erasmus, 2004). AHSV was reported by Theiler in 1921 to be closely associated with erythrocytes. More specifically, it has since been found to be associated with the cellular fraction, i.e. the erythrocytes and lymphocytes, with very little in the plasma. This phenomenon may be similar to BTV infections where the virus is requisitioned in the cell membrane of infected erythrocytes (Mellor & Hamblin, 2004). The damage caused by AHSV on mammalian cells is likely due to the damaging exit mechanisms from the cell that the virus

employs (Mellor, 2000). In a study on the AHS virus and its effects on capillaries, it was found that the virus was most common in the myocardial vessels and least common in the lung, while endothelial cell infection was rare in the spleen and liver (Gomez-Villamandos *et al.*, 1999).

In a chicken embryo model, AHSV was confirmed to have a definite tropism for microvascular endothelia and the mononuclear phagocyte system. Endothelial tissue was the first to be damaged 12 hours post-inoculation. This was most obvious in the spleen, lung and mesenchymal connective tissue of the neck 24 hours post-inoculation. In addition, damage continued to the tissues of skeletal and cardiac muscle, gastrointestinal smooth muscle, mesonephric glomeruli, liver and subcutis. The exorbitant costs and welfare concerns of using horses for AHSV studies has invariably led to severely reduced levels of research. The chicken embryo model represents a viable alternate which can hopefully be exploited in the near future to realise its full potential (Maartens *et al.*, 2011).

Since 1921, when Theiler first described AHS, four 'forms' of AHS have been used to categorise the disease. In ascending order of severity, these are the horse sickness fever form, the subacute/oedematous or cardiac ('dikkop') form, the mixed form and the peracute or pulmonary ('dunkop') form. It has since become apparent that most infections are of the 'mixed' form (Coetzer & Erasmus, 1994).

Horse sickness fever is the mildest form of the disease and occurs in animals with some level of immunity. Mortality is rare and usually involves a mild fever and slight oedema of the supraorbital fossae. It is the only form seen in zebras and donkeys. In the *cardiac form* (Figure 1.6, left), a fever may persist for a few weeks and there is significant subcutaneous oedema, particularly of the supraorbital fossae, but none in the lower limbs. Petechial and ecchymotic haemorrhaging (of the eyes and of the tongue respectively) may be present and mortality may exceed 50%. Colic symptoms are often a feature. The most severe form is the *pulmonary form* (Figure 1.6, right), where there is a mortality rate of 95%. It develops very rapidly with a fever of up to 41˚C followed by signs of respiratory distress. Foam exudes from the nostrils as the animal dies. The pulmonary and cardiac forms are often found to afflict the animals simultaneously. This *mixed form* is the most common with a mortality rate of 70%. Animals usually die within 3-6 days after infection (Coetzer & Erasmus, 1994).

Figure 1.6: Cardiac form (left) and pulmonary form (right) of the African horse sickness disease (Aklilu *et al*., 2012).

Laegreid *et al.* (1993) observed that the infecting serotype determines to some extent the form of the disease that is exhibited in the animal. Sailleau *et al.* (1997a) added to this observation when horses experimentally infected with serotype 4 developed the pulmonary form and those infected with serotype 9 developed the cardiac form. Aklilu *et al.* (2012), however, found that there was no obvious association between form and infecting serotype.

1.8. Differential diagnoses

It is important to distinguish AHS from other similarly presenting diseases as their consequences differ greatly. AHS shares many of the clinical signs and symptoms that are seen following infections by the closely related orbivirus, equine encephalosis virus (EEV). It is estimated that up to 40% of reported AHS cases are not actually confirmed as AHS – many are equine encephalosis (van Dam, 2012). The diseases have similar epidemiological patterns and occur simultaneously in South Africa, both being vectored by *Culicoides*, although mortality is higher for AHS and may occur simultaneously in the same animal (Lord *et al.*, 2002; Venter *et al.*, 2002). A standardised test must be used to confirm either diagnosis. An indirect sandwich ELISA with anti-EEV antibodies has been developed to indentify EEV antigens (Crafford *et al.*, 2003). In addition, the transmission dynamics of these two closely related viruses are not fully understood and additional data on their outbreak dynamics will assist in understanding the geographical variation in transmission (Lord *et al.*, 2002).

Other differential diagnoses for AHS include babesiosis, purpura haemorrhagica, equine viral arteritis, equine infectious anaemia and equine morbillivirus pneumonia (OIE, 2008). Purpura haemorrhagica and equine viral arteritis share similar symptoms to the pulmonary form of AHS (Coetzer & Erasmus, 1994).

1.9. Aetiology

1.9.1. AHSV taxonomy

The African horse sickness virus was first described as an ultravisible organism (Theiler, 1921). AHSV is a member of the *Reoviridae* family and is classified in the *Orbivirus* genus, which was initially described in 1971 to define arthropod-borne viruses with distinctive morphologies and physically and chemically identical characteristics (Gorman, 1979; Verwoerd *et al.*, 1979). Other closely related orbiviruses include the bluetongue (BTV) and equine encephalosis viruses (EEV) (Spence *et al.*, 1984; OIE, 2008). *Reoviridae* have a double-stranded RNA (dsRNA) genome encapsulated by a single viral particle that is quasi-spherical and displays icosahedral symmetry (Bremer, 1976; Gorman, 1979). AHSV is classified as an arbovirus since it is transmitted biologically to vertebrates through blood-sucking arthropod vectors, namely the biting midges of the *Culicoides* genus (Mellor, 2000; Kuno & Chang, 2005). Theiler (1921) alluded to the presence of more than one type of the virus as equines supposedly immune to the virus could become fatally re-infected. Nine immunologically distinct serotypes have since been found to exist, numbered 1-9, the last being isolated in 1960 (Howell, 1962; Hamblin *et al.*, 1991). The lack of any new serotypes being discovered since is indicative of a genetically stable virus with little to no antigenic changes (Howell, 1962; Erasmus, 2004). No complete cross-neutralisation is evident between any two strains although there are varying degrees of cross-neutralisation between serotypes 1 and 2, 3 and 7, 5 and 8 and 6 and 9 Field evidence suggests that there is no intratypic variation (Howell, 1962; Coetzer & Erasmus, 1994).

1.9.2. AHSV properties

The 68-70 nm diameter virion (Figure 1.7) is unenveloped with a double-layered capsid consisting of 32 capsomeres (Oellermann *et al.*, 1970; Bremer, 1976; Gorman, 1979) with the outer capsid more diffuse and less discernible (Wood, 1973). The physico-chemical properties of the virion appear to be common to all orbiviruses (Gorman, 1979). The virus is relatively heat-stable, but can be inactivated at 50°C for 3 hours and 60°C for 15 minutes. It can survive at 37°C for 37 days (OIE, 2009). Moreover, the virus may maintain its infectivity if isolated from putrid blood (Theiler, 1921). Infected blood samples may still yield virions for up to a year if stored at 4°C (House *et al.*, 1990). The virus can survive in the pH range of 6.5 –

8.5, and is more sensitive to acidity than to alkalinity. AHSV is inactivated by 0.4% ß-propiolactone, 0.1% formalin, binary ethyleneimine, 2% acetic acid, 3% sodium hypochlorite or 1% potassium peroxymonosulfate/sodium chloride-Virkon® S (Erasmus, 2004; OIE, 2009).

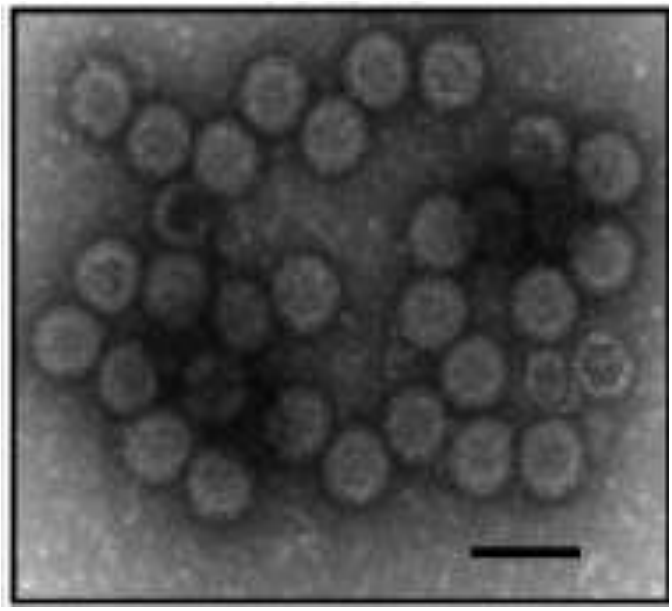

Figure 1.7: Electron micrographs of African horse sickness virus core particles stained with 2% uranyl acetate. Bar represents 100 nm (Matsuo *et al.*, 2010).

1.9.3. AHSV structure

AHSV is a double-stranded RNA virus made up of ten genome segments (Grubman & Lewis, 1992). This was first demonstrated when RNA was analysed on polyacrylamide gels resulting in 10 bands (Bremer, 1976; Gorman, 1979; Spence *et al.*, 1984). Orbiviruses contain segmented genomes, which may allow for genome segment re-assortment and antigenic diversity. However this is contradictory to earlier reports that AHSV is a very stable virus (Howell, 1962). Genome segment numbers were assigned on the basis of molecular weight data (Spence *et al.*, 1984; Bremer *et al.*, 1990) and are numbered in order of their migration (Roy *et al.*, 1994). However, there is some discrepancy in the literature and amongst published sequences with regard to coding assignments for segments 6, 7, 8, 9 and 10. This is due to the fact that the genome segments are of almost identical molecular weight, hindering their differentiation on gel systems (Bremer *et al.*, 1990). The coding assignments of Grubman and Lewis (1992) have segment 6 coding for VP5 and VP6 and an additional protein, NS4 for segment 10. However, this view is an isolated one and is incompatible with systems used for the bluetongue virus, the prototype orbivirus (Burroughs *et al.*, 1994). The two proteins encoded in segment 6 have since been found to be related,

the smaller protein being a truncated version of the larger protein (Roy *et al.*, 1994). Table 1.1 gives the coding assignments from four sources for comparative purposes. For the purposes of this dissertation, the coding assignments of Mertens *et al.* (2006) shall be used.

The core particle is composed of the major proteins (VP3 and VP7) and the minor proteins (VP1, VP4 and VP6) and encloses the 10 genome segments (Bremer *et al.*, 1990; Laviada *et al.*, 1993; Roy *et al.*, 1994; Maree *et al.*, 1998a; Manole *et al.*, 2012). The outer capsid is made up of VP2 and VP5 (Roy *et al.*, 1994; Manole *et al.*, 2012) (Figure 1.8).

Table 1.1: Coding assignments of Grubman and Lewis (1992), Roy *et al.* (1994) and Mertens *et al.* (2006) for the ten genome segments of the African horse sickness virus. Bold entries indicate where discrepancies have occurred in the literature with regard to **genome** segment and protein nomenclature.

Genome segment	Protein Nomenclature			Size (bp)
	Grubman and Lewis (1992)	**Roy *et al.* (1994)**	**Mertens *et al.* (2006)**	**(Mertens *et al.*, 2006)**
1	VP1	VP1	VP1	3965
2	VP2	VP2	VP2	3205
3	VP3	VP3	VP3	2792
4	VP4	VP4	VP4	1978
5	NS1	NS1	NS1	1748
6	**VP5/VP6**	**VP5**	**VP5**	1566
7	**VP7**	**VP7**	**VP6**	1169
8	**NS2**	**NS2**	**VP7**	1167
9	**NS3**	**VP6**	**NS2**	1166
10	**NS4/NS4a**	**NS3/NS3a**	**NS3/NS3a**	756

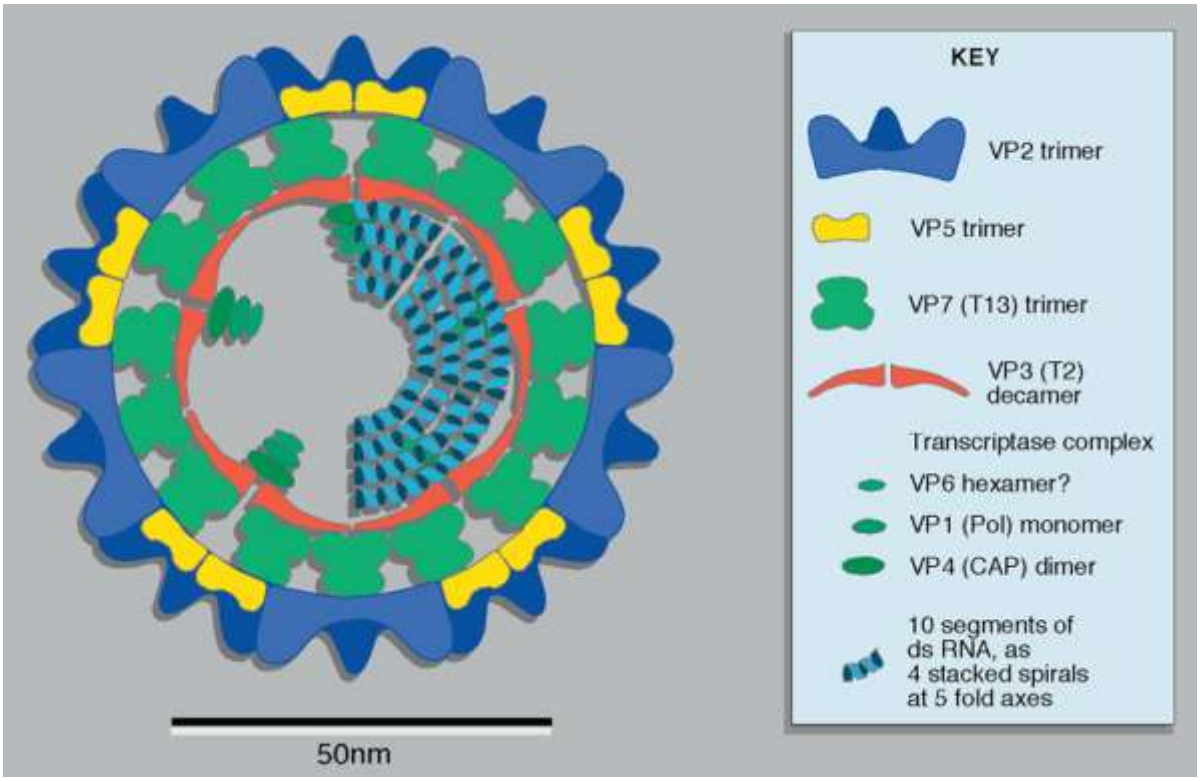

Figure 1.8: Schematic diagram of the structure of an orbivirus showing the organisation of the major and minor structural proteins (Wilson *et al.*, 2009).

VP2 is the most variable among the nine serotypes (Burrage & Laegreid, 1994) with almost 90% of the sequences varying between 46% and 52% on a pair-wise alignment in one study (Huismans *et al.*, 2004). As such, it is responsible for serotype diversity and specificity (Roy *et al.*, 1994; Venter *et al.*, 2000). VP2 and VP5 are together responsible for virus neutralisation activity (Martinez-Torrecuadrada *et al.*, 1999). In addition to the structural or viral proteins (VP), three non-structural proteins are present, namely NS1, NS2 and NS3 (Laviada *et al.*, 1995) and are mainly concerned with enzymatic activities (Table 1.2). It has been found that after VP2, NS3 is the second most variable protein (Venter *et al.*, 2000).

Table 1.2: Data derived from a number of sources describing the accepted functions of the ten proteins common to all orbiviruses and their molecular weights.

Protein	MW (kDa)	Accepted function(s)	Conserved in AHSV?	Reference
VP1	150	RNA-directed RNA polymerase	Yes	Stauber *et al.* (1997); Ramadevi *et al.* (1998); Ramadevi and Roy (1998); Huismans *et al.* (2004)
VP2	122-124	Outer capsid structure	No	Martinez-Torrecuadrada *et al.* (1996); Huismans *et al.* (2004); Mertens *et al.* (2006)
		Serotype-specificity		Huismans and Erasmus (1981); Burrage *et al.* (1993); Hassan and Roy (1999)
		Receptor binding		Martinez-Torrecuadrada *et al.* (1996); Bhattacharya *et al.* (2007)
		Haemagglutinating activity		Bhattacharya *et al.* (2007)
		Host-specific immunity		Bhattacharya *et al.* (2007)
		Cell attachment, virus penetration		Hassan and Roy (1999); Huismans *et al.* (2004)
		Induction of neutralisation specific antibody response		Martinez-Torrecuadrada *et al.* (1996); Potgieter *et al.* (2003); Huismans *et al.* (2004)
VP3	103	Inner capsid structure	Yes	Maree *et al.* (1998b); Lourenco and Roy (2011)
VP4	34	Guanylyl transferase	Yes	Le Blois *et al.* (1992); Turnbull *et al.* (1996)
		RNA capping		Stauber *et al.* (1997); Ramadevi *et al.* (1998); Ramadevi and Roy (1998); Huismans *et al.* (2004)
VP5	57	Outer capsid structure	Yes	Mertens (2004)
		Destabilisation of endocytosed vesicle membranes		Hassan *et al.* (2001); Huismans *et al.* (2004)
		Cell penetration		Huismans *et al.* (2004); Mertens *et al.* (2006)
VP6	38-46	Helicase	Yes	Stauber *et al.* (1997); Ramadevi *et al.* (1998); Ramadevi and Roy (1998); Huismans *et al.* (2004)
VP7	38	Major component of inner core	Yes	Martinez-Torrecuadrada *et al.* (1996); Maree *et al.* (1998b); Mertens (2004); Maree and Paweska (2005)
NS1	63	Major component of tubules in host cell	Yes	Maree and Huismans (1997); Mertens (2004)
NS2	41	Form inclusion bodies in host cells	Yes	Mertens (2004)
		ssRNA affinity		Mertens (2004)
NS3/3a	24	Possibly involved in the release of virions from cell	No	Hyatt *et al.* (1993); de Sa *et al.* (1994); Huismans *et al.* (2004)

More work has been done on BTV than AHSV, but all orbiviruses share many of the same characteristics. Indeed, previous BTV studies have helped to guide the interpretation of AHSV protein homology modelling and potential binding sites (Manole *et al.*, 2012). However, there are some notable differences: NS3 is the second most variable protein after VP2 in AHSV, but is one of the most conserved in BTV (Huismans *et al.*, 2004). The BTV subcore assembly is made up as follows: VP1, VP4, VP6 and VP3 constitute the subcore, with VP7 being added to form the core and protect the RNA genome. VP4 interacts with each of the subcore components, while VP6 interacts with VP4 and VP1. Importantly, the inclusion of all ten ssRNA molecules is required for the correct assembly to occur, after which they form templates for the generation of the dsRNA genome (Lourenco & Roy, 2011).

1.9.4. AHSV replication

Once the virus has entered a mammalian cell, VP2 and VP5 are removed. The removal of these two outer proteins causes the RNA polymerase to be activated with an associated loss in infectivity (Gorman, 1979). The core structure that remains is transcriptionally active and protects the genome from host cell detection. The core particles assume the responsibility of transcribing the ssRNA molecules into mRNA molecules that act as a template for the synthesis of the viral proteins and the new dsRNA genome (Matsuo *et al.*, 2010). Replication occurs in the cytoplasm of the host cell after the virion has depressed host cell protein synthesis (Gorman, 1979).

Tubules and inclusion bodies are formed by NS1 and NS2 respectively. It is believed that NS2 may be involved in recruiting core proteins and single-stranded viral RNA into the inclusion bodies. The minor proteins (VP1, VP4 and VP6) form the transcriptase complex that is encapsulated by VP3. This subcore acts as a foundation for VP7 proteins to attach and form the stable core structure. It is not known at what point VP5 and VP2 attach to the subcore to complete the virus particle. NS3 appears to interact with VP2 to facilitate virus release (Wood, 1973; Spence *et al.*, 1984; Bhattacharya *et al.*, 2007). In studies done on the bluetongue virus, it was found that the virus binds to glycophorins in human and porcine erythrocytes (Eaton & Crameri, 1989).

1.9.5. AHSV serotypes

The role of serotypes in the epidemiology of AHS is poorly understood. The relationship between serotypes, geographical distribution, virulence and transmission is all unknown. One of the first studies of the basic reproduction number, R_0, was an attempt to understand the implication of serotypes on the epidemiology of the disease (Lord *et al.*, 1996a). R_0 is a measure of the probability of transmission of a pathogen. R_0 can be used in the calculation of control strategies such as vaccination and the coverage required for halting an epidemic.

However, R_0 depends on the independence of the transmission of each serotype. It also depends on whether an infection by one serotype affects infection by a second serotype.

A study conducted on zebras found that the distribution of serotypes was non-independent, implying some sort of relationship between the serotypes that has yet to be elucidated (Lord *et al.*, 1997a; Lord *et al.*, 1998a). Cross-immunity, biting rates, spatial and temporal variations and genetic susceptibilities may all be responsible. A very high R_0 is indicative of the likely differences in infectivity of different serotypes for midges or zebras or both (Lord *et al.*, 1996a; Lord *et al.*, 1997b). As far as immunity to the different serotypes is concerned, a horse that recovers from an infection from a particular serotype develops a life-long immunity to that serotype, but may remain susceptible to other serotypes (Mellor, 1993). A strain of AHSV that occurred in Kenya in the early 1990s was not neutralised by antiserum of any of the nine previously defined serotypes, leading to speculation that a tenth serotype may exist (Mellor, 1993). However, only nine recognised serotypes exist today, which indicates the genetic stability of the virus. Table 1.3 shows the nine recognised serotypes accepted as reference strains.

Table 1.3: AHSV Serotypes and historical isolates/reference strains (Ozawa & Dardiri, 1970).

Serotype	Historical name
1	A501
2	OD
3	L
4	Vryheid
5	VH
6	114
7	Karen
8	18/60
9	S2

The distribution of serotypes in South Africa is not well studied, although between 2004 and 2006, all nine serotypes were sent to the Equine Research Centre (Onderstepoort, South Africa) (Figure 1.9) (Quan *et al.*, 2008). Although all nine serotypes were detected across southern Africa, each province has an unequal distribution compared to each other. In the Eastern Cape, for example, only three serotypes were detected, while in Gauteng, all nine serotypes were detected. Generally, the state veterinarian will only serotype one sample per

outbreak. This has led to a significant lack of data, but the Equine Research Centre has embarked on a validation campaign (Guthrie *et al.*, 2013) for the RT-PCR assay of Quan *et al.* (2010) and is simultaneously serotyping the samples received.

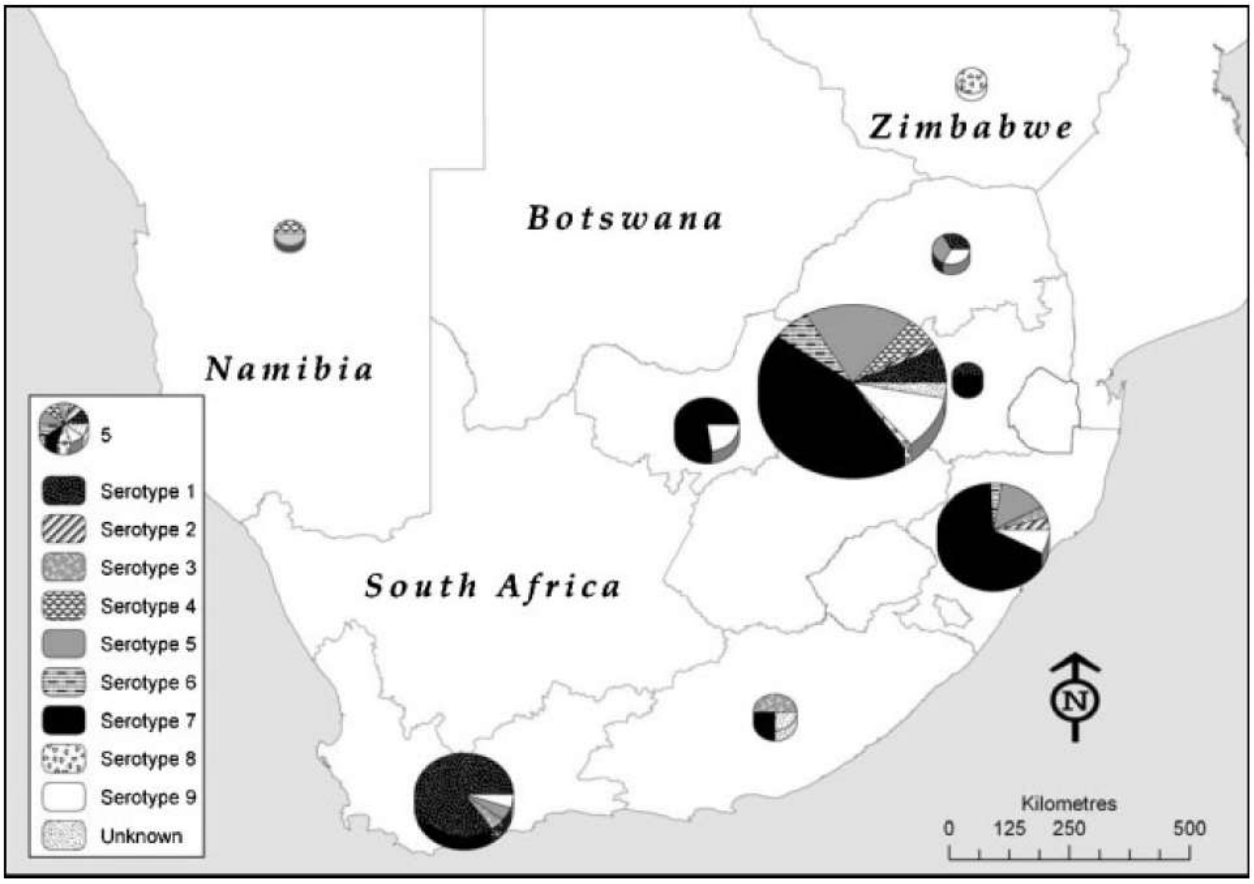

Figure 1.9: African horse sickness virus serotype distribution between 2004 and 2006 per province as determined by the number of samples sent to the Equine Research Centre, Onderstepoort. Pie chart in key indicates relative number of cases (Quan *et al.*, 2008).

1.9.6. AHSV stability

Genetic re-assortment of the genome is always a concern when dealing with viruses (Mumford, 2007). Segmented genomes, as exist in orbiviruses, are thought to facilitate genetic re-assortment. New virus types may therefore arise if a cell is co-infected with multiple serotypes. However, Gorman (1979) noted that in a study by Howell in 1966, only one strain of the bluetongue virus was ever found in infected sheep over a number of years. This, combined with the fact that no additional AHSV serotypes have been described since the 1960s, lends itself to the idea that the AHS virus is genetically stable.

However, the AHS virus is an RNA virus and is therefore expected to have a high mutation rate, in keeping with other RNA viruses, such as the influenza virus (Brown *et al.*, 1998;

Belshaw *et al.*, 2008). Additionally, there is recent evidence of BTV reassortment occurring in Europe in 2008 (Maan *et al.*, 2010b), likely by co-infection by two different serotypes. In a reverse genetics study, transfection with core transcripts from two serotypes resulted in reassorted viruses (Matsuo *et al.*, 2010).

Historically, there is considerable genetic heterogeneity of isolated field strains, possibly determining the course of the disease. Maclachlan and Guthrie (2010) suggest that this diversity may be accounted for by both genetic shift and drift. The authors further considered that genetic drift may be due to reassortment that occurs through the evolution of quasispecies in the equine host, followed by founder effects in the *Culicoides* spp. vectors. Negative or purifying selection may also occur over time for individual genome segments (Burrage & Laegreid, 1994; Quan *et al.*, 2010). However, it would be pertinent to note that since 2008, two new serotypes of BTV have been identified that appear to have arisen since the virus' dramatic incursion into Europe (Chaignat *et al.*, 2009).

1.10. Control and prevention

There is no specific treatment for African horse sickness (Mellor & Hamblin, 2004). As early as Theiler (1921), it was reported that the best treatment might be to leave the animal alone. Combating AHS therefore requires the prevention of an infected *Culicoides* spp. bite and control by 'rendering the animals immune' (Theiler, 1921). Foremost among these measures are introducing good husbandry practices, controlling the *Culicoides* midge vector and vaccination (Meiswinkel *et al.*, 1994; Jenkins, 2008; Simpkin, 2008). The large number of horses that transverse international boundaries in today's modern equine industry constitute an increasing concern due to the threat of various viral diseases of equines. Vaccination is seen as key to protecting the global nature of the equine industry (MacLachlan *et al.*, 2007; von Teichman *et al.*, 2010; Backer & Nodelijk, 2011; Lo Iacono *et al.*, 2013).

1.10.1. Control

Since *Culicoides* spp. midges are crepuscular (Wittmann & Baylis, 2000), husbandry measures include housing animals from before dusk to after dawn and preventing access of midges to stables (Wittmann *et al.*, 2001; Erasmus, 2004). The application of insecticides to the animals' coats may deter the midge from biting. These measures aim to limit the amount of time the animals can be exposed to the vector. Even before the vector species was identified, these measures were found to be highly effective at preventing infections (Theiler, 1921) and are still effective today (Simpkin, 2008; Page *et al.*, 2009). Controlling vector populations aims to reduce the number of potential bites that susceptible animals receive. Eradicating the midge population entirely is not possible, nor is it wise, from an ecological

perspective. Controlling the vector population includes altering their habitat, adultciding, larvaciding and the use of repellents (Jenkins, 2008; Simpkin, 2008). Additionally, in the case of AHS outbreaks, equine movement restrictions may be put in place and slaughter policies introduced in the case of currently AHS-free countries (Portas *et al.*, 1999; Anonymous, 2009).

1.10.2. Vaccination

The most practical approach and primary means to the prevention of viral diseases is vaccination (MacLachlan *et al.*, 2007; OIE, 2009; Gordon *et al.*, 2013). The nine AHSV serotypes are distributed throughout South Africa, although they may differ temporally (Coetzer & Erasmus, 1994). For this reason, a polyvalent, attenuated vaccine was developed by Onderstepoort Biological Products.

There have been a number of different vaccines developed for AHS over the last century. Before 1930, the approach was to confer active immunity by inoculating horses with virulent AHSV and passive immunity by administering anti-AHSV sera (MacLachlan *et al.*, 2007). Early vaccines were produced in the 1930s by passaging the virus approximately 100 times intracerebrally in suckling mouse brain (horsesickness neurotropic mouse brain vaccines). Despite the good protection that these vaccines provided, they occasionally resulted in serious side-effects with some horses dying of encephalitis (Nobel & Neumann, 1961; Pavri & Anderson, 1963) and proved to be infectious to humans (MacLachlan *et al.*, 2007). These problems were solved in the 1960s by passaging the virus in cell cultures instead (Mirchamsy & Taslimi, 1964; Mirchamsy & Taslimi, 1968). Also in the 1960s live-virus and killed-virus vaccines were investigated (Ozawa *et al.*, 1965; Ozawa & Bahrami, 1966). In 1974, however, these vaccines began to be replaced with plaque variants of AHSV grown in Vero cells (Coetzer & Erasmus, 1994).

The current vaccine produced by Onderstepoort Biological Products remains the best and most practical means of protection against AHS. However, the vaccine cannot be relied upon to give full protection to the animal. Individual horses' responses may vary, there may be some interference between the serotypes in the polyvalent vaccine or over attenuation of some of the vaccine strains, leading to weakly immunogenic vaccine strains (Coetzer & Erasmus, 1994). Historically, however, the development of the polyvalent vaccine has significantly reduced the losses associated with AHS (Guthrie, 2008). In a model of Lord *et al.* (2002), examining infection of a naïve herd with AHSV, it was determined that 50% of epidemics may be avoided if 75% of horses and donkeys or 90% of horses only were vaccinated before the introduction of the virus. Importantly, donkeys needed to be included in vaccination programmes to reduce overall losses. However, this model was based on a two

host, one vector system in Spain. This is far removed from the situation in South Africa, but gives an indication of the importance of vaccination.

Annual immunisation is recommended in early summer each year, before the peak AHS season, with yearlings normally receiving two vaccinations in the first year - the timing of these vaccinations has been found to be crucial (Anthony *et al.*, 2004; Crow, 2005; OBP, 2012). Onderstepoort Biological Products manufactures two quadrivalent vaccines containing live, attenuated strains. The seed virus is selected from genetically stable macroplaques from Vero cells (OIE, 2008). The first vaccine contains serotypes 1, 3 and 4 (AHS1), while the second vaccine contains serotypes 2, 6, 7 and 8 (AHS2) (MacLachlan *et al.*, 2007). The vaccines must be administered at least three weeks apart. Serotype 9 is not included in the vaccine as it is very rare in South Africa and serotype 6 affords sufficient cross-protection. Serotype 5 was removed from the vaccine in 1993 due to reports of severe reactions in workers and deaths in horses and is cross protected by serotype 8 (Mellor & Hamblin, 2004; von Teichman & Smit, 2008; von Teichman *et al.*, 2010). However, over the last few seasons, both serotype 5 and 9 have been increasingly detected in outbreaks. *In vivo* cross protection was therefore confirmed between serotypes 5 and 8 and serotypes 6 and 9 (von Teichman *et al.*, 2010). Repeated vaccinations over time are believed to assist the animal in gaining greater immunity to the serotypes contained in the vaccines (Coetzer & Erasmus, 1994; OBP, 2012). It is interesting to note, that in the last outbreak on the Iberian Peninsula from 1987 to 1991, a polyvalent vaccine was initially used. It has been claimed by some workers, (H. Hooghuis, personal communication in Mellor & Hamblin, 2004), that subsequent to these polyvalent vaccinations, different serotypes began appearing in animals that were not the initial serotype 4. This suggests that the polyvalent vaccine produced a viraemia in the vaccinated animals and the virus was then transmitted by the resident vectors. This has, however, yet to be substantiated.

Vaccination timing of pregnant mares and their offspring is of critical importance and more research is needed (Crow, 2005; Crafford *et al.*, 2013). Immunity to AHS is only transferred passively via colostrum after foaling, which requires the timing of the dam's vaccination to coincide with the greatest concentration of antibodies in the colostrum at the expected time of birth. Interestingly, the concentrations of antibodies to the serotypes differ in the colostrum as well as their longevity in the offspring. However, this may be due to the polyvalency of the vaccine.

Some anecdotal comments suggest that the vaccine itself may be responsible for inducing a fatal viraemia, particularly in younger horses (MacLachlan *et al.*, 2007). There is little literature to back up this claim and the vaccines used to control the last epizootic in Spain

have ‘never been known to revert to virulence’ (Mellor, 1993). ‘Vaccine-related deaths’ during the Iberian outbreak of 1987-1991 were later said to be due to the vaccination of already infected horses or that, due to a lack of education, the horses were worked after vaccination (Portas *et al.*, 1999). An ELISA assay has been developed that could be used to differentiate a vaccine viraemia from a natural viraemia based on NS3 (Laviada *et al.*, 1995), but it has not found widespread acceptance. In 2008, a study was conducted to determine whether the vaccine manufactured by Onderstepoort Biological Products could induce clinical symptoms. The study concluded that “assumptions of virulence or reversion to virulence of vaccine re-assortments post-vaccination in horses could not be substantiated” (von Teichman & Smit, 2008).

It would, however, be advantageous to conclusively trace the origin of the virus in an infected horse, be it wild type or vaccine strain. Vaccine and wild-type strains of the avian pathogen *Mycoplasma gallisepticum* have successfully been differentiated with standard PCR techniques (Evans & Leigh, 2008). More importantly, field and vaccine strains of the bluetongue virus were differentiated rapidly using real-time RT-PCR following reports of vaccine virulence in European outbreaks (Elia *et al.*, 2008).

Inactivated vaccines are an alternative to live, attenuated vaccines. They are advantageous in that they do not contain a potentially dangerous live agent. However, they are expensive to produce and require multiple inoculations. Complete vaccine inactivation may also be difficult (Mirchamsy & Taslimi, 1964; Guthrie *et al.*, 2009).

Howell (1962) recognised the advantages of monovalent vaccines over polyvalent vaccines, especially when outbreaks occurred in non-endemic regions. Monovalent vaccine production is simplified and expedient and allows for the reduction of economic losses in an outbreak. Inactivated monovalent vaccines are used extensively in West Africa, where serotype 9 is the dominant circulating serotype (National Laboratory, Senegal) (Mellor & Hamblin, 2004). Whenever AHSV appeared outside Africa, monovalent vaccines have successfully been used for the particular serotype involved. In the Spanish outbreak of 1987-1991, an inactivated monovalent serotype 4 vaccine was produced from the attenuated vaccine strain and the outbreak was eventually halted (OIE, 2008).

Although popular and efficacious, live attenuated and inactivated vaccines are perceived to have many flaws. As far as AHS-free countries are concerned, the use of a live, attenuated vaccine as a preventative measure against an outbreak is equal to declaring that the AHS virus itself was present (Portas *et al.*, 1999). Recombinant vaccines represent a modern alternative, but few have reached a commercial phase (MacLachlan *et al.*, 2007). A

considerable amount of research has been done on sub-unit vaccines, albeit for BTV (Savini *et al.*, 2007). Subunit vaccines have also been tested successfully with AHSV, although they are no longer commercially available. VP2, VP5 and VP7 of serotype 4 were expressed in baculovirus expression systems and used to immunise horses (Martinez-Torrecuadrada *et al.*, 1996). A completely protective immune response was achieved, although only VP2 was soluble and produced neutralising antibodies. Recombinant VP2 from serotypes 3, 4, 5 and 9 have since also been used to successfully immunise horses (Bentley *et al.*, 2000; Martinez-Torrecuadrada *et al.*, 2001; van Niekerk, 2001; Scanlen *et al.*, 2002).

Many workers expressed their concern over the continued use of live vaccines (Mirchamsy & Taslimi, 1968; Mellor & Hamblin, 2004; Guthrie *et al.*, 2009). In response to a growing call for a modern vaccine candidate, Guthrie *et al.* (2009) developed a recombinant canarypox-vectored monovalent vaccine for serotype 4, which has subsequently been patented (Minke *et al.*, 2012). The genes of the outer capsid proteins VP2 and VP5 of AHSV were cloned into a canarypox vector, recombinantly expressed and, when inoculated into horses, induced neutralising antibodies, while remaining avirulent. An identical method had been successfully used previously for bluetongue virus, West Nile virus and equine influenza virus (Minke *et al.*, 2004; Boone *et al.*, 2007; Minke *et al.*, 2007).

AHSV VP2, VP7 and NS3 have also been used as vaccine candidates by using a recombinant modified vaccina Ankara vaccine (MVA) (Chiam *et al.*, 2009). In trials with ponies, MVA-vectored VP2 induced a strong antibody response, followed by MVA-vectored VP7. Anti-NS3 antibodies could not be detected. In 2011, the VP2-recombinant MVA vaccine (of serotype 4), was also successfully tested, albeit only in a mouse model (Castillo-Olivares *et al.*, 2011). Vaccination of horses with this new vaccine prevented the horses from becoming viraemic after inoculation with live AHS virus and resulted in appropriate levels of circulating antibodies. This vaccine represents a significant advance in the successful prevention of AHS, but it is monovalent and the infecting serotype will have to be determined prior to immunisation with the vaccine. de la Poza *et al.* (2013) used the recombinant modified vaccina virus Ankara (rMVA) and naked DNAs which expressed AHSV VP2 and NS1. Mice inoculated with the naked DNA and rMVA-VP2, -NS1 produced appropriate amounts of neutralising antibody. Unfortunately, however, the complete development of a veterinary vaccine, from proof of concept to marketing authorisation, will take many years and must overcome many obstacles after rigorous research such as complying with veterinary authorities' regulations and national legislation (Heldens *et al.*, 2008).

The design of modern vaccines, with a tendency to be serotype specific, must be based on a sound understanding of the molecular biology and pathogenesis of each serotype within the

horse (MacLachlan *et al.*, 2007). Serotyping assays are crucial to provide this required knowledge.

Of concern with any viral disease and its control by vaccination is the antigenic diversity that exists because of mutation, recombination or re-assortment between different strains. Although AHSV appears to be a relatively stable virus genetically, surveillance programmes to monitor the circulating serotypes continue to be important (Mumford, 2007). Rapid serotyping assays would have the potential to identify shifting genotypes during an outbreak and facilitate monitoring of its progress in real time.

Apart from the vaccines mentioned in the previous paragraph, virus-like particles (VLPs) have also been used to induce an immune response. VLPs are effectively replicas of the virion, without a genome – in essence, a protein shell without the ability to replicate and induce a viraemia. This takes into account the disadvantages and shortcomings of other vaccine types, such as immunogenicity (sometimes experienced with sub-unit and recombinant vaccines) and incomplete attenuation of some viruses in inactivated vaccines. It also cannot revert to virulence due to its lack of (or partial lack of) a genome. VLPs have been developed for BTV and in a trial using sheep, all of the animals were protected against BTV post-challenge (French *et al.*, 1990; French & Roy, 1990; Crawford *et al.*, 1994; Noad & Roy, 2003).

Another vaccination strategy evaluated AHSV VP7 as an antigen delivery system for foreign peptides where both foot and mouth disease virus (FMDV) VP1 (36 aa) and AHSV VP2 (110 aa) immunogenic regions were cloned into VP7 (Rutkowska *et al.*, 2011). There was a good, specific immunogenic response to the inserted peptide of the fusion proteins when evaluated in guinea pigs.

As mentioned previously, inactivated monovalent vaccines are often regarded as the safest and most effective vaccine against a virus serotype. With this in mind, Ronchi *et al.* (2012), tested the adjuvants ISA 27 VG and Montanide™ gel (SEPPIC Srl, Milan, Italy) in combination with serotype 5 and 9 monovalent, inactivated vaccines on guinea pigs. ISA 27 VG was favoured due to the lack of reaction at the inoculation site. Furthermore, Castillo-Olivares *et al.* (2011) described the guinea pig as an ideal trial animal for AHS vaccines, although the mouse model (IFNAR -/-) has also been successfully used for both vaccine trials and infection models (Castillo-Olivares *et al.*, 2011). Following on from the work of Ronchi *et al.* (2012), the same inactivated-adjuvanted vaccine was successfully extrapolated to horses that were adequately protected from infection (Lelli *et al.*, 2013).

In the latter half of 2012, a new vaccine emerged manufactured by Disease Control Africa (Pretoria, South Africa). Anecdotal reports suggest that many horse-owners have used it in reaction to what is perceived to be an ineffective Onderstepoort Veterinary Products vaccine. However, there is no published data on the vaccine, nor any data about its manufacture or contents, besides being described as an 'inactivated field isolate vaccine'. The manufacturers claim to have done field trials, but none of this data is made available, either in peer-reviewed scientific journals or elsewhere, nor has a patent (provisional or complete) been issued (Carlisle, 2012).

Although not much work has been done on how the equine immune system responds to both vaccination and infection of AHSV, it would appear that the response is primarily humoral (Pretorius *et al.*, 2012). Peripheral blood mononuclear cells were collected from naïve horses vaccinated with live, attenuated virus. These cells were stimulated with viral antigen and this led to an increase in B-cells and IL-4 production from lymphocytes. In addition, virus specific CD8+ T-cells were stimulated with virulent virus, but the toxicity of these cells towards virus-infected cells remains to be determined, as does the particular antigen responsible.

1.11. AHS in rural, subsistence communities

One of the major problems in South Africa with regard to the outbreaks of AHS is the large population of unvaccinated equids living in the rural parts of the country, away from the concentrated racing and sport horse communities (Gerdes, 2006). Many of these rural and subsistence horses, mules and donkeys are used as traction animals. It is estimated that over 100 million equines are still used and relied upon for draught and transport in subsistence agricultural communities around the world. Despite the enormous role that these equines play in their communities, little attention is given to the health and welfare of these animals and veterinary authorities largely ignore these populations that may play an important role in endemic and non-endemic instances of AHS (El Idrissi & Lubroth, 2006).

In a survey carried out in 1994, it was established that in the rural areas of South Africa, 40 – 80% of the smallholder farmers visited were using animal power for transport and cultivation (Simalenga & Joubert, 1997). Although the observed mortality rate for horses is up to 90%, the length of time that these rural, unvaccinated horse populations have existed, and survived, could be suggestive of an immunity to AHSV having developed. Thus, when an outbreak occurs, these populations could provide a reservoir for the disease.

It has been recognised, particularly in eastern Africa, that community involvement in animal disease control provides an effective channel through which rural, subsistence communities

can be reached. Vaccinations and diagnostics can be performed by community based health care workers with success (Catley & Leyland, 2001). With regard to AHS, communities that rely on horses, mules or donkeys should be targeted such that a more effective national campaign to control AHS might enjoy more success. Teshome *et al.* (2012) indicated that only 25% of their horse-owning respondents in Ethiopia were aware of AHS, while Ayelet *et al.* (2013) found that owners do recognise the disease, but have little knowledge of its mode of transmission.

1.12. Overview of local and international policies to control AHS

The increase in the international movement of horses for the racing and sport horse industries has made AHS a very important disease to researchers and animal disease control officials around the world (Sakamoto *et al.*, 2000; Maclachlan & Guthrie, 2010). In recent years, the archetype orbivirus, the bluetongue virus, has been detected in increasingly northern regions in Europe that were historically free of bluetongue, suggesting that AHSV could readily be introduced to other parts of the world (Mullens *et al.*, 2004; Vellema, 2008; Maclachlan & Guthrie, 2010). The vector, *Culicoides imicola,* has expanded its range northwards through Europe, most likely as a result of climate change, and this is the most probable cause of the bluetongue outbreaks in Europe in recent years (Guthrie *et al.*, 2009; Maclachlan *et al.*, 2009). The importance of a rapid assay for diagnostics becomes exceptionally important should an outbreak of AHS occur in a country free of the disease and with an equine population naïve to the virus.

AHS is considered to be the most important disease of equines to be evaluated when moving horses across international borders (Guthrie, 2008). The OIE has defined a number of zones for the control of AHS globally. A 'free country' is a country where no confirmed infection has occurred for the last two years and where no horse has been vaccinated in the last year. In a country where the disease is endemic, a free zone may be declared in the same way as for a free country, and should preferably be delineated by substantial geographic boundaries with suitable animal movement controls (OIE, 2009). In countries previously free of the disease, determining the serotype and producing a monovalent vaccine is a priority, should there be an outbreak. A monovalent vaccine is the most successful control measure as it results in long-lasting immunity in most animals.

The equine industry (racing, sport and leisure) has been estimated to have an economic impact of £7 billion with more than 70,000 jobs dependant on it in the UK. Allison *et al.* (2009) suggested that a sustained outbreak could halve the value of the industry in less than two years, especially as the impact is likely to last at least 12 months. In Europe, the

horseracing industry alone has an economic impact of €6 billion (Bélinguier, 2009) including jobs and taxation (Bruggnik, 2009). Diagnosis of the correct infecting serotype and subsequent implementation of suitable control measures is therefore of great importance.

1.12.1. South African controls to prevent the spread AHS

In South Africa, after the European Commission Decision in 1997 (97/10/EC), exports were allowed to move directly out of the Cape Town Metropolitan area as long as the AHS free zone was defined (Parker, 2008). The free zone is located in Cape Town with appropriate buffer zones throughout the Western Cape (Figure 1.10). However, this has not been foolproof as AHS cases occurred in the controlled area in 1999, 2004, 2006 (Parker, 2008) and in 2010 (AHS-Trust, 2012).

Figure 1.10: South African African horse sickness Controlled Area. Devised in 2001 for the continued export of horses from South Africa. Red – Infected zone. Orange – protection zone. Blue – Surveillance zone. Green – free zone (Bührmann, 2011).

Export of horses from an infected country must take place through quarantine stations within the free zone (OIE, 2009). Under the EC Protocol of 1997, horses must spend 60 days in quarantine in the free zone in Cape Town before being shipped to the EU. However, when an outbreak occurs in any of the control zones, direct imports into the EU from South Africa

are banned and horses must spend 21 days in quarantine in Cape Town, followed by 90 days in Mauritius. However, Racing SA was recently able to lobby the OIE to revise the AHS code. Under the new code, horses will spend a minimum 14 days in quarantine and be allowed direct entry into the EU. Should an outbreak occur, and an OIE-acceptable containment zone be established, exports could resume after 80 days. However, if a containment zone cannot be established, the EU will automatically impose a two year ban (RacingSA, 2012).

1.12.2. European controls to prevent an AHSV incursion

Following the bluetongue outbreaks in 1998 and 2004-2006 in Europe and the Schmallenburg virus in Great Britain in 2011 (both orbiviruses with identical vectors to that of AHSV), there is a real concern in many European countries that AHSV could easily follow (McCarthy, 2012). Countries that have either drafted legislation or published possible scenarios of AHS outbreaks include the United Kingdom, the Netherlands, Ireland and Bulgaria (Backer & Nodelijk, 2011; Chenchev *et al.*, 2011; de Vos *et al.*, 2012; McCarthy, 2012; Thompson *et al.*, 2012). In policy documents, the United Kingdom 'government will act rapidly to kill infected horses' and those showing clinical symptoms on the initially infected premises and those neighbouring it. Owners will only receive compensation if the animal is found to be disease free after euthanasia, and only up to £2500. Equidae in the protection zone will be vaccinated; however, the type of vaccine or valency is not stipulated as no vaccine is currently registered for use in the UK. However, the European Commission has stockpiled monovalent live vaccines, although the source of the vaccine is not known (DEFRA, 2012). Additionally, the UK is reluctant to use live vaccines due to their perceived possible ability to revert to virulence (Allison *et al.*, 2009).

1.13. African horse sickness virus molecular diagnostics

Primarily as a means of detecting AHSV in equines and as part of surveillance programmes to track possibly infected vectors and hosts, AHSV diagnostics have developed from virus neutralization techniques in the 1960s to modern real-time PCR techniques. However, in the author's opinion, serotyping of the virus remains a neglected facet to the ongoing diagnostic work.

1.13.1. Reverse transcription PCR (RT-PCR)

The AHS virus is a double-stranded RNA virus and as such requires a reverse transcriptase step before standard PCR. In single tube, one-step RT-PCR protocols, the synthesis of cDNA and PCR occur sequentially but uninterrupted (Lee *et al.*, 1994). Where possible, one-step protocols are the preferred method for RNA diagnostics due to their one-tube, simplified

and expedited nature. In a two-step protocol, reverse transcription occurs in a separate tube from the one intended for PCR. In most RT-PCR reactions, a reverse transcriptase is used to transcribe RNA into cDNA and then a DNA polymerase synthesises the DNA amplicons.

1.13.2. Using RT-PCR to detect AHS

A number of researchers have developed RT-PCR assays to detect the AHS virus since the early 1990s and a brief overview of their experimental designs and differences between the assays are described.

1.13.2.1. Isolation of AHSV genomic material

Stone-Marschat *et al.* (1994) purified viral dsRNA from infected Vero cell lysates by phenol extraction and lithium chloride precipitation. Zientara *et al.* (1995b) and Bremer (2012) isolated total AHSV RNA from cell cultures and spleen tissue samples using the guanidinium-thiocyanate-phenol-chloroform method of Chomczynski and Sacchi (1987). Commercial kits based on this method are now available, such as the TRIzol™ group of reagents (Rodriguez-Sanchez *et al.*, 2008). The quantity of AHSV genomic dsRNA can be determined spectrophotometrically at 260 nm, as is standard for all RNA (Wade-Evans *et al.*, 1990).

In terms of field samples, it has been reported that the AHS viral genome was successfully extracted and purified from clotted blood. This has the potential to reduce costs further since special blood collection vials containing anti-coagulants may no longer be needed (Fasina, 2008; Fasina *et al.*, 2008). In addition, direct PCR from whole blood may be possible by modifying the initial viral capsid denaturation steps (Mercier *et al.*, 1990; McCusker *et al.*, 1992).

However, the possibility exists to eliminate viral RNA extraction procedures by using specially prepared filter paper (Whatman FTA® cards) for collection of small blood samples. In 1997, this was achieved with the Human Immunodeficiency Virus (HIV) Type 1 (Cassol *et al.*, 1997). In addition, RNA levels on the filter paper had not decreased after two weeks at 20°C and three days at 37°C. This has important consequences for field studies and the development of field applicable diagnostic assays. FTA cards have also been examined for their ability to inactivate pathogens and for their storage ability and stability of nucleic acids, all of which revealed promising results for reducing field assay costs (Roy & Nassuth, 2005; Purvis *et al.*, 2006). In 2007, real-time RT-PCR was performed on RNA from porcine reproductive and respiratory virus collected on FTA® cards (Inoue *et al.*, 2007). By using a higher pH PCR buffer, Bu *et al.* (2008) were able to amplify genomic DNA directly from blood that had dried on the filter paper. This has an enormous potential to reduce costs involved in

such diagnostic assays, as expensive reagents to extract genomic material will no longer be needed.

1.13.2.2. Primer selection for AHSV RT-PCR

Previous workers have selected a range of sequences from different genome segments of the AHS virus to design primers for RT-PCR. The genome segment encoding NS2 was used in the first PCR published to detect the AHS virus (Stone-Marschat *et al.*, 1994). The genome segment encoding NS2 has high sequence similarity within the serogroup, but was divergent enough among serogroups not to detect other orbiviruses. A single-tube RT-PCR was developed targeting regions on the genome segments encoding VP7 and NS3 a year later and all nine serotypes were detected (Zientara *et al.*, 1995b). Following on from that work, the genome segment encoding NS3 (segment 10) was used to differentiate the nine serotypes using restriction fragment length polymorphism (RFLP). In a 1997 study, VP7 was targeted again, coupled with a dot-blot hybridisation technique (Sailleau *et al.*, 1997a). In 2000, all nine serotypes were individually identified using 15 different primers in different combinations, but in nine separately optimised PCR assays (Sailleau *et al.*, 2000). In South Africa, the first PCR assay was developed in 2004: the assay could be used to serotype the virus using 16 primers under identical reaction conditions (Koekemoer & van Dijk, 2004). However, it required lengthy post-PCR analysis. Rodriguez-Sanchez *et al.* (2008) used the genome segment encoding NS1 as a target and combined it with gel-based techniques. The genome segment encoding VP7 was used to develop an assay for AHS coupled with probe-based technologies (Fernández-Pinero *et al.*, 2009). However, all of these assays require lengthy post-PCR analysis, such as agarose gel electrophoresis or use comparatively expensive reagents such as fluorescent probes.

1.13.2.3. AHSV cDNA synthesis from viral RNA

When double-stranded RNA is the starting nucleic material, such as is the case for the AHS virus, it must be denatured so that cDNA can be synthesised from it. This is achieved by either heat denaturation or adding a methyl mercuric hydroxide solution to the dsRNA material (Wade-Evans *et al.*, 1990; Zientara *et al.*, 1995b). Compared to heat denaturation, methyl mercuric hydroxide increases the sensitivity of RT-PCR ten-fold (Wilson & Chase, 1993). However, in recent years, heat denaturation is the most often used due to its ease and simplicity. Methyl mercuric hydroxide is also difficult to obtain. Depending on the reverse transcriptase to be used, the solution is incubated from 5-60 minutes at temperatures from 37-55°C to allow the enzyme to reverse transcribe the viral RNA.

1.13.2.4. AHSV RT-PCR diagnostic assays

A number of RT-PCR assays have been developed for the detection of AHSV since the first one by Stone-Marschat *et al.* (1994), which is still one of the OIE recommended protocols.

This is a simple, straightforward assay and terminates in an agarose gel analysis of the amplicons. Many of the more recent assays (Table 1.4) have switched to real-time, probe based technology. Although real-time assays reduce the need for agarose gel analysis, the cost of using probes negates that advantage. In addition, later assays have tended towards kit-based PCR protocols such as the Brilliant® QRT-PCR Master Mix One-Step kit (Rodriguez-Sanchez *et al.*, 2008), the Applied Biosystems GeneAmp Gold RNA PCR core kit (Quan *et al.*, 2008) or the Qiagen One Step RT-PCR kit (Fernández-Pinero *et al.*, 2009).

Table 1.4: Summary of recent RT-PCR assays for the African horse sickness virus.

Approach	Genome segment	Advantages	Disadvantages	Reference
AHSV +/- RT-PCR				
Real-time RT-PCR	7	Real-time, 1000-fold increase in sensitivity	TaqMan® probes expensive	Agüero *et al.* (2008)
	8	Able to amplify RNA from 0.0001 - 1.5 fg.	FAM-labelled TaqMan-MGB probe would add cost	Monaco *et al.* (2011)
Nested RT-PCR	3	Detect 0.1 fg of viral RNA (6 viral particles) Tested successfully on crude samples	Two PCR reactions effectively doubles time and cost	Aradaib (2009)
Duplex RT-PCR	8, 9	No probe	Two-step protocol	Quan *et al.* (2010); Guthrie *et al.* (2013)
Serotyping RT-PCR				
Probe-based hybridisation	2	Result in 24 hours	Probe-based, requires post-PCR reverse line blot	Koekemoer *et al.* (2000)
Conventional RT-PCR	2	Result in 24 hours	Gel-based and nine sets of primers	Maan *et al.* (2011a)

However, despite the advances of PCR technology, some institutions prefer to use more conventional, PCR technologies, with an agarose gel analysis as an endpoint, due to the small number of samples they receive and the relatively low cost of the reagents (Bremer, 2012). Considering the serotyping assays summarised in Table 1.4, none render a result immediately post-PCR. Both require additional steps to achieve the end-point. In addition, the probe-based assays, whilst recorded as being very sensitive, add to the cost of the assay. The conventional PCR, while lacking probes, uses nine sets of primers and would require nine different PCRs to achieve a result, effectively increasing the cost nine-fold.

Despite the minimal work done on AHSV RT-PCR assays, a significant amount more work has been done using other orbiviruses and is considered in the Section 1.13.2.5 as the results achieved are mostly directly translatable to AHSV.

1.13.2.5. Using RT-PCR to detect other orbiviruses

RT-PCR has been used successfully to amplify genomic material from other orbiviruses. In a study done in 1995 on epizootic haemorrhagic disease virus, PCR assays were already being identified as equal to, if not superior to the “cumbersome and time-consuming” virus neutralisation assays (Aradaib *et al.*, 1995). These include the bluetongue virus (Zientara *et al.*, 2004; Jimenez-Clavero *et al.*, 2006; Monaco *et al.*, 2006); epizootic haemorrhagic disease virus (Abdalla *et al.*, 2002; Aradaib *et al.*, 2003a; Aradaib *et al.*, 2003b) and the Chuzan and Ibaraki viruses (Ohashi *et al.*, 2004). Importantly the sensitivity of these RT-PCR assays compares very favourably with the conventionally accepted norm of virus isolation (Abdalla *et al.*, 2002).

Epizootic haemorrhagic disease virus (EHDV) was serotyped using a RT-PCR protocol with an agarose gel analysis as an endpoint (Maan *et al.*, 2010a). The methodologies are much the same as for the AHSV gel-based serotyping RT-PCR (Maan *et al.*, 2011a) in that two primer pairs were designed based on segment 2 for each of the seven EHDV serotypes and the best pair chosen. The presence of the correctly sized band on an electrophoresed agarose gel was an indication of the RT-PCR’s success, despite a number of other bands often being present. Due to this, these primers would not be suitable for High Resolution Melt (HRM) analysis (Section 1.14).

The emergence of highly sensitive and specific virus detection methods bode well for diagnosis prior to the movement of equines from infected regions to non-infected regions. Lengthy quarantine protocols were developed to allow an animal to display any symptoms of a disease if infected. As assays became more sensitive and specific, the need for lengthy

quarantine protocols diminishes (Maclachlan & Guthrie, 2010). Thus the evolution of a rapid assay could effectively reduce the costs involved in moving horses globally. As part of this evolution in molecular diagnostics, the relatively recent technique of High Resolution Melting has not yet been assessed for diagnosing, or indeed serotyping, an orbivirus.

1.14. High Resolution Melt analysis

1.14.1. Brief history and technique overview

High Resolution Melting (HRM) was introduced in 2002 through the collaborative efforts of academia (University of Utah) and industry (Idaho Technology) to detect genetic variations of double-stranded DNA (Reed *et al.*, 2007). Various methods have previously been developed to detect DNA sequence variation of PCR products. However, these involved additional, lengthy processing and separation steps subsequent to the PCR run and included additional apparatus (Reed *et al.*, 2007). Gundry *et al.* (2003) described the ability of melting temperatures to distinguish unique variants in a homogenous, closed tube procedure performed automatically after PCR. HRM analysis requires normal PCR reagents, a fluorescing dsDNA dye and approximately 10-15 minutes of closed-tube, post-PCR analysis (Reed & Wittwer, 2004). High Resolution Melting is the simplest method of determining DNA sequence variation and has consequently gained popularity (Reed *et al.*, 2007).

Historically, DNA melting was monitored by UV absorbance, requiring microgram amounts of DNA and very slow melting rates. High Resolution Melting, on the other hand, requires only nanogram amounts of DNA provided by PCR (Reed *et al.*, 2007). Earlier HRM applications used primers as well as various labelled probes. However, these proved to be too limiting for routine use (Wittwer *et al.*, 2003; Liew *et al.*, 2004). Following standard PCR, which results in a high copy number of a purified amplicon, HRM analysis is an advancement of previous melting analyses based on DNA denaturation or dissociation. It is based on the release of a DNA-intercalating fluorescent dye that is released from dsDNA as it is denatured or dissociated into ssDNA with increasing temperature (Figure 1.11). The melt curve is generated by heating the sample through a range of temperatures as fluorescence data is continuously collected. At low temperatures, the dsDNA fluoresces strongly. As the temperature is increased, the dye is released from the dsDNA structures, and at a characteristic point, the fluorescence drops rapidly, indicating the dissociation of the dsDNA into single strands, also known as the melting temperature of the DNA (T_m).

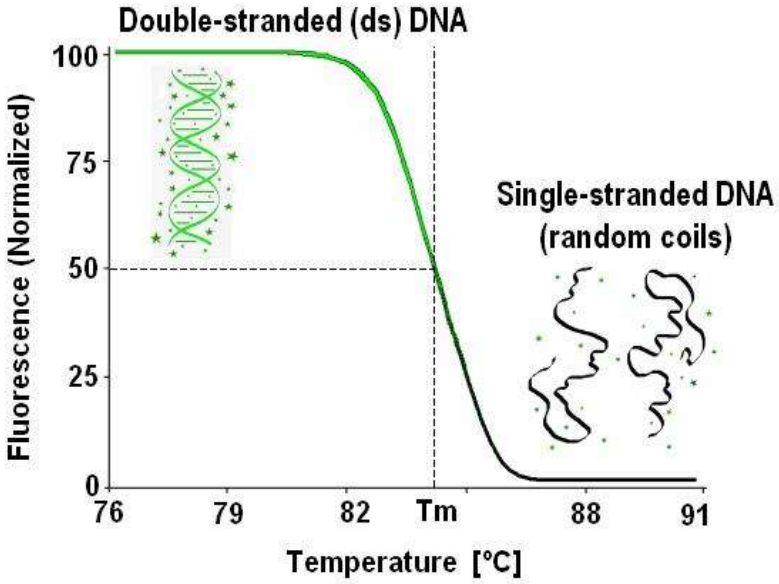

Figure 1.11: Simplified melt profile demonstrating the release of a fluorescent dye as the double-stranded DNA is denatured into single-stranded DNA. The dye is intercalated into the strands of the dsDNA at low temperatures, where it fluoresces strongly. As the temperature is increased, the dsDNA structure begins to dissociate into ssDNA and the dye is released and no longer fluoresces (Anonymous, 2006).

The characteristic melting of a DNA sequence is defined by the relative stabilities and kinetic melting rates that are dependent on sequence length, GC content and sequence complementarity, which are unique among genetic variants of the same genome segment. Based on this, HRM analysis has a number of applications including mutation detection, genotyping and species identification (Gundry *et al.*, 2003; Corbett, 2006; Hubbart *et al.*, 2007; Reed *et al.*, 2007). The decrease in fluorescence is measured with a high degree of optical and thermal precision and is analysed *in silico* (Corbett, 2006). HRM analysis is simple, cost-effective and requires no post-PCR processing such as agarose gel electrophoresis. It also compares favourably with other similar, expensive techniques such as DNA sequencing (Corbett, 2006; White & Potts, 2006).

Part of the recent success of HRM analysis is the introduction of third generation fluorescent dsDNA dyes. SYTO®9 (Invitrogen Corp., Carlsbad, CA), LCGreen® (Idaho Technologies, Salt Lake City, UT) and EvaGreen® (Biotium Inc, Hayward, CA) have lower toxicity levels than previous, older dyes (e.g. SYBR® Green I) and, as such, can be used at higher concentrations that ensure saturation of the dsDNA. (Gundry *et al.*, 2003; Wittwer *et al.*, 2003; Corbett, 2006). Previously used dyes also had a tendency to preferentially bind to sequences with a higher melting temperature (T_m) and GC-rich regions (Zhou *et al.*, 2004). Older dyes, such as SYBR® Green I, had to be optimised further when used in standard PCR buffers by the addition of dimethyl sulfoxide (DMSO), bovine serum albumin or Triton X-100.

In addition, the dye was reported to inhibit the PCR reaction without an increase in $MgCl_2$ and interferes in multiplex PCRs. SYTO®9 supports PCR in a wide range of applications, produces robust melting curves unaffected by DNA or dye concentration and can be used in multiplex PCR reactions (Monis *et al.*, 2005). However, SYBR® Green I is reported to be better suited to rapid detection and for larger amplicons (Pornprasert & Sukunthamala, 2010). In most instances, the choice of dye is dependent on the commercial system chosen.

The sensitivity of HRM analysis is evident in its ability to detect the smallest genetic changes such as single base changes (single nucleotide polymorphisms, SNPs). In general, the greater the number of changes, the easier they are to detect using HRM analysis (Corbett, 2006; White & Potts, 2006). HRM analysis is best performed on highly pure PCR products of less than 250 base pairs (bp), although 44-304 bp amplicons have been analysed previously (Gundry *et al.*, 2003; Corbett, 2006). Amplicons of up to 1000 bp have also been successfully analysed using HRM (Reed & Wittwer, 2004) The largest recorded amplicon for HRM application has been 1330 bp (Chateigner-Boutin & Small, 2007). The larger the amplicon, the lower the resolution as the differences between the sequences decreases. This can be overcome to some extent by melting at slower rates at the expense of an extended analysis time (Gundry *et al.*, 2003). Additionally, certain sequence motifs (e.g. hairpin loops or other secondary structures), localised regions of high or low GC content or repeat sequences can all affect the results unpredictably (Corbett, 2006).

An HRM analysis must be preceded by a good quality and accurate PCR, as would be a normal real-time PCR assay. This includes the design phase where the target sequence and primers are identified and the reactions are set up. Interestingly, HRM analysis has been successfully performed on samples from dried blood spots (Gundry *et al.*, 2003; Corbett, 2006).

The post-PCR/HRM analysis results are viewed as fluorescence versus temperature graphs and mathematical derivatives of these (Figure 1.12). The graphs are normalised for each sample by defining linear baselines before and after the melting transition. The fluorescence for each acquisition within the sample is calculated as a percentage between the top and bottom baselines at the acquisition temperature (Gundry *et al.*, 2003). Normalised curves represent the basic interpretation for sequence variation and are based on curve shifting, shape change and position (Wittwer *et al.*, 2003). These authors also described fluorescence difference as a useful method of differentiation. This allows better visual grouping of genotypes. One melting curve is chosen as the reference and the rest are plotted against it as a difference. The HRM analysis software now also allows for the automatic calling of genotypes with a set confidence interval (Corbett, 2006).

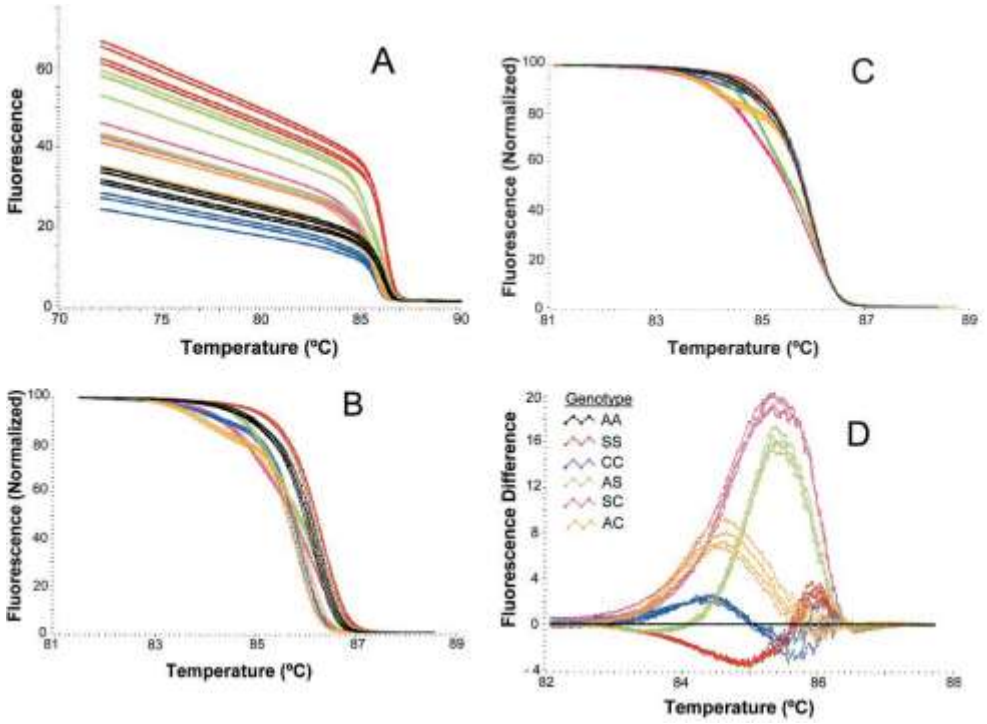

Figure 1.12: Variations of the interpretations of fluorescence data post HRM analysis. A) Raw fluorescence data in real-time. B) Normalised fluorescence. C) Temperature shifted normalised fluorescence. D) Difference plots of the normalised, temperature shifted data (Wittwer *et al.*, 2003)**.**

In studies that used HRM analysis to detect mutations, DNA sequencing confirmed that normal melting curves correlated with normal DNA sequences and abnormal melting curves correlated with abnormal DNA sequences (Willmore *et al.*, 2004). In a study performed in 2004, large sequence differences were found to be detectable by HRM analysis (Vaughn & Elenitoba-Johnson, 2004). Previously, only single point mutations had been studied. Using HRM analysis, amplicons of 335 to 431 bp in length were analysed for insertions of 6-102 bp in length. A concordance of 100% was achieved compared to more standard methods such as capillary electrophoresis-based fragment analysis, temperature gradient capillary electrophoresis detection and sequencing. High Resolution Melt analysis was also found to be effective at detecting mutations across the length of the amplicon, despite the mutations occurring at various positions.

Various computer programmes have been developed to produce melt curves entirely *in silico*, such as POLAND, MELTSIM and uMELT^{SM}. The programmes, while successful in accurately typing the samples, are, however, best suited to assay design (Rasmussen *et al.*, 2007; Dwight *et al.*, 2011). Although uMELT^{SM} does not produce an actual melt profile, it

illustrates where and when the double-stranded DNA products dissociate. It also has the added advantage of allowing the user to choose from different melting algorithms.

The standard software that is provided with the Corbett Rotor-Gene™ 6000 rotary analyser (Rotor-Gene™ 6000 Series Software) has a number of genotyping options. Using the melt profiles, 'bins' may be applied to certain peaks and all peaks that fall within a set range are similarly assigned that 'bin'. A 'bin' can be defined as a range of temperatures where a peak may be found. A second method, the more sensitive one, uses defined regions of the normalised melt profile, where a reference genotype is selected, and based on the HRM profile, the software will 'genotype' the remainder of the samples relative to the reference sample/melt profile and apply a confidence level to them. However, in some instances, the power of resolution is not enough. ScreenClust HRM® Software is a step up to the standard software and uses Principal Component Analysis (PCA), a statistical interrogation technique, to further define, statistically, the genotype (Reja *et al.*, 2010). Principal component analysis operates by identifying a number of factors in a data set and determining which of them contribute more or less to differentiating the sample set. These features are then combined in up to three principal component (PC) scores and plotted. In ScreenClust HRM® Software, the HRM raw data is normalised first. From the normalised data, a composite mean is calculated by averaging all of the vertical data points (fluorescence). This composite mean is then differentiated (subtracted) from the normalised profile to result in the residual plot (Figure 1.13). Certain features (unknown due to the software's proprietary nature) are extracted to calculate the PC scores. Suitably differentiated scores produce a number of clusters or discriminate groups. The power of PCA to resolve melt curves is demonstrated in Figure 1.14. In the left hand panel, the difference plot is shown, direct from the Corbett Rotor-Gene™ 6000 Series Software. Three profiles are evident, aided by the colours, although it would prove difficult to assess. The differentiation of these profiles is made very apparent in the PCA analysis in the right hand panel.

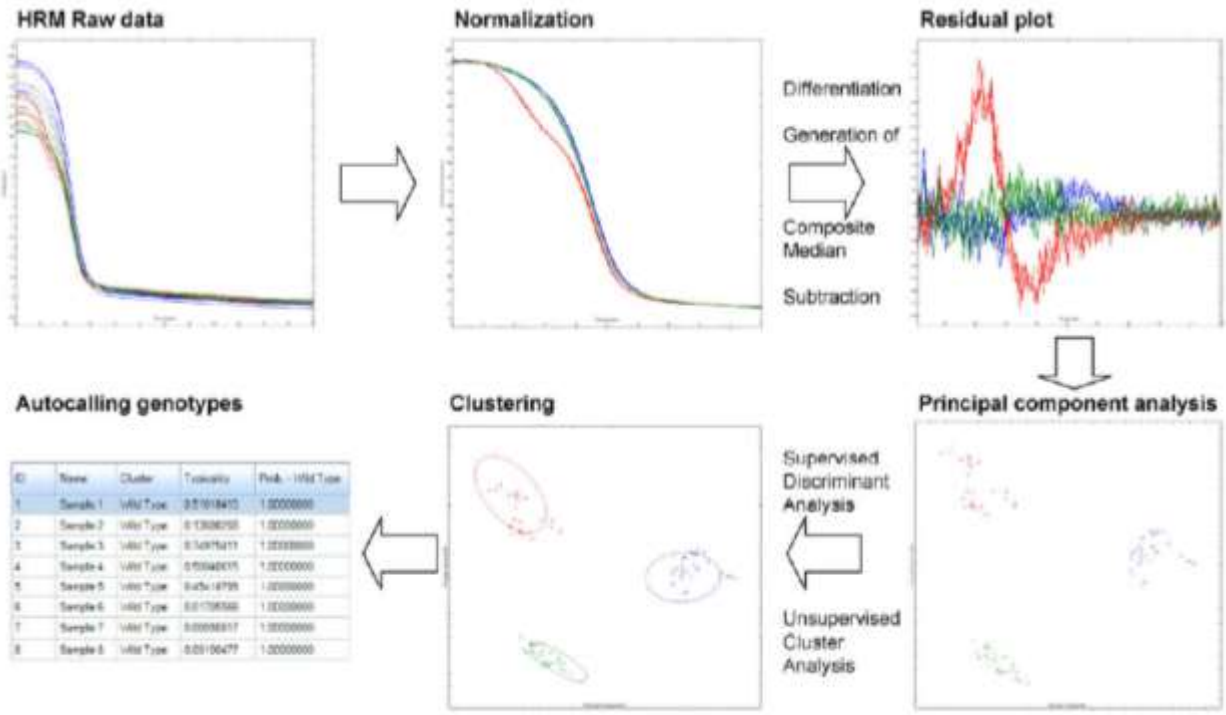

Figure 1.13: The basic steps involved in the analysis of HRM curves using the ScreenClust HRM® Software. See text for details of steps (Reja *et al.*, 2010).

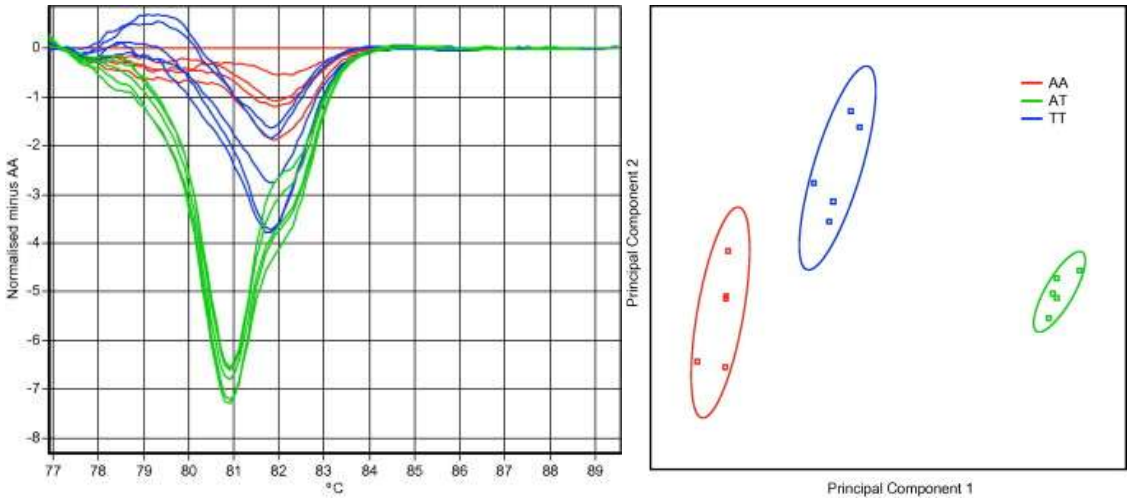

Figure 1.14: Comparison of Corbett Rotor-Gene™ 6000 Series Software and ScreenClust HRM® Software for single nucleotide polymorphism (SNP) analysis. Standard difference plot (left) of Corbett Rotor-Gene™ 6000 Series Software and PCA cluster analysis (right) of the ScreenClust HRM®. The differentiation of the three profiles is made very apparent by the PCA analysis (Reja et al., 2010).

ScreenClust HRM® Software, however, is not without its drawbacks. It can only analyse data from single runs – additional runs cannot be added and an experiment is therefore limited by the number of samples the rotor can accommodate in the Corbett Rotor-Gene™ (Gurtler *et al.*, 2012). In an attempt to circumvent this, Gurtler *et al.* (2012) opted to gather data from

many runs by recording the difference in fluorescence at 81°C, 82°C and 83°C, pooling this data and creating a 3D scatter graph (Figure 1.15). In the same study, another method recorded the fluorescence differences at 81°C, 82°C and 83°C in standard graphs over time (samples from patients taken over a few days/months). Both methods made it possible to use HRM profiles to distinguish samples taken over time, rather than having to run all of the samples at the completion of the trial.

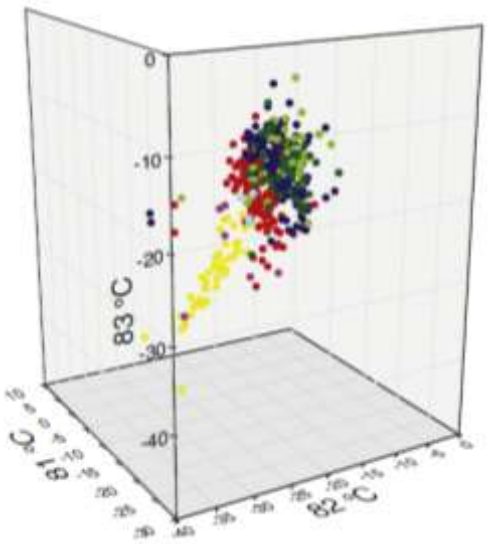

Figure 1.15: Using 3D scatter plots to utilise HRM profiles taken over time. Three temperature values taken from a normalised difference graph are used to create a 3D scatter plot (Gurtler *et al.*, 2012).

1.14.2. High Resolution Melt and species/genotype differentiation

Most HRM applications have sought the detection of single point mutations. Robinson *et al.* (2006) successfully and reproducibly differentiated between species of the amoebaflagellate genus *Naegleria* using a single primer set. The melting curves that resulted were distinguishable and unique for each species due to the differences seen in the positions and relative heights of the peaks (Figure 1.16). Feline caliciviruses (Helps *et al.*, 2002), *Cryptosporidium* spp. (Limor *et al.*, 2002; Tanriverdi *et al.*, 2002), *Leishmania* spp. (Nicolas *et al.*, 2002), Mycobacteria spp. (Odell *et al.*, 2005), *Plasmodium* spp. (Mangold *et al.*, 2005), *Campylobacter jejuni* (Price *et al.*, 2007) and *Pseudomonas aeruginosa* (Anuj *et al.*, 2011) have also all been successfully differentiated using HRM analysis. However, HRM analysis has not yet been tested on any orbiviruses.

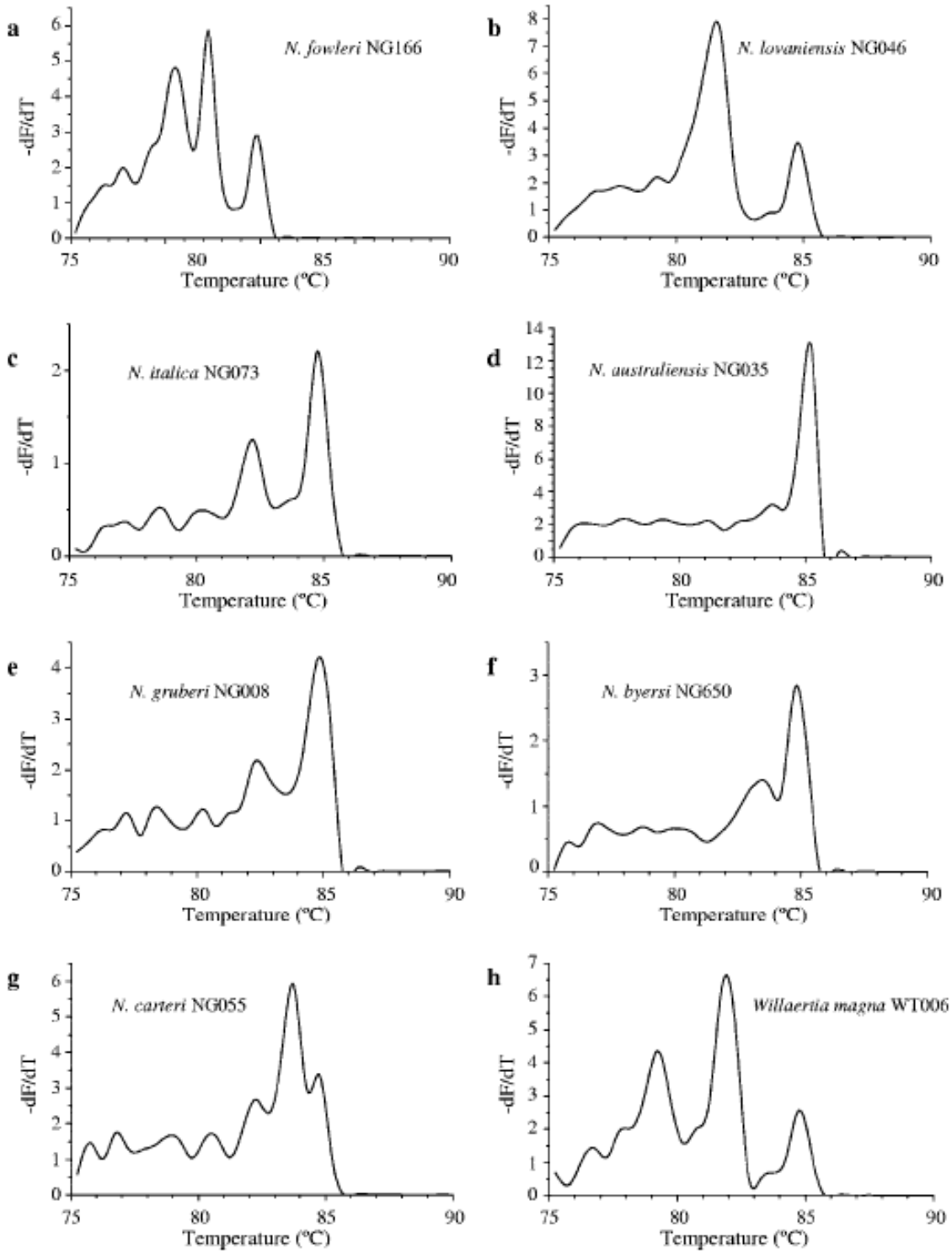

Figure 1.16: Melt curves obtained from *Naegleria* spp. using HRM analysis demonstrating unique positions and relative heights of peaks between the species. Each graph represents a different species and shows a unique profile (Robinson *et al.*, 2006).

In 2009, the use of HRM analysis combined with a unique mathematical model was used to differentiate strains of infectious bronchitis virus (IBV) on 230-436 bp products such that the most effective vaccination programme could be applied and hence rapidly control IBV

outbreaks (Figure 1.17) (Hewson *et al.*, 2009). A similar approach is envisaged for AHS, either in South Africa or internationally, where an infecting serotyping can be determined with minimal cost and time using HRM analysis and appropriate vaccine controls can subsequently be enforced.

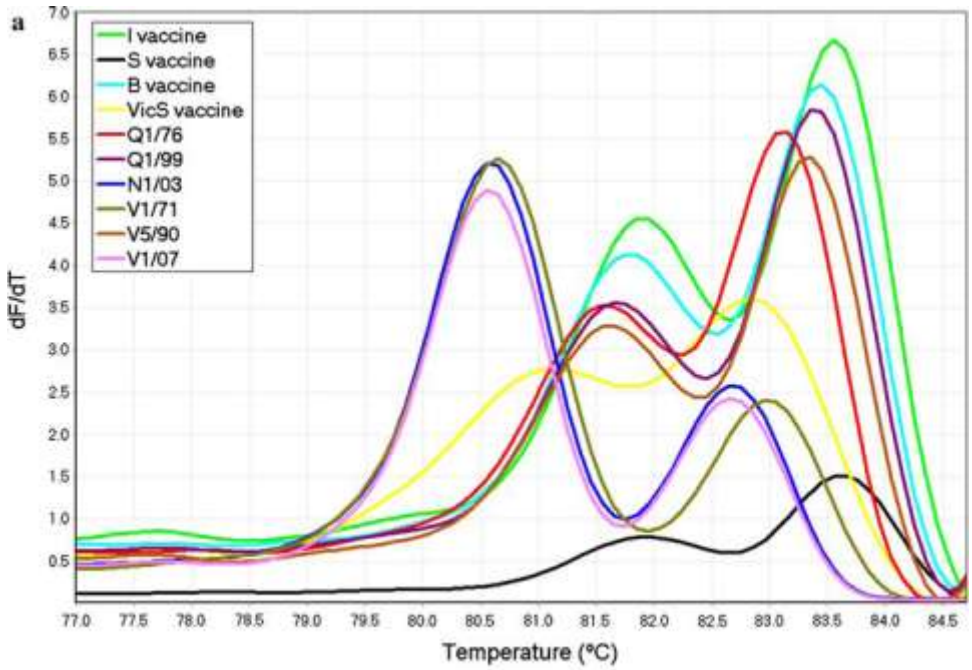

Figure 1.17: Conventional melt curves of various wild-type and vaccine strains of IBV (Hewson *et al.*, 2009).

The poultry pathogen *Mycoplasma synoviae*, with 35 different strains, was grouped into ten different HRM profiles (Jeffery *et al.*, 2007). As an intermediate step, this may have applications for AHSV where an initial PCR may not resolve all nine serotypes individually. Importantly, the authors claimed that the HRM curve analysis of *M. synoviae* is a 'rapid and effective technique that can be performed in a single test tube in less than two hours'.

Grando *et al.* (2012) explored the possibility of typing virulent and non-virulent strains of *Clostridium difficile* by comparing a conventional PCR ribotyping assay, HRM analysis and ScreenClust HRM® Software. Eighty-eight samples were used, but only two genotypes were sought. One of the isolates in the Grando *et al.* (2012) study was described as having had a similar shape curve as another, despite much lower signal strength. The authors did find HRM analysis to be more effective at genotyping the samples, with ScreenClust HRM® Software also producing similar results, although ScreenClust HRM® Software was not

valued any more over standard HRM analysis. The African horse sickness virus, on the other hand, has nine genotypes and far fewer available samples.

High Resolution Melt analysis has also been used to analyse JAK2 exon 12 mutations involved in erythrocytosis (Carillo et al., 2011). Although up to nine mutants were identifiable, the regions under question only spanned 33 bp. Beta-lactamases of *Escherichia coli* have also been detected by HRM analysis. However, all three β-lactamases considered in the study were detected with three unique sets of primers, producing various combinations of products that were easily distinguished by both visual inspection and the ScreenClust HRM® Software (Chroma *et al.*, 2011). Interestingly, no ScreenClust HRM® Software results were actually shown. The authors were less than satisfied with ScreenClust HRM® Software claiming one sample was clearly of a particular genotype; both by visual inspection of the melt curves and sequencing, yet ScreenClust HRM® Software had called it otherwise.

Infectious bursal disease virus (IBDV) has also successfully been serotyped using HRM analysis (Ghorashi *et al.*, 2011). IBDV is also a double-stranded RNA virus, but is only bi-segmented and only two serotypes have been identified (Becht *et al.*, 1988; Bayliss *et al.*, 1990). In the Ghorashi *et al.* (2011) study, a single primer pair was used which amplified a 474 bp IBDV product. Nine different IBDV reference strains were used plus three vaccine strains and each produced a unique melt profile in accordance with their sequences and the differences contained therein. Despite being tested a number of times, it would appear that it was the same isolate being re-tested, rather than testing different isolates of the same strain. The melt curves were described visually: peaks and shoulders, their relative heights and respective positions on the X-axis (temperature). Runs on different days and from different RNA extractions of the same isolate appeared to shift, however the shape and relative positions remained unchanged, an important consideration when setting up a genotype reference ‘bank’ of profiles (Ghorashi *et al.*, 2011).

High Resolution Melt analysis has proved to be more sensitive, more efficient and less time consuming than conformation sensitive gel electrophoresis for the detection of breast cancer gene mutations in breast cancer patients (de Juan Jimenez *et al.*, 2011). In a comparison of three techniques for distinguishing monoclonality from polyclonality in B-cell non-Hodgkin lymphoma, HRM analysis was found to be superior for cost, time and ease (Kummalue *et al.*, 2010).

1.15. African horse sickness virus phylogenetics

An important consideration in viral research, in particular when it involves various types of the virus, is the stability of the viral genome. A semblance of the genome's stability over time could be inferred from a phylogenetic study.

1.15.1. Phylogenetic studies of the African horse sickness virus and other orbiviruses

1.15.1.1. African horse sickness virus

Relationships between serotypes of the AHS virus have not been studied to a large degree. The first phylogenetic analysis was conducted using segment 10 (de Sa *et al.*, 1994). Segment 10 of serotypes 1, 4 and 8 was sequenced and compared to previously sequenced segment 10 of serotypes 3 and 9. Serotypes 1 and 8 appeared to be closely related, as well as serotypes 4 and 9. Serotype 3 was more closely related to serotypes 4 and 9 than serotypes 1 and 8 (Figure 1.18). It was found that segment 10 of AHSV was far more variable than segment 10 of the bluetongue virus or equine encephalosis virus (de Sa *et al.*, 1994).

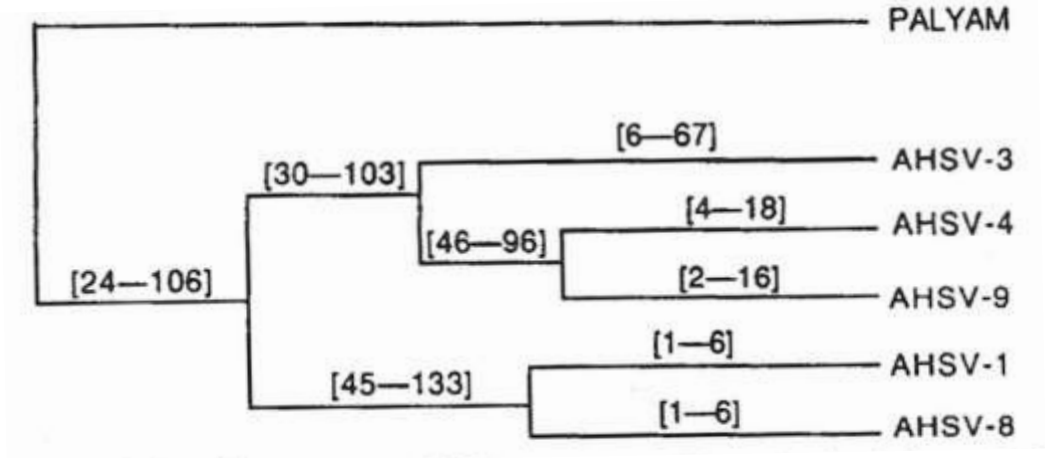

Figure 1.18: Relationships between serotypes 1, 3, 4, 8 and 9 of AHSV segment 10. Relationships based on the coding sequences of segment 10. Tree length = 379, consistency index = 0.868, values above branches correspond to the range of branch lengths under all character optimisation. As outgroup, Palyam represents another virus of the *Orbivirus* genus (de Sa *et al.*, 1994).

In another study in which segment 10 sequences of various orbiviruses were analysed phylogenetically, using only the reference strain sequences of AHSV (designated 'Jane'), the clades cluster as follows: serotypes 1 and 2, serotypes 3 and 7 and serotypes 4, 5, 6, 8 and 9 (Figure 1.19). When the field isolates were analysed, the clustering was slightly modified:

serotypes 6, 8 and 9, 3 and 7, and 2 all clustering into single clades. Serotypes 1, 4 and 5, however, clustered into multiple clades (Figure 1.20). In both cases, three clades were evident. The models used – a general time reversible (GTR) model with a proportion of invariable (I) sites and a gamma-shaped distribution of rates across the sites (Γ) – were calculated *in silico*. The GTR model is one of the most complex and parameter rich models, while the gamma-shaped distribution refers to the proportion of sites that contribute to the evolutionary rate (Quan *et al.*, 2008). However, the number of iterations used (1×10^6) is too small and the phylogeny should be treated with care. Although using fewer sequences, Koekemoer *et al.* (2003) also found that serotype 3 clusters with serotype 7.

Maan *et al.* (2011a), while developing a gel-based RT-PCR serotyping technique, included a few AHSV samples taken from east Africa (Senegal and Kenya) in a phylogenetic analysis. Despite the distance from South Africa, all of the serotypes closely clustered with their South African reference strain counterparts, with their sequences being taken from GenBank. There were, however, some notable differences, seen in the serotype's individual branching patterns. The eastern African isolates were distinctly separated from the South African isolates, although, this distance was negligible compared to the distance to the closest serotype on the tree (Figure 1.21).

Both serotype 2 Senegalese isolates (AHSV-2/SEN2007/02 and AHSV-2/SEN2007/05) showed a 97% identity with the South African serotype 2 strain (AY163332). The serotype 7 Senegalese isolate (AHSV-7/SEN2007/06) showed a 92% identity to the serotype 7 South African strain (AY163330), the serotype 9 Senegalese isolate (AHSV-9/SENyyyy/09) showed a 98.8% identity to the South African serotype 9 isolate (AF043926) and the serotype 4 Kenyan isolate (AHSV-4/KEN2007/01) showed a 96% identity to the South African isolate (M90697).

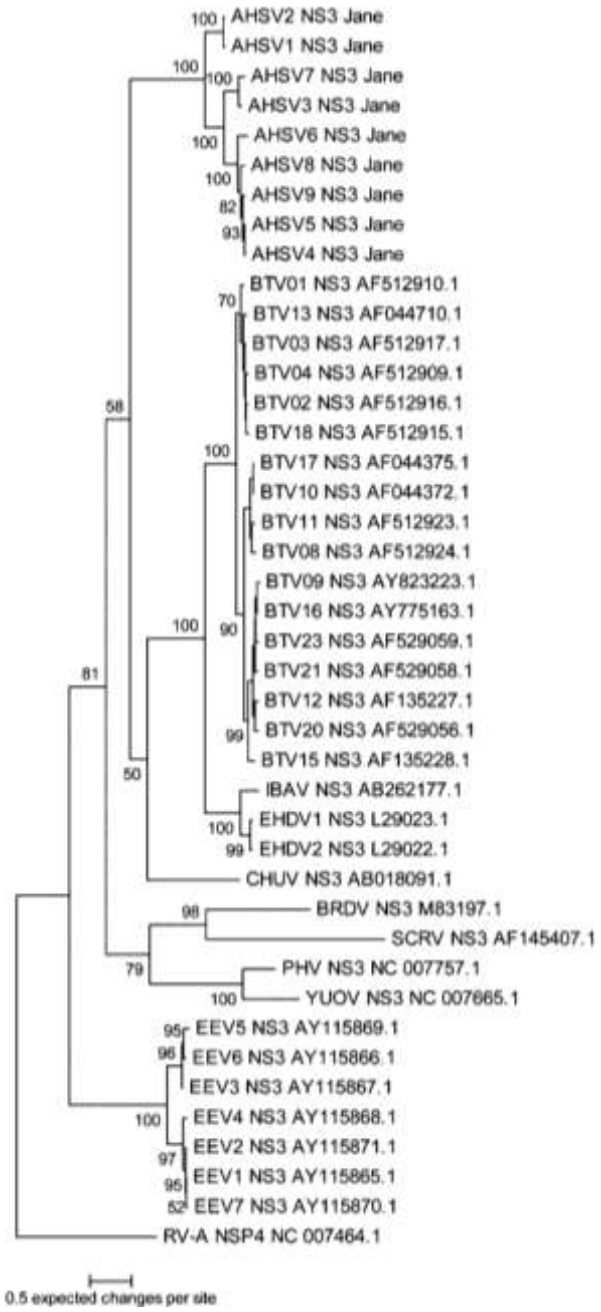

Figure 1.19: Phylogenetic analysis of segment 10 of various orbiviruses. Phylogram calculated by Bayesian inference, GTR+I+Γ substitution model and 5×10^6 iterations. AHSV – African horse sickness virus; BRDV – Broadhaven virus (Great Island virus group); BTV – bluetongue virus; CHUV – Chuzan virus (Palyam virus group); EEV – equine encephalosis virus; EHDV – epizootic haemorrhagic disease virus; IBAV – Ibaraki virus; PHV – Peruvian horse virus; RV-A – rotavirus A; SCRV – St Croix River virus; YUOV – Yunnan orbivirus. Where available, virus acronyms are followed by the serotype, genome segments and accession number. Posterior probabilities are shown on the nodes of the tree. The NSP4 gene of RV-A (family *Reoviridae*) was used as an outgroup (Quan *et al.*, 2008).

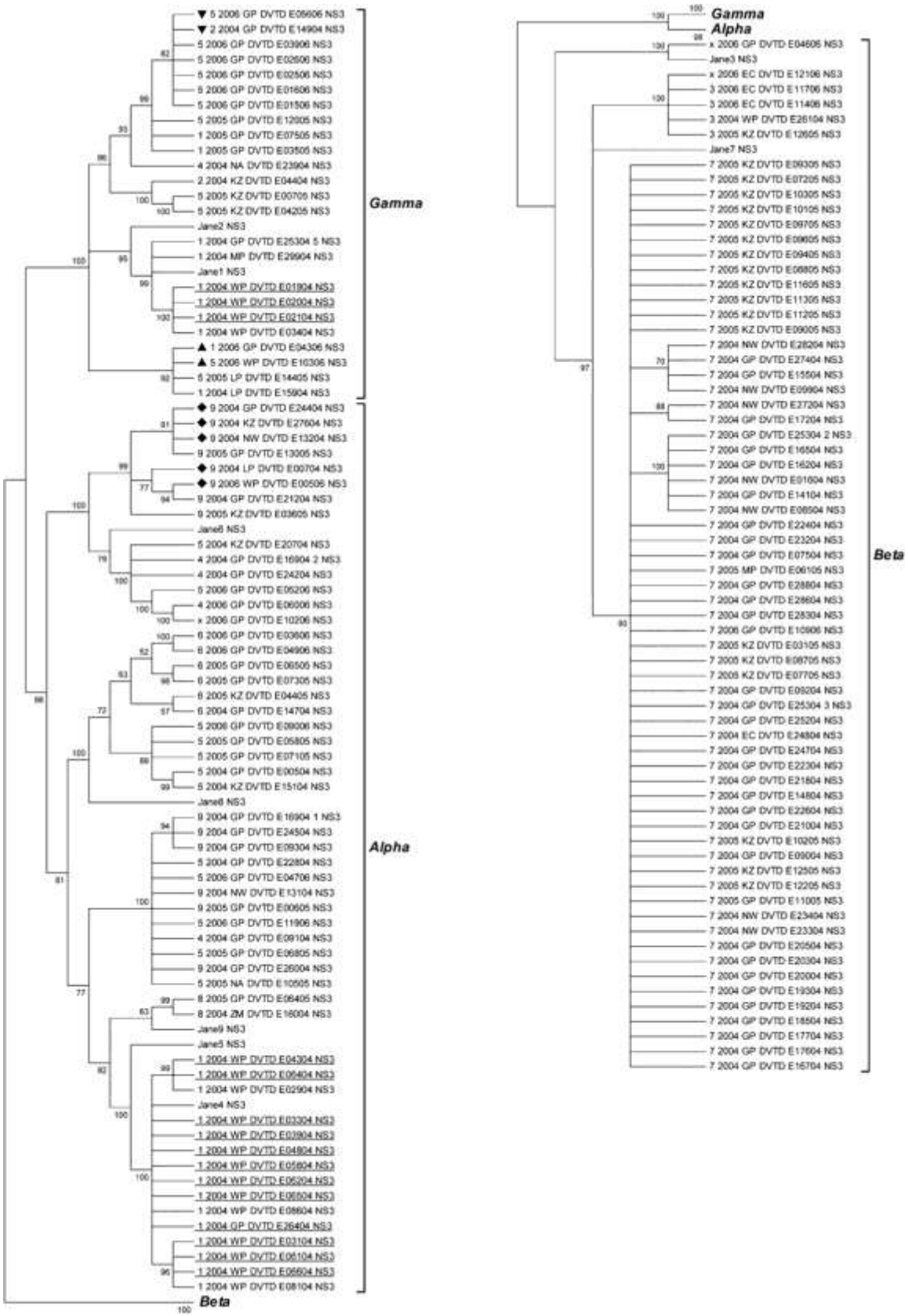

Figure 1.20: Unrooted phylogenetic analysis of AHSV segment 10 sequences isolated from southern African field samples between 2004 and 2006 using Bayesian inference and 1 × 106 iterations. The three distinct clades are indicated by alpha, beta and gamma. OTU labels indicate the serotype, followed by the year of isolation and the province where isolated (EC, Eastern Cape; GP, Gauteng; KZ, KwaZulu-Natal; LP, Limpopo; MP, Mpumalanga; NA, Namibia; NW, North-West; WP, Western Cape; ZM, Zimbabwe) (Quan *et al.*, 2008).

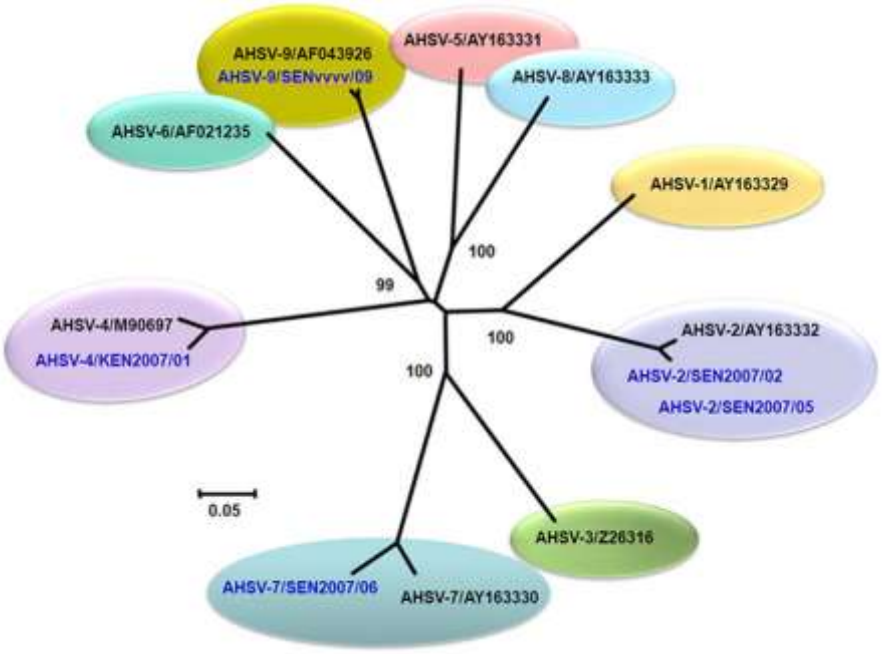

Figure 1.21: Phylogenetic analysis of segment 2 of five East African field strains of AHSV and reference strains from South Africa. The neighbour-joining tree was constructed using distance matrices, generated using the p-distance determination algorithm in MEGA 4.1 (500 bootstrap replicates) (Tamura et al., 2011). Bar represents number of substitutions per site. Values at major branching points represent neighbour-joining bootstraps. SEN – Senegal; KEN – Kenya. (Maan *et al.*, 2011a).

1.15.1.2. Phylogenetic studies of other orbiviruses

Phylogenies can be useful in identifying new strains or serotypes among orbiviruses. After an outbreak of EEV in Israel in 2008-2009, the infecting virus was profiled phylogenetically using segment 10 (NS3) (Aharonson-Raz *et al.*, 2011). The results indicated that a new cluster had emerged that did not cluster with other known isolates (Figure 1.22). Previously, two South African clusters had developed and each corresponded to a different geographic region in South Africa (van Niekerk *et al.*, 2003). Further observations revealed that this represented the two different distributions of the two vectors *C. imicola* and *C. bolitinos*. Although the new cluster of Israeli strains were 92% similar to serotype 3 of the South African isolates, it was suggested that the virus, being isolated from South Africa and resident long enough in Israel, had evolved into a separate cluster.

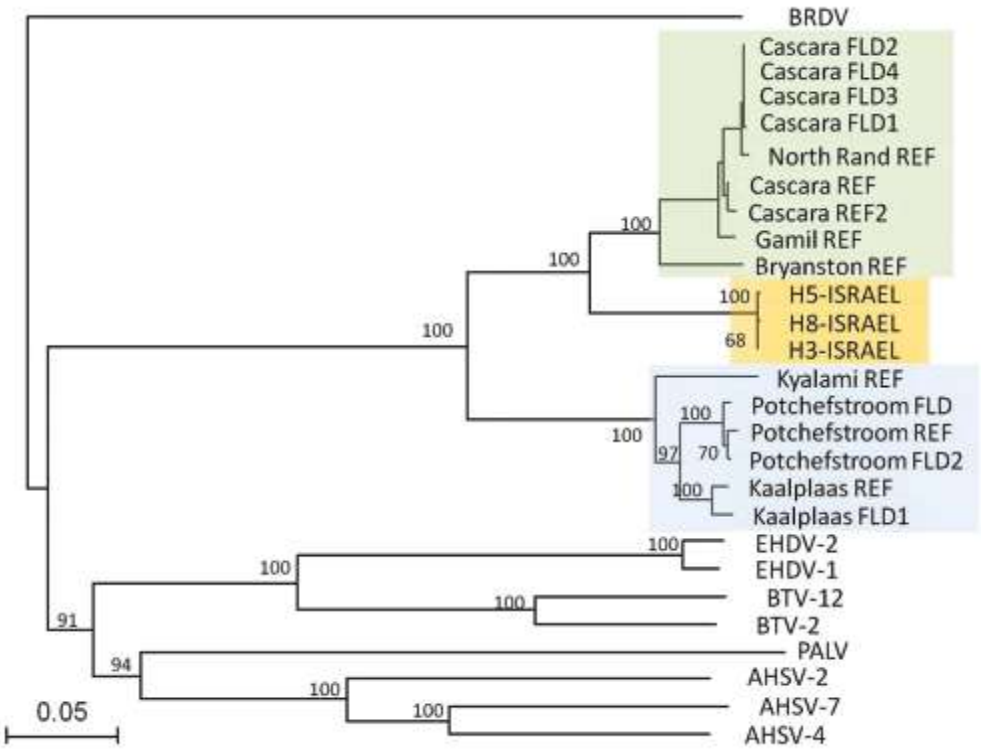

Figure 1.22: Phylogenetic analysis of equine encephalosis virus (EEV) segment 10 (NS3) isolated from horses in Israel in 2009. The phylogenetic tree was constructed by using the neighbour-joining method and bootstrapped with 100 replicates. EHDV – epizootic haemorrhagic disease virus; BTV – bluetongue virus; PALV – Palyam virus; AHSV – African horse sickness virus. Scale bar indicates number of substitutions per site (Aharonson-Raz *et al.*, 2011).

Phylogenetic analysis has also revealed the existence of completely new viruses (Attoui *et al.*, 2001; Attoui *et al.*, 2005). St. Croix River virus (SCRV) and Yunnan orbivirus (YOUV) were both determined to be orbiviruses, but were clearly distinct from all of the other type species (Figure 1.23).

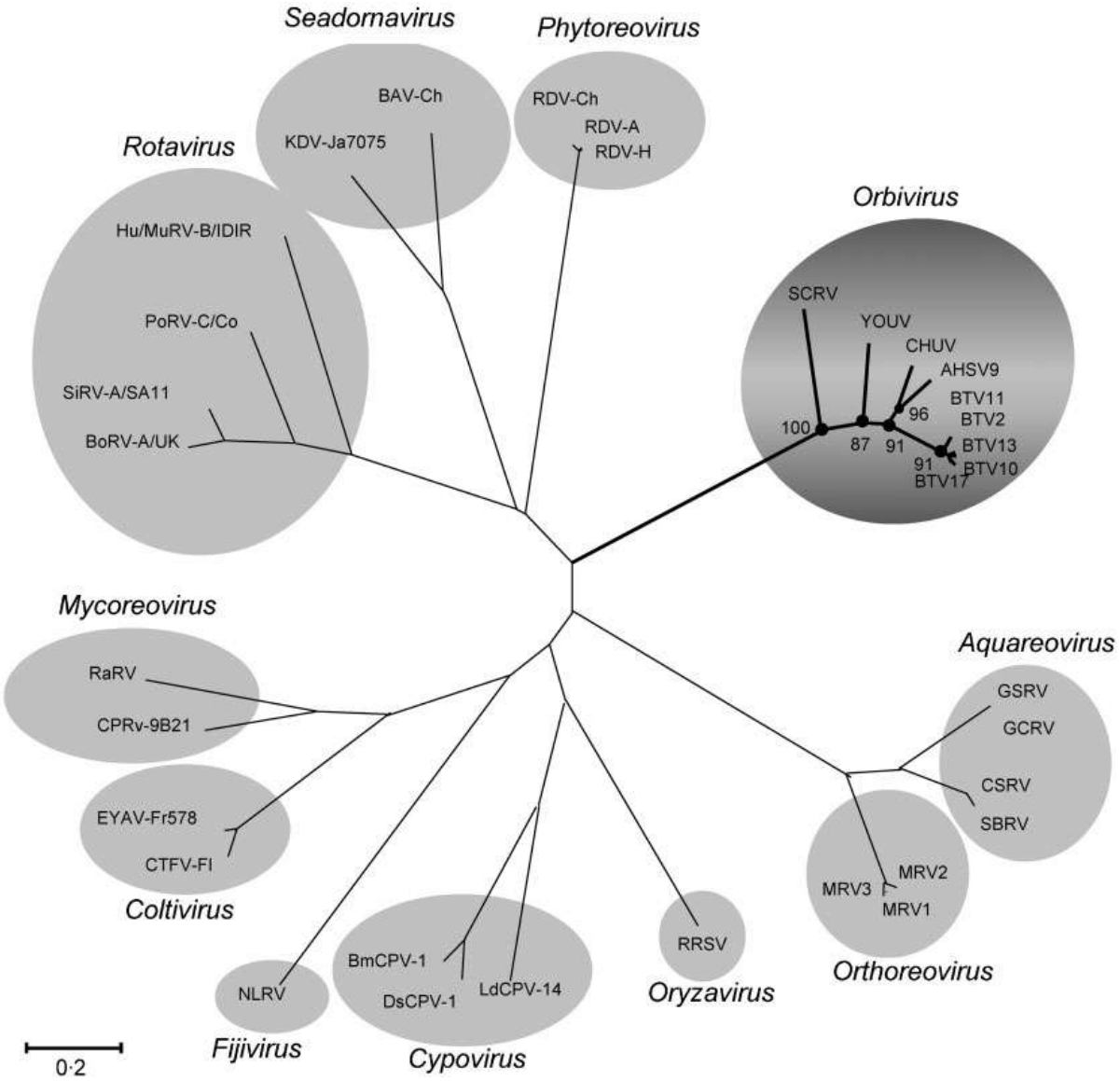

Figure 1.23: Phylogenetic analysis of the genome encoding VP1 sequences from the *Reoviridae* family. The orbivirus group is shown with new species, St. Croix River virus (SCRV) and Yunnan orbivirus (YOUV). This radial tree was constructed using the p-distance method and only branches with a bootstrap value of >85% were retained (Attoui *et al.*, 2005).

In recent years, phylogenetic analysis has been used to establish the presence of new strains, in this case, two new serotypes of BTV (Figure 1.24), serotypes 25 (Toggenburg virus) (Hofmann *et al.*, 2008; Planzer *et al.*, 2011) and 26 (Maan *et al.*, 2011b). Both isolates failed to neutralize any of the existing 24 anti-serotype antibodies in virus neutralisation tests. Using phylogenetic analysis, it became apparent that the novel isolate from Kuwait ('I') is a BTV serotype, but does not cluster with any of the other serotypes, topotypes (distinct geographical strain) or nucleotypes (distinct grouping within a serotype/genome segment) (Maan *et al.*, 2011b).

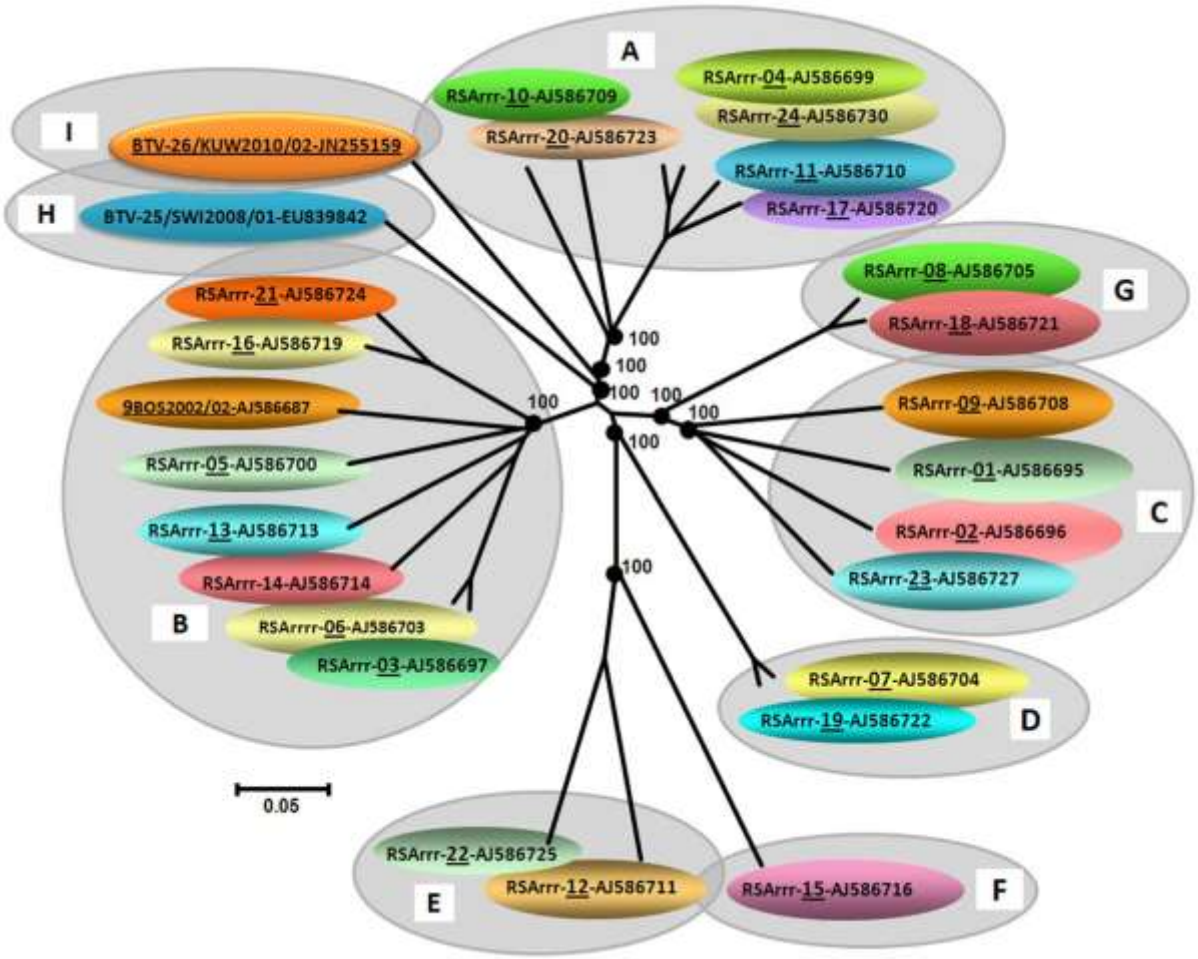

Figure 1.24: Phylogenetic analysis of a novel BTV serotype with the twenty-five reference strains of different BTV serotypes based on segment 6. Neighbour-joining tree constructed using distance matrices, generated using the p-distance determination algorithm in MEGA 5 (500 bootstrap replicates) (Tamura et al., 2011). Bar indicates the number of substitutions per site. Values at the nodes indicate bootstrap confidence. The circles indicate nucleotypes based on segment 6 (A-H). The novel serotype is in nucleotype 'I' (Maan *et al.*, 2011b).

1.16. Research objectives

The present study forms part of an ongoing research program that aims to ultimately develop an assay for the rapid serotyping of the African horse sickness virus using High Resolution Melt (HRM) analysis. A previous study discovered that the separation of AHSV serotypes using HRM analysis was aligned with the separation of the amplicons on a phylogram. This provided proof of concept and a patent was subsequently granted (Groenink 2009; Groenink *et al.*, 2009; Appendix A). The present study set out to develop the proof of concept through designing a set of primers to maximise the assay's efficiency in terms of cost and time and thereby arrive at a potential protocol for the future diagnostic assay. Future studies will involve in-depth sensitivity, specificity and field trials.

The objectives of the present study were:

1. to design a primer set targeting segments 2 and 10 of all nine serotypes of the AHSV genome simultaneously;
2. to propagate reference and recent field-collected AHSV strains and confirm their identification as such;
3. to identify and solve a number of anomalies that arose during the course of the present study involving the serotype of the available AHSV strains;
4. to propose a potential combination of primers and assay conditions for a future rapid serotype assay using HRM analysis;
5. to enhance the proposed assay by increasing the integrity of the results obtained using post-HRM principal component and discriminant analysis; and
6. to conduct a phylogenetic analysis using historical and recent AHSV sequences found in GenBank to establish the likelihood of a new serotype evolving.

The first objective was to design a set of primers to separate all nine AHSV serotypes based on genome segments 2 and 10, the two most serotype-divergent genome segments. After a bioinformatic analysis of the AHSV serotypes, the primers were designed and analysed *in silico* to target different serotype groupings in different primer pair combinations. These ranged from a single primer pair to a combination of primer pairs based on each genome segment to using both genome segments as primer design targets. To this end, a range of bioinformatics software was used as described in Chapter 2:

- The sequence data was collected from GenBank;
- Sequences were aligned using Clustal X2 and phylogenetic trees were produced with MEGA;
- Phylogenetic trees were viewed with TreeView ;

- Primaclade and BLASTn were used to assist in primer design across multiple sequences and to ensure their specificity respectively;
- Manual visual appraisal of the individual alignments was also conducted.

The second objective was to establish stocks of AHSV and confirm the identity of the isolated RNA as belonging to AHSV. A set of reference serotypes from the National Institute of Communicable Disease and two sets of recently collected field isolates from the Onderstepoort Veterinary Institute were obtained and cultured on Vero cell monolayers. Total RNA was subsequently extracted using the widely used guanidinium-thiocyanate-based reagents. The extracted total RNA was verified as AHSV genomic material using OIE approved primers that target genome segment 7. The extracted RNA was subsequently analysed using the primers designed as described in Chapter 2 using standard RT-PCR and RT-PCR coupled with HRM. During the course of this part of the study, various serotype anomalies were identified and necessitated further investigation. This was achieved using both HRM analysis and nucleotide sequencing. As the fourth objective, a potential protocol for a rapid serotyping assay using HRM analysis was proposed. Assay conditions were optimised and analysis conducted using the Corbett Rotor-Gene™ 6000 Series Software. Using the primers designed in this and a previous study, the grouping of the nine serotypes into three clades, followed by attempts to separate them into individual serotypes is described. These results are described Chapter 3.

Due to certain limitations of the standard Rotor-Gene® 6000 Series Software that became apparent, the fifth objective involved testing two additional methods to identify melt profile patterns. These methods involved the use of ScreenClust HRM® Software and GenStat®, where principal component analysis and discriminate analysis were assessed. The results are reported in Chapter 4. .

The final objective was realised by conducting a phylogenetic study using all available sequences for all AHSV genome segments and serotypes to identify the presence or absence of any patterns of genetic drift between sequences isolated in the 1960s and sequences isolated in the 2000s. These results are presented in Chapter 5.

The implications of the present study, in light of previous studies and future objectives, are discussed in Chapter 6.

The patent certificate based on work previous to the present study is located in Appendix A. Sequences used in this study that were downloaded from GenBank are listed in Appendix B as hyperlinks. Relevant alignments of AHSV segments 2 and 10 can be viewed in Appendices C, D and E.

CHAPTER 2: BIOINFORMATIC ANALYSIS OF AFRICAN HORSE VIRUS GENOME SEGMENTS 2 AND 10 FOR THE DESIGN OF PRIMERS TO SEROTYPE THE VIRUS USING HIGH RESOLUTION MELT ANALYSIS

2.1. Introduction

The African horse sickness virus (AHSV) genome is composed of ten double-stranded RNA segments (Grubman & Lewis, 1992). Only nine serotypes have been identified (Howell, 1962), with two of the genome segments displaying considerable genetic diversity amongst the serotypes, namely segment 2 (VP2) and 10 (NS3) (Roy *et al.*, 1994; Venter *et al.*, 2000). VP2 is both serotype-divergent and serotype-specific, while NS3 is serotype-divergent, but not necessarily serotype-specific. Segment 2 is approximately 3205 bp in length, while segment 10 is approximately 756 bp in length (Mertens *et al.*, 2006).

Many PCR assays have been designed for the detection of AHSV since the 1990s (Zientara *et al.*, 1993; Stone-Marschat *et al.*, 1994; Zientara *et al.*, 1994; Zientara *et al.*, 1995a; Zientara *et al.*, 1995b; Zientara *et al.*, 1998a; Rodriguez-Sanchez *et al.*, 2008), but few have used PCR as a potential serotyping assay. None have attempted to use High Resolution Melt (HRM) analysis as a potential serotyping route. The introduction of HRM analysis to post-PCR processing presents different challenges to standard primer design and is especially important in view of the diagnostic aspects this study aims to achieve.

Sailleau *et al.* (2000) described the first use of an RT-PCR technique for serotyping the AHS virus. The basic design was to use three forward primers and nine reverse primers to amplify regions of segment 2. Serotypes 1, 2, 3 and 9 all had unique reverse primers designed around nucleotide position 228, while serotypes 4, 5, 6 and 7 had unique reverse primers designed around nucleotide position 360. Serotype 8 had a primer pair designed to amplify the region of 2100-2882 bp. All of these primers were non-degenerate and were designed based on segment 2 sequences of serotypes 3 and 4 only. All of the RT-PCR results were consistent with virus neutralisation tests and cross-reactivity appeared negligible. There was no multiplexing involved – each set of primers would be run in a separate reaction (i.e. nine reactions to serotype an isolate). In total, the authors used 15 primers in their study. However, the end-point was still agarose gel electrophoresis. Despite the successful PCRs on all nine serotypes with negligible cross-reactions, the lack of degeneracies in the primers could potentially lead to false negatives due to the primer regions found in field strains not being identical.

Another method developed in South Africa initially used 16 primers to amplify a 520 bp region of segment 2 of all nine serotypes of AHSV (Koekemoer & van Dijk, 2004). Subsequently, the protocol was amended to include hybridisation probes (Koekemoer, 2008). Invariably, the addition of probes will significantly increase the final cost of the assay. The authors concluded that due to various genetic variations, the probe-based melting analysis could not be used to serotype AHSV. However, the advantage of HRM analysis, without probes, is that an entire amplicon contributes to the melt profile, not just a short sequence of approximately 40 bp, as the case would be with a probe. Variations in a short sequence will significantly affect the melt profile, whereas variations over a 200-300 bp amplicon will have less of an effect on the final melt profile and allow, to a degree, a broader confidence interval for the features of the melt profile that would come under consideration. In addition, since the melt results were obtained using primers previously designed for terminal reverse line blot hybridisation, the AHSV genome is unlikely to have been effectively searched for alternate regions offering a better region for melt analysis.

In the present study, the design of primers needed to achieve multiple purposes: the primer pair must amplify more than just a single sequence and the resulting amplicons should be divergent enough to distinguish them from each other in downstream HRM analysis. Figure 2.1 represents an over-simplistic graphical illustration of the approach that was taken in this study to primer design such that a single primer pair may result in amplification products with all nine serotypes yet each amplicon would be divergent and unique. This does present certain complications that need to be considered. The length of the final primer would be dependent on the length that all sequences under consideration were identical over in a particular region. However, this would seldom be a perfect alignment and would necessitate the introduction of degenerate bases into the final primer sequence that could have the effect of lowering the annealing temperature and a resulting loss in specificity. In Figure 2.1, the identical regions on the left and right represent the potential primer regions. In this ideal situation, the primer pairs could be used to amplify all nine ‘sequences’. On the other hand, the sequences of the amplicon region would be different for each sequence. This would ultimately result in nine different melt profiles in the downstream and terminal HRM analysis, providing the means by which each ‘sequence’ is to be ‘typed’.

In addition to the constraints of primer design for a multiple sequence alignment, the final end-point of the PCR to be developed here was an HRM analysis. Amplicons to be used for HRM analysis were aimed to be only a few hundred base pairs long, although, due to the nature of the DNA intercalating dye-release process, the smaller the amplicon, the more sensitive the HRM analysis would become (Vossen *et al.*, 2009; Stanzer *et al.*, 2010).

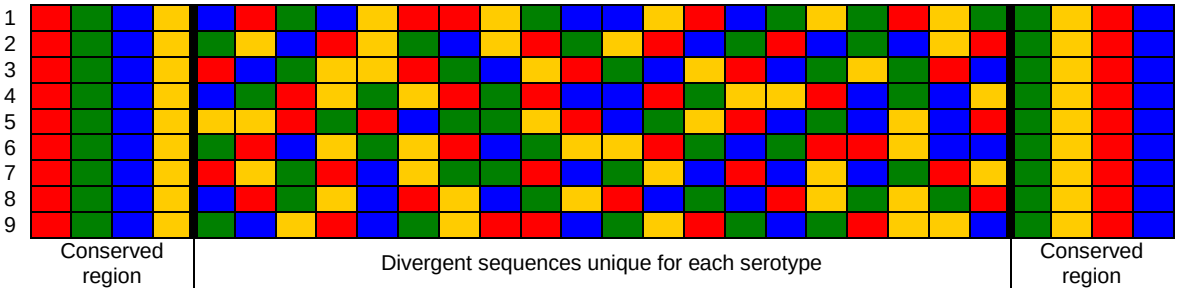

Figure 2.1: Schematic representation showing the ideal primer design across multiple sequences, such as that sought for all of the nine African horse sickness virus serotypes to develop a serotyping assay.

Between 2008 and 2009, a preliminary study into the feasibility of an assay to serotype AHSV based on HRM analysis was undertaken. Using the principles outlined above, a primer pair was designed that would amplify an amplicon from nucleotides 10-190 of segment 10 of the AHSV genome (hereafter referred to as the 10-190 bp region). Using the available AHSV segment 10 sequences in GenBank[1], a phylogeny was drawn (Figure 2.2), which formed three distinct clades. Using a set of purported AHSV reference strains, three distinct melt profiles resulted after HRM analysis (Figure 2.3), which coincided with the three clades in the phylogeny (Figure 2.2) (Groenink, 2009; Groenink *et al.*, 2010).

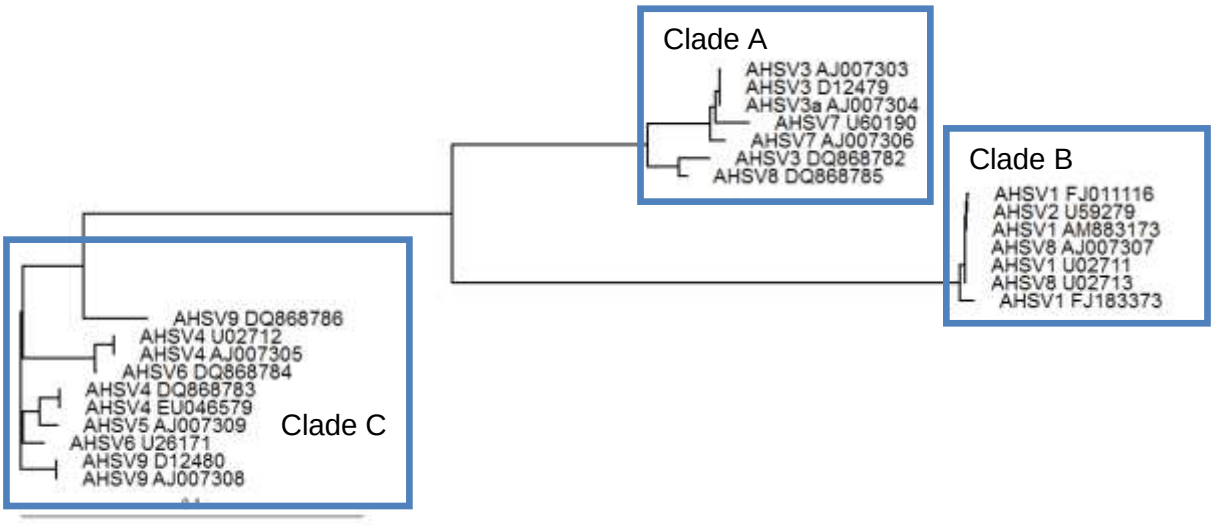

Figure 2.2: The phylogeny produced from the ClustalX2 alignment of the 10-190 bp region of segment 10 of the African horse sickness virus genome and viewed using TreeView. Clade A consists of serotypes 3 and 7, Clade B contains serotypes 1, 2 and 8 and Clade C contains serotypes 4, 5, 6 and 9. 'AHSV8 DQ868785' has been incorrectly annotated and is a serotype 3 isolate. The bar represents 0.1 substitutions per site (Groenink, 2009).

[1] http://www.ncbi.nlm.nih.gov/genbank/

This provided proof of concept such that a phylogeny of the sequences of the isolates used could translate into the melt profiles seen in Figure 2.3 (Groenink, 2009). However, the primer design and melt profiles were not ideal as a serotyping assay as they were only able to 'type' the AHSV serotypes into three clades, not all nine serotypes. As a result, a more intensive, integral primer design strategy needed to be defined. The protocol needed to be developed from one primer pair resulting in three clades and melt profiles to a protocol that would result in nine clades and/or nine melt profiles.

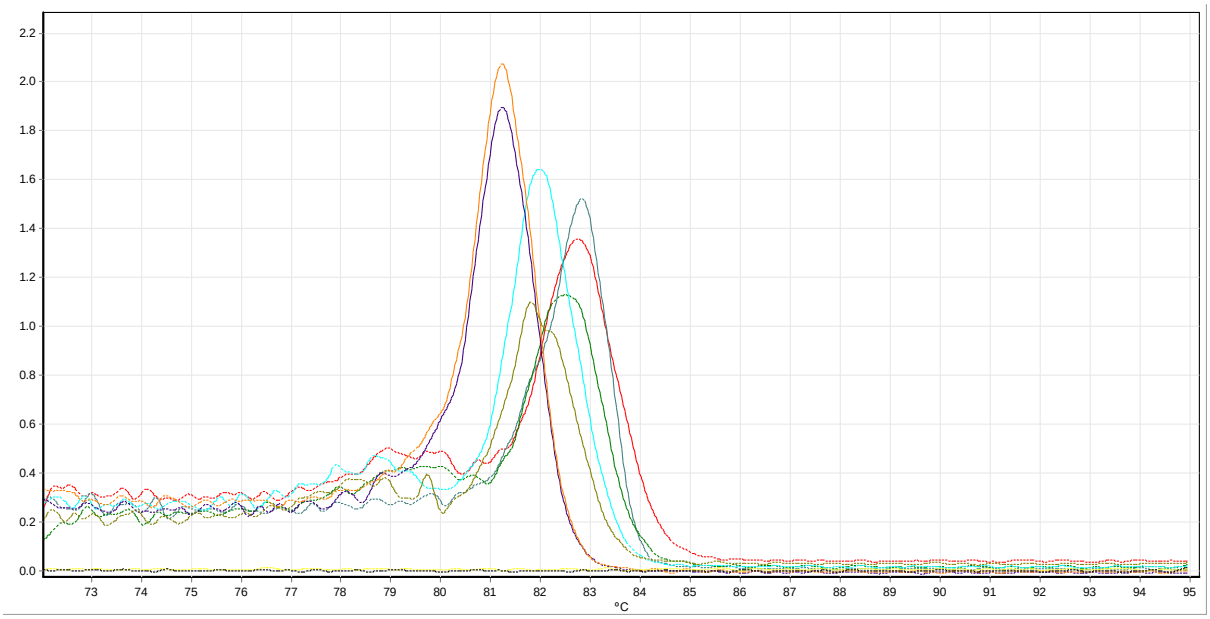

Figure 2.3: HRM profiles of the product of the 10-190 bp region of AHSV segment 10 using the Corbett Rotor-Gene™ 6000 Series Software (Groenink, 2009).

A large variety of programmes are available for designing primers. One of the simplest and most widely used freeware programmes is Primer3[2] (Rozen & Skaletsky, 2000). Primer3 is designed to pick a single primer pair for one sequence at a time. As mentioned previously, the assay depends on the ability to find primers that are common to all nine serotypes. Recognising this inadequacy of Primer3, Gadberry et al. (2005) designed a web-based application 'to find conserved PCR primers across multiple species'. In essence, the

[2] http://frodo.wi.mit.edu/

programme, called Primaclade[3] runs a Primer3 analysis on each sequence entered and then merges the results.

The success of the proposed assay is entirely dependent on the design of a primer pair and the characteristics of the amplicon. The approach in this study was to build on the work done previously, where the nine serotypes were 'typed' into three clades using segment 10 (Groenink *et al.*, 2009). Segment 2 was explored exhaustively for suitability (as in Figure 2.1), as was a combination of both segments 10 and 2.

The analysis of segments 2 and 10 of the AHSV genome was begun with the collection and collation of all available sequences in GenBank (Burks *et al.*, 1985; Benson *et al.*, 2009). A variety of selected sequences were then aligned using the Clustal programme (Chenna *et al.*, 2003; Larkin *et al.*, 2007) and a phylogeny drawn using TreeView (Page, 1996) to reveal the extent of sequence divergence. Using a variety of bioinformatics software programmes and visual inspection, primer regions were explored and the amplicons tested *in silico* to determine their suitability for serotyping via HRM analysis.

2.2. Materials and methods

2.2.1. Sequence retrieval

All sequences of AHSV segment 2 and 10 used in the design of primers were obtained from the GenBank database of the National Centre for Biotechnology Information (NCBI) (Benson *et al.*, 2012); only full-length sequences were considered. The accession numbers of the sequences used are contained in Appendix B. The applicable sequences were downloaded in FASTA format and saved as a text file. Unique identifiers were added into the header to assist with identification in downstream analysis in the following format: `AHSV`(serotype)`_`(accession number) (e.g. `AHSV6_U26171`).

2.2.2. Multiple sequence alignment

Multiple alignments were performed using ClustalX2 (Larkin *et al.*, 2007), using the following standard, software-derived parameters: Gap opening penalty = 15. Gap extension = 6.66. Delay divergent sequences = 30. DNA Transition = 0.5. The DNA weight matrix used was IUB.

[3] http://www.umsl.edu/~biology/Kellogg/Primaclade.html

2.2.3. Phylogenetic analysis and phylogeny visualisation

A phylogeny was drawn by bootstrapping a neighbour-joining tree with 1000 trials and a random number seed generator of 111. TreeView (Page, 1996) was used to visualise the resulting phylogeny and infer any sequence similarity.

2.2.4. Primer design strategies

2.2.4.1. Segment 10

Segment 10 encodes NS3, which is serotype-divergent, but not serotype specific. It was unlikely that alternate primers would be found which would result in nine clades/melt profiles as this was exhausted previously (Groenink, 2009). However, additional primers based on each clade (i.e. three primer pairs) were considered. Probe methodologies were also explored where short regions of the amplicon were explored such that a degenerate probe could be designed to reveal SNPs that could define the serotype.

2.2.4.2. Segment 2

Segment 2 encodes for the viral protein 2 (VP2), which is serotype-divergent and serotype-specific (Bremer *et al.*, 1990) and does naturally present the best possibilities in terms of the aims of the original assay to design a PCR/HRM serotyping assay. However, the sequences were considerably more divergent than those of segment 10 were. This prevented a single primer pair from being designed across all nine serotypes. Various strategies were investigated in which the VP2 sequences were split into one or more clades (without primers) and primers were designed based on the newly discovered clades.

2.2.4.3. Combination of segment 10 and segment 2

An additional primer design strategy was also possible that made use of the relative sequence depth, albeit limited serotype-divergence, of segment 10 combined with the vast sequence divergence, but limited sequence depth, of segment 2.

The greatest resolution to be achieved from segment 10 was amplifying the 10-190 bp region that resulted in three clades (Figure 2.2) and three melt profiles (Figure 2.3). It was envisaged that when each segment 10 clade (Clade A, B and C) was considered in the context of segment 2, with its greater degree of serotype divergence, suitable primers could be found that would separate out each clade into its individual serotypes (Figure 2.4).

The full-length segment 2 sequences of the serotypes of each of the clades resolved using segment 10 were downloaded from GenBank and aligned using Clustal X2. The resulting alignment files were visually inspected and run through Primaclade to identify possible primer regions.

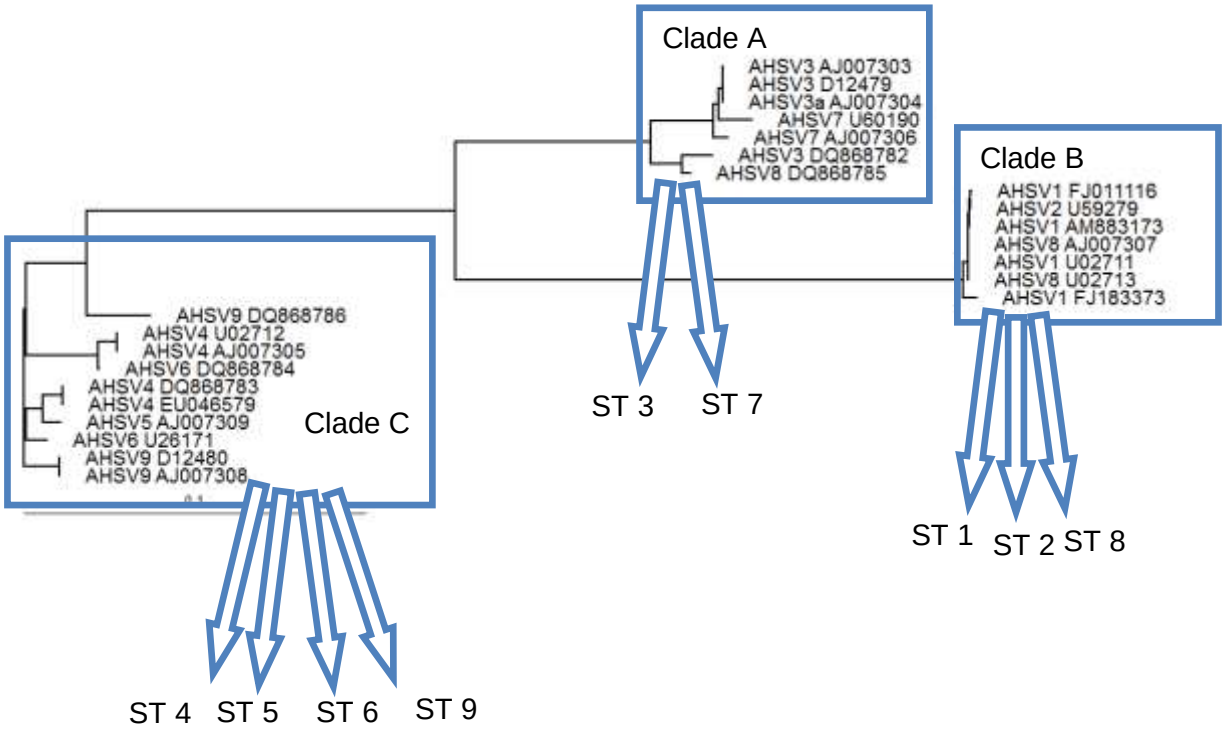

Figure 2.4: The phylogeny produced from the ClustalX2 alignment of the 10-190 bp region of segment 10 of the African horse sickness virus genome and viewed using TreeView. The blue boxes represent the three resulting clades (and subsequent HRM melt profiles). The arrows represent the proposed separation of the serotypes (ST) based on segment 2. 'AHSV8 DQ868785' has been incorrectly annotated and is a serotype 3 isolate. The bar represents 0.1 substitutions per site.

2.2.5. Primaclade

Primaclade (Gadberry *et al.*, 2005) is a web-based programme hosted by the Kellogg Laboratory[4] and the Santos Laboratory[5]. The input file is a recognised multiple sequence alignment file. The programme creates a consensus sequence and indicates possible primer sites of varying degeneracies based on previously adjusted settings. These settings include number of degeneracies, number of gaps and the minimum, maximum and optimum primer annealing temperature and GC content. In most circumstances, the settings were left as standard. However, when few or no primers were found, the conditions were relaxed to include five degeneracies and the minimum annealing temperature was adjusted to 50°C.

2.2.6. BLAST analysis

Each of the proposed primers were tested for their specificity by subjecting them to a BLAST analysis (BLASTn; word size = 7; match/mismatch scores = 1, -3, gap costs = 5.2) (Altschul *et al.*, 1997; Johnson *et al.*, 2008; Benson *et al.*, 2012). This served to highlight and confirm which regions of the genome segment the primer would most likely bind to and confirm that

[4] http://www.umsl.edu/services/kellogg/primaclade.html

[5] http://www.auburn.edu/~santosr/primaclade.htm

the primer would only target the intended serotype. It was also important to ascertain whether the primers would be inclined to amplify any Vero cell sequences as they are to be used as the host cell for the propagation of the virus.

2.3. Results

2.3.1. Sequence retrieval

At the time of the initial search of the nucleotide database of GenBank (NCBI) on 20 May 2010, “African horse sickness NS3” retrieved 201 sequences. Twenty-six were full-length sequences and 175 were coding sequences. Correspondingly, a search of the GenBank database on 30 June 2010 for “African horse sickness VP2” retrieved 65 sequences, 20 of which were full-length sequences. However, it must be noted that there were misnomers in the database. The sequence with accession number DQ868785 is described as serotype 8. However, it can be seen in Figure 2.5 and the BLASTn analysis of the sequence that it has been incorrectly annotated and should be described as serotype 3. In addition, the segment 2 sequence with accession number Z26316, described as serotype 1, should be annotated as serotype 3 (Figure 2.12). Accession numbers of the segment 10 and segment 2 sequences used are presented in Appendix B.

2.3.2. Bioinformatic analysis of segment 10 (NS3)

Only full-length sequences were included in the multiple alignment and downstream analysis. The full-length sequences were aligned using Clustal X2 and phylogenies viewed using TreeView.

Initially, segment 10 was considered further to the work of Groenink (2009). An alignment of the full-length sequences available was performed. The clades seen in Figure 2.5 were identical to the three clades formed using the 10-190 bp region of segment 10 (Figure 2.2). However, two clades can also be defined: one clade would consist of Clade A and B (Clade AB), whilst the second clade would consist of Clade C (Clade C). Should Clade AB and Clade C contain regions suitable for primer design, the protocol may be extended by using two primer pairs in an attempt to produce nine unique melt profiles.

2.3.2.1. Approach A – The use of two primer pairs for two clades of segment 10

Combining Clades A and B into Clade AB (Serotypes 1, 2, 3, 7 and 8), shown in Figure 2.5, sequences were realigned and the alignment examined manually with Primaclade for possible primer sites. Two suitable regions were located from nucleotides 153-174 and nucleotides 742-761 due to their extended conservation across all of the sequences under

consideration – these regions are shown in Appendix C1 in red font. The phylogeny of the theoretical amplicon is shown in Figure 2.6.

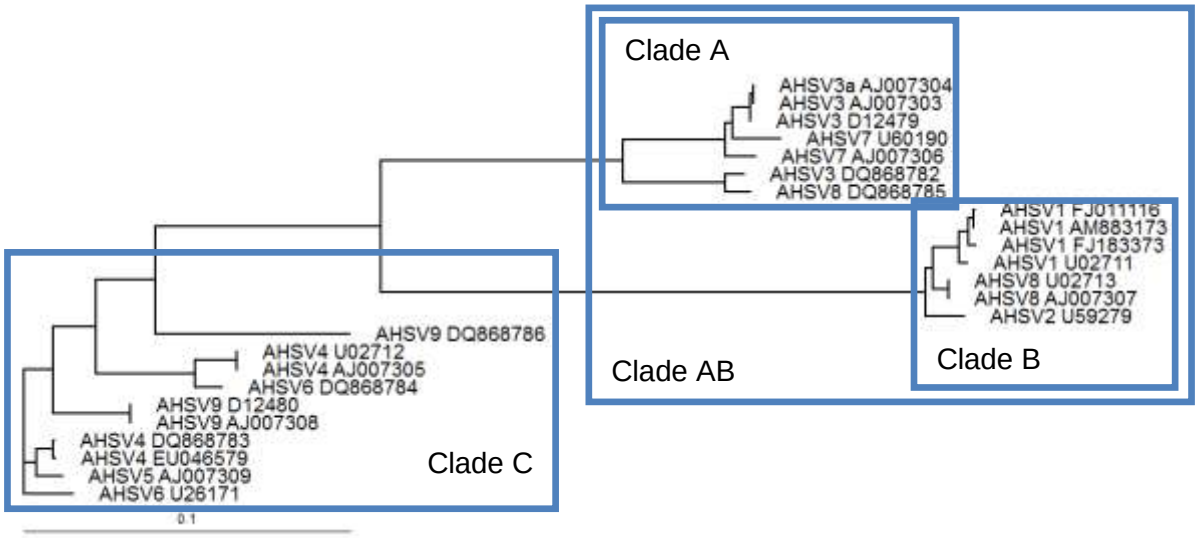

Figure 2.5: The phylogeny produced from the ClustalX2 alignment of the 10-190 bp region of segment 10 of the African horse sickness virus genome and viewed using TreeView showing the identification of ether two or three clades. 'AHSV8 DQ868785' has been incorrectly annotated and is a serotype 3 isolate. The bar represents 0.1 substitutions per site.

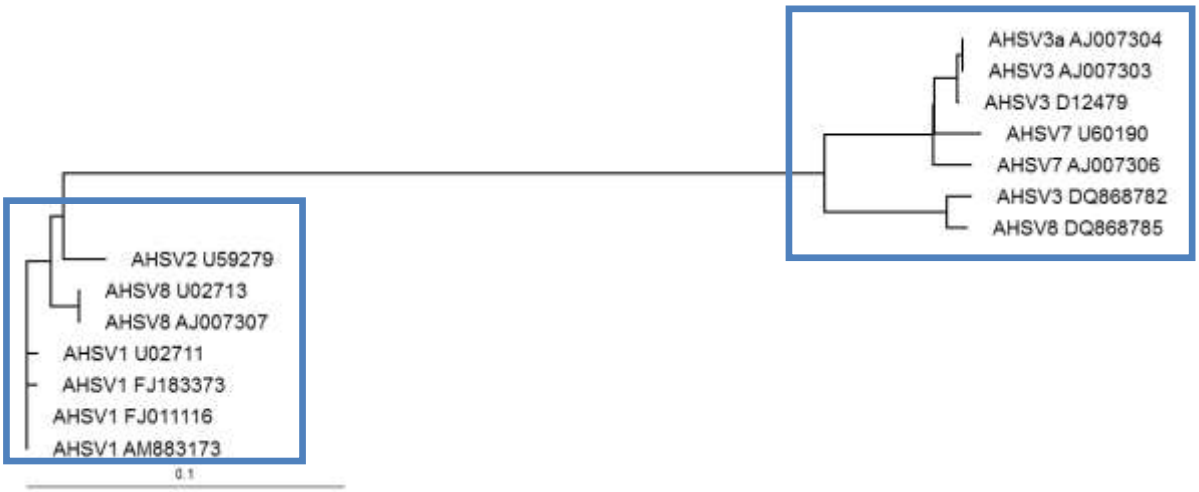

Figure 2.6: The phylogeny produced from the ClustalX2 alignment of nucleotides 153-761 of AHSV segment 10 serotypes 1, 2, 3, 7 and 8 (Clade AB) and viewed using TreeView showing the separation of the region into two clades. 'AHSV8 DQ868785' has been incorrectly annotated and is a serotype 3 isolate. The bar represents 0.1 substitutions per site.

In the same manner, Clade C was examined for possible primer sites. Potential sites were located at positions 153-174 bp and 689-712 bp. These are shown in Appendix C2 in red font. In Figure 2.7, the resulting theoretical amplicon has been aligned and viewed as a phylogeny.

An assessment of Clade C (Figure 2.7) reveals better separation of the sequences, although the serotypes themselves do not cluster together. In addition, the substitution bar is considerably longer than in Figure 2.6, indicating a higher degree of conservation and there are no distinct clades for any of the serotypes.

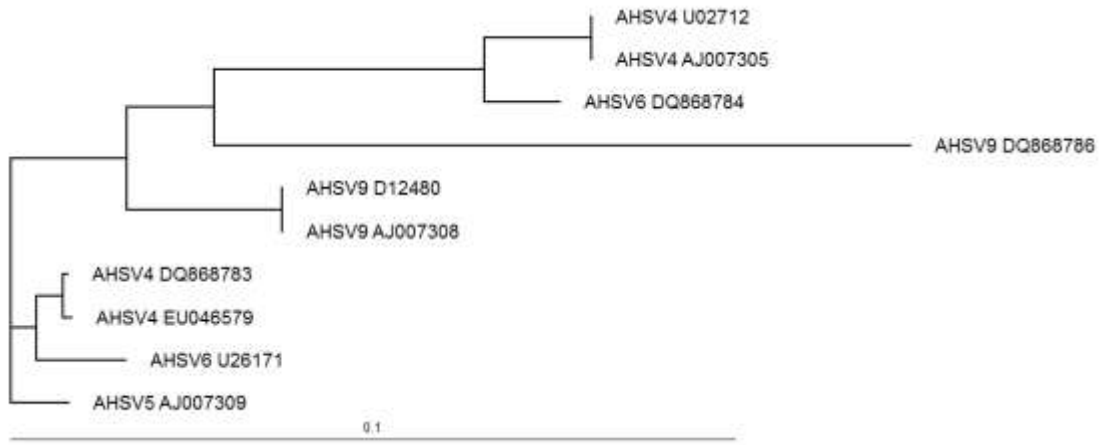

Figure 2.7: The phylogeny produced from the ClustalX2 alignment of nucleotides 153-712 of AHSV segment 10 serotypes 4, 5, 6 and 9 and viewed using TreeView showing the lack of clear clades for Clade C. The bar represents 0.1 substitutions per site.

2.3.2.2. Approach B – Using three primer pairs for three clades of segment 10

The full-length sequences of Clades A, B and C were aligned separately and assessed for regions of possible primer design after identifying unique positions that might aid in the identification of serotypes. Clade C's assessment would be identical to Approach A (Section 2.3.2.1, Figure 2.7) and so only Clades A and B were assessed here. Possible primers for Clade A were found at nucleotide positions 153-174 and 338-358 (Appendix D1) and for Clade B at nucleotide positions 153-174 and 261-284 (Appendix D2). The alignment files were subsequently edited to assess only these regions and phylogenies drawn for Clade A (Figure 2.8) and Clade B (Figure 2.9).

Using the approach of a primer pair per clade, Clade A appears to be well separated (Figure 2.8) and clustered to produce unique melt profiles. However, on closer inspection, serotype 3 is located within two clades. Clade B is also well-separated (Figure 2.9) and each serotype has clustered well. However, the difference apparent in the serotype 1 sequences is concerning given the scale of the phylogeny. It is therefore considered doubtful that this approach would lead to a unique and clear melt profile for each serotype.

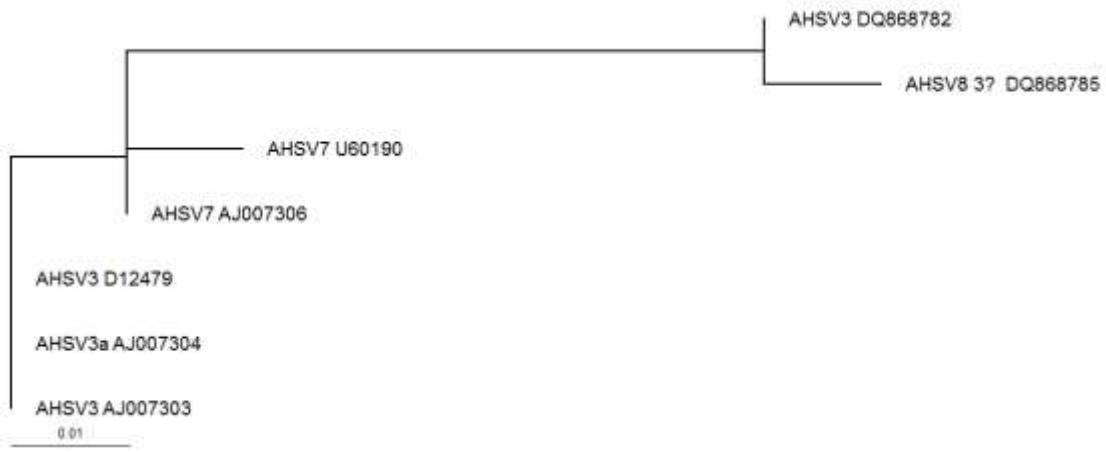

Figure 2.8: The phylogeny produced from the ClustalX2 alignment of nucleotides 153-358 of AHSV segment 10 serotypes 3 and 7 (Clade A) and viewed using TreeView to show the potential extent of the separation of the individual serotypes. 'AHSV8 3? DQ868785' has been incorrectly annotated and is a serotype 3 isolate. The bar represents 0.01 substitutions per site.

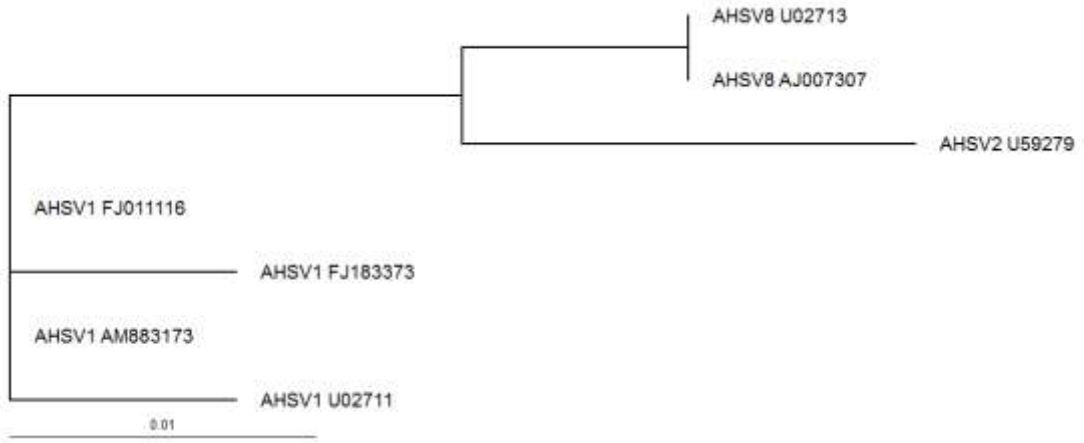

Figure 2.9: The phylogeny produced from the ClustalX2 alignment of nucleotides 153-284 of AHSV segment 10 serotypes 1, 2 and 8 (Clade B) and viewed using TreeView to show the potential extent of the separation of the individual serotypes. The bar represents 0.01 substitutions per site.

2.3.2.3. Approach C – The use of a probe within the 10-190 bp region of segment 10

As a starting point for exploring possible probe options, the original amplicon from Groenink (2009) was considered. This amplicon was located between nucleotides 10-190 of segment 10. The alignment file of the amplicon was therefore reviewed for possible probe locations containing unique positions that might aid in the identification of serotypes. The most suitable region would have been located from 33-62 bp of the amplicon. The alignment file of positions 10-69 bp of segment 10 is represented in Figure 2.10. The Boxshade version (Figure 2.11) is an alternative method to represent an alignment when short, semi-conserved regions are being considered. An inspection of the alignment files of the 10-190 bp region of

segment 10 revealed a potential region from 33-62 bp. Although it appears that there is greater differentiation (Figure 2.10), represented as a Boxshade file (Figure 2.11), the region becomes easier to analyse. Lines have been placed where there is a separation of unique sequences. However, these lines do not separate the serotypes, either individually or in alternate clades. Serotypes 3 and 7 (Clade A) are indistinguishable, as are serotypes 1, 2 and 8 (Clade B). Based on the GenBank sequences available, it would appear that serotypes 4, 5, 6 and 9 would not be able to anneal to a serotype-unique probe sequence.

```
                    10                  33                              62      69
AHSV3_D12479        ATCCCTTGTCATGAGTCTAGCTACGATCGCCGAAAATTATATGATGCATAATGGAAATCA
AHSV3_AJ007303      ATCCCTTGTCATGAGTCTAGCTACGATCGCCGAAAATTATATGATGCATAATGGAAATCA
AHSV3_AJ007304      ATCCCTTGTCATGAGTCTAGCTACGATCGCCGAAAATTATATGATGCATAATGGAAATCA
AHSV7_U60190        ATCCCTTGTCATGAGTCTAGCTACGATCGCCGAAAATTATATGATGCATAATGAAACTCA
AHSV7_AJ007306      ATCCCTTGTCATGAGTCTAGCTACGATCGCCGAAAATTATATGATGCATAATGGAAATCA
AHSV4_Z48735        -ATCCTTGTCATGAATCTAGCTACAATCGCCAAGAATTATAGCATGCATAATGGAGAGTC
AHSV5_AJ007309      ATCCCTTGTCATGAATCTAGCTGCAATCGCCAAGAATTATAGCATGCATAATGGAGAGTC
AHSV9_D12480        ATCCCTTGTCATGAATCTAGCTGCAATCGCCGAAAATTATAGTATGCATAATGGAGAGTC
AHSV9_AJ007308      ATCCCTTGTCATGAATCTAGCTGCAATCGCCGAAAATTATAGTATGCATAATGGAGAGTC
AHSV4_U02712        ATCCCTTGTCATGAATCTAGCTGCAATCGCCAAGAATTATAGTATGCATAATGGAGAGTC
AHSV4_AJ007305      ATCCCTTGTCATGAATCTAGCTGCAATCGCCAAGAATTATAGTATGCATAATGGAGAGTC
AHSV4_Z48734        ATCCCTTGTCATGAATCTAGCTGCAATCGCCAAGAATTATAGTATGCATAATGGAGAGTC
AHSV6_U26171        ATCCCTTGTCATGAATCTAGCTGCAATCGCCAAGAATTATAGTATGCATAATGGAGAGTC
AHSV6_U60189        ATCCCTTGTCATGAATCTAGCTGCAATCGCCAAGAACTACAGTATGCATAATGGAGAGCA
AHSVref_AM883173    ATCCCTTGTCATGAATCTTGCTAGCATCTCCCAAAGCTATATGTCACATAATGAGAATGA
AHSV1_U02711        ATCCCTTGTCATGAATCTTGCTAGCATCTCCCAAAGCTATATGTCACATAATGAGAATGA
AHSV8_AJ007307      ATCCCTTGTCATGAATCTTGCTAGCATCTCCCAAAGCTATATGTCACATAATGAGAATGA
AHSV2_AFU59279      ATCCCTTGTCATGAATCTTGCTAGCATCTCCCAAAGCTATATGTCACATAATGAGAATGA
AHSV8_U02713        ATCCCTTGTCATGAATCTTGCTAGCATCTCCCAAAGCTATATGTCACATAATGAGAATGA
                       *********** *** ***   *** ** * *  ** *     *******
```

Figure 2.10: Alignment of nucleotides 10-69 of segment 10 for full-length AHSV sequences using ClustalX2 to show the extent of the conservation over the potential probe region. The potential probe region (33-62 bp) is shown in red.

```
AHSV3_DQ868782      CGATCGCCGAAAATTATATGATGCATAATG
AHSV8_DQ868785      ............................
AHSV3_AJ007303      ............................
AHSV3_D12479        ............................
AHSV3a_AJ007304     ............................
AHSV7_U60190        ............................
AHSV7_AJ007306      ............................
AHSV9_D12480        .A..............GT..........
AHSV9_AJ007308      .A..............GT..........
AHSV4_DQ868783      .A......A.G.......GC........
AHSV4_EU046579      .A......A.G.......GC........
AHSV5_AJ007309      .A......A.G.......GC........
AHSV6_U26171        .A......A.G.......GT........
AHSV4_U02712        .A......A.G.......GT........
AHSV4_AJ007305      .A......A.G.......GT........
AHSV6_DQ868784      .A......A.G.......GT........
AHSV9_DQ868786      .A......A.........GC........
AHSV1_FJ011116      GC...T..C...GC......TCA.....
AHSV2_U59279        GC...T..C...GC......TCA.....
AHSV1_AM883173      GC...T..C...GC......TCA.....
AHSV8_AJ007307      GC...T..C...GC......TCA.....
AHSV1_U02711        GC...T..C...GC......TCA.....
AHSV8_U02713        GC...T..C...GC......TCA.....
AHSV1_FJ183373      GC...T..C...GC......TCA.....
```

Figure 2.11: Boxshade version of the 33-62 bp position region of segment 10 for all nine available full-length AHSV sequences to investigate the separation of the serotypes into 'unique' probe sequence groups.

2.3.3. Bioinformatic analysis of segment 2 (VP2)

2.3.3.1. Approach A – clade-specific primers for segment 2 clades

In a similar fashion to approaches A and B for the analysis of segment 10 (Sections 2.3.2.1 and 2.3.2.2), the available full-length sequences of segment 2 were aligned and the resulting phylogeny (Figure 2.12) analysed for potential clades. Beginning with a potential 'two primer pair' approach, two clades can be distinguished in Figure 2.12, shown by the blue line. Serotypes 1, 2, 3, 4 and 7 and serotypes 6, 8 and 9 cluster together. These two clades' respective alignment files were analysed manually and with Primaclade, but no uniform regions suitable for primer design were found.

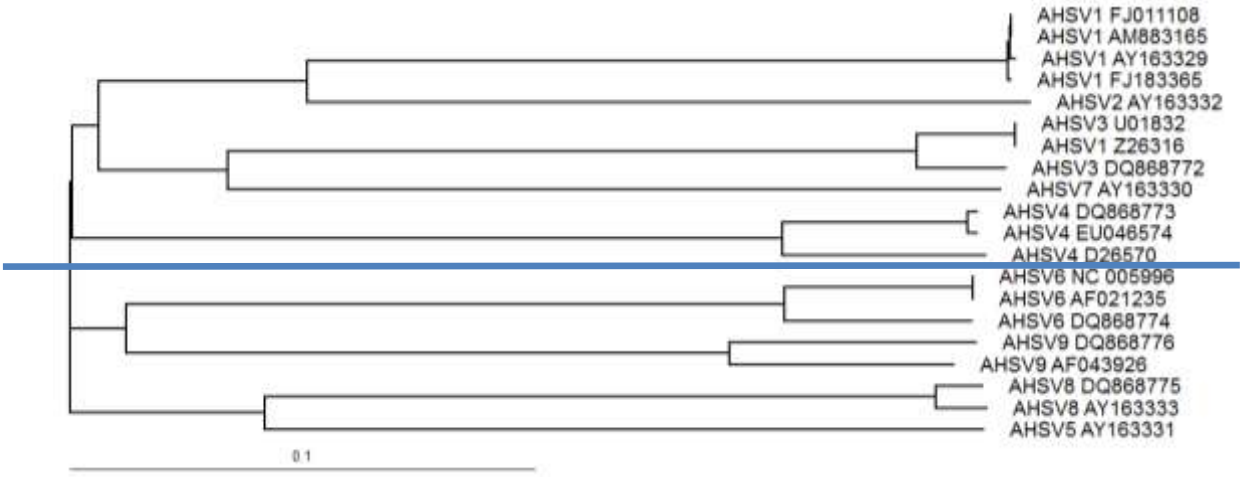

Figure 2.12: The phylogeny produced from the ClustalX2 alignment of the full-length sequences of AHSV segment 2 and viewed using TreeView to investigate potential clades for focused primer design. The blue line represents the separation of the phylogeny into two principle clades. 'AHSV1 Z26316' has been incorrectly annotated and is a serotype 3 isolate. The bar represents 0.1 substitutions per site.

2.3.3.2. Approach B – Primers based on the work of Sailleau et al. *(2000)*

Sailleau *et al.* (2000) investigated a number of regions for an AHSV serotyping RT-PCR. In particular, a number of primers were designed to bind to the regions spanning the approximate nucleotide positions of 209-228 and 339-360. For this study, both the 1-228 bp and the 1-360 bp regions were examined across all nine serotypes for primer design. Although a potential forward primer existed in the 1-17 bp region (Figure 2.13), no one suitable reverse primer could be found (Figure 2.14; Figure 2.15) as there was not enough conservation over the range of serotypes included. In Figure 2.13, these regions of all nine serotypes were aligned from positions 1-17 bp. The potential primer is indicated in red below the alignment as a consensus sequence, albeit with four degenerate primers. In Figure 2.14,

only five positions were conserved. In Figure 2.15, nine positions were conserved. This lack of conservation is highly unsuitable for the design of a primer.

```
AHSV4_DQ868773        GTTTAATTCACCATGGC
AHSV4_EU046574        GTTTAATTCACCATGGC
AHSV4_D26570          GTTTAATTCACCATGGC
AHSV3_U01832          GTTTAATTCACCATGGC
AHSV1_Z26316          GTTTAATTCACCATGGC
AHSV3_DQ868772        GTTTAATTCACCATGGC
AHSV8_DQ868775        GTTTAATTCATCATGGC
AHSV8_AY163333        GTTTAATTCATCATGGC
AHSV5_AY163331        GTTTATTTCATCATGGC
AHSV9_DQ868776        GTTTAATTCACCATGGC
AHSV9_AF043926        GTTTAATTCACCATGGC
AHSV6_NC_005996       GTTAAATTCACCATGGC
AHSV6_AF021235        GTTAAATTCACCATGGC
AHSV6_DQ868774        GTTAAATTCACCATGGC
AHSV1_FJ183365        GTTTATTTCAGCATGGC
AHSV1_FJ011108        GTTTATTTCAGCATGGC
AHSV1_AM883165        GTTTATTTCAGCATGGC
AHSV1_AY163329        GTTTATTTCAGCATGGC
AHSV2_AY163332        GTTTATTTCAGCATGGC
AHSV7_AY163330        GTTTAATTCACTATGGC
                      *** * ****  *****
                      GTTWAWTTCABYATGGC
```

Figure 2.13: Potential forward primer region (1-17 bp) of AHSV segment 2 based on Sailleau *et al.* (2000) for all nine serotypes. The red, bottommost sequence is the degenerate consensus sequence and possible primer sequence. AHSV1_Z26316 has been incorrectly annotated and is a serotype 3 isolate. The * represent conserved positions.

```
AHSV3_U01832          AGAATGATTTATGAACAGATT
AHSV1_Z26316          AGAATGATTTATGAACAGATT
AHSV3_DQ868772        AGAATGATTTATGAACAGATT
AHSV9_DQ868776        GATTTTGTGTATAAACAAACG
AHSV9_AF043926        GATTTTATGTACAAACAAACG
AHSV1_FJ183365        GATACGATGTATTGCCAAACA
AHSV1_FJ011108        GATACGATGTATTGCCAAACA
AHSV1_AM883165        GATACGATGTATTGCCAAACA
AHSV1_AY163329        GATACGATGTATTGCCAAACA
AHSV2_AY163332        GAAACCATGTATTGCCAAATT
AHSV7_AY163330        GAGTTCATGTATGAACAAATT
                             * **     * *
```

Figure 2.14: Potential reverse primer region (207-228 bp) of AHSV segment 2 based on Sailleau *et al.* (2000) for serotypes 1, 2, 3, 7 and 9 using ClustalX2. AHSV1_Z26316 has been incorrectly annotated and is a serotype 3 isolate. The * represent conserved positions.

```
AHSV4_DQ868773        GAAATGAGGAAAATATTGATA
AHSV4_EU046574        GAAATGAGGAAAATATTGATA
AHSV4_D26570          GAAATGAGGAAAATATTGATA
AHSV8_DQ868775        GAGTTAGGAAAGATTTTGATC
AHSV8_AY163333        GAATTAGGAAAGATTTTGATC
AHSV5_AY163331        GAGCTAAGCAAAATATTGATA
AHSV6_NC_005996       AGTATTGGAAAAATCCAGATT
AHSV6_AF021235        AGTATTGGAAAAATCCAGATT
AHSV6_DQ868774        AGTATTGGAAAAATCCAGATT
                          *  * ** **   ***
```

Figure 2.15: Potential reverse primer region (339-360 bp) of AHSV segment 2 based on Sailleau *et al.* (2000) for serotypes 4, 5, 6 and 8 using ClustalX2. The * represent conserved positions.

2.3.3.3. Other approaches

Other primer design approaches based on segment 2 investigated using one forward primer and nine reverse primers or nine forward primers and nine reverse primers, but neither could provide the means by which primers could be realistically designed (data not shown).

2.3.4. Bioinformatic analysis of segment 10 in combination with segment 2

The best resolution that could be achieved, in terms of the aims of the present study, from segment 10, was three clades. No suitable primer regions could be found within segment 2 using the approaches of Section 2.3.3.1 – 2.3.3.3 either. What remained was to limit the number of serotypes in a segment 2 analysis to provide enough conservation to design primers. This could be achieved by using the clades of segment 10 (i.e. Clades A, B and C) to provide multiple starting points for the design of primers based on segment 2 using the serotypes contained within each segment 10 clade (Figure 2.4). Considering each clade in turn, the serotypes contained in each were aligned based on full-length segment 2 sequences. This initial alignment of segment 2 sequences of each clade (i.e. Clade A, B and C) revealed that there was substantial divergence among each of the serotypes. This divergence warranted further investigation into the possibility of segregating the serotypes of each clade based on segment 2 sequences (Figure 2.16; Figure 2.17; Figure 2.18).

Figure 2.16: The phylogeny produced from the full-length ClustalX2 alignment of AHSV segment 2 serotypes 3 and 7 (Clade A) and viewed using TreeView to show the potential separation of the individual serotypes. 'AHSV1 3 Z26316' has been incorrectly annotated and is a serotype 3 isolate. The bar represents 0.1 substitutions per site.

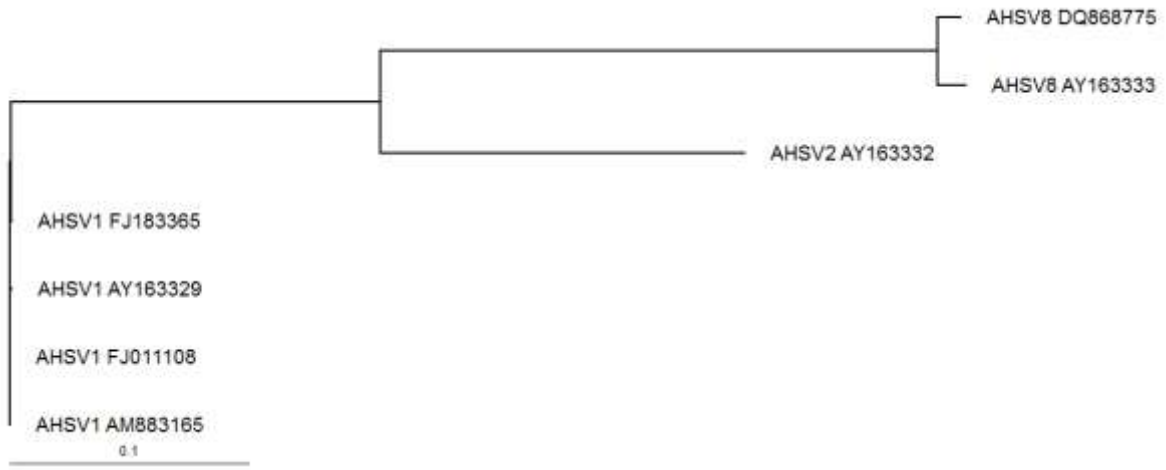

Figure 2.17: The phylogeny produced from the full-length ClustalX2 alignment of AHSV segment 2 serotypes 1, 2 and 8 (Clade B) and viewed using TreeView to show the potential separation of the individual serotypes. The bar represents 0.1 substitutions per site.

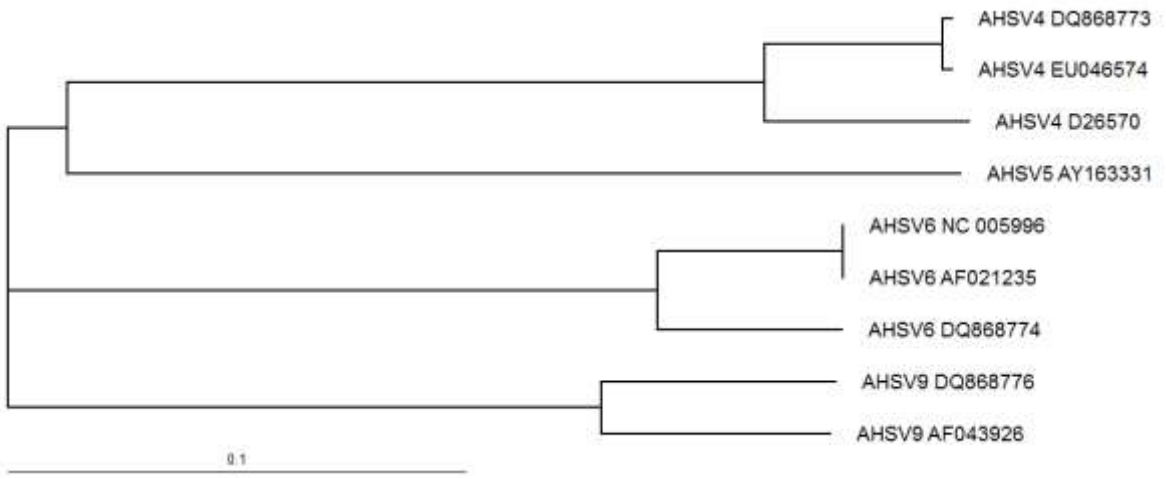

Figure 2.18: The phylogeny produced from the full-length ClustalX2 alignment of AHSV segment 2 serotypes 4, 5, 6 and 9 (Clade C) and viewed using TreeView to show the potential separation of the individual serotypes. The bar represents 0.1 substitutions per site.

After an exhaustive *in silico* and manual inspection of these alignments, (Appendices E1-E3) primers were selected (Table 2.1) and their respective phylogenies viewed (Figure 2.19).

2.3.5. BLAST analysis

All of the primers were subjected to a BLASTn analysis. Among the results of each primer BLAST were the sequences of the primers respective serotype. Some of the BLAST searches of the primer sequences returned results that contained sequences of serotypes not related to the intended serotype of the primer design. However, this was confined to the forward or the reverse primer only, not both.

Table 2.1: AHSV segment 2 primers to separate segment 10 clades into individual serotypes

Clade A: (serotypes 3, 7)	**Sequence (5′ → 3′)**	**Position (+length)**	**T_m**
Fwd:	ATT CAC YAT GGC TTC KGA	6 (+18)	52.5-58.9°C
Rev:	CYA CYC TTA YTT GRT TRT CAT TTC	302 (+23)	51.8-58.9°C
Clade B: (serotypes1, 2, 8)			
Fwd:	TTG GGT TGA WTG GGT YGT	1302 (+18)	55.3-58.3°C
Rev:	TTT GGR AAC ATY TGK GAW ACD G	1529 (+22)	54.9-57.9°C
Clade C: (serotypes 4, 5, 6, 9)			
Fwd:	AGY GGN TGG MTY CCD TA	2873 (+19)	52.4-58.8°C
Rev:	CAR TTY GAR CCR ATC CAN G	2703 (+17)	57.4-61.5°C

2.4. Discussion

Primer design is one of the most important aspects for a successful diagnostic RT-PCR with downstream HRM analysis. However, when considering primers across a range of sequences in a multiple sequence alignment, their design becomes rather limiting. In addition, downstream use of the PCR products needs to be taken into account. In this study, the PCR products were intended to be used to create a unique melt profile for each sequence. The primer design therefore has an added requirement to produce unique amplicons (Figure 2.1).

Many of the first phylogenetic studies of the African horse sickness virus were rather limited due to the lack of sequences available (de Sa *et al.*, 1994) or the fact that only one sequence per serotype was considered (Sailleau *et al.*, 2000). Recent research on serotype determination using segment 2 and segment 10 (Quan *et al.*, 2008; Quan *et al.*, 2010; Maan *et al.*, 2011a) has greatly increased the database of AHSV serotypes in GenBank, which consequently improved the integrity of primer design selection for this study. Various approaches were considered in the present study; however, it was a combination of segment 10 primers and segment 2 primers that were eventually decided upon as the best possible primer design.

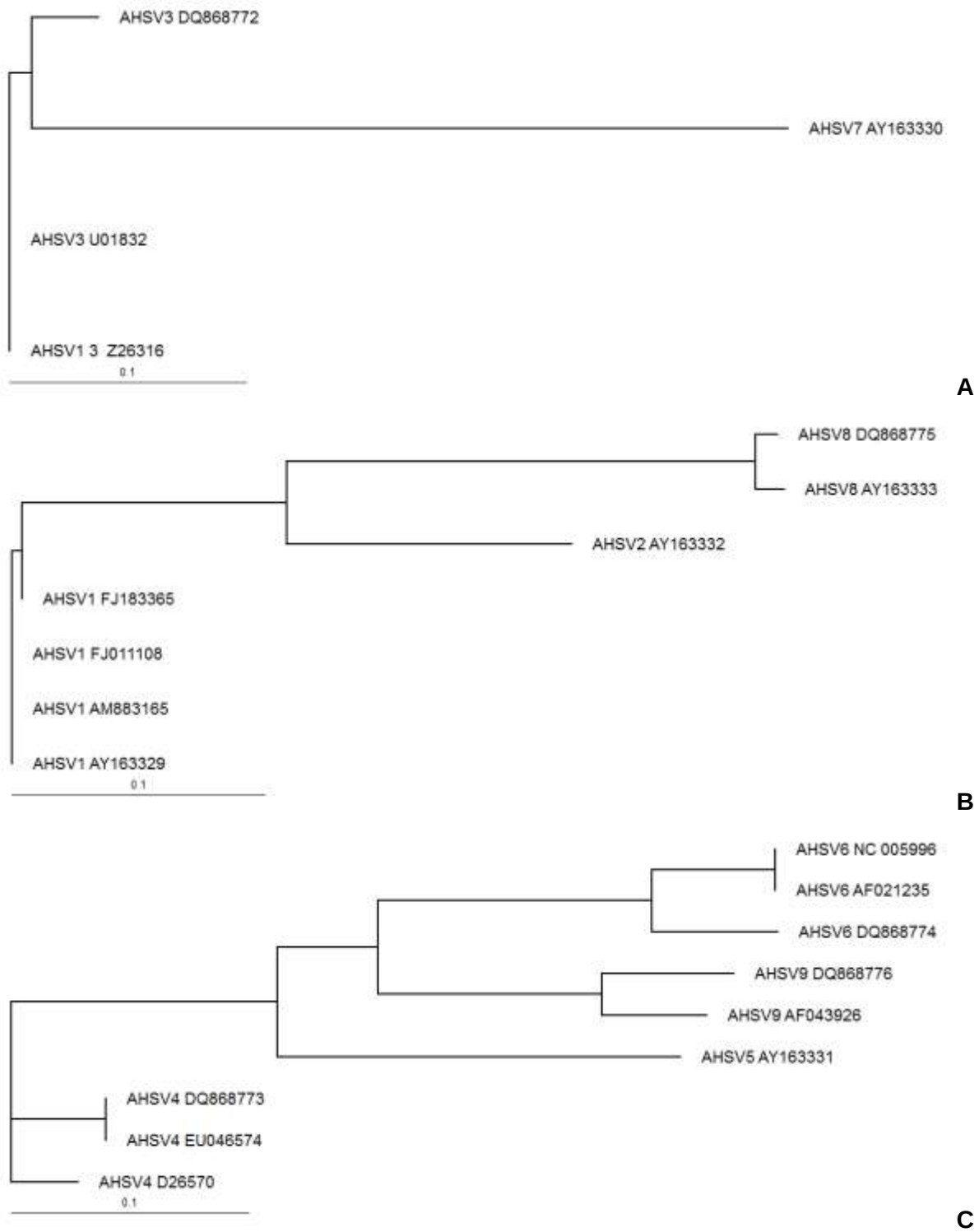

Figure 2.19: Based on the primers in Table 2.1, phylogenies were drawn based on the theoretical amplicons to assess the ability of the amplicons to be distinguishable using HRM in downstream analysis of the RT-PCR. Alignments were produced using ClustalX2 and the phylogenies viewed using TreeView. A – the phylogeny of the 6-326 bp region of AHSV segment 2 of serotypes 3 and 7 (Clade A). B – the phylogeny of the 1302-1551 bp region of AHSV segment 2 of serotypes 1, 2 and 8 (Clade B). C – the phylogeny of the 2703-2894 bp region of AHSV segment 2 of serotypes 4, 5, 6 and 9 (Clade C). The bars represent 0.1 substitutions per site.

Subsequent to this, and based on the findings of Groenink (2009) where one primer pair resolved the nine serotypes into three groupings, segment 10 was explored for additional primer design regions. When all of the most recent segment 10 sequences were aligned and a phylogeny drawn (Figure 2.5), two distinct groupings are apparent (Clade AB and Clade C). Considering Clade AB and then Clade C in turn, it was thought possible that if there were suitable regions for primer design among the serotype sequences of each clade, the assay could be based on two primer pairs (i.e. one pair for Clade AB and one pair for Clade C).

Very few possibilities for primer design existed, but two suitable regions were located from positions 153-174 bp and 742-761 bp on segment 10 (Appendix C1). Initially, however, an amplicon of 608 bp was considered too long for effective HRM analysis, but not impossible. Ideally, amplicons for HRM analysis need to be between 100 bp an up to a maximum of 600 bp, although 150-250 bp is preferred (Gundry *et al.*, 2003; Corbett, 2006). Due to the nature of the dye-release process, the smaller the amplicon, the more sensitive HRM analysis can become (Vossen *et al.*, 2009; Stanzer *et al.*, 2010; Levesque *et al.*, 2011). The phylogeny compiled from the alignment of position 153-761 bp for segment 10 (Figure 2.6) showed that the two clades present in the phylogeny were each representative of the initial Clades A and B. Further separation of the serotypes was highly unlikely due to the limited and exhausted availability of primer design regions.

Ideally, as few as possible primer pairs that can result in nine melt profiles should be aimed for. Since the approach where two primer pairs based on Clade AB and Clade C of segment 10 was identified as providing no additional resolution of the serotypes, an alternative approach involving three primer pairs was assessed. These three primer pairs were based on each of the clades represented in Figure 2.5. Using this approach, the serotypes failed to cluster into serotype unique clades.

Although not an ideal approach, given the aims of the assay for a rapid, cost-effective protocol, probes were still evaluated for the sake of completeness. Probes are short primer-type oligonucleotides that prime to the actual amplicon. Under HRM conditions, this adds additional HRM depth as the probe will dissociate from the amplicon independently. Previous work using up to eighteen different probes to serotype AHSV was considered unsuccessful due to apparent peak melt temperature shifts between laboratory and field strains (Koekemoer, 2008). The probes, however, were designed based on the nine reference strain sequences only, as opposed to a more inclusive set of available reference and field strain sequences. The chosen methodology for a potential probe in the present study was that one probe will generate nine unique melt profiles. It would be degenerate such that each serotype had its own unique sequence and, ultimately, its own ‘unique’ probe. Using this approach, a

suitable degenerate probe sequence could not be identified that would provide a unique sequence for each serotype and therefore a unique melt profile. In addition, potential probe regions per clade that would separate out the serotypes of each clade could not be found either (data not shown).

Having exhausted the chances of designing primers for segment 10 to concur with the aims of this study, focus was shifted to segment 2. It was hoped to exploit the advantages of segment 2 encoding VP2, the serotype determining protein. However, the very large sequence divergence between all of the serotypes rendered a single primer pair incapable of generating nine unique melt profiles. The two clades (serotypes 1, 2, 3, 4 and 7 and serotypes 6, 8 and 9) that were identified in a full-length alignment and phylogeny of segment 2 were unable to yield suitable primer regions either by manual inspection or via Primaclade.

In the study of Sailleau *et al.* (2000) 15 primers were used and it was decided to begin a more in-depth examination of segment 2 sequences starting with these primer building sites. The alignments of serotypes 1, 2, 3 and 9 and serotypes 4, 5, 6 and 8 produced a single degenerate forward primer (position 1-17 bp). However, no common reverse primer could be designed based on these groupings. Although it would be quite possible to design nine unique reverse primers, this was a departure from the original concept of using the minimum number of primers across the largest possible range of sequences and was therefore not pursued.

Following the relatively exhaustive efforts of designing primers focused exclusively on segment 10 and then segment 2, a combined approach was adopted using the advantages offered by targeting both segment 10 and segment 2. segment 10 provided for a greater sequence depth, while sequence 2 provided the serotype specificity to resolve a potential assay to individual serotypes.

In a preliminary study, the greatest resolution to be achieved from segment 10 was by amplifying the 10-190 bp region (Figure 2.5) (Groenink, 2009). It was envisaged that with the greater degree of serotype divergence observed in segment 2, now combined with fewer serotypes (those of each clade), suitable primers could be found that would separate out each clade into its individual serotypes.

Using segment 10 primers followed by segment 2 primers presented a number of possibilities for a future assay:

1. A two-tube assay where the segment 10 clade was determined in the first tube and the serotype determined in a subsequent tube (based on segment 2) depending on the resulting clade.

2. A three-tube assay where the segment 10 and segment 2 primers were used simultaneously in each tube: each tube would contain the segment 10 primers and then each of the three tubes would contain one of the segment 2 primers
3. A three-tube assay where only the segment 2 primers were used.

Subsequent to the full-length segment 2 alignment and phylogenetic analysis, an initial analysis of potential primers for segment 2 of each of the segment 10 clades (A, B and C) revealed a good separation of the serotypes on their respective clade-specific phylogenies, but the inherent primer properties were poor. Primaclade was only able to select very few primers under the default settings, but making the conditions less stringent increased the number of integral primers. These additional primers, combined with an intensive manual analysis of the alignments, successfully resulted in primers being designed for each of the clades, as shown in Table 2.1. The design of these primers would thus successfully cause the serotypes of each clade to separate out.

2.5. Conclusion

The combination of GenBank, ClustalX2, Primaclade, TreeView and BLASTn represent an ideal suite of programmes for bioinformatic analysis and primer design for multiple, divergent sequences sourced from GenBank. In addition, the programmes are all available online at no cost. Following the inadequacies of singularly using segment 10 and segment 2 to produce nine unique clades and therefore melt profiles, a combination of segment 10 primers and segment 2 primers were likely to be able to distinguish the nine serotypes based on their melt profiles. The design of a single primer pair based on either segment 10 or segment 2 was not possible, and nor were two or three primer pairs based on the various clades formed. A probe based on the 10-190 bp region of segment 10 was unlikely to give conclusive results. A probe-based technology was not pursued further due to the cost implications.

CHAPTER 3: AFRICAN HORSE SICKNESS VIRUS SEROTYPE IDENTIFICATION AND ANOMOLY RESOLUTION USING HIGH RESOLUTION MELT ANALYSIS

3.1. Introduction

Cell culture remains the easiest and most practical method for viral propagation for the extraction of large amounts of genetic material. The AHS virus has been successfully propagated in the brains of mice and embryonated chicken eggs (Howell, 1962; Goldsmit, 1967). More recently, the majority of published studies on the subject have used either Vero cells or baby hamster kidney (BHK) cells to propagate either the African horse sickness virus (AHSV) or other orbiviruses (Chaignat *et al.*, 2009; Maan *et al.*, 2010b; Maan *et al.*, 2011a). Zientara *et al.* (1995b) isolated total RNA from cell cultures using the guanidinium-thiocyanate-phenol-chloroform method of Chomczynski and Sacchi (1987). Commercial systems based on this method are now available such as the TRIzol™ and TriFast™ group of reagents (Rodriguez-Sanchez *et al.*, 2008).

For the objectives of the present study, serotyped reference viral isolates would be required. Particularly in the case of AHSV, viral isolates obtained from the field would be difficult to obtain. Collection of field strains is time-consuming, impractical and yields are low. In addition, all nine serotypes would have to be located. Due to the apparent random distribution of serotypes in time and space in South Africa, not all nine serotypes would be available at one time and it may have taken several years to collect all nine serotypes. Stocks of reference and field strains of the most economically important viruses reside in OIE Reference Laboratories around the world from where researchers should be able to obtain the necessary strains and seed stocks. One of the African horse sickness virus Reference Laboratories is the Onderstepoort Veterinary Institute of the Agricultural Research Council (OVI-ARC) of South Africa (OIE, 2008). In future studies and trials relating to the present study, it will become necessary to gather all nine serotypes from the field.

For this study, two molecular approaches for verifying the presence of AHSV in cell culture supernatants were used: firstly, an RT-PCR protocol using primers published in the OIE Diagnostic Manual which target the genome segment encoding VP7 (OIE, 2008; Fernández-Pinero *et al.*, 2009) and secondly, a duplex RT-PCR protocol using primers which targeted the VP7 and NS2 genes (Quan *et al.*, 2010; Guthrie *et al.*, 2013). OIE primers would have greater international significance, but were designed based on older isolates and do not appear to have been tested on South African field strains or recently collected strains. The genome segment encoding VP7 is a popular target for serogroup-specific (species-specific)

AHSV diagnostic assays as it is the most conserved genome segment amongst all nine serotypes of AHSV, yet it is divergent amongst serogroups, i.e. AHSV and BTV or EEV (Bremer *et al.*, 1990; Zientara *et al.*, 1993; Zientara *et al.*, 1994; Laviada *et al.*, 1997).

Fernández-Pinero *et al.* (2009) developed what would subsequently become the recognised OIE RT-PCR diagnostic assay protocol. Although all nine serotypes were represented, the study only used 12 isolates. The primers were designed using sequences from serotypes 3, 4, 6 and 9 only. In the duplex RT-PCR protocol, which targeted the VP7 and NS2 genes, developed by Quan *et al.* (2010), recent South African isolates were included. This work was conducted at the Equine Research Centre (University of Pretoria, Onderstepoort), but was, at the time of writing, yet to be validated due to the above mentioned difficulties of finding all nine serotypes in the field. These primers were designed based on 52 sequenced field samples (and subsequently submitted to GenBank), plus nine reference strains. The OIE method is accepted for international control purposes, as it carries more weight in the international arena, and is a simpler primer set test.

High Resolution Melt (HRM) analysis is a highly sophisticated method used to detect differences in DNA sequences. One of the important advantages of HRM analysis is that the influence of template concentrations is drastically minimised (Corbett, 2006; KAPA, 2010). This has important consequences for rapid diagnostic scenarios that aim to eliminate pre-analysis processes without reducing the accuracy of the result.

In previous studies involving HRM analysis, a relatively conserved region of the genome was considered. These regions invariably contained few, but significant, differences between the genotypes. In the present study, the amplicons were particularly divergent along their entire length, with even the primers being noticeably degenerate. The use of HRM analysis for amplicons of such diversity as encountered in the present study of AHSV, has not been tested before. Furthermore, HRM analysis has not been used for the successful genotyping of any orbivirus. Although some efforts have been made, the results were inconclusive (Koekemoer, 2008).

Serotypes evolved as a pathogen's mechanism to outwit the host's immune system. The basic premise of a serotype is that the epitopes recognised by the host's antibodies are different to those of other serotypes of the same species. Thus, to neutralise a serotype of a specific pathogen, the host requires a serotype-specific antibody. Any relationships between the serotype and the proteins involved in pathogenicity are likely to have evolved because of geographic isolation over time. In addition, despite occurring in similar regions, some pathogens display a relationship between pathogenicity and infecting serotype,. An example

is infectious bursal disease virus (Ghorashi *et al.*, 2011). The relationship between serotype and pathogenicity is not well understood in AHSV (Huismans *et al.*, 2004).

Genetic re-assortment of the genome or antigenic drift is always a concern when dealing with viruses. Segmented genomes, particularly RNA based ones, as exist in orbiviruses, are thought to favour genetic re-assortment (Mumford, 2007). New types may therefore arise if a cell is co-infected with more than one serotype. Re-assortment has, however, been documented in BTV, possibly due to infection of multiple serotypes (Maan *et al.*, 2010b). However, and to the author's knowledge, no case of AHS has been identified where more than one serotype has been detected in one individual simultaneously. The AHS viral genome appears to be genetically stable. This is demonstrated by the lack of additional AHSV serotypes being described since the ninth serotype was described in the 1960s (Howell, 1962).

Two genome segments are responsible for serotype divergence in AHSV. Segment 2 encodes the outer capsid protein (VP2) that contains the epitopes recognised by neutralising antibodies. Serotyping techniques, such as virus neutralisation, are based on this (Grubman & Lewis, 1992; Roy *et al.*, 1994). Segment 10, encoding the non-structural protein 3 (NS3), has no defined role as yet, but is thought to be involved in virulence (Mertens *et al.*, 2006). In AHSV, it is markedly divergent between the nine serotypes, while in BTV, it is fairly conserved amongst the 24 serotypes (Huismans *et al.*, 2004; Quan *et al.*, 2008). VP7 is the most conserved protein per orbivirus serogroup and is thus commonly used as a diagnostic target to confirm the presence of AHSV and the absence of other orbiviruses (Fernández-Pinero *et al.*, 2009).

Based on the results obtained from the design of primers described in Chapter 2, a proposed assay to serotype the AHS virus would involve all nine serotypes being segregated into three clades using segment 10 primers targeting nucleotide positions 10-190 (hereafter referred to as the 10-190 bp region). Following this, the serotypes could be determined from each clade using clade-specific primers targeting various regions of segment 2, as discussed in Chapter 2, using HRM analysis. To confirm the serotype of the isolate from which the PCR products are produced, the amplicons can be sequenced. Modern molecular diagnostics, including HRM analysis, will be able to detect sequence aberrations, and therefore the serotype, in real time. This will aid early warning systems for AHSV and preventative actions in the case of an outbreak.

As a necessary precursor to further molecular analysis of AHSV RNA for diagnostic purposes, it was necessary to propagate the AHS virus in Vero cells, extract the total RNA and validate the RNA as containing AHS viral RNA using the OIE sanctioned RT-PCR

method combined with HRM analysis. This would also serve to be the first study where the OIE recognised VP7 primers of Fernández-Pinero *et al.* (2009) were tested on South African field isolates.

Using three sets of AHSV serotypes from the Onderstepoort Veterinary Institute of the Agricultural Research Council (OVI-ARC) and the National Institute of Communicable Diseases (NICD) from two different isolation periods, primers targeting the genes of VP7, VP2 and NS3 were tested and the RT-PCR and HRM analysis protocols were described. These were used to ascertain and confirm the isolates as being particular AHSV serotypes and further develop the HRM analysis protocols that sought to distinguish between the serotypes.

Additionally, due to AHSV being an RNA virus, two RT-PCR protocols were compared: a one-step RT-PCR protocol using viral RNA contained in a total RNA extraction; or a two-step RT-PCR protocol using cDNA of the viral RNA. Following that, primers based on the 10-190 bp region of AHSV segment 10 were tested against all 27 isolates of AHSV to determine the clades. After confirmation of the clades, the isolates of each clade were tested against the segment 2 clade-specific primers in an attempt to determine the serotype.

3.2. Materials and methods

3.2.1. AHSV material

Reference strains of AHSV in South Africa reside at OIE Reference Laboratories and other associated governmental institutions. Two such laboratories exist in South Africa – the Onderstepoort Veterinary Institute of the Agricultural Research Council (OVI-ARC) and the National Institute of Communicable Diseases (NICD). Reference strains of the AHS virus were obtained from Prof. Janusz Paweska of the NICD (Special Pathogens Unit, Johannesburg, South Africa). The details of these strains are found in Table 3.1. These reference strains represent the original field virus isolates identified in the 1960s and are preserved as reference material in OIE Reference Laboratories across the world. They also serve to confirm the genetic conservation of the virus through time. The reference strains at the NICD were received from Prof. P. G. Howell (University of Pretoria) in 2000 who originally obtained the strains from the Onderstepoort Veterinary Institute and from the National Institute of Virology. The freeze-dried pellets obtained from the NICD are the product of a succession of mouse brain passages, baby hamster kidney (BHK) cell culture and Vero cell culture (Paweska, J. T., *personal communication*, June 2009). Two sets of

recent field isolates, isolated in the early 2000s, were purchased from OVI-ARC (Table 3.2) and are designated OVIA and OVIB.

Table 3.1: Details of the AHS virus reference strains from the NICD used in Vero cell culture for viral RNA isolation and subsequent RT-PCR and HRM analysis.

Serotype	Isolate	Year of original field isolation	Year of last culture isolation
1	A501	1965	1997
2	OD	1965	1997
3	L	1965	1997
4	Vry 47/58	1965	1997
5	VH	1965	2000
6	114	1965	1997
7	Karen	1965	1997
8	18/60/22	1962	1998
9	AHS 9	1995	2000

Table 3.2: Two sets of field isolated virus material supplied by OVI-ARC (designated OVIA and OVIB). The codes refer to the isolates' source and how many and which type of passage it has undergone. EQ – equine. BLD – blood; SPL – spleen; LU – lung; CLT – unknown. V – Vero cell; B – BHK cell; S – Suckling mouse brain.

Serotype	OVIA	OVIB
1	EQ BLD 5V	EQ BLD CLT 1V
2	EQ SPL B 1V	EQ SPL 2V
3	EQ BLD 1V	EQ BLD 2V
4	EQ BLD 3V	EQ SPL 1V
5	EQ SPL A 1V	EQ SPL 1V
6	EQ LU 2V	EQ SPL 2V
7	EQ BLD 4V	EQ LU 2V
8	1S 2V	EQ SPL 1S 4BHK
9	EQ SPL 1V	EQ LU 1V

3.2.2. Vero cell culture

All work involving the AHS virus was conducted under bio-safety level two (BSL2) conditions. A 2 mL vial of Vero cells, originally obtained from the NICD, was split into three T75 flasks

(75 cm^2) and 10 mL growth medium [10% (v/v) foetal bovine serum (FBS) (Lonza, Walkersville, USA or Delta Bioproducts, Johannesburg, RSA); 1% (w/v) Pen/Strep/Amphotericin B 100x (10,000 U penicillin/mL, 10,000 µg Streptomycin/mL, 25 µg Amphotericin B/mL) (Lonza, Walkersville, USA); 1% (w/v) non-essential amino acid (NEAA) mixture 100x (Lonza, Walkersville, USA) and 1% (w/v) L-glutamine (2 mM final concentration) (Lonza, Walkersville, USA) in Eagle's Minimum Essential Medium (EMEM) with Earle's Balanced Salt Solution (EBSS) and 25 mM Hepes and without L-glutamine] was added to each. Once 80-90% confluent, the cells were trypsinised, harvested and spun down. 6 mL of growth medium was added to the cell pellet. 2 mL was subsequently aliquoted into three T75 flasks (a 1:3 ratio). The cells were split in this manner of 1:3 ratios, until the required number of flasks was reached (Paweska *et al.*, 2003; Paweska, J. T., National Institute of Communicable Diseases, *personal communication*, June 2009).

The freeze-dried pellets of each of the NICD, OVIA and OVIB sets of AHSV were re-suspended in 250 µL of sterile phosphate buffered saline (PBS), pH 7.2; aliquoted into 50 µL volumes and stored at -70°C. To inoculate a T75 flask, 950 µL of growth medium was added to a 50 µL aliquot (1:20 dilution) and transferred to a ± 90% confluent monolayer of Vero cells. A negative control flask was inoculated with 1 mL EMEM. The flasks were placed in a Gallenkamp Orbital Incubator (60 rpm) for 1 hour at 37°C, subsequently overlaid with 10 mL growth medium and returned to the incubator (40 rpm). Flasks were monitored daily for non-specific cytopathic effects (CPE) that involved the cells rounding and lifting off the surface of the flask (Paweska, J. T., National Institute of Communicable Diseases, *personal communication*, June 2009). When the flasks showed 90% CPE after 5-7 days post-inoculation, the supernatants and cells, were aliquoted directly into 1 mL volumes and stored at -70°C..

3.2.3. AHSV RNA extraction

The extraction of total RNA from the cell culture supernatants and cells was achieved using TRIzol® LS Reagent (Invitrogen, Carlsbad, USA) or peqGOLD TriFast™ (peqlab, United Kingdom) following the manufacturer-provided protocols. Final RNA pellets were re-suspended in 50 µL of DEPC-treated water. Absorbance readings of the suspension, after extraction with TRIzol® or TriFast™, at 230, 260 and 280 nm were recorded using a using a NanoDrop™ 2000 UV-Vis Spectrophotometer (Thermo Scientific, Wilmington, USA) and used to determine the presence and relative quantity of RNA (Wade-Evans *et al.*, 1990). Total RNA extracted using guanidine-thiocyanate-based extraction methods has been used in various other HRM and RNA-based virus studies (Hewson *et al.*, 2010; Ghorashi *et al.*, 2011; Varillas *et al.*, 2011).

3.2.4. RT-PCR of AHSV

3.2.4.1. Primers

A number of primers were designed for the AHSV genome segments 2 and 10 (as discussed in Chapter 2) and are listed in Table 3.3. Serotype-specific primers based on segment 2 were adapted from Maan *et al.* (2011a) with a number of modifications. These modifications were due to the increased number of sequences used during primer design in the present study, compared to those used by Maan *et al.* (2011a), which necessitated the alteration of some bases to create improved primers (indicated in Table 3.3 in red font).

Segment 10 primers, 10F and 10R, resolve the nine serotypes into three clades (Table 3.4). Segment 2 clade-specific primers were then used on each resultant clade. VP7 primers were adapted from Fernández-Pinero *et al.* (2009) and have been recognised by the OIE for use in a standardised test for AHSV for equine trade purposes (OIE, 2008). As such, they were used in the present study to confirm the presence of AHSV RNA extracted from cell culture in a conventional gel-based RT-PCR.

3.2.4.2. RT-PCR for genome segment 7

The KAPA™ SYBR® FAST One-Step qRT-PCR system (Cape Town, South Africa) was used with slight modifications to take into account the double-stranded nature of the AHSV RNA genome. For a duplicate 20 µL reaction using the OIE segment 7 primer pair (7F and 7R), 7.6 µL of DEPC-treated water, 0.8 µL each of 10 µM forward and reverse primers (final concentration of 400 nM) and 10 µL TRIzol®/TriFast™-extracted total RNA (10-52 ng/µL) from AHSV-infected Vero cell cultures was combined and heated to 95°C for 5 min followed by immediate chilling on ice. Once cooled, 20 µL of the qPCR master mix was added followed by 0.8 µL of the RT mix. The tubes were briefly vortexed, spun down and split into two 20 µL volumes and loaded into a Corbett Rotor-Gene™ 6000 rotary analyser (Corbett, Sydney, Australia). The following PCR conditions were used: 42°C for 5 min for cDNA synthesis followed by a hold of 95°C for 2 min to deactivate the reverse transcriptase and activate the DNA polymerase. This was followed by 35 repeats of an incubation at 95°C for 5 s for denaturation and 60°C for 30 s for annealing and extension simultaneously. The no template controls (NTC) contained 10 µL of DEPC-treated water instead of extracted RNA.

Table 3.3: List of primers used for the analysis of AHSV by HRM. Red font indicates the changes made by the author to the primers of Maan *et al.* (2011a). dg – degeneracy.

	Name	Short	Sequence (5'-3')	T_m (°C)	Size (bp)	dg*
Segment 2: Clade-specific	AHSV_VP2AF_0006_0024_SG	AF	ATTCACYATGGCTTCKGA	51.8	319	4
	AHSV_VP2AR_0302_0325_SG	AR	CYACYCTTAYTTGRTTRTCATTTC			32
	AHSV_VP2BF_1302_1320_SG	BF	TTGGGTTGAWTGGGTYGT	54.9	249	4
	AHSV_VP2BR_1529_1551_SG	BR	TTTGGRAACATYTGKGAWACDG			48
	AHSV_VP2CF_2703_2720_SG	CF	AGYGGNTGGMTYCCDTA	52.4	189	48
	AHSV_VP2CR_2873_2892_SG	CR	CARTTYGARCCRATCCANG			64
Segment 2: Serotype specific	AHSV_VP2_1F_0508_0531_NM	2.1F_NM	GGTGTGTTGAATGGAAATAAACAG	60.3	1793	0
	AHSV_VP2_1R_2301_2280_NM	2.1R_NM	GCTCAATCCTTCACGGTTAAGG			0
	AHSV_VP2_2F_0456_0476_NM	2.2F_NM	RTATCCATTTGATATAAGATG	49.7	1098	2
	AHSV_VP2_2R_1554_1535_NM	2.2R_NM	GATGATATCTCCACGGAAG			0
	AHSV_VP2_3F_0447_0466_NM	2.3F_NM	GGTTTCTCGTTCAATTATAG	52.3	751	0
	AHSV_VP2_3R_1198_1176_NM	2.3R_NM	YCAAAAWCTTCTTAACTTCCGYT			8
	AHSV_VP2_4F_0441_0460_NM	2.4F_NM	GCTTGATCGRATTCGGARTT	54.3	1267	4
	AHSV_VP2_4R_1708_1687_NM	2.4R_NM	TCACCGCGAAGCCATCCCTACG			0
	AHSV_VP2_5F_0714_0735_NM	2.5F_NM	CAAAGGAGGTTTGATAGCYAAC	58.4	1139	2
	AHSV_VP2_5R_1853_1828_NM	2.5R_NM	TCAAAGACCCTATCTGGCYTRTYAAC			8
	AHSV_VP2_6F_0473_0496_NM	2.6F_NM	GRATGCGARRGATTGARGCYAGG	57.5	1154	32
	AHSV_VP2_6R_1627_1606_NM	2.6R_NM	GCATCGTCGYTCRACGAATAR			8
	AHSV_VP2_7F_0573_0593_NM	2.7F_NM	GATGGAGGGCCAACAAGAGA	59.4	1426	0
	AHSV_VP2_7R_1999_1978_NM	2.7R_NM	GAATATCGATTCTCGCCATCG			0
	AHSV_VP2_8F_0586_0609_NM	2.8F_NM	GTGGGAAAGARAGTGTGTGTAAG	60.1	1754	2
	AHSV_VP2_8R_2343_2321_NM	2.8R_NM	GTCTTTCTTAGTYAGTCCGCTG			2
	AHSV_VP2_9F_0487_0509_NM	2.9F_NM	GAGCGAGARTTARGKRSTGGRG	60.1	1483	64
	AHSV_VP2_9R_1970_1947_NM	2.9R_NM	GARGTBTGAACCTGTCGAACTCG			6
Segment 7 - OIE	AHSV_VP7F_0815_0837_JFP	7F	GGCTCCAACACTCACAAGATGT	59.0	102	0
	AHSV_VP7R_0896_0917_JFP	7R	GGCGGATTAATAGGCTGCATA			0
Segment 10	AHSV_NS3_F_0010_0031_SG	10F	ATCCCTTGTCATGARTCTWGCT	57.7	180	4
	AHSV_NS3_R_0165_0190_SG	10R	CTTGACATKGCTTGRTTAAGTATCC			4

Table 3.4: Serotypes per clade as defined in Groenink (2009).

Clade	Serotypes
A	3, 7
B	1, 2, 8
C	4, 5, 6, 9

3.2.4.3. Gradient PCR

A gradient PCR was performed on the clade-specific primers to establish the optimum annealing temperature. The PCR was set out according to Table 3.5 and was performed in a G-storm thermal cycler (Somerset, UK). Each clade was represented by a single serotype from the OVIA set and their respective clade specific primers. Only a single serotype representative was used due to space constraints in the cycler. The serotype per clade was selected based on the lowest theoretical annealing temperature of that serotype and its corresponding primer sequence in the degenerate primer. Total RNA concentrations for each representative isolate were: OVIA7 – 18 ng/µL (Clade A); OVIA8 – 20 ng/µL (Clade B) and OVIA9 – 26 ng/µL (Clade C). Final primer concentrations were 800 nM. The subsequent High Resolution Melt, from 70-90˚C, was performed in the Corbett Rotor-Gene™ 6000 rotary analyser.

A second gradient PCR was conducted to determine the optimum primer concentration and annealing temperature for the segment 10 primers (10F and 10R). OVIB1 was chosen for the template (28 ng/µL) as the unique sequence of serotype 1 corresponded to the lowest theoretical annealing temperature of the degenerate primers. Primer concentrations tested were 200, 400 and 800 nM with annealing temperatures from 55.1-66.2°C and set up according to Table 3.6. Again, as this was conducted on the non-real time-enabled G-storm thermal cycler; the High Resolution Melt, from 70-90˚C, was performed in the Corbett Rotor-Gene™ 6000 rotary analyser.

In both gradient PCRs, the reactions were set up as described in Section 3.3.4.2, but had an annealing step at the appropriate temperature for 30 s and an extension step at 72˚C for 5 s.

Table 3.5: Layout of gradient PCR for the determination of the optimum annealing temperature of the clade-specific primers (AF/AR, BF/BR, CF/CR). The first digit indicates the serotype (serotype 7, 8 or 9) and the last digit indicates the duplicate (1/2). The middle digit(s) corresponds to the column that the reaction was loaded in and therefore the temperature at which the primers would anneal as indicated by the top row.

Temp (°C)	**52.1**	**52.4**	**53.1**	**54.2**	**55.6**	**57.1**	**58.7**	**60.3**	**62.1**	**63.2**	**63.8**	**64.2**
Row/Col	**1**	**2**	**3**	**4**	**5**	**6**	**7**	**8**	**9**	**10**	**11**	**12**
A	711	721	731	741	751	761	771	781	791	7101	7111	7121
B	712	722	732	742	752	762	772	782	792	7102	7112	7122
C	811	821	831	841	851	861	871	881	891	8101	8111	8121
D	812	822	832	842	852	862	872	882	892	8102	8112	8122
E	911	921	931	941	951	961	971	981	991	9101	9111	9121
F	912	922	932	942	952	962	972	982	992	9102	9112	9122

Table 3.6: Layout of gradient PCR for the determination of the optimum primer concentration and annealing temperature for the segment 10 primers (10F/10R). The primer concentration is represented by the first digit – 2 is 200 nM, 4 is 400 nM and 8 is 800 nM, while the last digit(s) correspond to the column that the reaction was loaded in and therefore the temperature at which the primers would anneal as indicated by the top row.

Temp (°C)	**55.1**	**55.4**	**56.0**	**57.0**	**58.3**	**59.7**	**51.1**	**62.6**	**64.3**	**65.3**	**65.8**	**66.2**
Row/Col	**1**	**2**	**3**	**4**	**5**	**6**	**7**	**8**	**9**	**10**	**11**	**12**
B	21	22	23	24	25	26	27	28	29	210	211	212
C	41	42	43	44	45	46	47	48	49	410	411	412
D	81	82	83	84	85	86	87	88	89	810	811	812

3.2.4.4. One-step vs. two-step RT-PCR protocols

A comparison of one-step and two-step protocols was carried out. A one-step protocol involved the reverse transcription of the viral RNA and amplification of the cDNA in a single tube. It was a faster and simpler protocol and is more easily applied to rapid diagnostic assays. It would also be more efficient and more cost-effective than a two-step method, which involved reverse transcribing the viral RNA into cDNA in a separate protocol. However, the advantages of a two-step protocol also needed to be considered. Approximately the same amount of RNA was used in both the one-step and two-step protocols. However, in the two-step protocol, a cDNA stock can be maintained and would allow repeated sampling from the original sample, without diminishing it.

3.2.4.5. One-step RT-PCR protocol

The one-step protocol was performed according to Section 3.2.4.2 using serotype 3 isolate total RNA that ranged from 9.1-40 ng/µL and primer pair AF/AR, but scaled down for 10 µL reactions. The following conditions were applied: 42°C for 5 minutes for cDNA synthesis followed by a hold of 95°C for 2 minutes to deactivate the RT and activate the DNA polymerase. This was followed by 40 repeats of 95°C for 5 seconds for denaturation and 60°C for 30 seconds for annealing and extension simultaneously. Immediately after the RT-PCR, the samples were subjected to a High Resolution Melt (HRM) from 70-95°C in the same machine.

3.2.4.6. Two-step RT-PCR protocol

Where a two-step protocol was required, viral RNA was reverse transcribed into cDNA using the SuperScript® III First-Strand Synthesis SuperMix (Invitrogen, Carlsbad, CA). Random hexamers were used, according to the manufacturers protocol, but with slight modifications: 15% (v/v) DMSO was initially added to the total RNA preparations and incubated at 99˚C for

two minutes followed by immediate chilling on ice (Chatzinasiou *et al.*, 2010). The resulting cDNA was then amplified using the KAPA™ SYBR® FAST qPCR system. For duplicate 10 µL reactions, 6.4 µL of DEPC-treated water, 0.8 µL each of 10 µM forward and reverse primer (400 nM final concentrations), 10 µL of qPCR master mix and 2 µL of cDNA was combined. As for the one-step protocol above, the tubes were briefly vortexed, the contents spun down and split into two 10 µL volumes and loaded into a Corbett Rotor-Gene™ 6000 rotary analyser. The conditions and subsequent protocols remained as described above.

3.2.4.7. Influence of RNA template concentration on HRM

Due to a choice to use maximum total RNA, the effect of template concentration on the ability of HRM to resolve the serotypes downstream was assessed. Total RNA preparations of the OVIA2, OVIA5, OVIB1 and OVIB2 isolates were adjusted to contain 50 ng/µL (except OVIB1, which contained 48 ng/µL), 10 ng/µL, 2 ng/µL, 1 ng/µL and 0.5 ng/µL. The two-step protocol was followed, using the segment 10 primer pair at 400 nM final concentration at the above-mentioned conditions.

3.2.4.8. Anomaly identification

Where serotype anomalies were detected, the standard RT-PCR protocol was used (Section 3.2.4.2) for Clade B with a range of 8-52 ng/µL total RNA. Where Clade C was analysed, a 2-step protocol was used with the total initial RNA concentration ranging from 27-36 ng/µL.

3.2.4.9. Serotype-specific primer analysis

All of the serotype-specific primer analysis was conducted according to Section 3.2.4.2. Total RNA ranged from 10-52 ng/µL.

3.2.4.10. Segment 10 analysis

The two-step RT-PCR was conducted according to Section 3.2.4.4 with initial total RNA concentrations ranging from 10-52 ng/µL.

3.2.4.11. Clade determination of the segment 10 analysis

Following the rectification of serotype anomalies, the identification and classification of clades based on the segment 10 10-190 bp region was carried out on the results achieved in Section 3.2.4.10/3.3.8.

3.2.4.12. Serotype determination

Once the clades of the isolates had been determined, the serotypes of each clade were separated based on clade-specific primers. A two-step RT-PCR protocol was followed. The total RNA concentrations of Clade A isolates ranged from 9.1-40 ng/µL, Clade B isolates ranged from 11-29 ng/µL and Clade C isolates ranged from 9.4-53 ng/µL.

3.2.4.13. HRM analysis in the Corbett Rotor-Gene™ 6000 Series Software (Version 1.7)

Fluorescence and HRM curves of each isolate were compared visually, aided by the genotyping capabilities of the Corbett Rotor-Gene™ 6000 Series Software. Where applicable, 'bins' are applied by the user to identify melt peaks in the melt curve analysis and are used by the Rotor-Gene™ software in downstream genotyping. A 'bin' can be defined as 'an area (or a temperature range set by the user) where peaks are expected to occur' (Qiagen, 2009). The default bin width is 4°C. This was decreased to 0.6°C to make the bins more sensitive. A threshold may be applied to exclude the pre-melting noise.

In a secondary analysis, genotypes were then defined. HRM analysis begins with the normalisation of the raw fluorescence curves. The normalisation windows were set to be approximately 0.5°C wide and were adjusted such that the temperature range between them contained the unique melt characteristics. For the HRM analysis, genotypes were defined based on a control sample, which was nominated by the user.

The samples were therefore simply genotyped according to the bins they fitted into, which is based on their melt peak temperature. HRM analysis uses more sophisticated algorithms to associate a normalised HRM curve to one of the chosen control/reference samples and was therefore more sensitive (Gurtler *et al.*, 2012). In the case of the HRM analysis, the genotypes were assigned a confidence percentage, which is not synonymous to statistical confidence. Confidence percentages as low as 60% and 70% have been used (Toi & Dwyer, 2008; Steer *et al.*, 2011; Grando *et al.*, 2012) although 80% or 90% values are more commonly considered an acceptable level (Ghorashi *et al.*, 2011; Granados-Cifuentes & Rodriguez-Lanetty, 2011; Tanaka *et al.*, 2011; Grando *et al.*, 2012). However, the homogeneity of the sequences needs to be considered. Highly similar sequences are expected to have high correlations and therefore the confidence threshold can be set quite high. However, in the present study, in which fairly diverse sequences with highly degenerate primers were considered, the confidence thresholds need to be relaxed somewhat to account for the variations over the length of the amplicon.

3.2.4.14. Electrophoresis

To confirm that the correct region was being amplified, a 1.2 or 2.5 % agarose gel containing 1 µg/µL ethidium bromide in 0.5 × TBE was loaded with the amplified samples and was run at 120 V for 1 hour. Samples were prepared by adding 1 µL of the respective loading buffer and 2 µL of the PCR product to 3 µL of water. In some instances, the gel was post-stained in a bath of 0.5 µg/µL ethidium bromide for 15-20 minutes followed by 5 minutes in water on a shaker set to 25 rpm. The Fermentas O'GeneRuler™ 100 bp Plus DNA Ladder, the Fermentas O'GeneRuler™ Low Range DNA Ladder or the New England Biolabs® Low

Molecular Weight DNA Ladder were used as molecular weight markers. Product size was determined by plotting the log of the size of each molecular weight marker band against the distance travelled from the well. The distances that sample products had migrated were then extrapolated to a molecular weight (bp) according to the resulting log graph (data not shown).

3.2.4.15. Nucleotide sequencing

Where differences to the expected melt curves were observed, sequencing of the amplified DNA products was performed by Inqaba Biotec™ (Pretoria, South Africa) using an Applied Biosystems 3130XL sequencer with both forward and reverse primers. The chromatograms were checked and the resulting sequences edited to contain only reliable bases. The forward and reverse reads were merged into a single sequence where appropriate. These edited sequences were then subjected to a BLAST analysis against the NCBI nucleotide database (BLASTn; word size = 7/11/28; match/mismatch scores = 1, -3/2, -3/1, -2, gap costs = 5.2/5.2/0.0) (Altschul *et al.*, 1997; Johnson *et al.*, 2008; Benson *et al.*, 2012). This was to confirm the actual genome sequence and serotype that was present. A table was generated in which each of the isolates from the three sets were identified according to its named serotype, HRM analysis-derived serotype, and sequencing results. The sequences were submitted to the European Nucleotide Archive under accession numbers HG779544 – HG779580[6].

3.3. Results

3.3.1. AHSV culture on Vero cell monolayers

All AHSV isolates inoculated onto the Vero cell monolayers achieved a CPE of >80% between 64 and 96 hours.

3.3.2. Confirmation of the presence of AHSV RNA using OIE recognised primers

Due to the nature of virus propagation, total RNA extraction results in extraction of Vero cell RNA together with AHSV RNA. To ensure that AHSV RNA is present, it was necessary to test the RNA using recognised AHSV primers to validate its presence for further molecular analysis.

The cDNA derived from RNA of the OVIA Clade A AHSV isolates were amplified using primers that target the serogroup-conserved genome segment 7 (Figure 3.1).. There is a faint band shown for the NTC, but the fluorescence curve has a substantially higher C_T value than the samples (data not shown). Importantly, the negative control samples (OVIAC) did

[6] http://www.ebi.ac.uk/ena/data/view/HG779544-HG779580

not show amplification. Amplification of AHSV cDNA derived from RNA from OVIA serotypes 3 and 7 gave a product of the expected size of approximately 102 bp.

cDNA derived from RNA of serotypes 2 and 8 isolates of the OVIB set amplified well, but the serotype 1 isolate RNA failed to amplify and produce the required 102 bp-sized band (Figure 3.2). Serotype 2 and 8 isolates' cDNA derived from RNA did amplify and resulted in an approximately 102 bp-sized band. The NTC and negative controls showed no amplification products.

cDNA derived from RNA of serotypes 4, 5, 6, and 9 isolates of the OVIA set amplified well showing approximately 102 bp products (Figure 3.3), while no amplification products were observed with the NTC or negative controls.

cDNA derived from RNA of the OVIB set of the field strain isolates was amplified using the OIE primers designed for the 102 bp region of the genome segment encoding VP7 of AHSV (Figure 3.4). There is a faint band shown for the NTC, although this has a much lower molecular weight. No amplification products were evident in the negative controls and all the serotypes produced the expected approximate 102 bp product on the agarose gels.

Amplification products were produced for all nine serotypes of the NICD reference strains and all showed an approximate 102 bp product on an agarose gel (Figure 3.5).

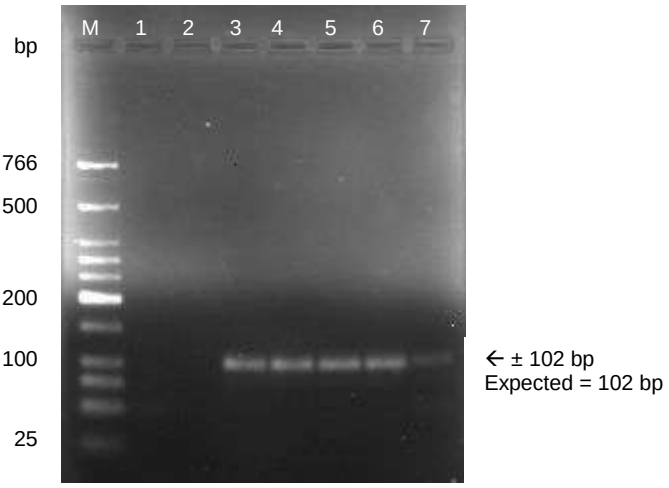

Figure 3.1: Analysis of RT-PCR products of AHSV RNA of OVIA serotypes 3, 7 and the negative control using VP7 OIE primers to amplify a 102 bp product of the genome segment encoding VP7. A 2.5% agarose gel was pre-stained with ethidium bromide. Lane M – New England Biolabs® Low Molecular Weight DNA Ladder ; Lanes 1 and 2 – OVIAC; Lanes 3 and 4 – OVIA3; Lanes 5 and 6 – OVIA7; Lane 7 – No template control.

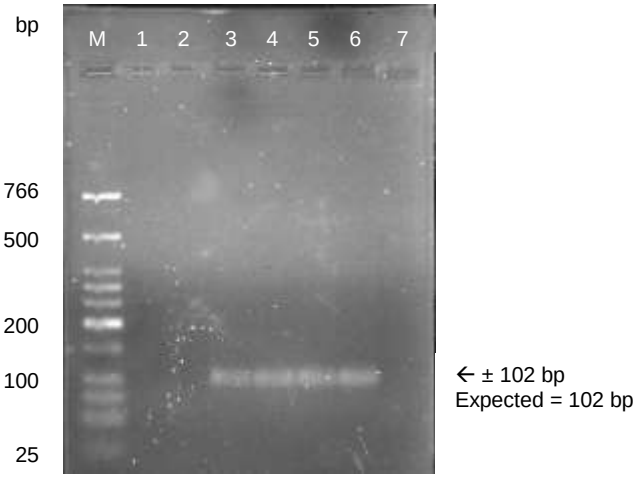

Figure 3.2: Analysis of RT-PCR products of AHSV RNA of OVIA serotypes 1, 2, 8 and the negative control using VP7 OIE primers to amplify a 102 bp product of the genome segment encoding VP7. A 2.5% agarose gel was pre-stained with ethidium bromide. Lane M – New England Biolabs® Low Molecular Weight DNA Ladder ; Lane 1 – OVIAC; Lane 2 – OVIA1; Lanes 3 and 4 – OVIA2; Lanes 5 and 6 – OVIA8; Lane 7 – No template control.

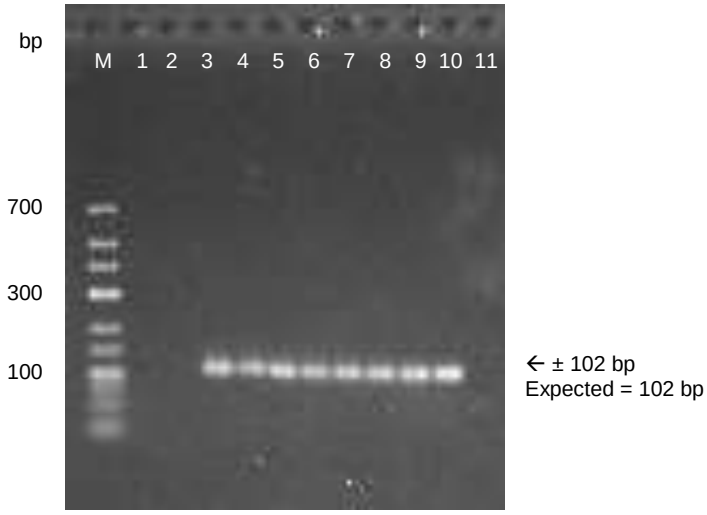

Figure 3.3: Analysis of RT-PCR products of AHSV RNA of OVIA serotypes 4, 5, 6, 9 and the negative control using VP7 OIE primers to amplify a 102 bp product of the genome segment encoding VP7. A 2.5% agarose gel was pre-stained with ethidium bromide. Lane M – Fermentas O'GeneRuler™ Low Range DNA Ladder; Lanes 1 and 2 – OVIAC; Lanes 3 and 4 – OVIA4; Lanes 5 and 6 – OVIA5; Lanes 7 and 8 – OVIA6; Lanes 9 and 10 – OVIA9; Lane 11 – No template control.

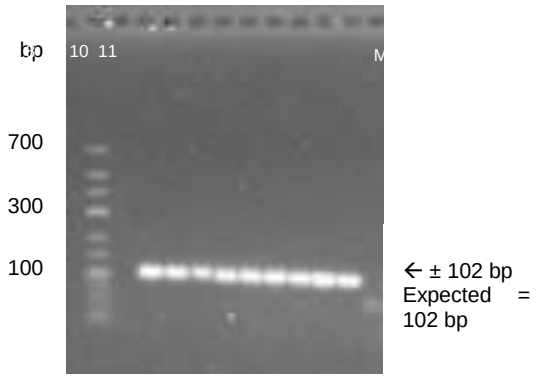

Figure 3.4: Analysis of RT-PCR products of AHSV OVIB serotypes 1-9 and the negative control using VP7 OIE primers to amplify a 102 bp product of the genome segment encoding VP7. A 2.5% agarose gel was pre-stained with ethidium bromide. Lane M – Fermentas O'GeneRuler™ Low Range DNA Ladder; Lane 1 – OVIBC; Lane 1 – OVIB1; Lane 3 – OVIB2; Lane 4 – OVIB3; Lane 5 – OVIB4; Lane 6 – OVIB5; Lane 7 – OVIB6; Lane 8 – OVIB7; Lane 9 – OVIB8; Lane 10 – OVIA9; Lane 11 – No template control.

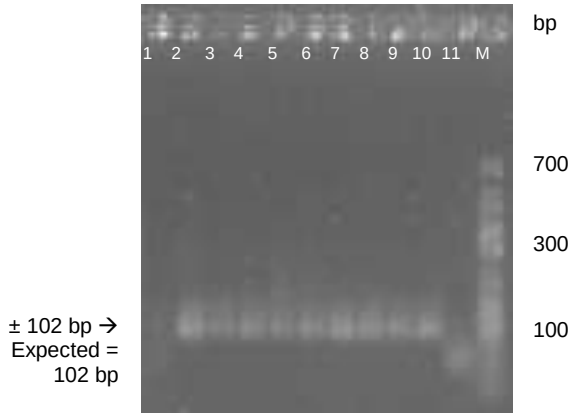

Figure 3.5: Analysis of RT-PCR products of AHSV NICD serotypes 1-9 and the negative control using VP7 OIE primers to amplify a 102 bp product of the genome segment encoding VP7. A 2.5% agarose gel was pre-stained with ethidium bromide. Lane 1 – NICDC; Lane 1 – NICD1; Lane 3 – NICD2; Lane 4 – NICD3; Lane 5 – NICD4; Lane 6 – NICD5; Lane 7 – NICD6; Lane 8 – NICD7; Lane 9 – NICD8; Lane 10 – NICD9; Lane 11 – No template control; Lane M – Fermentas O'GeneRuler™ Low Range DNA Ladder.

3.3.3. Optimisation of the clade-specific primers and segment 10 primers for RT-PCR

Clade-specific primers were tested on serotypes 7 (Clade A), 8 (Clade B), and 9 (Clade C). Gradient PCRs revealed optimised conditions for each clade-specific primer and are summarised in Table 3.7.

Table 3.7: Optimisation of RT-PCRs through gradient PCRs using AHSV clade-specific primers.

Clade (serotypes)	Isolate	Tm (°C)
A (3, 7)	OVIA7	52.1-60.3
B (1, 2, 8)	OVIA8	52.1-58.7
C (4, 5, 6, 9)	OVIA9	52.1-57.1

3.3.3.1. Clade A (serotype 7, OVIA, AF/AR primer pair)

The higher, more defined melt peaks are located between the annealing temperatures of 52.1°C and 60.3°C (Figure 3.6) with approximately 320 bp amplicons (expected size of 324 bp) produced to an annealing temperature of 63.8°C (Figure 3.7). The "smearing" seen in Figure 3.7 is likely due to the proliferation of product at the lower annealing temperatures. The additional bands may be due to the degeneracy of the primers. For Clade A, the raw melt data is displayed in panel A and the HRM curves, after normalisation, are presented in panel B. Only the HRM curves are presented in subsequent figures.

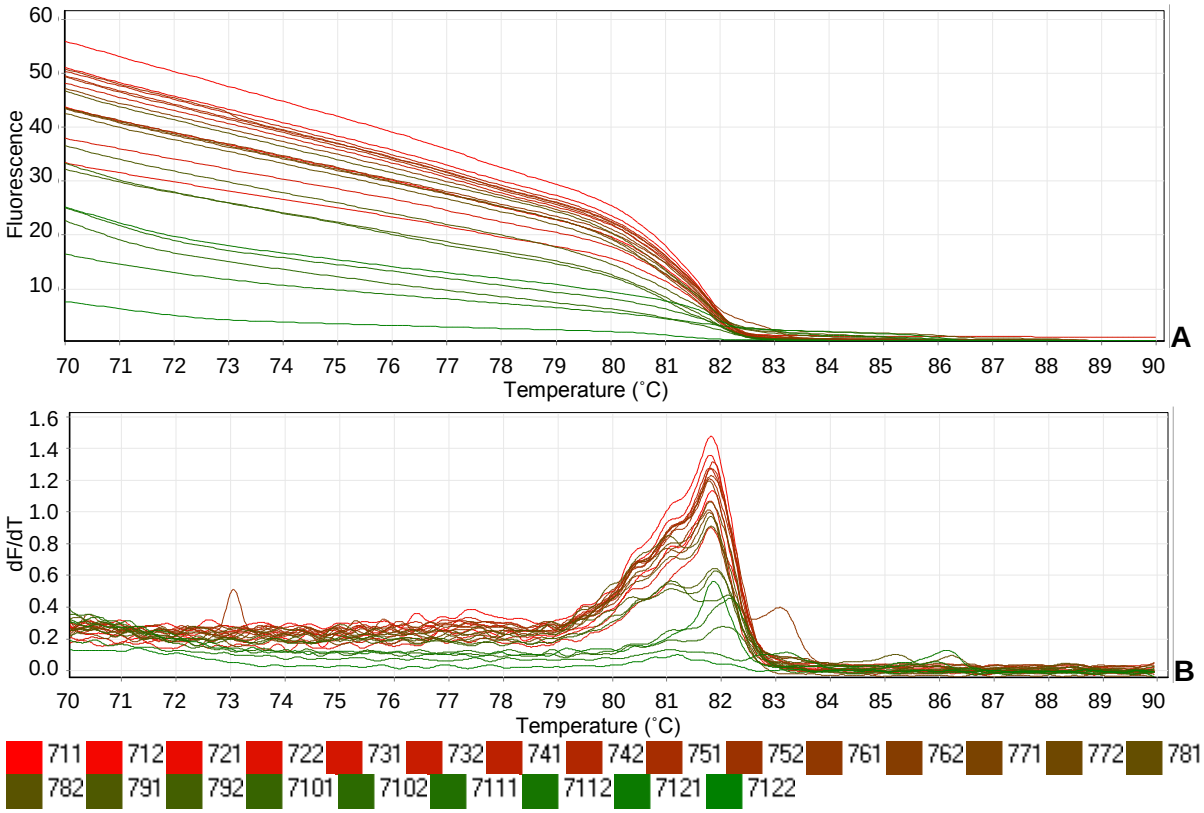

Figure 3.6: Melt analysis of the amplification of AHSV serotype 7 of the OVIA set as an isolate representative of Clade A using its clade-specific primer pair, AF and AR. A – melt curve; B – dF/dT (rate of change of fluorescence with respect to temperature) of melt curve. 711-7122 – increments in annealing temperature 52.1-64.2°C (Table 3.5).

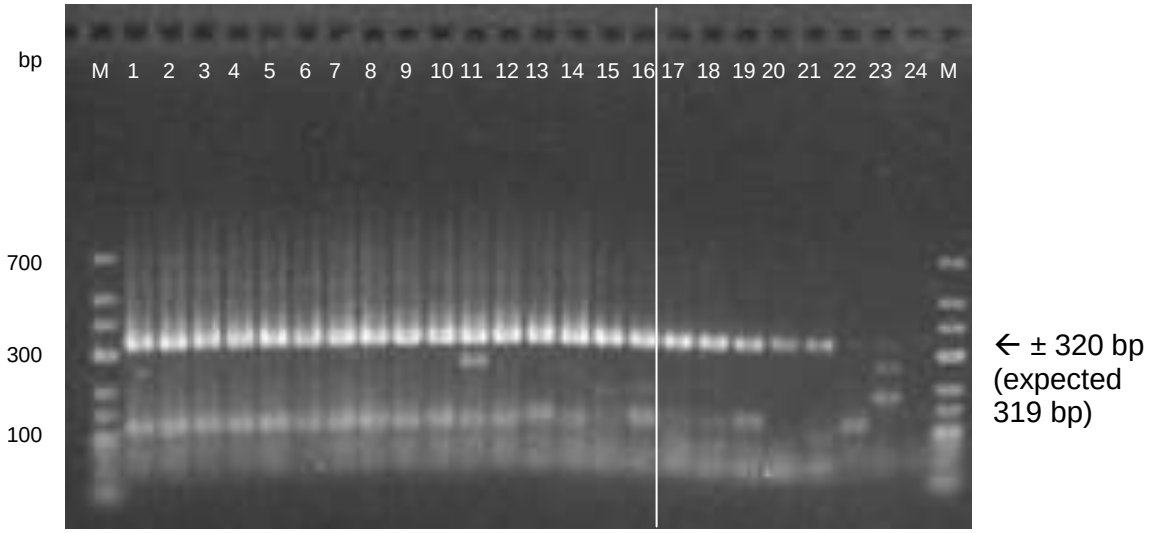

Figure 3.7: Analysis of gradient RT-PCR products of AHSV serotype 7 of the OVIA set using primer pair AF and AR to amplify a 319 bp product. A 2.5% agarose gel was pre-stained with ethidium bromide. Lane M – Fermentas O'GeneRuler™ Low Range DNA Ladder; Lane 1-24 – 711-7122 (Table 3.5 and Figure 3.6). The white line indicates the appropriate temperature cut off.

3.3.3.2. Clade B (serotype 8, OVIA, BF/BR primer pair)

Higher and clearer melt peaks were observed at temperatures of 52.1-58.7°C (Figure 3.8). The melt peaks for annealing temperatures greater than 58.7°C started to develop 'shoulders' and the peaks broadened to form double peaks. This produced two extra bands of approximately 680 and 350 bp (expected size of 676 and 347 bp respectively) on the agarose gel (Figure 3.9) and indicated the unsuitability of an annealing temperature greater than 60°C.

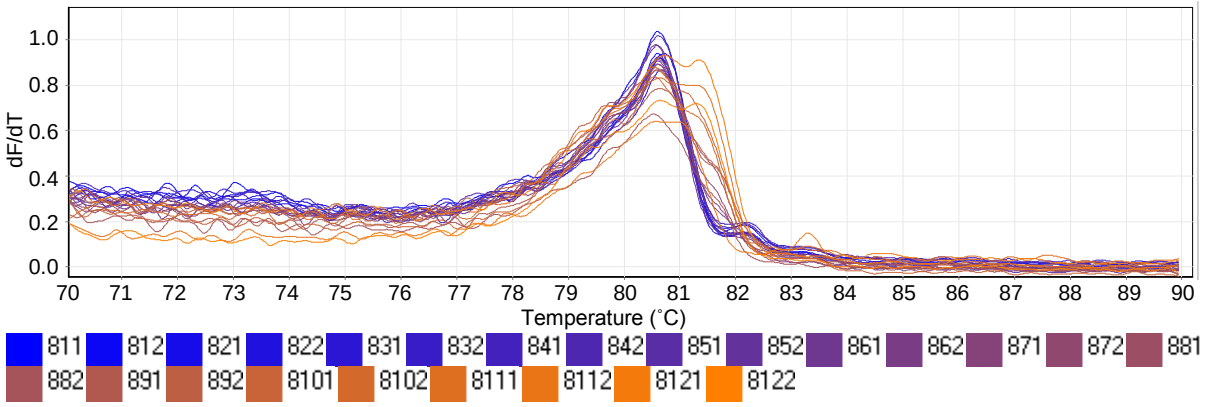

Figure 3.8: Melt analysis of the amplification of AHSV serotype 8 of the OVIA set as an isolate representative of Clade B using its clade-specific primer pair, BF and BR. dF/dT (rate of change of fluorescence with respect to temperature) of melt curve. 811-8122 – increments in annealing temperature 52.1-64.2°C (Table 3.5).

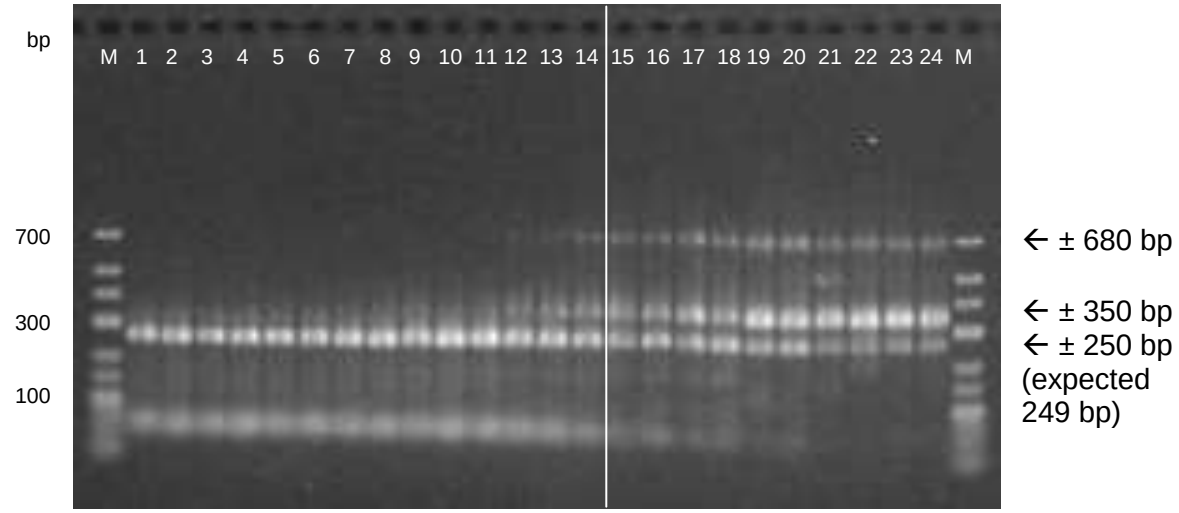

Figure 3.9: Analysis of gradient RT-PCR products of AHSV serotype 8 of the OVIA set using primer pair BF and BR to amplify a 249 bp product. A 2.5 % agarose gel was post-stained with ethidium bromide. Lane M – Fermentas O'GeneRuler™ Low Range DNA Ladder; Lane 1-24 – 811-8122 (See Table 3.5 and Figure 3.8). The white line indicates the appropriate temperature cut off.

3.3.3.3. Clade C (serotype 9, OVIA, CF/CR primer pair)

Products were observed at annealing temperatures up to 60.3°C (Figure 3.10). However, the more defined and higher melt peaks were discernible between 52.1°C and 57.1°C (Figure 3.11).

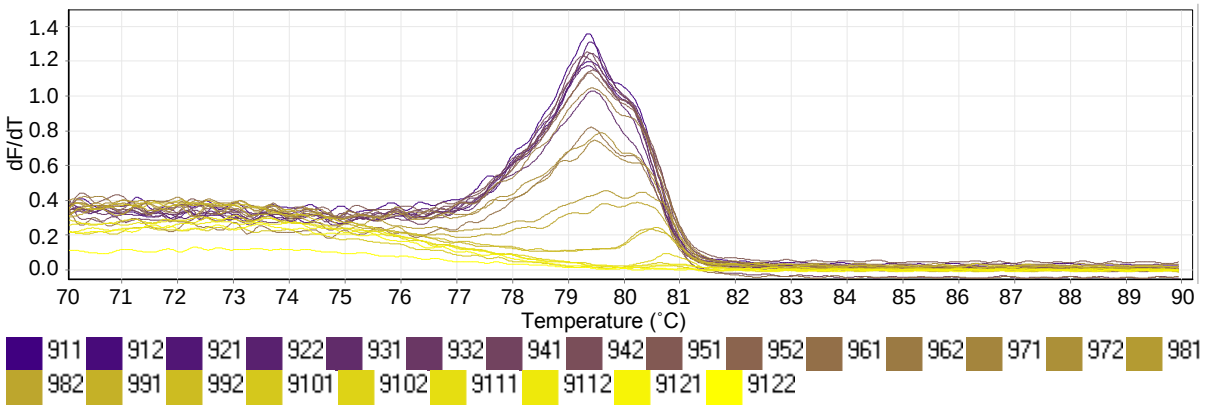

Figure 3.10: Melt analysis of the amplification of AHSV serotype 9 of the OVIA set as an isolate representative of Clade C using its clade-specific primer pair, CF and CR. dF/dT (rate of change of fluorescence with respect to temperature) of melt curve. 911-9122 – increments in annealing temperature 52.1-64.2°C (Table 3.5).

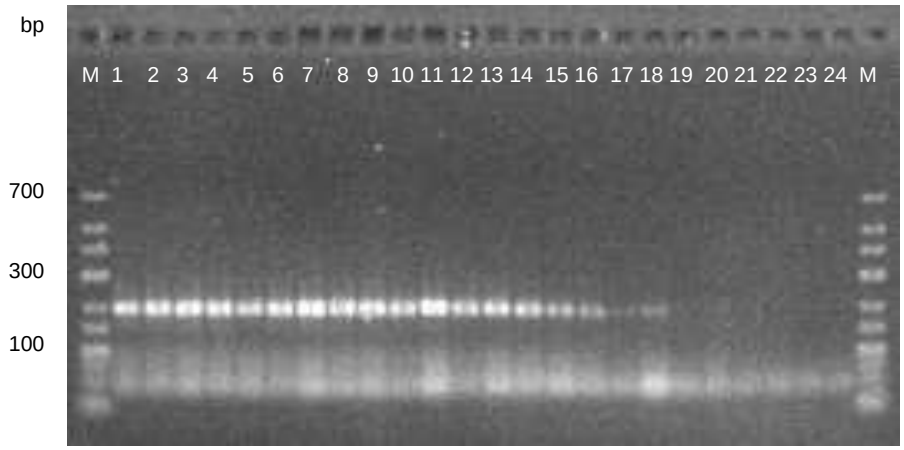

Figure 3.11: Analysis of gradient RT-PCR products of AHSV serotype 9 of the OVIA set using primer pair CF and CR to amplify a 189 bp product. A 2.5 % agarose gel was post-stained with ethidium bromide. Lane M – Fermentas O'GeneRuler™ Low Range DNA Ladder; Lane 1-24 – 911-9122 (See Table 3.5 and Figure 3.10). The white line indicates the appropriate temperature cut off.

3.3.3.4. Optimisation of segment 10 primers (10F and 10R)

Primer concentrations of 800 nM resulted in the most pronounced melt peaks and for all of the temperatures (Figure 3.12). However, primer concentrations of 400 nM gave adequate amplification products up to 61˚C. Primer concentrations of 200 nM, the recommended concentration of the KAPA protocol gave less than satisfactory results (KAPA, 2012).

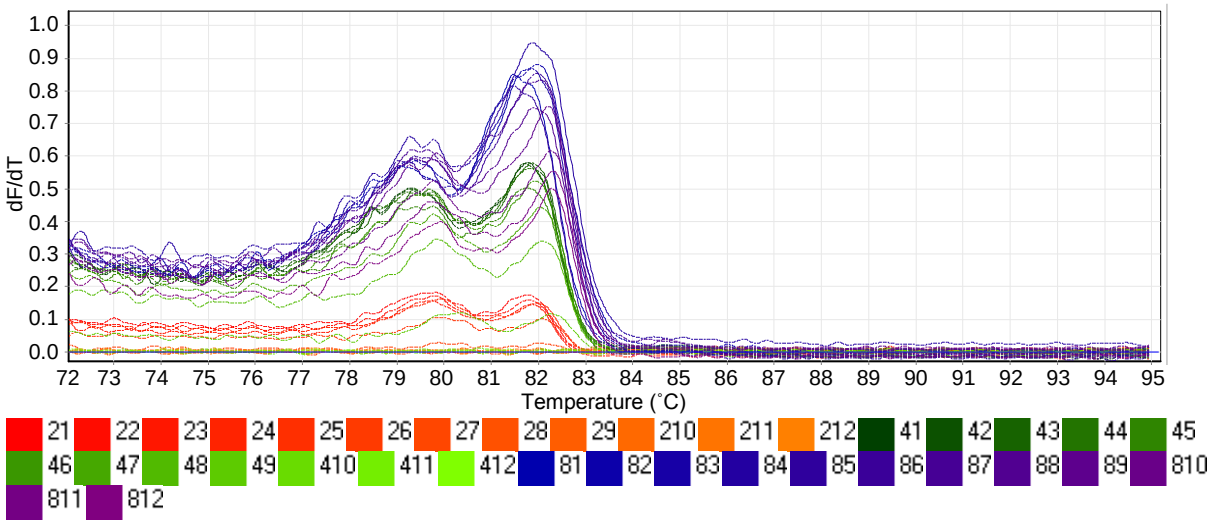

Figure 3.12: Melt analysis of the amplification of AHSV serotype 1 of the OVIB set using primer pair 10F and 10R to determine optimum primer concentration. dF/dT (rate of change of fluorescence with respect to temperature) of melt curve. 2 – 200 nM; 4 – 400 nM; 8 – 800 nM. 1-12 – increments in annealing temperature 55.1-66.2°C (Table 3.6).

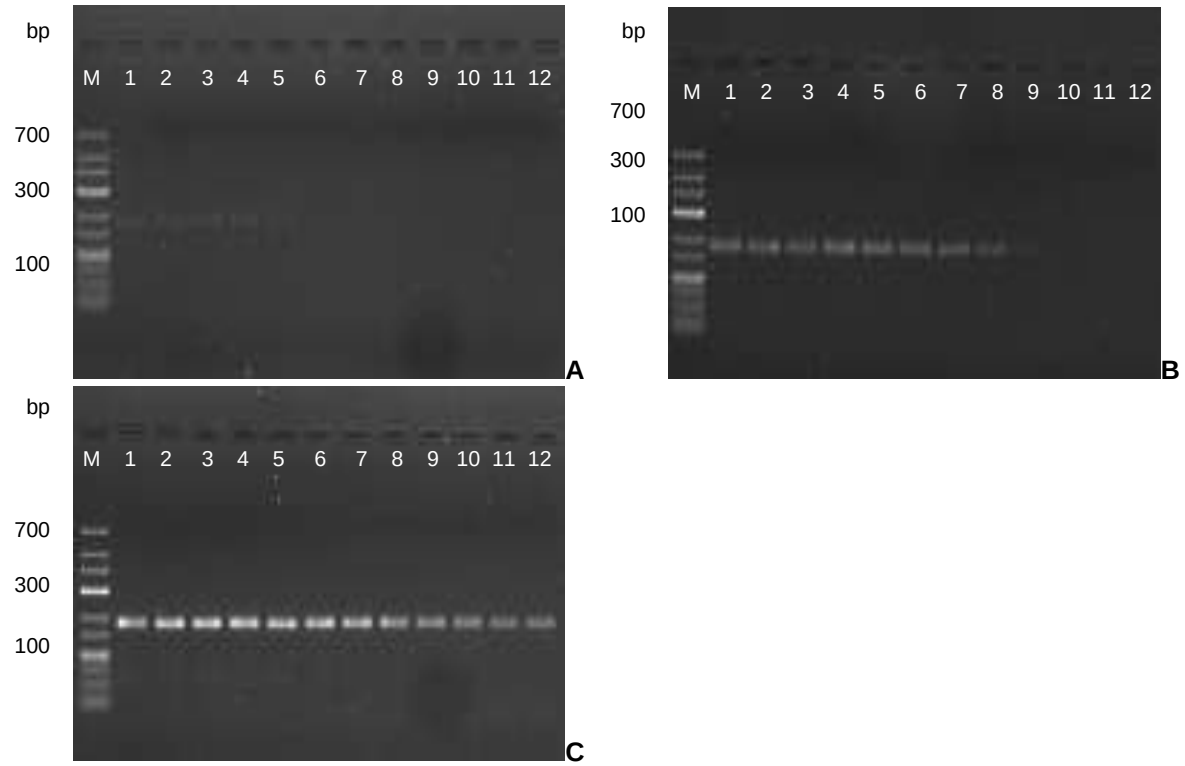

Figure 3.13: Analysis of gradient RT-PCR products of AHSV serotype 1 of the OVIB set using primer pair 10F and 10R to determine optimum primer concentration and amplify a 181 bp product. A 2.5 % agarose gel was post-stained with ethidium bromide. Panel A – 200 nM primer concentration; Panel B – 400 nm primer concentration; Panel C – 800 nM primer concentration. Lane M – Fermentas O'GeneRuler™ Low Range DNA Ladder; Lane 1-12 – 55.1-66.2˚C (See Table 3.6 and Figure 3.12).

3.3.4. One-step vs. two-step RT-PCR protocol

The one-step protocol was tested on serotype 3 isolates of the OVIA, OVIB and NICD sets using Clade A-specific primers, AF and AR. All isolates produced amplification products and melted accordingly. The C_T values are all within three cycles of each other and are below 20. All of the samples reached maximum fluorescence. However, the disparity between the individual isolates' duplicates was noted (Figure 3.14).

All of the isolates produced amplification products for the two-step protocol and melted accordingly in the same manner as the one-step protocol. The C_T values for all three samples and the duplicates are again within three cycles of each other. The C_T values are approximately five to six cycles later in the two-step protocol, but are below 30, with all samples reaching maximum fluorescence. However, in this case, the duplicates of each isolate were notably more synchronised than the one-step protocol represented in Figure 3.15.

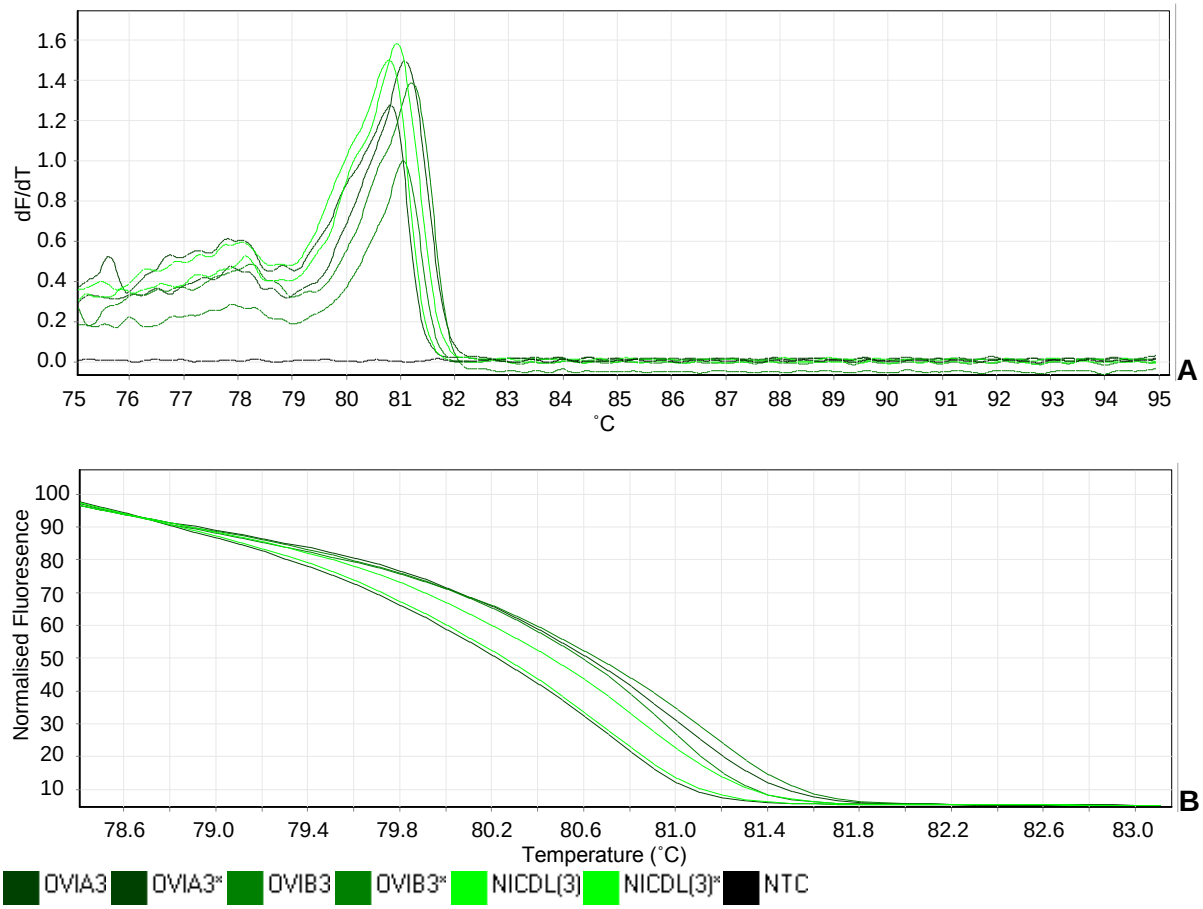

Figure 3.14: Amplification and High Resolution Melt of RNA of serotype 3 isolates of the OVIA, OVIB and NICD sets using clade A-specific primers AF/AR and a one-step protocol. A – dF/dT (rate of change of fluorescence with respect to time) of the melt curve; B – normalised High Resolution Melt analysis. OVIA3 – serotype 3 of OVIA set; OVIB3 – serotype 3 of OVIB set; NICDL(3) – serotype 3 of NICD set; NTC – no template control; * represents duplicates.

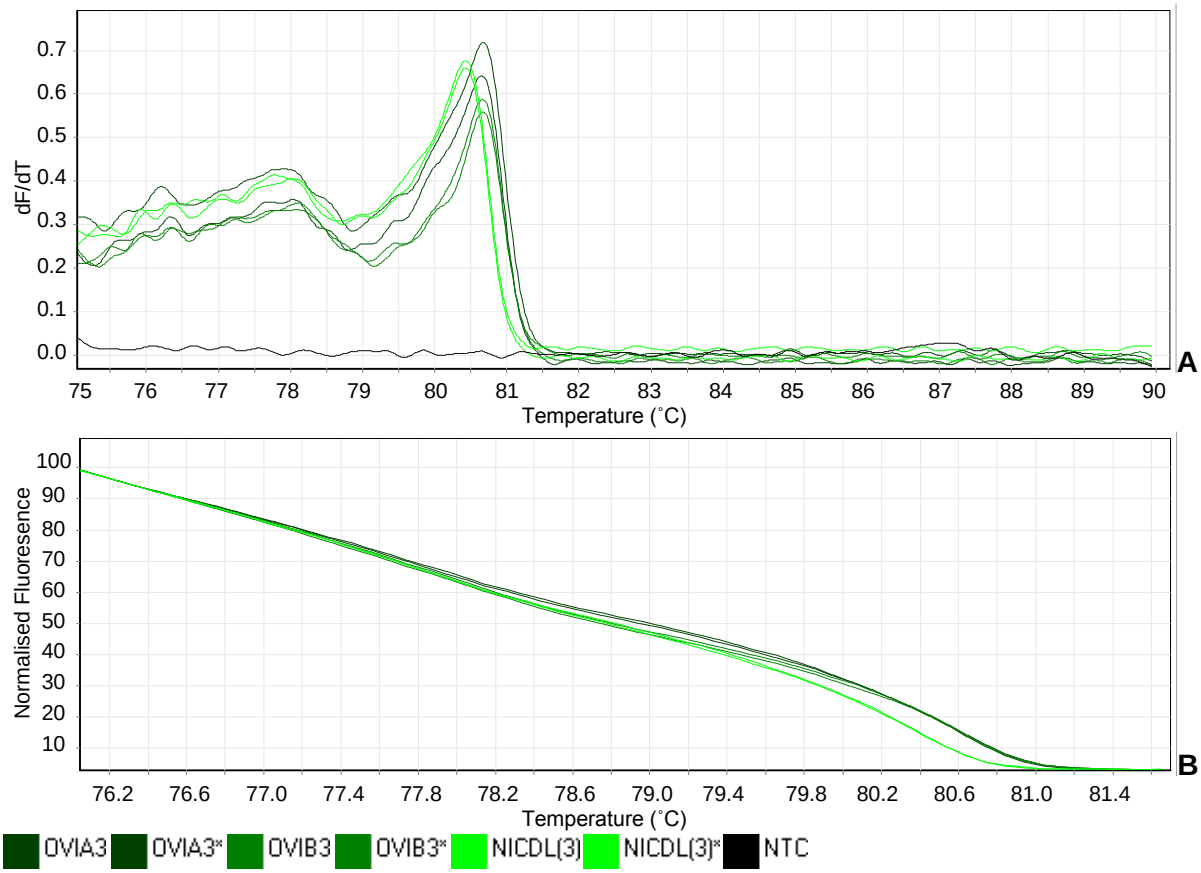

Figure 3.15: Amplification and High Resolution Melt of cDNA of serotype 3 isolates of the OVIA, OVIB and NICD sets using clade A-specific primers AF/AR and a two-step protocol. A - dF/dT (rate of change of fluorescence with respect to temperature) of the melt curve; B – normalised High Resolution Melt analysis. OVIA3 – serotype 3 of OVIA set; OVIB3 – serotype 3 of OVIB set; NICDL(3) – serotype 3 of NICD set; NTC – no template control; * represents duplicates.

3.3.5. Influence of RNA template concentration

Concentrations of total RNA ranging from 0.5 to 50 ng/µL were tested in a two-step protocol to ascertain their influence on the downstream HRM analysis. Despite some difference in the melt peak height related to the difference in starting concentration, all of the isolates are clearly distinguishable with the HRM analysis.

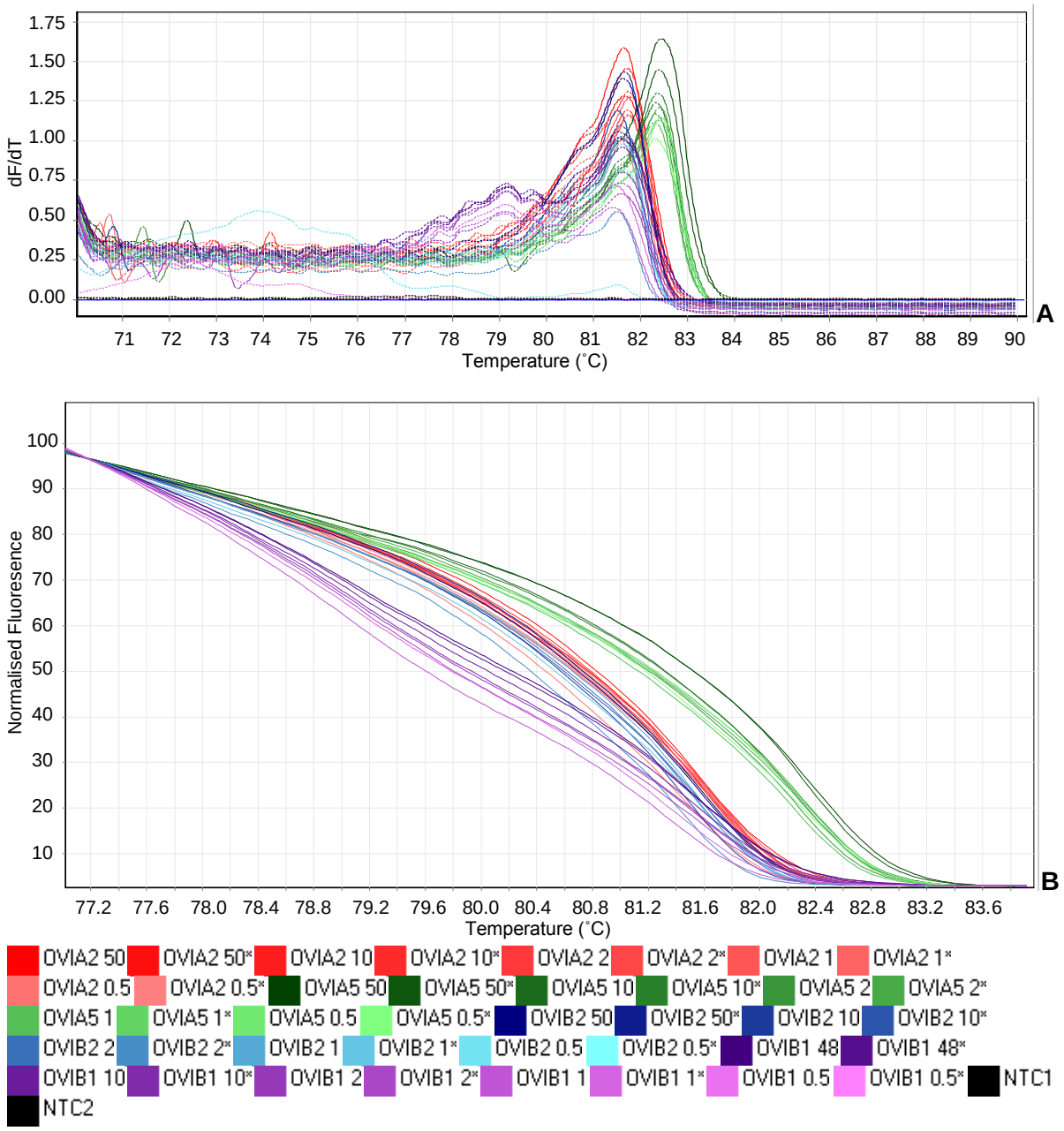

Figure 3.16: High Resolution Melt of cDNA of from varying concentrations of template total RNA from OVIA2, OVIA5, OVIB1 and OVIB2 to assess the influence of starting RNA concentration on HRM analysis using segment 10 primers 10F/10R and a two-step protocol. A – dF/dT (rate of change of fluorescence with respect to temperature) of the melt curve; B – High Resolution Melt analysis. OVIA2 – serotype 2 of OVIA set; OVIA5 – serotype 5 of OVIA set; OVIB1 – serotype 1 of OVIB set; OVIB2 – serotype 2 of OVIB set; NTC – no template control; 50, 10, 2, 1 and 0.5 refer to the starting concentration of total RNA in ng/µL; * represents duplicates.

3.3.6. Identification of anomalies

During routine testing of the primers, a number of anomalies became apparent. cDNA derived from RNA for isolates of Clade B serotypes 1, 2 and 8 were tested using their clade-specific primers, BF and BR (data not shown). cDNA from serotype 1 from the OVIA set did not amplify; neither did cDNA from either serotype 2 isolate of the OVIA and OVIB set.

Serotype 1 RNA of the OVIB set and serotype 8 RNA of both the OVIA and OVIB set amplified well and produced unique, but disparate, melt profiles (data not shown). Both serotype 2 isolates were therefore identified as possible anomalies. It is interesting to note that both serotype 2 isolates from the OVI sets failed to amplify with the Clade B-specific primers BF and BR. The possibility that a simple mix up would be responsible was considered. However, the likelihood that both serotype 2 isolates, from each OVI set, would be mixed up seems highly unlikely. The inability of both isolates labelled serotype 2 to amplify products with the primer pair BF and BR indicates the possibility of an anomaly requiring further investigation as the implications are serious and noteworthy.

cDNA from isolates of serotypes 4, 5, 6 and 9 (Clade C) were also subjected to their clade-specific primers, CF and CR. Of the OVIB set, cDNA derived from RNA from all isolates amplified. Due to the non-amplification of serotype 2 cDNA of the OVIB set (data not shown), these isolates were included in this preliminary Clade C analysis. cDNA from all serotypes of Clade C of the OVIB set amplified with CF/CR primers (Figure 3.17) and produced products of approximately 191 bp (expected size of 189 bp, Figure 3.18). The melt curves of serotypes 2 (purple; panel A) and 6 (red) gave almost identical melt profiles, with matching temperatures for their peaks, and it was concluded that the isolate labelled serotype 2 may be serotype 6. The melt curves of serotypes 5 (orange) and 9 (green) may appear similar, but do not have identical melt peak temperatures, nor are their profiles similar.

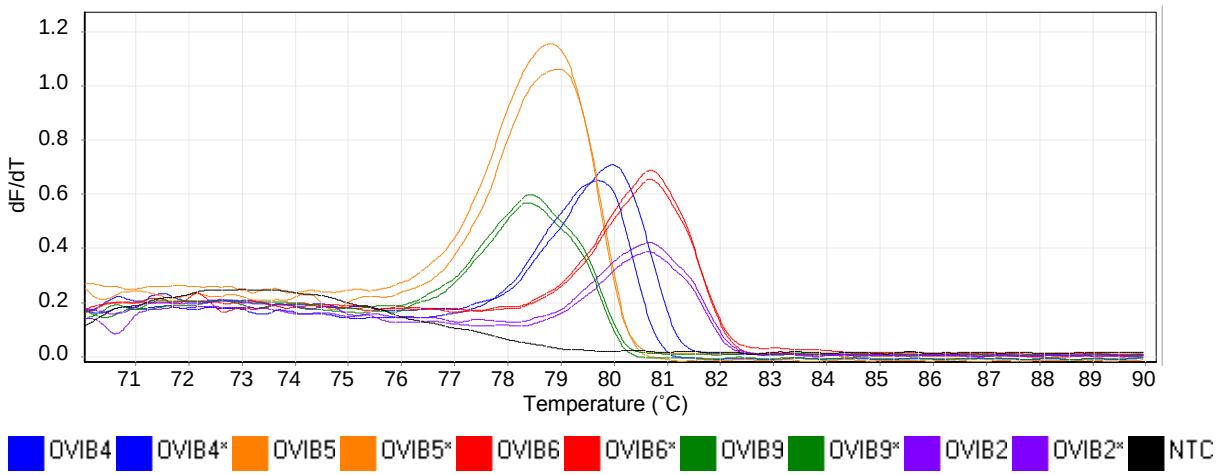

Figure 3.17: Rate of change of fluorescence with respect to temperature of the genome segment encoding VP2 of Clade C isolates using the CF/CR primer pair. A – amplification curve; B – Melt curve; C – dF/dT of melt curve. OVIB4 – Serotype 4 of OVIB set; OVIB5 – Serotype 5 of OVIB set; OVIB6 – Serotype 6 of OVI B set; OVIB9 – Serotype 9 of OVIB set; NTC – No template control; * represents duplicates.

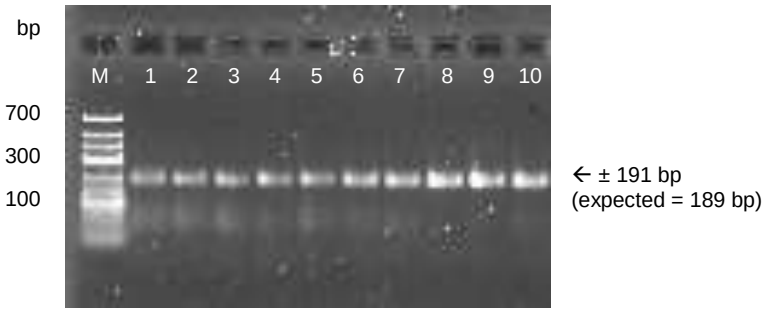

Figure 3.18: Analysis of RT-PCR products of Clade C isolates using the CF/CR primer pair. A 2.5% agarose gel was post-stained with ethidium bromide. Lane M: Fermentas O'GeneRuler™ Low Range DNA Ladder. Lanes 1, 2 – serotype 4 of OVIB set; Lanes 3, 4 – serotype 5 of OVIB; Lanes 5, 6 – serotype 6 of OVIB set; Lanes 7, 8 – serotype 9 of OVIB set; Lanes 9, 10 – the isolates labelled serotype 2 of the OVIB set.

3.3.7. Serotype-specific primer analysis

3.3.7.1. Serotype 2

Of the cDNA derived from RNA for OVIA, OVIB and NICD isolates of serotype 2, only the NICD isolate produced a product of approximately 1100 bp (expected size of 1098 bp, Figure 3.19). All of the isolates produced a barely visible product of approximately 300 bp.

3.3.7.2. Serotype 3

Apart from an OVIB duplicate RNA sample failing to amplify, bands of approximately the correct size of 775 bp were shown on the agarose gel analysis of the PCR products (expected size of 751 bp, Figure 3.20).

3.3.7.3. Serotype 4

Amplification products of approximately 1290 bp were detected for OVIA and OVIB isolates (expected size of 1267 bp, Figure 3.21), but no equivalent product was detected for the cDNA of serotype 4 of NICD set. Although not clearly visible, faint bands can be seen at approximately 450 bp.

3.3.7.4. Serotype 5

Using serotype 5-specific primers based on the genome segment encoding VP2 (after Maan *et al.*, 2011a), cDNA of serotype 5 from OVIA failed to amplify, while cDNA of serotype 5 isolates from OVIB and NICD produced the amplification products of approximately 1200 bp (expected size of 1139 bp, Figure 3.22). All nine serotype-specific primers were used in an additional amplification of the OVIA serotype 5 isolate cDNA and produced amplification products only with the serotype 8-specific primers, suggesting that the isolate known as serotype 5 of the OVIA set was, in fact, serotype 8 (data not shown).

3.3.7.5. Serotype 6

Positive amplification of an approximately 1190 bp product (expected size of 1154 bp) occurred for all three sources of serotype 6 (OVIA, OVIB and NICD) with the serotype 6-specific primers. The serotype 6 isolate of the NICD set had a weaker amplification product of and an additional amplicon at approximately 300 bp (Figure 3.23).

3.3.7.6. Serotypes 1, 7, 8 and 9

cDNA of serotypes 1, 7, 8 and 9 did not give amplification products using the serotype-specific primers of Maan *et al.* (2011a). The primers were expected to produce amplicons of 1793 bp for serotype 1, 1426 bp for serotype 7, 1754 bp for serotype 8 and 1483 bp for serotype 9.

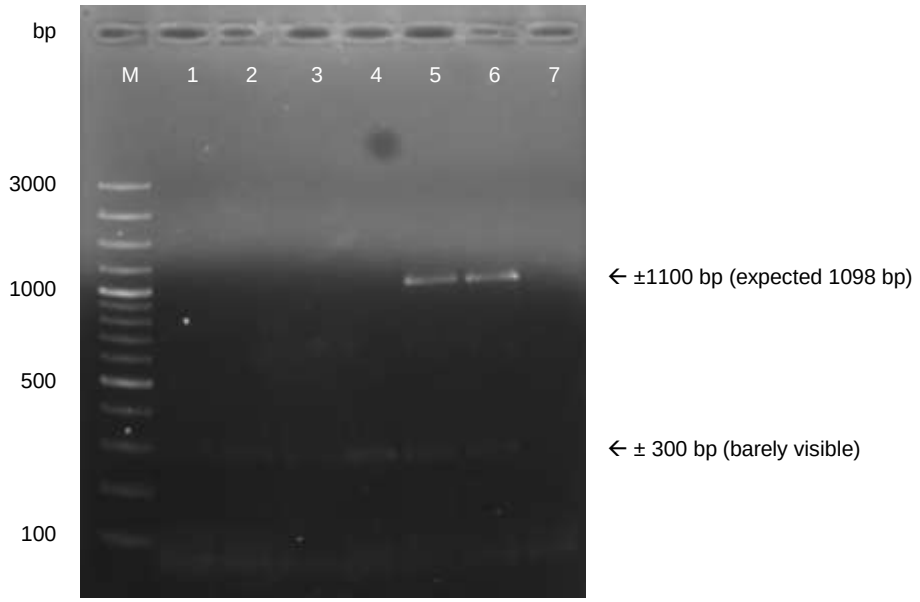

Figure 3.19: Analysis of serotype 2 isolates of OVIA, OVIB and NICD sets using serotype 2 specific primers (2.2F_NM and 2.2R_NM). A 1.2% agarose gel was pre-stained with ethidium bromide. The arrow shows the main product at approximately 1096 bp, the expected size being 1098 bp. Lane M - Fermentas O'GeneRuler™ 100 bp Plus DNA Ladder; Lane 1, 2 – OVIA2; Lane 3, 4 – OVIB2; Lane 5, 6 – NICDOD; Lane 7 – No template control.

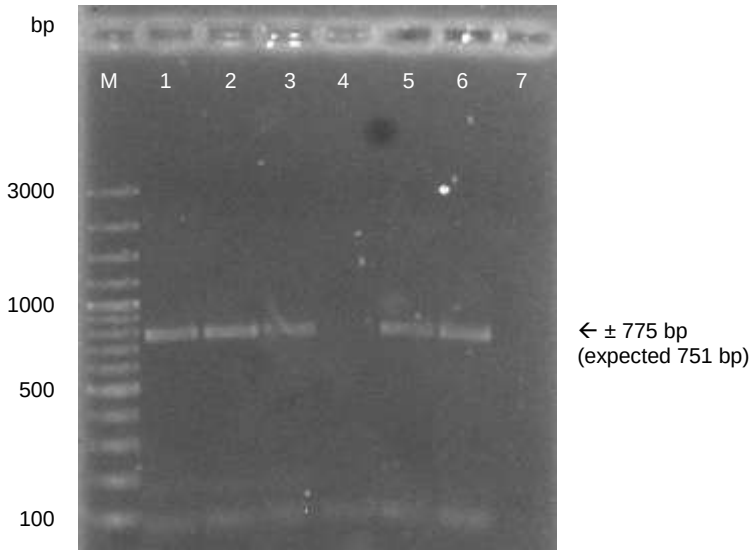

Figure 3.20: Analysis of serotype 3 isolates of OVIA, OVIB and NICD sets using serotype 3-specific primers (2.3F_NM and 2.3R_NM). A 1.2% agarose gel was post-stained with ethidium bromide. The arrow shows the main product at approximately 776 bp, the expected size being 751 bp. Lane M – Fermentas O'GeneRuler™ 100 bp Plus DNA Ladder; Lane 1, 2 – OVIA3; Lane 3, 4 – OVIB3; Lane 5, 6 – NICDL; Lane 7 – No template control.

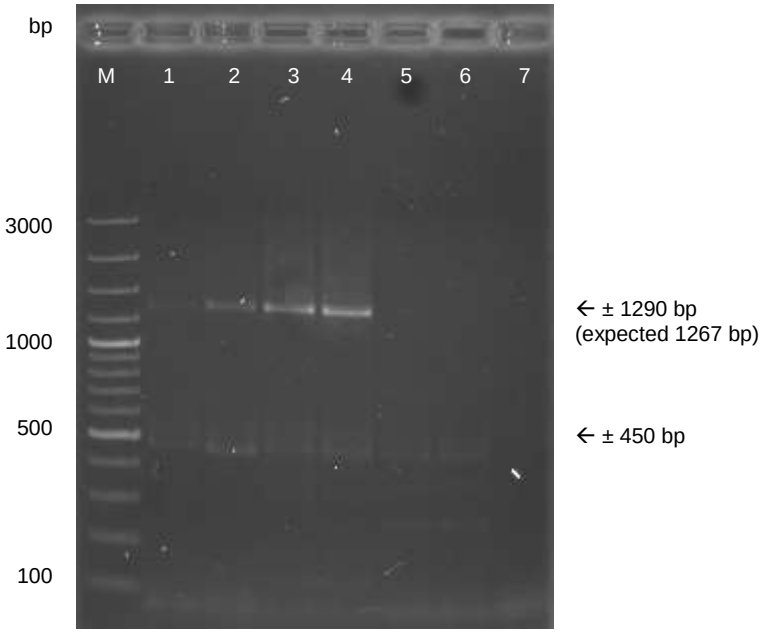

Figure 3.21: Analysis of serotype 4 isolates of OVIA, OVIB and NICD sets using serotype 4-specific primers (2.4F_NM and 2.4R_NM). A 1.2% agarose gel was post-stained with ethidium bromide. The arrow shows the main product at approximately 1288 bp, the expected size being 1267 bp. Lane M - Fermentas O'GeneRuler™ 100 bp Plus DNA Ladder; Lane 1, 2 – OVIA4; Lane 3, 4 – OVIB4; Lane 5, 6 – NICDV; Lane 7 – No template control.

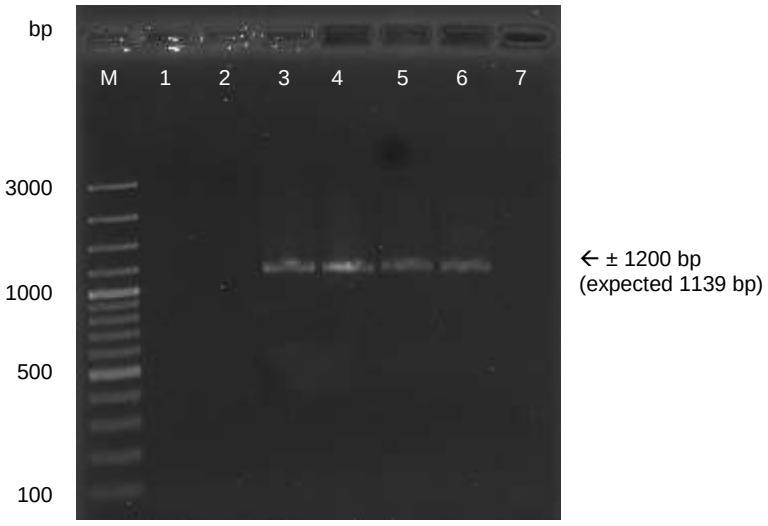

Figure 3.22: Analysis of serotype 5 isolates of OVIA, OVIB and NICD sets using serotype 5-specific primers (2.5F_NM and 2.5R_NM). A 1.2% agarose gel was post-stained with ethidium bromide. The arrow shows the main product at approximately 1288 bp, the expected size being 1267 bp. Lane M - Fermentas O'GeneRuler™ 100 bp Plus DNA Ladder; Lane 1, 2 – OVIA4; Lane 3, 4 – OVIB4; Lane 5, 6 – NICDV; Lane 7 – no template control.

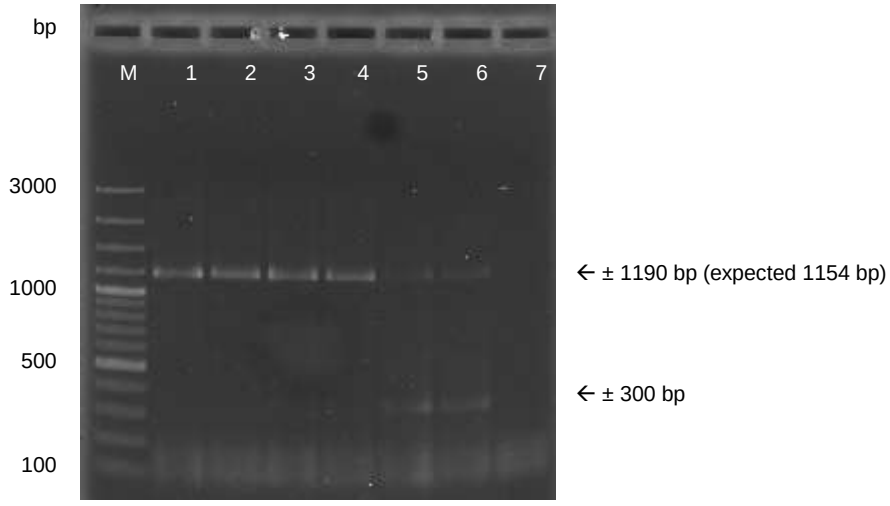

Figure 3.23: Analysis of serotype 6 isolates of OVIA, OVIB and NICD sets using serotype 6-specific primers (2.6F_NM and 2.6R_NM). A 1.2% agarose gel was post-stained with ethidium bromide. The arrow shows the main product at approximately 1190 bp, the expected size being 1154 bp. Lane M - Fermentas O'GeneRuler™ 100 bp Plus DNA Ladder; Lane 1, 2 – OVIA6; Lane 3, 4 – OVIB6; Lane 5, 6 – NICD114; Lane 7 – No template control.

3.3.8. Segment 10 analysis

Following the initial analysis of the serotypes per clade using the clade-specific primers, all of the isolates were analysed using the segment 10 primers, 10F and 10R. These primers were designed to separate the nine serotypes into three clades (Groenink, 2009). All 27 isolates would now be directly comparable in a single PCR run. It was envisaged that three melt profiles would develop and be easily distinguished. Failing that, identification of the three

clades might be possible through the genotyping capabilities of the Rotor-Gene™ 6000 Series Software. However, given the previously mentioned observation of serotype anomalies (Sections 3.3.6 and 3.3.7), the exercise was also performed in an attempt to further distil the serotype irregularity situation. Using AHSV cDNA, good melt curves were achieved (Figure 3.24) and there was good product retrieval (Figure 3.25). Serotype 1 of the OVIA set failed to amplify.

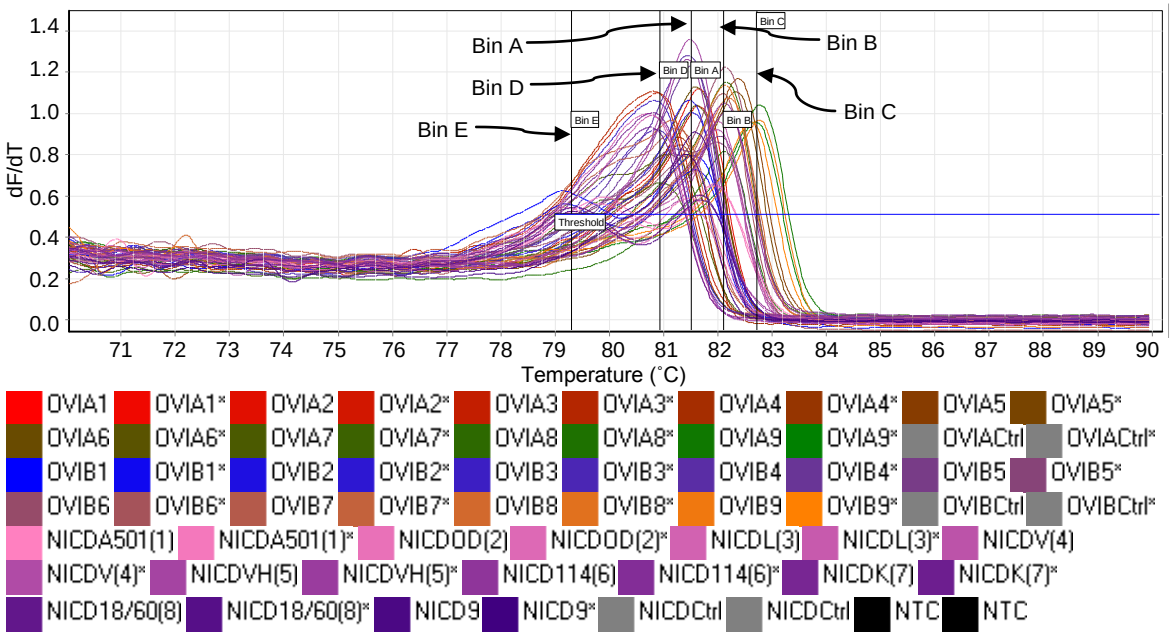

Figure 3.24: Amplification and High Resolution Melt of serotypes 1-9 of the OVIA, OVIB and NICD sets using the 10F and 10R primer pairs. dF/dT (rate of change of fluorescence with respect to temperature) of melt curve. Bins have been applied and defined by the user to identify important peaks and a threshold of 0.51 dF/dT and 75˚C was applied to exclude the pre-melt noise. OVIA1 – Serotype 1 of OVI A set; OVIA2 – Serotype 2 of OVI A set; OVIA3 – Serotype 3 of OVI A set; OVIA4 – Serotype 4 of OVI A set; OVIA5 – Serotype 5 of OVI A set; OVIA6 – Serotype 6 of OVI A set; OVIA7 – Serotype 7 of OVI A set; OVIA8 – Serotype 8 of OVI A set; OVIA9 – Serotype 9 of OVI A set; OVIAC – negative control; OVIB1 – Serotype 1 of OVI B set; OVIB2 – Serotype 2 of OVI B set; OVIB3 – Serotype 3 of OVI B set; OVIB4 – Serotype 4 of OVI B set; OVIB5 – Serotype 5 of OVI B set; OVIB6 – Serotype 6 of OVI B set; OVIB7 – Serotype 7 of OVI B set; OVIB8 – Serotype 8 of OVI B set; OVIB9 – Serotype 9 of OVI B set; OVIBC – negative control; NICD1 – Serotype 1 of NICD set; NICD2 – Serotype 2 of NICD set; NICD3 – Serotype 3 of NICD set; NICD4 – Serotype 4 of NICD set; NICD5 – Serotype 5 of NICD set; NICD6 – Serotype 6 of NICD set; NICD7 – Serotype 7 of NICD set; NICD8 – Serotype 8 of NICD set; NICD9 – Serotype 9 of NICD set; NICDC – negative control; NTC – No template control; * represents duplicates.

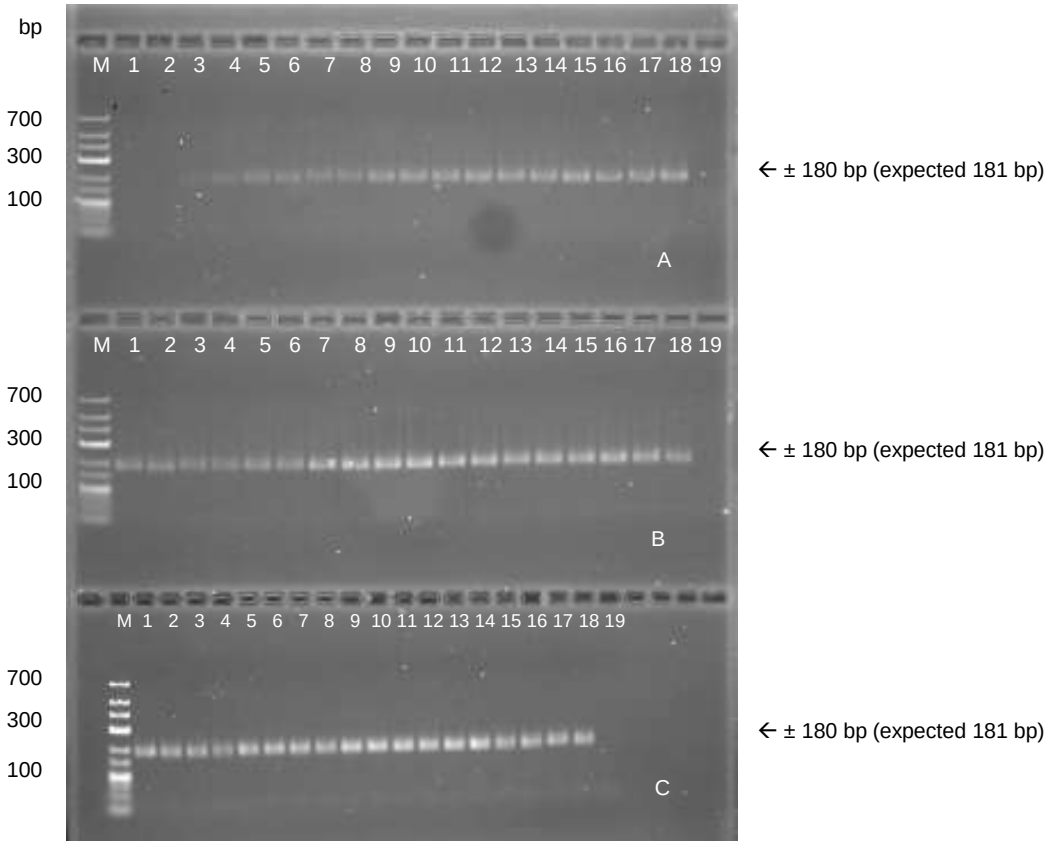

Figure 3.25: Analysis of RT-PCR products of all nine serotypes of OVIA, OVIB and NICD sets using segment 10 primers 10F and 10R. A 2.5% agarose gel was post-stained with ethidium bromide. A – OVIA set; B – OVIB set; C – NICD set. Lane M: Fermentas O'GeneRuler™ Low Range DNA Ladder. Lane 1, 2 - serotype 1; lane 3, 4 – serotype 2; lane 5, 6 – serotype 3; lane 7, 8 – serotype 4; lane 9, 10 – serotype 5; lane 11, 12 – serotype 6; lane 13, 14 – serotype 7; lane 15, 16 – serotype 8; lane 17, 18 – serotype 9, lane 19 – no template control.

All isolates amplified and plateaued with C_T values ranging from 17-24 (Figure 3.24). All are below a C_T value of 30 indicating adequate amounts of template (Corbett, 2006; KAPA, 2010). A negative control duplicate did have a positive fluorescence curve, but is substantially late and no amplification product was detected after gel electrophoresis (data not shown). At first glance, numerous melt profiles exist. Separating the profiles into their respective clades revealed the following:

OVIA3, OVIB3, NICD3 and NICD7 all have nearly identical melt peaks and profiles (Figure 3.26). Bin D was assigned to describe the peak for the Clade A isolates and the software was able to correctly call all but one of the isolates as Clade A (Table 3.8 – blue shading). The software relies on the user-defined 'bins' or melt temperature ranges, which isolate important peaks, and will assign samples to a bin based on this user-defined range.

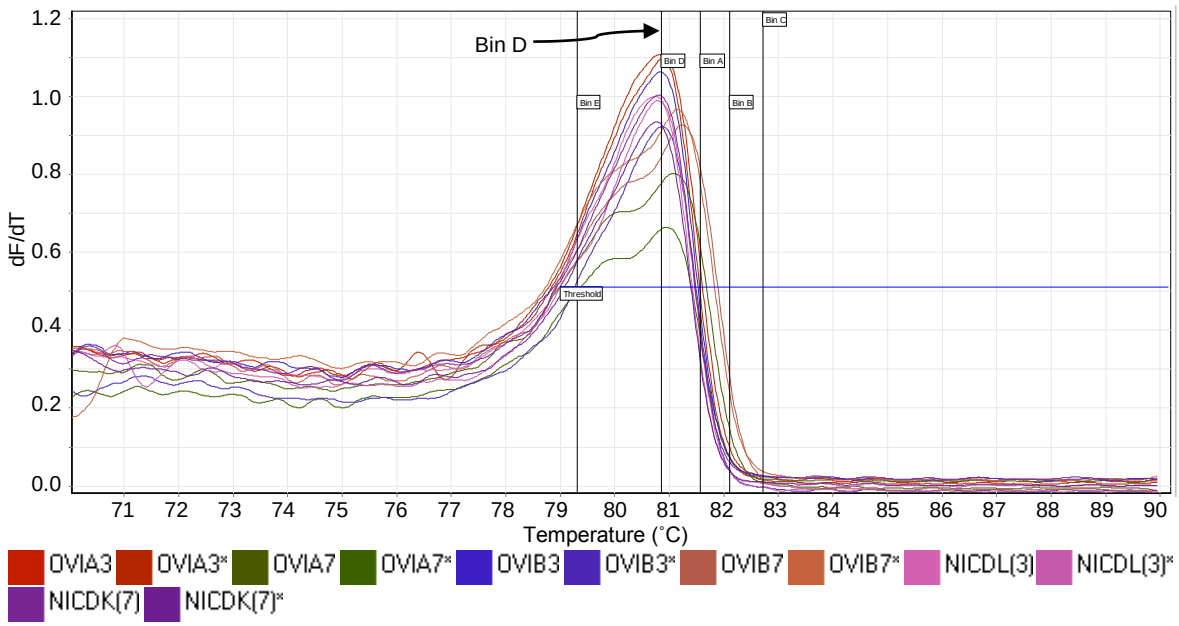

Figure 3.26: The High Resolution Melt analysis of the Clade A labelled isolates using the 10F and 10R primer pair. A melt threshold of 0.51 dF/dT and 75˚C was applied to exclude the pre-melt noise. Bins (melt regions) were defined and applied by the user to isolate important peaks.

Clade B labelled isolates' melt profiles are presented in Figure 3.27. OVIA1 cDNA failed to amplify. Considering that the cDNA of OVIA2 and OVIB2 did not amplify, and their near perfect singular assignment into Bin A in Figure 3.27, it is highly likely that they are not serotype 2, nor are they a Clade B isolate. OVIA8 and OVIB8 fall into Bin B, but not NICD 8. Both OVIA8 and OVIB8 were therefore suspected of being anomalies. OVIB1, NICD1, NICD2 and NICD8 all produced a melt profile with two peaks. Clade B is defined as having a peak in Bin A and E (Table 3.8, shaded red).

Clade C labelled isolates, when separated, are shown in Figure 3.28. At first glance, an untidy profile for Clade C appears. However, it is pertinent to note that all of these isolates fall into either Bin A, B or C exclusively, and not into any of the already defined genotypes for Clade A or B (i.e. Bin D and Bin A and E). When the phylogeny for the 10-190 bp region of segment 10 is re-examined (Figure 3.29), Clades A and B resolve into monophyletic clades, while Clade C is polyphyletic. This could account for the multiple melt profiles seen in Figure 3.28

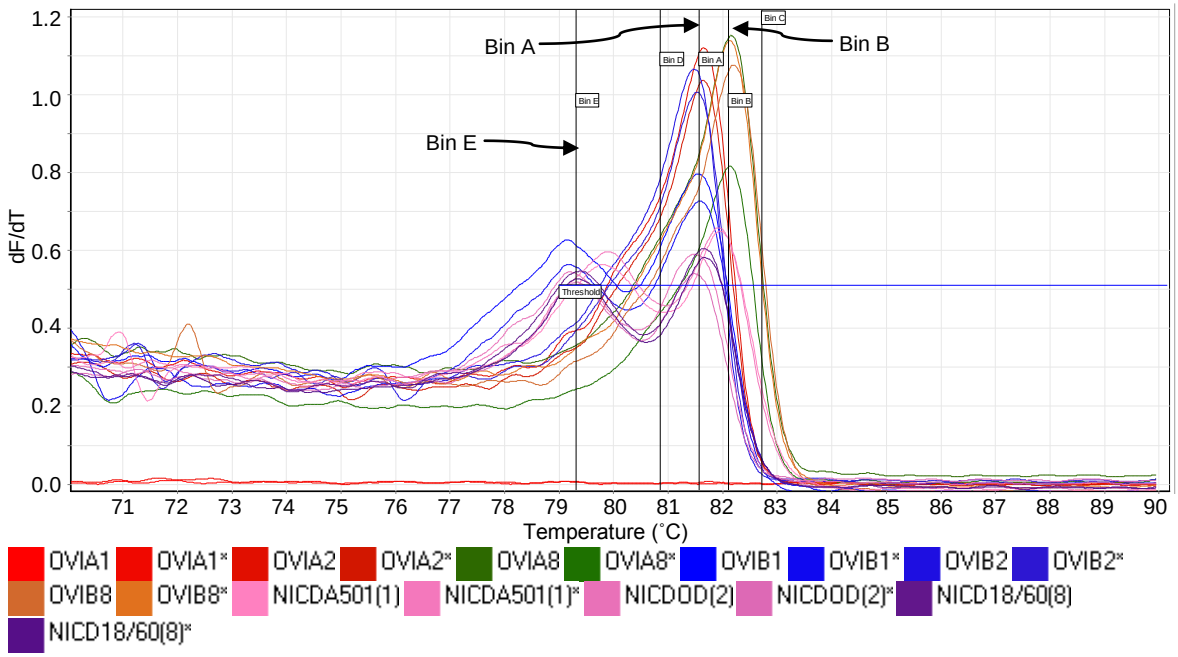

Figure 3.27: The High Resolution Melt analysis of the Clade B labelled isolates using the 10F and 10R primer pair. A melt threshold of 0.51 dF/dT and 75˚C was applied to exclude the pre-melt noise. Bins (melt regions) were defined and applied by the user to isolate important peaks.

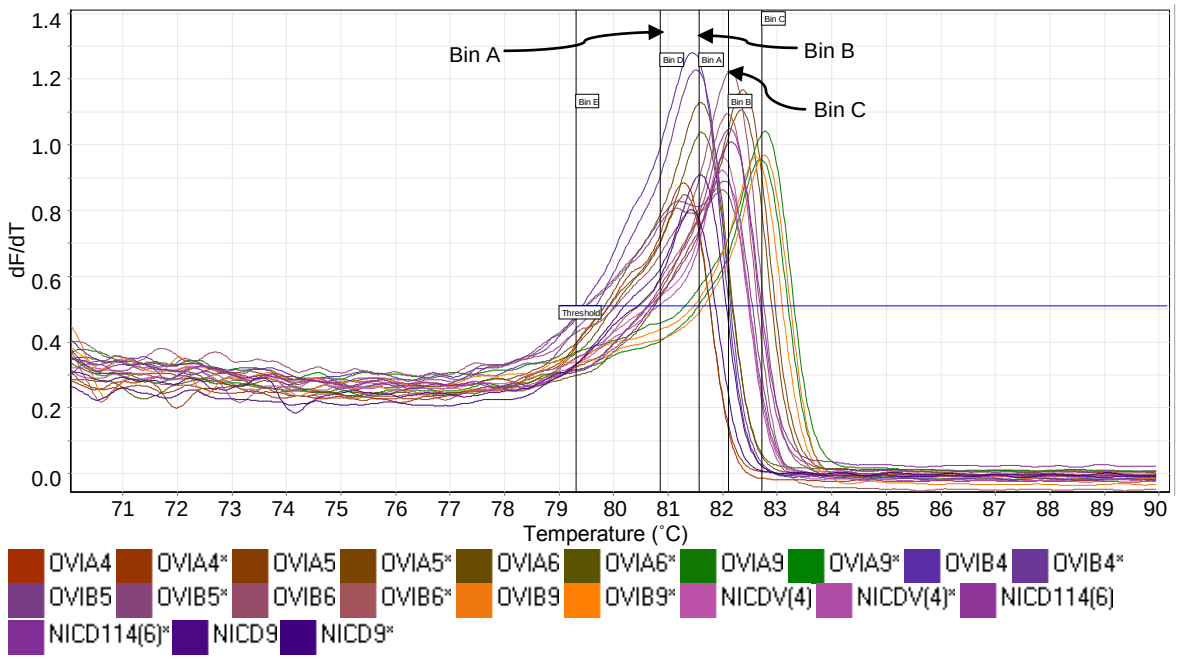

Figure 3.28: The High Resolution Melt analysis of the Clade C labelled isolates using the 10F and 10R primer pair. A melt threshold of 0.51 dF/dT and 75˚C was applied to exclude the pre-melt noise. Bins (melt regions) were defined and applied by the user to isolate important peaks.

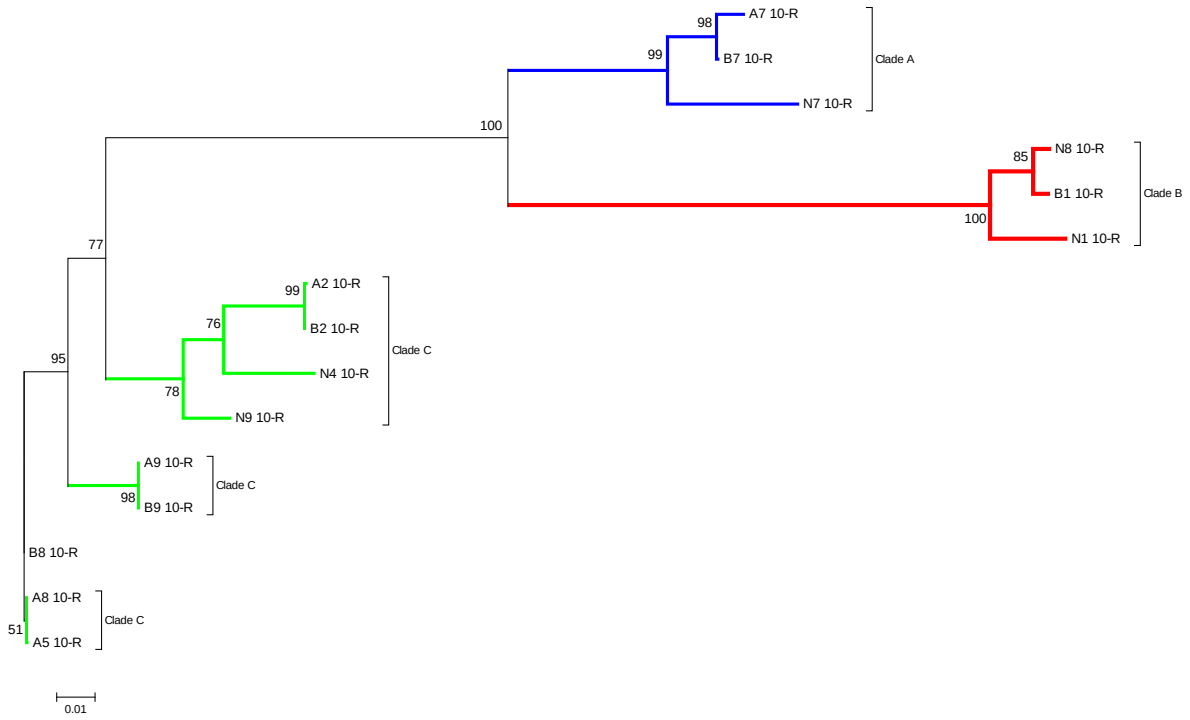

Figure 3.29: Phylogeny of the sequenced 10-190 bp region of AHSV segment 10 from the OVIA, OVIB and NICD sets showing clades A, B and C. Clade A is represented by the blue sub-tree, Clade B by the red sub-tree and Clade C by the green sub-tree. Sequences were aligned using ClustalX2 (Larkin et al., 2007) and the tree drawn using the neighbour-joining method of MEGA5 (Tamura et al., 2004; Tamura et al., 2011) with 1000 bootstrap replicates. Bootstrap percentages are shown on the nodes. The bar represents 0.01 substitutions per site (Felsenstein, 1985; Saitou & Nei, 1987).

It was clear that both serotype 2 isolates of the OVI sets were serotype 6 (Figure 3.30). The serotype 5 isolate of the OVIA set was very likely to be serotype 8 according to the melt curves in Figure 3.31.

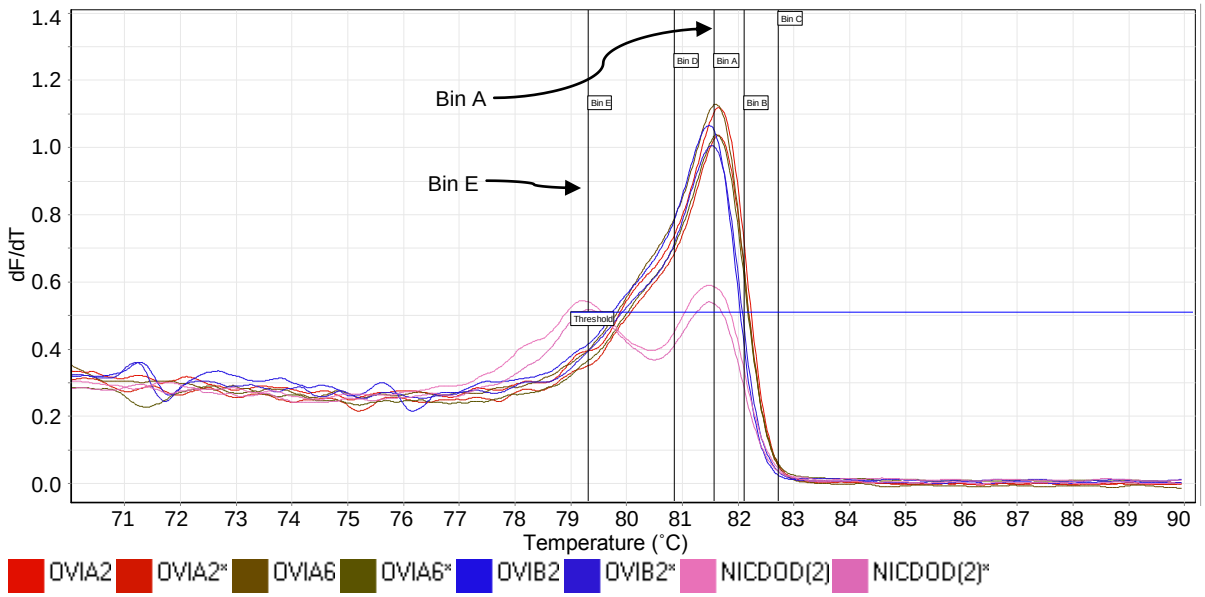

Figure 3.30: Melt curve analysis comparison of the 10-190 bp region of segment 10 of the isolates labelled OVIA2, OVIB2, OVIA6 and NICDOD(2) using primers 10F and 10R. Both serotype 2 OVI isolates align well with the confirmed serotype 6 isolate of OVIA, which all fall into Bin A only. NICDOD(2) is a confirmed serotype 2 isolate and falls into Bin A and Bin E. A melt threshold of 0.51 dF/dT and 75˚C was applied to exclude pre-melt noise. An * represents a duplicate.

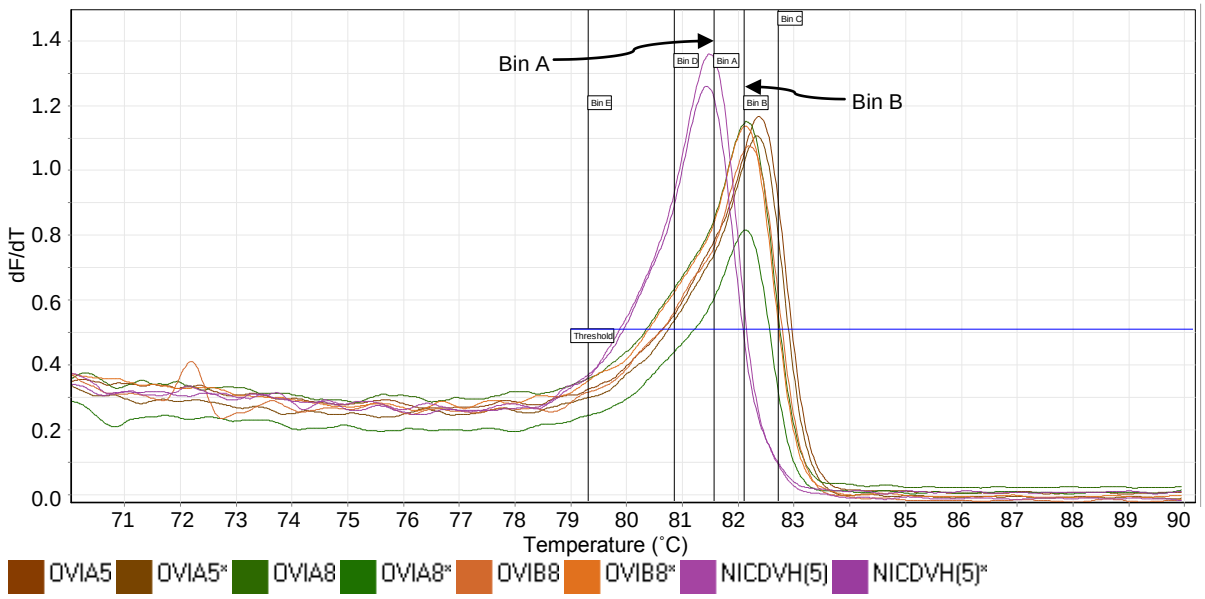

Figure 3.31: Melt curve analysis comparison of the 10-190 bp region of segment 10 of the isolates labelled OVIA5, OVIA8, OVIB8 and NICDVH(5) using primers 10F and 10R. Both serotype 8 OVI isolates align well with the serotype 5 isolate of OVIA, which all fall into Bin B. NICDVH(5) falls into Bin A. A melt threshold of 0.51 dF/dT and 75˚C was applied to exclude pre-melt noise. An * represents a duplicate.

The double-peaked profiles of the OVIB1 and NICD1 melts are very similar, although they have shifted (Figure 3.32). The NICD serotype 4 isolate's melt peak has shifted to the right, as was the case for NICD1 (Figure 3.33). NICD7 appears to shift slightly from the OVI

isolates in the melt curves (Figure 3.34). The difference between the serotype 8 NICD and OVI isolates' melt curves is pronounced in Figure 3.35. The NICD isolate of serotype 9 has an obvious shift in its melt peak (Figure 3.36).

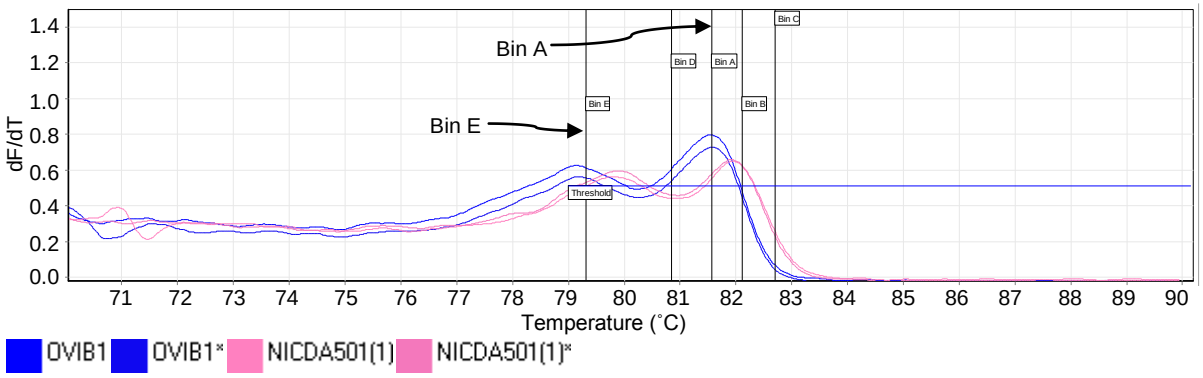

Figure 3.32: Melt curve analysis comparison of the 10-190 bp region of segment 10 of the isolates labelled OVIB1 and NICD1 using primers 10F and 10R. OVIB1 falls into Bin A and Bin E. NICD501(1) falls into Bin B, but is double-peaked. A melt threshold of 0.51 dF/dT and 75˚C was applied to exclude pre-melt noise. An * represents a duplicate.

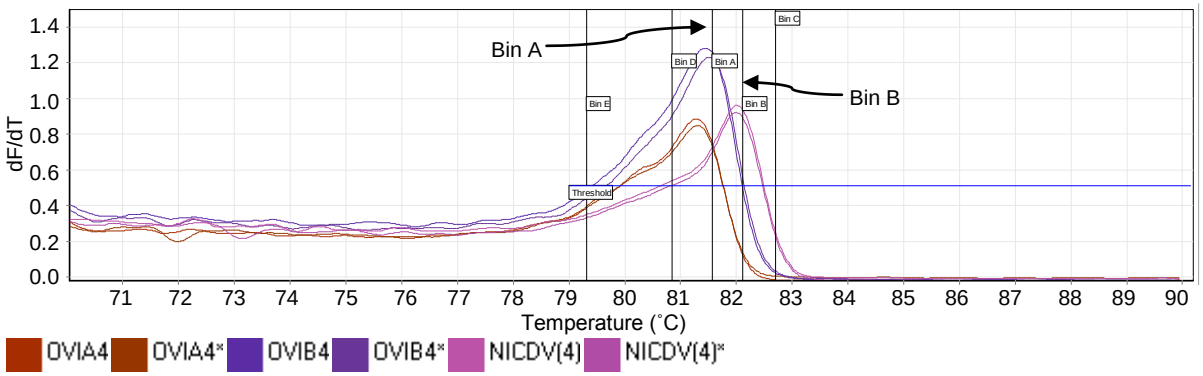

Figure 3.33: Melt curve analysis comparison of the 10-190 bp region of segment 10 of the isolates labelled OVIA4, OVIB4 and NICDV(4) using primers 10F and 10R. OVIA4 and OVIB4 fall into Bin A. NICDV(4) falls into Bin B. A melt threshold of 0.51 dF/dT and 75˚C was applied to exclude pre-melt noise. An * represents a duplicate.

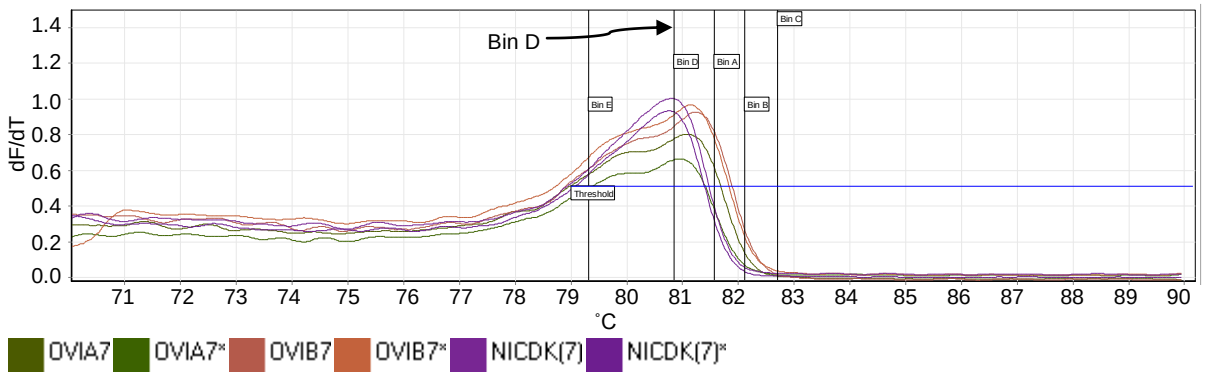

Figure 3.34: Melt curve analysis comparison of the 10-190 bp region of segment 10 of the isolates labelled OVIA7, OVIB7 and NICDK(7) using primers 10F and 10R. OVIA7, OVIB7 and NICDK(7) fall into Bin D. A melt threshold of 0.51 dF/dT and 75˚C was applied to exclude pre-melt noise. An * represents a duplicate.

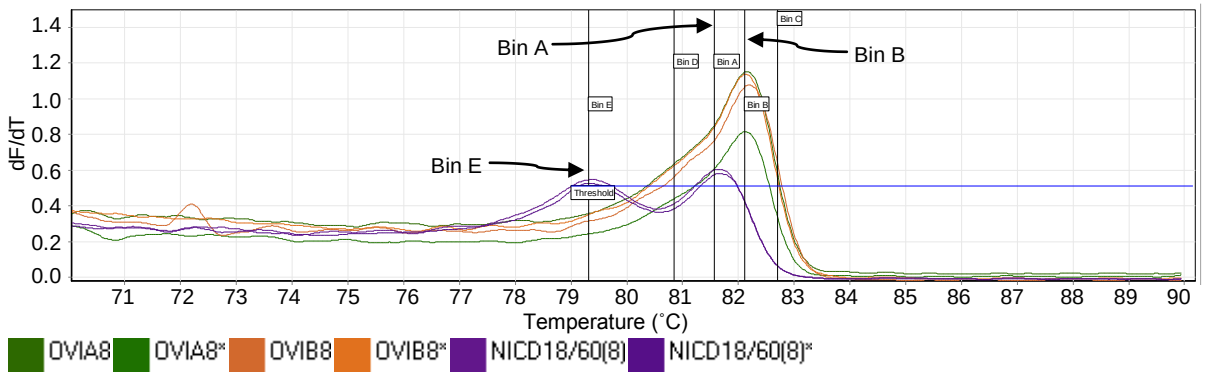

Figure 3.35: Melt curve analysis comparison of the 10-190 bp region of segment 10 of the isolates labelled OVIA8, OVIB8 and NICD18/60(8) using primers 10F and 10R. OVIA8 and OVIB8 fall into Bin B. NICD18/60(8) falls into Bin A and Bin E. A melt threshold of 0.51 dF/dT and 75˚C was applied to exclude pre-melt noise. An * represents a duplicate.

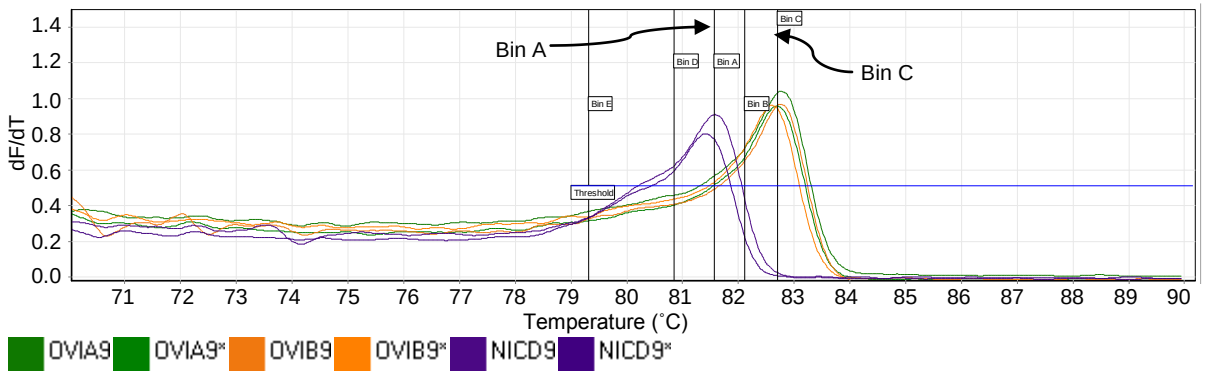

Figure 3.36: Melt curve analysis comparison of the 10-190 bp region of segment 10 of the isolates labelled OVIA9, OVIB9 and NICD9 using primers 10F and 10R. OVIA9 and OVIB9 fall into Bin C. NICD9 falls into Bin A. A melt threshold of 0.51 dF/dT and 75˚C was applied to exclude pre-melt noise. An * represents a duplicate.

Exhaustive examination of the melt curves of the 10-190 bp region of segment 10 from all 27 OVIA, OVIB and NICD AHSV isolates, as well as utilising the RT-PCR results of segment 2 indicated a number of anomalies in the serotypes identified and are recorded in Table 3.8. The Rotor-Gene™ 6000 Series Software identified the peaks and assigned them to bins based on the bin window defined by the user. The software nominates the genotype based on the bin. Clade A was defined as Bin D and Clade B was defined as Bin A and Bin E. Clade C was described as Bin A or Bin B or Bin C. The software is incapable of defining a genotype based on the Boolean operator 'OR', and will only assign genotypes based on the operator 'AND' (Corbett, 2006).

In Table 3.8, the genotype is nominated by the software according to the definitions described in the previous paragraph. The three 'genotypes' were Clade A, Clade B or Clade C. This was determined by the temperature at which the melt peak occurred and its bin. However, as the software was primarily developed to identify SNPs and short, invariant amplicons, it proved limited with respect to the 27 melt curves of the 10-190 bp region of segment 10 of AHSV. Visual inspection of the melt curves and results of the HRM analysis, the serotype designation of each isolate was assessed as being 'suspected' (possible incorrect assignment or anomaly) or 'none' (where there was no evidence of a possible misassignment). Possible reasons for this are given under the comment column.

Table 3.8: Summary of AHSV serotype profiling following Rotor-Gene™ software genotype calling using the 10-190 bp region of segment 10 and clade-specific primers. Blue – Clade A; Red – Clade B; Green – Clade C.

Name	Genotype	Peak 1 (°C)	Peak 2 (°C)	Serotype anomaly?	Comments
OVIA1				Suspected	Non-amplification
OVIA2		81.65 (Bin A) 81.65 (Bin A)		Suspected	VP2 st-sp PCR –ve, melt profile does not align, wrong bin
OVIA3	Clade A Clade A	80.90 (Bin D) 80.82 (Bin D)		None	
OVIA4		81.28 (Bin A) 81.30 (Bin A)		None	
OVIA5		82.37 (Bin B) 82.33 (Bin B)		Suspected	VP2 st-sp PCR –ve
OVIA6		81.60 (Bin A) 81.60 (Bin A)		None	

Name	Genotype	Peak 1 (°C)	Peak 2 (°C)	Serotype anomaly?	Comments
OVIA7	Clade A Clade A	80.12 80.10	81.08 (Bin D) 80.95 (Bin D)	None	
OVIA8		82.15 (Bin B) 82.13 (Bin B)		Suspected	Melt profiles do not align
OVIA9		82.78 (Bin C) 82.70 (Bin C)		None	
OVIB1	Clade B Clade B	79.15 (Bin E) 79.17 (Bin E)	81.55 (Bin A) 81.58 (Bin A)	None	
OVIB2		81.48 (Bin A) 81.53 (Bin A)		Suspected	VP2 st-sp PCR –ve
OVIB3	Clade A Clade A	80.83 (Bin D) 80.87 (Bin D)		None	
OVIB4		81.45 (Bin A) 81.52 (Bin A)		None	
OVIB5		81.20 81.15 (Bin D)	82.03 (Bin B) 82.00 (Bin B)	None	
OVIB6		82.15 (Bin B) 82.10 (Bin B)		None	
OVIB7	Clade A	81.25 81.15 (Bin D)		None	
OVIB8		82.20 (Bin B) 82.13 (Bin B)		Suspected	Melt profiles do not align
OVIB9		82.75 (Bin C) 82.60 (Bin C)		None	
NICDA501(1)		79.8 79.9	81.95 (Bin B) 81.93 (Bin B)	None	
NICDOD(2)	Clade B Clade B	79.20 (Bin E) 79.33 (Bin E)	81.50 (Bin A) 81.48 (Bin A)	None	
NICDL(3)	Clade A Clade A	80.75 (Bin D) 80.78 (Bin D)		None	
NICDV(4)		82.00 (Bin B) 82.00 (Bin B)		Suspected	VP2 st-sp PCR –ve
NICDVH(5)		81.48 (Bin A) 81.43 (Bin A)		None	
NICD114(6)		82.13 (Bin B) 82.15 (Bin B)		None	
NICDK(7)	Clade A Clade A	80.80 (Bin D) 80.77 (Bin D)		None	
NICD18/60(8)	Clade B Clade B	79.40 (Bin E) 79.35 (Bin E)	81.65 (Bin A) 81.68 (Bin A)	None	
NICD9		81.60 (Bin A) 81.42 (Bin A)		Suspected	Melt profiles do not align

st-sp – serotype-specific

3.3.9. Sequencing of the 10-190 bp region of segment 10 and the clade-specific and serotype-specific amplicons of segment 2

Due to the non-amplification of some isolates encountered in using the serotype-specific primers to determine the identity of the isolates, the PCR products of the 10-190 bp region of segment 10 and the clade-specific and serotype-specific amplicons of segment 2 were sequenced using both forward and reverse primers following the Sanger dideoxy method. Although next generation sequencing technologies, such as pyrosequencing, would have provided greater read depth and other advantages, these were, unfortunately unavailable for the present study. The sequences were subjected to a BLASTn analysis to identify the serotype of the isolate in question (Table 3.9). The serotype-specific primers were based on those designed by Maan *et al.* (2011a) while the clade-specific primers were described in Chapter 2. The segment 10 primers (10F and 10R) were designed by Groenink (2009). After reviewing the BLAST output for each sequence, a determination was made, based on the portion of sequence submitted, of the most likely serotype of that isolate. Due to the serotype-specificity of segment 2 (Roy *et al.*, 1994), this was generally unequivocal. However, in the case of segment 10, which is more conserved between the serotypes (Venter *et al.*, 2000), there was often no clear consensus – this is indicated in Table 3.9 by suggesting more than one serotype with question marks.

The results of the sequencing of segments 2 and 10 for all isolates of AHSV are summarised in Table 3.9, with the relevant accession numbers. Blank spaces in the table indicate that no PCR product was available for sequencing, or it was not deemed necessary. Serotype 1 of the OVIA set failed to amplify on all accounts. The two serotype 2 isolates of the OVI sets, sequenced using both segment 2 and 10 primers, revealed them to be serotype 6. The isolate known as serotype 5 of the OVIA set was sequenced and based on the sequence was identified as serotype 9 using segment 10 or serotype 8 using segment 2. NICD4 does, after failing to show amplification products with serotype-specific primers, prove to be serotype 4 after sequencing alternate amplicons. OVIA7, OVIB7 and NICD7 were all confirmed to be serotype 7, despite only being sequenced using segment 10 primers. OVIA8 and OVIB8, initially thought to be suspect isolates following sequencing of the 180 bp product of segment 10 were confirmed to be serotype 8 after the clade-specific amplicons of segment 2 were sequenced.

Once the anomalies had been rectified, the clade determination of the AHSV isolates is as seen in Figure 3.37 (Clade A), Figure 3.38 (Clade B) and Figure 3.39 (Clade C).

Table 3.9: Results of sequencing amplicons of both segments 2 and 10 for all isolates and allocation of the most likely serotype after BLASTn analysis of the edited sequences. The blue-highlighted rows indicate suspected anomalies in serotypes assigned to isolates that were reassigned a serotype post HRM analysis and sequencing in the present study.

Isolate	Serotype-specific primers[1]				Segment 10 primers[2]				Clade-specific primers[3]			
	Segment	Region (bp)	Serotype	Accession #*	Segment	Region (bp)	Serotype	Accession #*	Segment	Region (bp)	Serotype	Accession #*
OVIA1												
OVIB1					10	10-190	1 (2?)	HG779560	2	1302-1551	1	HG779574
NICDA501					10	10-190	1 (2?)	HG779565	2	1302-1551	1	HG779578
OVIA2					10	10-190	6	HG779555	2	1302-1551	6	HG779570
OVIB2					10	10-190	6	HG779561	2	1302-1551	6	HG779575
NICDOD	2	456-1535	2	HG779544								
OVIA3	2	447-1176	3	HG779545								
OVIB3	2	447-1176	3	HG779546								
NICDL	2	447-1176	3	HG779547								
OVIA4	2	441-1687	4	HG779548								
OVIB4	2	441-1687	4	HG779549								
NICDV					10	10-190	4?	HG779566	2	2703-2892	4	HG779579
OVIA5					10	10-190	9	HG779556	2	2703-2892	8	HG779571
OVIB5	2	714-1828	5	HG779550								
NICDVH	2	714-1828	5	HG779551								

Isolate	Serotype-specific primers[1]				Segment 10 primers[2]				Clade-specific primers[3]			
	Segment	Region (bp)	Serotype	Accession #*	Segment	Region (bp)	Serotype	Accession #*	Segment	Region (bp)	Serotype	Accession #*
OVIA6	2	473-1606	6	HG779552								
OVIB6	2	473-1606	6	HG779553								
NICD114	2	473-1606	6	HG779554								
OVIA7					10	10-190	3/7	HG779557				
OVIB7					10	10-190	3/7	HG779562				
NICDK					10	10-190	7	HG779567				
OVIA8					10	10-190	9? 5?	HG779558	2	1302-1551	8	HG779572
OVIB8					10	10-190	9? 5?	HG779563	2	1302-1551	8	HG779576
NICD18/60					10	10-190	1?	HG779568	2	1302-1551	8	HG779580
OVIA9					10	10-190	9	HG779559	2	2703-2892	9	HG779573
OVIB9					10	10-190	9	HG779564	2	2703-2892	9	HG779577
NICD9					10	10-190	9?	HG779569	2	2703-2892	9	

[1] Serotype-specific primers are based on those of Maan *et al.* (2011a) (Section 3.3.7).

[2] Segment 10 primers refer to the primers that amplify the 10-190 bp region of segment 10 (Groenink, 2009).

[3] Clade-specific primers refer to those segment 2 primers that aim to separate out the serotypes of each segment 10 clade (Section 2.3.4).

*European Nucleotide Archive: http://www.ebi.ac.uk/ena/data/view/HG779544-HG779580

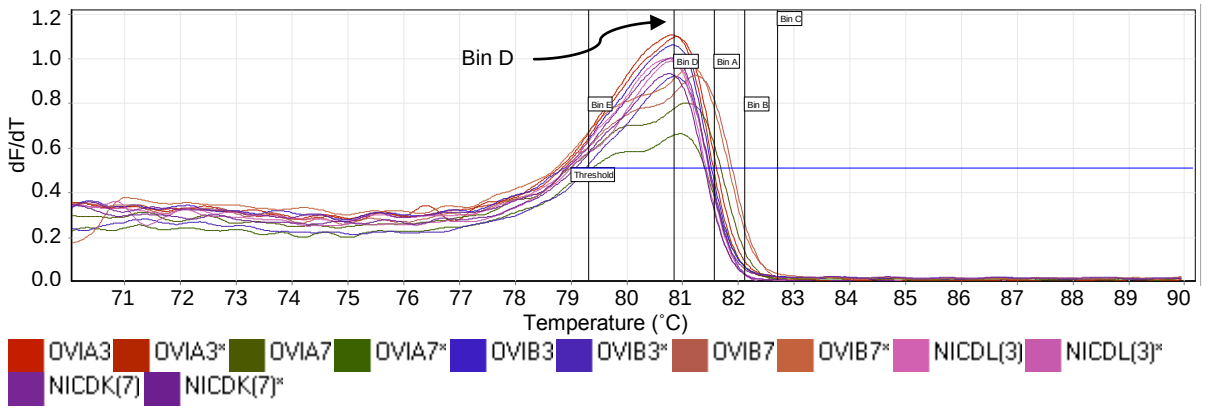

Figure 3.37: The High Resolution Melt analysis of the Clade A labelled isolates using the 10F and 10R primer pair. Bins (melt regions) were defined and applied by the user to identify important peaks. A melt threshold of 0.51 dF/dT and 79˚C was applied to exclude the pre-melt noise. The melt peaks fall into Bin D. An * represents a duplicate.

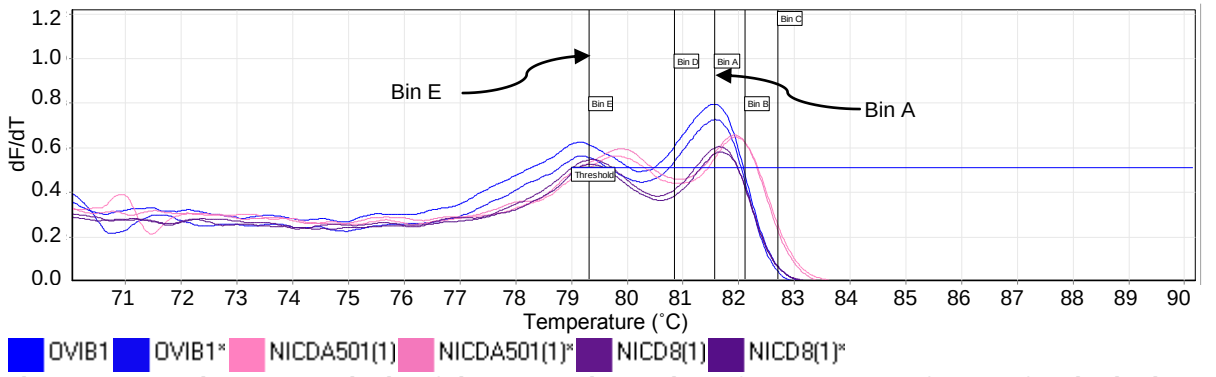

Figure 3.38: Melt curve analysis of the 10-190 bp region of segment 10 of AHSV for the isolates labelled OVIB1 and NICD1 using primers 10F and 10R. Bins (melt regions) were defined and applied by the user to identify important peaks. OVIB1 and NICD8(1) fell into Bin A and Bin E. NICD501(1) fell into Bin B, but was double-peaked. A melt threshold of 0.51 dF/dT and 79˚C was applied to exclude the pre-melt noise. An * represents a duplicate.

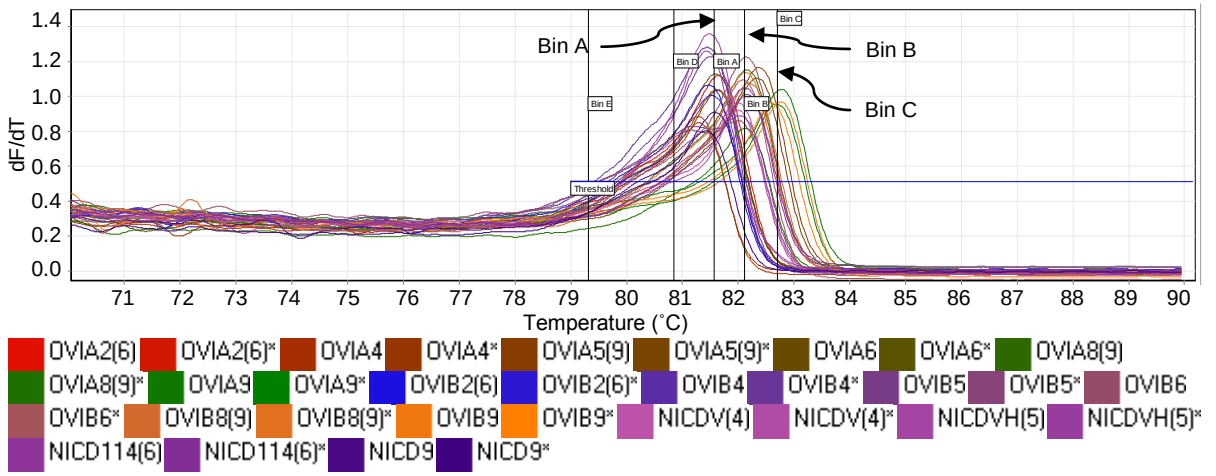

Figure 3.39: The High Resolution Melt analysis of the Clade C labelled and suspected isolates using the 10F and 10R primer pair. Bins were applied and defined by the user to identify important peaks and a threshold of 0.51 dF/dT and 79˚C was applied to exclude the pre-melt noise. The melt peaks fell into Bin A, B or C.

3.3.10. Serotype determination

Once isolates were determined to be in a specific clade, they could be subjected to a clade-specific serotype determination protocol.

3.3.10.1. The separation of clade A serotypes 3 and 7

Using the clade-specific segment 2 primers AF and AR, a 319 bp product from the RNA of serotype 3 and 7 isolates was amplified using the two-step protocol. C_T values ranged from 24-29 and all samples plateaued. There was a clear distinction between serotypes 3 (green) and serotypes 7 (blue) in the melt profile (Figure 3.40). There was a clear difference in peak shape and a secondary peak was seen in the region of 78°C for serotype 3 isolates. A higher degree of differentiation could be seen in the HRM analysis (panel B). In both panel A and B, the NICD isolates (light green and light blue) could be seen to have slightly different profiles to the OVI isolates and in panel B were shown to diverge from the OVI isolate melt profiles.

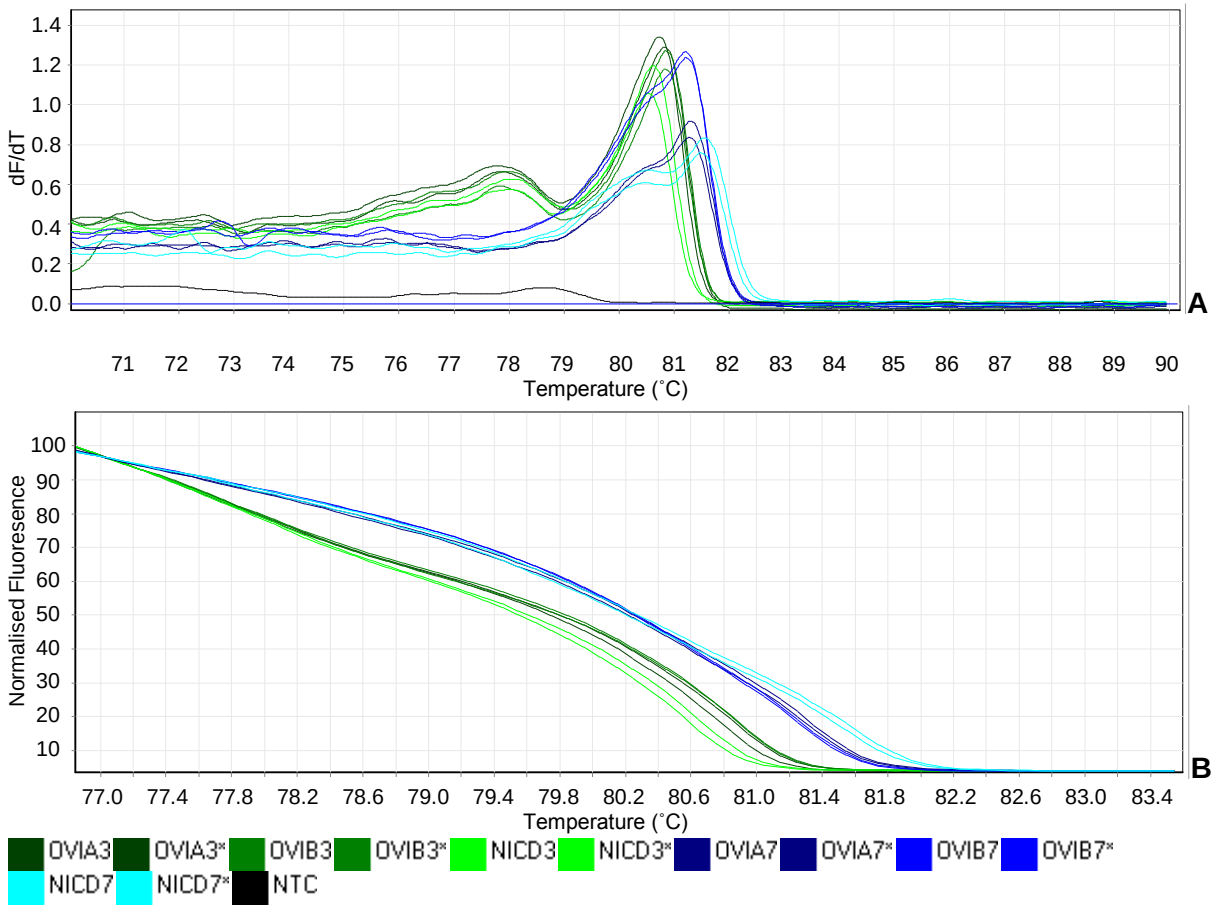

Figure 3.40: Amplification and High Resolution Melt of cDNA of serotype 3 and 7 isolates of the OVIA, OVIB and NICD sets using clade A-specific primers AF/AR and a two-step protocol. A – dF/dT (rate of change of fluorescence with respect to temperature) of the melt curve; B – High Resolution Melt analysis. OVIA3 – serotype 3 of OVIA set; OVIB3 – serotype 3 of the OVIB set; NICDL(3) – serotype 3 of the NICD set; OVIA7 – serotype 7 of OVIA set; OVIB7 – serotype 7 of the OVIB set; NICD7 – serotype 7 of NICD set; NTC – no template control; * represents duplicates.

3.3.10.2. The separation of clade B serotypes 1, 2 and 8

Using the primers BF and BR, a 249 bp product from segment 2 from RNA-derived cDNA of serotype 1, 2 and 8 isolates was amplified using the two-step protocol (Figure 3.41). C_T values ranged from 18-23. OVIA1 has been confirmed as non-AHSV so no amplification was expected. cDNA from NICD8, however, although amplifying well in previous RT-PCRs amplified weakly here, despite having the same C_T values as the NICD1 and NICD2 isolates that reached maximum fluorescence. Serotypes 1 and 2 appeared to be indistinguishable in the melt curves (panel A) and HRM (panel B). Serotype 8 was clearly and consistently distinguishable in all panels. Although the cDNA of the serotype 8 isolate did not amplify well, a distinct melt peak is seen to the right of the other melt peaks. The HRM analysis (panel B) also showed a clear difference, with the serotype 8 isolate's melt profile reaching zero fluorescence much later than the serotype 1 and 2 isolates.

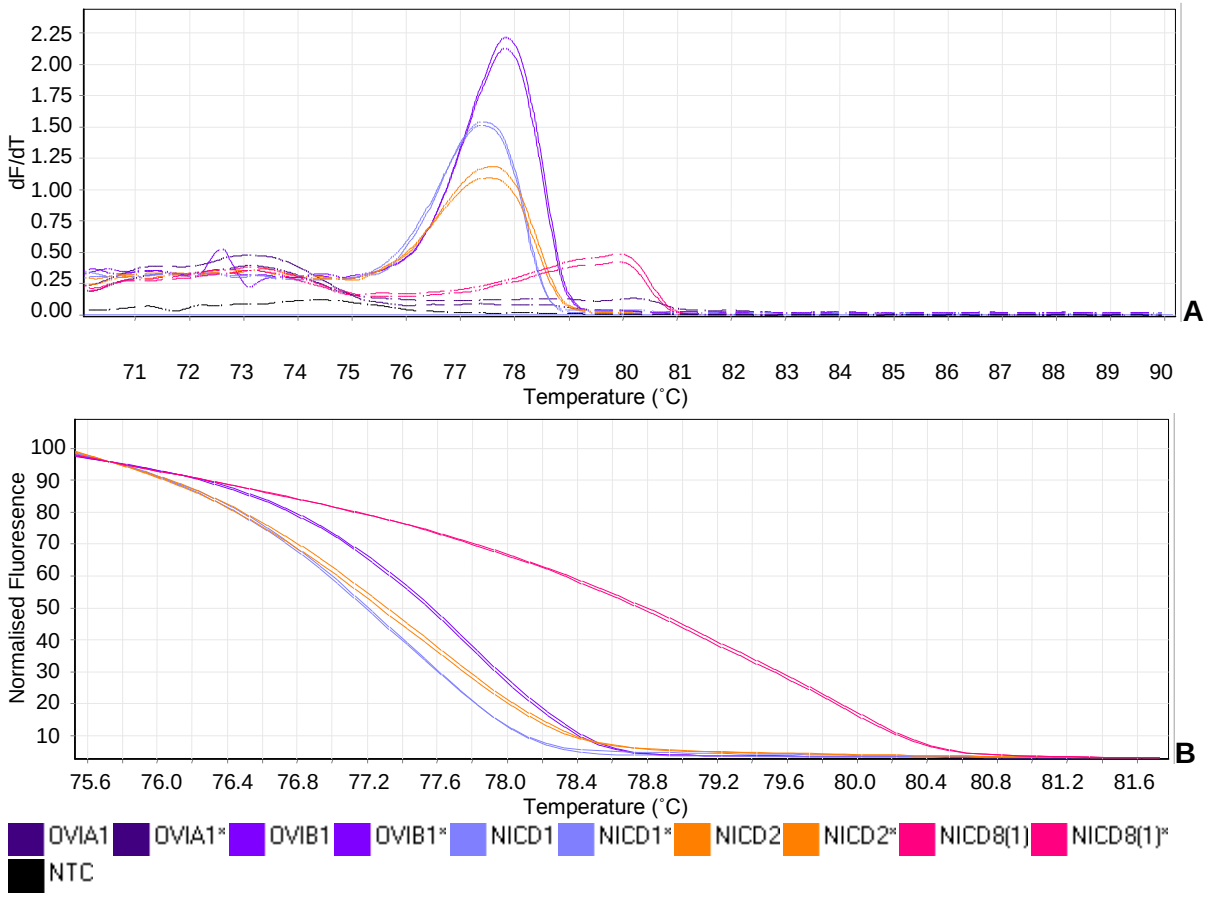

Figure 3.41: Amplification and High Resolution Melt of cDNA of serotypes 1, 2 and 8 of the OVIA, OVIB and NICD sets using clade B-specific primers BF/BR and a two-step protocol. A – dF/dT (rate of change of fluorescence with respect to temperature) of the melt curve; B – High Resolution Melt analysis. OVIA1 – serotype 1 of OVIA set; OVIB1 – serotype 1 of the OVIB set; NICD1 – serotype 1 of the NICD set; NICD2 – serotype 2 of NICD set; NICD8(1) – serotype 8 of NICD set; NTC – no template control; * represents duplicates.

3.3.10.3. The separation of clade C serotypes 4, 5, 6 and 9

Using the primers CF and CR, a 189 bp product from segment 2 from RNA of serotype 4, 5, 6 and 9 isolates was amplified using the two-step protocol (Figure 3.42). C_T values ranged from 15-23 and all samples reached maximum fluorescence. It can be seen that the melt curves (panel A) for the OVIA2 and OVIB2 isolates appeared in the same bin (Bin C) as the serotype 6 isolates. Although not distinct, three melt profile groupings can be seen (panel A). However, serotype 9 may be difficult to distinguish from serotype 5 in terms of melt peaks. In panel A, the melt profiles of the serotype 4 isolates (blue) were rather dispersed, while the OVI serotype 6- and OVI serotype 2-labelled (brown/pink and purple) isolates' melt profiles showed identical profiles. Serotype 4 fell into Bin A, serotype 5 into Bin B, serotype 6 into Bin C and serotype 9 into Bin D.

3.3.10.4. Comparison of PCRs using segment 2 clade-specific AF/AR, BF/BR and CF/CR primers

The PCRs using segment 2 clade-specific AF/AR, BF/BR and CF/CR primers with annealing temperatures of 55°C were compared. Each clade was analysed both manually (visually) and using the Rotor-Gene™ 6000 Series Software's genotyping methods. The net result obtained with Clade A, B and C is shown in Table 3.10, Table 3.11 and Table 3.12 respectively (for HRM genotyping). Blue shading represents the selected reference sample (which the other samples were compared to), while pink shading indicates low confidence. Orange shading represents possible serotype anomalies, while green represents confirmed anomalies. Table 3.10 shows the results of Clade A (serotypes 3 and 7). The isolates of the OVIA set for each serotype were chosen as the reference samples. The Rotor-Gene™ 6000 Series Software categorised all of the samples consistently with their labels (under the column 'Genotype') and the confidence of this result (as calculated by the software algorithms) is indicated under the 'Confidence (%)' column. Despite confidence in the NICD3 isolate's identification being low, it remains as a serotyped serotype 3. The genotyping results of Clade B isolates (serotypes 1, 2 and 8) are shown in Table 3.11 where the NICD isolates were selected as the genotyping reference samples for each serotype. OVIB1, the only OVI isolate, has been serotyped incorrectly although the confidence in this identification is low.

The HRM analysis genotyping for Clade C is the most complicated (Table 3.12). OVIB4 has a single duplicate with a low confidence. OVIA5 has been consistently serotyped with a high confidence. OVIB5 has been serotyped as serotype 5 in only one duplicate reaction, while the other duplicate reaction has been serotyped as serotype 9. Both OVI serotype 6 isolates were labelled as such, but NICD6 was genotyped as serotype 4. OVIA2, OVIB2, OVIA8 and OVIB8 were all labelled inconsistently following HRM analysis. OVIA2 and OVIB2 have been

genotyped as serotype 6 with high confidence. OVIB8 has been genotyped as serotype 5. OVIA8, while genotyped as serotype 5, has a very low confidence.

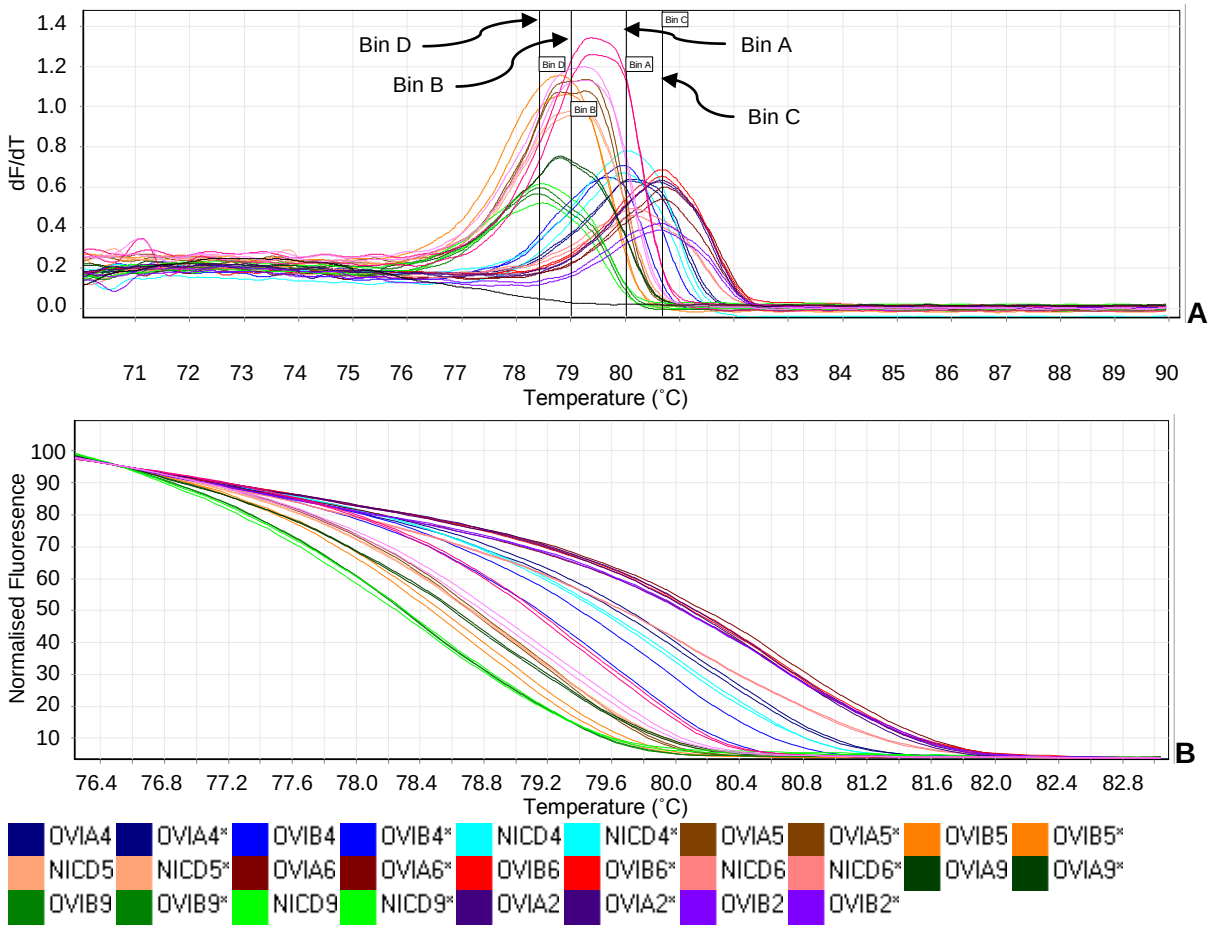

Figure 3.42: Amplification and High Resolution Melt of cDNA of serotype 4, 5, 6 and 9 of the OVIA, OVIB and NICD sets using clade C-specific primers CF/CR and a two-step protocol. A – dF/dT (rate of change of fluorescence with respect to temperature) of the melt curve; B – High Resolution Melt analysis. OVIA4 – serotype 4 of OVIA set; OVIB4 – serotype 4 of the OVIB set; NICD4 – serotype 4 of the NICD set; OVIA5 – serotype 5 of the OVIA set; OVIB5 – serotype 5 of the OVIB set; NICD5 – serotype 5 of NICD set; OVIA6 – serotype 6 of the OVIA set; OVIB6 – serotype 6 of the OVIB set; NICD6 – serotype 6 of NICD set; OVIA9 – serotype 9 of the OVIA set; OVIB9 – serotype 9 of the OVIB set; NICD9 – serotype 9 of the NICD set; OVIA2 – serotype 2 of the OVIA set; OVIB2 – serotype 2 of the OVIB set; NTC – no template control; * represents duplicates.

Table 3.10: Clade A HRM analysis genotyping for OVIA, OVIB and NICD using the Corbett Rotor-Gene™ 6000 Series Software 1.7™.

Name	Genotype	Confidence (%)
OVIA3	Serotype 3	100.00
OVIA3*	Serotype 3	90.22
OVIB3	Serotype 3	99.01
OVIB3*	Serotype 3	98.11
NICD3	Serotype 3	32.74
NICD3*	Serotype 3	55.87
OVIA7	Serotype 7	100.00
OVIA7*	Serotype 7	95.88
OVIB7	Serotype 7	94.27
OVIB7*	Serotype 7	90.73
NICD7	Serotype 7	71.17
NICD7*	Serotype 7	83.87

* indicates duplicates

Table 3.11: Clade B HRM analysis genotyping for OVIA, OVIB and NICD using the Corbett Rotor-Gene™ 6000 Series Software 1.7™.

Name	Genotype	Confidence %
OVIB1	Serotype 2	15.32
OVIB1*	Serotype 2	10.76
NICD1	Serotype 1	100.00
NICD1*	Serotype 1	98.00
NICD2	Serotype 2	100.00
NICD2*	Serotype 2	95.75
NICD8(1)	Serotype 8	100.00
NICD8(1)*	Serotype 8	98.04

* indicates duplicates

Table 3.12: Clade C HRM analysis genotyping for OVIA, OVIB and NICD using the Corbett Rotor-Gene™ 6000 Series Software 1.7™.

Name	Genotype	Confidence %	Name	Genotype	Confidence %
OVIA4	Serotype 4	85.71	NICD6	Serotype 4	33.85
OVIA4*	Serotype 4	68.47	NICD6*	Serotype 4	37.14
OVIB4	Serotype 5	3.42	OVIA9	Serotype 5	72.00
OVIB4*	Serotype 4	56.29	OVIA9*	Serotype 5	78.15
NICD4	Serotype 4	100.00	OVIB9	Serotype 9	100.00
NICD4*	Serotype 4	97.87	OVIB9*	Serotype 9	99.66
OVIA5	Serotype 5	95.29	NICD9	Serotype 9	97.90
OVIA5*	Serotype 5	96.17	NICD9*	Serotype 9	91.60
OVIB5	Serotype 5	39.13	OVIA2	Serotype 6	98.18
OVIB5*	Serotype 9	54.27	OVIA2*	Serotype 6	98.53
NICD5	Serotype 5	99.54	OVIB2	Serotype 6	93.13
NICD5*	Serotype 5	100.00	OVIB2*	Serotype 6	90.49
OVIA6	Serotype 6	88.85	OVIA8	Serotype 5	6.71
OVIA6*	Serotype 6	92.11	OVIA8*	Serotype 5	3.68
OVIB6	Serotype 6	100.00	OVIB8	Serotype 5	90.48
OVIB6*	Serotype 6	98.34	OVIB8*	Serotype 5	71.50

* indicates duplicates

3.4. Discussion

High Resolution Melt analysis has been identified as a powerful tool for the typing or species determination of various pathogens such as *Mycoplasma synoviae*, *Bartonella* spp., fowl adenoviruses and infectious bursal disease virus (Corbett, 2006; Jeffery *et al.*, 2007; Morick *et al.*, 2009; Steer *et al.*, 2009; Vossen *et al.*, 2009; Ghorashi *et al.*, 2011). Melt curves were both characteristic and unique, being based on sequence length, guanidine-cytosine content and sequence complementarity (Gundry *et al.*, 2003; Wittwer *et al.*, 2003), and were therefore thought to be able to discriminate between differences in the genetic sequence in any of the serotypes of AHSV. The results of this study showed the applicability of High Resolution Melt analysis to AHSV studies.

When differential diagnoses are considered for AHSV (e.g. equine encephalosis virus (EEV)), the gold standard is viral neutralisation. RT-PCR is an effective initial method for rapid diagnosis of AHSV (OIE, 2008; Aharonson-Raz *et al.*, 2011) and a negative AHSV RT-PCR test can be followed up by tests for differential diagnoses, such as an EEV RT-PCR. In

rapid diagnostic assays for AHSV, primers targeting the genome segment encoding VP7 are used. These primers are designed to be serogroup-conserved (Fernández-Pinero *et al.*, 2009) or the serotype-specific genome segment encoding VP2 primers (Maan *et al.*, 2011a). However, these primers were not designed with HRM analysis in mind and the end point result of these RT-PCR protocols is a product in an agarose gel post-electrophoresis. In time, it may be possible to use post-PCR HRM analysis for rapid detection of diseases that present similar symptoms in the field.

Three sets of the nine AHSV serotypes were obtained from two sources: the NICD isolates were original reference strains isolated in the 1960s, while the OVIA and OVIB isolates were recent field-isolated strains from the early 2000s. The AHS virus has been cultured in Vero cells in a number of studies (Paweska *et al.*, 2003; Fernández-Pinero *et al.*, 2009; Guthrie *et al.*, 2009). AHSV cultures grown in the present study were ready for harvesting between five and seven days post inoculation. There was no indication that the reference or field strains (NICD or OVI) or a particular serotype was more virulent than another was. Other studies have reported harvesting the cultures between two and eight days (OIE, 2008) and between two and four days (Paweska *et al.*, 2003).

Total RNA was extracted without further processing. This served to test the ease with which the RT-PCR protocol of the future assay could be set up. dsRNA isolation steps were considered (Akin *et al.*, 1998; Potgieter *et al.*, 2003), however, they invariably require lengthy incubation times that are unsuitable for a rapid assay. Future work on this assay will involve sensitivity studies where exact concentrations of pure viral dsRNA will be required.

The OIE established a primer set that amplified a sequence from the genome segment of VP7 (OIE, 2008; Fernández-Pinero *et al.*, 2009) and a positive amplification from this primer pair would indicate that AHSV was present. Serotype 1 cDNA or RNA of the OVIA set (OVIA1) did not produce amplification products using the OIE VP7 primers. The isolate was possibly not viable to begin with or an incorrect species of virus was labelled as AHSV. It is highly unlikely that the RNA extraction failed since the method used was particularly successful here and in other studies (Rodriguez-Sanchez *et al.*, 2008). Furthermore, spectrophotometer readings indicated that genomic material was present – this genomic material would be of Vero cell origin. All remaining isolates of the OVIA, OVIB and NICD strains amplified correctly and produced a single band of approximately 102 bp on agarose gels. The appearance of a amplification product on an agarose gel post electrophoresis was the method used by Fernández-Pinero *et al.* (2009) to positively identify the presence of the virus and is a recognised diagnostic technique (Stone-Marschat *et al.*, 1994; Sailleau *et al.*, 2000; Zientara *et al.*, 2004). This served to confirm that genomic material was extracted from

the Vero cell monolayers and it was of AHSV origin. The lack of amplification products for the negative controls in all of the PCRs performed in this study indicates that all of the primers thus designed, as described in Chapter 2, and obtained from other sources for the purposes of this study, did not bind to Vero cell genomic material, and only portions of the AHS viral genome were being amplified. Post-PCR, it would therefore follow that melt curves were only produced by AHSV amplicons. As an aside, despite the recommended reaction volume of 20 µL in a 200 µL PCR tube, 10 µL reactions in 100 µL PCR tubes performed equally well. This effectively allows for a doubling in the number of reactions from a particular commercial system and makes the Corbett Rotor-Gene™ 6000 rotary analyser vastly more cost-efficient compared to systems where only 200 µL PCR tubes can be used.

Optimisation protocols for the clade-specific primers (AF/AR, BF/BR, CF/CR), which target segment 2, indicated that AHSV amplicons were most successfully produced from 52.1°C to 60.3°C. The additional bands seen in the agarose gels are likely due to the high concentration of primer. Anomalies were already being identified and primer concentrations were increased to reduce the effect of the degenerate primers (Kwok *et al.*, 1994). Template concentration was not considered an issue due to the successful amplification of the isolates using the OIE genome segment 7 primers. In a second optimisation, reproducible melt curves were obtained using primers at a concentration of 400 nM. The standard values thus adopted were an annealing temperature of 60°C and a primer concentration of 400 nM each. The manufacturer-recommended protocol suggests a primer concentration of 50-400 nM. The degenerate nature of the primers used in this study would decrease the actual concentration of suitable primer, hence, the primer concentration was maximised. This is recommended in both Kwok *et al.* (1994) and Roux (1995).

Another aspect to be investigated was the use of a one-step or two-step protocol for the final assay. A one-step protocol was overwhelmingly favoured in previous studies of AHSV (Aradaib, 2009; Fernández-Pinero *et al.*, 2009; Hoffmann *et al.*, 2009; Maan *et al.*, 2011a; Monaco *et al.*, 2011; Bremer, 2012; Weyer *et al.*, 2013). Amplification of the VP2-encoding genome segment (with amplicons ranging from 345-2441 bp) from either AHSV or BTV was previously achieved using the Qiagen or Invitrogen SuperScript III one-step systems (Jimenez-Clavero *et al.*, 2006; Mertens, 2007; Hofmann *et al.*, 2008; OIE, 2008; Fernández-Pinero *et al.*, 2009; Potgieter *et al.*, 2009; Maan *et al.*, 2010b; Matsuo *et al.*, 2010; von Teichman *et al.*, 2010; Castillo-Olivares *et al.*, 2011; Maan *et al.*, 2011a; Monaco *et al.*, 2011).

However, despite the popularity and advantages of the one-step protocol for AHSV and BTV amplification, the improvements of the HRM analysis in this study using the two-step protocol

negated the advantages of the one-step protocol. A review of the literature pertaining to HRM analysis and virus classification revealed that two-step protocols were favoured by most workers and again, Invitrogen and Qiagen systems were preferred (Chateigner-Boutin & Small, 2007; Tajiri-Utagawa *et al.*, 2009; Hewson *et al.*, 2010; Towler *et al.*, 2010; Ghorashi *et al.*, 2011; Tong *et al.*, 2011; Varillas *et al.*, 2011).

Although no published studies have been conducted on the advantages and disadvantages of either protocol for HRM analysis, it would appear that the two-step protocol was significantly more reliable in this study. This was especially noticeable when one considers that in the two-step protocol the duplicates were better correlated than the one-step protocol. This was indicative of a pattern that emerged during the present study where two-step protocols were consistently more reliable in terms of the amplification, melt curves, melt curve analysis and the HRM analysis than one-step protocols. It is unfortunate that, at this stage, two-step protocols would be preferred. One-step protocols are quicker to perform and more practical in a rapid diagnostic setting.

One of the concerns with using total RNA as the starting template is the proportion of viral dsRNA present and the effect that this might have on downstream HRM analysis. Four different isolates were thus tested under various concentrations of starting RNA. Ranging from 0.5 – 50 ng/µL, all of the reactions produced easily discernible, by visual appraisal, melt and HRM curves. Template RNA concentration was thus concluded to have little effect on downstream HRM analysis. Indeed, the strength of HRM in this regard is its insensitivity to template concentration. This is important from a diagnostic point of view, as the time taken to purify dsRNA would negate the rapidity that the present study is attempting to espouse. However, future studies on sensitivity will require purified dsRNA as starting template.

Both the segment 10 and segment 2 clade-specific primers resulted in amplification products with their respective serotype isolates. However, Clade B-specific primers were not as successful. Serotype 1 of the OVIA set and serotype 2 of both OVI sets failed to give amplification products. Sequencing was used to understand and solve the serotype anomalies. The lack of a product after amplification indicated that the genomic material was not present or would not readily bind to the primers due to a lack of sequence complementarity.

After the preliminary identification that some isolates appeared not to be the serotype they were labelled with through analysis using the VP2 clade-specific PCRs, a method to definitively serotype the isolates was required. Virus neutralisation was considered, however, the lack of available serum rendered that approach unsuitable. Ideally, serotype-specific primers that target segment 2 would provide the answers. Segment 2, encoding VP2, the

outer capsid protein and the serotype-specific sequence, is the serotype benchmark. Segment 10, which encodes NS3, does not define the serotype of the virus – it is merely serotype divergent. It is unclear why this is so in AHSV as it is fairly conserved in BTV (Maan *et al.*, 2010b).

Maan *et al.* (2011a) designed a number of primers to serotype AHSV. These primers were tested on serotype confirmed isolates, negating the need for any further validation in this study. These primers were designed with an end-point being an agarose gel and were not designed with HRM analysis in mind. In addition, despite the number of alternate products being present in the gels of the Maan *et al.* (2011a) study, only the presence of a band at the correct size was sufficient for a positive identification. However, positive amplifications could only be achieved for serotypes 2 – 6 (which have amplicons ranging from 751-1267 bp). This was likely due to the fact that serotypes 1, 7, 8 and 9 have larger amplicons (1426-1793 bp) and the PCR system employed in this study suggested that the engineered polymerase was only suitable for amplicons from 60-400 bp (KAPA, 2012). At 1267 bp (for serotype 4), the polymerase is already operating at three times its stated limit. The KAPA system was used as a preliminary assessment with the intention of using a better-suited polymerase. However, the failure of OVIA2, OVIB2, NICDV(4) and OVIA5 cDNA or RNA to give amplification products with their respective primers indicated additional and further evidence of serotype anomalies. The primers of Maan *et al.* (2011a) were unable to expose subtle differences in the genome sequences, as evidenced by the corresponding melt profiles using the serotype-specific and clade-specific primers. Sequencing was thus pursued as a more suitable means to determine the serotype identity of the isolates as opposed to further RT-PCRs.

To generate additional HRM data on the isolates and further clarify the serotype of the remaining isolates, segment 10 primers 10F and 10R were used on all 27 isolates. Although the C_T values range from 17-24, all reactions plateaued. For quantitative purposes, it would be important to maintain the C_T values to within three cycles. However, quantitative aspects are not being explored in this study. The wider C_T range seen in this study is likely due to the varied amounts of viral RNA in the total RNA extractions. Total RNA is an accepted starting material for various HRM studies (Hewson *et al.*, 2010; Ghorashi *et al.*, 2011; Varillas *et al.*, 2011). Three melt profiles were evident in the segment 10 melt curve analysis. However, they were difficult to distinguish. This could be explained by the phylogeny in Figure 3.29, where the Clade C isolates (green) are present in three well-supported monophyletic clades. This is juxtaposed with the individual and resolved phylogenies of Clade A and B (red and blue). The phylogenies of segment 10 in Quan *et al.* (2008) reveal similarly disparate sub-clades. It would be expected that the more conserved clades would produce more uniform melt profiles due to the sensitivity of HRM analysis.

The Rotor-Gene™ software assigns ‘bins’ that can be set within a melt temperature region and the software will label any other melt peaks that exist in that window. The temperature window was set at 0.6°C in the present study for melt curves of the amplicons of the 10F and 10R primers. The bins were represented as labelled, vertical black lines. A threshold is normally assigned which limits the peaks detected to above a certain, defined value and is represented as a horizontal blue line. Bins are used to confirm serotype identification, but are also useful in identifying sequence divergence, as may have happened over the last 40-50 years in the AHS virus. BTV, through genetic drift or reassortment, has evolved new serotypes, although there is no evidence that the same is occurring with AHSV, despite the possible subtle drifting apparent in the melt curves (Chaignat *et al.*, 2009; Maan *et al.*, 2011b).

High Resolution Melt analysis therefore presents an effective means of separating the serotypes. The Rotor-Gene™ software does provide a tool for the distinction of the melt curves, but it is unable to accurately take into account shoulders, inflections and double peaks. For this reason, the use of the threshold and bin facility in the software is considered limited in its application. The software is also incapable of defining a genotype based on the Boolean operator ‘OR’ but will assign genotypes based on the operator ‘AND’. These restrictions become apparent in the profiles produced of the segment 10 primers where a clade could be defined using more than one ‘bin’. The Rotor-Gene™ software has the ability to genotype using the normalised HRM data, but the disparate nature of the melt profile within each clade renders this tool unusable. The software relies on the allocation of a single control profile as opposed to a statistical rendering of all the samples in a grouping – which is the outcome in this instance. Only when the individual serotypes of the clades are closely aligned, is this possible.

Concerning the serotype 2 OVI isolates being serotype 6, a possible mix-up would have likely resulted in a simple swop of two isolates, but there was no other serotype 2 isolate in either OVI set. The same could be said for the OVIA serotype 5 isolate. OVIB1 and NICD1 have been confirmed as serotype 1. NICD4 does, after failing to give amplification products with serotype-specific primers, prove to be serotype 4 after sequencing alternate amplicons. Although not designed with HRM in mind, the serotype-specific primers of Maan *et al.* (2011a) revealed that the NICD isolates of serotypes 1, 4, 7 and 9 had all shifted marginally, while maintaining the same melt profile. This may be due to small mutations of the virus over approximately 40 years and is apparent here due to the sensitivity of HRM analysis. However, additional bands seen in the gel may also have influenced the shift in melt profile. Interestingly, the number of additional products seen in this study is considerably less than those seen in the original study of (Maan *et al.*, 2011a). All of these isolates were confirmed

as being their respective serotype by sequencing. OVIA7, OVIB7 and NICD7 are all confirmed to be serotype 7 by sequencing, despite only being sequenced using segment 10 primers. OVIA8 and OVIB8, initially thought to be suspect isolates following sequencing of the 180 bp product of segment 10 (Table 3.9) were confirmed to be serotype 8 after the clade-specific amplicons of segment 2 were sequenced..

One of the advantages of HRM analysis is that the melt curves are characteristic of the actual product melted. Subtle differences in the melt curves indicate that the sequences under consideration are divergent to some extent. Where small differences in melt peak or shape are evident, a tool in the Rotor-Gene™ software can be used to define these. Given that the NICD isolates were originally isolated in the 1960s, and the OVI isolates more recently, the shifts could be attributed to the difference in isolation period and indicate a degree of genetic drift.

The NICD set of isolates was the most complete and reliable set of AHSV isolates available at the time the present study was undertaken. Some genetic drift was possibly evidenced in the shifting of melt profiles and this would indicate that any future application of HRM analysis for the serotyping or identification of AHSV or other related pathogens would necessitate a robust stock of recent field-collected isolates for control and validation purposes. Sequence analysis of these sequenced amplicons did reveal various degrees of substitution between the OVI (recent) and NICD (historical) isolates (data not shown). The final allocation of serotypes to the isolates is shown in Table 3.13. Upon investigation of the anomalies, it was discovered that the problem with the OIE reference strains has been acknowledged since 2004, but the results remain unpublished (Potgieter & Wright, 2010). Furthermore, it was acknowledged that a large number of AHSV sequences on the NCBI databases contain errors. The authors also acknowledge that many of the OVI reference strains contain mixed serotypes. Although no known case of natural mixed infections has been documented, whole genome sequence analysis would be an invaluable exercise during the annual outbreaks. In studies of rotaviruses, serotype-unique genotypes were defined and mixed infections identified through whole genome sequencing (Matthijnssens *et al.*, 2008; Jere *et al.*, 2011). In addition, the application of whole genome sequencing to the OVI reference strains would be highly advantageous.

Table 3.13: Final allocation of serotypes, through sequencing, to the OVI and NICD isolates with anomalies highlighted.

Isolate	FINAL SEROTYPE
OVIA1	?
OVIB1	1
NICDA501	1
OVIA2	6
OVIB2	6
NICDOD	2
OVIA3	3
OVIB3	3
NICDL	3
OVIA4	4
OVIB4	4
NICDV	4
OVIA5	8
OVIB5	5
NICDVH	5
OVIA6	6
OVIB6	6
NICD114	6
OVIA7	7
OVIB7	7
NICDK	7
OVIA8	8
OVIB8	8
NICD18/60	8
OVIA9	9
OVIB9	9
NICD9	9

All of the sequencing performed in this study was completed through the Sanger chain-termination method. Compared to the more advanced and modern next generation sequencing technologies, the Sanger method has some disadvantages such as low output

and rapidity and high cost per base, although remains useful for its extended reads (Wicker *et al.*, 2006; Rothberg & Leamon, 2008). Sequencing reactions in this study were, however, performed using both forward and reverse primers. In addition, the HRM curves would give anomalous and uninterpretable curves with two amplicon species, depending on their respective ratios, should a mixed infection be present. In addition, following the identification of the anomalous isolates post-sequencing, the melt curves are resolved into the respective bins and groupings of the actual serotype.

High Resolution Melt analysis is a powerful tool to display not only genetic drift, but using a combination of segment 10 primers and segment 2 clade-specific primers, it was possible that the simultaneous detection of AHSV and serotyping of the virus would be made. Some improvements have to be made to the allocation of serotypes in the Rotor-Gene™ software. HRM analysis has potential for the epidemiological profiling of AHSV in South Africa, and for rapid serotyping in the devastating event of an AHS outbreak in non-endemic zones.

It is unfortunate that the isolates received from OVI stalled the further development of a serotyping assay using HRM analysis. An unfortunate set of circumstances has resulted in the serotype anomalies described here. The history of each of the isolates is not clear, but it is presumed that they were serotyped by viral neutralisation.

It can be confirmed, through the sequencing of portions of the segment 2 genome, that all the isolates labelled serotype 2 from OVI are serotype 6 isolates. One of the isolates labelled serotype 5 from OVI is a serotype 8 isolate. The apparent shift in many of the melt curves for the NICD isolates could be accounted for by genetic drift.

With primer design and the optimisation of the primers completed previously, and the serotype anomalies largely solved, a basic protocol for the potential rapid serotyping assay could be developed. Using the segment 10 primers (10F and 10R), which could be used to amplify the 10-190 bp region, it was envisaged that the nine serotypes could be classified into three clades, according to the phylogeny in Figure 3.43.

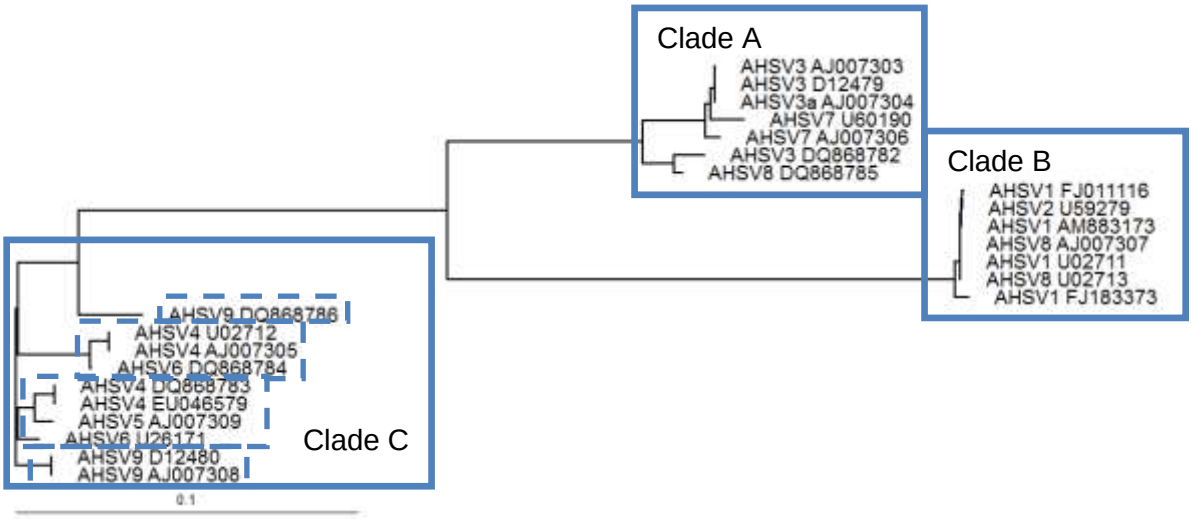

Figure 3.43: The phylogeny produced from the ClustalX2 alignment of the 10-190 bp region of segment 10 of the African horse sickness virus genome and viewed using TreeView. Dashed boxes represent the internal clades of Clade C. The bar represents 0.1 substitutions per site.

Using the 'bin' genotyping methods of the Corbett Rotor-Gene™ 6000 Series Software for melt curves, all of the isolates fell into one of the three clades. Clade A was defined as Bin D (Figure 3.37), Clade B was defined simultaneously by both Bin A and B (Figure 3.38), while Clade C was defined as either Bin A, B, or C (Figure 3.40). Clade B's double peaked profile may be due to the presence of two melting domains, while the multiple bins to define Clade C could be due to the polyphyletic nature of Clade C in Figure 3.43.

While all serotypes correctly fitted their clade profiles, serotype 8 proved to be problematic. The serotype 8 NICD isolate (NICD8) was easily classified as Clade B with its double peaked profile. However, the two serotype 8 OVI isolates (OVIA8 and OVIB8) were classified into Clade C. Initially suspected of being an additional serotype anomaly, sequencing the segment 2 amplicons (Section 3.3.9) revealed all three of the serotype 8 isolates (OVIA, OVIB and NICD) to be serotype 8. Sequencing the segment 10 amplicons was less conclusive than the results of segment 2. Quan *et al.* (2008) also experienced problems with serotype 8 when attempting to classify it into a clade based on segment 10. Additionally, earlier phylogenetic work placed serotype 8 in varying clades (Martin *et al.*, 1998; van Niekerk *et al.*, 2003).

When the Clade B sequences were isolated and only the 10-190 bp regions considered, there was a group of serotype 8 isolates that clustered on a long branch away from the rest of the sequences (Figure 3.44). The serotype 8 sequences that appeared to be outliers were also dated later (2000 onwards) than the other serotype 8 sequences.

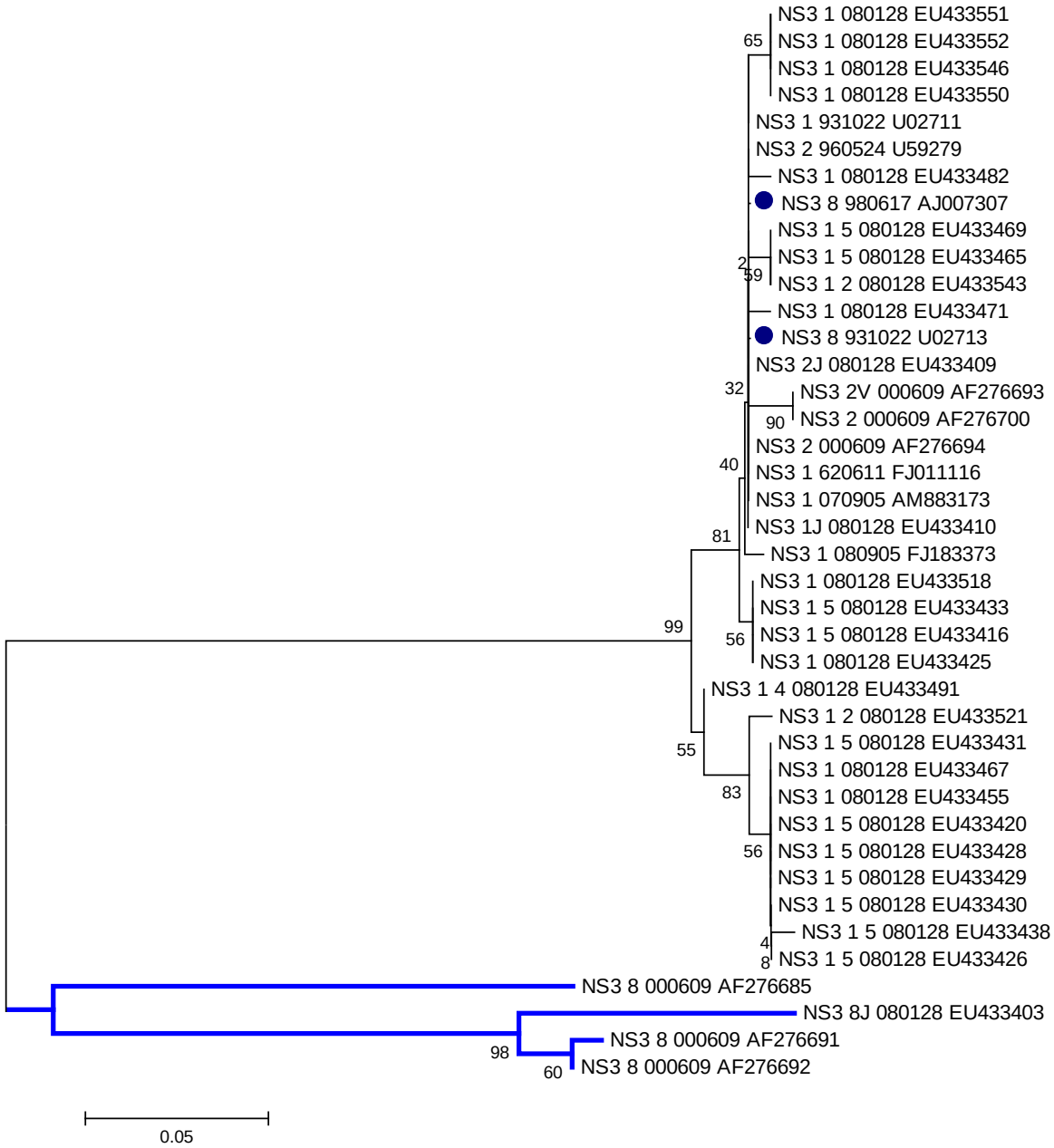

Figure 3.44: Phylogeny of Clade B serotypes based on the segment 10 10-190 bp region. Sequences were aligned using ClustalX2 (Larkin et al., 2007) and the tree drawn using the neighbour-joining method of MEGA5 (Tamura et al., 2004; Tamura et al., 2011) with 100 bootstrap replicates (Felsenstein, 1985; Saitou & Nei, 1987). The clade (shown in blue) indicated the serotype 8 outliers, while the solid blue indicated the serotype 8 sequences used for the design of the 10F and 10R primers.

Once classified into clades, the individual serotypes could be profiled and identified using the clade-specific primers (AF/AR, BF/BR and CF/CR) that target segment 2. Clade A was easily separated into serotype 3 and serotype 7 by visually inspecting the melt profiles. All three serotype 3 isolates (OVIA, OVIB and NICD) had similar profiles with a primary peak at 80-81°C and a secondary peak at 78°C. This double peak was likely due to two melting domains

in the amplicon. The serotype 7 isolates also all had similar melt profiles (panel A) with a primary peak at 81-82°C and a shoulder to the left of the peak. The distinction became clearer in the HRM analysis where there was a clear separation of the serotype 3 isolates (green) and the serotype 7 isolates (blue).

The separation of Clade B isolates was not as successful. It would appear that serotype 1 and 2 may be indistinguishable although serotype 1 has been reported to cross-react with serotype 2 (Coetzer & Erasmus, 1994). The non-amplification of RNA from serotype 1 of the OVIA set and the removal of the isolates labelled as serotype 2 of the OVI sets (OVIA2 and OVIB2) from Clade B (due to them being reclassified as serotype 6) resulted in a lack of isolates available for Clade B. Serotype 8 was well and consistently separated from serotype 1 and 2, although there was now only one serotype 8 isolate to consider. According to the phylogeny in Figure 3.45, the amplicons of serotype 1 and 2 are phylogenetically more similar to each other than to the amplicons of serotype 8, which may explain the close proximity of the melt curves of serotypes 1 and 2 in Figure 3.41.

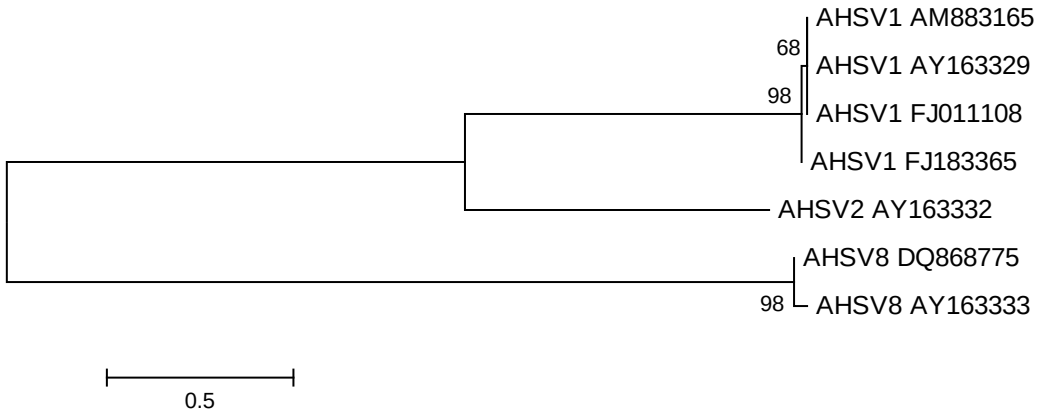

Figure 3.45: Phylogeny of Clade B serotypes based on the segment 2 1302-1551 bp region. Sequences were aligned using ClustalX2 (Larkin et al., 2007) and the tree drawn using the neighbour-joining method of MEGA5 (Tamura et al., 2004; Tamura et al., 2011) with 100 bootstrap replicates. Bar represents 0.5 substitutions per base (Felsenstein, 1985; Saitou & Nei, 1987).

Clade C serotype profiling was the least simple. Four distinct profiles could be observed in panel A of Figure 3.42. The OVI serotype 2 isolates' melt curves were the same as those of serotype 6. The serotype 9 isolate of the OVIA set fell into the same bin as serotype 5, but it had a different melt profile. The HRM analysis in panel B showed the OVI serotype 2 profiles in parallel with the serotype 6 profiles. The OVIA serotype 9 isolate had an HRM profile that occurred between the serotype 5 isolate profiles.

In many instances, the NICD isolates melt curves have marginally shifted peaks or altered melt profiles. This could be because they were isolated in the 1960s while the OVI isolates were collected during the early 2000s. This difference in isolation periods could have contributed towards some genetic drifting that is being detected over these relatively short amplicons, despite the virus being considered genetically stable. This aspect is further explored in Chapter 6, which takes into account the entire genome segment.

Table 3.10 – Table 3.12 demonstrate the capacity of the Rotor-Gene™ 6000 Series Software to genotype the sequences following post-PCR processing. The algorithms that the software applies to the calculation of the confidence percentages are proprietary, but the confidence percentage indicates the level of certainty that the allocation to a genotype was not by chance. Confidence levels as low as 60% have been used previously for highly conserved sequences, where the allocation to genotype was self-evident (Toi & Dwyer, 2008; Steer *et al.*, 2011; Grando *et al.*, 2012). The disparate nature of the amplicons in the present study suggests that a lower confidence could be accepted, but that the genotype could still be confidently separated from another at that level.

3.5. Conclusion

AHSV was successfully propagated in Vero cells and the viral RNA was extracted using a commercial phenol and guanidine isothiocyanate solution. AHSV RNA was found in all but one isolate. At the time of writing, this study represents the first successful use of the OIE mandated primers for the detection of AHSV via RT-PCR on South African field strain isolates.

High Resolution Melt analysis is a very sensitive technique that contributed to the organisation of the AHSV isolates into their correct serotypes, where applicable, using total RNA. HRM analysis also indicated that there have been some changes in the sequences from the 1960 NICD isolates to the more recent OVI isolates. This is more pronounced in some serotypes, but does not necessarily infer a new serotype. The application of HRM analysis to a rapid serotyping assay would, therefore, be a welcome and much needed addition to the current repertoire of diagnostic assays.

The combination of AHSV segment 10 10-190 bp primers and segment 2 clade-specific primers represent an ideal opportunity to serotype the AHS virus using HRM analysis from total RNA. Despite some of the serotypes not being exclusively serotyped, protocols could be applied to serotype the majority of the serotypes. Importantly, recent and large numbers of AHSV isolates would be vital to validating a serotyping assay based on HRM analysis.

CHAPTER 4: SEROTYPING THE AFRICAN HORSE SICKNESS VIRUS USING MULTIVARIATE ANALYSIS POST-HIGH RESOLUTION MELT ANALYSIS

4.1. Introduction

The African horse sickness (AHS) virus genome contains ten segments with segment 2, encoding VP2, being the most serotype-divergent and the antigenic determinant. Segment 10, encoding NS3, is the next most serotype-divergent genome segment. The AHS virus has evolved into nine different serotypes which are considered to be highly conserved due to the lack of any new serotypes being discovered since 1962 (Howell, 1962). Consequently, it is highly unlikely that enough mutations would occur to initiate the evolution of a new serotype. However, should a new serotype evolve, it would be highly advantageous to be able to detect this as rapidly as possible.

Of more immediate concern, though, is the correct identification of the serotype involved in an outbreak of AHSV. The gold standard test, according to the OIE, is the virus neutralisation test, although other end-point PCR-based tests are available (Sailleau *et al.*, 2000; OIE, 2008; Maan *et al.*, 2011a). The legislated protocol in South Africa requires that the consulting veterinarian send samples to the Onderstepoort Veterinary Institute (OVI), via the state veterinarian. There are various NGOs, industry partners and citizens groups that attempt to facilitate this process (AHS-Trust, 2008). The OVI confirms the presence or absence of AHS viral antigens through serogroup-specific (i.e. AHSV- or bluetongue-specific) serum and only one sample per outbreak is sent for serotype-specific virus neutralisation (VN) tests (DAFF, 2009).

A powerful genotyping tool is High Resolution Melt (HRM) analysis conducted in the Corbett Rotor-Gene™ 6000 rotary analyser. The Rotor-Gene™ is equipped with software that identifies the melt peaks in the post-PCR process, and assigns them to 'bins' based on the temperature at which the maximum rate of change in fluorescence is achieved. The Rotor-Gene® 6000 Series Software is, however, incapable of defining a genotype using the defined 'bins' based on the Boolean operator 'OR', but will assign genotypes based on the operator 'AND'. Although the Rotor-Gene® 6000 Series Software can define a genotype using the normalised HRM data, the disparate nature of the melt profiles obtained with the selected AHS virus PCR amplicons used in the present study renders this tool ineffective (as outlined in previous chapters). The genotyping process of the software relies on the identification of a single control or reference sample and melt profile as opposed to a statistical rendering of all samples in a group. In the present study, none of the isolates could be selected reliably as a

reference sample. All of the isolates of a particular serotype should define that serotype. When the individual melt curves of the samples are closely aligned is it possible to use a single control sample and melt profile.

The standard Corbett Rotor-Gene™ 6000 Series Software is limited when working with complex amplicons and melt profiles. Associated with the Rotor-Gene® is the ScreenClust HRM® Software, which works with the output files of an HRM run, but at a cost preclusive to most users. Only one run can be analysed at a time and there is no allowance for data from separate runs to be compared (Gurtler *et al.*, 2012). Another drawback of ScreenClust HRM® Software is that the domains are defined by the user, instead of using a statistical approach to calculate the most probable domains. These 'domains of probability' are based on quantitative variables of the melt curves. The number of clusters is determined by the gap statistic which takes into account the dispersion of the data points and recommends a cluster number as a result (Tibshirani *et al.*, 2001): the lower the number of clusters, the lower the gap statistic inferring the localised nature of the data points and *vice versa*. As the domains are defined by the user, isolates can erroneously be included in the domains. Analysis of HRM data using ScreenClust HRM® Software or the Rotor-Gene® software does not provide a statistical probability that genotype sequences should exist together in the same domain (Reja *et al.*, 2010).

Multivariate analysis is a component of several commercial statistical software packages. By definition, principal component analysis (PCA) reduces the dimensionality of several inter-correlated quantitative dependent variables to extract and "represent (them) as a set of new orthogonal variables called principal components, and to display the pattern of similarity of the observations and of the variables as points in maps" (Abdi & Williams, 2010). In particular, discriminant analysis can identify and describe clusters of related observations.

The determination of 'domains of probability' for each of the AHS virus serotypes using PCA, would provide a means of a) detecting; b) serotyping and c) confirming sequence conservation of the AHSV genome. Sequence divergence has occurred in the closely related BTV orbivirus (Maan *et al.*, 2011b). Rapid diagnostic assays should be used to gather data of all cases in the event of an outbreak in real time. Divergence from reference strains should be investigated and recorded, and field strain isolates should be evaluated for their statistical probability of departure from the reference strain to detect sequence divergence. In the event that field strain isolates could immediately be identified, new monovalent, killed-virus vaccine programmes could be employed to minimise the effects of an AHS outbreak in endemic and, more importantly, in non-endemic zones.

As mentioned in previous chapters, sequencing of various amplicons of the isolates received from OVI and NICD has revealed some anomalies in their serotyping. This poses a challenge, as it is imperative that the true serotype be identified – either for reporting purposes with respect to the index (first diagnosed) case, or for epidemiological analysis of the seroprevalence of AHSV and its continued research. The need for the reference virus and test neutralising serum, against which a diagnosis is made, to be correct is therefore critical. Identification of the serotype by HRM analysis, particularly in real-time, will facilitate an increased understanding of the correlation of the serotype to the four forms of AHS and correlate the movement of horses with severity indices and previous infections (Burne, 2011). In addition, this will enable researchers to determine whether new infections with a new serotype influence the form of the disease manifested and, most importantly, whether a new serotype has evolved. From a preventative point of view, this will theoretically enable the rapid deployment of monovalent, killed-virus vaccines after the confirmation of the index case locally, or internationally, in non-endemic and therefore serologically naïve zones.

Response time is critical in the event of an index case and subsequent outbreak. A result via real-time RT-PCR and HRM analysis could preclude a devastating outbreak in serologically naïve areas. However, equal to the rapidity of the test is the accuracy of the test. The standard Corbett Rotor-Gene™ 6000 Series Software proved to be limited when working with diverse amplicons and melt profiles. For this reason, data from the HRM analysis of the nine serotypes of AHS from three sources was subjected to multivariate analysis to detect and serotype the AHS virus. This study, therefore, introduces the concept of a statistical analysis performed in real-time such that the presence or absence of the virus is confirmed, the serotype of the virus is determined and any possible mutations are identified. Using the features of the derivative melt curves, the use of principal component analysis (PCA) is used to corroborate the ability of HRM analysis to distinguish between serotypes.

4.2. Materials and methods

4.2.1. AHSV material and data source

The nine AHS serotypes from the three sources (two sets from OVI – OVIA and OVIB – and one set from the National Institute of Communicable Diseases – NICD), were used to produce the characteristic melt curves which were used in a post-PCR *in silico* analysis. Melt curves were produced using amplification products of the 10-190 bp region of segment 10 and the clade specific primers outlined in Chapter 2.

4.2.2. ScreenClust HRM® Software

ScreenClust HRM® Software is proprietary software that prevents a user from following the process the input data undergoes. For this study, the trial version was made available by Whitehead Scientific (Cape Town, South Africa).

Raw data (as a .rex file) was exported from the Corbett Rotor-Gene™ 6000 Series Software and used in the proprietary software, ScreenClust HRM® Software (Reja *et al.*, 2010). ScreenClust HRM® Software algorithms normalise and then differentiate the HRM raw data. A composite median of the differentiated curves is then calculated and all the normalised, differentiated curves are subtracted from the composite median. The resulting residual plot is used for basic principal component analysis (Figure 1.13) (Grando *et al.*, 2012). However, the features of the curve that are used to calculate the principle components are not revealed and have proved impossible to establish due to the proprietary nature of the software. The principal component analysis can then follow a supervised discriminate analysis or an unsupervised cluster analysis for the endpoint clusters. The 'gap' statistic determines the number of clusters based on the dispersion of the data points and not the intuitive number of clusters that it should detect. If the number of genotypes is known, the user can coerce the software to find a certain number of clusters based on the known genotypes. A table describes the typicality, which indicates how well a sample fits into the assigned cluster (ranging from 0-1), the cluster it appears in and the probability of the sample occurring in that cluster, given the remaining clusters (Qiagen, 2009; Reja *et al.*, 2010).

4.2.3. GenStat® (14th edition)

ScreenClust HRM® Software potentially presents a problem should an incorrectly serotyped isolate be examined and the results are defined erroneously, by the user, to include the incorrectly serotyped isolate. Alternatively, a statistical protocol, akin to the methodologies used by the ScreenClust HRM® Software was developed using GenStat® (14th edition) to interpret the HRM analysis outputs and, importantly, assign probabilities that a melt curve represented a particular serotype based on the characteristics and features of its melt curve. Previous work does not provide the same level of statistical probability, but merely focuses on differential plots which form part of the commercial software (Reja *et al.*, 2010).

Data was exported to Microsoft® Excel® directly from the Rotor-Gene® software. The normalised HRM curves were used to obtain a number of parameters (Figure 4.1). The derivatives of the normalised HRM curves were used to obtain the maximum dF/dT (rate of change of fluorescence with respect to temperature), dF/dT variance, average dF/dT, median dF/dT, the temperature at maximum dF/dT, the number of peaks, the area under the curve, and the slope to peak. Normalised data is used so as to remove the influence of template

concentration in the analyses. These features were submitted to GenStat® in a PCA and the principal component (PC) scores were generated from the correlation matrix, which is equivalent to the variance-covariance matrix of standardised values. Average dF/dT, median dF/dT and slope to peak were highly correlated to the area under the curve, and did not influence the PC scores, and were thus excluded to avoid multi-colinearity. The PC scores thus obtained explained the variation between the serotypes in respect of the features of their differentiated fluorescence curves very well. These features were maximum dF/dT, area under the curve, number of peaks, dF/dT variance and temperature at maximum dF/dT.

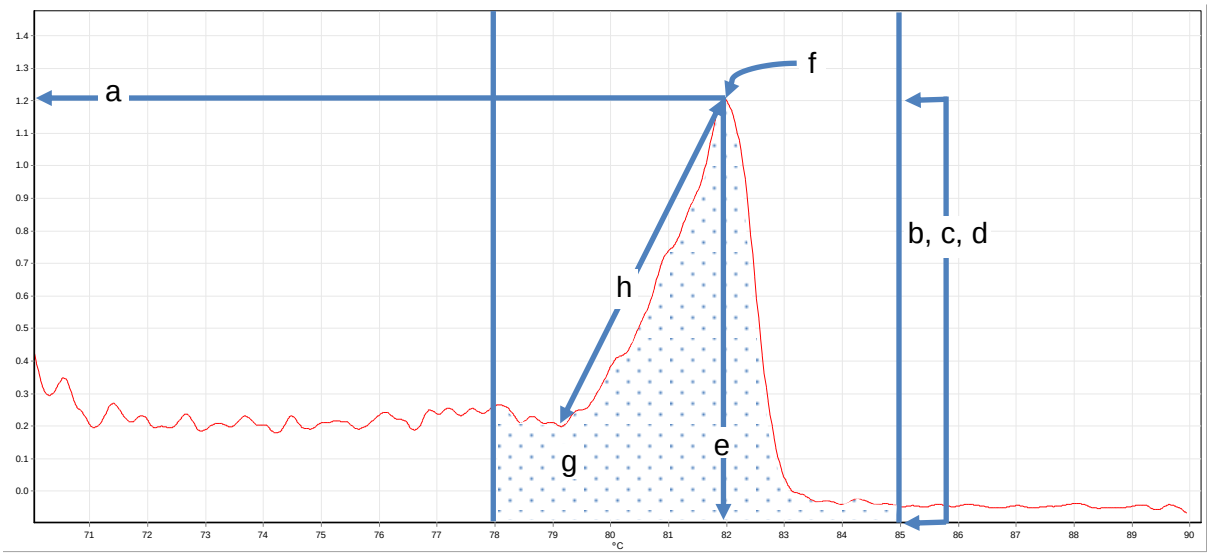

Figure 4.1: Features of the melt curve included in the principal component analysis (PCA). a – maximum dF/dT (rate of change of fluorescence with respect to temperature); b – dF/dT variance; c – average dF/dT; d – median dF/dT; e – temperature at maximum dF/dT; f – number of peaks; g – area under the curve (dotted area) and h – slope to peak.

The unsupervised cluster analysis in the ScreenClust HRM® Software is equivalent to the PCA done by first principles in GenStat®, but the variables used in the PCA in GenStat® can be customised for analysis. Being proprietary commercial software, the methodologies, although explained in Reja *et al.* (2010), cannot be manipulated in the ScreenClust HRM® Software.

HRM data from the amplification of segment 2 of AHSV using the clade-specific primers for the three serogroups (Groenink, 2009) were evaluated in ScreenClust HRM® Software and GenStat®. Representative reference strains were used in supervised analysis (ScreenClust HRM® Software) and in discriminant analysis (GenStat®).

4.3. Results

4.3.1. Analysis of the melt curve data from the 10-190 bp region amplicon of segment 10 using the ScreenClust HRM® Software

From the ScreenClust HRM® Software, using the raw fluorescence data from the melt curves of segment 10, three serogroups (clusters) were apparent (Table 4.1) (Groenink, 2009). Typicality indicates how well the sample fits into the assigned cluster: a sample that fits well tends to 1.000. ScreenClust HRM® Software, which works with the output files of an HRM analysis run, can only analyse one run at a time and there is no allowance for data from separate runs to be compared (Gurtler *et al.*, 2012). ScreenClust HRM® Software domains are defined by the user, instead of using a statistical approach to calculate the most probable domains. The number of clusters is determined by the gap statistic which takes into account the dispersion of the data points and recommends a cluster number as a result (Tibshirani *et al.*, 2001). The lower the number of clusters there are, the lower the gap statistic, which infers the localised nature of the data points and vice versa. These domains do not necessarily equal the most statistically robust number of clusters. The data in the table indicate that that some typicality is low in the groups. The ScreenClust HRM® Software User Guide indicates that typicalities of 0.05 or lower should be treated with caution (Qiagen, 2009) Three serogroups were expected as described in Groenink (2009). Cluster 1 contained only Clade B isolates (serotypes 1, 2 or 8), while Clusters 2 and 3 contained isolates from more than one clade. However, due to the proprietary nature of the software, the reasons for this could not be examined, and the results could not be improved upon by manipulating the attributes of the curves used and their respective influence. It was thus decided to assess each set of isolates separately, while dictating the number of clusters to equal the number of genotypes (serotypes) in each set.

Table 4.1: The cluster values of the nine AHS serotypes OVIA, OVIB and NICD. The values were derived from High Resolution Melt analysis post RT-PCR using the segment 10 10-190 bp amplicon and subsequent ScreenClust HRM® Software analysis. * indicates duplicates.

ID	Name	Cluster	Typicality	Prob. Cluster 1	Prob. Cluster 2	Prob. Cluster 3
21	OVIB1	**Cluster 1**	0.5498	1.0000	0.0000	0.0000
22	OVIB1*	**Cluster 1**	0.3665	1.0000	0.0000	0.0000
41	NICD1	**Cluster 1**	0.4020	1.0000	0.0000	0.0000
42	NICD1*	**Cluster 1**	0.4850	1.0000	0.0000	0.0000
43	NICD2	**Cluster 1**	0.7085	1.0000	0.0000	0.0000
44	NICD2*	**Cluster 1**	0.2673	1.0000	0.0000	0.0000
55	NICD8	**Cluster 1**	0.6127	1.0000	0.0000	0.0000
56	NICD8*	**Cluster 1**	0.3621	1.0000	0.0000	0.0000
9	OVIA5	**Cluster 2**	0.4206	0.0000	1.0000	0.0000
10	OVIA5*	**Cluster 2**	0.4030	0.0000	1.0000	0.0000
15	OVIA8	**Cluster 2**	0.8005	0.0000	1.0000	0.0000
16	OVIA8*	**Cluster 2**	0.7828	0.0000	1.0000	0.0000
17	OVIA9	**Cluster 2**	0.3094	0.0000	1.0000	0.0000
18	OVIA9*	**Cluster 2**	0.3891	0.0000	1.0000	0.0000
29	OVIB5	**Cluster 2**	0.0683	0.0000	1.0000	0.0000
30	OVIB5*	**Cluster 2**	0.0557	0.0000	1.0000	0.0000
31	OVIB6	**Cluster 2**	0.9088	0.0000	1.0000	0.0000
32	OVIB6*	**Cluster 2**	0.8938	0.0000	1.0000	0.0000
35	OVIB8	**Cluster 2**	0.8458	0.0000	1.0000	0.0000
36	OVIB8*	**Cluster 2**	0.8662	0.0000	1.0000	0.0000
37	OVIB9	**Cluster 2**	0.2951	0.0000	1.0000	0.0000
38	OVIB9*	**Cluster 2**	0.2938	0.0000	1.0000	0.0000
47	NICD4	**Cluster 2**	0.1596	0.0000	1.0000	0.0000
48	NICD4*	**Cluster 2**	0.1685	0.0000	1.0000	0.0000
51	NICD6	**Cluster 2**	0.8643	0.0000	1.0000	0.0000
52	NICD6*	**Cluster 2**	0.8484	0.0000	1.0000	0.0000
3	OVIA2	**Cluster 3**	0.1503	0.0000	0.0002	0.9998
4	OVIA2*	**Cluster 3**	0.2351	0.0000	0.0000	1.0000
5	OVIA3	**Cluster 3**	0.5494	0.0000	0.0000	1.0000
6	OVIA3*	**Cluster 3**	0.5304	0.0000	0.0000	1.0000
7	OVIA4	**Cluster 3**	0.3457	0.0000	0.0000	1.0000
8	OVIA4*	**Cluster 3**	0.3402	0.0000	0.0000	1.0000
11	OVIA6	**Cluster 3**	0.5002	0.0000	0.0000	1.0000
12	OVIA6*	**Cluster 3**	0.4346	0.0000	0.0000	1.0000
13	OVIA7	**Cluster 3**	0.2857	0.0000	0.0000	1.0000
14	OVIA7*	**Cluster 3**	0.2089	0.0000	0.0000	1.0000
23	OVIB2	**Cluster 3**	0.5861	0.0000	0.0000	1.0000
24	OVIB2*	**Cluster 3**	0.7150	0.0000	0.0000	1.0000
25	OVIB3	**Cluster 3**	0.5669	0.0000	0.0000	1.0000
26	OVIB3*	**Cluster 3**	0.4608	0.0000	0.0000	1.0000
27	OVIB4	**Cluster 3**	0.5281	0.0000	0.0000	1.0000
28	OVIB4*	**Cluster 3**	0.7246	0.0000	0.0000	1.0000
33	OVIB7	**Cluster 3**	0.5792	0.0000	0.0000	1.0000
34	OVIB7*	**Cluster 3**	0.4875	0.0000	0.0000	1.0000
45	NICD3	**Cluster 3**	0.3804	0.0000	0.0000	1.0000
46	NICD3*	**Cluster 3**	0.5642	0.0000	0.0000	1.0000
49	NICD5	**Cluster 3**	0.2329	0.0000	0.0000	1.0000
50	NICD5*	**Cluster 3**	0.1542	0.0000	0.0000	1.0000
53	NICD7	**Cluster 3**	0.5170	0.0000	0.0000	1.0000
54	NICD7*	**Cluster 3**	0.3820	0.0000	0.0000	1.0000
57	NICD9	**Cluster 3**	0.5772	0.0000	0.0000	1.0000
58	NICD9*	**Cluster 3**	0.3590	0.0000	0.0000	1.0000

The features of the curves that constitute PC 1, 2 and 3 are effectively able to produce three distinct clusters, with more commonality in the features between PC 2 and 3 (indicated by the large overlap in the clusters in the top rand hand panel) than between PC 1 and 2 or PC 1 and 3 (Figure 4.2). The reproducibility between the duplicates indicates integrity in the curves produced, but because of the proprietary nature of the software, the attributes that are included in the principal component scores cannot be discerned, or altered, and the overlap in PC 1 and 3 and the commonality in PC 2 and 3 cannot be unpacked.

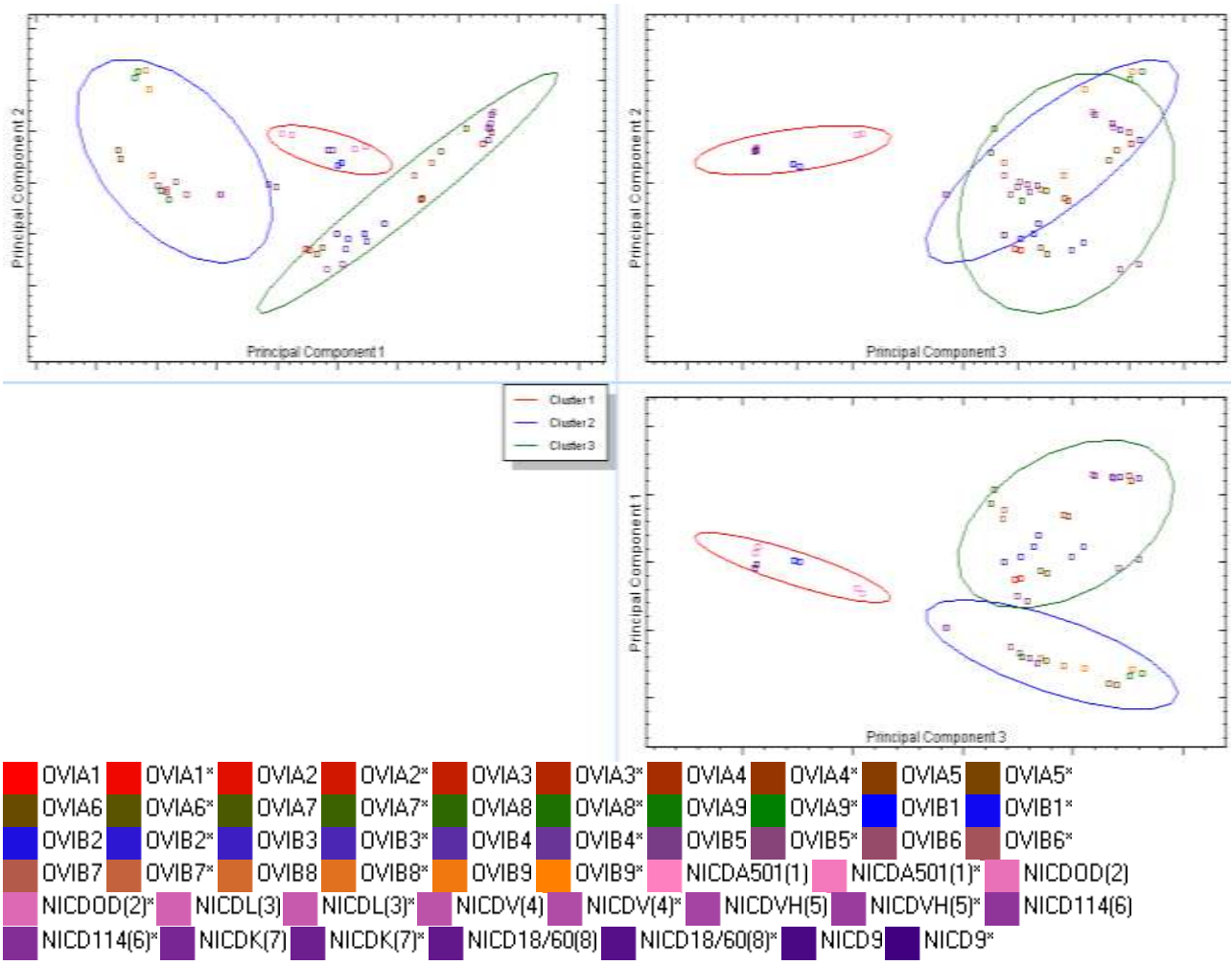

Figure 4.2: ScreenClust HRM® Software graphical output of the principal component scores for the 10-190 bp region of segment 10 of AHSV for the OVIA, OVIB and NICD sets.

It is also apparent from Table 4.1 and Figure 4.2 that there are some discrepancies in the nomenclature of the OVIA, OVIB and NICD isolates, leading to the low typicalities within a group. For this reason, the isolates that have historically been used together (i.e. each AHSV

set of isolates) were analysed separately in ScreenClust HRM® Software, using the primers that amplify the 10-190 bp region of segment 10. Groenink (2009) found that the 10-190 bp region of segment 10 produced three distinct clades of AHSV serotypes. Serotypes 3 and 7, serotypes 1, 2 and 8, and serotypes 4, 5, 6 and 9 should reside in Clades A, B and C respectively (Figure 4.3). It was intended that a ScreenClust HRM® Software analysis using HRM curve data derived from the amplicons of the 10-190 bp region of segment 10 should produce three clusters that correlate to each of the clades (Clade A, B and C).

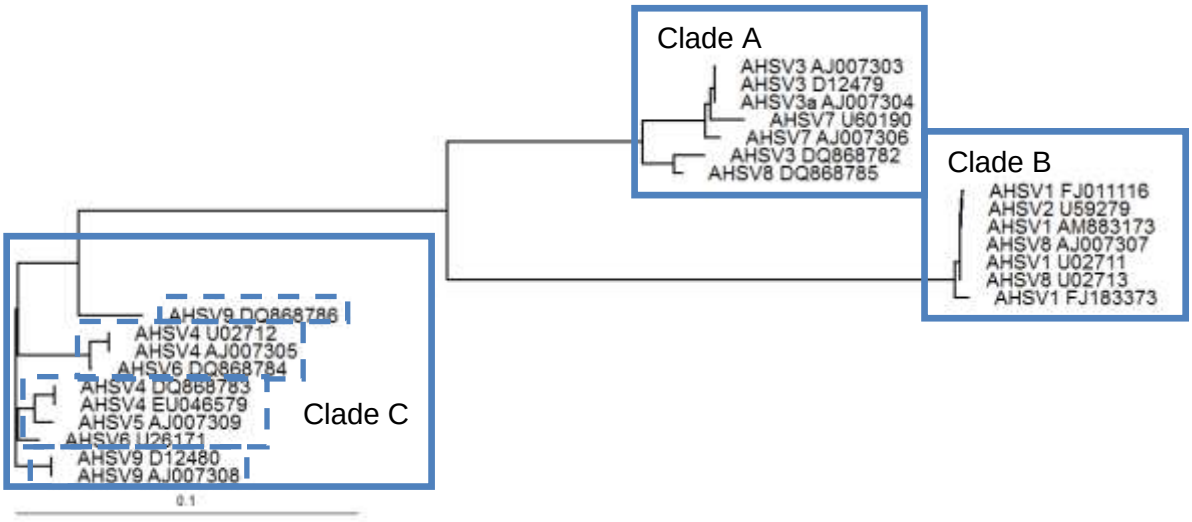

Figure 4.3: The phylogeny produced from the ClustalX2 alignment of the 10-190 bp region of segment 10 of the African horse sickness virus genome and viewed using TreeView. Dashed boxes represent the internal clades of Clade C. The bar represents 0.1 substitutions per site.

The OVIA set of isolates does not contain a serotype 1 isolate. Figure 4.4 and Table 4.2 contain the results of the OVIA isolates from the ScreenClust HRM® Software with the clusters set at 8 (equal to the number of serotypes from OVIA). It is evident from an analysis of both Table 4.2 and Figure 4.4 that the OVIA isolate labelled as serotype 2 (OVIA2) is in fact serotype 6 (both appear in Cluster 7), and the isolate OVIA8, which was suspected of being serotype 9, is serotype 8 (Table 3.9). OVIA5, previously suspected of being a serotype anomaly and possibly serotype 9, is not clustered with serotype 9 (OVIA9). There is an issue with the duplicate sample runs of OVIA serotypes 3 and 7, which exist in three different clusters (Clusters 2, 5 and 6), but are, however, in very close proximity to each other (Figure 4.4). These anomalies are not detected by the gap statistic allocated automatically by the software, which only flags serotype 7 in two different clusters, and not group it with serotype 3.

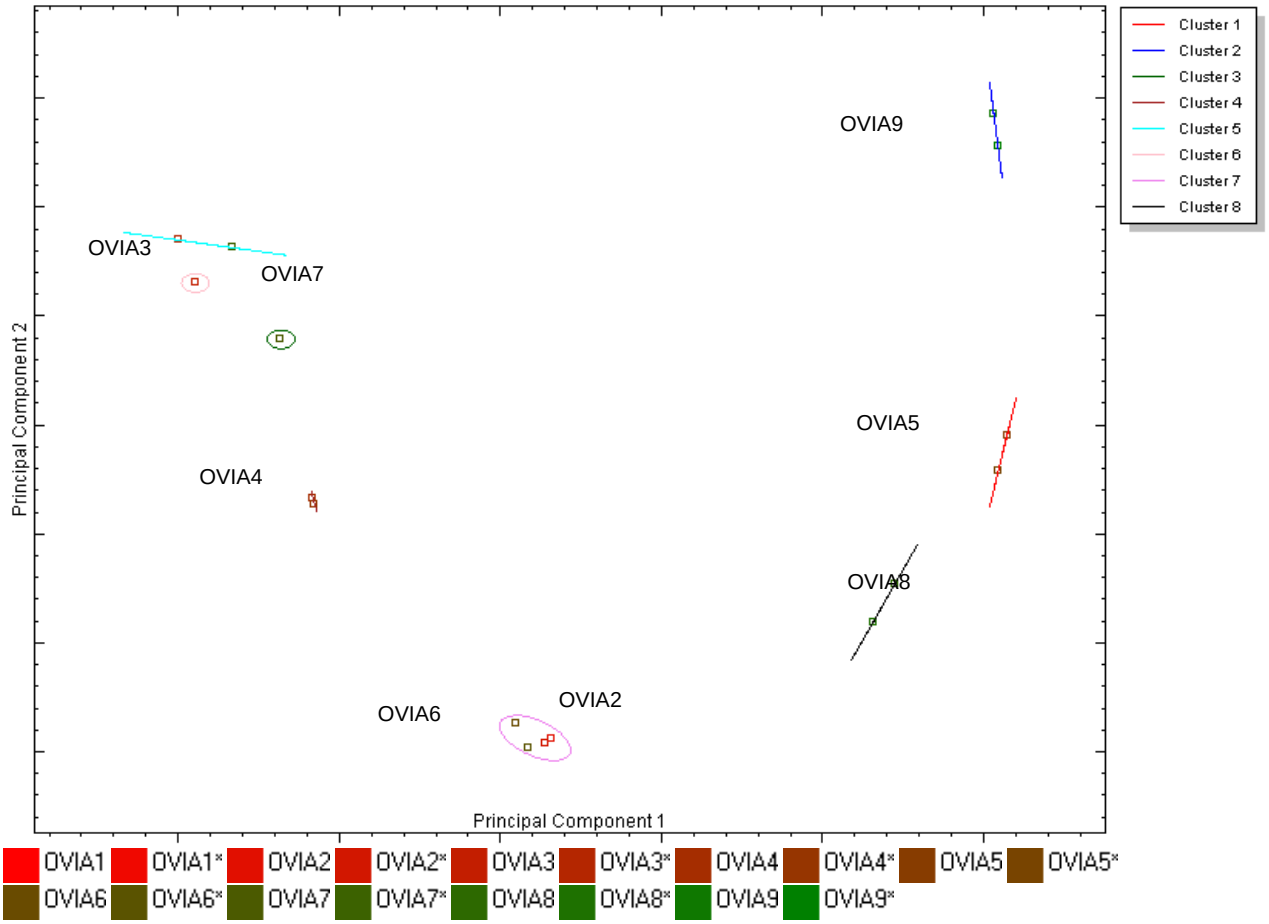

Figure 4.4: Cluster assignments for the segment 10 10-190 bp region for the OVIA isolates. The number of clusters is set to 8 to segregate the 8 serotypes of the AHSV included in this set.

Table 4.2: Cluster assignments of the 10-190 bp region of segment 10 for the OVIA set of AHSV using the ScreenClust HRM® Software. The number of clusters was set to 8 to segregate the 8 serotypes of the AHSV included in this set. * represents duplicates.

ID	Name	Cluster	Typicality	ID	Name	Cluster	Typicality
3	OVIA2	Cluster 7	0.5160	11	OVIA6	Cluster 7	0.3260
4	OVIA2*	Cluster 7	0.8119	12	OVIA6*	Cluster 7	0.3646
5	OVIA3	Cluster 6	1.0000	13	OVIA7	Cluster 3	1.0000
6	OVIA3*	Cluster 5	0.7788	14	OVIA7*	Cluster 5	0.7788
7	OVIA4	Cluster 4	0.7788	15	OVIA8	Cluster 8	0.7788
8	OVIA4*	Cluster 4	0.7788	16	OVIA8*	Cluster 8	0.7788
9	OVIA5	Cluster 1	0.7788	17	OVIA9	Cluster 2	0.7788
10	OVIA5*	Cluster 1	0.7788	18	OVIA9*	Cluster 2	0.7788

When the serotypes in the OVIB set were considered independently, the ScreenClust HRM® Software determined the number of clusters to be two from the gap statistic. The gap statistic is based on the dispersion of the data points, and increasing the number of clusters reduces the error measure for within-cluster dispersion (Tibshirani *et al.*, 2001). Table 4.3 indicates the clusters for the nine serotypes. Data from the melt curve analysis of the amplicons of the 10-190 bp region of segment 10 resulted in serotype 2 of the OVIB set clustering with serotype 6 in the ScreenClust HRM® Software analysis. With the OVI isolate labelled serotype 2 (OVIB2) confirmed to be serotype 6 (Table 3.13), the number of clusters was reduced to eight. This resulted in the serotype 2 (which is serotype 6) isolate, clustering with the serotype 4 isolate. According to Figure 4.3, serotype 4 and 6 are both in Clade C. The ScreenClust HRM® Software analysis, however, cannot elucidate these anomalies with its default algorithms or, in fact, detect them.

The results of the ScreenClust HRM® Software analysis for the NICD set are shown in Table 4.4. Serotype 9 duplicate runs appear in two clusters, and serotypes 3 and 7 were both placed in cluster 9 for the NICD set, although they are both in Clade A with similar amplicons.

Table 4.3: Cluster assignments of the 10-190 bp region of segment 10 for the OVIB set of AHSV using the ScreenClust HRM® Software. The number of clusters was set to 9 to segregate the 9 serotypes of the AHSV included in this set. * represents duplicates.

ID	Name	Cluster	Typicality	ID	Name	Cluster	Typicality
5	OVIB3	Cluster 1	0.9189	32	OVIB6*	Cluster 5	0.7212
26	OVIB3*	Cluster 1	0.9189	36	OVIB8*	Cluster 5	0.7212
23	OVIB2	Cluster 2	0.9189	33	OVIB7	Cluster 6	0.9189
24	OVIB2*	Cluster 2	0.9189	34	OVIB7*	Cluster 6	0.9189
37	OVIB9	Cluster 3	0.9189	35	OVIB8	Cluster 7	1.0000
38	OVIB9*	Cluster 3	0.9189	27	OVIB4	Cluster 8	0.9189
21	OVIB1	Cluster 4	0.9189	28	OVIB4*	Cluster 8	0.9189
22	OVIB1*	Cluster 4	0.9189	29	OVIB5	Cluster 9	0.9189
31	OVIB6	Cluster 5	0.9189	30	OVIB5*	Cluster 9	0.7212

Table 4.4: Cluster assignments of the 10-190 bp region of segment 10 for the NICD set of AHSV using the ScreenClust HRM® Software. The number of clusters was set to 9 to segregate the 9 serotypes of the AHSV included in this set. * represents duplicates.

ID	Name	Cluster	Typicality	ID	Name	Cluster	Typicality
55	NICD8	Cluster 1	0.9189	52	NICD6*	Cluster 6	0.9189
56	NICD8*	Cluster 1	0.9189	49	NICD5	Cluster 7	0.9189
58	NICD9*	Cluster 2	1.0000	50	NICD5*	Cluster 7	0.9189
47	NICD4	Cluster 3	0.9189	41	NICD1	Cluster 8	0.9189
48	NICD4*	Cluster 3	0.9189	42	NICD1*	Cluster 8	0.9189
43	NICD2	Cluster 4	0.9189	45	NICD3	Cluster 9	0.5222
44	NICD2*	Cluster 4	0.9189	46	NICD3*	Cluster 9	0.5222
57	NICD9	Cluster 5	1.0000	53	NICD7	Cluster 9	0.5222
51	NICD6	Cluster 6	0.9189	54	NICD7*	Cluster 9	0.9189

4.3.2. Analysis of the normalised HRM curve data from the 10-190 bp region of segment 10 using GenStat®

Exporting the attributes of the HRM curves to Microsoft® Excel® and performing a PCA in GenStat® produced the following output in terms of the melt profiles of the 10-190 bp region of segment 10. Using all of the variables indicated in Figure 4.1, a correlation matrix for the isolates was calculated (data not shown). This matrix indicated that high correlations exist between the average dF/dT, median dF/dT, number of peaks, area under the curve and slope to peak and that these can be replaced with the area under the curve, maximum dF/dT, number of peaks, dF/dT variance and the temperature at maximum fluorescence without a significant loss in information. The relative contribution of an attribute of the melt curve to the PC score that segregates the clusters is indicated by the latent vectors (Table 4.5). Table 4.5 shows that for these three variables, PC 1 and PC 2 account for 92.56% of the variation present between the melt curves. It also indicates that maximum dF/dT, variance, number of peaks and area under the curve are important in PC 1, while the variance, temperature at maximum dF/dT and area under the curve are important in PC 2.

Using two PC scores of segment 10 HRM data, the PCA is displayed in Figure 4.5. Distinct groupings are discernible, but there is a need to produce a clearer grouping of the three clades/clusters. Clade A isolates are seen in the bottom middle of the figure, Clade B isolates are located to the right of the figure, while the Clade C isolates are clustered in multiple clusters from the top centre anti-clockwise to left centre.

Table 4.5: Latent vectors of AHSV isolates in a principal component analysis in GenStat®. The vectors indicate the relative importance of each feature in the principal component (PC) scores.

	PC 1	PC 2
Maximum dF/dT (MAX)	-0.56699	0.02695
Variance	-0.41598	-0.52504
Temp. at max. dF/dT (TEMPatMax)	0.03522	0.73877
Number of peaks (PEAKS)	0.53584	-0.06539
Area under the curve (AUC)	0.46596	-0.41658

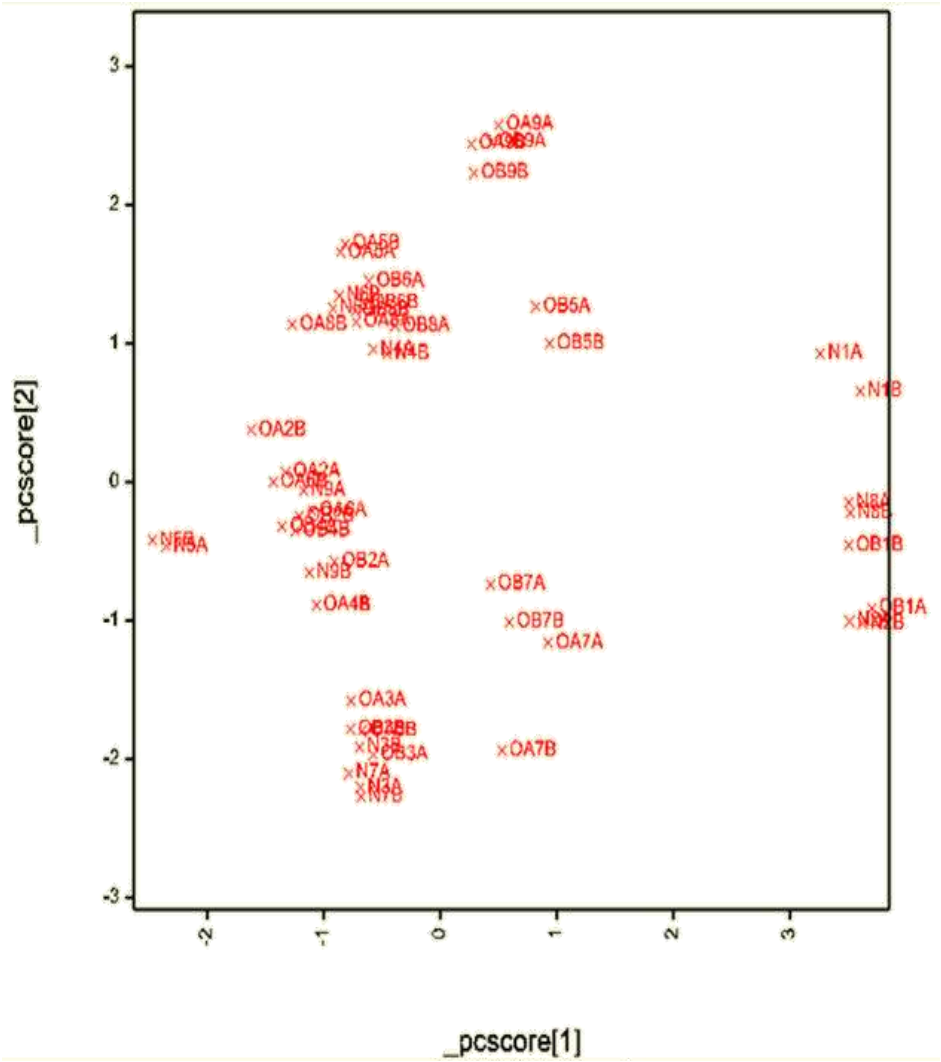

Figure 4.5: PCA of all AHSV isolated based on segment 10 HRM normalised data. OA – OVIA set; OB – OVIB set; N – NICD set; 1-9 – serotypes 1-9; A/B – duplicates.

4.3.3. Analysis of the melt curve and normalised HRM data from the 10-190 bp region of segment 10 using supervised analysis (ScreenClust HRM® Software) and multivariate discriminant analysis (GenStat®)

A supervised analysis, conducted with the ScreenClust HRM® Software, is akin to a multivariate discriminant analysis. This requires that reference samples are identified, and the proximity of the remaining samples to the reference sample will indicate relatedness. Using the PCA results of the analysis of segment 10 from Section 4.3.2, a representative for each of the nine serotypes of AHSV was selected based on its proximity to its duplicate and consistency of grouping across the three sets of reference strains (Table 4.6).

Table 4.6: Choice of isolates for references of each serotype for a supervised analysis in ScreenClust HRM® Software or a multivariate discriminant analysis in GenStat®.

Serotype	Choice
1	OVIB
2	NICD
3	OVIB
4	OVIA
5	OVIB
6	OVIA
7	OVIB
8	NICD
9	OVIA

A ScreenClust HRM® Software output of a supervised analysis based on the chosen representatives as references (Table 4.6), or 'supervisors' is shown in Table 4.7. The ScreenClust HRM® Software technique still does not permit enough resolution of isolates that have similar melt profiles. Serotype 7 isolates of the NICD set (NICD7) were clustered with all of the serotype 3 isolates (ST3), although these are of the same Clade A. The serotype 9 duplicates of the NICD set (NICD9) were located in two different clusters (ST4 and ST6); neither of them clustered with the remaining serotype 9 isolates of the OVI sets (ST9). Again, these are all in Clade C. In the serotype 5 cluster (ST5), the serotype 8 isolates of the OVIA set (OVIA8), serotype 6 isolates of the OVIB set (OVIB6), serotype 8 isolates of the OVIB set (OVIB8), serotype 4 isolates of the NICD set (NICD4) and serotype 6 isolates of the NICD (NICD6) are all found. Both serotype 2 isolates of the OVI sets (OVIA2 and OVIB2) are found in the serotype 6 cluster (ST6), along with serotype 4 of the OVIB set (OVIB4) and serotype 5 of the NICD set (NICD5), all of which are Clade C. Both serotype 7 isolates of the OVI sets

cluster in the serotype 7 cluster (ST7). These overlapping clusters with low typicalities rendered ScreenClust HRM® Software unsuitable for this purpose.

Table 4.7: A supervised ScreenClust HRM® Software analysis of the three sets of AHSV isolates (OVIA, OVIB and NICD) using the selected representatives in Table 4.6. * indicates duplicates; ST represents serotype.

ID	Name	Cluster	Typicality	ID	Name	Cluster	Typicality
21	OVIB1	ST1	1.0000	47	NICD4	ST5	0.1511
22	OVIB1*	ST1	0.3916	48	NICD4*	ST5	0.1535
41	NICD1	ST1	0.3916	51	NICD6	ST5	0.6184
42	NICD1*	ST1	0.3916	52	NICD6*	ST5	0.7170
43	NICD2	ST2	1.0000	3	OVIA2	ST6	0.7513
44	NICD2*	ST2	0.8013	4	OVIA2*	ST6	0.5909
5	OVIA3	ST3	0.0930	11	OVIA6	ST6	1.0000
6	OVIA3*	ST3	0.3132	12	OVIA6*	ST6	0.7870
25	OVIB3	ST3	1.0000	23	OVIB2	ST6	0.2712
26	OVIB3*	ST3	0.5769	24	OVIB2*	ST6	0.2186
45	NICD3	ST3	0.1406	27	OVIB4	ST6	0.2442
46	NICD3*	ST3	0.8633	28	OVIB4*	ST6	0.6943
53	NICD7	ST3	0.8898	49	NICD5	ST6	0.1238
54	NICD7*	ST3	0.5303	50	NICD5*	ST6	0.2052
7	OVIA4	ST4	1.0000	57	NICD9	ST6	0.6764
8	OVIA4*	ST4	0.5724	13	OVIA7	ST7	0.3916
58	NICD9*	ST4	0.5724	14	OVIA7*	ST7	0.3916
10	OVIA5*	ST5	0.1072	33	OVIB7	ST7	1.0000
15	OVIA8	ST5	0.5102	34	OVIB7*	ST7	0.3916
16	OVIA8*	ST5	0.2169	55	NICD8	ST8	1.0000
29	OVIB5	ST5	1.0000	56	NICD8*	ST8	0.8013
30	OVIB5*	ST5	0.9958	9	OVIA5	ST9	0.2615
31	OVIB6	ST5	0.5943	17	OVIA9	ST9	1.0000
32	OVIB6*	ST5	0.6717	18	OVIA9*	ST9	0.5632
35	OVIB8	ST5	0.5105	37	OVIB9	ST9	0.5271
36	OVIB8*	ST5	0.6319				

A discriminant analysis was performed in GenStat® using the melt curve data from the 10-190 bp region of segment 10 (Figure 4.6). The same representatives of the serotypes across the nine serotypes were used (Table 4.6). The black cluster, labelled ‘1’ is Clade A, the red cluster, labelled ‘2’ is Clade B and the green cluster, labelled ‘3’ is Clade C. Figure 4.6 indicates that using the normalised HRM data for segment 10, all nine serotypes of all three sets of isolates were discriminated into their respective clades. Based on two PC scores, GenStat®, in a supervised analysis, was able to discriminate more effectively between the serotypes than the ScreenClust HRM® Software analysis could.

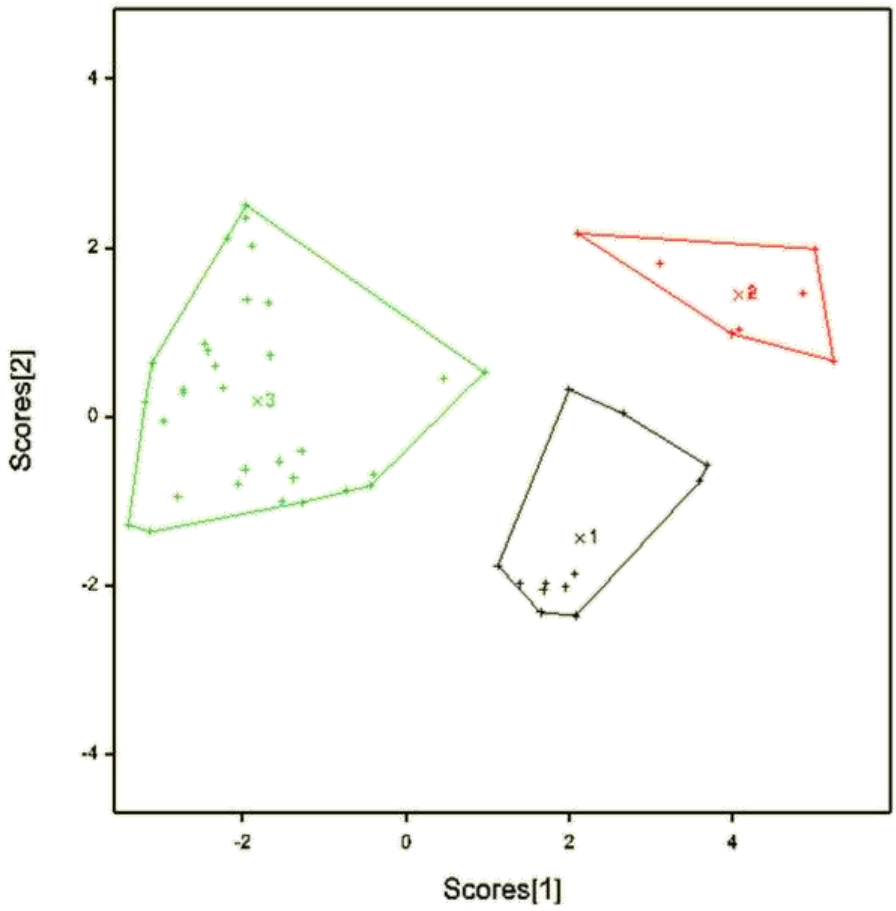

Figure 4.6: Discriminant analysis in GenStat® of OVIA, OVIB and NICD sets of AHSV using five attributes. Representatives of the nine serotypes of AHSV were used as a means of clustering all other serotypes from the OVIA, OVIB and NICD isolates, based on two PC scores calculated from the classifying variables of HRM curves of the isolates. Black (1) – Clade A; red (2) – Clade B; green (3) – Clade C. The representatives of the serotypes across the nine serotypes are represented by the × symbols. The remaining isolates of each serotype are indicated by + symbols.

Considering the resultant DA correlations, the analysis was further refined by removing the dF/dT variance, as there was a strong correlation to the maximum dF/dT (Figure 4.7). Using only four variables resulted in additional data points being included in the 95% confidence spheres (data not shown).

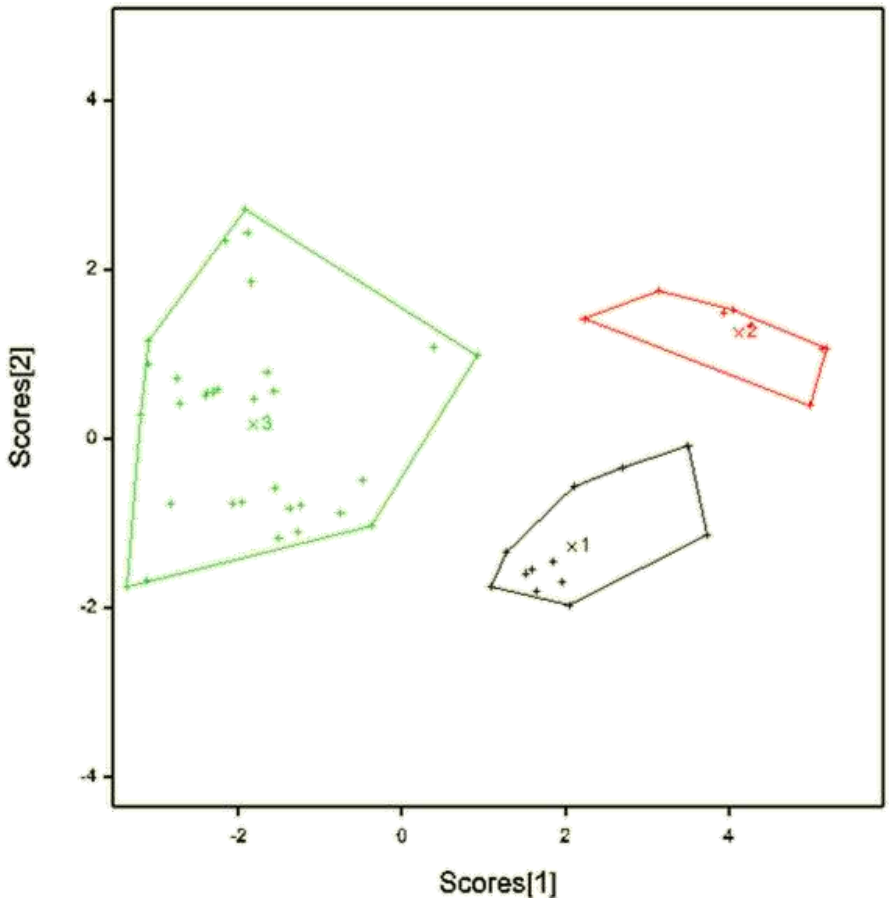

Figure 4.7: Discriminant analysis in GenStat® of OVIA, OVIB and NICD sets of AHSV using four attributes. Representatives of the nine serotypes of AHSV were used as a means of clustering all other serotypes from the OVIA, OVIB and NICD isolates, based on two PC scores calculated from the classifying variables of HRM curves of the isolates. Black (1) – Clade A; red (2) – Clade B; green (3) – Clade C. The representatives of the serotypes across the nine serotypes are represented by the × symbols. The remaining isolates of each serotype are indicated by + symbols.

When a PCA biplot is drawn using the identical data used to achieve the discriminant analysis in Figure 4.7, the separation of the isolates is again discernible (Figure 4.8). Clade A isolates are shown in the top centre of the figure and the temperature at which their maximum dF/dT occurs influencing their separation the most. Clade B isolates appear in the left of the figure with the number of peaks and maximum dF/dT responsible for the most influence. Clade C appears towards the right centre of the figure and is largely influenced by area under the curve and maximum dF/dT.

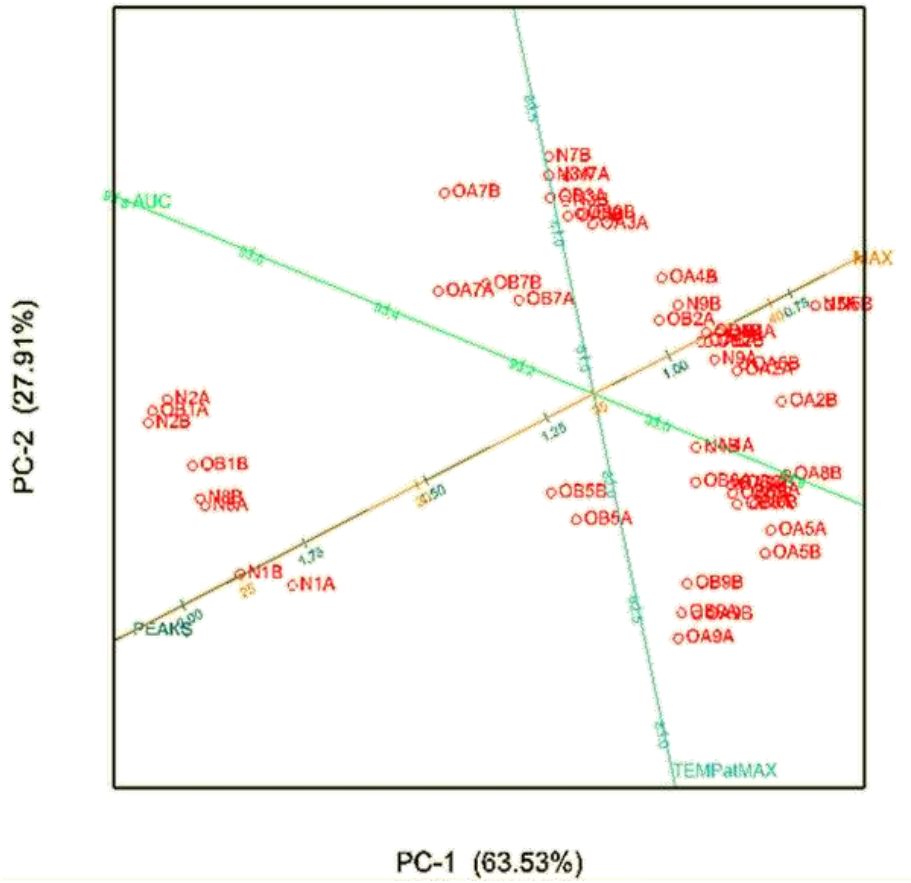

Figure 4.8: PCA biplot for the discriminant analysis using four attributes of the segment 10 HRM curve data. The PCA biplot indicates how each of the variables or attributes have contributed to the scores that distinguish between the serotypes. AUC (green) – area under the curve; TEMPatMAX (light blue) – temperature at maximum dF/dT; MAX (brown) – maximum dF/dT; PEAKS (dark blue – number of peaks).OA – OVIA set; OB – OVIB set; N – NICD set; 1-9 – serotypes 1-9; A/B – duplicates.

4.3.4. Analysis of the normalised HRM data from the clade-specific amplicons of segment 2 using multivariate discriminant analysis (GenStat®)

Because of the lack of absolute resolution between the nine serotypes in Figure 4.8, and the inability of the ScreenClust HRM® Software to compare more than one HRM run in an analysis, the clade-specific primers designed in Chapter 2 were used in a discriminant analysis, similar to the method employed in Section 4.3.3.

Using a combination of PC biplots and correlation matrices, variables selected for the clades are as follows: Clade A – slope to peak, area under the curve, number of peaks and temperature at maximum dF/dT. Clade B – area under the curve. Clade C – area under the curve, maximum dF/dT, temperature at maximum dF/dT and variance.

Considering each of the clades individually, it is possible to predict, with a reasonable degree of certainty, what the serotype is of a field strain viral infection Figure 4.9. The same process

that was followed in Section 4.3.3 was applied, in this instance, to the individual clades. The resolution that is obtainable using the discriminant analysis of GenStat® to resolve the classifying variables obtained from derivatised HRM normalised curves from the clade-specific primers is clearly illustrated. When viral RNA of a field strain is amplified and melted under the same conditions, melt data can be used to calculate melt curve features, which, next to reference serotypes in GenStat®, can be used to statistically evaluate the probability of its serotype, whilst simultaneously verifying the infection as AHSV.

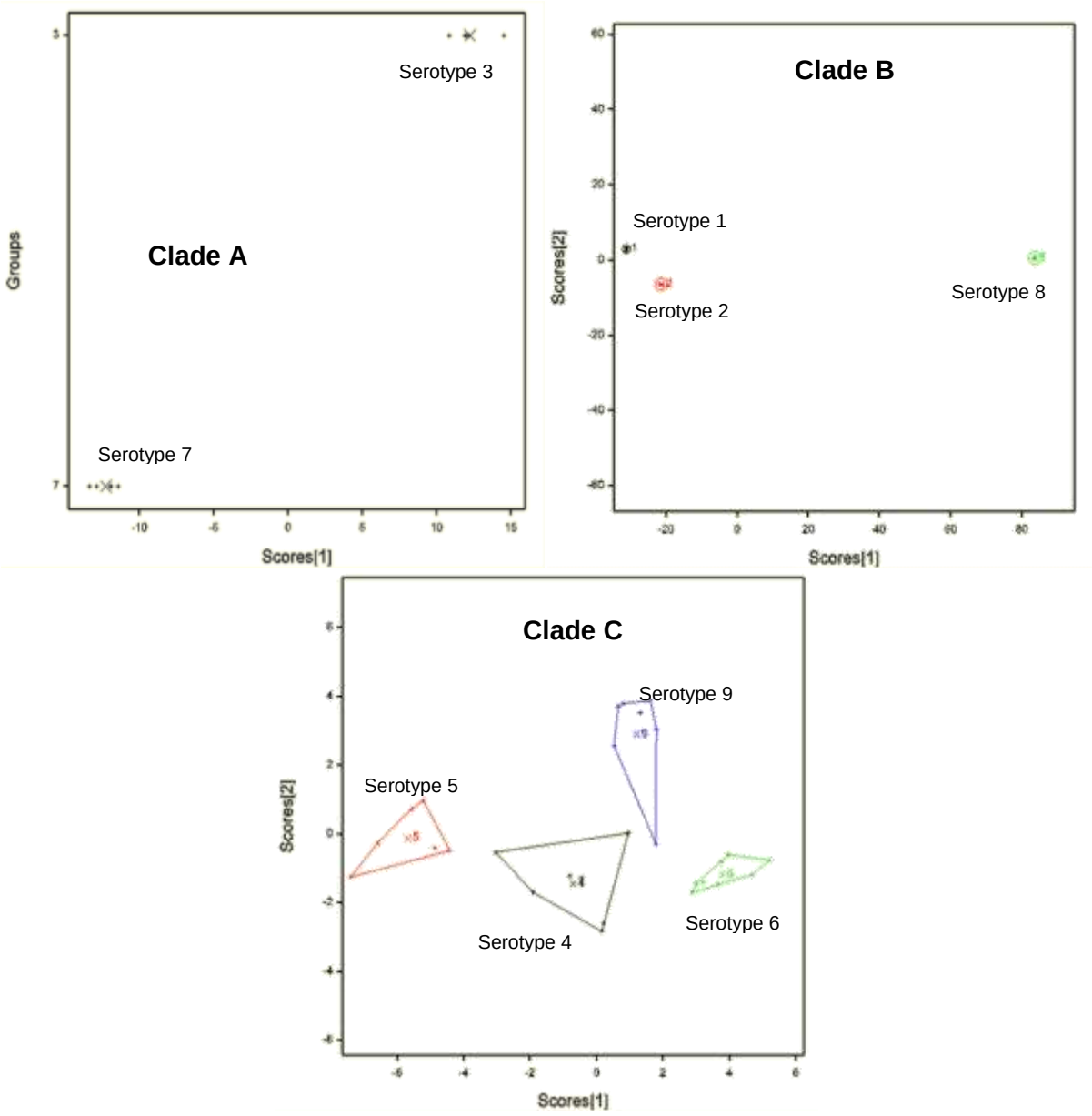

Figure 4.9: Discriminant analysis of clade-specific amplicons of segment 2 using GenStat®. Clade A (serotypes 3 and 7), Clade B (serotypes 1, 2 and 8) and Clade C (serotypes 4, 5, 6 and 9).

Melt curve features from field strain isolates treated identically to the reference serotypes would be computed by a discriminant analysis in GenStat® post-HRM analysis to belong to a specific serotype. The production of a melt curve with specific AHSV primers would confer a positive AHSV diagnosis in the first instance.

4.3.5. Influence of template concentration

To ascertain the effect of template concentration on the PCA or discriminant analysis, normalised HRM data from Section 3.3.5 was analysed in an identical fashion and the results displayed in Figure 4.10. The isolates used are clearly identifiable, despite template RNA concentrations of 100-fold difference.

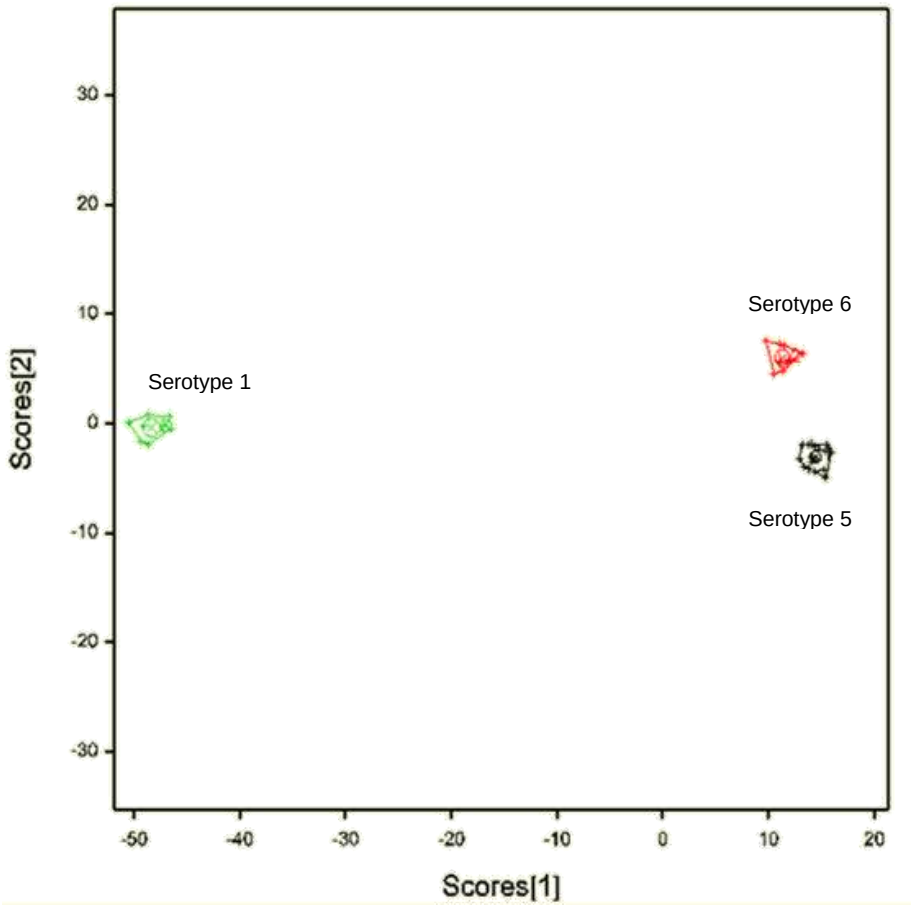

Figure 4.10: Discriminant analysis of OVIB1, OVIA2, OVIB2 and OVIA5 using initial starting template concentrations ranging from 0.5 – 50 ng/µL using GenStat®. OVIB1 – green; OVIA2/OVIB2 (= serotype 6) – red; OVIA5 – black.

4.4. Discussion

In clinical and diagnostic laboratories, successful implementation of an assay often relies on its ease of interpretation (Roth & Hanson, 2013). Traditional PCR relies on the presence of a

band of the correct size on an agarose gel. Real-time PCR relies on a positive amplification curve. The ease with which an HRM analysis is interpreted depends on the specific amplicon that is to be melted and the resultant melt curve. Where this is a simple SNP, or where the amplicons are conserved, the interpretation of a HRM analysis is straightforward. Some amplicons, as in the present study, produce an array of melt curves that the standard Rotor-Gene 6000 Series Software fails to adequately deconstruct. ScreenClust HRM® Software was developed to improve the interpretation of the results and generate a statistical interpretation of HRM results (Reja *et al.*, 2010). A number of studies have successfully used ScreenClust HRM® Software to provide an extra tier of analysis. The differentiation of *Klebsiella pneumoniae* carbapenemase gene variants in Gram-negative pathogens, ribotypes of *Clostridium difficile* and methylation of DNA have all successfully employed ScreenClust HRM® Software (Rodríguez López *et al.*, 2010; Grando *et al.*, 2012; Roth & Hanson, 2013). However, the present study was not the first to describe the limitations of ScreenClust HRM® Software. Gurtler *et al.* (2012) developed a secondary method of interpreting the data and separating the melt curves and clusters using a series of difference plots related to three temperature points and representing this information in a three dimensional graph. The present study has demonstrated that the interrogation of the algorithms in the ScreenClust HRM® Software precludes its application in the identification of AHSV serotypes. ScreenClust HRM® Software is able to successfully separate closely aligned melt curves (primarily SNPs), but the melting domains are largely conserved (Reja *et al.*, 2010; Roth & Hanson, 2013). GenStat®, on the other hand, can be used to extend analysis of the melt curves obtained in the Corbett Rotor-Gene™ 6000.

The analysis of the 10-190 bp region of segment 10 in the ScreenClust HRM® Software did not produce new information, although three clusters were produced. The three clusters produced by ScreenClust HRM® Software were not in agreement with the three clades expected from the AHSV phylogeny. According to the typicality values and the posterior class probabilities shown in Table 4.1, cluster 1 contains serotypes 1 and 2 (roughly equivalent to Clade B). Cluster 2 contains serotypes 4, 5, 6 and 9 (roughly equivalent to Clade C). Cluster 3, however, is considerably disparate and contains serotypes 3, 4, 5, 6, 7 and 9, whereas Clade A should contain only serotypes 3 and 7. There is a high coefficient of variation of 48% among the typicality values, which tends to indicate that while clusters have been ascribed, the fitting of the data into that cluster is somewhat less confident, as also evidenced by the PC biplots data. The outliers in these biplots correspond to low typicalities. A possible, and very likely, explanation for this is that the melt curve features used by the PCA in the ScreenClust HRM® Software could be improved for the type of disparate data used in the present study. However, the features that the PCA in the ScreenClust HRM®

Software uses cannot be accessed or identified. Another possible explanation for the disparate nature of these outliers, and indeed other outliers seen in this study, is that those particular serotypes are more divergent than others are, or that perhaps there has been a greater degree of genetic drift over the years between the NICD reference isolates and the recent isolates of the OVI. This point is given some validity when each of the sets (OVIA, OVIB and NICD) are considered separately and the serotypes separate out more distinctly, based on the 10-190 bp region of segment 10, although there are still a few serotypes that do not cluster separately.

Each AHSV set was also subjected to a PCA in GenStat®, using the derivatised HRM normalised curves rather than the normalised, differentiated median features that the ScreenClust HRM® Software uses. Despite some separation of the serotypes, clade separation was more defined, especially for the NICD set.

Following on from the unsupervised cluster analysis in the ScreenClust HRM® Software and the PCA in GenStat®, supervised discriminant analysis (ScreenClust HRM® Software) and multivariate discriminant analysis (GenStat®) was performed. Both of these methods call for the reference samples to be identified. A reference for each serotype was chosen from all three sets of isolates based on their performance in the unsupervised cluster analysis and the PCA. This resulted in a clear separation of the serotypes, based on their respective clades.

The clade-specific amplicons, designed for separation of the serotypes, were employed in a multivariate discriminant analysis in GenStat®. Analysing each clade individually, the serotypes separated out entirely. It was apparent from the analysis of the OVI sets of AHSV that the two serotype 2 isolates (OVIA2 and OVIB2) are, in reality, serotype 6. Prior to sequencing the amplicons, it was suspected that OVIA8 may be serotype 9, but it is indeed serotype 8, as confirmed by sequencing of segment 2 regions of the isolate and further confirmed by the PCA analysis of the ScreenClust HRM® Software.

A concern regarding the use of total RNA as the starting material for the RT-PCR assay discussed in previous chapters was that the variable amount of AHSV dsRNA present would negatively influence the statistical analyses. When ScreenClust HRM® Software is used, built in algorithms normalise the data before being subjected to a PCA. This effectively negates the influence of the concentration of starting material by ensuring that all samples are normalised to the same starting fluorescence. Before the statistical analyses (either PCA or discriminant analysis) is performed in GenStat®, normalised fluorescence data is exported from the Rotor-Gene 6000 Series Software, before being derivatised in Microsoft® Excel®. Again, this process has removed the influence of the starting concentration of template. This

has important considerations for a future diagnostic assay where normalised and pure dsRNA would not be used. However, ongoing validation and field trials will need to investigate this aspect further.

It was possible to use a PCA in GenStat® to verify the identification of reference strain serotypes. Setting serotype representatives of the reference strains in a discriminant analysis was a successful means of serotyping AHSV isolates. In particular, using clade-specific primers on segment 2 amplicons was highly successful in segregating serotypes, and provides a novel and highly accurate means of firstly, detecting the AHSV and secondly, serotyping it in real time in the case of outbreaks. Using PCA in this manner could also provide further evidence for the intra-serotype variation and this information can be used to inform vaccine production concerning circulating field serotype strains.

4.5. Conclusion

The work reported in Chapter 5 demonstrates the limited suitability of the standard Corbett Rotor-Gene™ 6000 Series Software to fully comprehend the melt curves for AHSV serotyping. Despite using the melt curves to accurately serotype the virus in some respects, there remained some inefficiency with regard to separating closely aligned melt curves. The lack of any real statistical interrogation was also a cause for concern. However, with the ScreenClust HRM® Software and the application of PCA to the melt curves, a greater degree of separation was found for the serotypes. However, in some instances this proved difficult to interpret and was made more so by the inability of the user to access the algorithms or methods behind the proprietary PCA software. For this reason, a generic software programme, GenStat® was used to analyse the data of the melt curves using the PCA and discriminant analysis options.

Following the analysis of both segments 2 and 10 on all sets of AHSV (OVIA, OVIB and NICD) with both ScreenClust HRM® Software and GenStat®, the use of ScreenClust HRM® Software is by far the most user friendly and does, to most degrees adequately separate the serotypes, especially for the melt data from the clade-specific segment 2 amplicons. However, the lack of interrogation of the methods and algorithms means that should a rogue isolate appear, or be included accidently, the ability of ScreenClust HRM® Software to identify it is limited. The PCA used in GenStat® is a basic statistical application and is widely available in other statistical software packages. For the PCA in GenStat®, the most suitable and reliable reference isolates were selected. These isolates could form the basis of the endpoint of a rapid serotyping assay for AHSV. AHSV can be diagnosed and simultaneously

serotyped using a discriminant analysis in GenStat® following the creation of melt curve data post-PCR.

CHAPTER 5: HISTORICAL PHYLOGENETIC ANALYSIS OF THE AFRICAN HORSE SICKNESS VIRUS

5.1. Introduction

The ability of a virus to evolve into variations of a type through accumulated mutations or reassortment, notably serotypes, is well documented. This is particularly apparent for the influenza viruses (Webster *et al.*, 1992; Castrucci *et al.*, 1993; Zhou *et al.*, 1999; Peiris *et al.*, 2001; Holmes *et al.*, 2005; Garten *et al.*, 2009), but has been documented for BTV (Samal *et al.*, 1987a; Samal *et al.*, 1987b; Stott *et al.*, 1987; Maan *et al.*, 2010b) . It is in their inherent nature and it would therefore be feasible to assume that AHSV also has the ability to mutate and/or re-assort and produce a new serotype, which no neutralising antibodies would be able to recognise, either *in situ* or *in vitro* (Worobey & Holmes, 1999; Attoui *et al.*, 2001; von Teichman & Smit, 2008). The prototype species of the *Orbivirus* genus is the Bluetongue virus (BTV). Prior to 2009, 24 serotypes had existed for many years (Maan *et al.*, 2011b). However, since 2008, two new serotypes have been identified in Switzerland and Kuwait, which are in geographical areas different to the classical distribution of the virus. The mechanism of this process is not fully understood, although it is believed that general BTV evolution is driven by a purifying positive selection. (Chaignat *et al.*, 2009; Maan *et al.*, 2011b). Additionally, reassortment events have been recorded BTV (Maan *et al.*, 2010b), which suggests that reassortment is a real possibility for AHSV. Phylogenetic analyses of the 'new' BTV serotypes confirmed that they are indeed BTV and can be identified in unique clades when compared to the other BTV serotypes. A new strain of Equine encephalosis virus (EEV) was identified by phylogenetic methods in Israel (Aharonson-Raz *et al.*, 2011). Phylogenetics is a tool, therefore, that can be applied to analysing sequence variation in AHSV.

African horse sickness virus can be separated into nine serotypes. The last of these serotypes was identified and isolated in 1962 (Howell, 1962). Despite regular isolation of the virus from outbreaks since then, no new serotype has been identified by either virus neutralisation tests or molecular techniques. However, despite this, anecdotal, unsubstantiated and often sensational claims have been made during a particularly intense outbreak that a new serotype had evolved (author's observations). This could largely be due to the insistence of media statements of Onderstepoort Biological Products that the vaccine is effective for all nine serotypes (Howell, 1962; Bremer, 1976; Bremer *et al.*, 1990; Mellor & Hamblin, 2004; von Teichman *et al.*, 2010) yet devastating outbreaks continue to occur periodically.

The AHSV genome is made up of 10 double-stranded RNA segments, each encoding a structural or a non-structural protein (Grubman & Lewis, 1992; Roy *et al.*, 1994). Each genome segment encodes a separate protein with unique structural and enzymatic functions in the virus. Exact functions for AHSV proteins have yet to be conclusively proven, but it is highly likely that they would have the same functions as the corresponding BTV proteins (Table 1.2). Segment 2 encodes the VP2 protein, the outer capsid protein that is responsible for cell attachment and the determination of the serotype (Roy *et al.*, 1994; Mertens *et al.*, 2006; OIE, 2008). For a new serotype to evolve, segment 2 would need to undergo significant mutations to effect this. However, the non-structural proteins (mostly involved in viral replication) could also, theoretically, evolve to become more virulent over the years such that a weak immunogenic response to VP2 could trigger the onset of greater morbidity, and therefore imitate the evolution of a new serotype. It is not known what role segment 10 (NS3) plays in serotype determination, although a role in virulence or pathogenicity has been elucidated (Martin *et al.*, 1998; Meiring *et al.*, 2009). Despite VP2 being the serotype determinant, and NS3 being serotype divergent, all of the genome segments were analysed in the present study in an effort to identify any other historical patterns of clustering between the serotypes. Strength of the infection is possibly determined by a number of different proteins and mutations, genetic shifts or reassortment in the sequences of any of them could affect the virus' virulence. Vaccines would therefore be less effective against those strains.

Molecular phylogenetic analysis has seen an explosion in popularity in recent years, aided by the ease with which genomes can now be sequenced (Baldauf, 2003). The ability to track infectious diseases of both humans and animals has become invaluable to study the evolution of a virus (Ebert & Bull, 2003). It is a pity that more full-length sequences were not available for AHSV. A basic protocol for a phylogenetic analysis consists of data retrieval and organisation, the alignment of all sequences, and phylogenetic analysis. Although phylogenetic studies were done on AHSV on a small scale in the 1990s (de Sa *et al.*, 1994; Williams *et al.*, 1998), and specific outbreaks have been studied more recently (van Niekerk *et al.*, 2001b; Koekemoer *et al.*, 2003; Quan *et al.*, 2008), it has not yet been performed on a large scale, taking into account historical and more recent isolations.

Relationships between serotypes of the AHS virus have not been studied to a large degree. The first phylogenetic analysis was performed on segment 10 sequences (de Sa *et al.*, 1994) which was found to be more variable than segment 10 of the bluetongue virus or equine encephalosis virus. In a later study of segment 10, three clades were evident. An AHSV outbreak in the Western Cape, South Africa, was tracked as a result (Quan *et al.*, 2008). A small phylogenetic study of east African AHSV isolates found that, despite the distance from

South Africa, all of the serotypes comfortably clustered with their South African reference strain counterparts (Maan *et al.*, 2011a).

Phylogenetic analysis was also used in the 2011 outbreak of AHSV in the Western Cape of South Africa to determine the serotype of the infecting virus (Grewar *et al.*, 2013). Portions of both segment 10 and segment 2 were sequenced and the phylogenetic relationships of the segment 2 sequences are shown in Figure 5.1.

However, it is unfortunate that the number of sequences available on GenBank is relatively limited compared to other economically important viruses. In addition, the number of full-length sequences is severely limited. Born out of a need to address anecdotal "assumptions" that a new serotype has evolved, the present study attempted to phylogenetically analyse each of the AHSV genome segments to create a series of phylogenetic trees that might document the evolution within each. Three different periods are identified and compared: 1960s, pre-2000 and 2000 onwards. These periods were chosen based on their availability on GenBank. Additionally, this study sought to identify a possible genetic shift in the VP2 protein (responsible for serotype determination) that would result in the vaccine becoming less effective than anticipated.

5.2. Materials and methods

5.2.1. Method outline

The analysis was done in a four-part process. Firstly, the sequences were retrieved from the GenBank database[7] and the headers (or labels) adjusted to a consistent format. Secondly, the sequences were aligned per genome segment using ClustalX2 (Larkin *et al.*, 2007). The alignment files were then, thirdly, analysed phylogenetically using MEGA5 (Tamura *et al.*, 2011) and finally the phylogenies were analysed and the sequences marked according to the approximate period of isolation.

5.2.2. Data retrieval

All available AHSV nucleotide sequences were downloaded from GenBank[7] on 15 May 2012 in FASTA format (Benson *et al.*, 2011). Both partial and full-length sequences were used in subsequent analyses. The headers downloaded from GenBank were adjusted to a consistent operational taxonomic unit (OTU), or terminal node, format. For example: `VP7_8J_100325_HM035402`. VP7 refers to the genome segment; 8J refers to serotype 8 (the J refers to the Jane sequences – a set of reference strains. Alternatively, V would refer

[7] http://www.ncbi.nlm.nih.gov/genbank/

to vaccine strains). 100325 refers to the date that best represents the date of isolation, i.e. 25 March 2010 in this example. Where no isolation dates were available, dates of submission were used. Although this is not an ideal categorisation, it seems a reasonable way of organising the somewhat chaotic GenBank data set. HM035402 refers to the accession number of that sequence. In the phylogenies, the underscores (_) are removed.

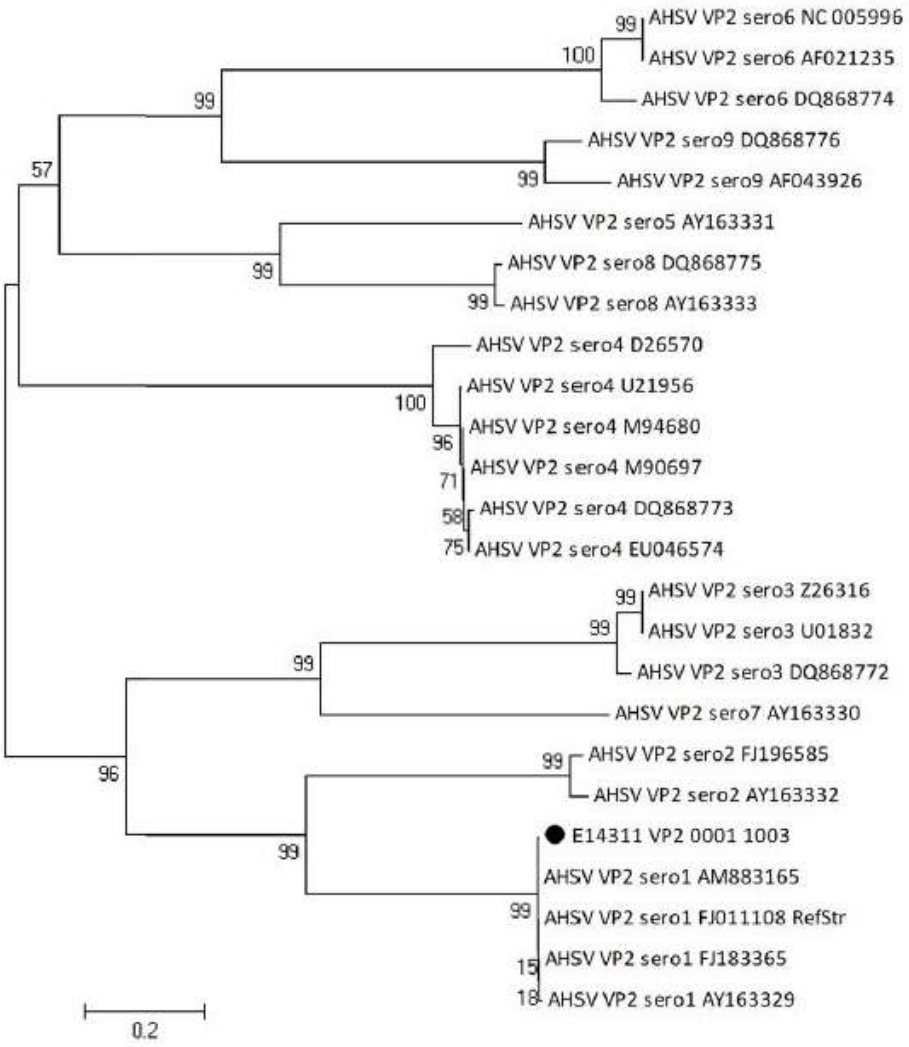

Figure 5.1: AHSV segment 2 phylogenetic tree to identify the serotype of an isolate from the 2011 outbreak in the Western Province compared to segment 2 sequences from GenBank. A neighbour-joining phylogenetic tree of 1000 bootstrap replicates of approximately 1000 nucleotides of the 5‘ end of AHSV genome segment encoding VP2. The isolate of the outbreak is indicated by a ●. GenBank accession labels are indicated in the labels (Grewar et al., 2013).

5.2.3. Sequence alignment

Sequence alignment was performed using ClustalX2 (Chenna *et al.*, 2003; Larkin *et al.*, 2007) with the following standard software-derived parameters: Gap opening penalty of 15; Gap extension penalty of 6.66 and DNA transition weight of 0.5.

5.2.4. Tree construction

The Clustal alignment files were analysed phylogenetically in MEGA 5.05 (Tamura *et al.*, 2011) using the neighbour-joining technique and clade support computed by bootstrapping (Maan *et al.*, 2011a; Grewar *et al.*, 2013). The Maximum Composite Likelihood method was used with transitions and transversions taken into account at a uniform rate. Gaps were deleted, but all coding and non-coding positions included. All trees were unrooted. The sequences were identified as being 1960s, pre-2000 (1970-1999) or post-2000.

5.2.5. Phylogenetic analysis

Analysis of the trees was performed by visual appraisal for each genome segment.

5.3. Results

A total of 488 AHSV nucleotide sequences were downloaded from GenBank on 15 May 2012. Table 5.1 lists the number of sequences available for each genome segment. The largest number of available sequences was for segment 10 (encoding for NS3). Although not a serotype determinant, it is serotype-divergent and is also the shortest genome segment allowing easier sequencing. VP2 has the next largest number of available sequences due to its importance in serotype determination and therefore its role in vaccine production.

Table 5.1: AHSV sequences available on GenBank as at 15 May 2012.

Genome segment	Sequence length (bp)	Number of sequences available	
		Full length	Partial
1 (VP1)	3965	5	
2 (VP2)	3205	18	32
3 (VP3)	2792	7	12
4 (VP4)	1978	5	13
5 (VP5)	1748	18	12
6 (VP6)	1566	6	
7 (VP7)	1169	11	45 (cds*)
8 (NS1)	1167	7	54
9 (NS2)	1166	4	37 (cds*)
10 (NS3)	756	27	175 (cds*)

*cds, coding sequences.

A phylogeny of VP1 sequences resolves serotypes 1 and 9 into two different clades (Figure 5.2).

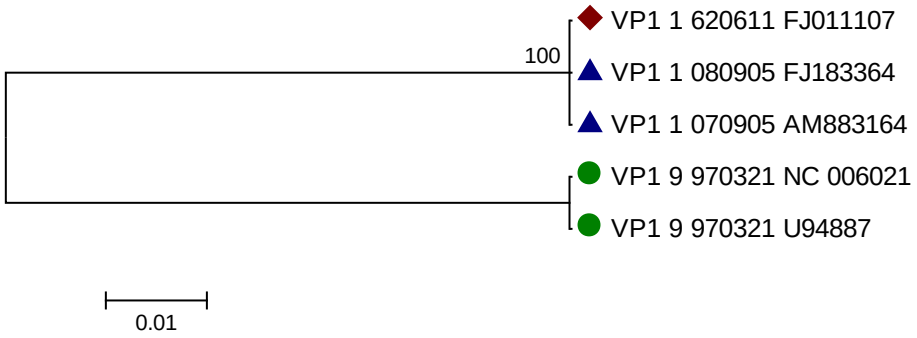

Figure 5.2: Phylogenetic tree of all available VP1 sequences of AHSV to identify potential serotype and/or isolate period relationships over time. Sequences dated in the 1960s (◆); pre-2000 (●) and from 2000 onwards (▲). The evolutionary history was inferred using the Neighbour-Joining method (Saitou & Nei, 1987). The optimal tree with the sum of branch length = 0.11178091 is shown. The percentage of replicate trees in which the associated taxa clustered together in the bootstrap test (100 replicates) are shown next to the branches (Felsenstein, 1985). The tree is drawn to scale, with branch lengths in the same units as those of the evolutionary distances used to infer the phylogenetic tree. The evolutionary distances were computed using the Maximum Composite Likelihood method (Tamura *et al.*, 2004) and are in the units of the number of base substitutions per site. The scale bar represents 0.01 base substitutions per site. The analysis involved 5 nucleotide sequences. Codon positions included were 1st+2nd+3rd+Noncoding. All positions containing gaps and missing data were eliminated. There were a total of 3965 positions in the final dataset. Evolutionary analyses were conducted in MEGA5 (Tamura *et al.*, 2011).

The nucleotide sequence of the genome segment encoding VP2 (Figure 5.3), the serotype determining genome segment, resolves groups into monophyletic and strongly supported clades that represent each serotype, with bootstrap support ranging from 77-100%. In most clades, older (maroon and green) sequences cluster amongst recent (blue) isolates. In the ST6 (serotype 6) clade, the pre-2000 sequences (green) are separated from the post-2000 sequences (blue). This is the identical pattern seen for the ST9 (serotype 9) clade. Based on the full-length sequences, the segment 2 sequences of serotypes 1 and 2 (Clade B) cluster monophyletically, with serotype 8 clustering with weak support. Although the segment 2 sequences of serotypes 3 and 7 (Clade A) and serotypes 4, 5, 6 and 9 cluster together, there is poor support for these clades.. Interestingly, the clades are based on segment 10 full-length sequences.

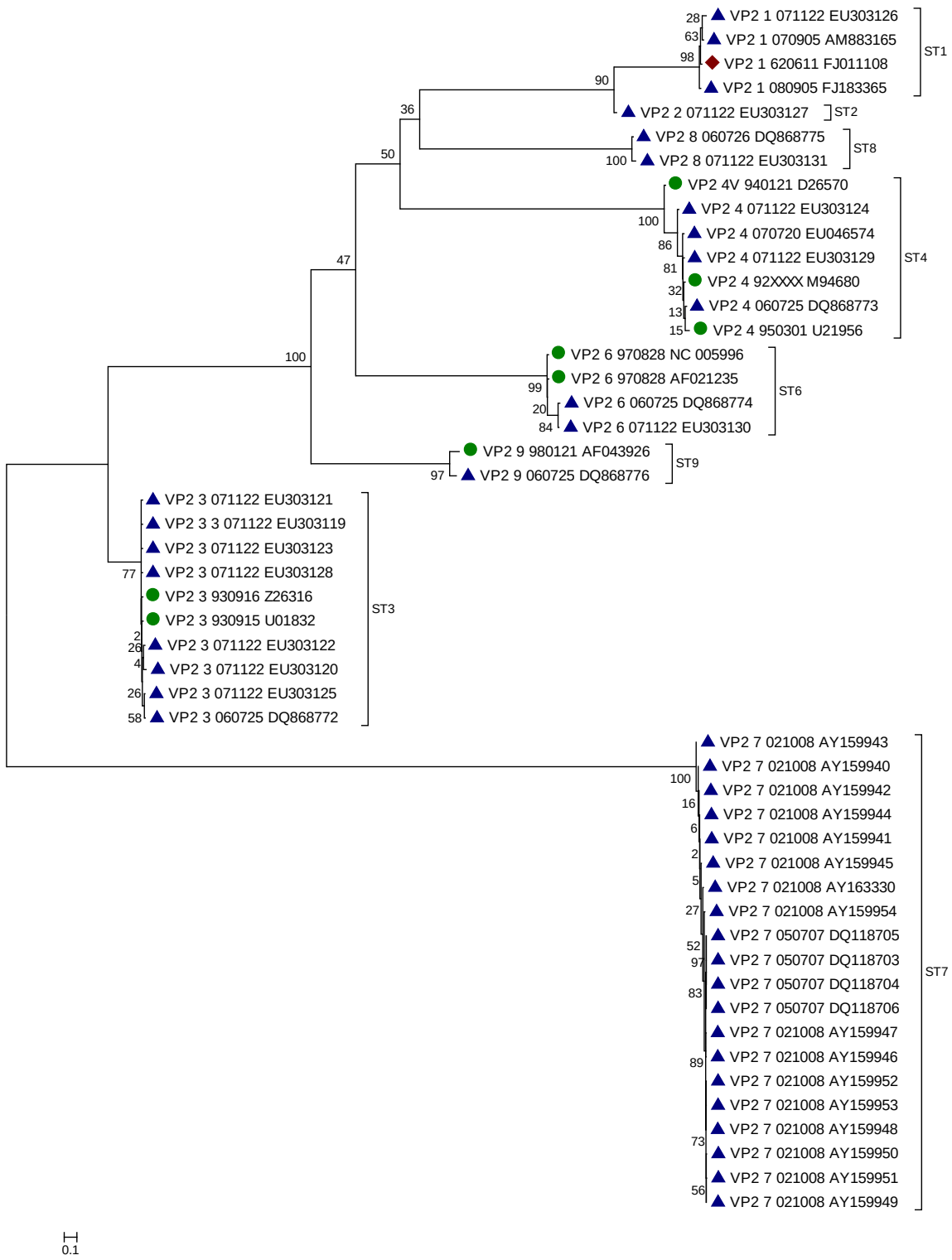

Figure 5.3: Phylogenetic tree of all available VP2 sequences of AHSV to identify potential serotype and/or isolate period relationships over time. Sequences dated in the 1960s (◆); pre-2000 (●) and from 2000 onwards (▲).The evolutionary history was inferred using the Neighbour-Joining method (Saitou & Nei, 1987). The optimal tree with the sum of branch length = 18.11039297 is shown. The percentage of replicate trees in which the associated taxa clustered together in the bootstrap test (100 replicates) are shown next to the branches (Felsenstein, 1985). The tree is drawn to scale, with branch lengths in the same units as those of the evolutionary distances used to infer the phylogenetic tree. The evolutionary distances were computed using the Maximum Composite Likelihood method (Tamura *et al.*, 2004) and are in the units of the number of base substitutions per site. The analysis involved 50 nucleotide sequences. Codon positions included were 1st+2nd+3rd+Noncoding. All positions containing gaps and missing data were eliminated. There were a total of 771 positions in the final dataset. Evolutionary analyses were conducted in MEGA5 (Tamura *et al.*, 2011).

Despite the branching evident in Figure 5.4, representing the phylogeny of genome segment encoding VP3 sequences, the scale bar of 0.01 indicates that the genome segment encoding VP3 is highly conserved and any differences between the sequences are not significant. The older sequence (maroon) is 100% identical to recent (2007 and 2008) isolates. The sequences for the genome segment encoding VP4 display similar results (Figure 5.5). The older (maroon) sequence is 100% identical to a 2007 isolate. The serotypes found amongst the genome segment encoding VP4 sequences do not cluster exclusively.

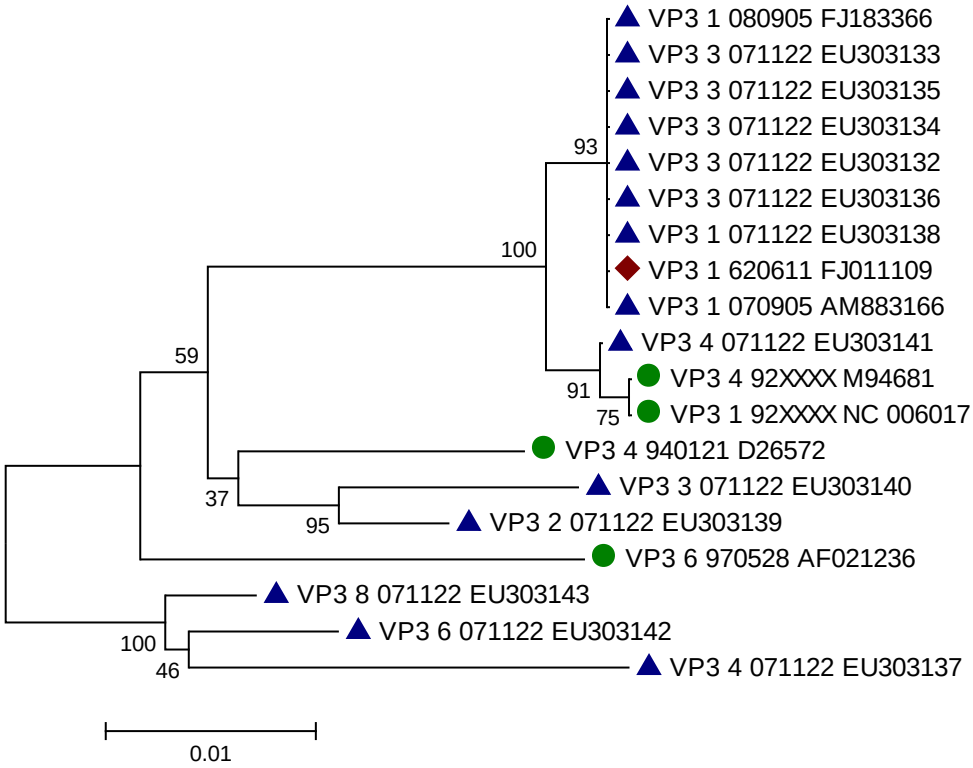

Figure 5.4: Phylogeny of all available VP3 sequences of AHSV to identify potential serotype and/or isolate period relationships over time. Sequences dated in the 1960s (◆); pre-2000 (●) and from 2000 onwards (▲). The evolutionary history was inferred using the Neighbour-Joining method (Saitou & Nei, 1987). The optimal tree with the sum of branch length = 0.13112856 is shown. The percentage of replicate trees in which the associated taxa clustered together in the bootstrap test (100 replicates) are shown next to the branches (Felsenstein, 1985). The tree is drawn to scale, with branch lengths in the same units as those of the evolutionary distances used to infer the phylogenetic tree. The evolutionary distances were computed using the Maximum Composite Likelihood method (Tamura *et al.*, 2004) and are in the units of the number of base substitutions per site. The analysis involved 19 nucleotide sequences. Codon positions included were 1st+2nd+3rd+Noncoding. All positions containing gaps and missing data were eliminated. There were a total of 735 positions in the final dataset. Evolutionary analyses were conducted in MEGA5 (Tamura *et al.*, 2011).

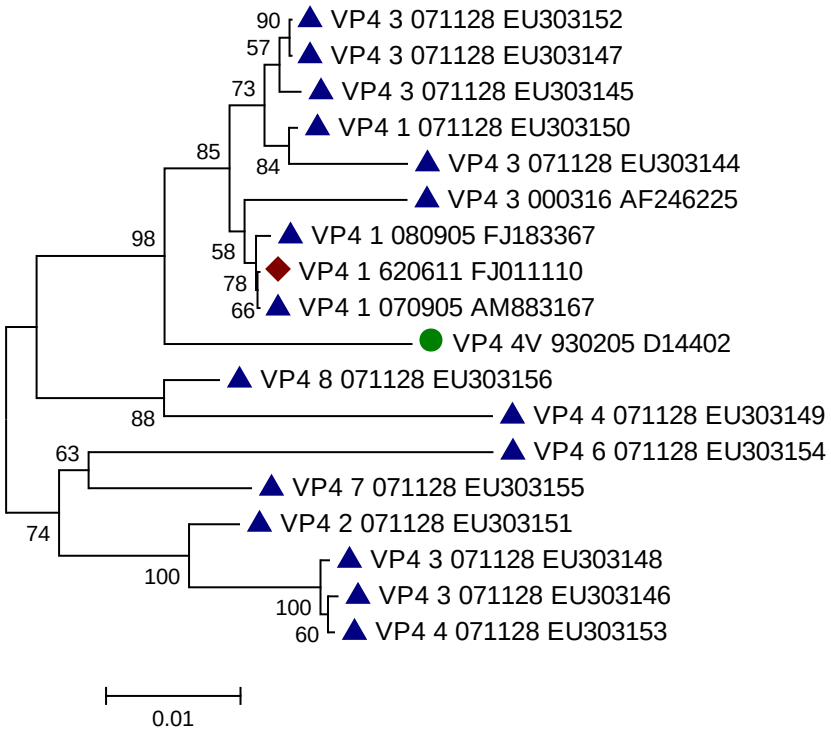

Figure 5.5: Phylogeny of all available VP4 sequences of AHSV to identify potential serotype and/or isolate period relationships over time. Sequences dated in the 1960s (◆); pre-2000 (●) and from 2000 onwards (▲).The evolutionary history was inferred using the Neighbour-Joining method (Saitou & Nei, 1987). The optimal tree with the sum of branch length = 0.17920273 is shown. The percentage of replicate trees in which the associated taxa clustered together in the bootstrap test (100 replicates) are shown next to the branches (Felsenstein, 1985). The tree is drawn to scale, with branch lengths in the same units as those of the evolutionary distances used to infer the phylogenetic tree. The evolutionary distances were computed using the Maximum Composite Likelihood method (Tamura *et al.*, 2004) and are in the units of the number of base substitutions per site. The analysis involved 18 nucleotide sequences. Codon positions included were 1st+2nd+3rd+Noncoding. All positions containing gaps and missing data were eliminated. There were a total of 863 positions in the final dataset. Evolutionary analyses were conducted in MEGA5 (Tamura *et al.*, 2011).

The sequences for the genome segment encoding VP5 appear substantially more divergent than those for VP3 and VP4 (Figure 5.6). The pre-2000 (green) sequences indicated by the arrows do not cluster with their respective serotype sequences. The remaining pre-2000 sequences (green) are clustered with the post-2000 (blue) sequences. Furthermore, there is some notable clustering of serotypes. Serotype 3 sequences are resolved except two sequences, which cluster within a multi-serotype clade (red box). The only serotype 7 sequence is within its own clade, but clustered close to serotype 3. Sequences of serotypes 8, 4, 2 and 1 cluster in serotype exclusive clades.

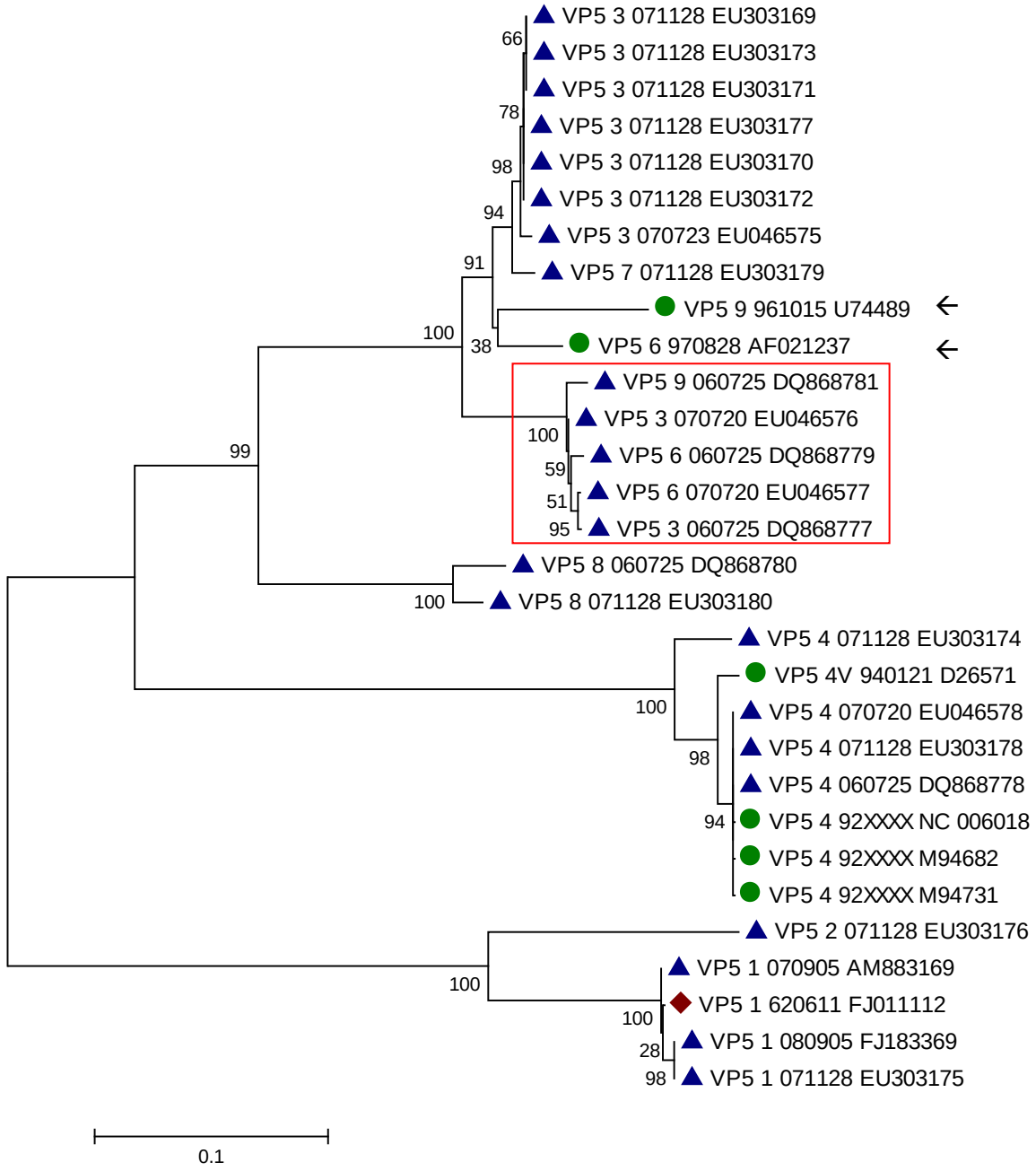

Figure 5.6: Phylogeny of all available VP5 sequences of AHSV to identify potential serotype and/or isolate period relationships over time. Sequences dated in the 1960s (◆); pre-2000 (●) and from 2000 onwards (▲). The arrows indicate sequences that do not cluster with their respective serotypes. The red box indicates a multi-serotype clade. The evolutionary history was inferred using the Neighbour-Joining method (Saitou & Nei, 1987). The optimal tree with the sum of branch length = 1.19616825 is shown. The percentage of replicate trees in which the associated taxa clustered together in the bootstrap test (100 replicates) are shown next to the branches (Felsenstein, 1985). The tree is drawn to scale, with branch lengths in the same units as those of the evolutionary distances used to infer the phylogenetic tree. The evolutionary distances were computed using the Maximum Composite Likelihood method (Tamura *et al.*, 2004) and are in the units of the number of base substitutions per site. The analysis involved 30 nucleotide sequences. Codon positions included were 1st+2nd+3rd+Noncoding. All positions containing gaps and missing data were eliminated. There were a total of 859 positions in the final dataset. Evolutionary analyses were conducted in MEGA5 (Tamura *et al.*, 2011).

It is shown in Figure 5.7 that the sequences for the genome segment encoding VP6, of which there were only six available, have clustered per serotype (serotypes 1, 3 and 6), although the overall similarity is very high. The 1960s' (maroon) sequences are similarly clustered with the more recent, post-2000 (blue) sequences.

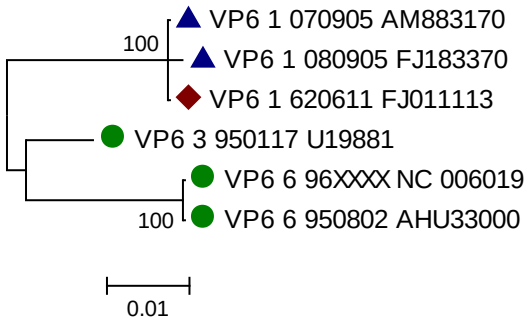

Figure 5.7: Phylogeny of all available VP6 sequences of AHSV to identify potential serotype and/or isolate period relationships over time. Sequences dated in the 1960s (◆); pre-2000 (●) and from 2000 onwards (▲). The evolutionary history was inferred using the Neighbour-Joining method (Saitou & Nei, 1987). The optimal tree with the sum of branch length = 0.05076176 is shown. The percentage of replicate trees in which the associated taxa clustered together in the bootstrap test (100 replicates) are shown next to the branches (Felsenstein, 1985). The tree is drawn to scale, with branch lengths in the same units as those of the evolutionary distances used to infer the phylogenetic tree. The evolutionary distances were computed using the Maximum Composite Likelihood method (Tamura *et al.*, 2004) and are in the units of the number of base substitutions per site. The analysis involved 6 nucleotide sequences. Codon positions included were 1st+2nd+3rd+Noncoding. All positions containing gaps and missing data were eliminated. There were a total of 1168 positions in the final dataset. Evolutionary analyses were conducted in MEGA5 (Tamura *et al.*, 2011).

Large numbers of recent isolates (blue) for segment 7 (encoding VP7), the most conserved genome segment, were available (Figure 5.8). This is likely due to the popularity of the genome segment encoding VP7 as a PCR target for serogroup specific assays (Fernández-Pinero *et al.*, 2009; Quan *et al.*, 2010). Where obtained, older sequences were identical to recent isolates. No appreciable clustering of the serotypes is evident.

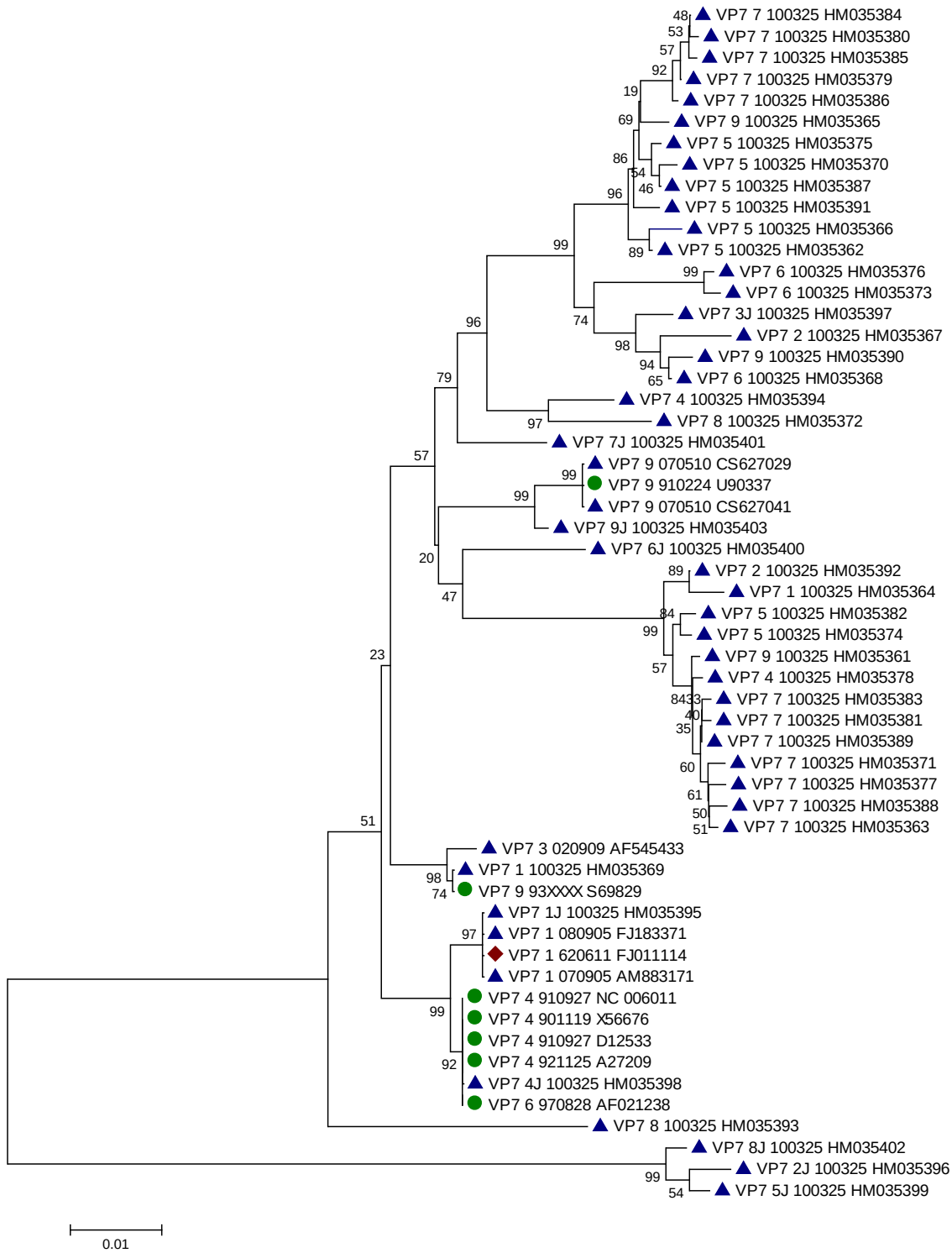

Figure 5.8: Phylogeny of all available VP7 sequences of AHSV to identify potential serotype and/or isolate period relationships over time. Sequences dated in the 1960s (◆); pre-2000 (●) and from 2000 onwards (▲). The evolutionary history was inferred using the Neighbour-Joining method (Saitou & Nei, 1987). The optimal tree with the sum of branch length = 0.05076176 is shown. The percentage of replicate trees in which the associated taxa clustered together in the bootstrap test (100 replicates) are shown next to the branches (Felsenstein, 1985). The tree is drawn to scale, with branch lengths in the same units as those of the evolutionary distances used to infer the phylogenetic tree. The evolutionary distances were computed using the Maximum Composite Likelihood method (Tamura *et al.*, 2004) and are in the units of the number of base substitutions per site. The analysis involved 56 nucleotide sequences. Codon positions included were 1st+2nd+3rd+Noncoding. All positions containing gaps and missing data were eliminated. There were a total of 1050 positions in the final dataset. Evolutionary analyses were conducted in MEGA5 (Tamura *et al.*, 2011).

The scale bar for the genome segment encoding NS1 sequences indicates a high degree of conservation (Figure 5.9). As NS1 is involved in tubule formation in the host cell (Mertens *et al.*, 2006), it is unlikely that there is a large degree of selective pressure on it. There is minimal to no clustering of either serotypes or isolation periods. However, the one 1960s (maroon) isolate appears individually in a clade separated from other isolates (arrow) The scale bar further indicates the conservation of the genome segment encoding NS1 across serotypes and isolation periods.

The available sequences of NS2 contain very few older isolates (1960s or pre-2000), as shown in Figure 5.10. However, the two that are available (indicated by arrows), are identical to other recent isolates. As for the NS1 sequences, there is minimal to no clustering of the serotypes and the scale bar indicates the conservation of the genome segment encoding NS1 across serotypes and isolation periods. NS2 forms inclusion bodies in host cells (Mertens, 2004).

Segment 10 (NS3) has been extensively studied due to its unique divergence amongst serotypes and relatively short length. As such, there is a much greater sequence depth for NS3 with over 200 gene sequences available on genomic databases. As described previously (Groenink, 2009), segment 10 sequences can be divided into three distinct clades (Clade A – serotypes 3 and 7; Clade B – serotypes 1, 2 and 8; Clade C – serotypes 4, 5, 6 and 9). Due to the number of sequences available, and ease of display, Clade A is shown in Figure 5.11 with Clade B and C collapsed, Clade B is shown in Figure 5.12 with Clade A and C collapsed and Clade C is shown in Figure 5.13 with Clade A and B collapsed. Segment 10 is serotype divergent although it has no known bearing on serotype determination. However,NS3 is involved in virion release from the infected cell (Hyatt *et al.*, 1993; de Sa *et al.*, 1994; Huismans *et al.*, 2004).

In Figure 5.11 – 5.13, the older sequences (maroon and green) are evenly distributed throughout all three clades. They do not cluster together at any point on the phylogenetic trees that would indicate some sequence conservation since the 1960s. Closer inspection of the OTU labels reveals that a number of the isolates may have two possible serotypes associated with them. The first number (after the genome segment description) represents the inferred serotype from BLASTn searching the actual sequence. The second number (before the date) represents the named serotype according to the GenBank annotations of that sequence and any related published studies. An example is shown in Figure 5.11 by the arrow: a BLASTn analysis of the sequence indicates that this isolate is serotype 3. However, the GenBank entry's annotations suggest that it is serotype 5.

The sequences in the phylogenies have clustered according to the former serotype, inferred from a BLASTn analysis, rather than the named, annotated serotype. In the above example, the isolate clusters with serotype 3, not serotype 5. Segment 10 does indicate serotype divergence in each of the main clades produced by the phylogenetic analysis. In Figure 5.11 (Clade A), there is a separation of serotypes 3 and 7, albeit with poor support, but no separation of isolates with different isolation periods. Some of the serotype 7 sequences (red box) are closely related to some serotype 3 sequences, supported with a bootstrap of 86. In Figure 5.12 (Clade B), there is a clear separation of serotype 8 isolates from serotype 1 and 2 isolates. Furthermore, serotype 2 isolates appear throughout the principal clade of serotype 1. There is no separation of the isolates based on isolation period. In Figure 5.13 (Clade C), although distinct serotype-specific clustering is initially evident, further investigation reveals that this is not so. What is apparent though is that the clustering of serotypes that is evident is based on the serotype determined by BLASTn analysis rather than the annotated serotype.

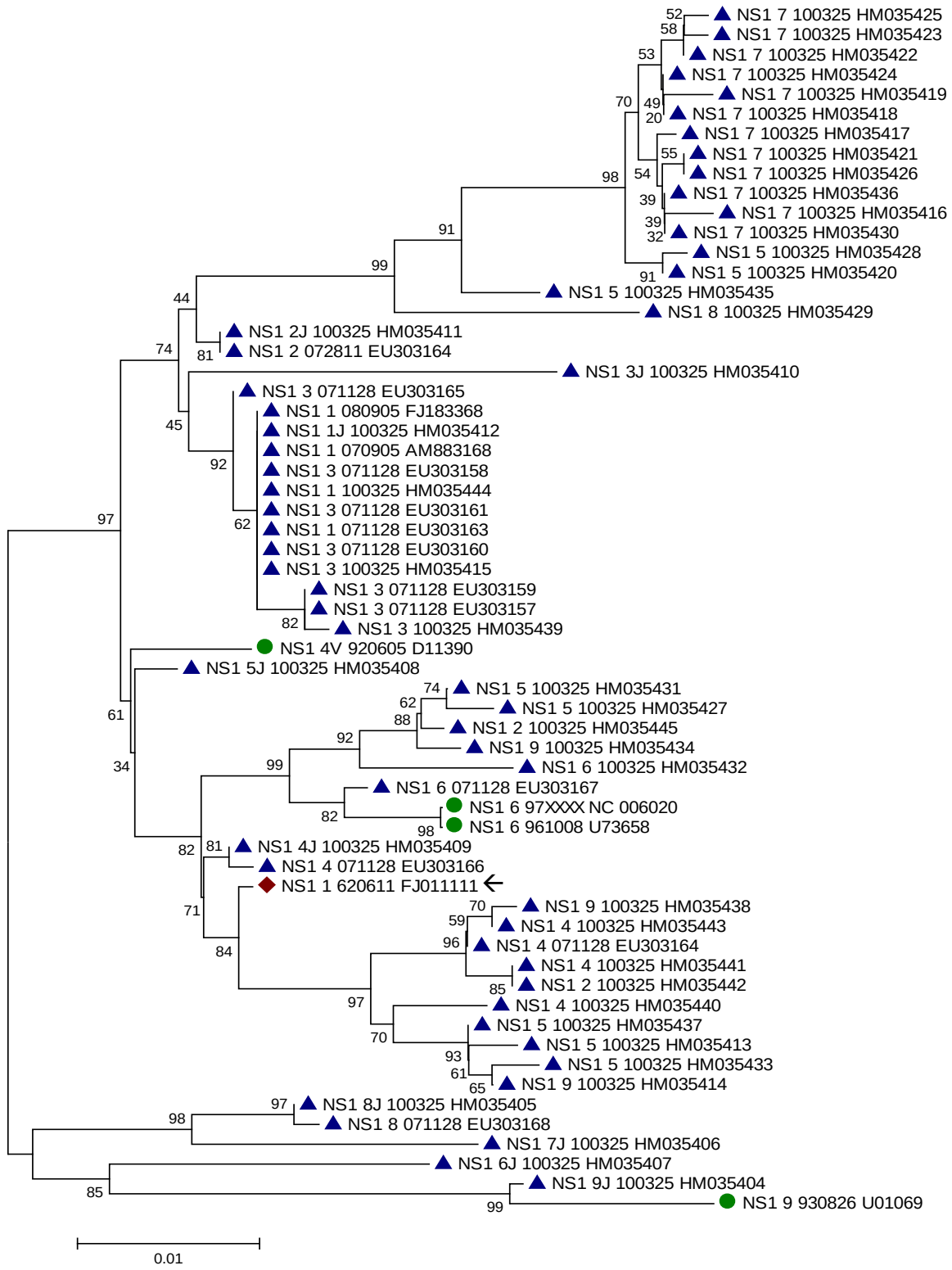

Figure 5.9: Phylogeny of all available NS1 sequences of AHSV to identify potential serotype and/or isolate period relationships over time. Sequences dated in the 1960s (◆); pre-2000 (●) and from 2000 onwards (▲). The evolutionary history was inferred using the Neighbour-Joining method (Saitou & Nei, 1987). The optimal tree with the sum of branch length = 0.27928831 is shown. The percentage of replicate trees in which the associated taxa clustered together in the bootstrap test (100 replicates) are shown next to the branches (Felsenstein, 1985). The tree is drawn to scale, with branch lengths in the same units as those of the evolutionary distances used to infer the phylogenetic tree. The evolutionary distances were computed using the Maximum Composite Likelihood method (Tamura *et al.*, 2004) and are in the units of the number of base substitutions per site. The analysis involved 61 nucleotide sequences. Codon positions included were 1st+2nd+3rd+Noncoding. All positions containing gaps and missing data were eliminated. There were a total of 767 positions in the final dataset. Evolutionary analyses were conducted in MEGA5 (Tamura *et al.*, 2011).

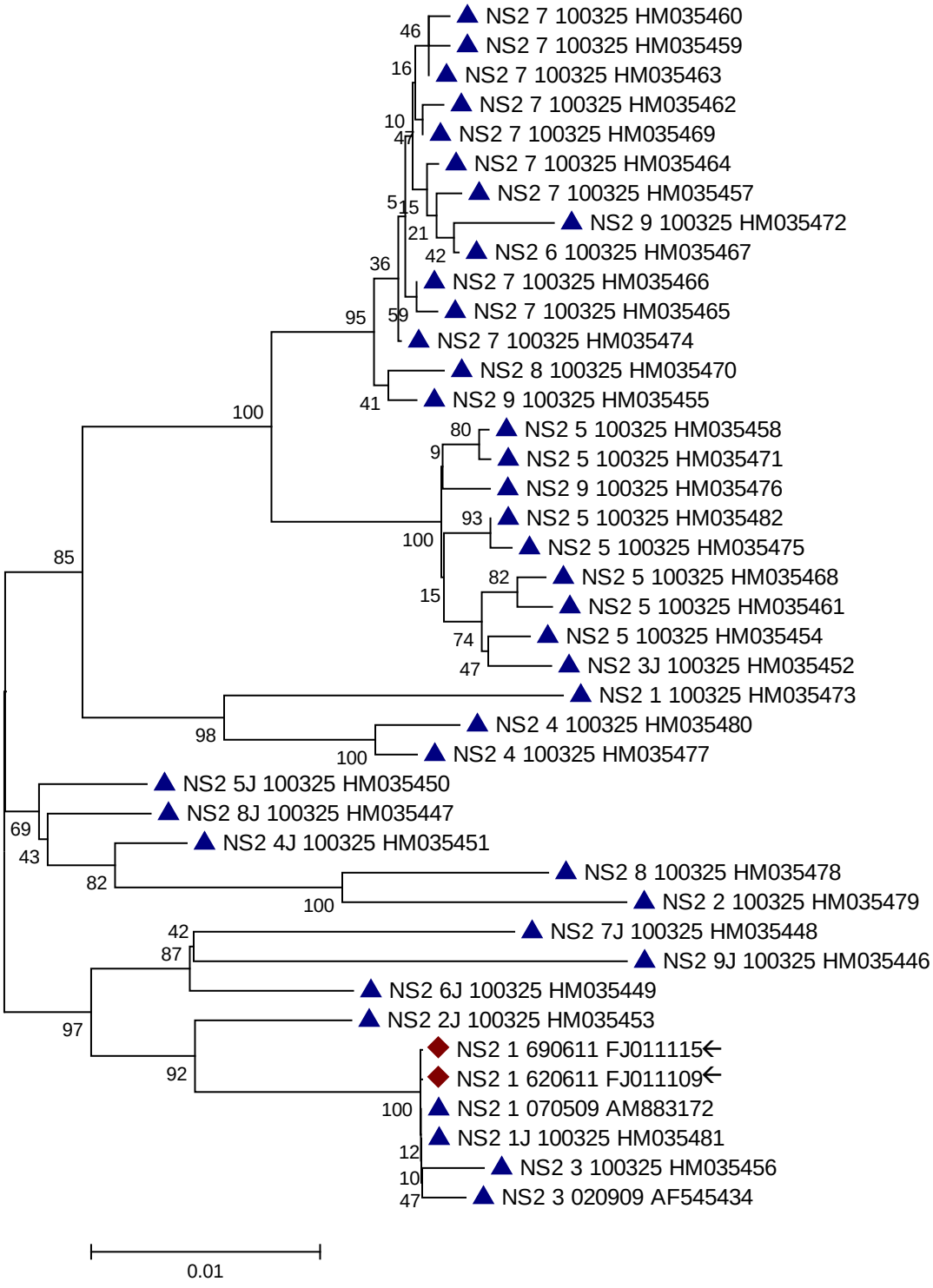

Figure 5.10: Phylogeny of all available NS2 sequences of AHSV to identify potential serotype and/or isolate period relationships over time. Sequences dated in the 1960s (◆); pre-2000 (●) and from 2000 onwards (▲). The evolutionary history was inferred using the Neighbour-Joining method (Saitou & Nei, 1987). The optimal tree with the sum of branch length = 0.21686496 is shown. The percentage of replicate trees in which the associated taxa clustered together in the bootstrap test (100 replicates) are shown next to the branches (Felsenstein, 1985). The tree is drawn to scale, with branch lengths in the same units as those of the evolutionary distances used to infer the phylogenetic tree. The evolutionary distances were computed using the Maximum Composite Likelihood method (Tamura *et al.*, 2004) and are in the units of the number of base substitutions per site. The analysis involved 41 nucleotide sequences. Codon positions included were 1st+2nd+3rd+Noncoding. All positions containing gaps and missing data were eliminated. There were a total of 1098 positions in the final dataset. Evolutionary analyses were conducted in MEGA5 (Tamura *et al.*, 2011).

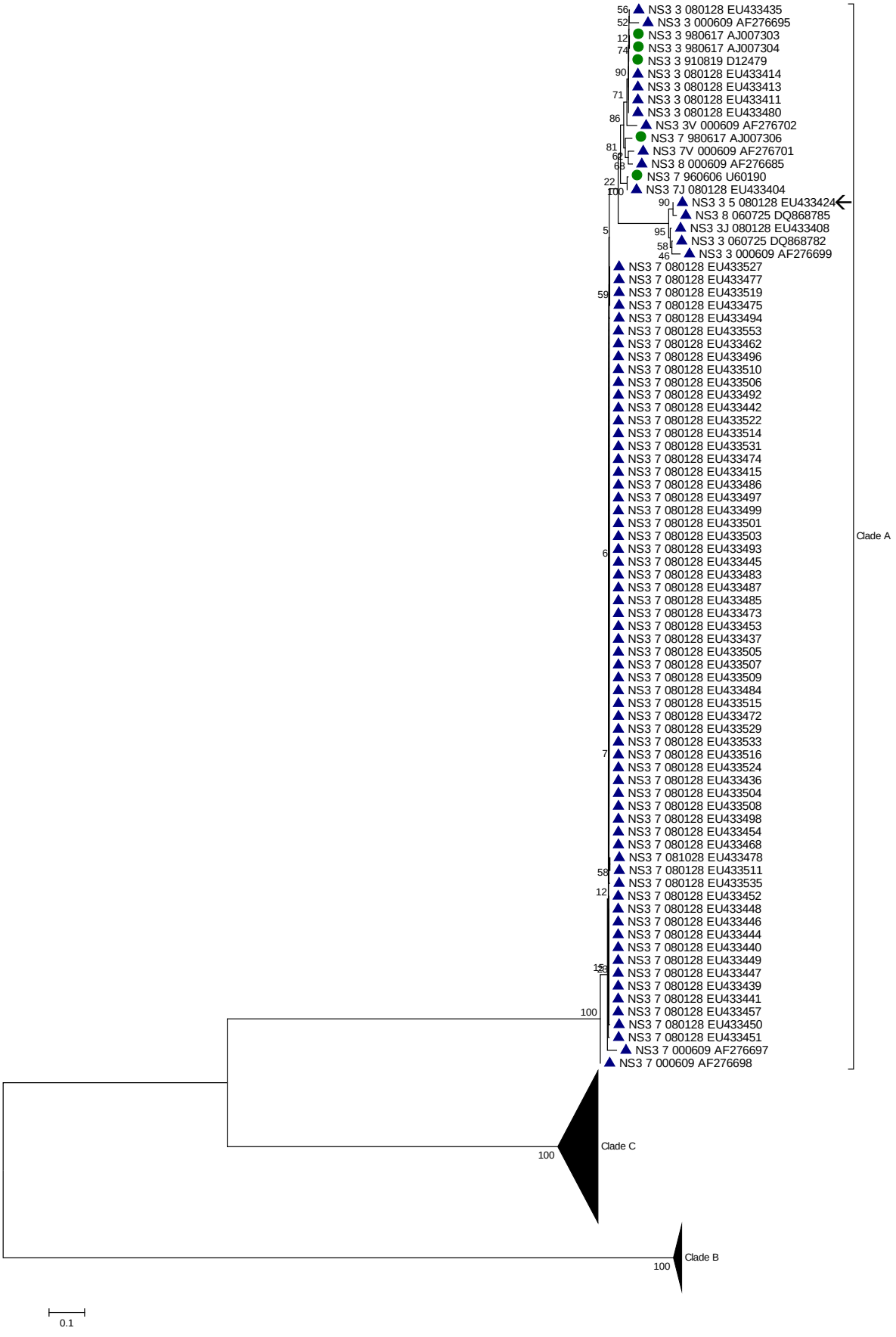
NS3 3 080128 EU433435
NS3 3 000609 AF276695
NS3 3 980617 AJ007303
NS3 3 980617 AJ007304
NS3 3 910819 D12479
NS3 3 080128 EU433414
NS3 3 080128 EU433413
NS3 3 080128 EU433411
NS3 3 080128 EU433480
NS3 3V 000609 AF276702
NS3 7 980617 AJ007306
NS3 7V 000609 AF276701
NS3 8 000609 AF276685
NS3 7 960606 U60190
NS3 7J 080128 EU433404
NS3 3 5 080128 EU433424
NS3 8 060725 DQ868785
NS3 3J 080128 EU433408
NS3 3 060725 DQ868782
NS3 3 000609 AF276699
NS3 7 080128 EU433527
NS3 7 080128 EU433477
NS3 7 080128 EU433519
NS3 7 080128 EU433475
NS3 7 080128 EU433494
NS3 7 080128 EU433553
NS3 7 080128 EU433462
NS3 7 080128 EU433496
NS3 7 080128 EU433510
NS3 7 080128 EU433506
NS3 7 080128 EU433492
NS3 7 080128 EU433442
NS3 7 080128 EU433522
NS3 7 080128 EU433514
NS3 7 080128 EU433531
NS3 7 080128 EU433474
NS3 7 080128 EU433415
NS3 7 080128 EU433486
NS3 7 080128 EU433497
NS3 7 080128 EU433499
NS3 7 080128 EU433501
NS3 7 080128 EU433503
NS3 7 080128 EU433493
NS3 7 080128 EU433445
NS3 7 080128 EU433483
NS3 7 080128 EU433487
NS3 7 080128 EU433485
NS3 7 080128 EU433473
NS3 7 080128 EU433453
NS3 7 080128 EU433437
NS3 7 080128 EU433505
NS3 7 080128 EU433507
NS3 7 080128 EU433509
NS3 7 080128 EU433484
NS3 7 080128 EU433515
NS3 7 080128 EU433472
NS3 7 080128 EU433529
NS3 7 080128 EU433533
NS3 7 080128 EU433516
NS3 7 080128 EU433524
NS3 7 080128 EU433436
NS3 7 080128 EU433504
NS3 7 080128 EU433508
NS3 7 080128 EU433498
NS3 7 080128 EU433454
NS3 7 080128 EU433468
NS3 7 081028 EU433478
NS3 7 080128 EU433511
NS3 7 080128 EU433535
NS3 7 080128 EU433452
NS3 7 080128 EU433448
NS3 7 080128 EU433446
NS3 7 080128 EU433444
NS3 7 080128 EU433440
NS3 7 080128 EU433449
NS3 7 080128 EU433447
NS3 7 080128 EU433439
NS3 7 080128 EU433441
NS3 7 080128 EU433457
NS3 7 080128 EU433450
NS3 7 080128 EU433451
NS3 7 000609 AF276697
NS3 7 000609 AF276698
Clade A
Clade C
Clade B
0.1

Figure 5.11 (previous page): Phylogeny of all available NS3 sequences of AHSV to identify potential serotype and/or isolate period relationships over time. Clade B and C branches have been collapsed. Sequences dated in the 1960s (◆); pre-2000 (●) and from 2000 onwards (▲). The evolutionary history was inferred using the Neighbour-Joining method (Saitou & Nei, 1987). The optimal tree with the sum of branch length = 6.50509277 is shown. The percentage of replicate trees in which the associated taxa clustered together in the bootstrap test (100 replicates) are shown next to the branches (Felsenstein, 1985). The tree is drawn to scale, with branch lengths in the same units as those of the evolutionary distances used to infer the phylogenetic tree. The evolutionary distances were computed using the Maximum Composite Likelihood method (Tamura *et al.*, 2004) and are in the units of the number of base substitutions per site. The analysis involved 202 nucleotide sequences. Codon positions included were 1st+2nd+3rd+Noncoding. All positions containing gaps and missing data were eliminated. There were a total of 646 positions in the final dataset. Evolutionary analyses were conducted in MEGA5 (Tamura *et al.*, 2011).

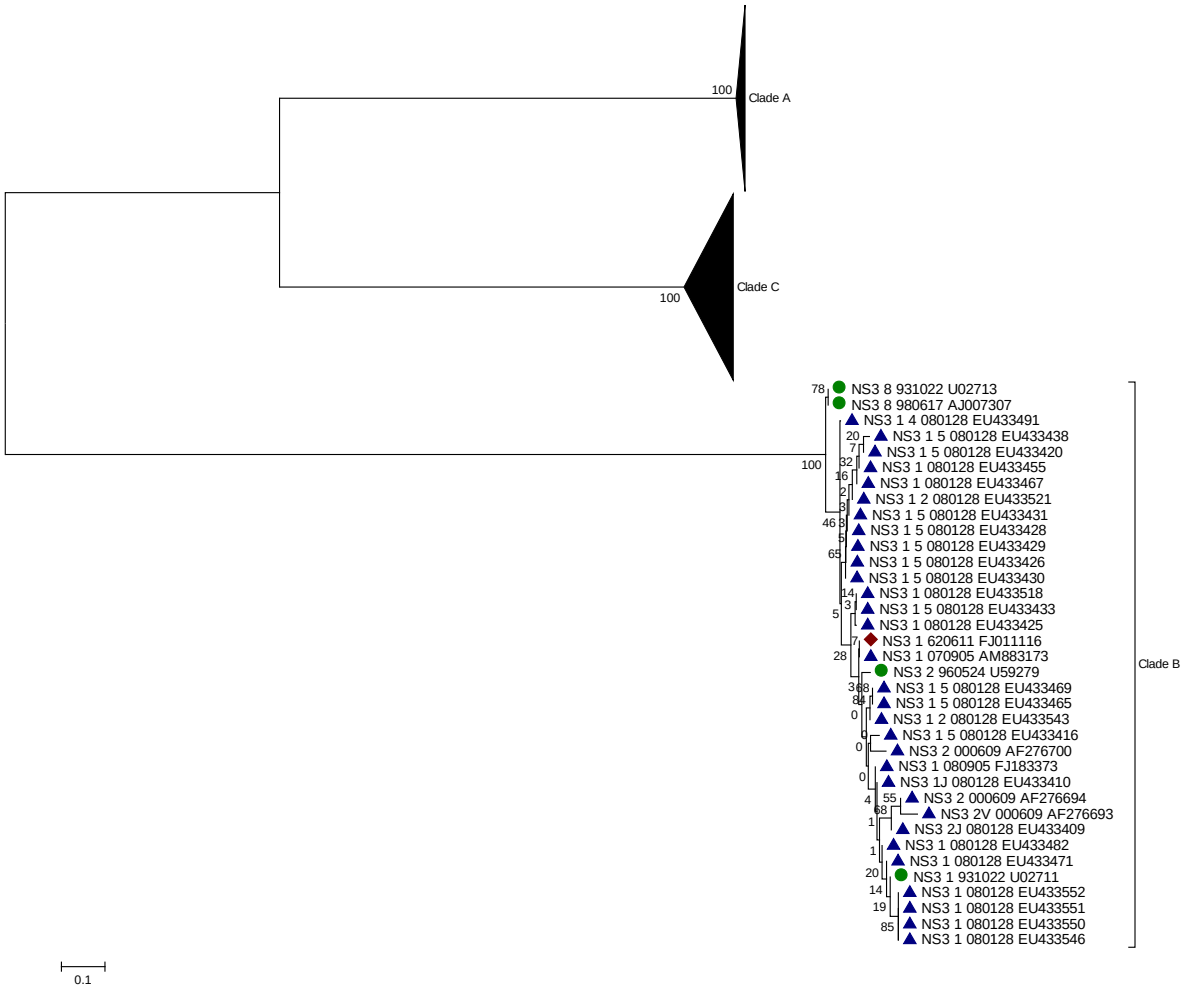

Figure 5.12: Phylogeny of all available NS3 sequences of AHSV to identify potential serotype and/or isolate period relationships over time. Clade A and C branches have been collapsed. Sequences dated in the 1960s (◆); pre-2000 (●) and from 2000 onwards (▲). The evolutionary history was inferred using the Neighbour-Joining method (Saitou & Nei, 1987). The optimal tree with the sum of branch length = 6.50509277 is shown. The percentage of replicate trees in which the associated taxa clustered together in the bootstrap test (100 replicates) are shown next to the branches (Felsenstein, 1985). The tree is drawn to scale, with branch lengths in the same units as those of the evolutionary distances used to infer the phylogenetic tree. The evolutionary distances were computed using the Maximum Composite Likelihood method (Tamura *et al.*, 2004) and are in the units of the number of base substitutions per site. The analysis involved 202 nucleotide sequences. Codon positions included were 1st+2nd+3rd+Noncoding. All positions containing gaps and missing data were eliminated. There were a total of 646 positions in the final dataset. Evolutionary analyses were conducted in MEGA5 (Tamura *et al.*, 2011).

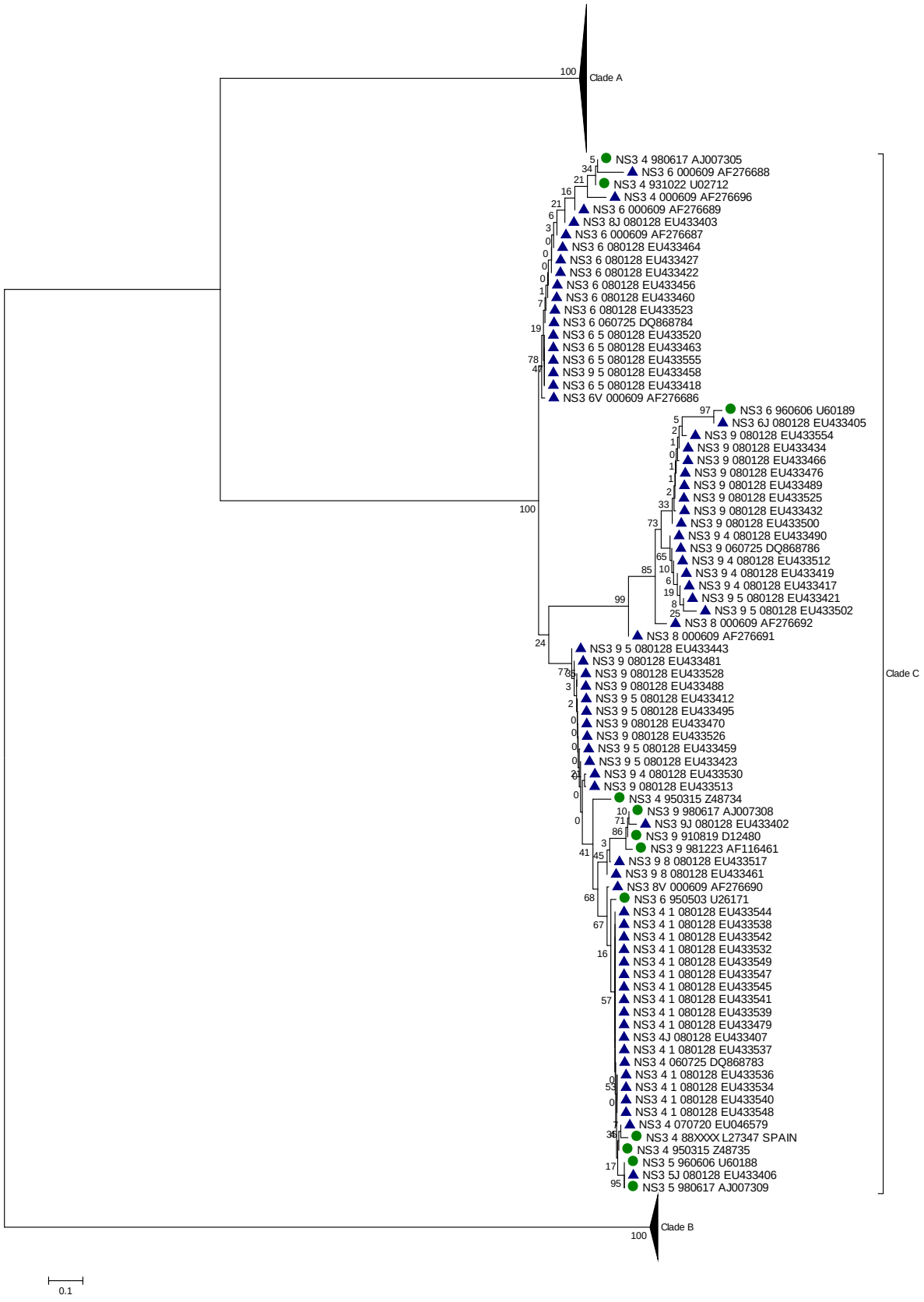
Clade A
Clade B
Clade C
NS3 4 980617 AJ007305
NS3 6 000609 AF276688
NS3 4 931022 U02712
NS3 4 000609 AF276696
NS3 6 000609 AF276689
NS3 8J 080128 EU433403
NS3 6 000609 AF276687
NS3 6 080128 EU433464
NS3 6 080128 EU433427
NS3 6 080128 EU433422
NS3 6 080128 EU433456
NS3 6 080128 EU433460
NS3 6 080128 EU433523
NS3 6 060725 DQ868784
NS3 6 5 080128 EU433520
NS3 6 5 080128 EU433463
NS3 6 5 080128 EU433555
NS3 9 5 080128 EU433458
NS3 6 5 080128 EU433418
NS3 6V 000609 AF276686
NS3 6 960606 U60189
NS3 6J 080128 EU433405
NS3 9 080128 EU433554
NS3 9 080128 EU433434
NS3 9 080128 EU433466
NS3 9 080128 EU433476
NS3 9 080128 EU433489
NS3 9 080128 EU433525
NS3 9 080128 EU433432
NS3 9 080128 EU433500
NS3 9 4 080128 EU433490
NS3 9 060725 DQ868786
NS3 9 4 080128 EU433512
NS3 9 4 080128 EU433419
NS3 9 4 080128 EU433417
NS3 9 5 080128 EU433421
NS3 9 5 080128 EU433502
NS3 8 000609 AF276692
NS3 8 000609 AF276691
NS3 9 5 080128 EU433443
NS3 9 080128 EU433481
NS3 9 080128 EU433528
NS3 9 080128 EU433488
NS3 9 5 080128 EU433412
NS3 9 5 080128 EU433495
NS3 9 080128 EU433470
NS3 9 080128 EU433526
NS3 9 5 080128 EU433459
NS3 9 5 080128 EU433423
NS3 9 4 080128 EU433530
NS3 9 080128 EU433513
NS3 4 950315 Z48734
NS3 9 980617 AJ007308
NS3 9J 080128 EU433402
NS3 9 910819 D12480
NS3 9 981223 AF116461
NS3 9 8 080128 EU433517
NS3 9 8 080128 EU433461
NS3 8V 000609 AF276690
NS3 6 950503 U26171
NS3 4 1 080128 EU433544
NS3 4 1 080128 EU433538
NS3 4 1 080128 EU433542
NS3 4 1 080128 EU433532
NS3 4 1 080128 EU433549
NS3 4 1 080128 EU433547
NS3 4 1 080128 EU433545
NS3 4 1 080128 EU433541
NS3 4 1 080128 EU433539
NS3 4 1 080128 EU433479
NS3 4J 080128 EU433407
NS3 4 1 080128 EU433537
NS3 4 060725 DQ868783
NS3 4 1 080128 EU433536
NS3 4 1 080128 EU433534
NS3 4 1 080128 EU433540
NS3 4 1 080128 EU433548
NS3 4 070720 EU046579
NS3 4 88XXXX L27347 SPAIN
NS3 4 950315 Z48735
NS3 5 960606 U60188
NS3 5J 080128 EU433406
NS3 5 980617 AJ007309
0.1

Figure 5.13 (previous page): Phylogeny of all available NS3 sequences of AHSV to identify potential serotype and/or isolate period relationships over time. Clade A and B branches have been collapsed. Sequences dated in the 1960s (◆); pre-2000 (●) and from 2000 onwards (▲). The evolutionary history was inferred using the Neighbour-Joining method (Saitou & Nei, 1987). The optimal tree with the sum of branch length = 6.50509277 is shown. The percentage of replicate trees in which the associated taxa clustered together in the bootstrap test (100 replicates) are shown next to the branches (Felsenstein, 1985). The tree is drawn to scale, with branch lengths in the same units as those of the evolutionary distances used to infer the phylogenetic tree. The evolutionary distances were computed using the Maximum Composite Likelihood method (Tamura *et al.*, 2004) and are in the units of the number of base substitutions per site. The analysis involved 202 nucleotide sequences. Codon positions included were 1st+2nd+3rd+Noncoding. All positions containing gaps and missing data were eliminated. There were a total of 646 positions in the final dataset. Evolutionary analyses were conducted in MEGA5 (Tamura *et al.*, 2011).

5.4. Discussion

The sequencing and tracking of viral genomes plays an important role in the identification of new or unidentified viruses and tracking mixed infections, such as the St Croix River virus, the Wongorr virus, the Yunnan orbivirus, the Toggenburg virus and Rotavirus species (Parkes & Gould, 1996; Attoui *et al.*, 2001; Attoui *et al.*, 2005; Hofmann *et al.*, 2008; Matthijnssens *et al.*, 2008; Jere *et al.*, 2011; Jere *et al.*, 2012). Phylogenetics also lends itself to the identification of new BTV strains (Maan *et al.*, 2011b). Additionally, fowl adenoviruses have been classified based on phylogenetic methods (Marek *et al.*, 2010). Phylogenetics has also been used on a number of occasions to study the relatedness of *Culicoides* spp. vectors (Dallas *et al.*, 2003; Gomulski *et al.*, 2006; Perrin *et al.*, 2006; Calvo *et al.*, 2009). It has been found that the relationship between different HRM curves and phylogenetic groupings correlate in *Listeria monocytogenes* strains (Pietzka *et al.*, 2011). By identifying AHSV sequences according to their isolation period, it was envisaged that, if present, any relationship between older and more recently isolated sequences could be identified. Simultaneously, the phylogenies could be used to confirm current serotype groupings per genome segment or identify possible new patterns.

Reviewing the phylogeny of all VP1 sequences, no pattern was evident for either the isolation period or serotype. Older sequences were an exact match with recent sequences. VP1 is the RNA-directed RNA polymerase (Stauber *et al.*, 1997; Ramadevi *et al.*, 1998; Ramadevi & Roy, 1998; Huismans *et al.*, 2004) and as such is expected to be under strong selective pressure due to its central role in the replication of the viral genome. VP1 also forms part of the inner capsid as one of the three minor proteins (Roy *et al.*, 1994). In addition, it is the largest AHSV genome segment, at 3965 bp (Mertens *et al.*, 2006) and would require notable genetic drift to alter its function.

Potentially the most interesting phylogeny is the phylogenetic tree of all the VP2 sequences. VP2 contains the antigenic regions that define the serotype of the virus and is thus responsible for receptor binding, haemagglutination and invoking host-specific immunity (Bremer *et al.*, 1990; Burrage *et al.*, 1993; Burrage & Laegreid, 1994; Roy *et al.*, 1994;

Bentley *et al.*, 2000; Bhattacharya *et al.*, 2007). VP2 is thus the target for serotyping assays (Koekemoer *et al.*, 2000; Maan *et al.*, 2011a). Under the most selective pressure due to its location on the outer viral capsid (Lewis & Grubman, 1991), the evolution of a new serotype would ultimately need to occur through the continued mutation and genetic drift of the genome segment encoding VP2. However, there is no indication that this has occurred or is occurring. The older sequences were evenly distributed amongst the more recent sequences, within their respective serotypes. However, for the serotype 6 and 9 (ST6 and ST9) clades, the older sequences were separated from the more recent sequences. The distance between the old and new clades is very small, for both. Interestingly, serotype 6 cross protects for the absence of serotype 9 in the Onderstepoort Biological Products' vaccines (von Teichman *et al.*, 2010). Historically, serotype 9 has been confined to West Africa (Mellor & Hamblin, 2004) and this may have resulted in some differentiation between older and more recent sequences.

The lack of any evident genetic drift for VP2 has important consequences for vaccine development focused on the hosts' serotype-specific antibody responses to VP2 (Martinez-Torrecuadrada *et al.*, 1996; Roy *et al.*, 1996; du Plessis *et al.*, 1998; Chiam *et al.*, 2009; Guthrie *et al.*, 2009; Castillo-Olivares *et al.*, 2011). Interestingly, a truncated VP2 protein has been reported to alter the growth dynamics of AHSV *in vitro* (Manole *et al.*, 2012). Cleaved VP2 molecules have also resulted in an increase in infectivity in the *Culicoides* spp. vector suggesting that VP2 plays an important role in the vector-AHSV relationship (Marchi *et al.*, 1995). The sustained vector-host cycle could thus be dependent on the conservation of this region. Martinez-Torrecuadrada and Casal (1995) and Martinez-Torrecuadrada *et al.* (2001) reported that there are 15 sites, mostly found in the central region of the VP2 protein, that are immunogenic. The evolution of a new serotype would likely occur in these regions and perhaps a future study could focus on these regions and their susceptibility to mutations.

Using genome segment encoding VP2 sequences, an outbreak of serotype 7 was accurately characterised geographically and an origin of the outbreak was inferred (Koekemoer *et al.*, 2003). In a previous phylogenetic study of VP2, besides confirming that VP2 was the most variable AHSV protein, it also resulted in the grouping together of the serotypes reported to have cross-reactions and therefore afford some degree of cross-protection in the polyvalent vaccine (Potgieter *et al.*, 2003). However, only one sequence of each serotype was considered. Serotype 5 cross-reacts with serotype 8, while serotype 6 cross-reacts with serotype 9 (von Teichman *et al.*, 2010). Unfortunately, no sequences of serotype 5 were available on GenBank. In the present study serotype 6 and serotype 9 did not appear in the same clade.

For VP3 (inner capsid structure), VP4 (RNA capping), VP6 (helicase), NS1 (host cell tubules) and NS2 (host cell inclusion bodies) sequences, the phylogenies' scale bars indicate that the degree of change inferred from the branch length is very small and there does not appear to be any significant phylogenetic divergence. All of these sequences, despite the small number of available sequences or information, all appear relatively stable and are unlikely to mutate to a high degree that could result in a change to the virus. Iwata *et al.* (1992) described VP3 as being the most conserved of the capsid proteins. VP3 is also serogroup divergent, which makes it an attractive target for some diagnostic assays (Sakamoto *et al.*, 1994). VP4, one of the inner minor capsid proteins (Roy *et al.*, 1994) has not been a popular research target, hence the dearth of available sequences. VP6, being a helicase and responsible for interacting with the double-stranded RNA genome is not expected to be under much selective pressure (de Waal & Huismans, 2005). VP6 is also one of the earliest serological markers, and combined with its relative conservation, makes it an attractive target for early serological diagnosis (Martinez-Torrecuadrada *et al.*, 1997). A comparison of the VP6 amino acid sequences confirmed its high degree of conservation (Turnbull *et al.*, 1996). However, the resolution of the serotypes based on the sequences available make it an attractive genome segment for further study. Despite the high degree of similarity, a small and diverse region may be accounting for the resolution seen and would thus prove to be an attractive target for serotyping assays.

VP5 shows some moderate sequence changes, with some degree of clustering based on serotype but not on the same scale as either VP2 or NS3. The majority of older and newer sequences cluster randomly, although two pre-2000 sequences appear to fall within different clusters (indicated by the arrows). However the bootstrap value of this node is 38 rendering this cluster unreliable. VP5 is a component of the outer capsid protein with VP2 (Roy *et al.*, 1994). However, unlike VP2, it is much more conserved and can be used in serological assays for the detection of AHSV (Laviada *et al.*, 1993; Roy *et al.*, 1996; Bougrine *et al.*, 1998). The relative conservation of VP5, combined with the divergence of VP2 (Guthrie *et al.*, 2009), was used successfully in the development of potential vaccines. VP5 is also the earliest serological marker identified, making it an important target for serological diagnostic assays (Martinez-Torrecuadrada *et al.*, 1997). VP5 contains some regions that remain highly conserved between different *Orbivirus* species (Martinez-Torrecuadrada *et al.*, 1999). Compared to VP2, the genome segment encoding VP5 is substantially more conserved, based on the scale bar dimensions, but the clustering of the serotypes would suggest that VP5 could play a role in future, more sensitive serotyping diagnostic assays.

The VP7 genome segment and protein is the choice for serogroup-specific PCRs (Sailleau *et al.*, 1997a; Agüero *et al.*, 2008; Fernández-Pinero *et al.*, 2009; Quan *et al.*, 2010) and

serological assays (du Plessis *et al.*, 1990; Chuma *et al.*, 1992; Laviada *et al.*, 1992; Ranz *et al.*, 1992; Bremer *et al.*, 1994; House *et al.*, 1996; du Plessis *et al.*, 1999; Kweon *et al.*, 2003; Maree & Paweska, 2005) to differentially diagnose AHSV. This is due to its conservation amongst all nine AHSV serotypes, but its divergence from other orbivirus VP7 proteins (only 44% identical to BTV VP7) (Roy *et al.*, 1991). Interestingly, however, VP7-specific antibodies are only detected much later during the course of the infection making the serologic detection of VP7 unsuitable for early diagnosis (Martinez-Torrecuadrada *et al.*, 1997). Additionally, VP7, with VP3, makes up the inner capsid of the virus (Nason *et al.*, 2004) and would thus be protected from any influences that would favour mutations. The VP7 genome segment is known to be genetically stable (Basak *et al.*, 1996) and thus little to no divergence is expected to be seen between the serotypes. No pattern emerged that would indicate any genetic drift between isolation periods, despite the extensive branching seen in the phylogeny.

NS3 is possibly involved in the release of the virions into the host cell and would be an important virulence factor (Stoltz *et al.*, 1996; O'Hara *et al.*, 1998; van Niekerk *et al.*, 2001a; Meiring *et al.*, 2009). The genome segment encoding NS3 is also the second most variable genome segment after the genome segment encoding VP2, unique among the orbiviruses (Roy *et al.*, 1994; van Niekerk *et al.*, 2001b). In all three clades, older and newer sequences do not cluster separately, but are dispersed throughout. NS3 has been identified as a marker protein for the detection of live (attenuated vaccine or field infection) virus (Laviada *et al.*, 1995; Bougrine *et al.*, 1998; el Hasnaoui *et al.*, 1998; van Niekerk *et al.*, 2001b), although some studies found no evidence of this (Idrissi Bougrine *et al.*, 1999). Interestingly, Laviada *et al.* (1995) found a higher degree of similarity between serotypes 4 and 9 (both Clade C) than between serotypes 4 and 3 (Clade C and A). In a phylogenetic study of segment 10, Martin *et al.* (1998) grouped all nine serotypes in an identical fashion as did Sailleau *et al.* (1997b) and Zientara *et al.* (1998b). In addition, individual serotypes of each clade were shown to have different phenotypes in Vero cells (Meiring *et al.*, 2009). The importance of NS3 for diagnostics was described in Quan *et al.* (2008), where an outbreak was tracked using segment 10 sequences and a database of segment 10 sequences was suggested to gain an enhanced understanding of AHSV epidemiology. NS3 has also played an important role in related orbiviruses: using segment 10, a new strain of EEV was identified in Israel (Aharonson-Raz *et al.*, 2011). Considering that all nine serotypes easily and consistently fall into three unique clades, it would follow that the identification of a new strain or serotype might occur by tracking the sequences of segment 10 and its position in a phylogeny, with or without an associated change in the genome segment encoding VP2 sequence.

As an additional opportunity, by analysing the individual genome segments phylogenetically and possibly relating to the genome segment-encoding protein, divergences amongst the serotypes per genome segment could be related to the form of disease an equine manifests and, by extrapolation, the functions of the viral proteins. This in turn could have consequences for future epidemiological studies focused on the molecular and genetic aspects of the disease. Due to the limited number of sequences available, the inferences contained in this chapter cannot be considered definitive.

5.5. Conclusion

In all ten genome segments, there was a lack of evidence for any significant genetic drift that might account for the development of a new serotype.. There was comparatively little genetic change by means of mutation for each of genome segments. Furthermore, a high degree of variation shown between sequences of segment 2 and 10 was confirmed, while the lack of variation between the sequences of the remaining genome segments was also shown. The three clades evident for full-length sequences of segment 10 was reaffirmed. There was a distinct lack of sequence depth for the genome sequences of VP1 and VP6, which should be a target for future research. However, a large-scale isolation and full genome-sequencing project would be highly advantageous in order to better understand the dynamics of AHSV evolution where reassortment is concerned. In addition, it would be valuable to deduce the genetic variants of each of the ten genome segments that are common to each of the nine serotypes. A combined analysis of all ten genome segments would also be able to establish the relationships between the serotypes and outbreak isolates.

CHAPTER 6: GENERAL DISCUSSION AND CONCLUSION

African horse sickness (AHS) is fast becoming one of the greater animal scourges of our time. AHS is a fatal viral disease that afflicts all equines and has a 90% mortality rate in unvaccinated horses. The AHS virus (AHSV) belongs to the *Orbivirus* genus in the family *Reoviridae* and is thus closely related to the Bluetongue virus (BTV), sharing many epidemiological and aetiological features (Spence *et al.*, 1984; OIE, 2008). A brief history of the disease reveals its capacity to exact enormous losses to national herds, especially in serologically naïve herds if left unchecked. The virus, although endemic to sub-Saharan Africa, has made appearances in Europe (Lubroth, 1988; Lord *et al.*, 1998b) and the Middle East (Massie, 1962) and there are currently stringent controls of equine transport from South Africa to prevent the virus' permanent incursion into Europe (RacingSA, 2012). In South Africa, the virus occurs naturally in all areas, except the metropolitan area of Cape Town, which is defined as an OIE free zone and is essential to the continued trade of equines from South Africa (DoA, 2003; Mellor & Hamblin, 2004). AHS has a devastating effect on export and international competitiveness in equine trade, and impacts significantly on the South African racehorse and performance horse industries.

AHS is predominant during the late summer and autumn months and is positively correlated to the amount of rainfall received (Burne, 2011). Serotype distribution of AHSV in South Africa is largely unknown and unpredictable. This is likely due to the inconvenience, time and expense of serotyping each sample that is confirmed positive for AHSV, which has led to a significant gap in that sphere of understanding. The need for a rapid serotyping assay is essential to provide the necessary data for further research into AHS epidemiology. This is further underscored by the development of monovalent vaccines that can be rapidly deployed in the event of an outbreak to create a specific buffer/containment zone according to the serotype of the outbreak.

Modelling efforts have been numerous (Lord *et al.*, 1996b; Lord *et al.*, 1997b; Lord *et al.*, 1998b; Baylis *et al.*, 2001; Burne, 2011), but are largely hampered by the large gaps in knowledge of the virus' epidemiology such as seroprevalence, the relationship between serotype, pathogenicity and form of disease and the overwintering mechanisms of the virus (Lord *et al.*, 1997a; Mellor *et al.*, 1998; Cramer, 2010; Aklilu *et al.*, 2012; Thompson *et al.*, 2012). The afflicted hosts of the AHS virus include all equine species, with zebras having been accepted as the natural reservoir of the disease (Bosman *et al.*, 1995; OIE, 2008). The virus is vectored by the *Culicoides* spp. of biting midge and is transferred to the bloodstream

of equines through their salivary glands (Meiswinkel *et al.*, 1994; Meiswinkel & Paweska, 2003; Venter *et al.*, 2010). The virus' tropism for erythrocytes and endothelial tissue results in its two most serious manifestations of the cardiac and pulmonary form (Laegreid *et al.*, 1993; Gomez-Villamandos *et al.*, 1999). Unlike BTV, the AHS virus has only nine serotypes, the last being identified in the 1960s (Howell, 1962). The AHS virus is thus largely considered a genetically stable virus. The control of the disease is largely related to the control of its vector, the *Culicoides* midge, and includes various husbandry and related practices, such as stabling and vector-deterrent spray applications (Jenkins, 2008; Simpkin, 2008). The prevention of the disease is largely effected by the use of a reliable and registered vaccine (OIE, 2008). Currently, the only registered vaccine in South Africa is manufactured by Onderstepoort Biological Products and is polyvalent. This vaccine is, however, plagued by user's suggestions of vaccine failure and a number of workers have attempted to develop an improved vaccine (Martinez-Torrecuadrada *et al.*, 1996; Bentley *et al.*, 2000; Martinez-Torrecuadrada *et al.*, 2001; Scanlen *et al.*, 2002; Chiam *et al.*, 2009; Guthrie *et al.*, 2009; Castillo-Olivares *et al.*, 2011). One of the major challenges in combating and controlling the disease in South Africa, which cannot be overlooked, is the large population of equines used in rural communities for traction and transport (El Idrissi & Lubroth, 2006; Gerdes, 2006).

Using various serological techniques, AHSV has been diagnosed since the mid 20th century (du Plessis *et al.*, 1990; House *et al.*, 1990; Adeyefa, 1996; du Plessis *et al.*, 1999). Molecular techniques, particularly RT-PCR assays came to the fore in the mid-1990s with a number of different protocols having been described since and targeting different genome segments (Mizukoshi *et al.*, 1994; Sakamoto *et al.*, 1994; Zientara *et al.*, 1994; Agüero *et al.*, 2008; Koekemoer, 2008; Aradaib, 2009; Fernández-Pinero *et al.*, 2009; Monaco *et al.*, 2011). The AHS virus has been serotyped by virus neutralisation since the 1960s (Hazrati & Ozawa, 1965; OIE, 2008), but this is a tedious process. An RT-PCR serotyping protocol was first developed by Sailleau *et al.* (2000) and again by Maan *et al.* (2011a). However, both use post-PCR agarose gels as an end-point. Recently, sequencing and phylogenetics have been used to serotype AHSV (Grewar *et al.*, 2013), with advanced pyrosequencing techniques being an important development. Aklilu *et al.* (2012) used an as yet unpublished RT-PCR protocol and Ayelet *et al.* (2013) sent samples from Ethiopia to the Institute for Animal Health (Pirbright, UK) for serotyping. The rapid serotyping assay proposed here will greatly reduce the time and cost to achieve a result.

As an extension to RT-PCR, High Resolution Melt (HRM) analysis was developed in the 2000s for single nucleotide polymorphism (SNP) analysis and has since been extrapolated to a mechanism to distinguish amplicons from each other based on their sequence (Corbett, 2006; White & Potts, 2006). HRM analysis is a powerful and sensitive technique that

accurately discriminates between the differences in PCR amplicons by producing melt curves based on the sequence and length of the amplicons. Organisms such as feline caliciviruses (Helps *et al.*, 2002), *Leishmania* species (Nicolas *et al.*, 2002), *Plasmodium* species (Mangold *et al.*, 2005), *Campylobacter jejuni* (Price *et al.*, 2007), infectious bronchitis virus (Hewson *et al.*, 2009), infectious bursal disease virus (IBDV) (Ghorashi *et al.*, 2011), *Clostridium difficile* (Grando *et al.*, 2012) and *Enterococcus* species (Gurtler *et al.*, 2012) have all been typed using HRM analysis. HRM analysis has been used previously for AHSV in an attempt to separate serotypes based on melt profiles, but was based on a single, short probe, as opposed to an entire amplicon, and limited experimental evidence (Koekemoer, 2008). HRM analysis presents a number of advantages over other systems and is a potentially powerful tool in the gathering of vital epidemiological data to support AHS studies.

Due to the nature of the rapid serotyping assay proposed in the present study, the design of primers to effect this was of particular importance and was given due importance in a discrete chapter. The nine distinct serotypes and two serotype-divergent genome segments precluded a simple primer selection process that a conserved set of sequences with a SNP would require. The present study necessitated an in-depth analysis of various primer design strategies and the testing of them extensively *in silico*. The protocol for the design of primers for highly divergent amplicons for downstream HRM analysis was thus articulated in Chapter 2[8]. Of the AHSV genome, segment 2, which is serotype-specific, is extensively divergent and has minimal sequence depth in the relevant databases. Segment 10, on the other hand, while being serotype-divergent, has a much greater sequence depth and is considerably less divergent amongst the serotypes than segment 2 (Grubman & Lewis, 1992). While segment 2 may be the natural choice to develop a genotyping system to assay the serotype, the level of divergence renders it virtually impossible to design a single set of primers that prime to all nine serotypes. Other assays based on HRM analysis that aim to genotype a particular pathogen have far fewer genotypes than the number considered in the present study. Alternatively, the pathogen's genome is substantially less divergent, enabling a single primer pair to be designed that produces an amplicon with few, yet significant changes per serotype or genotype (Helps *et al.*, 2002; Nicolas *et al.*, 2002; Mangold *et al.*, 2005; Price *et al.*, 2007; Hewson *et al.*, 2009; Ghorashi *et al.*, 2011; Grando *et al.*, 2012; Gurtler *et al.*, 2012). Sailleau

[8] Sequences used for the design of primers were downloaded from GenBank (Appendix B). There was a temporal distance between the collation of these sequences and the sequences collated for the phylogenetic study of Chapter 5. This presented the possibility of additional sequences being available that may have influenced the primer design. An additional full-length sequence was available for both segment 2 and 10. The relevant primer sequences were checked against these additional sequences using BLASTn and found to be identical.

et al. (2000) designed a number of primers for AHSV segment 2 that aimed to produce serotype-unique products on agarose gels, without HRM analysis. However, the end point of this assay was gel-based and the methodology behind the design of the primers did not include all nine serotypes, which may have the potential to result in mispriming when used in other applications. Koekemoer (2008) attempted to use HRM analysis to serotype AHSV, but only considered the melting of probes with expensive fluorescent tags. The assay was not considered successful likely due to the relatively short sequence of the probe that was intended to generate melt data. The sensitivity of HRM analysis would have caused a single base pair change to exert enough influence on the melt curve so as to skew the results. In normal HRM analysis, where entire amplicons (generally much larger than probes) are melted, single base pair changes have much less influence than a short probe. In the present study, entire amplicons were melted and reflect the balance between decreasing the influence of single nucleotide changes, whilst still harnessing the inherent differences in each amplicon to produce a unique melt curve.

Hence, in the present study, the advantages of using primers for each genome segment were exploited to provide a primer strategy that encompassed both viral genome segments. Three primer pairs that target genome segment 2 were thus designed to complement the primer pair already designed targeting genome segment 10. The net result of this process was the combination of segment 10 (where a primer pair divided the nine serotypes into three clades), combined with the three primer pairs, based on segment 2, that would separate out the individual clades into their serotypes (Figure 2.4, Table 2.1). The primers designed as described in Chapter 2 are considered the best compromise in this respect and the protocol followed would be recommended in similar primer design scenarios. Due to the unique nature of primer design in this study, namely diverse amplicons, multiple genome segments and nine serotypes, the protocol followed could be extrapolated to other similar pathogens where HRM analysis has not been attempted for these reasons. In particular, other members of the *Orbivirus* genus could be explored for the applicability of HRM analysis to type their serotypes. In the case of BTV, where up to 26 serotypes have been described (Maan *et al.*, 2011b), only serotypes known to circulate in particular regions would need to be included initially.

Due to the apparent stochasticity of AHSV serotype distribution in the field over space and time, the virus was propagated from reference and field stocks obtained from the Onderstepoort Veterinary Institute (OVI) and the National Institute of Communicable Disease (NICD) as detailed in Chapter 3. The AHS virus has been propagated successfully and consistently using Vero cell culture as per Paweska *et al.* (2003) and Lelli *et al.* (2013), although some workers have used baby hamster kidney cells (BHK) (Wade-Evans *et al.*,

1993; Venter *et al.*, 1999; Paweska *et al.*, 2003). AHSV RNA from Vero cell monolayers was successfully extracted via total RNA using commercial preparations of guanidine-thiocyanate (Paweska *et al.*, 2003). The extraction of total RNA via commercial guanidine-thiocyanate reagents has become common for other orbiviruses (Hofmann *et al.*, 2008; Chaignat *et al.*, 2009; Maan *et al.*, 2011b; Planzer *et al.*, 2011). The availability of materials, ease and success of both these methods make them commonplace for the propagation of the virus and subsequent RNA extraction. Confirmation that AHS viral RNA was extracted was achieved by the use of primers that target the genome segment encoding VP7. These primers were developed by Fernández-Pinero *et al.* (2009) and were adopted by the OIE (2008) for international trade purposes. The genome segment encoding VP7 is the most common target for serogroup-specific ELISA and RT-PCR assays (Chuma *et al.*, 1992; Bremer *et al.*, 1994; Kweon *et al.*, 2003; Agüero *et al.*, 2008; Rodriguez-Sanchez *et al.*, 2008; Quan *et al.*, 2010). Using these primers, 26 of the 27 isolates were confirmed to be AHSV. The isolates labelled serotype 1 of the OVIA set failed to yield amplification products throughout the study.

The segment 2 clade-specific primers, having been designed *in silico* as described in Chapter 2*,* required some optimisation and confirmation of their specificity. Primer concentration and annealing temperatures were optimised and they were confirmed to amplify their respective targets in segment 2. The concentration of the primers was higher than the recommended protocol, but due to their degenerate nature, this was necessary to increase the amount of viable primer per reaction. Kwok *et al.* (1994) suggested both raising the primer concentration and lowering the annealing temperature when using degenerate primers. Roux (1995), in explaining modifications to touchdown PCRs, also suggested lowering initial annealing temperatures to as low as 35˚C in the case of degenerate or mismatched primers. Importantly, the use of HRM analysis in conjunction with these primers revealed the possibility that some serotype anomalies may exist in the AHSV isolates from the OVI. Not only was the serotype 1 isolate of the OVIA set not giving amplification products, but both serotype 2 isolates and the OVIA isolate of serotype 8 were also resulting in amplification products. The serotype 2 isolates both had almost identical melt profiles to serotype 6 and the serotype 8 isolate had a very similar melt profile to serotype 5. The isolates of Clade C (serotypes 4, 5, 6 and 9) also presented multiple melt profiles, rather than a single unique profile, due to the polyphyletic nature of the clade. A number of melt profiles resulted and each represented a serotype of Clade C.

High Resolution Melting has been used numerous times to type various pathogens in an *in vitro* situation where the types were known. However, HRM analysis has not been used, in the first instance, to type isolates that were unknown. The power and usefulness of HRM

analysis is emphasised in this scenario. Serotype-specific primers that targeted segment 2 were used in an attempt to ascertain the correct serotype assignment of the irregular isolates. As an advancement on the primers used by Sailleau *et al.* (2000), Maan *et al.* (2011a) designed a set of primers per serotype, but again, the end result was gel based and not intended for HRM analysis. Using these primers, albeit slightly modified, isolates of serotypes 2, 3, 4, 5 and 6 were identified in the present study. This confirmed that the serotype 2 isolates of the OVI sets were not serotype 2 and likewise for serotype 5 of the OVIA set. The engineered polymerase of the RT-PCR system used, the KAPA™ SYBR® FAST qPCR system, had a theoretical maximum of 600 bp (KAPA, 2012). The amplicons of serotypes 1, 7, 8 and 9 all had amplicons of over 1400 bp and thus were not amplifiable with the polymerase contained in this system. The largest amplicon amplified here was 1267 bp – this represents the largest known amplicon that the KAPA® polymerase has amplified. No other published literature exists that describes the KAPA Biosystems' engineered polymerase's limits. Further attempts to amplify the larger amplicons were abandoned in favour of sequencing to ascertain the correct identification of the isolates.

Segment 10 primers that targeted the 10-190 bp region generated additional HRM data. Studying the melt curves from these primers, it became clear that the serotype 2 OVI isolates were highly likely to be serotype 6 (Figure 3.30) and the serotype 5 OVIA isolate appeared to be serotype 8 (Figure 3.31). These results were later confirmed through sequencing and the sequences submitted to the European Nucleotide Archive (Table 3.9). It was suggested that some other isolates might have some anomalies as evidenced by the segment 10 melt profiles. Although sequencing confirmed these to be correct, it became apparent that the disparate nature of Clade C (Figure 3.43) might offer an explanation for the disparate melt profiles seen. Despite this, using the Rotor-Gene® software, Clade A was suitably defined based on the bins. Clade B and Clade C isolates were similarly defined. Due to the limitations of the Rotor-Gene® software however, it was unable to accurately identify the serotypes.

Using HRM analysis to establish the identity of the isolates, verified by sequencing, a protocol was designed for the rapid serotyping of AHSV as described in Chapter 4. One-step (cDNA synthesis and PCR performed in the same tube) and two-step (cDNA and PCR performed separately) protocols were compared: two-step protocols produced more consistent HRM curves despite the added time and effort. The majority of RT-PCR studies of orbiviruses have tended towards the one-step RT-PCR protocol, likely due to its ease of use. Both BTV (Jimenez-Clavero *et al.*, 2006; Mertens *et al.*, 2007; Hofmann *et al.*, 2008; OIE, 2008; Potgieter *et al.*, 2009; Maan *et al.*, 2010b; Monaco *et al.*, 2011) and AHSV (Fernández-Pinero *et al.*, 2009; Matsuo *et al.*, 2010; von Teichman *et al.*, 2010; Castillo-Olivares *et al.*,

2011; Maan *et al.*, 2011a) studies have used the one-step protocol. However, none of those studies involved the use of HRM analysis. When HRM analysis studies are considered, two-step protocols are preferred such as the differentiation of chloroplast mutants with multiple SNPs (Chateigner-Boutin & Small, 2007), norovirus genotyping (Tajiri-Utagawa *et al.*, 2009), infectious bronchitis virus classification (Hewson *et al.*, 2010), HIV diversity (Towler *et al.*, 2010), infectious bursal disease virus strain differentiation (Ghorashi *et al.*, 2011), influenza A SNP mutation (Tong *et al.*, 2011) and influenza neuraminidase gene variation (Varillas *et al.*, 2011). The only study to attempt HRM analysis on AHSV also used a two-step protocol (Koekemoer, 2008). No study has compared the two protocols specifically for HRM analysis, but the results presented in the present study indicate that two-step protocols produce more consistent melt curves with better reproducibility between duplicates. This is likely due to the lack of extraneous genomic material that would normally be present due to total RNA being extracted and used as the starting material in a one-step protocol and would thus affect the ultimate melting temperature.

The use of total and variable RNA as the starting template was decided upon due to the future role that the proposed assay is envisaged to play. Variable amounts of RNA in tissue samples would be received. In both the Rotor-Gene® 6000 Series Software and downstream statistical analysis in GenStat®, the influence of starting material concentration was negligible.

As described in Chapter 4, the Rotor-Gene® 6000 Series Software was used to define clades as 'bins' (in the language of the software) and subsequently the serotypes were defined as best as possible using the available tools. A protocol for the rapid serotyping assay based on HRM analysis was outlined in Chapter 4 and the clades and serotypes defined. The distribution of the melt profiles for each of the clades reflects the clustering seen on the phylogenies (Figure 3.43), but the Rotor-Gene® 6000 Series Software cannot adequately distinguish them.

The Rotor-Gene® 6000 Series Software is unable to utilise the Boolean operator 'OR' in distinguishing between the multiple melt profiles of the Clade C serotypes. The software is also incapable of statistically considering a range of reference samples in its genotyping protocol – only one sample may be selected as the reference sample. This caused the exclusion or low confidence of some isolates. The software was unable to define AHSV serotypes according to the author's opinion and alternate protocols were sought. Other studies have also found the Rotor-Gene® 6000 Series Software to be lacking in these aspects and have resorted to alternate renderings of the data to be more statistically relevant (Chroma *et al.*, 2011; Grando *et al.*, 2012; Roth & Hanson, 2013).

One of the principal drawbacks of the Rotor-Gene® genotyping abilities was the lack of statistical rigor and interrogation and a system that required too narrow a definition of a genotype. This was explored and is reported in Chapter 5. To counter this problem, Corbett (subsequently Qiagen) developed the ScreenClust HRM® Software that is based on principal component analysis to add statistical rigour to HRM analysis (Abdi & Williams, 2010; Reja *et al.*, 2010). By transforming the normalised melt curves and identifying various characteristics of the transformed data, samples are collated based upon the variables that most likely group them together. The differentiation of *Klebsiella pneumoniae* carbapenemase gene variants in Gram-negative pathogens, ribotypes of *Clostridium difficile* and methylation of DNA have all successfully employed ScreenClust HRM® Software (Rodríguez López *et al.*, 2010; Grando *et al.*, 2012; Roth & Hanson, 2013), although their amplicons under consideration are relatively conserved. The propriety nature of the software prevented a detailed appraisal of its algorithms and it was found to be limited in its application. The AHSV amplicons under investigation in the present study are considerably more diverse than other known amplicons for HRM analysis, such as above. In addition, degenerate primers have been used. Grando *et al.* (2012) developed a secondary method of interpreting the data and separating the melt curves and clusters using a series of difference plots related to three temperature points and represented this information in a three dimensional graph. Using the derivative of the normalised fluorescence (dF/dT vs. temperature) and identifying various attributes that the Rotor-Gene® software and ScreenClust HRM® Software could not, AHS melt curves were analysed using a combination of principal component analysis and discriminant analysis in GenStat®. Importantly, the derivative of the normalised fluorescence, rather than the normalised fluorescence curve data, was used for the calculation of the principal components due to the inherently more information that they contained. Discriminant analysis was, however, preferred because it separates data based on previously defined and statistically chosen reference characteristics and it separated the AHSV isolates based on what makes them different. AHSV could thus be diagnosed and simultaneously serotyped using a discriminant analysis in GenStat® following the creation of melt curve data post-PCR in a very effective, resolute manner.

One of the advantages of using HRM analysis to serotype AHSV is that a new strain (or serotype) could be detected quicker than traditional methods where a false negative could result. A new melt curve that does not fit into any previously defined genotypes, using either the Rotor-Gene® software or the more statistically reliable discriminant analysis protocol, could prove to be a new strain and/or serotype. This is a point of discussion amongst equestrian communities trying to make sense of the perceived ineffectiveness of the OBP vaccine.

In the last part of the study, an effort was made to establish the likelihood of a new serotype evolving through phylogenetic analysis of all publicly available sequences of AHSV, notwithstanding the larger evolutionary events such as genetic reassortment or recombination that could lead to a new serotype. Although a study of this kind should preferably be linked to the bioinformatic analysis of Chapter 2, the phylogenetic study could not add further information to the bioinformatic study. The bioinformatic analysis resulted in a very limited number of regions for primer design and information such as nucleotide positions with high rates of mutation could not have altered the primer design findings. Furthermore, the concept for this study developed over the course of the entire study when various anomalies were detected. de Sa *et al.* (1994) analysed the primitive relationships between AHSV serotypes using segment 10 and placed serotypes 4 and 9 and serotypes 1 and 8 together, the same groupings encountered throughout the present study. Quan *et al.* (2008) developed these further by adding numerous field isolates. Although three distinct clades were evident, serotypes 1, 4 and 5 were distributed between two clades. Koekemoer *et al.* (2003) conducted a phylogenetic analysis on segment 2, but only on serotype 7, during the 1999 Western Province outbreak. A comparison of South African and East African AHSV isolates revealed subtle differences based on their segment 2 sequences, but nine clades resulted corresponding to the nine serotypes (Maan *et al.*, 2011a). Two new serotypes have been identified through phylogenetic studies for BTV, which indicates the ability of an orbivirus to evolve new serotypes (Hofmann *et al.*, 2008; Chaignat *et al.*, 2009; Maan *et al.*, 2011b). No study has analysed all ten AHSV genome segments, or compared sequences of different isolation periods, and represented them in phylogenies to identify any patterns. The most recent use of phylogenetics for AHSV was to serotype the outbreak of 2011 in the Western Province where Grewar *et al.* (2013) used a neighbour-joining tree and portions of segment 10 and segment 2 to determine the infecting serotype was serotype 1. The appearance of a new serotype would have important consequences for AHSV vaccination strategies, which currently rely on a dual polyvalent attenuated vaccine system. A number of anecdotal reports suggest that the recent increase in AHS incidence may be due to a new serotype and consequent lack of provision for it in the vaccine. In the present study, all genome segments were assessed together for the first time using all available sequences located on international databases to ascertain whether genetic drift might be occurring in the viral genome. Sequences were marked uniquely for being isolated in the 1960s, pre-2000 or post-2000. In all of the genome segments analysed, there was no indication of any significant genetic drift that would constitute the emergence of a new serotype or indicate a reason for the lack of efficacy of the vaccine.

The disadvantage of developing a protocol for a serotyping assay of this nature is the need to validate it in the field across all nine serotypes when their distribution is unpredictable and inconsistent. However, the protocol described in this dissertation presented the first opportunity to serotype an orbivirus using HRM analysis, and without post-PCR processing. The implications of this are the ability to serotype an isolate in less than a day and deploy suitable strategies, particularly monovalent vaccination for surrounding equines, to contain an outbreak. The primer design strategies employed here can easily be transcribed to other pathogens where a similar outcome is required. High Resolution Melt analysis is a powerful tool that if directed towards pathogen typing could prove to be a valuable tool in fast-acting epidemics and zoonoses (Steer *et al.*, 2009; Steer *et al.*, 2011). Using principal component analysis and discriminant analysis, greater statistical interrogation is achieved and thus greater confidence could reside in the results. Although the phylogenetic analysis revealed no indication of a new serotype developing, the combination of HRM analysis and discriminant analysis proved to be an able and rapid detector of the serotype anomalies reported in this study. This has important repercussions for new serotype detection in the field.

The nature of the proposed assay calls for an extensive field trial as the next step that involves all nine serotypes to be collected over a number of years from across South Africa. This would involve sensitivity studies using highly pure dsRNA viral preparations (Potgieter *et al.*, 2003; Potgieter *et al.*, 2009) and specificity studies using closely related orbivirus species such as EEV, which is also an important differential diagnosis. The collection and storage of samples in this regard should be a high priority. With this in mind, various options need to be considered in terms of collecting and storing these samples. Whatman™ FTA cards could be considered. The collection and sequencing of AHSV field samples should also be undertaken and fast tracked to add to a database that is considerably underrepresented across all AHSV genome segments. This would enable more extensive phylogenetic studies to be conducted and recorded. The added advantage of this would be the ability to constantly update primer designs – either searching for new sites or improving the current primers. The production of melt curves for field-collected isolates would assist in improving the features and characteristics that are used in the discriminant analysis. It would also seem pertinent to attempt a follow up of the serotype anomalies discovered in the OVI isolates.

The African horse sickness virus can therefore be serotyped using primers that target the 10-190 bp region of genome segment 10 and three additional primer pairs that target specific regions of genome segment 2 of the serotypes in each clade. Using the segment 10 primers, the nine serotypes are resolved into three clades. Additional HRM data was generated using the genome segment 2 primer pairs. Although HRM analysis is not on record as having been

used for as complicated an assay as the one described here, it remains a powerful tool and was instrumental in solving the OVI serotype anomalies. While the Rotor-Gene® 6000 Series Software was useful, it failed in this instance to fully type the samples. ScreenClust is an improvement, but ultimately, a fresh statistical approach, using discriminant analysis, provided the ultimate segregation of the serotypes based on HRM analysis. The HRM data from each of the four primer pairs was exported from the Rotor-Gene 6000 Series Software to Microsoft Excel. Various statistical analyses were performed and this data was used to develop the serotyping results through discriminant analysis. Phylogenetically, the virus remains stable, with no evidence of any significant genetic drift in any of the ten genome segments..

This represents the first study where a pathogen has been differentiated based on its genotypes using generic discriminant analysis protocols. While many pathogens have been adequately separated using the standard Rotor-Gene® software, such as infectious bursal disease virus (Ghorashi *et al.*, 2011), some have required the use of the proprietary ScreenClust HRM® software for enhanced discrimination (Grando *et al.*, 2012). Gurtler *et al.* (2012), as in the present study, found ScreenClust HRM® software inadequate and developed a complicated three-dimensional graph and difference curves to discriminate melt profiles.

The present study has made innovative use of the application of melt curves produced by HRM analysis on the Corbett Rotor-Gene™ 6000 rotary analyser. A patent was awarded for the development of primers based on segment 10 of AHSV (Groenink *et al.*, 2010, Appendix A). A patent of addition for the clade-specific primers and discriminant analysis protocol is pending. By using the clade-specific primers to segregate serotypes within a clade, and by extending the diagnosis of the AHS virus with a serotyping assay using discriminant analysis, a strong platform for the production of data for surveillance and research purposes is provided. These data can inform vaccine programmes, while advancing epidemiological modelling of African horse sickness. Better management of vaccine distribution to rural equines would also facilitate a more integrated approach to herd immunity across South Africa. Crow (2005) elucidated the critical relationship between the timing of vaccination in pregnant Thoroughbred mares and the passive immunity transfer to the foals and the foals' variation in individual serotype immunity. This emphasises the importance of adherence to vaccination protocols, as well as serotype immunity. Burne (2011) has suggested that this serotype-specific data would also be crucial in developing accurate predicative models of AHS incidence. Both of these studies provide important applications for the principles outlined in the present study regarding the diagnosis and serotyping of the AHSV. This would also lead to an enhanced understanding of the seroprevalence of the virus and facilitate a

greater understanding of pathogenicity. The net result of these outcomes would also involve the improvement of quarantine protocols for the export of race and sport horses, a potentially lucrative economic sector in South Africa.

African horse sickness is a devastating disease. Future control of the disease lies in simultaneous diagnosis and serotyping which would lead to the development of surveillance and prophylactic strategies that focus on herd immunity concepts, effective vaccination and detection. Ultimately, protecting the national herd against AHS through vaccination requires a thorough understanding of the serotypes of AHSV, their individual epidemiologies and the relationships between them. This dissertation sought to propose a possible and preliminary protocol for the rapid detection of the infecting serotype, using the advanced technique of HRM, such that knowledge of seroprevalence is expounded and data is substantially increased. Subsequent to this study, validation studies are to be carried out that would seek to identify sensitivity levels and specificity and begin field trial work

The projection of this research into the future espouses a multidisciplinary approach to the socio-economic, epidemiological and molecular elucidation of the impacts of AHS on South African horses. Due to the fear of infected vector excursions into non-endemic, European zones, and the devastation that this would bring to the global horse population, the imperative is provided for South Africa to be at the forefront of this research. If South Africa can develop the early warning systems, and develop the required monovalent vaccines and have systems and policies in place that engage stakeholders and role players in the industry, South Africa can transpose itself from its historical role as the endemic source of African Horse Sickness, to presenting the global solution to the disease.

REFERENCES

Abdalla, M., Aradaib, I. E. & Osburn, B. I. 2002. Evaluation of RT-PCR for detection of Sudanese serotypes of epizootic hemorrhagic disease virus serogroup. *Vet Arhiv,* 72, 311-318.

Abdi, H. & Williams, L. J. 2010. Principal component analysis. *WIREs Comput Stat,* 2, 433-459.

Abu Elzein, E. M. E., Mirghani, M. E. & Ali, B. E. 1989. Observations on African horse sickness in donkeys in the Sudan. *Rev. - Off. Int. Epizoot.,* 8, 785-787.

Adeyefa, C. A. 1996. Rapid diagnosis of African horse sickness. *Rev Elev Med Vet Pays Trop,* 49, 295-8.

Agüero, M., Gomez-Tejedor, C., Angeles Cubillo, M., Rubio, C., Romero, E. & Jimenez-Clavero, A. 2008. Real-time fluorogenic reverse transcription polymerase chain reaction assay for detection of African horse sickness virus. *J Vet Diagn Invest,* 20, 325-328.

Aharonson-Raz, K., Steinman, A., Bumbarov, V., Maan, S., Maan, N. S., Nomikou, K., Batten, C., Potgieter, C., Gottlieb, Y., Mertens, P. & Klement, E. 2011. Isolation and phylogenetic grouping of equine encephalosis virus in Israel. *Emerg Infect Dis,* 17, 1883-1886.

AHS-Trust. 2008. *African Horse Sickness Trust* [Online]. Newcastle. http://www.africanhorsesickness.co.za [Accessed 28 June 2008].

AHS-Trust. 2012. *AHS Early Warning System: 2011/2012 Outbreak* [Online]. African Horse Sickness Trust. http://www.africanhorsesickness.co.za/early_warning_new.asp?OutbreakID=8&OutbreakName=2011/2012 [Accessed 18 November 2012].

Akin, A., Wu, C. C. & Lin, T. L. 1998. A comparison of two RNA isolation methods for double-stranded RNA of infectious bursal disease virus. *J Virol Methods,* 74, 179-84.

Aklilu, N., Batten, C., Gelaye, E., Jenberie, S., Ayelet, G., Wilson, A., Belay, A., Asfaw, Y., Oura, C., Maan, S., Bachanek-Bankowska, K. & Mertens, P. P. 2012. African Horse Sickness Outbreaks Caused by Multiple Virus Types in Ethiopia. *Transbound Emerg Dis,* 10.1111/tbed.12024.

Alexander, K. A., Kat, P. W., House, J., House, C., O'Brien, S. J., Laurenson, M. K., McNutt, J. W. & Osburn, B. I. 1995. African horse sickness and African carnivores. *Vet Microbiol,* 47, 133-40.

Allison, K., Taylor, N., Upton, M. & Wilsmore, T. 2009. African Horse Sickness: Impact on the UK Horse Industry. University of Reading: Veterinary Epidemiology and Economics Research Unit.

Altschul, S. F., Madden, T. L., Schaffer, A. A., Zhang, J., Zhang, Z., Miller, W. & Lipman, D. J. 1997. Gapped BLAST and PSI-BLAST: a new generation of protein database search programs. *Nucleic Acids Res,* 25, 3389-402.

Anonymous. 2006. *High-Resolution Melting* [Online]. Utah: University of Utah. http://www.dna.utah.edu/Hi-Res/TOP_Hi-Res%20Melting.html [Accessed 6 June 2010].

Anonymous. 2008. *Risk Of New Horse Diseases Prompts Special Conference* [Online]. Speen: The Horse Trust. http://www.horsetrust.org.uk/Doc_News.aspx?id=c435bf82-f88c-4340-987a-2b2d5ce1f532 [Accessed 10 August 2008].

Anonymous. 2009. A Strategy for the Control of an Outbreak of African Horse Sickness in Great Britain

Anthony, S., Maan, S., Samuel, A. R., Mellor, P. S. & Mertens, P. P. 2004. Differential diagnosis of bluetongue virus using reverse transcriptase-polymerase chain reaction for genome segment 7. *Vet Ital,* 40, 546-551.

Anuj, S. N., Whiley, D. M., Kidd, T. J., Ramsay, K. A., Bell, S. C., Syrmis, M. W., Grimwood, K., Wainwright, C. E., Nissen, M. D. & Sloots, T. P. 2011. Rapid single-nucleotide polymorphism-based identification of clonal *Pseudomonas aeruginosa* isolates from patients with cystic fibrosis by the use of real-time PCR and high-resolution melting curve analysis. *Clin Microbiol Infect,* 17, 1403-8.

Aradaib, I. E., Akita, G. Y., Pearson, J. E. & Osburn, B. I. 1995. Comparison of polymerase chain reaction and virus isolation for detection of epizootic hemorrhagic disease virus in clinical samples from naturally infected deer. *J Vet Diagn Invest,* 7, 196-200.

Aradaib, I. E., Karrar, A., Abdalla, M. & Osburn, B. I. 2003a. Detection of United States Orbivirus serogroup using a multiplex RT-PCR. *Vet Arhiv,* 73, 63-71.

Aradaib, I. E., Smith, W. L., Osburn, B. I. & Cullor, J. S. 2003b. A multiplex PCR for simultaneous detection and differentiation of North American serotypes of bluetongue and epizootic hemorrhagic disease viruses. *Comp Immunol Microbiol Infect Dis,* 26, 77-87.

Aradaib, I. E. 2009. PCR detection of African horse sickness virus serogroup based on genome segment three sequence analysis. *J Virol Methods,* 159, 1-5.

Archer, R. K. 1974. International control of equine infectious diseases. *Vet Rec,* 95, 248-51.

Attoui, H., Stirling, J. M., Munderloh, U. G., Billoir, F., Brookes, S. M., Burroughs, J. N., de Micco, P., Mertens, P. P. & de Lamballerie, X. 2001. Complete sequence characterization of the genome of the St Croix River virus, a new orbivirus isolated from cells of *Ixodes scapularis*. *J Gen Virol,* 82, 795-804.

Attoui, H., Mohd Jaafar, F., Belhouchet, M., Aldrovandi, N., Tao, S., Chen, B., Liang, G., Tesh, R. B., de Micco, P. & de Lamballerie, X. 2005. Yunnan orbivirus, a new orbivirus species isolated from *Culex tritaeniorhynchus* mosquitoes in China. *J Gen Virol,* 86, 3409-17.

Awad, F. I., Amin, M. M., Salama, S. A. & Aly, M. M. 1981a. The incidence of African horse sickness antibodies in animals of various species in Egypt. *Bull Anim Health Prod Afr,* 29, 285-7.

Awad, F. I., Amin, M. M., Salama, S. A. & Khide, S. 1981b. The role played by Hyalomma dromedarii in the transmission of African horse sickness virus in Egypt. *Bull Anim Health Prod Afr,* 29, 337-40.

Ayelet, G., Derso, S., Jenberie, S., Tigre, W., Aklilu, N., Gelaye, E. & Asmare, K. 2013. Outbreak investigation and molecular characterization of African horse sickness virus circulating in selected areas of Ethiopia. *Acta Trop,* 127, 91-6.

Backer, J. A. & Nodelijk, G. 2011. Transmission and control of African horse sickness in The Netherlands: a model analysis. *PLoS One,* 6, e23066.

Baldauf, S. L. 2003. Phylogeny for the faint of heart: a tutorial. *Trends Genet,* 19, 345-51.

Barnard, B. J. 1993. Circulation of African horsesickness virus in zebra (*Equus burchelli*) in the Kruger National Park, South Africa, as measured by the prevalence of type specific antibodies. *Onderstepoort J Vet Res,* 60, 111-7.

Barnard, B. J., Bengis, R., Keet, D. & Dekker, E. H. 1994. Epidemiology of African horsesickness: duration of viraemia in zebra (*Equus burchelli*). *Onderstepoort J Vet Res,* 61, 391-3.

Barnard, B. J. 1998. Epidemiology of African horse sickness and the role of the zebra in South Africa. *Arch Virol Suppl,* 14, 13-9.

Basak, A. K., Gouet, P., Grimes, J., Roy, P. & Stuart, D. 1996. Crystal structure of the top domain of African horse sickness virus VP7: comparisons with bluetongue virus VP7. *J Virol,* 70, 3797-806.

Baylis, M., Mellor, P. S. & Meiswinkel, R. 1999. Horse sickness and ENSO in South Africa. *Nature,* 397, 574.

Baylis, M., Mellor, P. S., Wittmann, E. J. & Rogers, D. J. 2001. Prediction of areas around the Mediterranean at risk of bluetongue by modelling the distribution of its vector using satellite imaging. *Vet Rec,* 149, 639-43.

Bayliss, C. D., Spies, U., Shaw, K., Peters, R. W., Papageorgiou, A., Muller, H. & Boursnell, M. E. 1990. A comparison of the sequences of segment A of four infectious bursal disease virus strains and identification of a variable region in VP2. *J Gen Virol,* 71 (Pt 6), 1303-12.

Becht, H., Muller, H. & Muller, H. K. 1988. Comparative studies on structural and antigenic properties of two serotypes of infectious bursal disease virus. *J Gen Virol,* 69 (Pt 3), 631-40.

Bélinguier, B. 2009. Economic and social contribution of horseracing in Europe. *EU Equus 2009.* Uppsala, Sweden: Swedish University of Agricultural Sciences.

Belshaw, R., Gardner, A., Rambaut, A. & Pybus, O. G. 2008. Pacing a small cage: mutation and RNA viruses. *Trends Ecol Evol,* 23, 188-93.

Bengis, R. G., Kock, R. A. & Fischer, J. 2002. Infectious animal diseases: the wildlife/livestock interface. *Rev Sci Tech,* 21, 53-65.

Benson, D. A., Karsch-Mizrachi, I., Lipman, D. J., Ostell, J. & Sayers, E. W. 2009. GenBank. *Nucleic Acids Res,* 37, D26-31.

Benson, D. A., Karsch-Mizrachi, I., Lipman, D. J., Ostell, J. & Sayers, E. W. 2011. GenBank. *Nucleic Acids Res,* 39, D32-7.

Benson, D. A., Karsch-Mizrachi, I., Clark, K., Lipman, D. J., Ostell, J. & Sayers, E. W. 2012. GenBank. *Nucleic Acids Res,* 40, D48-53.

Bentley, L., Fehrsen, J., Jordaan, F., Huismans, H. & du Plessis, D. H. 2000. Identification of antigenic regions on VP2 of African horsesickness virus serotype 3 by using phage-displayed epitope libraries. *J Gen Virol,* 81, 993-1000.

Bhattacharya, B., Noad, R. J. & Roy, P. 2007. Interaction between Bluetongue virus outer capsid protein VP2 and vimentin is necessary for virus egress. *Virol J,* 4, 7.

Bigalke, R. 1994. The important role of wildlife in the occurrence of livestock diseases in southern Africa. *In:* Coetzer, J. A. W., Thomson, G. R. & Tustin, R. C. (eds.) *Infectious Diseases of Livestock with Special Reference to Southern Africa.* Cape Town: Oxford University Press.

Bitew, M., Andargie, A., Bekele, M., Jenberie, S., Ayelet, G. & Gelaye, E. 2011. Serological survey of African horse sickness in selected districts of Jimma zone, Southwestern Ethiopia. *Trop Anim Health Prod,* 43, 1543-7.

Boone, J. D., Balasuriya, U. B., Karaca, K., Audonnet, J. C., Yao, J., He, L., Nordgren, R., Monaco, F., Savini, G., Gardner, I. A. & Maclachlan, N. J. 2007. Recombinant canarypox virus vaccine co-expressing genes encoding the VP2 and VP5 outer capsid proteins of bluetongue virus induces high level protection in sheep. *Vaccine,* 25, 672-8.

Boorman, J., Mellor, P. S., Penn, M. & Jennings, M. 1975. The growth of African horse-sickness virus in embryonated hen eggs and the transmission of virus by *Culicoides variipennis* Coquillett (Diptera, Ceratopogonidae). *Arch Virol,* 47, 343-9.

Bosman, P., Bruckner, G. K. & Faul, A. 1995. African horse sickness surveillance systems and regionalisation/zoning: the case of South Africa. *Rev Sci Tech,* 14, 645-53.

Bouayoune, H., Touti, J., el Hasnaoui, H., Baylis, M. & Mellor, P. S. 1998. The *Culicoides* vectors of African horse sickness virus in Morocco: distribution and epidemiological implications. *Arch Virol Suppl,* 14, 113-25.

Bougrine, S. I., Fihri, O. F. & Fehri, M. M. 1998. Western immunoblotting as a method for the detection of African horse sickness virus protein-specific antibodies: differentiation between infected and vaccinated horses. *Arch Virol Suppl,* 14, 329-36.

Braverman, Y. & Chizov-Ginzburg, A. 1996. Role of dogs (*Canis domesticus*) as hosts for African horse sickness virus. *Vet Microbiol,* 51, 19-25.

Bremer, C. W. 1976. A gel electrophoretic study of the protein and nucleic acid components of African horsesickness virus. *Onderstepoort J Vet Res,* 43, 193-9.

Bremer, C. W., Huismans, H. & Van Dijk, A. A. 1990. Characterization and cloning of the African horsesickness virus genome. *J Gen Virol,* 71 (Pt 4), 793-9.

Bremer, C. W., du Plessis, D. H. & van Dijk, A. A. 1994. Baculovirus expression of non-structural protein NS2 and core protein VP7 of African horsesickness virus serotype 3 and their use as antigens in an indirect ELISA. *J Virol Methods,* 48, 245-56.

Bremer, C. W. 2012. A Comparison of Different PCR-Based Methods for the Detection of African Horsesickness Virus. *Open Vet Sci J,* 6, 8-14.

Brown, I. H., Harris, P. A., McCauley, J. W. & Alexander, D. J. 1998. Multiple genetic reassortment of avian and human influenza A viruses in European pigs, resulting in the emergence of an H1N2 virus of novel genotype. *J Gen Virol,* 79 (Pt 12), 2947-55.

Bruggnik, M. 2009. How to present interests of the horse industry in the European Union? *In:* International Federation of Horseracing Authorities, 29 October 2009 Uppsala, Sweden.

Bu, Y., Huang, H. & Zhou, G. 2008. Direct polymerase chain reaction (PCR) from human whole blood and filter-paper-dried blood by using a PCR buffer with a higher pH. *Anal Biochem,* 375, 370-2.

Bührmann, G. 2011. *Equine Census 2012* [Online]. Online. http://www.elsenburg.com/vets/downloads/equine_census_2012.pdf [Accessed].

Burks, C., Fickett, J. W., Goad, W. B., Kanehisa, M., Lewitter, F. I., Rindone, W. P., Swindell, C. D., Tung, C. S. & Bilofsky, H. S. 1985. The GenBank nucleic acid sequence database. *Comput Appl Biosci,* 1, 225-33.

Burne, R. 2011. *Statistical analysis of the incidence and mortality of African horse sickness in South Africa.* MSc Dissertation, University of KwaZulu-Natal, Pietermaritzburg.

Burrage, T. G., Trevejo, R., Stone-Marschat, M. & Laegreid, W. W. 1993. Neutralizing epitopes of African horsesickness virus serotype 4 are located on VP2. *Virology,* 196, 799-803.

Burrage, T. G. & Laegreid, W. W. 1994. African horsesickness: pathogenesis and immunity. *Comp Immunol Microbiol Infect Dis,* 17, 275-85.

Burroughs, J. N., O'Hara, R. S., Smale, C. J., Hamblin, C., Walton, A., Armstrong, R. & Mertens, P. P. 1994. Purification and properties of virus particles, infectious subviral particles, cores and VP7 crystals of African horsesickness virus serotype 9. *J Gen Virol,* 75 (Pt 8), 1849-57.

Calvo, J. H., Calvete, C., Martinez-Royo, A., Estrada, R., Miranda, M. A., Borras, D., Sarto, I. M. V., Pages, N., Delgado, J. A., Collantes, F. & Lucientes, J. 2009. Variations in the mitochondrial cytochrome c oxidase subunit I gene indicate northward expanding populations of *Culicoides imicola* in Spain. *Bull Entomol Res,* 99, 583-91.

Capela, R., Purse, B. V., Pena, I., Wittman, E. J., Margarita, Y., Capela, M., Romao, L., Mellor, P. S. & Baylis, M. 2003. Spatial distribution of *Culicoides* species in Portugal in relation to the transmission of African horse sickness and bluetongue viruses. *Med Vet Entomol,* 17, 165-77.

Carillo, S., Henry, L., Lippert, E., Girodon, F., Guiraud, I., Richard, C., Dubois Galopin, F., Cleyrat, C., Jourdan, E., Kralovics, R., Hermouet, S. & Lavabre-Bertrand, T. 2011. Nested high-resolution melting curve analysis a highly sensitive, reliable, and simple method for detection of JAK2 exon 12 mutations - clinical relevance in the monitoring of polycythemia. *J Mol Diagn,* 13, 263-70.

Carlisle, A. 2012. Uproar over new vaccine. Available: http://www.dispatch.co.za/exclusive-uproar-over-new-vaccine/ [Accessed 19 November 2012].

Carpenter, S., Wilson, A. & Mellor, P. S. 2009. *Culicoides* and the emergence of bluetongue virus in northern Europe. *Trends Microbiol,* 17, 172-8.

Carpenter, S., Wilson, A., Barber, J., Veronesi, E., Mellor, P., Venter, G. & Gubbins, S. 2011. Temperature dependence of the extrinsic incubation period of orbiviruses in *Culicoides* biting midges. *PLoS One,* 6, e27987.

Cassol, S., Gill, M. J., Pilon, R., Cormier, M., Voigt, R. F., Willoughby, B. & Forbes, J. 1997. Quantification of human immunodeficiency virus type 1 RNA from dried plasma spots collected on filter paper. *J Clin Microbiol,* 35, 2795-801.

Castillo-Olivares, J., Calvo-Pinilla, E., Casanova, I., Bachanek-Bankowska, K., Chiam, R., Maan, S., Nieto, J. M., Ortego, J. & Mertens, P. P. 2011. A modified vaccinia Ankara virus (MVA) vaccine expressing African horse sickness virus (AHSV) VP2 protects against AHSV challenge in an IFNAR -/- mouse model. *PLoS One,* 6, e16503.

Castrucci, M. R., Donatelli, I., Sidoli, L., Barigazzi, G., Kawaoka, Y. & Webster, R. G. 1993. Genetic reassortment between avian and human influenza A viruses in Italian pigs. *Virology,* 193, 503-6.

Catley, A. & Leyland, T. 2001. Community participation and the delivery of veterinary services in Africa. *Prev Vet Med,* 49, 95-113.

Chaignat, V., Worwa, G., Scherrer, N., Hilbe, M., Ehrensperger, F., Batten, C., Cortyen, M., Hofmann, M. & Thuer, B. 2009. Toggenburg Orbivirus, a new bluetongue virus: initial detection, first observations in field and experimental infection of goats and sheep. *Vet Microbiol,* 138, 11-9.

Chateigner-Boutin, A. L. & Small, I. 2007. A rapid high-throughput method for the detection and quantification of RNA editing based on high-resolution melting of amplicons. *Nucleic Acids Res,* 35, e114.

Chatzinasiou, E., Dovas, C. I., Papanastassopoulou, M., Georgiadis, M., Psychas, V., Bouzalas, I., Koumbati, M., Koptopoulos, G. & Papadopoulos, O. 2010. Assessment of bluetongue viraemia in sheep by real-time PCR and correlation with viral infectivity. *J Virol Methods,* 169, 305-15.

Chenchev, I., Rusenova, N. & Sandev, N. 2011. Seroepidemiology studies of donkey's blood for detection of some virus infections on ungulates. *Trakia Journal of Sciences,* 9, 82-86.

Chenna, R., Sugawara, H., Koike, T., Lopez, R., Gibson, T. J., Higgins, D. G. & Thompson, J. D. 2003. Multiple sequence alignment with the Clustal series of programs. *Nucleic Acids Res,* 31, 3497-500.

Chiam, R., Sharp, E., Maan, S., Rao, S., Mertens, P., Blacklaws, B., Davis-Poynter, N., Wood, J. & Castillo-Olivares, J. 2009. Induction of antibody responses to African horse sickness virus (AHSV) in ponies after vaccination with recombinant modified vaccinia Ankara (MVA). *PLoS One,* 4, e5997.

Chomczynski, P. & Sacchi, N. 1987. Single-step method of RNA isolation by acid guanidinium thiocyanate-phenol-chloroform extraction. *Anal Biochem,* 162, 156-9.

Chroma, M., Hricova, K., Kolar, M., Sauer, P. & Koukalova, D. 2011. Using newly developed multiplex polymerase chain reaction and melting curve analysis for detection and discrimination of beta-lactamases in *Escherichia coli* isolates from intensive care patients. *Diagn Microbiol Infect Dis,* 71, 181-91.

Chuma, T., Le Blois, H., Sanchez-Vizcaino, J. M., Diaz-Laviada, M. & Roy, P. 1992. Expression of the major core antigen VP7 of African horsesickness virus by a recombinant baculovirus and its use as a group-specific diagnostic reagent. *J Gen Virol,* 73 (Pt 4), 925-31.

Clift, S. J. & Penrith, M. L. 2010. Tissue and cell tropism of African horse sickness virus demonstrated by immunoperoxidase labeling in natural and experimental infection in horses in South Africa. *Vet Pathol,* 47, 690-7.

Coetzee, E. 2000. El Niño linked to horse sickness. *Farmer's Weekly.* 3 March 2000

Coetzer, J. A. W. & Erasmus, B. J. 1994. African horsesickness. *In:* Coetzer, J. A. W., Thomson, G. R. & Tustin, R. C. (eds.) *Infectious Diseases of Livestock with Special Reference to Southern Africa.* Cape Town: Oxford University Press.

Corbett. 2006. HRM™. *High Resolution Melt Assay Design and Analysis.* Online: Corbett Life Science.

Crafford, J. E., Guthrie, A. J., van Vuuren, M., Mertens, P. P., Burroughs, J. N., Howell, P. G. & Hamblin, C. 2003. A group-specific, indirect sandwich ELISA for the detection of equine encephalosis virus antigen. *J Virol Methods,* 112, 129-35.

Crafford, J. E., Lourens, C. W., Gardner, I. A., Maclachlan, N. J. & Guthrie, A. J. 2013. Passive transfer and rate of decay of maternal antibody against African horse sickness virus in South African Thoroughbred foals. *Equine Vet J,* 45, 604-7.

Cramer, T. J. 2010. *Monitoring the African horsesickness virus life cycle by real-time RT-PCR of viral dsRNA.* Magister Scientiae Dissertation, University of Pretoria, Online.

Crawford, S. E., Labbe, M., Cohen, J., Burroughs, M. H., Zhou, Y. J. & Estes, M. K. 1994. Characterization of virus-like particles produced by the expression of rotavirus capsid proteins in insect cells. *J Virol,* 68, 5945-52.

Crow, L. J. I. 2005. *Testing for passive transfer of immunity in foals, and an evaluation of the African horse sickness vaccination schedule.* Master of Science in Agriculture Dissertation, University of KwaZulu-Natal, Pietermaritzburg.

DAFF. 2009. *Department of Agriculture, Forestry and Fisheries* [Online]. Pretoria: Department of Agriculture, Forestry and Fisheries. http://www.daff.gov.za [Accessed 18 October 2009].

Dallas, J. F., Cruickshank, R. H., Linton, Y. M., Nolan, D. V., Patakakis, M., Braverman, Y., Capela, R., Capela, M., Pena, I., Meiswinkel, R., Ortega, M. D., Baylis, M., Mellor, P. S. & Mordue Luntz, A. J. 2003. Phylogenetic status and matrilineal structure of the biting midge, *Culicoides imicola*, in Portugal, Rhodes and Israel. *Med Vet Entomol,* 17, 379-87.

de Juan Jimenez, I., Cardenosa, E. E., Suela, S. P., Gonzalez, E. B., Trejo, D. S., Lluch, O. F. & Gilabert, P. B. 2011. Advantage of high-resolution melting curve analysis over conformation-sensitive gel electrophoresis for mutational screening of BRCA1 and BRCA2 genes. *Clin Chim Acta,* 412, 578-82.

de la Poza, F., Calvo-Pinilla, E., Lopez-Gil, E., Marin-Lopez, A., Mateos, F., Castillo-Olivares, J., Lorenzo, G. & Ortego, J. 2013. NS1 is a key protein in the vaccine composition to protect IFNAR(-/-) mice against infection with multiple serotypes of African horse sickness virus. *PLoS One,* 8, e70197.

de Sa, R. O., Zellner, M. & Grubman, M. J. 1994. Phylogenetic analysis of segment 10 from African horsesickness virus and cognate genes from other orbiviruses. *Virus Res,* 33, 157-65.

de Vos, C. J., Hoek, C. A. & Nodelijk, G. 2012. Risk of introducing African horse sickness virus into the Netherlands by international equine movements. *Prev Vet Med,* 106, 108-22.

de Waal, P. J. & Huismans, H. 2005. Characterization of the nucleic acid binding activity of inner core protein VP6 of African horse sickness virus. *Arch Virol,* 150, 2037-50.

DEFRA. 2012. African Horse Sickness Control Strategy for Great Britain. Department for Environment, Food and Rural Affairs, London.

Del Rio Lopez, R., Miranda, M. A., Paredes-Esquivel, C., Lucientes, J., Calvete, C., Estrada, R. & Venter, G. J. 2012. Recovery rates of bluetongue virus serotypes 1, 2, 4 and 8 Spanish strains from orally infected *Culicoides imicola* in South Africa. *Med Vet Entomol,* 26, 162-7.

DoA. 2003. African Horse Sickness (AHS) Control Policy

du Plessis, D. H., van Wyngaardt, W. & Bremer, C. W. 1990. An indirect sandwich ELISA utilising F(ab')2 fragments for the detection of African horsesickness virus. *J Virol Methods,* 29, 279-89.

du Plessis, D. H., van Wyngaardt, W., Romito, M., du Plessis, M. & Maree, S. 1999. The use of chicken IgY in a double antibody sandwich ELISA for detecting African horsesickness virus. *Onderstepoort J Vet Res,* 66, 25-8.

du Plessis, M., Cloete, M., Aitchison, H. & Van Dijk, A. A. 1998. Protein aggregation complicates the development of baculovirus-expressed African horsesickness virus serotype 5 VP2 subunit vaccines. *Onderstepoort J Vet Res,* 65, 321-9.

du Toit, R. M. 1944. The transmission of bluetongue and horse-sickness by *Culicoides*. *Onderstepoort J Vet Sci Anim Ind,* 19, 7-16.

Dwight, Z., Palais, R. & Wittwer, C. T. 2011. uMELT: prediction of high-resolution melting curves and dynamic melting profiles of PCR products in a rich web application. *Bioinformatics,* 27, 1019-20.

Eaton, B. T. & Crameri, G. S. 1989. The site of bluetongue virus attachment to glycophorins from a number of animal erythrocytes. *J Gen Virol,* 70 (Pt 12), 3347-53.

Eaton, B. T. & White, J. R. 2004. Developing new orbivirus diagnostic platforms. *Vet Ital,* 40, 525-30.

Ebert, D. & Bull, J. J. 2003. Challenging the trade-off model for the evolution of virulence: is virulence management feasible? *Trends Microbiol,* 11, 15-20.

Eksteen, S., Breetzke, G. D. & Eksteen, S. 2011. Predicting the abundance of African horse sickness vectors in South Africa using GIS and artificial neural networks. *S Afr J Sci,* 107.

El-Harrak, M., Martin-Folgar, R., Llorente, F., Fernandez-Pacheco, P., Brun, A., Figuerola, J. & Jimenez-Clavero, M. A. 2011. Rift Valley and West Nile virus antibodies in camels, North Africa. *Emerg Infect Dis,* 17, 2372-4.

el-Husseini, M. M., Salama, S. A., Abdallah, S. K., Abou Bakr, H. E. & Hassanein, M. M. 1986. Role of Culex pipiens L. in recovering latent African-horse-sickness virus from dogs. *J Egypt Soc Parasitol,* 16, 249-58.

el Hasnaoui, H., el Harrak, M., Zientara, S., Laviada, M. & Hamblin, C. 1998. Serological and virological responses in mules and donkeys following inoculation with African horse sickness virus serotype 4. *Arch Virol Suppl,* 14, 29-36.

El Idrissi, A. H. & Lubroth, J. 2006. Global Epidemiology of Infectious Diseases in Working Equine Animals. *In:* Bakkoury, M. & Dakkak, A. (eds.) *9th International Congress of World Equine Veterinary Association.* Marrakech, Morocco: International Veterinary Information Service.

Elia, G., Savini, G., Decaro, N., Martella, V., Teodori, L., Casaccia, C., Di Gialleonardo, L., Lorusso, E., Caporale, V. & Buonavoglia, C. 2008. Use of real-time RT-PCR as a rapid molecular approach for differentiation of field and vaccine strains of bluetongue virus serotypes 2 and 9. *Mol Cell Probes,* 22, 38-46.

Erasmus, B. J. 2004. *African horse sickness* [Online]. Onderstepoort: Onderstepoort Veterinary Institute. http://www.vet.uga.edu/VPP/gray_book02/fad/ahs.php [Accessed 12 March 2008].

Evans, J. D. & Leigh, S. A. 2008. Differentiation of *Mycoplasma gallisepticum* vaccine strains ts-11 and 6/85 from commonly used *Mycoplasma gallisepticum* challenge strains by PCR. *Avian Dis,* 52, 491-7.

Fasina, F. 2008. African Horse sickness expands to Northern Hemisphere. *European Veterinary Conference - Voorjaarsdagen.* Amsterdam, Netherlands: International Veterinary Information Service.

Fasina, F., Potgieter, A. C., Ibironke, A., Bako, B., Bwala, D. & Kumbish, P. 2008. First Report of an Outbreak of African Horsesickness Virus Serotype 2 in the Northern Hemisphere. *J Equine Vet Sci,* 28, 167-170.

Felsenstein, J. 1985. Confidence limits on phylogenies: an approach using the bootstrap. *Evolution*, 783-791.

Fernández-Pinero, J., Fernández-Pacheco, P., Rodríguez, B., Sotelo, E., Robles, A., Arias, M. & Sánchez-Vizcaíno, J. M. 2009. Rapid and sensitive detection of African horse sickness virus by real-time PCR. *Res Vet Sci,* 86, 353-358.

French, T. J., Marshall, J. J. & Roy, P. 1990. Assembly of double-shelled, viruslike particles of bluetongue virus by the simultaneous expression of four structural proteins. *J. Virol.,* 64, 5695-5700.

French, T. J. & Roy, P. 1990. Synthesis of bluetongue virus (BTV) corelike particles by a recombinant baculovirus expressing the two major structural core proteins of BTV. *J Virol,* 64, 1530-6.

Gadberry, M. D., Malcomber, S. T., Doust, A. N. & Kellogg, E. A. 2005. Primaclade - a flexible tool to find conserved PCR primers across multiple species. *Bioinformatics,* 21, 1263-4.

Garten, R. J., Davis, C. T., Russell, C. A., Shu, B., Lindstrom, S., Balish, A., Sessions, W. M., Xu, X., Skepner, E., Deyde, V., Okomo-Adhiambo, M., Gubareva, L., Barnes, J., Smith, C. B., Emery, S. L., Hillman, M. J., Rivailler, P., Smagala, J., de Graaf, M., Burke, D. F., Fouchier, R. A., Pappas, C., Alpuche-Aranda, C. M., Lopez-Gatell, H., Olivera, H., Lopez, I., Myers, C. A., Faix, D., Blair, P. J., Yu, C., Keene, K. M., Dotson, P. D., Jr., Boxrud, D., Sambol, A. R., Abid, S. H., St George, K., Bannerman, T., Moore, A. L., Stringer, D. J., Blevins, P., Demmler-Harrison, G. J., Ginsberg, M., Kriner, P., Waterman, S., Smole, S., Guevara, H. F., Belongia, E. A., Clark, P. A., Beatrice, S. T., Donis, R., Katz, J., Finelli, L., Bridges, C. B., Shaw, M., Jernigan, D. B., Uyeki, T. M., Smith, D. J., Klimov, A. I. & Cox, N. J. 2009. Antigenic and genetic characteristics of swine-origin 2009 A(H1N1) influenza viruses circulating in humans. *Science,* 325, 197-201.

Gerdes, G. 2006. Tracing African horse sickness outbreaks in South Africa. *In:* Bakkoury, M. & Dakkak, A. (eds.) *9th International Congress of World Equine Veterinary Association.* Marrakech, Morocco: International Veterinary Information Service.

Ghorashi, S. A., O'Rourke, D., Ignjatovic, J. & Noormohammadi, A. H. 2011. Differentiation of infectious bursal disease virus strains using real-time RT-PCR and high resolution melt curve analysis. *J Virol Methods,* 171, 264-71.

Goffredo, M. & Meiswinkel, R. 2004. Entomological surveillance of bluetongue in Italy: methods of capture, catch analysis and identification of *Culicoides* biting midges. *Vet Ital,* 40, 260-5.

Goldsmit, L. 1967. Growth Characteristics of Six Neurotropic and One Viscerotropic African Horse-Sickness Virus Strains in Fertilized Eggs. *Am J Vet Res,* 28, 19-24.

Gomez-Villamandos, J. C., Sanchez, C., Carrasco, L., Laviada, M. M., Bautista, M. J., Martinez-Torrecuadrada, J., Sanchez-Vizcaino, J. M. & Sierra, M. A. 1999. Pathogenesis of African horse sickness: ultrastructural study of the capillaries in experimental infection. *J Comp Pathol,* 121, 101-16.

Gomulski, L. M., Meiswinkel, R., Delecolle, J. C., Goffredo, M. & Gasperi, G. 2006. Phylogeny of the subgenus *Culicoides* and related species in Italy, inferred from internal transcribed spacer 2 ribosomal DNA sequences. *Med Vet Entomol,* 20, 229-38.

Gordon, S., Bolwell, C., Rogers, C., Guthrie, A., Magunda, F. & Hove, P. 2013. Descriptive epidemiology of African horse sickness in Zimbabwe. *Onderstepoort J Vet Res,* 80, E1-5.

Gorman, B. M. 1979. Variation in orbiviruses. *J Gen Virol,* 44, 1-15.

Granados-Cifuentes, C. & Rodriguez-Lanetty, M. 2011. The use of high-resolution melting analysis for genotyping *Symbiodinium* strains: a sensitive and fast approach. *Mol Ecol Resour,* 11, 394-9.

Grando, D., Said, M. M., Mayall, B. C. & Gurtler, V. 2012. High resolution melt analysis to track infections due to ribotype 027 *Clostridium difficile*. *J Microbiol Methods,* 89, 87-94.

Grewar, J. D., Weyer, C. T., Guthrie, A. J., Koen, P., Davey, S., Quan, M., Visser, D., Russouw, E. & Bührmann, G. 2013. The 2011 outbreak of African horse sickness in the African horse sickness controlled area in South Africa. *J S Afr Vet Assoc,* 84, 7 pages.

Groenink, S., Watson, G. & Young, M. 2009. Development of a rapid assay for African horse sickness virus serotyping through High Resolution Melt Analysis. *In:* Mann, J. & Dugmore, T., eds. Animal Science in a Changing Environment, 28-30 July 2009 Alpine Heath Conference Village, KwaZulu-Natal. South African Society for Animal Science.

Groenink, S. R. 2009. *Development of a protocol for the molecular serotyping of the African horse sickness virus.* Master of Science in Agriculture Dissertation, University of KwaZulu-Natal, Pietermaritzburg.

Groenink, S. R., Watson, G. M. F. & Young, M. B. 2010. *A method of serotyping the African horse sickness virus*. South Africa patent application 2010/04579.

Grubman, M. J. & Lewis, S. A. 1992. Identification and characterization of the structural and nonstructural proteins of African horsesickness virus and determination of the genome coding assignments. *Virology,* 186, 444-51.

Gundry, C. N., Vandersteen, J. G., Reed, G. H., Pryor, R. J., Chen, J. & Wittwer, C. T. 2003. Amplicon melting analysis with labeled primers: a closed-tube method for differentiating homozygotes and heterozygotes. *Clin Chem,* 49, 396-406.

Gurtler, V., Grando, D., Mayall, B. C., Wang, J. & Ghaly-Derias, S. 2012. A novel method for simultaneous *Enterococcus* species identification/typing and van genotyping by high resolution melt analysis. *J Microbiol Methods,* 90, 167-81.

Guthrie, A. J. 2008. AHS: Current perspectives. *47th British Equine Veterinary Association Congress.* Liverpool, United Kingdom: International Veterinary Information Services.

Guthrie, A. J., Quan, M., Lourens, C. W., Audonnet, J. C., Minke, J. M., Yao, J., He, L., Nordgren, R., Gardner, I. A. & Maclachlan, N. J. 2009. Protective immunization of horses with a recombinant canarypox virus vectored vaccine co-expressing genes encoding the outer capsid proteins of African horse sickness virus. *Vaccine,* 27, 4434-8.

Guthrie, A. J., Maclachlan, N. J., Joone, C., Lourens, C. W., Weyer, C. T., Quan, M., Monyai, M. S. & Gardner, I. A. 2013. Diagnostic accuracy of a duplex real-time reverse transcription quantitative PCR assay for detection of African horse sickness virus. *J Virol Methods,* 189, 30-5.

Haji Ende, H. T., Balcha, E., Amsalu, K. & Gizaw, D. 2013. Seroprevalence of African Horse Sickness at Central Highland of Ethiopia. *Adv Anim Vet Sci,* 1, 84-7.

Hamblin, C., Mertens, P. P., Mellor, P. S., Burroughs, J. N. & Crowther, J. R. 1991. A serogroup specific enzyme-linked immunosorbent assay for the detection and identification of African horse sickness viruses. *J Virol Methods,* 31, 285-92.

Hamblin, C., Salt, J. S., Mellor, P. S., Graham, S. D., Smith, P. R. & Wohlsein, P. 1998. Donkeys as reservoirs of African horse sickness virus. *Arch Virol. Supplementum,* 14, 37.

Hassan, S. H., Wirblich, C., Forzan, M. & Roy, P. 2001. Expression and functional characterization of bluetongue virus VP5 protein: role in cellular permeabilization. *J Virol,* 75, 8356-67.

Hassan, S. S. & Roy, P. 1999. Expression and functional characterization of bluetongue virus VP2 protein: role in cell entry. *J Virol,* 73, 9832-42.

Hazrati, A. & Ozawa, Y. 1965. Serologic Studies of African Horse-Sickness Virus with Emphasis on Neutralization Test in Tissue Culture. *Can J Comp Med Vet Sci,* 29, 173-8.

Heldens, J. G., Patel, J. R., Chanter, N., Ten Thij, G. J., Gravendijck, M., Schijns, V. E., Langen, A. & Schetters, T. P. 2008. Veterinary vaccine development from an industrial perspective. *Vet J,* 178, 7-20.

Helps, C., Lait, P., Tasker, S. & Harbour, D. 2002. Melting curve analysis of feline calicivirus isolates detected by real-time reverse transcription PCR. *J Virol Methods,* 106, 241-4.

Henning, M. W. 1956. African horsesickness, perdesiekte, pestis equorum. *Animal Diseases of South Africa.* Pretoria: Central News Agency.

Hewson, K., Noormohammadi, A. H., Devlin, J. M., Mardani, K. & Ignjatovic, J. 2009. Rapid detection and non-subjective characterisation of infectious bronchitis virus isolates using high-resolution melt curve analysis and a mathematical model. *Arch Virol,* 154, 649-60.

Hewson, K. A., Browning, G. F., Devlin, J. M., Ignjatovic, J. & Noormohammadi, A. H. 2010. Application of high-resolution melt curve analysis for classification of infectious bronchitis viruses in field specimens. *Aust Vet J,* 88, 408-13.

Hoffmann, B., Beer, M., Reid, S. M., Mertens, P., Oura, C. A., van Rijn, P. A., Slomka, M. J., Banks, J., Brown, I. H., Alexander, D. J. & King, D. P. 2009. A review of RT-PCR technologies used in veterinary virology and disease control: sensitive and

specific diagnosis of five livestock diseases notifiable to the World Organisation for Animal Health. *Vet Microbiol,* 139, 1-23.

Hofmann, M. A., Renzullo, S., Mader, M., Chaignat, V., Worwa, G. & Thuer, B. 2008. Genetic characterization of toggenburg orbivirus, a new bluetongue virus, from goats, Switzerland. *Emerg Infect Dis,* 14, 1855-61.

Holmes, E. C., Ghedin, E., Miller, N., Taylor, J., Bao, Y., St George, K., Grenfell, B. T., Salzberg, S. L., Fraser, C. M., Lipman, D. J. & Taubenberger, J. K. 2005. Whole-genome analysis of human influenza A virus reveals multiple persistent lineages and reassortment among recent H3N2 viruses. *PLoS Biol,* 3, e300.

House, C., Mikiciuk, P. E. & Berninger, M. L. 1990. Laboratory diagnosis of African horse sickness: comparison of serological techniques and evaluation of storage methods of samples for virus isolation. *J Vet Diagn Invest,* 2, 44-50.

House, J. A., Stott, J. L., Blanchard, M. T., LaRocco, M. & Llewellyn, M. E. 1996. A blocking ELISA for detection of antibody to a subgroup-reactive epitope of African horsesickness viral protein 7 (VP7) using a novel gamma-irradiated antigen. *Ann N Y Acad Sci,* 791, 333-44.

Howell, P. G. 1962. The isolation and identification of further antigenic types of African horsesickness virus. *Onderstepoort J Vet Res,* 29, 139-149.

Hubbart, C., Whittall, R., Scartezini, M. & Humphries, S. 2007. Development of an affordable, sensitive and rapid screening method for mutation detection in UK FH subjects. *Atherosclerosis 194,* 194, 279-286.

Huismans, H. & Erasmus, B. J. 1981. Identification of the serotype-specific and group-specific antigens of bluetongue virus. *Onderstepoort J Vet Res,* 48, 51-8.

Huismans, H., van Dijk, A. A. & Bauskin, A. R. 1987. *In vitro* phosphorylation and purification of a nonstructural protein of bluetongue virus with affinity for single-stranded RNA. *J Virol,* 61, 3589-95.

Huismans, H., van Staden, V., Fick, W., van Niekerk, M. & Meiring, T. 2004. A comparison of different orbivirus proteins that could affect virulence and pathogenesis. *Vet Ital,* 40, 417-425.

Hyatt, A. D., Zhao, Y. & Roy, P. 1993. Release of bluetongue virus-like particles from insect cells is mediated by BTV nonstructural protein NS3/NS3A. *Virology,* 193, 592-603.

Idrissi Bougrine, S., Fassi Fihri, O., el Harrak, M. & Fassi Fehri, M. M. 1999. Use of the immunoenzyme test ELISA-NS3 to distinguish horses infected by African horsesickness virus from vaccinated horses [Abstract]. *Rev Sci Tech,* 18, 618-26.

Inoue, R., Tsukahara, T., Sunaba, C., Itoh, M. & Ushida, K. 2007. Simple and rapid detection of the porcine reproductive and respiratory syndrome virus from pig whole blood using filter paper. *J Virol Methods,* 141, 102-6.

Iwata, H., Yamagawa, M. & Roy, P. 1992. Evolutionary relationships among the gnat-transmitted orbiviruses that cause African horse sickness, bluetongue, and epizootic hemorrhagic disease as evidenced by their capsid protein sequences. *Virology,* 191, 251-61.

Jeffery, N., Gasser, R. B., Steer, P. A. & Noormohammadi, A. H. 2007. Classification of *Mycoplasma synoviae* strains using single-strand conformation polymorphism and high-resolution melting-curve analysis of the vlhA gene single-copy region. *Microbiology,* 153, 2679-88.

Jenkins, A. B. 2008. *A study of the Culicoides (Diptera: Ceratopogonidae) vectors of African horse sickness to enhance current practical control measures and research methods.* Master of Science in Agriculture Dissertation, University of KwaZulu-Natal, Pietermarizburg.

Jere, K. C., Mlera, L., Page, N. A., van Dijk, A. A. & O'Neill, H. G. 2011. Whole genome analysis of multiple rotavirus strains from a single stool specimen using sequence-independent amplification and 454(R) pyrosequencing reveals evidence of intergenotype genome segment recombination. *Infect Genet Evol,* 11, 2072-82.

Jere, K. C., Mlera, L., O'Neill, H. G., Peenze, I. & van Dijk, A. A. 2012. Whole genome sequence analyses of three African bovine rotaviruses reveal that they emerged

through multiple reassortment events between rotaviruses from different mammalian species. *Vet Microbiol,* 159, 245-50.

Jimenez-Clavero, M. A., Aguero, M., San Miguel, E., Mayoral, T., Lopez, M. C., Ruano, M. J., Romero, E., Monaco, F., Polci, A., Savini, G. & Gomez-Tejedor, C. 2006. High throughput detection of bluetongue virus by a new real-time fluorogenic reverse transcription-polymerase chain reaction: application on clinical samples from current Mediterranean outbreaks. *J Vet Diagn Invest,* 18, 7-17.

Johnson, M., Zaretskaya, I., Raytselis, Y., Merezhuk, Y., McGinnis, S. & Madden, T. L. 2008. NCBI BLAST: a better web interface. *Nucleic Acids Res,* 36, W5-9.

KAPA. 2010. Introduction to High Resolution Melt Analysis. *Application Guide.* Cape Town, South Africa: KAPA Biosystems.

KAPA. 2012. KAPA™ SYBR® FAST qPCR Kit Technical Data Sheet. 4.10 ed. Cape Town, South Africa: KAPA Biosystems.

Koekemoer, J. J., Potgieter, A. C., Paweska, J. T. & van Dijk, A. A. 2000. Development of probes for typing African horsesickness virus isolates using a complete set of cloned VP2-genes. *J Virol Methods,* 88, 135-44.

Koekemoer, J. J., Paweska, J. T., Pretorius, P. J. & van Dijk, A. A. 2003. VP2 gene phylogenetic characterization of field isolates of African horsesickness virus serotype 7 circulating in South Africa during the time of the 1999 African horsesickness outbreak in the Western Cape. *Virus Res,* 93, 159-67.

Koekemoer, J. J. & van Dijk, A. A. 2004. African horsesickness virus serotyping and identification of multiple co-infecting serotypes with a single genome segment 2 RT-PCR amplification and reverse line blot hybridization. *J Virol Methods,* 122, 49-56.

Koekemoer, J. J. 2008. Serotype-specific detection of African horsesickness virus by real-time PCR and the influence of genetic variations. *J Virol Methods,* 154, 104-10.

Kummalue, T., Chuphrom, A., Sukpanichanant, S., Pongpruttipan, T. & Sukpanichanant, S. 2010. Detection of monoclonal immunoglobulin heavy chain gene rearrangement (FR3) in Thai malignant lymphoma by High Resolution Melting curve analysis. *Diagn Pathol,* 5, 31.

Kuno, G. & Chang, G. J. 2005. Biological transmission of arboviruses: reexamination of and new insights into components, mechanisms, and unique traits as well as their evolutionary trends. *Clin Microbiol Rev,* 18, 608-37.

Kweon, C. H., Kwon, B. J., Ko, Y. J. & Kenichi, S. 2003. Development of competitive ELISA for serodiagnosis on African horsesickness virus using baculovirus expressed VP7 and monoclonal antibody. *J Virol Methods,* 113, 13-8.

Kwok, S., Chang, S. Y., Sninsky, J. J. & Wang, A. 1994. A guide to the design and use of mismatched and degenerate primers. *PCR Methods Appl,* 3, S39-47.

Laegreid, W. W., Skowronek, A., Stone-Marschat, M. & Burrage, T. 1993. Characterization of virulence variants of African horsesickness virus. *Virology,* 195, 836-9.

Larkin, M. A., Blackshields, G., Brown, N. P., Chenna, R., McGettigan, P. A., McWilliam, H., Valentin, F., Wallace, I. M., Wilm, A., Lopez, R., Thompson, J. D., Gibson, T. J. & Higgins, D. G. 2007. Clustal W and Clustal X version 2.0. *Bioinformatics,* 23, 2947-8.

Laviada, M. D., Babin, M., Dominguez, J. & Sanchez-Vizcaino, J. M. 1992. Detection of African horsesickness virus in infected spleens by a sandwich ELISA using two monoclonal antibodies specific for VP7. *J Virol Methods,* 38, 229-42.

Laviada, M. D., Arias, M. & Sanchez-Vizcaino, J. M. 1993. Characterization of African horsesickness virus serotype 4-induced polypeptides in Vero cells and their reactivity in Western immunoblotting. *J Gen Virol,* 74 (Pt 1), 81-7.

Laviada, M. D., Roy, P., Sanchez-Vizcaino, J. M. & Casal, J. I. 1995. The use of African horse sickness virus NS3 protein, expressed in bacteria, as a marker to differentiate infected from vaccinated horses. *Virus Res,* 38, 205-18.

Laviada, M. D., Sanchez-Vizcaino, J. M., Roy, P. & Sobrino, F. 1997. Detection of African horsesickness virus by the polymerase chain reaction. *Invest. Agr. SA.,* 12, 97–102.

Le Blois, H., French, T., Mertens, P. P., Burroughs, J. N. & Roy, P. 1992. The expressed VP4 protein of bluetongue virus binds GTP and is the candidate guanylyl transferase of the virus. *Virology,* 189, 757-61.

Lee, L. H., Ting, L. J., Shien, J. H. & Shieh, H. K. 1994. Single-tube, noninterrupted reverse transcription-PCR for detection of infectious bursal disease virus. *J Clin Microbiol,* 32, 1268-72.

Lelli, R., Molini, U., Ronchi, G. F., Rossi, E., Franchi, P., Ulisse, S., Armillotta, G., Capista, S., Khaiseb, S., Di Ventura, M. & Pini, A. 2013. Inactivated and adjuvanted vaccine for the control of the African horse sickness virus serotype 9 infection: evaluation of efficacy in horses and guinea-pig model. *Vet Ital,* 49, 89-98.

Levesque, S., Michaud, S., Arbeit, R. D. & Frost, E. H. 2011. High-resolution melting system to perform multilocus sequence typing of *Campylobacter jejuni*. *PLoS One,* 6, e16167.

Lewis, S. A. & Grubman, M. J. 1991. VP2 is the major exposed protein on orbiviruses. *Arch Virol,* 121, 233-6.

Liew, M., Pryor, R., Palais, R., Meadows, C., Erali, M., Lyon, E. & Wittwer, C. 2004. Genotyping of single-nucleotide polymorphisms by high-resolution melting of small amplicons. *Clin Chem,* 50, 1156-64.

Limor, J. R., Lal, A. A. & Xiao, L. 2002. Detection and differentiation of Cryptosporidium parasites that are pathogenic for humans by real-time PCR. *J Clin Microbiol,* 40, 2335-8.

Linthicum, K. J., Anyamba, A., Chretien, J. P., Small, J., Tucker, C. J. & Britch, S. C. 2010. The Role of Global Climate Patterns in the Spatial and Temporal Distribution of Vector-Borne Disease. *Vector Biology, Ecology and Control*, 3-13.

Lo Iacono, G., Robin, C. A., Newton, J. R., Gubbins, S. & Wood, J. L. 2013. Where are the horses? With the sheep or cows? Uncertain host location, vector-feeding preferences and the risk of African horse sickness transmission in Great Britain. *J R Soc Interface,* 10, 20130194.

Lord, C. C., Woolhouse, M. E., Heesterbeek, J. A. & Mellor, P. S. 1996a. Vector-borne diseases and the basic reproduction number: a case study of African horse sickness. *Med Vet Entomol,* 10, 19-28.

Lord, C. C., Woolhouse, M. E., Rawlings, P. & Mellor, P. S. 1996b. Simulation studies of African horse sickness and *Culicoides imicola* (Diptera: Ceratopogonidae). *J Med Entomol,* 33, 328-38.

Lord, C. C., Woolhouse, M. E. & Barnard, B. J. 1997a. Transmission and distribution of virus serotypes: African horse sickness in zebra. *Epidemiol Infect,* 118, 43-50.

Lord, C. C., Woolhouse, M. E. & Mellor, P. S. 1997b. Simulation studies of vaccination strategies in African horse sickness. *Vaccine,* 15, 519-24.

Lord, C. C., Woolhouse, M. E. & Barnard, B. J. 1998a. Transmission and distribution of African horse sickness virus serotypes in South African zebra. *Arch Virol Suppl,* 14, 21-8.

Lord, C. C., Woolhouse, M. E. & Mellor, P. S. 1998b. Simulation studies of African horse sickness in Spain. *Arch Virol Suppl,* 14, 103-11.

Lord, C. C., Venter, G. J., Mellor, P. S., Paweska, J. T. & Woolhouse, M. E. 2002. Transmission patterns of African horse sickness and equine encephalosis viruses in South African donkeys. *Epidemiol Infect,* 128, 265-75.

Lourenco, S. & Roy, P. 2011. *In vitro* reconstitution of Bluetongue virus infectious cores. *Proc Natl Acad Sci U S A,* 108, 13746-51.

Lubroth, J. 1988. African horsesickness and the epizootic in Spain 1987. *Equine Pract,* 10, 26-33.

Maan, N. S., Maan, S., Nomikou, K., Johnson, D. J., El Harrak, M., Madani, H., Yadin, H., Incoglu, S., Yesilbag, K., Allison, A. B., Stallknecht, D. E., Batten, C., Anthony, S. J. & Mertens, P. P. 2010a. RT-PCR assays for seven serotypes of epizootic haemorrhagic disease virus & their use to type strains from the Mediterranean region and North America. *PLoS One,* 5, e12782.

Maan, N. S., Maan, S., Nomikou, K., Belaganahalli, M. N., Bachanek-Bankowska, K. & Mertens, P. P. 2011a. Serotype specific primers and gel-based RT-PCR assays for 'typing' African horse sickness virus: identification of strains from Africa. *PLoS One,* 6, e25686.

Maan, S., Maan, N. S., van Rijn, P. A., van Gennip, R. G., Sanders, A., Wright, I. M., Batten, C., Hoffmann, B., Eschbaumer, M., Oura, C. A., Potgieter, A. C., Nomikou, K. & Mertens, P. P. 2010b. Full genome characterisation of bluetongue virus serotype 6 from the Netherlands 2008 and comparison to other field and vaccine strains. *PLoS One,* 5, e10323.

Maan, S., Maan, N. S., Nomikou, K., Veronesi, E., Bachanek-Bankowska, K., Belaganahalli, M. N., Attoui, H. & Mertens, P. P. 2011b. Complete genome characterisation of a novel 26th bluetongue virus serotype from Kuwait. *PLoS One,* 6, e26147.

Maartens, L. H., Erasmus, B. J. & Clift, S. J. 2011. Tissue tropism of African horsesickness virus in the chicken embryo demonstrated with the avidin-biotin complex immunoperoxidase method. *Vet Pathol,* 48, 1085-93.

MacLachlan, N. J., Balasuriya, U. B., Davis, N. L., Collier, M., Johnston, R. E., Ferraro, G. L. & Guthrie, A. J. 2007. Experiences with new generation vaccines against equine viral arteritis, West Nile disease and African horse sickness. *Vaccine,* 25, 5577-82.

Maclachlan, N. J., Drew, C. P., Darpel, K. E. & Worwa, G. 2009. The pathology and pathogenesis of bluetongue. *J Comp Pathol,* 141, 1-16.

Maclachlan, N. J. & Guthrie, A. J. 2010. Re-emergence of bluetongue, African horse sickness, and other orbivirus diseases. *Vet Res,* 41, 35.

Madani, H., Casal, J., Alba, A., Allepuz, A., Cetre-Sossah, C., Hafsi, L., Kount-Chareb, H., Bouayed-Chaouach, N., Saadaoui, H. & Napp, S. 2011. Animal diseases caused by orbiviruses, Algeria. *Emerg Infect Dis,* 17, 2325-7.

Mangold, K. A., Manson, R. U., Koay, E. S., Stephens, L., Regner, M., Thomson, R. B., Jr., Peterson, L. R. & Kaul, K. L. 2005. Real-time PCR for detection and identification of Plasmodium spp. *J Clin Microbiol,* 43, 2435-40.

Manole, V., Laurinmaki, P., Van Wyngaardt, W., Potgieter, C. A., Wright, I. M., Venter, G. J., van Dijk, A. A., Sewell, B. T. & Butcher, S. J. 2012. Structural insight into African horsesickness virus infection. *J Virol,* 86, 7858-66.

Marchi, P. R., Rawlings, P., Burroughs, J. N., Wellby, M., Mertens, P. P., Mellor, P. S. & Wade-Evans, A. M. 1995. Proteolytic cleavage of VP2, an outer capsid protein of African horse sickness virus, by species-specific serum proteases enhances infectivity in *Culicoides*. *J Gen Virol,* 76 (Pt 10), 2607-11.

Maree, F. F. & Huismans, H. 1997. Characterization of tubular structures composed of nonstructural protein NS1 of African horsesickness virus expressed in insect cells. *J Gen Virol,* 78 (Pt 5), 1077-82.

Maree, S., Durbach, S. & Huismans, H. 1998a. Intracellular production of African horsesickness virus core-like particles by expression of the two major core proteins, VP3 and VP7, in insect cells. *J Gen Virol,* 79 (Pt 2), 333-7.

Maree, S., Durbach, S., Maree, F. F., Vreede, F. & Huismans, H. 1998b. Expression of the major core structural proteins VP3 and VP7 of African horse sickness virus, and production of core-like particles. *Arch Virol Suppl,* 14, 203-9.

Maree, S. & Paweska, J. T. 2005. Preparation of recombinant African horse sickness virus VP7 antigen via a simple method and validation of a VP7-based indirect ELISA for the detection of group-specific IgG antibodies in horse sera. *J Virol Methods,* 125, 55-65.

Marek, A., Gunes, A., Schulz, E. & Hess, M. 2010. Classification of fowl adenoviruses by use of phylogenetic analysis and high-resolution melting-curve analysis of the hexon L1 gene region. *J Virol Methods,* 170, 147-54.

Marlow, C. H. 2010. A brief history of equine private practice in South Africa. *J S Afr Vet Assoc,* 81, 190-200.

Martin, L. A., Meyer, A. J., O'Hara, R. S., Fu, H., Mellor, P. S., Knowles, N. J. & Mertens, P. P. 1998. Phylogenetic analysis of African horse sickness virus segment 10: sequence variation, virulence characteristics and cell exit. *Arch Virol Suppl,* 14, 281-93.

Martinez-Torrecuadrada, J. L. & Casal, J. I. 1995. Identification of a linear neutralization domain in the protein VP2 of African horse sickness virus. *Virology,* 210, 391-9.

Martinez-Torrecuadrada, J. L., Diaz-Laviada, M., Roy, P., Sanchez, C., Vela, C., Sanchez-Vizcaino, J. M. & Casal, J. I. 1996. Full protection against African horsesickness (AHS) in horses induced by baculovirus-derived AHS virus serotype 4 VP2, VP5 and VP7. *J Gen Virol,* 77 (Pt 6), 1211-21.

Martinez-Torrecuadrada, J. L., Diaz-Laviada, M., Roy, P., Sanchez, C., Vela, C., Sanchez-Vizcaino, J. M. & Casal, J. I. 1997. Serologic markers in early stages of African horse sickness virus infection. *J Clin Microbiol,* 35, 531-5.

Martinez-Torrecuadrada, J. L., Langeveld, J. P., Venteo, A., Sanz, A., Dalsgaard, K., Hamilton, W. D., Meloen, R. H. & Casal, J. I. 1999. Antigenic profile of African horse sickness virus serotype 4 VP5 and identification of a neutralizing epitope shared with bluetongue virus and epizootic hemorrhagic disease virus. *Virology,* 257, 449-59.

Martinez-Torrecuadrada, J. L., Langeveld, J. P., Meloen, R. H. & Casal, J. I. 2001. Definition of neutralizing sites on African horse sickness virus serotype 4 VP2 at the level of peptides. *J Gen Virol,* 82, 2415-24.

Massie, E. L. 1962. African horse sickness in the Middle East. *Mil Med,* 127, 143-6.

Matsuo, E., Celma, C. C. & Roy, P. 2010. A reverse genetics system of African horse sickness virus reveals existence of primary replication. *FEBS Lett,* 584, 3386-91.

Matthijnssens, J., Ciarlet, M., Heiman, E., Arijs, I., Delbeke, T., McDonald, S. M., Palombo, E. A., Iturriza-Gomara, M., Maes, P., Patton, J. T., Rahman, M. & Van Ranst, M. 2008. Full genome-based classification of rotaviruses reveals a common origin between human Wa-Like and porcine rotavirus strains and human DS-1-like and bovine rotavirus strains. *J Virol,* 82, 3204-19.

McCarthy, M. 2012. *Now horses are threatened by deadly foreign virus* [Online]. Online: The Indepenent. http://www.independent.co.uk/environment/nature/now-horses-are-threatened-by-deadly-foreign-virus-7468941.html [Accessed].

McCusker, J., Dawson, M. T., Noone, D., Gannon, F. & Smith, T. 1992. Improved method for direct PCR amplification from whole blood. *Nucleic Acids Res,* 20, 6747.

Meiring, T. L., Huismans, H. & van Staden, V. 2009. Genome segment reassortment identifies non-structural protein NS3 as a key protein in African horsesickness virus release and alteration of membrane permeability. *Arch Virol,* 154, 263-71.

Meiswinkel, R. & Braack, L. E. 1994. African horsesickness epidemiology: five species of *Culicoides* (Diptera: Ceratopogonidae) collected live behind the ears and at the dung of the African elephant in the Kruger National Park, South Africa. *Onderstepoort J Vet Res,* 61, 155-70.

Meiswinkel, R., Nevill, E. & Venter, G. 1994. Vectors: *Culicoides* spp. *In:* Coetzer, J. A. W., Thomson, G. R. & Tustin, R. C. (eds.) *Infectious Diseases of Livestock with Special Reference to Southern Africa.* Cape Town: Oxford University Press.

Meiswinkel, R. 1998. The 1996 outbreak of African horse sickness in South Africa - the entomological perspective. *Arch Virol Suppl,* 14, 69-83.

Meiswinkel, R. & Paweska, J. T. 2003. Evidence for a new field *Culicoides* vector of African horse sickness in South Africa. *Prev Vet Med,* 60, 243-53.

Mellor, P. S., Boorman, J. & Jennings, M. 1975. The multiplication of African horse-sickness virus in two species of *Culicoides* (Diptera, Ceratopogonidae). *Arch Virol,* 47, 351-6.

Mellor, P. S., Boned, J., Hamblin, C. & Graham, S. 1990a. Isolations of African horse sickness virus from vector insects made during the 1988 epizootic in Spain. *Epidemiol Infect,* 105, 447-54.

Mellor, P. S., Hamblin, C. & Graham, S. D. 1990b. African horse sickness in Saudi Arabia. *Vet Rec,* 127, 41-2.

Mellor, P. S. 1993. African horse sickness: transmission and epidemiology. *Vet Res,* 24, 199-212.
Mellor, P. S. 1994. Epizootiology and vectors of African horse sickness virus. *Comp Immunol Microbiol Infect Dis,* 17, 287-96.
Mellor, P. S., Rawlings, P., Baylis, M. & Wellby, M. P. 1998. Effect of temperature on African horse sickness virus infection in *Culicoides*. *Arch Virol Suppl,* 14, 155-63.
Mellor, P. S. 2000. Replication of arboviruses in insect vectors. *J Comp Pathol,* 123, 231-47.
Mellor, P. S. & Hamblin, C. 2004. African horse sickness. *Vet Res,* 35, 445-66.
Mercier, B., Gaucher, C., Feugeas, O. & Mazurier, C. 1990. Direct PCR from whole blood, without DNA extraction. *Nucleic Acids Res,* 18, 5908.
Mertens, P. P., Maan, N. S., Prasad, G., Samuel, A. R., Shaw, A. E., Potgieter, A. C., Anthony, S. J. & Maan, S. 2007. Design of primers and use of RT-PCR assays for typing European bluetongue virus isolates: differentiation of field and vaccine strains. *J Gen Virol,* 88, 2811-23.
Mertens, P. P. C. 2004. The dsRNA viruses. *Virus Res,* 101, 3-13.
Mertens, P. P. C., Attoui, H. & Bamford, D. H. 2006. The RNAs and Proteins of dsRNA Viruses [Online]. http://www.reoviridae.org/dsRNA_virus_proteins/. [Accessed: January 2008].
Mertens, P. P. C. 2007. Presentation: The Molecular Epidemiology of BTV. *European Community Reference Laboratory for Bluetongue virus - Institute for Animal Health Pirbright UK*. [Accessed: 24 April 2009].
Meyer, I. 2007. The role of zebra in the spread of AHS (Summary of Literature). July 2007.
Minke, J. M., Siger, L., Karaca, K., Austgen, L., Gordy, P., Bowen, R., Renshaw, R. W., Loosmore, S., Audonnet, J. C. & Nordgren, B. 2004. Recombinant canarypoxvirus vaccine carrying the prM/E genes of West Nile virus protects horses against a West Nile virus-mosquito challenge. *Arch Virol Suppl*, 221-30.
Minke, J. M., Toulemonde, C. E., Coupier, H., Guigal, P. M., Dinic, S., Sindle, T., Jessett, D., Black, L., Bublot, M., Pardo, M. C. & Audonnet, J. C. 2007. Efficacy of a canarypox-vectored recombinant vaccine expressing the hemagglutinin gene of equine influenza H3N8 virus in the protection of ponies from viral challenge. *Am J Vet Res,* 68, 213-9.
Minke, J. M., Audonnet, J. C., Guthrie, A. J., MacLachlan, J. N. & Yao, D. M. 2012. *Vaccine against African horse sickness virus*. United States patent application 13/357,755.
Mirchamsy, H. & Taslimi, H. 1964. Visualization of Horse Sickness Virus by the Fluorescent Antibody Technique. *Immunology,* 7, 213-6.
Mirchamsy, H. & Taslimi, H. 1968. Inactivated African horse sickness virus cell culture vaccine. *Immunology,* 14, 81-8.
Mizukoshi, N., Sakamoto, K., Iwata, A., Ueda, S., Kamada, M. & Fukusho, A. 1994. Detection of African horsesickness virus by reverse transcriptase polymerase chain reaction (RT-PCR) using primers for segment 5 (NS1 gene). *J Vet Med Sci,* 56, 347-52.
Monaco, F., Camma, C., Serini, S. & Savini, G. 2006. Differentiation between field and vaccine strain of bluetongue virus serotype 16. *Vet Microbiol,* 116, 45-52.
Monaco, F., Polci, A., Lelli, R., Pinoni, C., Di Mattia, T., Mbulu, R. S., Scacchia, M. & Savini, G. 2011. A new duplex real-time RT-PCR assay for sensitive and specific detection of African horse sickness virus. *Mol Cell Probes,* 25, 87-93.
Monis, P. T., Giglio, S. & Saint, C. P. 2005. Comparison of SYTO9 and SYBR Green I for real-time polymerase chain reaction and investigation of the effect of dye concentration on amplification and DNA melting curve analysis. *Anal Biochem,* 340, 24-34.
Morick, D., Baneth, G., Avidor, B., Kosoy, M. Y., Mumcuoglu, K. Y., Mintz, D., Eyal, O., Goethe, R., Mietze, A., Shpigel, N. & Harrus, S. 2009. Detection of *Bartonella* spp. in wild rodents in Israel using HRM real-time PCR. *Vet Microbiol,* 139, 293-7.
Moule, L. 1896. *Histoire de la Médecine Vétérinaire,* Paris, Maulde.

Mullens, B. A., Gerry, A. C., Lysyk, T. J. & Schmidtmann, E. T. 2004. Environmental effects on vector competence and virogenesis of bluetongue virus in *Culicoides*: interpreting laboratory data in a field context. *Vet Ital,* 40, 160-6.

Mumford, J. A. 2007. Vaccines and viral antigenic diversity. *Rev Sci Tech,* 26, 69-90.

Nason, E. L., Rothagel, R., Mukherjee, S. K., Kar, A. K., Forzan, M., Prasad, B. V. & Roy, P. 2004. Interactions between the inner and outer capsids of bluetongue virus. *J Virol,* 78, 8059-67.

Nicolas, L., Milon, G. & Prina, E. 2002. Rapid differentiation of Old World Leishmania species by LightCycler polymerase chain reaction and melting curve analysis. *J Microbiol Methods,* 51, 295-9.

Noad, R. & Roy, P. 2003. Virus-like particles as immunogens. *Trends Microbiol,* 11, 438-44.

Nobel, T. A. & Neumann, F. 1961. Vaccination against African horse sickness and postvaccination reactions in Israel. *Refu. Vet,* 18, 168–173.

O'Hara, R. S., Meyer, A. J., Burroughs, J. N., Pullen, L., Martin, L. A. & Mertens, P. P. 1998. Development of a mouse model system, coding assignments and identification of the genome segments controlling virulence of African horse sickness virus serotypes 3 and 8. *Arch Virol Suppl,* 14, 259-79.

OBP. 2012. African horse sickness vaccine for horses, mules and donkeys. *In:* Products, O. B. (ed.).

Odell, I. D., Cloud, J. L., Seipp, M. & Wittwer, C. T. 2005. Rapid species identification within the *Mycobacterium chelonae-abscessus* group by high-resolution melting analysis of hsp65 PCR products. *Am J Clin Pathol,* 123, 96-101.

Oellermann, R. A., Els, H. J. & Erasmus, B. J. 1970. Characterization of African horsesickness virus. *Arch Gesamte Virusforsch,* 29, 163-74.

Ohashi, S., Yoshida, K., Yanase, T., Kato, T. & Tsuda, T. 2004. Simultaneous detection of bovine arboviruses using single-tube multiplex reverse transcription-polymerase chain reaction. *J Virol Methods,* 120, 79-85.

OIE. 2008. African horse sickness. *Manual of Diagnostic Tests and Vaccines for Terrestrial Animals.* Paris: World Organisation for Animal Health.

OIE. 2009. *African horse sickness* [Online]. Paris: World Organisation for Animal Health. http://www.oie.int/eng/maladies/fiches/A_A110.HTM [Accessed 23 June 2010].

Ozawa, Y., Hazrati, A. & Erol, N. 1965. African Horse-Sickness Live-Virus Tissue Culture Vaccine. *Am J Vet Res,* 26, 154-68.

Ozawa, Y. & Bahrami, S. 1966. African horse-sickness killed-virus tissue culture vaccine. *Can J Comp Med Vet Sci,* 30, 311-4.

Ozawa, Y. & Dardiri, A. H. 1970. Transmission of African horse-sickness in mice (Abstract). *Arch Gesamte Virusforsch,* 29, 331-6.

Page, P. C., Labuschagne, K., Nurton, J. P., Venter, G. J. & Guthrie, A. J. 2009. Duration of repellency of N,N-diethyl-3-methylbenzamide, citronella oil and cypermethrin against *Culicoides* species when applied to polyester mesh. *Vet Parasitol,* 163, 105-9.

Page, R. D. 1996. TreeView: an application to display phylogenetic trees on personal computers. *Comput Appl Biosci,* 12, 357-8.

Parker, B. 2008. Presentation: African horse sickness in South Africa: An Update. *Racing South Africa*. [Accessed: 18 May 2012].

Parkes, H. & Gould, A. R. 1996. Characterisation of Wongorr virus, an Australian orbivirus. *Virus Res,* 44, 111-22.

Pavri, K. M. & Anderson, C. R. 1963. Isolation of a vaccine strain of African horse-sickness virus from brains of two horses given polyvalent vaccine. *Indian J Vet Sci,* 33, 215-219.

Paweska, J. T., Prinsloo, S. & Venter, G. J. 2003. Oral susceptibility of South African *Culicoides* species to live-attenuated serotype-specific vaccine strains of African horse sickness virus (AHSV). *Med Vet Entomol,* 17, 436-447.

Peiris, J. S., Guan, Y., Markwell, D., Ghose, P., Webster, R. G. & Shortridge, K. F. 2001. Cocirculation of avian H9N2 and contemporary "human" H3N2 influenza A viruses in pigs in southeastern China: potential for genetic reassortment? *J Virol,* 75, 9679-86.

Perrin, A., Cetre-Sossah, C., Mathieu, B., Baldet, T., Delecolle, J. C. & Albina, E. 2006. Phylogenetic analysis of *Culicoides* species from France based on nuclear ITS1-rDNA sequences. *Med Vet Entomol,* 20, 219-28.

Pietzka, A. T., Stoger, A., Huhulescu, S., Allerberger, F. & Ruppitsch, W. 2011. Gene Scanning of an Internalin B Gene Fragment Using High-Resolution Melting Curve Analysis as a Tool for Rapid Typing of *Listeria monocytogenes*. *J Mol Diagn,* 13, 57-63.

Planzer, J., Kaufmann, C., Worwa, G., Gavier-Widen, D., Hofmann, M. A., Chaignat, V. & Thur, B. 2011. *In vivo* and *in vitro* propagation and transmission of Toggenburg orbivirus. *Res Vet Sci,* 91, e163-8.

Pornprasert, S. & Sukunthamala, K. 2010. SYTO9 and SYBR GREEN1 with a high-resolution melting analysis for prenatal diagnosis of beta(0)-thalassemia/hemoglobin-E. *Eur J Haematol,* 85, 424-9.

Portas, M., Boinas, F. S., Oliveira, E. S. J. & Rawlings, P. 1999. African horse sickness in Portugal: a successful eradication programme. *Epidemiol Infect,* 123, 337-46.

Potgieter, A. C., Cloete, M., Pretorius, P. J. & van Dijk, A. A. 2003. A first full outer capsid protein sequence data-set in the *Orbivirus* genus (family Reoviridae): cloning, sequencing, expression and analysis of a complete set of full-length outer capsid VP2 genes of the nine African horsesickness virus serotypes. *J Gen Virol,* 84, 1317-26.

Potgieter, A. C., Page, N. A., Liebenberg, J., Wright, I. M., Landt, O. & van Dijk, A. A. 2009. Improved strategies for sequence-independent amplification and sequencing of viral double-stranded RNA genomes. *J Gen Virol,* 90, 1423-32.

Potgieter, A. C. & Wright, I. M. 2010. Presentation: Publicly funded research on AHSV and EEV at ARC-OVI from 2006-2009. *Onderstepoort Veterinary Institute*. [Accessed: 26 November 2010].

Pretorius, A., Van Kleef, M., Van Wyngaardt, W. & Heath, J. 2012. Virus-specific CD8(+) T-cells detected in PBMC from horses vaccinated against African horse sickness virus. *Vet Immunol Immunopathol,* 146, 81-6.

Price, E. P., Smith, H., Huygens, F. & Giffard, P. M. 2007. High-resolution DNA melt curve analysis of the clustered, regularly interspaced short-palindromic-repeat locus of *Campylobacter jejuni*. *Appl Environ Microbiol,* 73, 3431-6.

Purvis, L. B., Villegas, P. & Perozo, F. 2006. Evaluation of FTA paper and phenol for storage, extraction and molecular characterization of infectious bursal disease virus. *J Virol Methods,* 138, 66-9.

Qiagen. 2009. Rotor-Gene® ScreenClust HRM® Software User Guide.

Quan, M., van Vuuren, M., Howell, P. G., Groenewald, D. & Guthrie, A. J. 2008. Molecular epidemiology of the African horse sickness virus S10 gene. *J Gen Virol,* 89, 1159-68.

Quan, M., Lourens, C. W., MacLachlan, N. J., Gardner, I. A. & Guthrie, A. J. 2010. Development and optimisation of a duplex real-time reverse transcription quantitative PCR assay targeting the VP7 and NS2 genes of African horse sickness virus. *J Virol Methods,* 167, 45-52.

RacingSA. 2012. *Kenilworth Quarantine Station - News* [Online]. Online: Racing South Africa. http://www.racingsouthafrica.com [Accessed 27 April 2012 2012].

Ramadevi, N., Burroughs, N. J., Mertens, P. P., Jones, I. M. & Roy, P. 1998. Capping and methylation of mRNA by purified recombinant VP4 protein of bluetongue virus. *Proc Natl Acad Sci U S A,* 95, 13537-42.

Ramadevi, N. & Roy, P. 1998. Bluetongue virus core protein VP4 has nucleoside triphosphate phosphohydrolase activity. *J Gen Virol,* 79 (Pt 10), 2475-80.

Ramilo, D. W., Diaz, S., Pereira da Fonseca, I., Delecolle, J. C., Wilson, A., Meireles, J., Lucientes, J., Ribeiro, R. & Boinas, F. 2012. First report of 13 species of *Culicoides*

(Diptera: Ceratopogonidae) in mainland Portugal and Azores by morphological and molecular characterization. *PLoS One,* 7, e34896.

Ranz, A. I., Miguet, J. G., Anaya, C., Venteo, A., Cortes, E., Vela, C. & Sanz, A. 1992. Diagnostic methods for African horsesickness virus using monoclonal antibodies to structural and non-structural proteins. *Vet Microbiol,* 33, 143-53.

Rasmussen, J. P., Saint, C. P. & Monis, P. T. 2007. Use of DNA melting simulation software for *in silico* diagnostic assay design: targeting regions with complex melting curves and confirmation by real-time PCR using intercalating dyes. *BMC Bioinformatics,* 8, 107.

Reed, G. H. & Wittwer, C. T. 2004. Sensitivity and specificity of single-nucleotide polymorphism scanning by high-resolution melting analysis. *Clin Chem,* 50, 1748-54.

Reed, G. H., Kent, J. O. & Wittwer, C. T. 2007. High-resolution DNA melting analysis for simple and efficient molecular diagnostics. *Pharmacogenomics,* 8, 597-608.

Reja, V., Kwok, A., Stone, G., Yang, L., Missel, A., Menzel, C. & Bassam, B. 2010. ScreenClust: Advanced statistical software for supervised and unsupervised high resolution melting (HRM) analysis. *Methods,* 50, S10-4.

Robinson, B. S., Monis, P. T. & Dobson, P. J. 2006. Rapid, sensitive, and discriminating identification of *Naegleria* spp. by real-time PCR and melting-curve analysis. *Appl Environ Microbiol,* 72, 5857-63.

Rodriguez-Sanchez, B., Fernandez-Pinero, J., Sailleau, C., Zientara, S., Belak, S., Arias, M. & Sanchez-Vizcaino, J. M. 2008. Novel gel-based and real-time PCR assays for the improved detection of African horse sickness virus. *J Virol Methods,* 151, 87-94.

Rodríguez López, C. M., Guzmán Asenjo, B., Lloyd, A. J. & Wilkinson, M. J. 2010. Direct detection and quantification of methylation in nucleic acid sequences using high-resolution melting analysis. *Anal Chem,* 82, 9100-9108.

Ronchi, G. F., Ulisse, S., Rossi, E., Franchi, P., Armillotta, G., Capista, S., Peccio, A., Di Ventura, M. & Pini, A. 2012. Immunogenicity of two adjuvant formulations of an inactivated African horse sickness vaccine in guinea-pigs and target animals. *Vet Ital,* 48, 55-76.

Roth, A. L. & Hanson, N. D. 2013. Rapid detection and statistical differentiation of KPC gene variants in Gram-negative pathogens by use of high-resolution melting and ScreenClust analyses. *J Clin Microbiol,* 51, 61-5.

Rothberg, J. M. & Leamon, J. H. 2008. The development and impact of 454 sequencing. *Nat Biotechnol,* 26, 1117-24.

Roux, K. H. 1995. Optimization and troubleshooting in PCR. *PCR Methods Appl,* 4, S185-94.

Roy, P., Hirasawa, T., Fernandez, M., Blinov, V. M. & Sanchez-Vixcain Rodrique, J. M. 1991. The complete sequence of the group-specific antigen, VP7, of African horsesickness disease virus serotype 4 reveals a close relationship to bluetongue virus. *J Gen Virol,* 72 (Pt 6), 1237-41.

Roy, P., Mertens, P. P. & Casal, I. 1994. African horse sickness virus structure. *Comp Immunol Microbiol Infect Dis,* 17, 243-73.

Roy, P., Bishop, D. H., Howard, S., Aitchison, H. & Erasmus, B. 1996. Recombinant baculovirus-synthesized African horsesickness virus (AHSV) outer-capsid protein VP2 provides protection against virulent AHSV challenge. *J Gen Virol,* 77 (Pt 9), 2053-7.

Roy, Y. & Nassuth, A. 2005. Detection of Plant Genes, Gene Expression and Viral DNA from Tissue Prints on FTA® Cards. *Plant Molecular Biology Reporter,* 23, 383-395.

Rozen, S. & Skaletsky, H. 2000. Primer3 on the WWW for general users and for biologist programmers. *Methods Mol Biol,* 132, 365-86.

Rutkowska, D. A., Meyer, Q. C., Maree, F., Vosloo, W., Fick, W. & Huismans, H. 2011. The use of soluble African horse sickness viral protein 7 as an antigen delivery and presentation system. *Virus Res,* 156, 35-48.

Sailleau, C., Moulay, S., Cruciere, C., Laegreid, W. W. & Zientara, S. 1997a. Detection of African horse sickness virus in the blood of experimentally infected horses: comparison of virus isolation and a PCR assay. *Res Vet Sci,* 62, 229-32.

Sailleau, C., Moulay, S. & Zientara, S. 1997b. Nucleotide sequence comparison of the segments S10 of the nine African horsesickness virus serotypes. *Arch Virol,* 142, 965-78.

Sailleau, C., Hamblin, C., Paweska, J. T. & Zientara, S. 2000. Identification and differentiation of the nine African horse sickness virus serotypes by RT-PCR amplification of the serotype-specific genome segment 2. *J Gen Virol,* 81, 831-7.

Saitou, N. & Nei, M. 1987. The neighbor-joining method: a new method for reconstructing phylogenetic trees. *Mol Biol Evol,* 4, 406-25.

Sakamoto, K., Punyahotra, R., Mizukoshi, N., Ueda, S., Imagawa, H., Sugiura, T., Kamada, M. & Fukusho, A. 1994. Rapid detection of African horsesickness virus by the reverse transcriptase polymerase chain reaction (RT-PCR) using the amplimer for segment 3 (VP3 gene). *Arch Virol,* 136, 87-97.

Sakamoto, K., Kawashima, K., Narita, M., Kamada, M. & Fukusho, A. 2000. African Horsesickness Virus Infection in Adult Mice. *J Equine Sci,* 11, 107-112.

Salama, S. A., Dardiri, A. H., Awad, F. I., Soliman, A. M. & Amin, M. M. 1981. Isolation and identification of African horsesickness virus from naturally infected dogs in Upper Egypt. *Can J Comp Med,* 45, 392-6.

Samal, S. K., el-Hussein, A., Holbrook, F. R., Beaty, B. J. & Ramig, R. F. 1987a. Mixed infection of Culicoides variipennis with bluetongue virus serotypes 10 and 17: evidence for high frequency reassortment in the vector. *J Gen Virol,* 68 (Pt 9), 2319-29.

Samal, S. K., Livingston, C. W., Jr., McConnell, S. & Ramig, R. F. 1987b. Analysis of mixed infection of sheep with bluetongue virus serotypes 10 and 17: evidence for genetic reassortment in the vertebrate host. *J Virol,* 61, 1086-91.

Savini, G., Ronchi, G. F., Leone, A., Ciarelli, A., Migliaccio, P., Franchi, P., Mercante, M. T. & Pini, A. 2007. An inactivated vaccine for the control of bluetongue virus serotype 16 infection in sheep in Italy. *Vet Microbiol,* 124, 140-6.

Scanlen, M., Paweska, J. T., Verschoor, J. A. & van Dijk, A. A. 2002. The protective efficacy of a recombinant VP2-based African horsesickness subunit vaccine candidate is determined by adjuvant. *Vaccine,* 20, 1079-88.

Scheffer, E. G., Venter, G. J., Joone, C., Osterrieder, N. & Guthrie, A. J. 2011. Use of real-time quantitative reverse transcription polymerase chain reaction for the detection of African horse sickness virus replication in *Culicoides imicola*. *Onderstepoort J Vet Res,* 78, 1-4.

Scheffer, E. G., Venter, G. J., Labuschagne, K., Page, P. C., Mullens, B. A., MacLachlan, N. J., Osterrieder, N. & Guthrie, A. J. 2012. Comparison of two trapping methods for *Culicoides* biting midges and determination of African horse sickness virus prevalence in midge populations at Onderstepoort, South Africa. *Vet Parasitol,* 185, 265-73.

Sellers, R. F. & Mellor, P. S. 1993. Temperature and the persistence of viruses in *Culicoides* spp. during adverse conditions. *Rev Sci Tech,* 12, 733-55.

Simalenga, T. & Joubert, A. 1997. Developing agriculture with animal traction. Pretoria: University of Fort Hare.

Simpkin, T. L. 2008. *Prophylactic strategies in the control of African horse sickness.* Master of Science in Agriculture Dissertation, University of KwaZulu-Natal, Pietermaritzburg.

Spence, R. P., Moore, N. F. & Nuttall, P. A. 1984. The biochemistry of orbiviruses. Brief review. *Arch Virol,* 82, 1-18.

Stanzer, S., Balic, M., Strutz, J., Heitzer, E., Obermair, F., Hauser-Kronberger, C., Samonigg, H. & Dandachi, N. 2010. Rapid and reliable detection of LINE-1 hypomethylation using high-resolution melting analysis. *Clin Biochem,* 43, 1443-8.

Stauber, N., Martinez-Costas, J., Sutton, G., Monastyrskaya, K. & Roy, P. 1997. Bluetongue virus VP6 protein binds ATP and exhibits an RNA-dependent ATPase

function and a helicase activity that catalyze the unwinding of double-stranded RNA substrates. *J Virol,* 71, 7220-6.

Steer, P. A., Kirkpatrick, N. C., O'Rourke, D. & Noormohammadi, A. H. 2009. Classification of fowl adenovirus serotypes by use of high-resolution melting-curve analysis of the hexon gene region. *J Clin Microbiol,* 47, 311-21.

Steer, P. A., O'Rourke, D., Ghorashi, S. A. & Noormohammadi, A. H. 2011. Application of high-resolution melting curve analysis for typing of fowl adenoviruses in field cases of inclusion body hepatitis. *Aust Vet J,* 89, 184-92.

Stoltz, M. A., van der Merwe, C. F., Coetzee, J. & Huismans, H. 1996. Subcellular localization of the nonstructural protein NS3 of African horsesickness virus. *Onderstepoort J Vet Res,* 63, 57-61.

Stone-Marschat, M., Carville, A., Skowronek, A. & Laegreid, W. W. 1994. Detection of African horse sickness virus by reverse transcription-PCR. *J Clin Microbiol,* 32, 697-700.

Stott, J. L., Oberst, R. D., Channell, M. B. & Osburn, B. I. 1987. Genome segment reassortment between two serotypes of bluetongue virus in a natural host. *J Virol,* 61, 2670-4.

Tajiri-Utagawa, E., Hara, M., Takahashi, K., Watanabe, M. & Wakita, T. 2009. Development of a rapid high-throughput method for high-resolution melting analysis for routine detection and genotyping of noroviruses. *J Clin Microbiol,* 47, 435-40.

Tamura, K., Nei, M. & Kumar, S. 2004. Prospects for inferring very large phylogenies by using the neighbor-joining method. *Proc Natl Acad Sci U S A,* 101, 11030-5.

Tamura, K., Peterson, D., Peterson, N., Stecher, G., Nei, M. & Kumar, S. 2011. MEGA5: molecular evolutionary genetics analysis using maximum likelihood, evolutionary distance, and maximum parsimony methods. *Mol Biol Evol,* 28, 2731-9.

Tanaka, M., Takahahi, J., Hirayama, F. & Tani, Y. 2011. High-resolution melting analysis for genotyping Duffy, Kidd and Diego blood group antigens. *Leg Med (Tokyo),* 13, 1-6.

Tanriverdi, S., Tanyeli, A., Baslamisli, F., Koksal, F., Kilinc, Y., Feng, X., Batzer, G., Tzipori, S. & Widmer, G. 2002. Detection and genotyping of oocysts of *Cryptosporidium parvum* by real-time PCR and melting curve analysis. *J Clin Microbiol,* 40, 3237-44.

Teshome, M., Addis, M. & Temesgen, W. 2012. Seroprevalence and risk factors of African horse sickness in mules and donkeys in selected sites of West Amhara Region, Ethiopia. *Afr J Microbiol Res,* 6, 4146-4151.

Theiler, A. 1921. African Horse Sickness (*Pestis Equorum*). *Science Bulletin,* 19.

Thompson, G. M., Jess, S. & Murchie, A. K. 2012. A review of African horse sickness and its implications for Ireland. *Ir Vet J,* 65, 9.

Tibshirani, R., Walther, G. & Hastie, T. 2001. Estimating the number of clusters in a data set via the gap statistic. *J R Stat Soc Series B Stat Methodol,* 63, 411-423.

Toi, C. S. & Dwyer, D. E. 2008. Differentiation between vaccine and wild-type varicella-zoster virus genotypes by high-resolution melt analysis of single nucleotide polymorphisms. *J Clin Virol,* 43, 18-24.

Tong, S. Y., Dakh, F., Hurt, A. C., Deng, Y. M., Freeman, K., Fagan, P. K., Barr, I. G. & Giffard, P. M. 2011. Rapid detection of the H275Y oseltamivir resistance mutation in influenza A/H1N1 2009 by single base pair RT-PCR and high-resolution melting. *PLoS One,* 6, e21446.

Touil, N., Cherkaoui, Z., Lmrabih, Z., Loutfi, C., Harif, B. & El Harrak, M. 2012. Emerging viral diseases in dromedary camels in the Southern Morocco. *Transbound Emerg Dis,* 59, 177-82.

Towler, W. I., James, M. M., Ray, S. C., Wang, L., Donnell, D., Mwatha, A., Guay, L., Nakabiito, C., Musoke, P., Jackson, J. B. & Eshleman, S. H. 2010. Analysis of HIV diversity using a high-resolution melting assay. *AIDS Res Hum Retroviruses,* 26, 913-8.

Turnbull, P. J., Cormack, S. B. & Huismans, H. 1996. Characterization of the gene encoding core protein VP6 of two African horsesickness virus serotypes. *J Gen Virol,* 77 (Pt 7), 1421-3.

van Dam, P. 2012. Approaches to AHS treatment: special report. *SA Horsemen,* 7, 18-19.

van der Meyden, C. H., Erasmus, B. J., Swanepoel, R. & Prozesky, O. W. 1992. Encephalitis and chorioretinitis associated with neurotropic African horsesickness virus infection in laboratory workers. Part I. Clinical and neurological observations. *S Afr Med J,* 81, 451-4.

van Niekerk, M. 2001. *Association of nonstructural protein NS3 of African Horsesickness virus with cytotoxicity and virus virulence.* Philosophiae Doctor Dissertation, University of Pretoria, Pretoria.

van Niekerk, M., Smit, C. C., Fick, W. C., van Staden, V. & Huismans, H. 2001a. Membrane association of African horsesickness virus nonstructural protein NS3 determines its cytotoxicity. *Virology,* 279, 499-508.

van Niekerk, M., van Staden, V., van Dijk, A. A. & Huismans, H. 2001b. Variation of African horsesickness virus nonstructural protein NS3 in southern Africa. *J Gen Virol,* 82, 149-58.

van Niekerk, M., Freeman, M., Paweska, J. T., Howell, P. G., Guthrie, A. J., Potgieter, A. C., van Staden, V. & Huismans, H. 2003. Variation in the NS3 gene and protein in South African isolates of bluetongue and equine encephalosis viruses. *J Gen Virol,* 84, 581-90.

Van Rensberg, I. B., De Clerk, J., Groenewald, H. B. & Botha, W. S. 1981. An outbreak of African horsesickness in dogs. *J S Afr Vet Assoc,* 52, 323-5.

van Sittert, S. J., Drew, T. M., Kotze, J. L., Strydom, T., Weyer, C. T. & Guthrie, A. J. 2013. Occurrence of African horse sickness in a domestic dog without apparent ingestion of horse meat. *J S Afr Vet Assoc,* 84, 5 pages.

Varillas, D., Bermejo-Martin, J. F., Almansa, R., Rojo, S., Nogueira, B., Eiros, J. M., Rico, L., Iglesias, V. & de Lejarazu, R. O. 2011. A new method for detection of pandemic influenza virus using High Resolution Melting analysis of the neuraminidase gene. *J Virol Methods,* 171, 284-6.

Vaughn, C. P. & Elenitoba-Johnson, K. S. 2004. High-resolution melting analysis for detection of internal tandem duplications. *J Mol Diagn,* 6, 211-6.

Vellema, P. 2008. Bluetongue in sheep: Question marks on bluetongue virus serotype 8 in Europe. *Small Rumin Res,* 76, 141-148.

Venter, G. J., Nevill, E. M. & Van der Linde, T. C. 1996. Geographical distribution and relative abundance of stock-associated *Culicoides* species (Diptera: Ceratopogonidae) in southern Africa in relation to their potential as viral vectors. *Onderstepoort J Vet Res,* 63, 25-38.

Venter, G. J., Groenewald, D. M., Paweska, J. T., Venter, E. H. & Howell, P. G. 1999. Vector competence of selected South African *Culicoides* species for the Bryanston serotype of equine encephalosis virus. *Med Vet Entomol,* 13, 393-400.

Venter, G. J., Graham, S. D. & Hamblin, C. 2000. African horse sickness epidemiology: vector competence of South African *Culicoides* species for virus serotypes 3, 5 and 8. *Med Vet Entomol,* 14, 245-50.

Venter, G. J., Groenewald, D., Venter, E., Hermanides, K. G. & Howell, P. G. 2002. A comparison of the vector competence of the biting midges, *Culicoides* (*Avaritia*) *bolitinos* and *C. (A.) imicola*, for the Bryanston serotype of equine encephalosis virus. *Med Vet Entomol,* 16, 372-7.

Venter, G. J., Wright, I. M. & Paweska, J. T. 2010. A comparison of the susceptibility of the biting midge *Culicoides imicola* to infection with recent and historical isolates of African horse sickness virus. *Med Vet Entomol,* 24, 324-8.

Verwoerd, D. W., Huismans, H. & Erasmus, B. J. 1979. Orbiviruses. *In:* H., F.-C. & Wagner, R. R. (eds.) *Comprehensive Virology.* London: Plenum Press.

von Teichman, B. F. & Smit, T. K. 2008. Evaluation of the pathogenicity of African Horsesickness (AHS) isolates in vaccinated animals. *Vaccine,* 26, 5014-5021.

von Teichman, B. F., Dungu, B. & Smit, T. K. 2010. *In vivo* cross-protection to African horse sickness Serotypes 5 and 9 after vaccination with Serotypes 8 and 6. *Vaccine,* 28, 6505-17.

Vossen, R. H., Aten, E., Roos, A. & den Dunnen, J. T. 2009. High-resolution melting analysis (HRMA): more than just sequence variant screening. *Hum Mutat,* 30, 860-6.

Wade-Evans, A. M., Mertens, P. P. & Bostock, C. J. 1990. Development of the polymerase chain reaction for the detection of bluetongue virus in tissue samples. *J Virol Methods,* 30, 15-24.

Wade-Evans, A. M., Woolhouse, T., O'Hara, R. & Hamblin, C. 1993. The use of African horse sickness virus VP7 antigen, synthesised in bacteria, and anti-VP7 monoclonal antibodies in a competitive ELISA. *J Virol Methods,* 45, 179-88.

Webster, R. G., Bean, W. J., Gorman, O. T., Chambers, T. M. & Kawaoka, Y. 1992. Evolution and ecology of influenza A viruses. *Microbiol Rev,* 56, 152-79.

Wellby, M. P., Baylis, M., Rawlings, P. & Mellor, P. S. 1996. Effect of temperature on survival and rate of virogenesis of African horse sickness virus in *Culicoides variipennis sonorensis* (Diptera: Ceratopogonidae) and its significance in relation to the epidemiology of the disease. *Bulletin of entomological research,* 86, 715-720.

Wetzel, H., Nevill, E. M. & Erasmus, B. J. 1970. Studies on the transmission of African horsesickness. *Onderstepoort J Vet Res,* 37, 165-8.

Weyer, C. T., Quan, M., Joone, C., Lourens, C. W., MacLachlan, N. J. & Guthrie, A. J. 2013. African horse sickness in naturally infected, immunised horses. *Equine Vet J,* 45, 117-9.

White, H. & Potts, G. 2006. Mutation scanning by high resolution melt analysis. Evaluation of RotorGene™ 6000 (Corbett Life Science), HR1™ and 384 well LightScanner™ (Idaho Technology). Wessex: National Genetics Reference Laboratory.

Wicker, T., Schlagenhauf, E., Graner, A., Close, T. J., Keller, B. & Stein, N. 2006. 454 sequencing put to the test using the complex genome of barley. *BMC Genomics,* 7, 275.

Williams, C. F., Inoue, T., Lucus, A. M., Zanotto, P. M. & Roy, P. 1998. The complete sequence of four major structural proteins of African horse sickness virus serotype 6: evolutionary relationships within and between the orbiviruses. *Virus Res,* 53, 53-73.

Willmore, C., Holden, J. A., Zhou, L., Tripp, S., Wittwer, C. T. & Layfield, L. J. 2004. Detection of c-kit-activating mutations in gastrointestinal stromal tumors by high-resolution amplicon melting analysis. *Am J Clin Pathol,* 122, 206-16.

Wilson, A., Mellor, P. S., Szmaragd, C. & Mertens, P. P. 2009. Adaptive strategies of African horse sickness virus to facilitate vector transmission. *Vet Res,* 40, 16.

Wilson, W. C. & Chase, C. C. 1993. Nested and multiplex polymerase chain reactions for the identification of bluetongue virus infection in the biting midge, *Culicoides variipennis*. *J Virol Methods,* 45, 39-47.

Wittmann, E. J. & Baylis, M. 2000. Climate change: effects on *Culicoides* - transmitted viruses and implications for the UK. *Vet J,* 160, 107-17.

Wittmann, E. J., Mellor, P. S. & Baylis, M. 2001. Using climate data to map the potential distribution of *Culicoides imicola* (Diptera: Ceratopogonidae) in Europe. *Rev Sci Tech,* 20, 731-40.

Wittwer, C. T., Reed, G. H., Gundry, C. N., Vandersteen, J. G. & Pryor, R. J. 2003. High-resolution genotyping by amplicon melting analysis using LCGreen. *Clin Chem,* 49, 853-60.

Wood, H. A. 1973. Viruses with double-stranded RNA genomes. *J Gen Virol,* 20, Suppl:61-85.

Worobey, M. & Holmes, E. C. 1999. Evolutionary aspects of recombination in RNA viruses. *J Gen Virol,* 80 (Pt 10), 2535-43.

Zhou, L., Myers, A. N., Vandersteen, J. G., Wang, L. & Wittwer, C. T. 2004. Closed-tube genotyping with unlabeled oligonucleotide probes and a saturating DNA dye. *Clin Chem,* 50, 1328-35.

Zhou, N. N., Senne, D. A., Landgraf, J. S., Swenson, S. L., Erickson, G., Rossow, K., Liu, L., Yoon, K., Krauss, S. & Webster, R. G. 1999. Genetic reassortment of avian, swine, and human influenza A viruses in American pigs. *J Virol,* 73, 8851-6.

Zientara, S., Sailleau, C., Moulay, S., Plateau, E. & Cruciere, C. 1993. Diagnosis and molecular epidemiology of the African horse sickness virus by the polymerase chain reaction and restriction patterns. *Vet Res,* 24, 385-95.

Zientara, S., Sailleau, C., Moulay, S. & Cruciere, C. 1994. Diagnosis of the African horse sickness virus serotype 4 by a one-tube, one manipulation RT-PCR reaction from infected organs. *J Virol Methods,* 46, 179-88.

Zientara, S., Sailleau, C., Moulay, S. & Cruciere, C. 1995a. Differentiation of African horse sickness viruses by polymerase chain reaction and segments 10 restriction patterns. *Vet Microbiol,* 47, 365-75.

Zientara, S., Sailleau, C., Moulay, S., Wade-Evans, A. & Cruciere, C. 1995b. Application of the polymerase chain reaction to the detection of African horse sickness viruses. *J Virol Methods,* 53, 47-54.

Zientara, S., Sailleau, C., Moulay, S., Cruciere, C., el-Harrak, M., Laegreid, W. W. & Hamblin, C. 1998a. Use of reverse transcriptase-polymerase chain reaction (RT-PCR) and dot-blot hybridisation for the detection and identification of African horse sickness virus nucleic acids. *Arch Virol Suppl,* 14, 317-27.

Zientara, S., Sailleau, C., Plateau, E., Moulay, S., Mertens, P. P. & Cruciere, C. 1998b. Molecular epidemiology of African horse sickness virus based on analyses and comparisons of genome segments 7 and 10. *Arch Virol Suppl,* 14, 221-34.

Zientara, S., Bréard, E. & Sailleau, C. 2004. Bluetongue diagnosis by reverse transcriptase-polymerase chain reaction. *Vet Ital,* 40, 531-7.

Appendices

Appendix A

REPUBLIC OF SOUTH AFRICA

REPUBLIEK VAN SUID AFRIKA

PATENTS ACT, 1978

CERTIFICATE

In accordance with section 44 (1) of the Patents Act, No. 57 of 1978, it is hereby certified that:

UNIVERSITY OF KWAZULU-NATAL

Has been granted a patent in respect of an invention described and claimed in complete specification deposited at the Patent Office under the number

2010/04579

A copy of the complete specification is annexed, together with the relevant Form P2.

testimony thereof, the seal of the Patent Office has been affixed at Pretoria with effect from the 30 day of March 2011

Registrar of Patents

Appendix B

AHSV segment 10 and 2 full length sequence accession numbers

Segment 10:

AJ007303	D12480	U02711
AJ007304	DQ868782	U02712
AJ007305	DQ868783	U02713
AJ007306	DQ868784	U26171
AJ007307	DQ868785	U59279
AJ007308	DQ868786	U60189
AJ007309	EU046579	U60190
AM883173	FJ011116	Z48734
D12479	FJ183373	

Segment 2:

AF021235	AY163333	EU046574
AF043926	D26570	FJ011108
AM883165	DQ868772	FJ783365
AY163329	DQ868773	NC_005996
AY163330	DQ868774	U01832
AY163331	DQ868775	Z26316
AY163332	DQ868776	

Appendix C1

AHSV segment 10 full length alignment of Clades A and B (Clade AB – serotypes 1, 2, 3, 7 and 8)

```
CLUSTAL 2.0.12 multiple sequence alignment (AHSV Seg10 260510 FL ST 1,2,3,7,8.aln)


AHSV8_U02713          GTTTAAATTATCCCTTGTCATGAATCTTGCTAGCATCTCCCAAAGCTATATGTCACATAA 60
AHSV8_AJ007307        GTTTAAATTATCCCTTGTCATGAATCTTGCTAGCATCTCCCAAAGCTATATGTCACATAA 60
AHSV1_FJ011116        -GTTTAATTATCCCT-GTCATGAATCTTGCTAGCATCTCCCAAAGCTATATGTCACATAA 58
AHSV1_AM883173        -GTTTAATTATCCCTTGTCATGAATCTTGCTAGCATCTCCCAAAGCTATATGTCACATAA 59
AHSV1_FJ183373        -GTTAAATTATCCCTTGTCATGAATCTTGCTAGCATCTCCCAAAGCTATATGTCACATAA 59
AHSV1_U02711          GTTTAAATTATCCCTTGTCATGAATCTTGCTAGCATCTCCCAAAGCTATATGTCACATAA 60
AHSV2_U59279          GTTTAAATTATCCCTTGTCATGAATCTTGCTAGCATCTCCCAAAGCTATATGTCACATAA 60
AHSV3_DQ868782        GTTTAAATTATCCCTTGTCATGAGTCTAGCTACGATCGCCGAAAATTATATGATGCATAA 60
AHSV8_DQ868785        GTTTAAATTATCCCTTGTCATGAGTCTAGCTACGATCGCCGAAAATTATATGATGCATAA 60
AHSV3a_AJ007304       GTTTAAATTATCCCTTGTCATGAGTCTAGCTACGATCGCCGAAAATTATATGATGCATAA 60
AHSV3_AJ007303        GTTTAAATTATCCCTTGTCATGAGTCTAGCTACGATCGCCGAAAATTATATGATGCATAA 60
AHSV3_D12479          GTTTAAATTATCCCTTGTCATGAGTCTAGCTACGATCGCCGAAAATTATATGATGCATAA 60
AHSV7_AJ007306        GTTTAAATTATCCCTTGTCATGAGTCTAGCTACGATCGCCGAAAATTATATGATGCATAA 60
AHSV7_U60190          GTTTAAATTATCCCTTGTCATGAGTCTAGCTACGATCGCCGAAAATTATATGATGCATAA 60
                        ** ********** ******* *** ****  *** ** ***  ******   *****

AHSV8_U02713          TGAGAATGAAAGATCAATTGTACCATACATTCCGCCACCGTAT---CATCCGACGGCTCC 117
AHSV8_AJ007307        TGAGAATGAAAGATCAATTGTACCATACATTCCGCCACCGTAT---CATCCGACGGCTCC 117
AHSV1_FJ011116        TGAGAATGAAAGATCAATTGTACCATACATTCCGCCACCGTAT---CATCCGACGGCTCC 115
AHSV1_AM883173        TGAGAATGAAAGATCAATTGTACCATACATTCCGCCACCGTAT---CATCCGACGGCTCC 116
AHSV1_FJ183373        TGAGAATGAAAGATCAATTGTACCATACATTCCGCCACCGTAT---CATCCGACGGCTCC 116
AHSV1_U02711          TGAGAATGAAAGATCAATTGTACCATACATTCCGCCACCGTAT---CATCCGACGGCTCC 117
AHSV2_U59279          TGAGAATGAAAGATCAATTGTACCATACATTCCGCCACCGTAT---CATCCGACGGCTCC 117
AHSV3_DQ868782        TGGAAATCAGAGGGCAATTGTACCGTATGTTCCGCCCCCTTATACGTATGCAAATGCTCC 120
AHSV8_DQ868785        TGGAAATCAGAGGGCAATCGTACCGTATGTTCCGCCCCCTTATACGTATGCAAATGCTCC 120
AHSV3a_AJ007304       TGGAAATCAGAGAGCAATTGTACCGTATGTTCCACCCCCTTATGCGTATGCAAATGCTCC 120
AHSV3_AJ007303        TGGAAATCAGAGAGCAATTGTACCGTATGTTCCACCCCCTTATGCGTATGCAAATGCTCC 120
AHSV3_D12479          TGGAAATCAGAGAGCAATTGTACCGTATGTTCCACCCCCTTATGCGTATGCAAATGCTCC 120
AHSV7_AJ007306        TGGAAATCAGAGAGCAATTGTGCCGTATGTTCCACCCCCTTATGCGTATGCAAATGCTCC 120
AHSV7_U60190          TGAAACTCAGAGAGCAATTGTACCGTATGTTCCACCCCCTTATGCGTATGCAAATGCTCC 120
                      **  * * * **  **** ** ** **  **** ** ** ***    ** * *  *****

AHSV8_U02713          GGCGCTTGCTGTATCCGCCAGTCAAATGGAGACCATGTCGCTTGGGATACTTAACCAAGC 177
AHSV8_AJ007307        GGCGCTTGCTGTATCCGCCAGTCAAATGGAGACCATGTCGCTTGGGATACTTAACCAAGC 177
AHSV1_FJ011116        GGCGCTTGCTGTATCCGCCAGTCAAATGGAGACCATGTCGCTTGGGATACTTAACCAAGC 175
AHSV1_AM883173        GGCGCTTGCTGTATCCGCCAGTCAAATGGAGACCATGTCGCTTGGGATACTTAACCAAGC 176
AHSV1_FJ183373        GGCGCTTGCTGTATCCGCCAGTCAAATGGAGACCATGTCGCTTGGGATACTTAATCAAGC 176
AHSV1_U02711          GGCGCTTGCTGTATCCGCCAGTCAAATGGAGACCATGTCGCTTGGGATACTTAACCAAGC 177
AHSV2_U59279          GGCGCTTGCTGTATCCGCCAGTCAAATGGAGACCATGTCGCTTGGGATACTTAACCAAGC 177
AHSV3_DQ868782        GACGCCTGGTGGTCAAGCGGGTGAAATGGAGTCCATGTCGCTTGGGATACTTAACCAAGC 180
AHSV8_DQ868785        GACGCTTGGTGGTCAAGCGGGTGAAATGGAGTCCATGTCGCTTGGGATACTTAACCAAGC 180
AHSV3a_AJ007304       GACGCTTGGTGGTCAGGCGGGTGAAATGGAGTCCATGTCGCTTGGGATACTTAATCAAGC 180
AHSV3_AJ007303        GACGCTTGGTGGTCAGGCGGGTGAAATGGAGTCCATGTCGCTTGGGATACTTAATCAAGC 180
AHSV3_D12479          GACGCTTGGTGGTCAGGCGGGTGAAATGGAGTCCATGTCGCTTGGGATACTTAATCAAGC 180
AHSV7_AJ007306        GACGCTTGGTGGTCAGGCGGGTGAAATGGAGTCCATGTCGCTTGGGATACTTAATCAAGC 180
AHSV7_U60190          GACGCTTGGTGGTCAGGCGGGTGAAATGGAGTCCATGTCGCTTGGGATACTTAATCAAGC 180
                      * *** ** **     **  ** ******** ********************** *****

AHSV8_U02713          AATGTCAAGTTCAGCTGGTGCGAGTGGCGCACTTAAGGATGAAAAGGCAGCGTTTGGAGC 237
AHSV8_AJ007307        AATGTCAAGTTCAGCTGGTGCGAGTGGCGCACTTAAGGATGAAAAGGCAGCGTTTGGAGC 237
AHSV1_FJ011116        AATGTCAAGTTCAGCTGGTGCGAGCGGAGCACTTAAGGATGAAAAGGCAGCGTTTGGAGC 235
AHSV1_AM883173        AATGTCAAGTTCAGCTGGTGCGAGCGGAGCACTTAAGGATGAAAAGGCAGCGTTTGGAGC 236
AHSV1_FJ183373        AATGTCAAGTTCAGCTGGTGCGAGCGGAGCACTTAAGGATGAAAAGGCAGCGTTTGGAGC 236
AHSV1_U02711          AATGTCAAGTTCAGCTGGTGCGAGCGGAGCACTTAAGGATGAAAAGGCAGCGTATGGAGC 237
AHSV2_U59279          AATGTCAAGTTCAGCTGGTGCGAGTGGCGCACTTAAGGACGAAAAGGCAGCGTTTGGAGC 237
AHSV3_DQ868782        CATGTCAAGTACAACTGGTGCGAGTGGGGCCCTTAAGGATGAAAAAGCAGCATTTGGTGC 240
AHSV8_DQ868785        CATGTCAAGTACAACTGGTGCGAGTGGGGCCCTTAAGGATGAAAAAGCAGCATTTGGTGC 240
AHSV3a_AJ007304       CATGTCAAGTACAACTGGTGCAAGTCGGGCTCTTAAGGATGAAAAAGCAGCGTTTGGTGC 240
AHSV3_AJ007303        CATGTCAAGTACAACTGGTGCAAGTCGGGCTCTTAAGGATGAAAAAGCAGCGTTTGGTGC 240
AHSV3_D12479          CATGTCAAGTACAACTGGTGCAAGTCGGGCTCTTAAGGATGAAAAAGCAGCGTTTGGTGC 240
AHSV7_AJ007306        CATGTCAAGTACAACTGGTGCAAGTGGGGCTCTTAAGGATGAAAAAGCAGCGTTTGGTGC 240
AHSV7_U60190          CATGTCAAGTACAACTGGTGCAAGTGGGGCTCTTAAGGATGAAAAAGCAGCGTTTGGTGC 240
                       ********* ** ******* **  * ** ******** ***** ***** * *** **
```

```
AHSV8_U02713         GGTGGCGGAGGCGTTGAGAGATCCGGAGCCGATCAGAAAAATTAAGCGACAAGTAGGTAT 297
AHSV8_AJ007307       GGTGGCGGAGGCGTTGAGAGATCCGGAGCCGATCAGAAAAATTAAGCGACAAGTAGGTAT 297
AHSV1_FJ011116       GGTGGCAGAGGCGTTGAGAGATCCGGAGCCGATCAGAAAAATTAAGCGACAAGTAGGTAT 295
AHSV1_AM883173       GGTGGCAGAGGCGTTGAGAGATCCGGAGCCGATCAGAAAAATTAAGCGACAAGTAGGTAT 296
AHSV1_FJ183373       GGTGGCAGAGGCGTTGAGAGATCCGGAGCCGATCAGAAAAATTAAGCGACAAGTAGGTAT 296
AHSV1_U02711         GGTGGCAGAGGCGTTGAGAGATCCGGAGCCGATCAGAAAAATTAAGCGACAAGTAGGTAT 297
AHSV2_U59279         GATGGCAGAGGCGTTGAGAGATCCGGAGCCGATCAGAAAAATTAAGCGACAAGTAGGTAT 297
AHSV3_DQ868782       GATGGCGGAAGCATTACGTGATCCAGAACCAATACGTCAAATTAAGAAAACCGTTGGATT 300
AHSV8_DQ868785       GATGGCGGAGGCATTACGTGATCCAGAACCAATACGTCAAATTAAGAAAACCGTTGGATT 300
AHSV3a_AJ007304      GATGGCGGAAGCATTACGTGATCCAGAACCGATACGTCAAATAAAGAAACATGTTGGATT 300
AHSV3_AJ007303       GATGGCGGAAGCATTACGTGATCCAGAACCGATACGTCAAATAAAGAAACATGTTGGATT 300
AHSV3_D12479         GATGGCGGAAGCATTACGTGATCCAGAACCGATACGTCAAATAAAGAAACATGTTGGATT 300
AHSV7_AJ007306       GATGGCGGAAGCATTACGTGATCCAGAACCGATACGTCAAATTAAGAAACATGTTGGATT 300
AHSV7_U60190         GATGGCGGAAGCACTACGTGATCCAGAACCGATTCGTCAAATTAAGAAACATGTTGGATT 300
                     * **** ** **  *  * ***** ** ** **  *  **** ***  *   ** **  *

AHSV8_U02713         CCAAACTCTAAAAACACTGAAAGTTGAATTGAGCGGGATGCGAAGGAAGAAATTGATTTT 357
AHSV8_AJ007307       CCAAACTCTAAAAACACTGAAAGTTGAATTGAGCGGGATGCGAAGGAAGAAATTGATTTT 357
AHSV1_FJ011116       CCAAACTCTAAAAACACTGAAAGTTGAATTGAGCGGGATGCGAAGGAAGAAATTGATTTT 355
AHSV1_AM883173       CCAAACTCTAAAAACACTGAAAGTTGAATTGAGCGGGATGCGAAGGAAGAAATTGATTTT 356
AHSV1_FJ183373       CCAAACTCTAAAAACACTGAAAGTTGAATTGAGCGGGATGCGAAGGAAGAAATTGATTTT 356
AHSV1_U02711         CCAAACTCTAAAAACACTGAAAGTTGAATTGAGCGGGATGCGAAGGAAGAAATTGATTTT 357
AHSV2_U59279         CCAAACTCTAAAAGCATTGAAAGTTGAATTGAGCGGGATGCGAAGGAAGAGATTGATTTT 357
AHSV3_DQ868782       AAGGACGCTTAAGCATTTAAAGATAGAGTTGGCGTCGATGAGACGTAGGTATGCGATATT 360
AHSV8_DQ868785       AAGGACACTTAAGCATTTAAAGATAGAGTTGGCGTCGATGAGACGTAGGTATGCGATATT 360
AHSV3a_AJ007304      AAGAACGCTCAAGCATTTAAAGATAGAGTTGGCGTCAATGAGACGTAGGTATGCGATACT 360
AHSV3_AJ007303       AAGAACGCTCAAGCATTTAAAGATAGAGTTGGCGTCAATGAGACGTAGGTATGCGATACT 360
AHSV3_D12479         AAGAACGCTCAAGCATTTAAAGATAGAGTTGGCGTCAATGAGACGTAGGTATGCGATACT 360
AHSV7_AJ007306       AAGAACGCTCAAGCATTTAAAGATAGAGTTGGCGTCAATGAGACGTAGGTATGCGATACT 360
AHSV7_U60190         AAGAACGCTCAAGCATTTAAAGATAGAGTTGGCGTCAATGAGACGTAGGTATGCGATACT 360
                         ** ** **     * **  * ** ***      *** ** * * *     ***  *

AHSV8_U02713         GAAAATAATTATGTTTATTTGCGCAAACGTAACTATGGCTACTTCTCTAGTTGGAGGTAT 417
AHSV8_AJ007307       GAAAATAATTATGTTTATTTGCGCAAACGTAACTATGGCTACTTCTCTAGTTGGAGGTAT 417
AHSV1_FJ011116       GAAAATAATTATGTTTATTTGCGCAAACGTAACTATGGCTACTTCTCTAGTTGGAGGTAT 415
AHSV1_AM883173       GAAAATAATTATGTTTATTTGCGCAAACGTAACTATGGCTACTTCTCTAGTTGGAGGTAT 416
AHSV1_FJ183373       GAAAATAATTATGTTTATTTGCGCAAACGTAACTATGGCTACTTCTCTAGTTGGAGGTAT 416
AHSV1_U02711         GAAAATAATTATGTTTATTTGCGCAAACGTAACTATGGCTACTTCTCTAGTTGGAGGTAT 417
AHSV2_U59279         GAAAATAATTATGTTTATTTGCGCAAACGTAACTATGGCTACTTCTCTAGTTGGAGGTAT 417
AHSV3_DQ868782       ACGAGTAGTCATTTTTATGAGTGGGTGCGTGACAATGGCTACCTCGATGGTGGGCGGGTT 420
AHSV8_DQ868785       ACGAGTAGTCACTTTTATGAGTGGGTGCGTGACAATGGCTACCTCGATGGTGGGCGGGTT 420
AHSV3a_AJ007304      ACGTGTAGTGATCTTAATGAGCGGGTGCGTAACGATGGCTACCTCGATGGCGGGCGGGTT 420
AHSV3_AJ007303       ACGTGTAGTGATCTTAATGAGCGGGTGCGTAACGATGGCTACCTCGATGGCGGGCGGGTT 420
AHSV3_D12479         ACGTGTAGTGATCTTTATGAGCGGGTGCGTAACGATGGCTACCTCGATGGCGGGCGGGTT 420
AHSV7_AJ007306       ACGTGTAGTGATCTTTATGAGCGGGTGCGTAACGATGGCTACCTCGATGGCGGGCGGGTT 420
AHSV7_U60190         ACGTGTAGTGATCTTAATGAGCGGGTGCGTAACGATGGCTACCTCGATGGCGGGCGGGTT 420
                          ** * *  ** **  * *    *** ** ******** **  * *  ** **  *

AHSV8_U02713         GTCGATCGTTGATGAGGATATTGCTAAGCATTTGGCGTTTGACGGAAAAGGGGATTGGGT 477
AHSV8_AJ007307       GTCGATCGTTGATGAGGATATTGCTAAGCATTTGGCGTTTGACGGAAAAGGGGATTGGGT 477
AHSV1_FJ011116       GTCAATCGTTGATGAGGATATTGCTAAGCATTTGGCGTTTGACGGAAAAGGGGATTGGGT 475
AHSV1_AM883173       GTCAATCGTTGATGAGGATATTGCTAAGCATTTGGCGTTTGACGGAAAAGGGGATTGGGT 476
AHSV1_FJ183373       GTCAATCGTTGATGAGGATATTGCTAAGCATTTGGCGTTTGACGGAAAAGGGGATTGGGT 476
AHSV1_U02711         GTCAATCGTTGATGAGGATATTGCTAAGCATTTGGCGTTTGACGGAAAAGGGGATTGGGT 477
AHSV2_U59279         ATCAATCGTTGATGAGGATATTGCTAAGCATTTGGCGTTTGACGGAAAGGGAGATTGGGT 477
AHSV3_DQ868782       AACGATTATTGATACAGAAAT------ATATAGGGATCTTAATAGTGATGG---ATGGCT 471
AHSV8_DQ868785       AACGATTATTGATACAGATAT------ATATAAGGATCTTAATAATGATGG---ATGGCT 471
AHSV3a_AJ007304      AACGATTATTGATAATGAAAT------ATATGAAGACCTTAGTGGAGATGG---TTGGCT 471
AHSV3_AJ007303       AACGATTATTGATAATGAAAT------ATATGAAGACCTTAGTGGAGATGG---TTGGCT 471
AHSV3_D12479         AACGATTATTGATAATGAAAT------ATATGAAGACCTTAGTGGAGATGG---TTGGCT 471
AHSV7_AJ007306       AACGATTATTGATAAAGAAAT------ATATGATGACCTTAGTGGAGATGG---TTGGCT 471
AHSV7_U60190         AACGATTATTGATAAAGATAT------ATATCAAGACCTTAATGGAGATGG---TTGGCT 471
                       * **  *****   ** **        **   *   **       * **    *** *

AHSV8_U02713         GTCAAAAACGGTCCATGGTTTAAATTTGTTATGTACCACAATGCTGCTAGCAGCGAATAA 537
AHSV8_AJ007307       GTCAAAAACGGTCCATGGTTTAAATTTGTTATGTACCACAATGCTGCTAGCAGCGAATAA 537
AHSV1_FJ011116       GTCAAAAACGGTCCATGGTTTAAATTTATTATGTACCACGATGCTGCTGGCAGCGAATAA 535
AHSV1_AM883173       GTCAAAAACGGTCCATGGTTTAAATTTATTATGTACCACGATGCTGCTGGCAGCGAATAA 536
AHSV1_FJ183373       GTCAAAAACGGTCCATGGTTTAAATTTATTATGTACCACGATGCTGCTGGCAGCGAATAA 536
AHSV1_U02711         GTCAAAAACGGTCCATGGTTTAAATTTATTATGTACCACGATGCTGCTGGCAGCGAATAA 537
AHSV2_U59279         GTCAAAAACGGTCCATGGTTTAAATTTGTTATGTACAACGATGCTGTTGGCAGCGAATAA 537
AHSV3_DQ868782       GTCGAAGACGGTTCACGGTCTGAATCTGCTGTGCACTACCATGTTGTTAGCAGCGGGAAA 531
AHSV8_DQ868785       GTCGAAGACGGTTCACGGTCTGAATCTGCTGTGCACCACCATGTTGTTAGCAGCGGGAAA 531
AHSV3a_AJ007304      GTCGAAGACGATTCACGGTTTGAATTTGCTGTGTACCACTATGTTGTTAGCGGCTGGAAA 531
AHSV3_AJ007303       GTCGAAGACGATTCACGGTTTGAATTTGCTGTGTACCACTATGTTGTTAGCGGCTGGAAA 531
```

```
AHSV3_D12479          GTCGAAGACGATTCACGGTTTGAATTTGCTGTGTACCACTATGTTGTTAGCGGCTGGAAA 531
AHSV7_AJ007306        GTCGAAGACGATTCACGGTTTGAATCTGCTGTGTACCACTATGTTGTTAGCGGCTGGAAA 531
AHSV7_U60190          GTCGAAGACGATTCACGGTTTGAATCTGCTGTGTACCACTATGTTGTTAGCGGCTGGAAA 531
                      *** ** *** * ** *** * *** *  * ** ** ** *** ** * ** **    **

AHSV8_U02713          AATATCGGAAAAAGTGAGAGAAGAGATTGCGAGGACAAAAAGAGACATCGCGAAAAGACA 597
AHSV8_AJ007307        AATATCGGAAAAAGTGAGAGAAGAGATTGCGAGGACAAAAAGAGACATCGCGAAAAGACA 597
AHSV1_FJ011116        AATATCGGAAAAGGTGAGAGAAGAGATTGCGAGGACAAAAAGAGACATCGCGAAAAGACA 595
AHSV1_AM883173        AATATCGGAAAAGGTGAGAGAAGAGATTGCGAGGACAAAAAGAGACATCGCGAAAAGACA 596
AHSV1_FJ183373        AATATCGGAAAAGGTGAGAGAAGAGATTGCGAGGACAAAAAGAGACATCGCGAAAAGACA 596
AHSV1_U02711          AATATCGGAAAAGGTGAGAGAAGAGATTGCGAGGACAAAAAGAGACATCGCGAAAAGACA 597
AHSV2_U59279          AATATCGGAAAAGGTGAGAGAAGAGATTGCGAGGACAAAAAGAGACATCGCGAAAAGACA 597
AHSV3_DQ868782        AATATCAGATAAAATACAGGAGGAGATATCACGGACAAAGCGGGATATAGCAAAAAGAGA 591
AHSV8_DQ868785        AATATCAGATAAAATACAGGAGGAGATATCACGGACAAAGCGGGATATAGCAAAAAGAGA 591
AHSV3a_AJ007304       AATATCAGATAAAATACAGGAGGAGATCTCACGCACAAAGCGGGATATAGCGAAGAGAGA 591
AHSV3_AJ007303        AATATCAGATAAAATACAGGAGGAGATCTCACGCACAAAGCGGGATATAGCGAAGAGAGA 591
AHSV3_D12479          AATATCAGATAAAATACAGGAGGAGATCTCACGCACAAAGCGGGATATAGCGAAGAGAGA 591
AHSV7_AJ007306        AATATCAGATAAAATACAGGAGGAGATCTCACGTACAAAGCGGGATATAGCGAAGAGAGA 591
AHSV7_U60190          AATATCAGATAAAATACAGGAGGAGATCTCACGCACAAAGCGGGATATAGCGAAGATAGA 591
                      ****** ** **  *    ** *****  *  * *****  * ** ** ** ** * * *

AHSV8_U02713          ATCGTACGTATCAGCTGCGACGATGTCTTGGGATGGCGATAGCGTAACTCTATTACGAGA 657
AHSV8_AJ007307        ATCGTACGTATCAGCTGCGACGATGTCTTGGGATGGCGATAGCGTAACTCTATTACGAGA 657
AHSV1_FJ011116        ATCGTACGTATCAGCTGCGACGATGTCTTGGGATGGCGATAGCGTAACTCTATTACGAGA 655
AHSV1_AM883173        ATCGTACGTATCAGCTGCGACGATGTCTTGGGATGGCGATAGCGTAACTCTATTACGAGA 656
AHSV1_FJ183373        ATCGTACGTATCAGCTGCGACGAAGTCTTGGGATGGCGATAGCGTAACTCTATTACGAGA 656
AHSV1_U02711          ATCGTACGTATCAGCTGCGACGATGTCTTGGGATGGCGATAGCGTAACTCAATTACGAGA 657
AHSV2_U59279          ATCGTACGTATCAGCTGCGACGATGTCTTGGGATGGCGATAGCGTAACTCCATTACGAGA 657
AHSV3_DQ868782        ATCATACGTTTCTGCGGCTAGTATGTCATGGAGTGGGGATACGAGCGTTTTGTTAAAAGA 651
AHSV8_DQ868785        ATCATACGTTTCTGCGGCTAGTATGTCATGGAGTGGGGATACGAGCGTTTTGTTAAGAGA 651
AHSV3a_AJ007304       ATCATATGTTTCCGCGGCTAGTATGTCTTGGAGTGGGGATACGAGCGTTCTATTAAAAGA 651
AHSV3_AJ007303        ATCATATGTTTCCGCGGCTAGTATGTCTTGGAGTGGGGATACGAGCGTTCTATTAAAAGA 651
AHSV3_D12479          ATCATATGTTTCCGCGGCTAGTATGTCTTGGAGTGGGGATACGAGCGTTCTATTAAAAGA 651
AHSV7_AJ007306        ATCATATGTCCCCGCGGCTAGTATGTCTTGGAGTGGGGATACGAGCGTTCTATTAAAAGA 651
AHSV7_U60190          ATCATATGTTTCCGCGGCTAGTATGTCTTGGAGTGGGGATACGAGCGTTCCACTAAAAGA 651
                      *** ** **  * ** ** * *  * *** ***  *** ****       *    **  ***

AHSV8_U02713          TGTAAAATGTGGAGACTAGCGGATAGACCTCCAAAAGCGGGATTCCGCTGGTGTTGCAGT 717
AHSV8_AJ007307        TGTAAAATGTGGAGACTAGCGGATAGACCTCCAAAAGCGGGATTCCGCTGGTGTTGCAGT 717
AHSV1_FJ011116        TGTAAAATATGGAGACTAGCGGATAGACCTCCAAAAGCGGGATTCCACTGGTGTTGCAGT 715
AHSV1_AM883173        TGTAAAATATGGAGACTAGCGGATAGACCTCCAAAAGCGGGATTCCACTGGTGTTGCAGT 716
AHSV1_FJ183373        TGTAAAATATGGAGACTAGCGGATAGACCTCCAAAAGCGGGATTCCACTGGTGTTGCAGT 716
AHSV1_U02711          TGTAAAATATGGAGACTAGCGGATAGACCTCCAAAAGCGGGATTCCACTGGTGTTGCAGT 717
AHSV2_U59279          TGTAAAATATGGAGACTAGCGGATAGACCTCCAAAAGCGGGATTCCGCTGGTGTTGCAGT 717
AHSV3_DQ868782        AGTGAAATATGGCGATAGCTAGAATGACCTCCATTTGTGGGAGATCCACAGTGTTG-GGT 710
AHSV8_DQ868785        AGTGAAATATGGCGATAGCTAGAATGACCTCCATTTGTGGGAGATCCACAGTGTTG-GGT 710
AHSV3a_AJ007304       GGTAAAATATGGCGACAGCTAGAATGACCTCCATTTGTGGGAGATCCACAGTGTTG-GGT 710
AHSV3_AJ007303        GGTAAAATATGGCGACAGCTAGAATGACCTCCATTTGTGGGAGATCCACAGTGTTG-GGT 710
AHSV3_D12479          GGTAAAATATGGCGACAGCTAGAATGACCTCCATTTGTGGGAGATCCACAGTGTTG-GGT 710
AHSV7_AJ007306        GGTAAATATTGGCGACAGCTAGAATGACCTCCATTAGTGGGAGATCCACAGTGTTG-GGT 710
AHSV7_U60190          GGTAAAATATGGCGACAGCTAGAATGACCTCCATTAGTGGGAGATCCACAGTGTTG-GGT 710
                       ** **   *** **      **  ********   * ****   *    ******  **

AHSV8_U02713          GGAT-AACCGCCTAGATCGTGTTCTAGGGAGCCGGGATAACGACTTAC 764
AHSV8_AJ007307        GGAT-AACCGCCTAGATCGTGTTCTAGGGAGCCGGGATAACGACTTAC 764
AHSV1_FJ011116        GGAT-AACCGCCTAGATCGTGTTCTAGGGAGCCGGGATAACAACTTAC 762
AHSV1_AM883173        GGAT-AACCGCCTAGATCGTGTTCTAGGGAGCCGGGATAACAACTTAC 763
AHSV1_FJ183373        GGAT-AACCGCCTAGATCGTGTTCTAGGGAGCCGGGATAACAACTTAC 763
AHSV1_U02711          GGAT-AACCGCCTAGATCGTGTTCTAGGGAGCCGGGATAACGACTTAC 764
AHSV2_U59279          GGAT-AACCGCCTAGATCGTGTTCTAGGGAGCCGGGATAACGACTTAC 764
AHSV3_DQ868782        GGATCAAACACCTAGATCGTTTTCTAGGGAGCCGGGATAACGACTTAC 758
AHSV8_DQ868785        GGATCAAACACCTAGATCGTTTTCTAGGGAGCCGGGATAACGACTTAC 758
AHSV3a_AJ007304       GGATCAAACACCTAGATCGTTTTCTAGGGAGCCGGGATAACGACTTAC 758
AHSV3_AJ007303        GGATCAAACACCTAGATCGTTTTCTAGGGAGCCGGGATAACGACTTAC 758
AHSV3_D12479          GGATCAAACACCTAGATCGTTTTCTAGGGAGCCGGGATAACGACTTAC 758
AHSV7_AJ007306        GGATCAAACACCTAGATCGTTTTCTAGGGAGCCGGGATAACGACTTAC 758
AHSV7_U60190          GGATCAAACACCTAGATCGTTTTCTAGGGAGCCGGGATAACGACTTAC 758
                      **** ** * ********** ******************** ******
```

Appendix C2

AHSV segment 10 full-length alignment of Clade C (serotypes 4, 5, 6 and 9)

```
CLUSTAL 2.0.12 multiple sequence alignment (AHSV Seg10 260510 FL ST 4,5,6,9.aln)

AHSV4_U02712        GTTTAAATTATCCCTTGTCATGAATCTAGCTGCAATCGCCAAGAATTATAGTATGCATAA 60
AHSV4_AJ007305      GTTTAAATTATCCCTTGTCATGAATCTAGCTGCAATCGCCAAGAATTATAGTATGCATAA 60
AHSV6_DQ868784      GTTTAAATTATCCCTTGTCATGAATCTAGCTGCAATCGCCAAGAATTATAGTATGCATAA 60
AHSV4_DQ868783      GTTTAAATTATCCCTTGTCATGAATCTAGCTACAATCGCCAAGAATTATAGCATGCATAA 60
AHSV4_EU046579      GTTTAAATTATCCCTTGTCATGAATCTAGCTACAATCGCCAAGAATTATAGCATGCATAA 60
AHSV5_AJ007309      GTTTAAATTATCCCTTGTCATGAATCTAGCTGCAATCGCCAAGAATTATAGCATGCATAA 60
AHSV6_U26171        GTTTAA-TTATCCCTTGTCATGAATCTAGCTGCAATCGCCAAGAATTATAGTATGCATAA 59
AHSV9_D12480        GTTTAA-TTATCCCTTGTCATGAATCTAGCTGCAATCGCCGAAAATTATAGTATGCATAA 59
AHSV9_AJ007308      GTTTAA-TTATCCCTTGTCATGAATCTAGCTGCAATCGCCGAAAATTATAGTATGCATAA 59
AHSV9_DQ868786      GTTTAAATTATCCCTTGTCATGAATCTAGCTGCAATCGCCAAAAATTATAGCATGCATAA 60
                    ****** ************************ ******** * ******** ********

AHSV4_U02712        TGGAGAGTCGGGGGCGATTGTCCCTTATGTGCCACCGCCATATAATTTCGCGAGCGCTCC 120
AHSV4_AJ007305      TGGAGAGTCGGGGGCGATTGTCCCTTATGTGCCACCGCCATATAATTTCGCGAGCGCTCC 120
AHSV6_DQ868784      TGGAGAGTCGGGGGCGATTGTCCCTTATGTGCCACCACCATATAATTTCGCGAGCGCTCC 120
AHSV4_DQ868783      TGGAGAGTCGGGGGCGATCGTCCCTTATGTGCCACCACCATACAATTTCGCAAGTGCTCC 120
AHSV4_EU046579      TGGAGAGTCGGGGGCGATCGTCCCTTATGTGCCACCACCATACAATTTCGCAAGTGCTCC 120
AHSV5_AJ007309      TGGAGAGTCGGGGACGATCGTCCCTTATGTGCCACCACCATACAATTTCGCAAGTGCTCC 120
AHSV6_U26171        TGGAGAGTCGGAGGCGATCGTCCCTTATGTGCCACCACCATACAATTTCGCAAGTGCTCC 119
AHSV9_D12480        TGGAGAGTCGGGGGCGATCGTCCCTTATGTGCCACCACCATACAATTTCGCAAGTGCTCC 119
AHSV9_AJ007308      TGGAGAGTCGGGGGCGATCGTCCCTTATGTGCCACCACCATACAATTTCGCAAGTGCTCC 119
AHSV9_DQ868786      TGGAGAGCAGGGGGCGATCGTCCCATATGTGCCGCCACCATACAATTTCGCAAGTGCTCC 120
                    *******  ** * **** ***** ******** ** ***** ******** ** *****

AHSV4_U02712        GACGTTTTCTCAGCGTACGAGTCAAATGGAGTCCGTGTCGCTTGGGATACTTAACCAAGC 180
AHSV4_AJ007305      GACGTTTTCTCAGCGTACGAGTCAAATGGAGTCCGTGTCGCTTGGGATACTTAACCAAGC 180
AHSV6_DQ868784      GACGTTTTCTCAGCGTACGAGTCAAATGGAGTCCGTGTCGCTTGGGATACTTAACCAAGC 180
AHSV4_DQ868783      GACGTTTTCTCAGCGTACGAGTCAAATGGAGTCCGTGTCGCTTGGGATACTTAACCAAGC 180
AHSV4_EU046579      GACGTTTTCTCAGCGTACGAGTCAAATGGAGTCCGTGTCGCTTGGGATACTTAACCAAGC 180
AHSV5_AJ007309      GACGTTTTCTCAGCGTACGAGTCAAATGGAGTCCGTGTCGCTTGGGATACTTAACCAAGC 180
AHSV6_U26171        GACGTTTTCTCAGCGTACGAGTCAAATGGAGTCCGTGTCGCTTGGGATACTTAACCAAGC 179
AHSV9_D12480        GACGTTTTCTCAGCGTACGAGTCAAATGGAGTCCGTGTCGCTTGGGATACTTAACCAAGC 179
AHSV9_AJ007308      GACGTTTTCTCAGCGTACGAGTCAAATGGAGTCCGTGTCGCTTGGGATACTTAACCAAGC 179
AHSV9_DQ868786      GGCGTTTACTCAGCGTACGAGTCAAATGGAGTCCGTGTCGCTTGGGATACTTAACCAAGC 180
                    * ***** ************************************************

AHSV4_U02712        CATGTCAAGTACAACTGGTGCGAGTGGGGCGCTTAAAGATGAAAAAGCAGCGTTCGGTGC 240
AHSV4_AJ007305      CATGTCAAGTACAACTGGTGCGAGTGGGGCGCTTAAAGATGAAAAAGCAGCGTTCGGTGC 240
AHSV6_DQ868784      CATGTCAAGTACAACTGGTGCGAGTGGGGCGCTTAAAGATGAAAAAGCAGCGTTTGGTGC 240
AHSV4_DQ868783      CATGTCAAGTACAACTGGTGCGAGTGGGGCGCTTAAAGATGAAAAAGCAGCATTCGGTGC 240
AHSV4_EU046579      CATGTCAAGTACAACTGGTGCGAGTGGGGCGCTTAAAGATGAAAAAGCAGCATTCGGTGC 240
AHSV5_AJ007309      CATGTCAAGTACAACTGGTGCGAGTGGGGCGCTTAAAGATGAAAAAGCAGCGTTCGGTGC 240
AHSV6_U26171        CATGTCAAGTACAACTGGTGCGAGTGGGGCGCTTAAAGATGAAAAAGCAGCATTCGGTGC 239
AHSV9_D12480        CATGTCAAGTACAACTGGTGCGAGTGGGGCGCTTAAAGATGAAAAAGCGGCATTTGGTGC 239
AHSV9_AJ007308      CATGTCAAGTACAACTGGTGCGAGTGGGGCGCTTAAAGATGAAAAAGCGGCATTTGGTGC 239
AHSV9_DQ868786      CATGTCAAGCACAACTGGTGCGAGTGGGGCACTTAAAGATGAAAAAGCAGCATTTGGTGC 240
                    ********* ******************* ***************** ** ** *****

AHSV4_U02712        TATGGCGGAACGATTGCGTGATCCAGAACCCATACGTCAAATTAAAAAGCAGGTGGGTAT 300
AHSV4_AJ007305      TATGGCGGAACGATTGCGTGATCCAGAACCCATACGTCAAATTAAAAAGCAGGTGGGTAT 300
AHSV6_DQ868784      TATGGCGGAAGCATTGCGTGATCCAGAACCCATACGTCAAATTAAAAAGCAGGTGGGTAT 300
AHSV4_DQ868783      TATGGCGGAAGCATTGCGTGATCCAGAACCCATACGTCAAATTAAAAAGCAGGTGGGTAT 300
AHSV4_EU046579      TATGGCGGAAGCATTGCGTGATCCAGAACCCATACGTCAAATTAAAAAGCAGGTGGGTAT 300
AHSV5_AJ007309      CATGGCGGAAGCATTGCGTGATCCAGAACCCATACGTCAAATTAAAAAGCAGGTGGGTAT 300
AHSV6_U26171        TATGGCGGAAGCATTGCGTGATCCAGAACCCATACGTCAAATTAAAAAGCAGGTGGGTAT 299
AHSV9_D12480        CATGGCGGAAGCATTGCGTGATCCAGAACCCATACGTCAAATTAAAAAGCAGGTGGGTAT 299
AHSV9_AJ007308      CATGGCGGAAGCATTGCGTGATCCAGAACCCATACGTCAAATTAAAAAGCAGGTGGGTAT 299
AHSV9_DQ868786      GATGGCGGAAGCATTACGTGATCCAGAACCCATACGTCAAATTAAGAAACAGGTAGGCAT 300
                     *********  *** ***************************** ** ***** ** **

AHSV4_U02712        CAGAACTTTAAAGAACTTGAAGATGGAGTTAGCAACAATGCGTCGAAAAAAGTCGGCATT 360
AHSV4_AJ007305      CAGAACTTTAAAGAACTTGAAGATGGAGTTAGCAACAATGCGTCGAAAAAAGTCGGCATT 360
AHSV6_DQ868784      CAGAACTTTAAAGAACTTAAAGATGGAGTTAGCGACAATGCGTCGAAAAAAGTCGGCATT 360
AHSV4_DQ868783      CAGAACTTTAAAGAACCTAAAGATGGAGTTAGCAACAATGCGTCGAAAGAAATCGGCATT 360
AHSV4_EU046579      CAGAACTTTAAAGAACCTAAAGATGGAGTTAGCAACAATGCGTCGAAAGAAATCGGCATT 360
```

```
AHSV5_AJ007309      CAGAACTTTAAAGAACCTAAAGATGGAGTTAGCAACAATGCGTCGAAAGAAATCGGCATT 360
AHSV6_U26171        CAGAACTTTAAAGAACCTAAAGATGGAGCTGGCAACAATGCGTCGAAAGAAATCGGCATT 359
AHSV9_D12480        CAGAACTTTAAAGAACTTAAAGATGGAGTTAGCAACAATGCGTCGAAAGAAATCGGCATT 359
AHSV9_AJ007308      CAGAACTTTAAAGAACTTAAAGATGGAGTTAGCAACAATGCGTCGAAAGAAATCGGCATT 359
AHSV9_DQ868786      TAGAACCTTGAAAAATTTGAAGACGGAGCTAACGACTATGCGCCGAAAGAAATCGGCATT 360
                     ***** ** ** **  * **** **** *  * ** ***** ***** ** ********

AHSV4_U02712        AAAAATAACGATTCTTATCAGCGGATGTGTGACGTTAGCAACATCGATGGTCGGGGGGTT 420
AHSV4_AJ007305      AAAAATAACGATTCTTATCAGCGGATGTGTGACGTTAGCAACATCGATGGTCGGGGGGTT 420
AHSV6_DQ868784      AAAAATAATGATTTTTATCAGCGGATGTGTGACGTTAGCAACATCGATGGTCGGAGGGTT 420
AHSV4_DQ868783      AAAAATAATGATCTTTATTAGTGGATGCGTAACGTTAGCTACATCGATGGTTGGGGGATT 420
AHSV4_EU046579      AAAAATAATGATCTTTATTAGTGGATGCGTAACGTTAGCTACATCGATGGTTGGGGGATT 420
AHSV5_AJ007309      AAAAATAATGATCTTTATTAGTGGATGCGTGACGTTAGCTACATCGATGGTTGGGGGATT 420
AHSV6_U26171        AAAGATAATGATCTTTATTAGTGGATGCGTAACGTTAGCTACATCGATGGTTGGGGGATT 419
AHSV9_D12480        AAAAATAATGATTTTTATTAGTGGGTGCGTGACGTTAGCTACATCGATGGTTGGGGGATT 419
AHSV9_AJ007308      AAAAATAATGATTTTTATTAGTGGGTGCGTGACGTTAGCTACATCGATGGTTGGGGGATT 419
AHSV9_DQ868786      GAAAATAACGATTTTTATCAGTGGGTGTGTGACTTTAGCAACCTCAATGGTTGGAGGATT 420
                     ** **** ***  **** ** ** ** ** ** ***** ** ** ***** ** ** **

AHSV4_U02712        AAGTATTGTCGATAACGAAATATTTGAAGATTATAAGAAGAACGATTGGTTAATGAAAGC 480
AHSV4_AJ007305      AAGTATTGTCGATAACGAAATATTTGAAGATTATAAGAAGAACGATTGGTTAATGAAAGC 480
AHSV6_DQ868784      AAGTATTGTTGATAACGAAATATTTGAAGATTATAAGAAGAACGATTGGTTAATGAAAAC 480
AHSV4_DQ868783      GAGTATCGTTGACGACGAAATATTAAGAGATTATAAGAACAACGATTGGTTAATGAAGAC 480
AHSV4_EU046579      GAGTATCGTTGACGACGAAATATTAAGAGATTATAAGAACAACGATTGGTTAATGAAGAC 480
AHSV5_AJ007309      GAGTATCGTTGACGACGAAATATTAGGAGATTATAAGAACAACGATTGGTTAATGAAGAC 480
AHSV6_U26171        GAGTATCGTTGATGACGAAATATTAAGAGATTATAAGAACAACGATTGGTTAATGAAGAC 479
AHSV9_D12480        GAGTATTGTTGATGACCAAATATTAGATGATTATAAGAAAAACGATTGGTTGATGAAGAC 479
AHSV9_AJ007308      GAGTATTGTTGATGACCAAATATTAGATGATTATAAGAAAAACGATTGGTTGATGAAGAC 479
AHSV9_DQ868786      AAGCATAGTTGATGACCAGATTTGGGGAGAGTATAAAGATAACGATTGGTTGATAAAAAC 480
                     ** ** ** **  ** * ** *     ** *****  * ********** ** **  *

AHSV4_U02712        GATACATGGGCTGAATTTGTTATGTACCACAGTTTTGTTGGCGGCGGGTAAGATTTCTGA 540
AHSV4_AJ007305      GATACATGGGCTGAATTTGTTATGTACCACAGTTTTGTTGGCGGCGGGTAAGATTTCTGA 540
AHSV6_DQ868784      GATACATGGGCTGAATTTGTTATGTACCACAGTTTTGTTGGCGGCAGGTAAGATTTCTGA 540
AHSV4_DQ868783      TATACATGGGCTGAATTTGTTATGTACTACAGTTTTGTTAGCGGCGGGTAAGATTTCCGA 540
AHSV4_EU046579      TATACATGGGCTGAATTTGTTATGTACTACAGTTTTGTTAGCGGCGGGTAAGATTTCCGA 540
AHSV5_AJ007309      TATACATGGGCTGAATTTGTTATGTACTACAGTTTTGTTAGCGGCGGGTAAGATTTCCGA 540
AHSV6_U26171        TATACATGGGCTGAATTTGTTGTGTACTACAGTTTTGTTAGCGGCGGGTAAGATTTCCGA 539
AHSV9_D12480        TATACATGGGCTGAATTTGTTATGTACTACAGTTTTGTTAGCTGCGGGTAAGATTTCTGA 539
AHSV9_AJ007308      TATACATGGGCTGAATTTGTTATGTACTACAGTTTTGTTAGCTGCGGGTAAGATTTCTGA 539
AHSV9_DQ868786      GATACATGGACTGAACTTATTATGTACAACAGTATTGCTGGCAGCGGGTAAGATTTCCGA 540
                     ******** ***** ** ** ***** ***** *** * ** ** ********** **

AHSV4_U02712        TAAAATACAAGAGGAGATTTCACGAACAAAGCGTGATATTGCGAAAAGAGAGTCTTACGT 600
AHSV4_AJ007305      TAAAATACAAGAGGAGATTTCACGAACAAAGCGTGATATTGCGAAAAGAGAGTCTTACGT 600
AHSV6_DQ868784      TAAAATCCAAGAGGAGATTTCACGAACAAAGCGTGATATTGCGAAAAGAGAGTCTTATGT 600
AHSV4_DQ868783      TAAAATGCAAGAGGAGATTTCACGGACTAAACGTGACATTGCGAAAAGAGAGTCTTACGT 600
AHSV4_EU046579      TAAAATGCAAGAGGAGATTTCACGGACTAAACGTGACATTGCGAAAAGAGAGTCTTACGT 600
AHSV5_AJ007309      TAAAATACAAGAGGAGATTTCACGGACTAAACGTGACATTGCGAAAAGAGAGTCTTACGT 600
AHSV6_U26171        TAAAATACAAGAGGAGATTTCACGGACTAAACGTGACATCGCGAAAAGAGAGTCTTACGT 599
AHSV9_D12480        TAAAATACAAGAAGAAATTTCACGGACTAAACGTGACATTGCAAAAAGAGAGTCTTACGT 599
AHSV9_AJ007308      TAAAATACAAGAAGAAATTTCACGGACTAAACGTGACATTGCAAAAAGAGAGTCTTACGT 599
AHSV9_DQ868786      TAAGATTCAAGAAGAAATTTCGCGGACGAAGCGTGACATTGCGAAGAGAGAGTCTTATGT 600
                    *** ** ***** ** ***** ** ** ** ***** ** ** ** ********** **

AHSV4_U02712        ATCTGCGGCGAGTATGTCATGGAATGGAGATACTGAAGTATTATTGCAAGGAATTAAGTA 660
AHSV4_AJ007305      ATCTGCGGCGAGTATGTCATGGAATGGAGATACTGAAGTATTATTGCAAGGAATTAAGTA 660
AHSV6_DQ868784      ATCTGCGGCGAGTATGTCATGGAGTGGAGATACTGAAGTATTATTGCAAGGAATTAAGTA 660
AHSV4_DQ868783      GTCAGCGGCGAGTATGTCGTGGAGTGGAGATACTGAGATGTTATTACAGGGAATTAAGTA 660
AHSV4_EU046579      GTCAGCGGCGAGTATGTCGTGGAGTGGAGATACTGAGATGTCATTACAGGGAATTAAGTA 660
AHSV5_AJ007309      GTCAGCGGCGAGTATGTCGTGGAACGGAGATACTGAGATGTCATTACAGGGAATTAAGTA 660
AHSV6_U26171        GTCAGCGGCGAGTATGTCGTGGAATGGAGATACTGAGATGTTATTACAGGGAATTAAGTA 659
AHSV9_D12480        ATCAGCGGCGAGTATGTCGTGGAATGGAGATACTGAGATGTTATTACAGGGAACTAAGTA 659
AHSV9_AJ007308      ATCAGCGGCGAGTATGTCGTGGAATGGAGATACTGAGATGTTATTACAGGGAACTAAGTA 659
AHSV9_DQ868786      GTCAGCAGCCAGTATGTCGTGGAGTGGAGATACTGAGATGTTATTACACGGAATTAAGTA 660
                     ** ** ** ******** ****  ***********  * * *** ** **** ******

AHSV4_U02712        TGGCGATAGCTAGTACGACCTCCACAAGCGGAAAATCCATCGTGTTGGATGGATGGAACG 720
AHSV4_AJ007305      TGGCGATAGCTAGTACGACCTCCACAAGCGGAAAATCCATCGTGTTGGATGGATGGAACG 720
AHSV6_DQ868784      TGGCGATAGCTAGTACGACCTCCACAAGCGGAAAATCCATCGTGTTGGATGGATGGAACG 720
AHSV4_DQ868783      TGGCGAGAGCTAGTATGACCTCCACGAGCGGAAAATCCATCGTGTTGGATGGATGGAACG 720
AHSV4_EU046579      TGGCGAGAGCTAGTATGACCTCCACGAGCGGAAAATCCATCGTGTTGGATGGATGGAACG 720
AHSV5_AJ007309      TGGCGAGAGCTAGTATGACCTCCACAAGCGGAAAATCCATCGTGTTGGATGGATGGAACG 720
AHSV6_U26171        TGGCGAGAGCTAGTATGACCTC-GCGAGCGGAAAATCCATCGTGTTGGATGGATGGAACG 718
AHSV9_D12480        TGGCGAAAGCTAGTATGACCTCCATGAGCGGAAAATCCATCGTGTTGGATGGATGGAACG 719
AHSV9_AJ007308      TGGCGAAAGCTAGTATGACCTCCATGAGCGGAAAATCCATCGTGTTGGATGGATGGAACG 719
```

```
AHSV9_DQ868786      TGGCGAAAGCTAGTATGACCTCCATGAGCGGAAAATCCATCGTGTTGGATGGATGGAACG 720
                    ****** ******** ******    **********************************

AHSV4_U02712        CCTAGATCGTTTTCTAGGGAGCCGGGATAACGACTTAC 758
AHSV4_AJ007305      CCTAGATCGTTTTCTAGGGAGCCGGGATAACGACTTAC 758
AHSV6_DQ868784      CCTAGATCGTCTTCTAGGGAGCCGGGATAACGACTTAC 758
AHSV4_DQ868783      CCTAGATCGTTTTCTAGGGAGCCGGGATAACGACTTAC 758
AHSV4_EU046579      CCTAGATCGTTTTCTAGGGAGCCGGGATAACGACTTAC 758
AHSV5_AJ007309      CCTAGATCGTTTTCTAGGGAGCCGGGATAACGACTTAC 758
AHSV6_U26171        CCTAGATCGTCTTCTAGGGAGT-GGGATAACAACTTAC 755
AHSV9_D12480        CCTAGATCGTTTTCTAGGGAGT-GGGATAACAACTTAC 756
AHSV9_AJ007308      CCTAGATCGTTTTCTAGGGAGT-GGGATAACAACTTAC 756
AHSV9_DQ868786      CCTAGATCGTTTTCTAGGGAGC-GGGATAACGACTTAC 757
                    ********** **********  ******** ******
```

Appendix D1

AHSV segment 10 full-length alignment of Clade A (Serotypes 3 and 7)

```
CLUSTAL 2.0.12 multiple sequence alignment (AHSV Seg10 260510 FL ST 3,7)


AHSV3a_AJ007304         GTTTAAATTATCCCTTGTCATGAGTCTAGCTACGATCGCCGAAAATTATATGATGCATAA 60
AHSV3_AJ007303          GTTTAAATTATCCCTTGTCATGAGTCTAGCTACGATCGCCGAAAATTATATGATGCATAA 60
AHSV3_D12479            GTTTAAATTATCCCTTGTCATGAGTCTAGCTACGATCGCCGAAAATTATATGATGCATAA 60
AHSV7_AJ007306          GTTTAAATTATCCCTTGTCATGAGTCTAGCTACGATCGCCGAAAATTATATGATGCATAA 60
AHSV7_U60190            GTTTAAATTATCCCTTGTCATGAGTCTAGCTACGATCGCCGAAAATTATATGATGCATAA 60
AHSV3_DQ868782          GTTTAAATTATCCCTTGTCATGAGTCTAGCTACGATCGCCGAAAATTATATGATGCATAA 60
AHSV8_3?__DQ868785      GTTTAAATTATCCCTTGTCATGAGTCTAGCTACGATCGCCGAAAATTATATGATGCATAA 60
                        ************************************************************

AHSV3a_AJ007304         TGGAAATCAGAGAGCAATTGTACCGTATGTTCCACCCCCTTATGCGTATGCAAATGCTCC 120
AHSV3_AJ007303          TGGAAATCAGAGAGCAATTGTACCGTATGTTCCACCCCCTTATGCGTATGCAAATGCTCC 120
AHSV3_D12479            TGGAAATCAGAGAGCAATTGTACCGTATGTTCCACCCCCTTATGCGTATGCAAATGCTCC 120
AHSV7_AJ007306          TGGAAATCAGAGAGCAATTGTGCCGTATGTTCCACCCCCTTATGCGTATGCAAATGCTCC 120
AHSV7_U60190            TGAAACTCAGAGAGCAATTGTACCGTATGTTCCACCCCCTTATGCGTATGCAAATGCTCC 120
AHSV3_DQ868782          TGGAAATCAGAGGGCAATTGTACCGTATGTTCCGCCCCCTTATACGTATGCAAATGCTCC 120
AHSV8_3?__DQ868785      TGGAAATCAGAGGGCAATCGTACCGTATGTTCCGCCCCCTTATACGTATGCAAATGCTCC 120
                        ** ** ****** ***** ** *********** ********* ****************

AHSV3a_AJ007304         GACGCTTGGTGGTCAGGCGGGTGAAATGGAGTCCATGTCGCTTGGGATACTTAATCAAGC 180
AHSV3_AJ007303          GACGCTTGGTGGTCAGGCGGGTGAAATGGAGTCCATGTCGCTTGGGATACTTAATCAAGC 180
AHSV3_D12479            GACGCTTGGTGGTCAGGCGGGTGAAATGGAGTCCATGTCGCTTGGGATACTTAATCAAGC 180
AHSV7_AJ007306          GACGCTTGGTGGTCAGGCGGGTGAAATGGAGTCCATGTCGCTTGGGATACTTAATCAAGC 180
AHSV7_U60190            GACGCTTGGTGGTCAGGCGGGTGAAATGGAGTCCATGTCGCTTGGGATACTTAATCAAGC 180
AHSV3_DQ868782          GACGCCTGGTGGTCAAGCGGGTGAAATGGAGTCCATGTCGCTTGGGATACTTAACCAAGC 180
AHSV8_3?__DQ868785      GACGCTTGGTGGTCAAGCGGGTGAAATGGAGTCCATGTCGCTTGGGATACTTAACCAAGC 180
                        ***** ********* ************************** *****

AHSV3a_AJ007304         CATGTCAAGTACAACTGGTGCAAGTCGGGCTCTTAAGGATGAAAAAGCAGCGTTTGGTGC 240
AHSV3_AJ007303          CATGTCAAGTACAACTGGTGCAAGTCGGGCTCTTAAGGATGAAAAAGCAGCGTTTGGTGC 240
AHSV3_D12479            CATGTCAAGTACAACTGGTGCAAGTCGGGCTCTTAAGGATGAAAAAGCAGCGTTTGGTGC 240
AHSV7_AJ007306          CATGTCAAGTACAACTGGTGCAAGTGGGGCTCTTAAGGATGAAAAAGCAGCGTTTGGTGC 240
AHSV7_U60190            CATGTCAAGTACAACTGGTGCAAGTGGGGCTCTTAAGGATGAAAAAGCAGCGTTTGGTGC 240
AHSV3_DQ868782          CATGTCAAGTACAACTGGTGCGAGTGGGGCCCTTAAGGATGAAAAAGCAGCATTTGGTGC 240
AHSV8_3?__DQ868785      CATGTCAAGTACAACTGGTGCGAGTGGGGCCCTTAAGGATGAAAAAGCAGCATTTGGTGC 240
                        ********************* *** **** ******************** ********

AHSV3a_AJ007304         GATGGCGGAAGCATTACGTGATCCAGAACCGATACGTCAAATAAAGAAACATGTTGGATT 300
AHSV3_AJ007303          GATGGCGGAAGCATTACGTGATCCAGAACCGATACGTCAAATAAAGAAACATGTTGGATT 300
AHSV3_D12479            GATGGCGGAAGCATTACGTGATCCAGAACCGATACGTCAAATAAAGAAACATGTTGGATT 300
AHSV7_AJ007306          GATGGCGGAAGCATTACGTGATCCAGAACCGATACGTCAAATTAAGAAACATGTTGGATT 300
AHSV7_U60190            GATGGCGGAAGCACTACGTGATCCAGAACCGATTCGTCAAATTAAGAAACATGTTGGATT 300
AHSV3_DQ868782          GATGGCGGAAGCATTACGTGATCCAGAACCAATACGTCAAATTAAGAAAACCGTTGGATT 300
AHSV8_3?__DQ868785      GATGGCGGAGGCATTACGTGATCCAGAACCAATACGTCAAATTAAGAAAACCGTTGGATT 300
                        ********* *** ***************** ** ******** ******   ********

AHSV3a_AJ007304         AAGAACGCTCAAGCATTTAAAGATAGAGTTGGCGTCAATGAGACGTAGGTATGCGATACT 360
AHSV3_AJ007303          AAGAACGCTCAAGCATTTAAAGATAGAGTTGGCGTCAATGAGACGTAGGTATGCGATACT 360
AHSV3_D12479            AAGAACGCTCAAGCATTTAAAGATAGAGTTGGCGTCAATGAGACGTAGGTATGCGATACT 360
AHSV7_AJ007306          AAGAACGCTCAAGCATTTAAAGATAGAGTTGGCGTCAATGAGACGTAGGTATGCGATACT 360
AHSV7_U60190            AAGAACGCTCAAGCATTTAAAGATAGAGTTGGCGTCAATGAGACGTAGGTATGCGATACT 360
AHSV3_DQ868782          AAGGACGCTTAAGCATTTAAAGATAGAGTTGGCGTCGATGAGACGTAGGTATGCGATATT 360
AHSV8_3?__DQ868785      AAGGACACTTAAGCATTTAAAGATAGAGTTGGCGTCGATGAGACGTAGGTATGCGATATT 360
                        *** ** ** ************************** ********************** *

AHSV3a_AJ007304         ACGTGTAGTGATCTTAATGAGCGGGTGCGTAACGATGGCTACCTCGATGGCGGGCGGGTT 420
AHSV3_AJ007303          ACGTGTAGTGATCTTAATGAGCGGGTGCGTAACGATGGCTACCTCGATGGCGGGCGGGTT 420
AHSV3_D12479            ACGTGTAGTGATCTTTATGAGCGGGTGCGTAACGATGGCTACCTCGATGGCGGGCGGGTT 420
AHSV7_AJ007306          ACGTGTAGTGATCTTTATGAGCGGGTGCGTAACGATGGCTACCTCGATGGCGGGCGGGTT 420
AHSV7_U60190            ACGTGTAGTGATCTTAATGAGCGGGTGCGTAACGATGGCTACCTCGATGGCGGGCGGGTT 420
AHSV3_DQ868782          ACGAGTAGTCATTTTTATGAGTGGGTGCGTGACAATGGCTACCTCGATGGTGGGCGGGTT 420
AHSV8_3?__DQ868785      ACGAGTAGTCACTTTTATGAGTGGGTGCGTGACAATGGCTACCTCGATGGTGGGCGGGTT 420
                        *** ***** *  ** ***** ******** ** ********************* *********

AHSV3a_AJ007304         AACGATTATTGATAATGAAATATATGAAGACCTTAGTGGAGATGGTTGGCTGTCGAAGAC 480
AHSV3_AJ007303          AACGATTATTGATAATGAAATATATGAAGACCTTAGTGGAGATGGTTGGCTGTCGAAGAC 480
```

```
AHSV3_D12479            AACGATTATTGATAATGAAATATATGAAGACCTTAGTGGAGATGGTTGGCTGTCGAAGAC 480
AHSV7_AJ007306          AACGATTATTGATAAAGAAATATATGATGACCTTAGTGGAGATGGTTGGCTGTCGAAGAC 480
AHSV7_U60190            AACGATTATTGATAAAGATATATATCAAGACCTTAATGGAGATGGTTGGCTGTCGAAGAC 480
AHSV3_DQ868782          AACGATTATTGATACAGAAATATATAGGGATCTTAATAGTGATGGATGGCTGTCGAAGAC 480
AHSV8_3?__DQ868785      AACGATTATTGATACAGATATATATAAGGATCTTAATAATGATGGATGGCTGTCGAAGAC 480
                        **************  ** ******   ** **** *   ***** **************

AHSV3a_AJ007304         GATTCACGGTTTGAATTTGCTGTGTACCACTATGTTGTTAGCGGCTGGAAAAATATCAGA 540
AHSV3_AJ007303          GATTCACGGTTTGAATTTGCTGTGTACCACTATGTTGTTAGCGGCTGGAAAAATATCAGA 540
AHSV3_D12479            GATTCACGGTTTGAATTTGCTGTGTACCACTATGTTGTTAGCGGCTGGAAAAATATCAGA 540
AHSV7_AJ007306          GATTCACGGTTTGAATCTGCTGTGTACCACTATGTTGTTAGCGGCTGGAAAAATATCAGA 540
AHSV7_U60190            GATTCACGGTTTGAATCTGCTGTGTACCACTATGTTGTTAGCGGCTGGAAAAATATCAGA 540
AHSV3_DQ868782          GGTTCACGGTCTGAATCTGCTGTGCACTACCATGTTGTTAGCAGCGGGAAAAATATCAGA 540
AHSV8_3?__DQ868785      GGTTCACGGTCTGAATCTGCTGTGCACCACCATGTTGTTAGCAGCGGGAAAAATATCAGA 540
                        * ******** ***** ******* ** ** *********** ** **************

AHSV3a_AJ007304         TAAAATACAGGAGGAGATCTCACGCACAAAGCGGGATATAGCGAAGAGAGAATCATATGT 600
AHSV3_AJ007303          TAAAATACAGGAGGAGATCTCACGCACAAAGCGGGATATAGCGAAGAGAGAATCATATGT 600
AHSV3_D12479            TAAAATACAGGAGGAGATCTCACGCACAAAGCGGGATATAGCGAAGAGAGAATCATATGT 600
AHSV7_AJ007306          TAAAATACAGGAGGAGATCTCACGTACAAAGCGGGATATAGCGAAGAGAGAATCATATGT 600
AHSV7_U60190            TAAAATACAGGAGGAGATCTCACGCACAAAGCGGGATATAGCGAAGATAGAATCATATGT 600
AHSV3_DQ868782          TAAAATACAGGAGGAGATATCACGGACAAAGCGGGATATAGCAAAAAGAGAATCATACGT 600
AHSV8_3?__DQ868785      TAAAATACAGGAGGAGATATCACGGACAAAGCGGGATATAGCAAAAAGAGAATCATACGT 600
                        ****************** ***** ***************** ** * ********* **

AHSV3a_AJ007304         TTCCGCGGCTAGTATGTCTTGGAGTGGGGATACGAGCGTTCTATTAAAAGAGGTAAAATA 660
AHSV3_AJ007303          TTCCGCGGCTAGTATGTCTTGGAGTGGGGATACGAGCGTTCTATTAAAAGAGGTAAAATA 660
AHSV3_D12479            TTCCGCGGCTAGTATGTCTTGGAGTGGGGATACGAGCGTTCTATTAAAAGAGGTAAAATA 660
AHSV7_AJ007306          CCCCGCGGCTAGTATGTCTTGGAGTGGGGATACGAGCGTTCTATTAAAAGAGGTAAATAT 660
AHSV7_U60190            TTCCGCGGCTAGTATGTCTTGGAGTGGGGATACGAGCGTTCCACTAAAAGAGGTAAAATA 660
AHSV3_DQ868782          TTCTGCGGCTAGTATGTCATGGAGTGGGGATACGAGCGTTTTGTTAAAAGAAGTGAAATA 660
AHSV8_3?__DQ868785      TTCTGCGGCTAGTATGTCATGGAGTGGGGATACGAGCGTTTTGTTAAGAGAAGTGAAATA 660
                          * ************** ********************    *** *** ** **

AHSV3a_AJ007304         TGGCGACAGCTAGAATGACCTCCATTTGTGGGAGATCCACAGTGTTGGGTGGATCAAACA 720
AHSV3_AJ007303          TGGCGACAGCTAGAATGACCTCCATTTGTGGGAGATCCACAGTGTTGGGTGGATCAAACA 720
AHSV3_D12479            TGGCGACAGCTAGAATGACCTCCATTTGTGGGAGATCCACAGTGTTGGGTGGATCAAACA 720
AHSV7_AJ007306          TGGCGACAGCTAGAATGACCTCCATTAGTGGGAGATCCACAGTGTTGGGTGGATCAAACA 720
AHSV7_U60190            TGGCGACAGCTAGAATGACCTCCATTAGTGGGAGATCCACAGTGTTGGGTGGATCAAACA 720
AHSV3_DQ868782          TGGCGATAGCTAGAATGACCTCCATTTGTGGGAGATCCACAGTGTTGGGTGGATCAAACA 720
AHSV8_3?__DQ868785      TGGCGATAGCTAGAATGACCTCCATTTGTGGGAGATCCACAGTGTTGGGTGGATCAAACA 720
                        ****** ****************** ********************************

AHSV3a_AJ007304         CCTAGATCGTTTTCTAGGGAGCCGGGATAACGACTTAC 758
AHSV3_AJ007303          CCTAGATCGTTTTCTAGGGAGCCGGGATAACGACTTAC 758
AHSV3_D12479            CCTAGATCGTTTTCTAGGGAGCCGGGATAACGACTTAC 758
AHSV7_AJ007306          CCTAGATCGTTTTCTAGGGAGCCGGGATAACGACTTAC 758
AHSV7_U60190            CCTAGATCGTTTTCTAGGGAGCCGGGATAACGACTTAC 758
AHSV3_DQ868782          CCTAGATCGTTTTCTAGGGAGCCGGGATAACGACTTAC 758
AHSV8_3?__DQ868785      CCTAGATCGTTTTCTAGGGAGCCGGGATAACGACTTAC 758
                        **************************************
```

Appendix D2

AHSV segment 10 full-length alignment of Clade B (Serotypes 1, 2 and 8)

```
CLUSTAL 2.0.12 multiple sequence alignment (AHSV Seg10 260510 FL ST 1,2,8)


AHSV8_U02713        GTTTAAATTATCCCTTGTCATGAATCTTGCTAGCATCTCCCAAAGCTATATGTCACATAA 60
AHSV8_AJ007307      GTTTAAATTATCCCTTGTCATGAATCTTGCTAGCATCTCCCAAAGCTATATGTCACATAA 60
AHSV1_FJ011116      -GTTTAATTATCCCT-GTCATGAATCTTGCTAGCATCTCCCAAAGCTATATGTCACATAA 58
AHSV1_AM883173      -GTTTAATTATCCCTTGTCATGAATCTTGCTAGCATCTCCCAAAGCTATATGTCACATAA 59
AHSV1_FJ183373      -GTTAAATTATCCCTTGTCATGAATCTTGCTAGCATCTCCCAAAGCTATATGTCACATAA 59
AHSV1_U02711        GTTTAAATTATCCCTTGTCATGAATCTTGCTAGCATCTCCCAAAGCTATATGTCACATAA 60
AHSV2_U59279        GTTTAAATTATCCCTTGTCATGAATCTTGCTAGCATCTCCCAAAGCTATATGTCACATAA 60
                      ** ********** ******************************************

AHSV8_U02713        TGAGAATGAAAGATCAATTGTACCATACATTCCGCCACCGTATCATCCGACGGCTCCGGC 120
AHSV8_AJ007307      TGAGAATGAAAGATCAATTGTACCATACATTCCGCCACCGTATCATCCGACGGCTCCGGC 120
AHSV1_FJ011116      TGAGAATGAAAGATCAATTGTACCATACATTCCGCCACCGTATCATCCGACGGCTCCGGC 118
AHSV1_AM883173      TGAGAATGAAAGATCAATTGTACCATACATTCCGCCACCGTATCATCCGACGGCTCCGGC 119
AHSV1_FJ183373      TGAGAATGAAAGATCAATTGTACCATACATTCCGCCACCGTATCATCCGACGGCTCCGGC 119
AHSV1_U02711        TGAGAATGAAAGATCAATTGTACCATACATTCCGCCACCGTATCATCCGACGGCTCCGGC 120
AHSV2_U59279        TGAGAATGAAAGATCAATTGTACCATACATTCCGCCACCGTATCATCCGACGGCTCCGGC 120
                    ************************************************************

AHSV8_U02713        GCTTGCTGTATCCGCCAGTCAAATGGAGACCATGTCGCTTGGGATACTTAACCAAGCAAT 180
AHSV8_AJ007307      GCTTGCTGTATCCGCCAGTCAAATGGAGACCATGTCGCTTGGGATACTTAACCAAGCAAT 180
AHSV1_FJ011116      GCTTGCTGTATCCGCCAGTCAAATGGAGACCATGTCGCTTGGGATACTTAACCAAGCAAT 178
AHSV1_AM883173      GCTTGCTGTATCCGCCAGTCAAATGGAGACCATGTCGCTTGGGATACTTAACCAAGCAAT 179
AHSV1_FJ183373      GCTTGCTGTATCCGCCAGTCAAATGGAGACCATGTCGCTTGGGATACTTAATCAAGCAAT 179
AHSV1_U02711        GCTTGCTGTATCCGCCAGTCAAATGGAGACCATGTCGCTTGGGATACTTAACCAAGCAAT 180
AHSV2_U59279        GCTTGCTGTATCCGCCAGTCAAATGGAGACCATGTCGCTTGGGATACTTAACCAAGCAAT 180
                    ****************************************** ********

AHSV8_U02713        GTCAAGTTCAGCTGGTGCGAGTGGCGCACTTAAGGATGAAAAGGCAGCGTTTGGAGCGGT 240
AHSV8_AJ007307      GTCAAGTTCAGCTGGTGCGAGTGGCGCACTTAAGGATGAAAAGGCAGCGTTTGGAGCGGT 240
AHSV1_FJ011116      GTCAAGTTCAGCTGGTGCGAGCGGAGCACTTAAGGATGAAAAGGCAGCGTTTGGAGCGGT 238
AHSV1_AM883173      GTCAAGTTCAGCTGGTGCGAGCGGAGCACTTAAGGATGAAAAGGCAGCGTTTGGAGCGGT 239
AHSV1_FJ183373      GTCAAGTTCAGCTGGTGCGAGCGGAGCACTTAAGGATGAAAAGGCAGCGTTTGGAGCGGT 239
AHSV1_U02711        GTCAAGTTCAGCTGGTGCGAGCGGAGCACTTAAGGATGAAAAGGCAGCGTATGGAGCGGT 240
AHSV2_U59279        GTCAAGTTCAGCTGGTGCGAGTGGCGCACTTAAGGACGAAAAGGCAGCGTTTGGAGCGAT 240
                    ******************** ** *********** ************* ******* *

AHSV8_U02713        GGCGGAGGCGTTGAGAGATCCGGAGCCGATCAGAAAAATTAAGCGACAAGTAGGTATCCA 300
AHSV8_AJ007307      GGCGGAGGCGTTGAGAGATCCGGAGCCGATCAGAAAAATTAAGCGACAAGTAGGTATCCA 300
AHSV1_FJ011116      GGCAGAGGCGTTGAGAGATCCGGAGCCGATCAGAAAAATTAAGCGACAAGTAGGTATCCA 298
AHSV1_AM883173      GGCAGAGGCGTTGAGAGATCCGGAGCCGATCAGAAAAATTAAGCGACAAGTAGGTATCCA 299
AHSV1_FJ183373      GGCAGAGGCGTTGAGAGATCCGGAGCCGATCAGAAAAATTAAGCGACAAGTAGGTATCCA 299
AHSV1_U02711        GGCAGAGGCGTTGAGAGATCCGGAGCCGATCAGAAAAATTAAGCGACAAGTAGGTATCCA 300
AHSV2_U59279        GGCAGAGGCGTTGAGAGATCCGGAGCCGATCAGAAAAATTAAGCGACAAGTAGGTATCCA 300
                    *** ****************************************************

AHSV8_U02713        AACTCTAAAAACACTGAAAGTTGAATTGAGCGGGATGCGAAGGAAGAAATTGATTTTGAA 360
AHSV8_AJ007307      AACTCTAAAAACACTGAAAGTTGAATTGAGCGGGATGCGAAGGAAGAAATTGATTTTGAA 360
AHSV1_FJ011116      AACTCTAAAAACACTGAAAGTTGAATTGAGCGGGATGCGAAGGAAGAAATTGATTTTGAA 358
AHSV1_AM883173      AACTCTAAAAACACTGAAAGTTGAATTGAGCGGGATGCGAAGGAAGAAATTGATTTTGAA 359
AHSV1_FJ183373      AACTCTAAAAACACTGAAAGTTGAATTGAGCGGGATGCGAAGGAAGAAATTGATTTTGAA 359
AHSV1_U02711        AACTCTAAAAACACTGAAAGTTGAATTGAGCGGGATGCGAAGGAAGAAATTGATTTTGAA 360
AHSV2_U59279        AACTCTAAAAGCATTGAAAGTTGAATTGAGCGGGATGCGAAGGAAGAGATTGATTTTGAA 360
                    ********** ** ******************************** ************

AHSV8_U02713        AATAATTATGTTTATTTGCGCAAACGTAACTATGGCTACTTCTCTAGTTGGAGGTATGTC 420
AHSV8_AJ007307      AATAATTATGTTTATTTGCGCAAACGTAACTATGGCTACTTCTCTAGTTGGAGGTATGTC 420
AHSV1_FJ011116      AATAATTATGTTTATTTGCGCAAACGTAACTATGGCTACTTCTCTAGTTGGAGGTATGTC 418
AHSV1_AM883173      AATAATTATGTTTATTTGCGCAAACGTAACTATGGCTACTTCTCTAGTTGGAGGTATGTC 419
AHSV1_FJ183373      AATAATTATGTTTATTTGCGCAAACGTAACTATGGCTACTTCTCTAGTTGGAGGTATGTC 419
AHSV1_U02711        AATAATTATGTTTATTTGCGCAAACGTAACTATGGCTACTTCTCTAGTTGGAGGTATGTC 420
AHSV2_U59279        AATAATTATGTTTATTTGCGCAAACGTAACTATGGCTACTTCTCTAGTTGGAGGTATATC 420
                    ************************************************************ **

AHSV8_U02713        GATCGTTGATGAGGATATTGCTAAGCATTTGGCGTTTGACGGAAAAGGGGATTGGGTGTC 480
AHSV8_AJ007307      GATCGTTGATGAGGATATTGCTAAGCATTTGGCGTTTGACGGAAAAGGGGATTGGGTGTC 480
AHSV1_FJ011116      AATCGTTGATGAGGATATTGCTAAGCATTTGGCGTTTGACGGAAAAGGGGATTGGGTGTC 478
AHSV1_AM883173      AATCGTTGATGAGGATATTGCTAAGCATTTGGCGTTTGACGGAAAAGGGGATTGGGTGTC 479
AHSV1_FJ183373      AATCGTTGATGAGGATATTGCTAAGCATTTGGCGTTTGACGGAAAAGGGGATTGGGTGTC 479
```

```
AHSV1_U02711        AATCGTTGATGAGGATATTGCTAAGCATTTGGCGTTTGACGGAAAAGGGGATTGGGTGTC 480
AHSV2_U59279        AATCGTTGATGAGGATATTGCTAAGCATTTGGCGTTTGACGGAAAGGGAGATTGGGTGTC 480
                     ****************************************** ** ***********

AHSV8_U02713        AAAAACGGTCCATGGTTTAAATTTGTTATGTACCACAATGCTGCTAGCAGCGAATAAAAT 540
AHSV8_AJ007307      AAAAACGGTCCATGGTTTAAATTTGTTATGTACCACAATGCTGCTAGCAGCGAATAAAAT 540
AHSV1_FJ011116      AAAAACGGTCCATGGTTTAAATTTATTATGTACCACGATGCTGCTGGCAGCGAATAAAAT 538
AHSV1_AM883173      AAAAACGGTCCATGGTTTAAATTTATTATGTACCACGATGCTGCTGGCAGCGAATAAAAT 539
AHSV1_FJ183373      AAAAACGGTCCATGGTTTAAATTTATTATGTACCACGATGCTGCTGGCAGCGAATAAAAT 539
AHSV1_U02711        AAAAACGGTCCATGGTTTAAATTTATTATGTACCACGATGCTGCTGGCAGCGAATAAAAT 540
AHSV2_U59279        AAAAACGGTCCATGGTTTAAATTTGTTATGTACAACGATGCTGTTGGCAGCGAATAAAAT 540
                    ************************ ******** ** ****** * **************

AHSV8_U02713        ATCGGAAAAAGTGAGAGAAGAGATTGCGAGGACAAAAAGAGACATCGCGAAAAGACAATC 600
AHSV8_AJ007307      ATCGGAAAAAGTGAGAGAAGAGATTGCGAGGACAAAAAGAGACATCGCGAAAAGACAATC 600
AHSV1_FJ011116      ATCGGAAAAGGTGAGAGAAGAGATTGCGAGGACAAAAAGAGACATCGCGAAAAGACAATC 598
AHSV1_AM883173      ATCGGAAAAGGTGAGAGAAGAGATTGCGAGGACAAAAAGAGACATCGCGAAAAGACAATC 599
AHSV1_FJ183373      ATCGGAAAAGGTGAGAGAAGAGATTGCGAGGACAAAAAGAGACATCGCGAAAAGACAATC 599
AHSV1_U02711        ATCGGAAAAGGTGAGAGAAGAGATTGCGAGGACAAAAAGAGACATCGCGAAAAGACAATC 600
AHSV2_U59279        ATCGGAAAAGGTGAGAGAAGAGATTGCGAGGACAAAAAGAGACATCGCGAAAAGACAATC 600
                    ********* ************************************************

AHSV8_U02713        GTACGTATCAGCTGCGACGATGTCTTGGGATGGCGATAGCGTAACTCTATTACGAGATGT 660
AHSV8_AJ007307      GTACGTATCAGCTGCGACGATGTCTTGGGATGGCGATAGCGTAACTCTATTACGAGATGT 660
AHSV1_FJ011116      GTACGTATCAGCTGCGACGATGTCTTGGGATGGCGATAGCGTAACTCTATTACGAGATGT 658
AHSV1_AM883173      GTACGTATCAGCTGCGACGATGTCTTGGGATGGCGATAGCGTAACTCTATTACGAGATGT 659
AHSV1_FJ183373      GTACGTATCAGCTGCGACGAAGTCTTGGGATGGCGATAGCGTAACTCTATTACGAGATGT 659
AHSV1_U02711        GTACGTATCAGCTGCGACGATGTCTTGGGATGGCGATAGCGTAACTCAATTACGAGATGT 660
AHSV2_U59279        GTACGTATCAGCTGCGACGATGTCTTGGGATGGCGATAGCGTAACTCCATTACGAGATGT 660
                    ******************** ************************** ************

AHSV8_U02713        AAAATGTGGAGACTAGCGGATAGACCTCCAAAAGCGGGATTCCGCTGGTGTTGCAGTGGA 720
AHSV8_AJ007307      AAAATGTGGAGACTAGCGGATAGACCTCCAAAAGCGGGATTCCGCTGGTGTTGCAGTGGA 720
AHSV1_FJ011116      AAAATATGGAGACTAGCGGATAGACCTCCAAAAGCGGGATTCCACTGGTGTTGCAGTGGA 718
AHSV1_AM883173      AAAATATGGAGACTAGCGGATAGACCTCCAAAAGCGGGATTCCACTGGTGTTGCAGTGGA 719
AHSV1_FJ183373      AAAATATGGAGACTAGCGGATAGACCTCCAAAAGCGGGATTCCACTGGTGTTGCAGTGGA 719
AHSV1_U02711        AAAATATGGAGACTAGCGGATAGACCTCCAAAAGCGGGATTCCACTGGTGTTGCAGTGGA 720
AHSV2_U59279        AAAATATGGAGACTAGCGGATAGACCTCCAAAAGCGGGATTCCGCTGGTGTTGCAGTGGA 720
                    ***** ************************************ ****************

AHSV8_U02713        TAACCGCCTAGATCGTGTTCTAGGGAGCCGGGATAACGACTTAC 764
AHSV8_AJ007307      TAACCGCCTAGATCGTGTTCTAGGGAGCCGGGATAACGACTTAC 764
AHSV1_FJ011116      TAACCGCCTAGATCGTGTTCTAGGGAGCCGGGATAACAACTTAC 762
AHSV1_AM883173      TAACCGCCTAGATCGTGTTCTAGGGAGCCGGGATAACAACTTAC 763
AHSV1_FJ183373      TAACCGCCTAGATCGTGTTCTAGGGAGCCGGGATAACAACTTAC 763
AHSV1_U02711        TAACCGCCTAGATCGTGTTCTAGGGAGCCGGGATAACGACTTAC 764
AHSV2_U59279        TAACCGCCTAGATCGTGTTCTAGGGAGCCGGGATAACGACTTAC 764
                    ************************************ ******
```

Appendix E1

AHSV segment 2 full-length alignment of Clade A (Serotypes 3 and 7)

```
CLUSTAL 2.0.12 multiple sequence alignment (AHSV 100630 FL Seg2 A ST3,7)


AHSV3_U01832          GTTTAATTCACCATGGCTTCGGAATTCGGGATCCTATTGACAAATCAAATATATGATCAA 60
AHSV1_3__Z26316       GTTTAATTCACCATGGCTTCGGAATTCGGGATCCTATTGACAAATCAAATATATGATCAA 60
AHSV3_DQ868772        GTTTAATTCACCATGGCTTCGGAATTCGGGATCTTATTGACAATTCAAATATATGATCAA 60
AHSV7_AY163330        GTTTAATTCACTATGGCTTCTGAGTTTGGAATTTTGTACACTGATCAGATCTACGAACAA 60
                      *********** ******** ** ** ** **  * *  **   *** ** ** ** ***

AHSV3_U01832          ACATATGAGAAAGAGATGTGTGATGTAATTATTACAGCGGAGAATGCAGTTAGAAGAGTT 120
AHSV1_3__Z26316       ACATATGAGAAAGAGATGTGTGATGTAATTATTACAGCGGAGAATGCAGTTAGAAGAGTT 120
AHSV3_DQ868772        ACATATGAGAAAGAGAAGTGCGATGTAATTATTACAGCGGAAAATGCAGTTAGAAGAGTT 120
AHSV7_AY163330        ACATTGGAGAAGACGAGCTGTGACGTGATCGTAACAAAAGAGAATGCTGTAAAGAGGGTC 120
                      ****  *****   **  ** ** ** **  * ***   ** ***** ** *  ** **

AHSV3_U01832          GAGGTTGCGGGAGTACATGGTTATGAGTGGGGTGCGACGAATCATAGGCTTGGGTTGTGT 180
AHSV1_3__Z26316       GAGGTTGCGGGAGTACATGGTTATGAGTGGGGTGCGACGAATCATAGGCTTGGGTTGTGT 180
AHSV3_DQ868772        GAGGTTGCGGGAGTATATGGTTATGAGTGGGGTGCGACGAATCATAGGCTCGGGTTGTGT 180
AHSV7_AY163330        GAAATCGATGGCGTGCTAGGGTATGAGTGGGGCGCAACAAATCACCGATTAGGACTATGC 180
                      **  * *  ** **    ** *********** ** ** *****  *  * **  * **

AHSV3_U01832          GAGGTAGAGAACACGAAGTCGATTGGGAGAATGATTTATGAACAGATTCGATGCGAAGGT 240
AHSV1_3__Z26316       GAGGTAGAGAACACGAAGTCGATTGGGAGAATGATTTATGAACAGATTCGATGCGAAGGT 240
AHSV3_DQ868772        GAGATAGAGAATACGAAGTCGATCGGGAGAATGATTTATGAACAGATTCGATGCGAAGGT 240
AHSV7_AY163330        GAAATAGAACACGTAAAGACGATATCTGAGTTCATGTATGAACAAATTAAATGTGAGGGT 240
                      **  ****  *    *** ****        * ** ******** ***  *** ** ***

AHSV3_U01832          GCGTACCCAATTTTTCCGCACTATATAACGGATACTCTAAAATATGGGAAATCAATTGAT 300
AHSV1_3__Z26316       GCGTACCCAATTTTTCCGCACTATATAACGGATACTCTAAAATATGGGAAATCAATTGAT 300
AHSV3_DQ868772        GCGTACCCAATTTTTCCGCACTATATAACAGATACTTTAAAATATGGGAAATCAATTGAT 300
AHSV7_AY163330        GCATATCCGGTGTTCCCTCATTATGTAATCGATGCCTTAAAATATAACAAAGTTATAGAG 300
                      ** ** **  * ** ** ** *** ***  *** *  ********   ***   ** **

AHSV3_U01832          AGAAATGACAACCAAATAAGGGTGGATAGGGATGATGAACGCGTCCGCAAAATAAAAATT 360
AHSV1_3__Z26316       AGAAATGACAACCAAATAAGGGTGGATAGGGATGATGAACGCGTCCGCAAAATAAAAATT 360
AHSV3_DQ868772        AGAAATGACAACCAAATAAGGGTGGATAGGGACGACGAACGGCTCCGCAAAATAAAAATC 360
AHSV7_AY163330        AGAAATGATAATCAAGTAAGAGTAGATAGAGATGATGAAAGACTACAAAAAATAAAGATC 360
                      ******** ** *** **** ** ***** ** ** *** *  * *  ******** **

AHSV3_U01832          CAGCCGTATTTTGGAGAAATGTACTTTTCACCAGAAAATTATATAACAGTTTTTTGTAAA 420
AHSV1_3__Z26316       CAGCCGTATTTTGGAGAAATGTACTTTTCACCAGAAAATTATATAACAGTTTTTTGTAAA 420
AHSV3_DQ868772        CAGCCGTATTTTGGAGAAATGTACTTCTCACCAGAAAATTATATAACAGTTTTTTGTAAA 420
AHSV7_AY163330        CAACCATATTTTGGAGAAGCGTTCTTCTCGCCGGAGACCTACTCTTCAACTTTTTGCAAA 420
                      ** ** ************  ** *** ** ** ** *  **     **  ****** ***

AHSV3_U01832          AGGCAGGCAATCAGTGGCCAAATTGAGGTTTCTCGTTCAATTATAGGTCGGCGGATGAAG 480
AHSV1_3__Z26316       AGGCAGGCAATCAGTGGCCAAATTGAGGTTTCTCGTTCAATTATAGGTCGGCGGATGAAG 480
AHSV3_DQ868772        AGGCAGGCAATCAGCGGCCAAATTGAGGTTTCTCGTTCAATTATAGGCCGGCGAATGAAG 480
AHSV7_AY163330        AGACAAGCGATTAGAGGGCACGTTGCGAAGATGCGAACGTTTGCAAAGGATAGGATTGAT 480
                      ** ** ** ** ** ** **  *** *      **  *  **  *       * **  *

AHSV3_U01832          TATGAAGAGAGTGCTGAACAGACGAAGGGAACGATAAACGCAAATAAATATCGATTGTTG 540
AHSV1_3__Z26316       TATGAAGAGAGTGCTGAACAGACGAAGGGAACGATAAACGCAAATAAATATCGATTGTTG 540
AHSV3_DQ868772        TATGAAGAGAGCGCTGAACAGACGAAGGGAACGATAAACGCAAATAAATATCGATTGTTG 540
AHSV7_AY163330        TTTGAAGAGAGTAGCGCACAGACGAAAT--ACG-TCAATGGAAATAAGGTTAAGATTTTA 537
                      * *********    * *********    *** * ** * ******   *    * **

AHSV3_U01832          GAGAAGTGGCGCGATCTGGCCTATGAACAAATTGAAATAGAACGTGATAATGAAAGATGT 600
AHSV1_3__Z26316       GAGAAGTGGCGCGATCTGGCCTATGAACAAATTGAAATAGAACGTGATAATGAAAGATGT 600
AHSV3_DQ868772        GAGAAGTGGCGTGATCTGGCTTATGAGCAAATTGAAATGGAAGGTAGTAGTGAAAGGTGT 600
AHSV7_AY163330        GAGGAGTGGAAGGGGCGGACTGATGCTAGAATGTTGATGGAGGGCCAACAAGAGAAGTGC 597
                      *** *****   *  * * *  ***    ***    ** **  *       ** *  **

AHSV3_U01832          TTGACGCATAACACCGACCCGATTTATCAATTGATAAAAAAGATGAGGTATGGAATGATG 660
AHSV1_3__Z26316       TTGACGCATAACACCGACCCGATTTATCAATTGATAAAAAAGATGAGGTATGGAATGATG 660
AHSV3_DQ868772        TTGACGCATAACACTGATCCGATTTATCAATTGATAAAGAAGATGAGGTTTGGAATGATG 660
AHSV7_AY163330        GTTGCACATGAGGTTGATCCGATTTACCAATTGATTAAAAAGATGAGATATGGAATGATG 657
                       *  * *** *    ** ******** ******** ** ******** * **********
```

```
AHSV3_U01832          TATCCAGTGCACTACATGCTAAACGATAGATATAAAGTTGTGCAAGAGCGCGCAGATATG 720
AHSV1_3__Z26316       TATCCAGTGCACTACATGCTAAACGATAGATATAAAGTTGTGCAAGAGCGCGCAGATATG 720
AHSV3_DQ868772        TATCCAGTGCATTACATACTAAACGATAAATACAAGGTCGTACAAGAGCGCGCAGATATG 720
AHSV7_AY163330        TATCCTACGCATTATATGTTGAGCCAGAGATATAGGATTATATCTGAACGTCGAAAAATG 717
                      *****   *** ** **  * * * * * *** *   *  *    ** **   * * ***

AHSV3_U01832          GGGGTTGAAAAGTGGCTTCTTCAAAAAATCGGAAGGGGTACCCAAAGGCGGAAGGCTGAC 780
AHSV1_3__Z26316       GGGGTTGAAAAGTGGCTTCTTCAAAAAATCGGAAGGGGTACCCAAAGGCGGAAGGCTGAC 780
AHSV3_DQ868772        GGGATTGAAAAGTGGCTTCTTCAAAAAATCGGAAGGGGTACCCAAAGGCGGAAGGCTGAC 780
AHSV7_AY163330        GGAATTGAGAAGTGGCTATTGGAGAAAGTTGAAAGGGGAGTACAGAGAGGAGTAGCCGGT 777
                      **  **** ********  *  * *** * * ******    ** **  *    ** *

AHSV3_U01832          GATGGCGATAATGATGCGCTCTTACAGCTAGAAAGAATGATGAGCAGTGAAGAGCTGGAA 840
AHSV1_3__Z26316       GATGGCGATAATGATGCGCTCTTACAGCTAGAAAGAATGATGAGCAGTGAAGAGCTGGAA 840
AHSV3_DQ868772        GATGGCGATAATGATACGCTCTTACAGCTAGAAAGAATGATGAGCAGTGAGGAGCTAGAA 840
AHSV7_AY163330        GCGAAAGGTAATGAATCGTTAGTACGGTTAGAAAAACTGATGCAGAAAGAAGAGCTTGAG 837
                      *     * ******  ** *  *** * ****** * *****   *  ** ***** **

AHSV3_U01832          AGATCCGTTATTGAGAGCGTCATAAGATTCGGTTCTTTATATAACGCGCACGCGGGCAAA 900
AHSV1_3__Z26316       AGATCCGTTATTGAGAGCGTCATAAGATTCGGTTCTTTATATAACGCGCACGCGGGCAAA 900
AHSV3_DQ868772        AGACCCGTTATTGAGAGCGTCATAAGATTCGGTTCCTTATATAACGCGCACGCGGGCAAG 900
AHSV7_AY163330        AATTCTGTGATCGAGAATGTAATACGCTACGGTTCGCAGTTTAGCACACACGCCGGAGAA 897
                      *   * ** ** ****  ** *** * * ******    * ** * * ***** **  *

AHSV3_U01832          AAGACAGGCGACATTCCATTAGAAGTCTTGATTAAATATTGCGATTCGCTTACTACATTC 960
AHSV1_3__Z26316       AAGACAGGCGACATTCCATTAGAAGTCTTGATTAAATATTGCGATTCGCTTACTACATTC 960
AHSV3_DQ868772        AAGACAGGCGACATTCCATTAGAAGTCTTGATAAAATATTGCGATTCGCTTACTACATTC 960
AHSV7_AY163330        AAGACTAATGATATGCCTCTGTCCGTTTTGATAAAATACTGCGAATCATTAACCACTTTT 957
                      *****    ** ** **  *    ** ***** ***** ***** **  * ** ** **

AHSV3_U01832          GTGCATAAAAAGAACAGAGAGGGAGGAGATAATCAGACCGCTCGCGACGAGATTAGGAGG 1020
AHSV1_3__Z26316       GTGCATAAAAAGAACAGAGAGGGAGGAGATAATCAGACCGCTCGCGACGAGATTAGGAGG 1020
AHSV3_DQ868772        GTGCATAAAAAGAACAGAGAGGGAGGAGATAATCAGACCGCTCGCGACGAGATTAGGAGG 1020
AHSV7_AY163330        GTACATAAAAAGAATCGCGAGGGAGGCGATAATCAGACGGCGCGTGATGAGATTAGAAAA 1017
                      ** ***********  * ******** ********** ** ** ** ******** *

AHSV3_U01832          GCAGTGGTAAAGAATATTCCATCGATGAAACAGGAGAATCAGATGAAAGTCACTCCTAAT 1080
AHSV1_3__Z26316       GCAGTGGTAAAGAATATTCCATCGATGAAACAGGAGAATCAGATGAAAGTCACTCCTAAT 1080
AHSV3_DQ868772        GCAATGGTAAAGAATATTCCATCGATGAAGCAGGAAAATCAGATGAAAGTCACTCCAAAT 1080
AHSV7_AY163330        GCTATGGTGCATAATATGCCGACCATGAATCACAACAACCCGATGAAGGTGACGAAGAAC 1077
                      **  ****  * ***** **  * ***** **  * ** * ****** ** **    **

AHSV3_U01832          ATCAGGAATTTTCTGTTTTTCGCATATTTAAACGGTTTTAAAAGGAATAATGGCGTTGAT 1140
AHSV1_3__Z26316       ATCAGGAATTTTCTGTTTTTCGCATATTTAAACGGTTTTAAAAGGAATAATGGCGTTGAT 1140
AHSV3_DQ868772        ATCAGGAATTTTCTGTTTTTCGCATATTTAAACGGTTTTAAAAGGAATAATGGTGTTGAT 1140
AHSV7_AY163330        TTTAAGAACTTTCTCTTTTTCGCGTATTTAGATGGCTTTAAAAGAAATAACGGCGTAGAT 1137
                       * * *** ***** ******** ****** * ** ******** ***** ** ** ***

AHSV3_U01832          ATCGACCCAAATAATGGTACGTGGAGTAAGCATAAAGCGGAAGTTAAGAAGTTTTTGAAC 1200
AHSV1_3__Z26316       ATCGACCCAAATAATGGTACGTGGAGTAAGCATAAAGCGGAAGTTAAGAAGTTTTTGAAC 1200
AHSV3_DQ868772        ATCGACCCAAATAATGGTACGTGGAGTAAGCATAAAACGGAAGTTAAGAAGATTTTGGAC 1200
AHSV7_AY163330        ATTAATCCTAACAATTCGACGTGGATCGAGCATAAGAAGAAGATGGCGGAAAAGCTAAAG 1197
                      **  * ** ** ***   *******   *******   * *  *   * *     *  *

AHSV3_U01832          GAGGAACAAAAGAAGAATGAAAATAAACCATTAAAGGTGTTGATTGATGGCGCGTACATA 1260
AHSV1_3__Z26316       GAGGAACAAAAGAAGAATGAAAATAAACCATTAAAGGTGTTGATTGATGGCGCGTACATA 1260
AHSV3_DQ868772        GAGGAACAAAAGAAGAATGAAAACAAACCATTAAAGGTGTTGATTGATGGCGCGTACATA 1260
AHSV7_AY163330        GATGAGCAACAGAAAAACCAAAATCGTCCGATGCTAGTGCCGATTGATGGTGTCTACGTC 1257
                      ** ** *** **** **  ****    **  *    ***  ********* *  *** *

AHSV3_U01832          TCAACCGATGCTGAGTACGGAACCGTAGCGCATTGGGTGGATTGGGTCGTTGATATCGTA 1320
AHSV1_3__Z26316       TCAACCGATGCTGAGTACGGAACCGTAGCGCATTGGGTGGATTGGGTCGTTGATATCGTA 1320
AHSV3_DQ868772        TCAACTGATGCTGAGTACGGAACCGTAGCGCATTGGGTGGACTGGGTCGTGGATATCATA 1320
AHSV7_AY163330        TCCACTAGTGTTGAGTATGGTACCGTTACACATTGGGTTGATTGGGTCGTTGATATTATA 1317
                      ** **   ** ****** ** *****  * ******** ** ******** *****  **

AHSV3_U01832          ATGATGACTCAAGTTAGCCGCATGATAAAAGAATATAATTTTATTAGATTAAAAAAGGAT 1380
AHSV1_3__Z26316       ATGATGACTCAAGTTAGCCGCATGATAAAAGAATATAATTTTATTAGATTAAAAAAGGAT 1380
AHSV3_DQ868772        ATGACGACTCAAGTTAGCCGCATGATAAAGGAATATAATTTTATTAGATTGAAAAAGGAT 1380
AHSV7_AY163330        ATGACAACGCAGGTTGAAAGAATGATAAAAGAGTATGATTTTAAACGATTGGAGAGAAAA 1377
                      ****  ** ** ***    * ******** ** *** ******   ****  * *   *

AHSV3_U01832          CAGCTAATCAGCGGTATGAATAAGTTGGAGGATGGGGTAAAATGCTACGCGTATTGTTTG 1440
AHSV1_3__Z26316       CAGCTAATCAGCGGTATGAATAAGTTGGAGGATGGGGTAAAATGCTACGCGTATTGTTTG 1440
AHSV3_DQ868772        CAGCTAATCAGCGGTATGAATAAATTAGAGGATGGGGTAAAATGCTACGCGTATTGTTTG 1440
```

```
AHSV7_AY163330       CAGCTAATTAGTGGTATGAACAAGCTCGAGGATGGAGTTAAATGTTATGCTTATTGCTTG 1437
                     ******** ** ******** **  * ******** ** ***** ** ** ***** ***

AHSV3_U01832         ATCCTCGCACTGTACGATTTTCATGGGCGTGACGTAGACGGCTTTGCGCAGGGGACGAGA 1500
AHSV1_3__Z26316      ATCCTCGCACTGTACGATTTTCATGGGCGTGACGTAGACGGCTTTGCGCAGGGGACGAGA 1500
AHSV3_DQ868772       ATCCTCGCATTATATGATTTTCATGGGCGTGAACTAGACGGCTTTGCGCAGGGAACGAGA 1500
AHSV7_AY163330       ATTTTGGCATTGTACGATTATTATGGAGATGCGATCGAGGGTTTCGCGCAAGGAACGCGT 1497
                     **  * *** * ** **** * ****   **   * ** ** ** ***** ** *** *

AHSV3_U01832         ACCGCAGCTATTGTTGAGACCGTCGCGCGAATGTTTCCTGATTTTCGCTCTGAGGTTTCG 1560
AHSV1_3__Z26316      ACCGCAGCTATTGTTGAGACCGTCGCGCGAATGTTTCCTGATTTTCGCTCTGAGGTTTCG 1560
AHSV3_DQ868772       ACCGCGGCTATTGTCGAGACCGTCGCACGAATGTTTCCCGATTTTCGCTCCGAGGTTTCG 1560
AHSV7_AY163330       GCGGGTTCGATTGTCGAGACAATCTCCCAGATGTTCCCTGAGTTCCGTTCAGACGTAGCG 1557
                      * *   * ***** *****  ** * *  ***** ** ** ** ** ** ** **  **

AHSV3_U01832         GAAAAATTCGGTATTGATTTAGCGGTGTCAGAGGAATCAGATGAACTATTCGTAAAGAAG 1620
AHSV1_3__Z26316      GAAAAATTCGGTATTGATTTAGCGGTGTCAGAGGAATCAGATGAACTATTCGTAAAGAAG 1620
AHSV3_DQ868772       GAAAAATTCGGCATTGATTTAGCGGTGTCAGAGGAATCAGATGAATTATTCGTGAAGAAA 1620
AHSV7_AY163330       GAAAAGTTTGGTATTAAACTGACTATAAAGGACGAATCAGAAGAGTTGTTCGTTCAAAAA 1617
                     ***** ** ** *** *  *  *  *    ** ******** **  * *****  * **

AHSV3_U01832         ACGATGGTCTCGAGTTTCTCTGACTCTGGGGAGATGGGTTACAAATTCATATTTGGATGG 1680
AHSV1_3__Z26316      ACGATGGTCTCGAGTTTCTCTGACTCTGGGGAGATGGGTTACAAATTCATATTTGGATGG 1680
AHSV3_DQ868772       ACGATGGTTTCGAGTTTCTCTGACTCTGGGGAGATGGGTTATAAATTCATATTCGGATGG 1680
AHSV7_AY163330       GATATGAATTCGGAGTTTTTGGATGAGGGAGAGATGGGCTATAAATTCGTGTTCGGGTGG 1677
                        ***   ***   ** *  **    ** ******** ** ****** * ** ** ***

AHSV3_U01832         AGGAAAACTGATTTCAAGGTTGAGACTGATTATGGAGAGATAGTTTCTGATGAAGTCCAT 1740
AHSV1_3__Z26316      AGGAAAACTGATTTCAAGGTTGAGACTGATTATGGAGAGATAGTTTCTGATGAAGTCCAT 1740
AHSV3_DQ868772       AGGAAAACTGATTTCAAGGTTGAGACTGATTATGGAGAGATAGTTTCTGACGAAGTTCAT 1740
AHSV7_AY163330       AAAAATACAGATTTTAAAGTACAGAGCAATTATGGCGAGATCGTTTCAGAGGAAGTTGAA 1737
                     *  ** ** ***** ** **  ***   ******* ***** ***** ** *****  *

AHSV3_U01832         CGGTTATATCAAGCAATTTTGGATGGCAAGGAATGGAGTAAAGAGGTTGATGACCCTGAA 1800
AHSV1_3__Z26316      CGGTTATATCAAGCAATTTTGGATGGCAAGGAATGGAGTAAAGAGGTTGATGACCCTGAA 1800
AHSV3_DQ868772       CGGTTATATCAAGCAATTTTGGATGGCAAAGAATGGAGTAAAGAGGTTGATGATCCAGAA 1800
AHSV7_AY163330       AGGTTATTCAAAGTGATTTTGGAAGGTAAGGAGTGGTCAAATGAGGTAGAGGACCCGGAG 1797
                      ******   ***  ******** ** ** ** ***   ** ***** ** ** ** **

AHSV3_U01832         AAATACTTCGTTGATGATTTATATAATAGATGCCCGGAGTCAATATATGTCAGGAACGGA 1860
AHSV1_3__Z26316      AAATACTTCGTTGATGATTTATATAATAGATGCCCGGAGTCAATATATGTCAGGAACGGA 1860
AHSV3_DQ868772       AAATACTTCGTTGATGATTTATATAATAGATGCCCGGAGTCAATATACGTTAGGAACGGA 1860
AHSV7_AY163330       GATTATTTCGTTGATAACTTGTTTAATAAAACACCGGATGCAGTGTTTGAGAGAGACGGA 1857
                      * ** ********* * ** * ***** *   *****  ** * *  *  **  *****

AHSV3_U01832         GTTGATCCTAATAATAAGATAATGATTAAGAAGCGAGGTTTAGTTGGGGAGAGCCAGCG- 1919
AHSV1_3__Z26316      GTTGATCCTAATAATAAGATAATGATTAAGAAGCGAGGTTTAGTTGGGGAGAGCCAGCG- 1919
AHSV3_DQ868772       GTTGATCCTGATAATAAGATAATGATTAAGAAGCGAGGTTTAGTTGGGGAGGGCCAACGG 1920
AHSV7_AY163330       ATGGACGGAAGCAACAGGATTATCGTTAAGAATAAAACTACACTTCGAGAGGGACAACGC 1917
                      * **       ** * *** **  *******   *  *  * ** * *** * ** **

AHSV3_U01832         CATTTTTCTGCGAGATTTGTCTCATATTGGTATGAATTTCAAAAAGTTACTATTGAGGCT 1979
AHSV1_3__Z26316      CATTTTTCTGCGAGATTTGTCTCATATTGGTATGAATTTCAAAAAGTTACTATTGAGGCT 1979
AHSV3_DQ868772       CATTTTTCCGCGAGATTCGTCTCATATTGGTATGAATTTCAAAAAGTTACTATTAAGGCT 1980
AHSV7_AY163330       CATTTTTCAGCTCGTTTTGTTTCGTATTGGTATACGTTTGAGAAGGTGGAGGTTG-GTCG 1976
                     ******** **  * ** ** ** *********   *** * ** **     **  * *

AHSV3_U01832         GAGTTCGAAGCGATTGCACGCACGTGGCGAACATATACAGTATCATGAGATAGATGTTGA 2039
AHSV1_3__Z26316      GAGTTCGAAGCGATTGCACGCACGTGGCGAACATATACAGTATCATGAGATAGATGTTGA 2039
AHSV3_DQ868772       GA-TTCGAAGCGATTGGACGCACGTGGCGAACATACACAGTATCATGAGATAGATGTTGA 2039
AHSV7_AY163330       GGCGATGGCGAGAATCGATATTCATGATCGAGAGACCAAGTTTTCCGAGTTCGATGTCGA 2036
                     *     *  * ** *  *    * **    * * *   *** *   *** * ***** **

AHSV3_U01832         AGATTTCAAACCTTGCGCGATTGCGGAACTTGGATTACATTGCTCAACCTATATTTATCA 2099
AHSV1_3__Z26316      AGATTTCAAACCTTGCGCGATTGCGGAACTTGGATTACATTGCTCAACCTATATTTATCA 2099
AHSV3_DQ868772       AGATTTCAAACCCTGCGCGATTGCGGAACTTGGATTACATTGCTCAACCTATATTTATCA 2099
AHSV7_AY163330       TGACTATAAACCATGTTCAGTGGCGGAAATGGGGCTACATTCATCAACTTATATCTATCA 2096
                      ** *  ***** **  *  * ****** * **  ******  ***** ***** *****

AHSV3_U01832         AGATTTGCTCGTTGGCGCGAACAGAGGTGAATATGTGAAGGATGCGAAGGAGCTCGTCTG 2159
AHSV1_3__Z26316      AGATTTGCTCGTTGGCGCGAACAGAGGTGAATATGTGAAGGATGCGAAGGAGCTCGTCTG 2159
AHSV3_DQ868772       AGATTTGCTCGTTGGCGCGAACAGAGGTGAATATGTGAAGGATGCGAAGGAGCTCGTTTG 2159
AHSV7_AY163330       AGATTTGTTGATAGGCCCAAATAGGGGAGAGCATGTGATTGATGCAAAAGAATTGGTTTG 2156
                     ******* *  * *** * ** ** ** **  ******  ***** ** **  * ** **

AHSV3_U01832         GTTCGATATCGCTAACACAAACTTCAACATCACGCGTCCTTTTGATAGATGCTGGCCTTC 2219
```

```
AHSV1_3__Z26316      GTTCGATATCGCTAACACAAACTTCAACATCACGCGTCCTTTTGATAGATGCTGGCCTTC 2219
AHSV3_DQ868772       GTTCGATATCGCTAACACAAACTACAACATCACGCGTCCCTTTGATAGATGCTGGCCTTC 2219
AHSV7_AY163330       GTATGATATTGCGTTAACAAATTATGGAACAACGCGCTATTTTGATCAGTGTTGGCCATC 2216
                     **  ***** **    ***** *     *  *****    ******   ** ***** **

AHSV3_U01832         TTCTTGCGCGGAGGCTGAGTTATCCTTGAGGTTTCATCTGATTACCAAGATCTTCACGAG 2279
AHSV1_3__Z26316      TTCTTGCGCGGAGGCTGAGTTATCCTTGAGGTTTCATCTGATTACCAAGATCTTCACGAG 2279
AHSV3_DQ868772       TTCTTGCGCGGAGGCTGAGTTATCCTTGAGATTTCATCTGATTACCAAGATCTTCACGAG 2279
AHSV7_AY163330       CTCATGTTCCACCACGGAATTATCAATGAGATATTTTTTGATTACTGAAATCTTTCAGAG 2276
                      ** **  *     * ** *****  **** * *  * *******  * *****   ***

AHSV3_U01832         ATATCGA---GGCGAAAGAACTTCGTTTGTCGATATAATTAATGAGTTGAGTGAGCATGG 2336
AHSV1_3__Z26316      ATATCGA---GGCGAAAGAACTTCGTTTGTCGATATAATTAATGAGTTGAGTGAGCATGG 2336
AHSV3_DQ868772       ATATCGA---GGCGAAAGAACTTCGTTTGTCGATATAATTAATGAGTTGAGTGAGCGAGG 2336
AHSV7_AY163330       ATATAGGACTGACGATAGATCATCTTTTGCGGATATCTTGGAGAGGATGCGTAAGAACGG 2336
                     **** *    * *** *** * ** ****  *****  *  *   * ** ** **   **

AHSV3_U01832         CTACGTGAAACACAATTTCCCGTCATATAAGCATTATTACCTCTCTGTTATTCAGACGGT 2396
AHSV1_3__Z26316      CTACGTGAAACACAATTTCCCGTCATATAAGCATTATTACCTCTCTGTTATTCAGACGGT 2396
AHSV3_DQ868772       CTACGTGAAACACAATTTCCCGTCATATAAGCATTATTACCTCTCTGTCATTCAGACGGT 2396
AHSV7_AY163330       GTATCCCCGTCGCAATTTTCTGACGTATAAACATTATTATGTCGCTGTCATTCAAGAGGT 2396
                      **       * ****** * * * ***** ********  ** **** *****   ***

AHSV3_U01832         TTTTGAGGATCAAAGAGCGATCGATCCGCTTGACTTTTGTGCAATGATTTCACGGAATGA 2456
AHSV1_3__Z26316      TTTTGAGGATCAAAGAGCGATCGATCCGCTTGACTTTTGTGCAATGATTTCACGGAATGA 2456
AHSV3_DQ868772       TTTTGAGGATCAAAGAGCAATCGATCCGCTTGACTTTTGTGCAATGATTTCACGGAATGA 2456
AHSV7_AY163330       ATTTGGTGATCAAAGACCGATCGATGTGTATAGTTTTTGTACCGATATCTTTAAGAAAGA 2456
                      ****  ********* * ******  *  *   ****** *    ** *    *** **

AHSV3_U01832         GACGCGAGAGAGCACGCTCAAGGGATTTAGTATGTTTACTGCAATTGTTAAAAGTGAGAG 2516
AHSV1_3__Z26316      GACGCGAGAGAGCACGCTCAAGGGATTTAGTATGTTTACTGCAATTGTTAAAAGTGAGAG 2516
AHSV3_DQ868772       GACGCGAGAGAGCACGCTCAAGGGATTTAGTATGTTTGCTGCAATTGTTAAGAGTGAGAG 2516
AHSV7_AY163330       GAGGCGCCGAGGGGTTTTGAGTATGTTTCCTACCTTTTCTACCTTAATCAAGAGCGAAAA 2516
                     ** ***     *     * *     ***  **  *** ** *  *  * ** ** ** *

AHSV3_U01832         ACTGATAGATACCCTGTTCTTGAATTTCTTGTTATGGATTGTCTTTGAAATGGAGAATGT 2576
AHSV1_3__Z26316      ACTGATAGATACCCTGTTCTTGAATTTCTTGTTATGGATTGTCTTTGAAATGGAGAATGT 2576
AHSV3_DQ868772       ACTGATAGATACCTTGTTTTTGAATTTCTTGTTATGGATTGTTTTTGAAATGGAGAATGT 2576
AHSV7_AY163330       ATTGATCGATGCTTTATTTCTTAATTTCTTCTTGTGGGTTGTTTTCGAGATGGAAAACGT 2576
                     * **** *** *  * **  * ******** ** *** **** ** ** ***** ** **

AHSV3_U01832         TGATGTGAGCGCTGCTAATAAGAGACATCCATTATTAATATCGCATGAAAAAGGATTACG 2636
AHSV1_3__Z26316      TGATGTGAGCGCTGCTAATAAGAGACATCCATTATTAATATCGCATGAAAAAGGATTACG 2636
AHSV3_DQ868772       TGATGTGAGCGCTGCTAATAAGAGACATCCATTATTAATATCGCATGAGAAAGGATTACG 2636
AHSV7_AY163330       TGACGTAAGTTTTGCAAATAAGCGTCATCCTTTATTGATATCGCACGATAAGGGTTTGCG 2636
                     *** ** **   *** ****** * ***** ***** ******** ** ** ** ** **

AHSV3_U01832         TTTAATTGGCGTAGATTTGTTTAATGGCGCGCTTTCGATTTCCACGGGGGGGGTGGATTCC 2696
AHSV1_3__Z26316      TTTAATTGGCGTAGATTTGTTTAATGGCGCGCTTTCGATTTCCACGGGGGGGGTGGATTCC 2696
AHSV3_DQ868772       TTTAATTGGCGTAGATTTGTTCAATGGCGCGCTTTCGATTTCCACGGGGGGGGTGGATTCC 2696
AHSV7_AY163330       ATTGATTGGTGTAGATTTGTTCAATAGTGCGTTATCCATTTCAATGGGTGGATGGATCCC 2696
                      ** ***** ********** *** * *** * ** ***** * *** ** ***** **

AHSV3_U01832         GTATCTAGAGAGGATATGTTCAGAGGAGAAAGCTCAGAGAAGGTTGAACGCGGATGAACT 2756
AHSV1_3__Z26316      GTATCTAGAGAGGATATGTTCAGAGGAGAAAGCTCAGAGAAGGTTGAACGCGGATGAACT 2756
AHSV3_DQ868772       GTATCTAGAGAGGATATGTTCAGAGGAGAAAGCTCAGAGAAGGTTGAACGCGGATGAACT 2756
AHSV7_AY163330       TTATGTTGAAAGGATATGCCATGCAGATCATGCAGCAAGAAAATTGAATGCGGACGAACT 2756
                      *** * ** ********    *  **  * **    ****  ***** ***** *****

AHSV3_U01832         GAAAATAAAAAGTTGGTTTTTAACGTATTATATGAATCTTTCGTTAGAAAGGAGAGCGGA 2816
AHSV1_3__Z26316      GAAAATAAAAAGTTGGTTTTTAACGTATTATATGAATCTTTCGTTAGAAAGGAGAGCGGA 2816
AHSV3_DQ868772       TAAAATAAAAAGTTGGTTTTTAACGTATTATATGAATCTTTCGTTAGAAAGAAGAGCGGA 2816
AHSV7_AY163330       GAAAATAAAGAGGTGGTTTATAGATTATTATATGGATCTAAGTTTAGATCGACGAGCAGA 2816
                      ******** ** ****** **   ********* ****    *****  *  **** **

AHSV3_U01832         GCCGCGTATGAGCTTTAAGTTCGAAGGGTTAACCACTTGGATCGGCTCAAATTGTGGTGG 2876
AHSV1_3__Z26316      GCCGCGTATGAGCTTTAAGTTCGAAGGGTTAACCACTTGGATCGGCTCAAATTGTGGTGG 2876
AHSV3_DQ868772       GCCGCGTATGAGCTTTAAGTTCGAAGGATTAACCACTTGGATTGGCTCAAATTGTGGTGG 2876
AHSV7_AY163330       GCCGAGAATGAGTTTCAAATATGAAGGACTAGCGACGTGGGTTGGATCGAACTGCGGTGG 2876
                     **** * ***** ** ** *  *****  ** * ** *** * ** ** ** ** *****

AHSV3_U01832         AGTTCGCGATTATGTCGTCCAAGCTCTACCGATGCGGAAACCAAAGCCTGGTTTATTGAT 2936
AHSV1_3__Z26316      AGTTCGCGATTATGTCGTCCAAGCTCTACCGATGCGGAAACCAAAGCCTGGTTTATTGAT 2936
AHSV3_DQ868772       AGTTCGCGATTATGTCGTCCAAGCTCTACCGATGCGGAAACCAAAGCCTGGTTTATTGAT 2936
AHSV7_AY163330       TGTTAGAGACTATATTATCCAGGAGTTGCCAATGCGAAAGCCAAAACCTGGACTTTTAAT 2936
                      *** * ** *** *  **** *   * ** ***** ** ***** *****  * ** **
```

```
AHSV3_U01832          GATAATTTATGGAGACGATGGGGACGCGCGTTGGGTAGAGTGGGCAATGAAGAATTTTAC 2996
AHSV1_3__Z26316       GATAATTTATGGAGACGATGGGGACGCGCGTTGGGTAGAGTGGGCAATGAAGAATTTTAC 2996
AHSV3_DQ868772        GGTAATTTATGGAGACGATGGGGACGCGCGTTGGGTAGAATGGGCAATGAAGAATTTTAC 2996
AHSV7_AY163330        ATTAGTGTATGGAGAAGATGGAGATCCAAAATGGGTTGAGTGGGCGATTAAGGATTTTAC 2996
                        ** * ******** ***** **  *    ***** ** ***** ** *** *******

AHSV3_U01832          AGCGGTTGATGGATCGTTGGGCTTCATTTATATCGATAGACATAAGCTGGTTAACAAGAG 3056
AHSV1_3__Z26316       AGCGGTTGATGGATCGTTGGGCTTCATTTATATCGATAGACATAAGCTGGTTAACAAGAG 3056
AHSV3_DQ868772        AGCGGTTGACGGATCGTTGGGCTTCATTTATATCGATAGACATAAGTTAGTTAATAAGAG 3056
AHSV7_AY163330        TCAAATTGAAGGCTCTCTTGGCTTTATATACATTGATCCGATTTCCGTTGTTAATAAGAG 3056
                           **** ** **  * ***** ** ** ** ***     *    * ***** *****

AHSV3_U01832          TGATTTCCGAGTCAGAGAAATGAAAATATATAACCGAGGACGTTTAGACCGTCTGATATT 3116
AHSV1_3__Z26316       TGATTTCCGAGTCAGAGAAATGAAAATATATAACCGAGGACGTTTAGACCGTCTGATATT 3116
AHSV3_DQ868772        TGATTTCCGAGTCAGAGAAATGAAAATATATAACCGAGGACGTTTAGACCGTCTGATATT 3116
AHSV7_AY163330        TACTTTTCGGACGAGAGAGATGAAGATTTATAATCGAGGAAGGTTAGATAGATTGATTTT 3116
                      *  *** **    ***** ***** ** ***** ****** * *****  *  **** **

AHSV3_U01832          GATATCTAGTGGTCATTATACATTTGGGAATAAGTTTCTAATGTCTAAGCTGCTTGCGAA 3176
AHSV1_3__Z26316       GATATCTAGTGGTCATTATACATTTGGGAATAAGTTTCTAATGTCTAAGCTGCTTGCGAA 3176
AHSV3_DQ868772        GATATCTAGCGGTCATTATACATTTGGGAATAAGTTTCTGATGTCTAAGCTGCTTGCGAA 3176
AHSV7_AY163330        GATATCAAGTGGGAATTACACATTCGGTAATAAGTTCTTATTATCCAAACTGTTATCCAA 3176
                      ****** ** **  **** ***** ** ********  *  * ** ** *** *  * **

AHSV3_U01832          AACTGAATAAGCGGAGTGACTCCCGCTCCATGTGAATCAACT-TAC 3221
AHSV1_3__Z26316       AACTGAATAAGCGGAGTGACTCCCGCTCCATGTGAATCAACT-TAC 3221
AHSV3_DQ868772        AACTGAATAAGCGGAGTGACTCCCGCTCCATGTGAATCAACT-TAC 3221
AHSV7_AY163330        GGCAGAGTAAGCGGTGTGACTACCGCTCCAAGTGAATCAGCCGTAC 3222
                        * ** ******* ****** ******** ******** *  ***
```

Appendix E2

AHSV segment 2 full-length alignment of Clade B (Serotypes 1, 2 and 8)

```
CLUSTAL 2.0.12 multiple sequence alignment(AHSV 100630 FL Seg2 B ST1,2,8)


AHSV1_FJ011108      GTTTATTTCAGCATGGCGTCTGAATTTGGAATTCTATTGACCGAGAGAATCTTTGACGAA 60
AHSV1_AM883165      GTTTATTTCAGCATGGCGTCTGAATTTGGAATTCTATTGACCGAGAGAATCTTTGACGAA 60
AHSV1_AY163329      GTTTATTTCAGCATGGCGTCTGAATTTGGAATTCTATTGACCGAGAGAATCTTTGACGAA 60
AHSV1_FJ183365      GTTTATTTCAGCATGGCGTCTGAATTTGGAATTCTATTGACCGAGAGAATCTTTGACGAA 60
AHSV2_AY163332      GTTTATTTCAGCATGGCGTCTGAATTTGGAATACTTTTCACCGAAAAGATCTATGACCAA 60
AHSV8_DQ868775      GTTTAATTCATCATGGCGTTCGAGTTTGGCATATTACTAACTGAGAAAGTAGAAGGTGAT 60
AHSV8_AY163333      GTTTAATTCATCATGGCGTCGGAGTTTGGCATATTACTAACTGAGAAAGTAGAAGGTGAT 60
                    ***** **** ********  ** ***** **  *  * ** ** *   *    *   *

AHSV1_FJ011108      ACATTGGAAAAAACAAATTGTGATGTTATTATAACCGAGGAGAAGAAAGTAAAACGGAAG 120
AHSV1_AM883165      ACATTGGAAAAAACAAATTGTGATGTTATTATAACCGAGGAGAAGAAAGTAAAACGGAAG 120
AHSV1_AY163329      ACATTGGGAAAAACAAATTGTGATGTTATTATAACCGAGGAGAAGAAAGTAAAACGGAAG 120
AHSV1_FJ183365      ACATTGGAAAAAACAAATTGTGATGTTATTATAACCGAGGAGAAGAAAGTAAAACGGAAG 120
AHSV2_AY163332      ACGTTGGAGAAAACGAATTGTGATGTGATTATCACTGAGGAGAGGAAAGTGAATCGGAGA 120
AHSV8_DQ868775      GCACTGGAAAAGACGAATTGTGAAGTGATAATAACGAAAAACGGGAGAGTGAAACATAAA 120
AHSV8_AY163333      GCACTGGAAAAGACGAATTGTGAAGTGATAATAACGAAAAACGGGAGAGTGAAACATAAA 120
                     *  ***  ** ** ******** ** ** ** **  *  *   ** *** ** *  *

AHSV1_FJ011108      GAGGTCGAGGGAGTGTTGGGTTACGTGTGGGAGGAAACTAACCATAGGTTCGGCTTATGC 180
AHSV1_AM883165      GAGGTCGAGGGAGTGTTGGGTTACGTGTGGGAGGAAACTAACCATAGGTTCGGCTTATGC 180
AHSV1_AY163329      GAGGTCGAGGGAGTGTTGGGTTACGTGTGGGAGGAAACTAACCATAGGTTCGGCTTATGC 180
AHSV1_FJ183365      GAGGTCGAGGGAGTGTTGGGTTACGTGTGGGAGGAAACTAACCATAGGTTCGGCTTATGC 180
AHSV2_AY163332      GAGGTGGAAGGAGTGCGGGGATATGTATGGGAAGAAACAAACCACCGTTTTGGATTATGT 180
AHSV8_DQ868775      GAGGTTGATGGAGTAAAAGGCTATGAGTGGGAATTTACAGACCATAGGCTGGGGCTCTGC 180
AHSV8_AY163333      GAGGTTGATGGAGTAAAAGGCTATGAGTGGGAGTTTACAGACCATAGGCTGGGGCTCTGC 180
                    ***** ** *****    ** ** *  *****    **  ****  *  * **  * **

AHSV1_FJ011108      GAAGGAAATTATGATTTGGCATTTTCAGATACGATGTATTGCCAAACAAAGTGCGACGGA 240
AHSV1_AM883165      GAAGGAAATTATGATTTGGCATTTTCAGATACGATGTATTGCCAAACAAAGTGCGACGGA 240
AHSV1_AY163329      GAAGGAAATTATGATTTGGCATTTTCAGATACGATGTATTGCCAAACAAAGTGCGACGGA 240
AHSV1_FJ183365      GAAGGAAATTATGATTTGGCATTTTCAGATACGATGTATTGCCAAACAAAGTGCGACGGA 240
AHSV2_AY163332      GAGAATTCATTTGACGAAAAAATATCGGAAACCATGTATTGCCAAATTAAGTGTGAAGGT 240
AHSV8_DQ868775      GAAGAGAGTTATCTGATGAAAATGGCGGAGTATGTGTATACGCAAACAAAATGCGAAGGT 240
AHSV8_AY163333      GAAGAGAGTTATCTGATGAAAATGGCGGAGTATGTGTATACGCAAACAAAATGCGAAGGT 240
                    **       * *        * *  * **     *****   ****  ** ** ** **

AHSV1_FJ011108      TCGTATCCAGTATTTCCGCATTATATAATTGATGCTTTAAGATATGGAGTTATGATTGAT 300
AHSV1_AM883165      TCGTATCCAGTATTTCCGCATTATATAATTGATGCTTTAAGATATGGAGTTATGATTGAT 300
AHSV1_AY163329      TCGTATCCAGTATTTCCGCATTATATAATTGATGCTTTAAGATATGGAGTTATGATTGAT 300
AHSV1_FJ183365      TCGTATCCAGTATTTCCGCATTATATAATTGATGCTTTAAGATATGGAGTTATGATTGAT 300
AHSV2_AY163332      GCTTACCCGATCTTTCCACATTATATTGTTGATGCGTTGAGGTATGGTAAGATGATCGAT 300
AHSV8_DQ868775      GCGTATCCGGTGTTTCCGCATTATATTACTGATGTTTTGAAGTATGGTGTCATGGTTGAT 300
AHSV8_AY163333      GCGTATCCGGTGTTTCCGCATTATATTACTGATGTTTTGAAGTACGGTGTCATGGTTGAT 300
                     * ** **  * ***** ********   *****  ** *  ** **    *** * ***

AHSV1_FJ011108      CGGAATGATAATCAAGTAAGAGTTGATCTAGATGACAAGCGATTAATGAAAATTAAGATT 360
AHSV1_AM883165      CGGAATGATAATCAAGTAAGAGTTGATCTAGATGACAAGCGATTAATGAAAATTAAGATT 360
AHSV1_AY163329      CGGAATGATAATCAAGTAAGAGTTGATCTAGATGACAAGCGATTAATGAAAATTAAGATT 360
AHSV1_FJ183365      CGGAATGATAATCAAGTAAGAGTTGATCTAGATGACAAGCGATTAATGAAAATTAAGATT 360
AHSV2_AY163332      AGAAATGATAACCAGGTTAGGGTTGATCAGGATGACAAGCGATTGATGAAAATTAAAATT 360
AHSV8_DQ868775      AGGAATGATCACCAAATAAGAGTGGATAGGGATGTGAAAGAGTTAGGAAAGATTTTGATC 360
AHSV8_AY163333      AGGAATGATCACCAAATAAGAGTGGATAGGGACGTGAAAGAATTAGGAAAGATTTTGATC 360
                     * ****** * **  * ** ** ***   ** *  **    **    ** ***   **

AHSV1_FJ011108      CAGCCGTATTTGGGTGAAATGTATTTTTCGCCGGAGAACTATTCAACTGTATTTTGCAAA 420
AHSV1_AM883165      CAGCCGTATTTGGGTGAAATGTATTTTTCGCCGGAGAACTATTCAACTGTATTTTGCAAA 420
AHSV1_AY163329      CAGCCGTATTTGGGTGAAATGTATTTTTCGCCGGAGAACTATTCAACTGTATTTTGCAAA 420
AHSV1_FJ183365      CAGCCGTATTTGGGTGAAATGTATTTTTCGCCGGAGAACTATTCAACTGTATTTTGCAAA 420
AHSV2_AY163332      CAGCCGTATATGGGTGAAATGTATTTCTCACCCGAGAGCTATTCTACCGTTTTCTGTAAG 420
AHSV8_DQ868775      CAACCGTACTTTGGAGAGGTGTTCTTTTCACCTGAGTTTTATACATCGACCTTTTTGAAA 420
AHSV8_AY163333      CAACCGTACTTTGGAGAGGTGTTCTTTTCACCTGAGTTTTATACATCGACCTTTTTGAAA 420
                    ** *****  * ** **  ***  ** ** ** ***   *** *  *    ** *  **

AHSV1_FJ011108      AGGCAAGCGCTGGCACTTGGAGTTGACGATCTAAGACATTCTGTT--GATGTAAG-GAAT 477
AHSV1_AM883165      AGGCAAGCGCTGGCACTTGGAGTTGACGATCTAAGACATTCTGTT--GATGTAAG-GAAT 477
```

```
AHSV1_AY163329      AGGCAAGCGCTGGCACTTGGAGTTGACGATCTAAGACATTCTGTT--GATGTAAG-GAAT 477
AHSV1_FJ183365      AGGCAAGCGCTGGCACTTGGAGTTGACGATCTAAGACATTCTGTT--GATGTAAG-GAAT 477
AHSV2_AY163332      AGACAAGCAGAGCTCATGTCAATTGAAGATCTAAGGTATCCATTT--GATATAAG-ATGC 477
AHSV8_DQ868775      AGACAAGCGATTAATAGTGATGTTGAGATGTTGAGGAGATCGATTCCGAAACGGATAAAA 480
AHSV8_AY163333      AGACAAGCGATTAATAGTGATGTTGAGATGTTGAGGAGATCGATTCCGAAACGGATAAAA 480
                    ** *****              ****     * **     *  **  **

AHSV1_FJ011108      GAGTTCGAAGAAACGAATCACCAAACGAAAGGTGTGTTGAATGGAAATAAACAGAGAGCG 537
AHSV1_AM883165      GAGTTCGAAGAAACGAATCACCAAACGAAAGGTGTGTTGAATGGAAATAAACAGAGAGCG 537
AHSV1_AY163329      GAGTTCGAAGAAACGAATCACCAAACGAAAGGTGTGTTGAATGGAAATAAACAGAGAGCG 537
AHSV1_FJ183365      GAGTTCGAAGAAACGAATCACCAAACGAAAGGTGTGTTGAATGGAAATAAACAGAGAGCG 537
AHSV2_AY163332      GACTTCGAAGAAACTTCGTTCCAAACGAAATCCTCTTTAGATGGTAAGAAGCTTAGATTA 537
AHSV8_DQ868775      TACTTTGAAGACCAGATGGAGTTAAGGAAAAGCG---TAAACGGAAATTGGATCGGTACG 537
AHSV8_AY163333      TACTTTGAAGATCAGATGGAGTTAAGGAAAAGCG---TAAATGGAAATTGGATCGGTACG 537
                     * ** *****            ** ****       *  * ** **        *

AHSV1_FJ011108      CTTGAAGTTTGGAAGGAAATGGCGTATCAACGGATGCGTAAGGAGGGATCGCGGGGTAG- 596
AHSV1_AM883165      CTTGAAGTTTGGAAGGAAATGGCGTATCAACGGATGCGTAAGGAGGGATCGCGGGGTAG- 596
AHSV1_AY163329      CTTGAAGTTTGGAAGGAAATGGCGCATCAACGGATGCGTAAGGAGGGATCGCGGGGTAG- 596
AHSV1_FJ183365      CTTGAAGTTTGGAAGGAAATGGCGTATCAACGGATGCGTAAGGAGGGATCGCGGGGTAG- 596
AHSV2_AY163332      TTGGAAAAATGGAAACGGGCTTCGCAAGAACGCATGCACGAAGAAAACGACCGTGGAAA- 596
AHSV8_DQ868775      TTACACAAATGGAAAGAGAGCGTAGATGCGCGTATGTTAGAGGAGGGAGTGGGAAAGAAA 597
AHSV8_AY163333      TTACACAAATGGAAAGAGAGCGTAGATGCGCGTATGTTAGAGGAGGGAGTGGGAAAGAGA 597
                     *  *    *****           *    ** ***    * **        *    *

AHSV1_FJ011108      --ATGTATCGGACACGATGATGATGTAATGTACCAACTGATAAAGAAATTGAGATATGGG 654
AHSV1_AM883165      --ATGTATCGGACACGATGATGATGTAATGTACCAACTGATAAAGAAATTGAGATATGGG 654
AHSV1_AY163329      --ATGTATCGGACACGATGATGATGTAATGTACCAACTGATAAAGAAATTGAGATATGGG 654
AHSV1_FJ183365      --ATGTATCGGACACGATGATGATGTAATGTACCAACTGATAAAGAAATTGAGATATGGG 654
AHSV2_AY163332      --GTGTGCTGGTCACGACGAAGATGTGTTGTATCAATTAGTTAAGAAATTAAGGTATGGC 654
AHSV8_DQ868775      GTGTGTGTAAGCCACGAAACTGATGTGGTATATCAGCTAATGAAAAAGATGCGGTTTGGT 657
AHSV8_AY163333      GTGTGTGTAAGCCACGAAACTGACGTGGTATATCAGCTAATGAAAGAGATGCGGTTTGGT 657
                       ***    * *****    ** **  * ** **  *  * **  *  *  * * ***

AHSV1_FJ011108      ATGATGTATCCTCATCATTACGCATTGAATGCTCGATATGAGGTTTCAAACCCAAGCGCG 714
AHSV1_AM883165      ATGATGTATCCTCATCATTACGCATTGAATGCTCGATATGAGGTTTCAAACCCAAGCGCG 714
AHSV1_AY163329      ATGATGTATCCTCATCATTACGCATTGAATGCTCGATATGAGGTTTCAAACCCAAGCGCG 714
AHSV1_FJ183365      ATGATGTATCCTCATCATTACGCATTGAATGCTCGATATGAGGTTTCAAACCCAAGCGCG 714
AHSV2_AY163332      CTACTGTATCCACATAGCTATACCCTTAACACGAAATATAAAATTGTCAACCCAAGCGTT 714
AHSV8_DQ868775      CTATTATACCCCCATTATTATATGCTAAACAATGAGTATGTAGTGAAGAAAGAGAATGTT 717
AHSV8_AY163333      CTATTATACCCCCATTATTATATGCTAAACAATGAGTATGTAGTGAAGAAAGAGAATGTT 717
                     *  * ** ** ***   **     * **       ***    *    **    *  *

AHSV1_FJ011108      G---CACGGATTAAAGATTGGCTGTTGAAGGTAAGGGTTAATGTAGGGAGGGCAC---AG 768
AHSV1_AM883165      G---CACGGATTAAAGATTGGCTGTTGAAGGTAAGGGTTAATGTAGGGAGGGCAC---AG 768
AHSV1_AY163329      G---CACGGATTAAAGATTGGCTGTTGAAGGTAAGGGTTAATGTAGGGAGGGCAC---AG 768
AHSV1_FJ183365      G---CACGGATTAAAGATTGGCTGTTGAAGGTAAGGGTTAATGTAGGGAGGGCAC---AG 768
AHSV2_AY163332      T---CACAGATTAAGGACTGGCTGTTAAAAACAAGGGATGGTATTAGAGAAGAAT---CT 768
AHSV8_DQ868775      GACGCGTTAATTGGTAGTTGGTTGATCAAGGAGAGATCGAGTGGAAAGGCAGAGTACTCC 777
AHSV8_AY163333      GACGCGTTAATTGGTAGTTGGTTGATCAAGGAGAGATCGAGTGGAAAGGCAGAGTACTCC 777
                        *    ***      *** ** * **    **      *         *

AHSV1_FJ011108      GAGAAAGCTGATCAAACAGGCCCGCTCGCCGAGATGGCTAGATCAATTGAAAACGATGAA 828
AHSV1_AM883165      GAGAAAGCTGATCAAACAGGCCCGCTCGCCGAGATGGCTAGATCAATTGAAAACGATGAA 828
AHSV1_AY163329      GAGAAAGCTGATCAAACAGGCCCGCTCGCCGAGATGGCTAGATCAATTGAAAACGATGAA 828
AHSV1_FJ183365      GAGAAAGCTGATCAAACAGGCCCGCTCGCCGAGATGGCTAGATCAATTGAAAACGATGAA 828
AHSV2_AY163332      GGAATATCAGATAAGCAGGGACCATTAGCGGAGTTGGTGAGTGCAATCAAAGACGAGGAG 828
AHSV8_DQ868775      CAGATGTATTCAGGGGTGGGACCGCTTAGTGGGTTACGCGAACGTATCGAAAAGGATGAG 837
AHSV8_AY163333      CAGATGTATTCAGGGGTAGGACCGCTTAGTGGGTTACGCGAACGTATTGAAAAGGATGAG 837
                       *             ** **  *    * * *          **  ** * ** **

AHSV1_FJ011108      TTAAGCCGTCAAGTGGTTGACCAAATTATACAATATGGTGGACAATTTAGTTCATGCTCA 888
AHSV1_AM883165      TTAAGCCGTCAAGTGGTTGACCAAATTATACAATATGGTGGACAATTTAGTTCATGCTCA 888
AHSV1_AY163329      TTAAGCCGTCAAGTGGTTGACCAAATTATACAATATGGTGGACAATTTAGTTCATGCTCA 888
AHSV1_FJ183365      TTAAGCCGTCAAGTGGTTGACCAAATTATACAATATGGTGGACAATTTAGTTCATGCTCA 888
AHSV2_AY163332      CTAAGTCGGGGAGTAATTGGGCGGATCGTACAATATGGCTCGCAATTTAGTTCGTGTGCA 888
AHSV8_DQ868775      TTGGACGAAAAAGTTATTCAAGAGATTATCGCCTATGGCTCAAAATTTAGCACATATACA 897
AHSV8_AY163333      TTGGATGAAAAAGTTATTCAAGAGATTATTGCCTATGGCTCAAAATTTAGCACATATACA 897
                     *         ***  **      **  *    *****     *******  * *   **

AHSV1_FJ011108      GGCGCACGTGAAGATGATATTCCGATAAATATTTTGTTGGAGTATTGTGAGTCCTTAACA 948
AHSV1_AM883165      GGCGCACGTGAAGATGATATTCCGATAAATATTTTGTTGGAGTATTGTGAGTCCTTAACA 948
AHSV1_AY163329      GGCGCACGTGAAGATGATATTCCGATAAATATTTTGTTGGAGTATTGTGAGTCCTTAACA 948
AHSV1_FJ183365      GGCGCACGTGAAGATGATATTCCGATAAATATTTTGTTGGAGTATTGTGAGTCCTTAACA 948
AHSV2_AY163332      GGGGAACGAGAAGATGATATCCCGATCGAAACATTGATTCGTTACTGCGACTCGCTGACG 948
AHSV8_DQ868775      GGTGCCAAGCACGGTGATATATCGCTAAAAGACTTAGTTGAGTATTGTGAAAGTTTAACC 957
```

```
AHSV8_AY163333      GGTACCAAGCGCGGTGATATATCGCTAAAAAACTTAGTTGAGTATTGTGAAAGTTTGACC 957
                    **          * ******  ** *  *    **  *    ** ** **     * **

AHSV1_FJ011108      ACATTTGTTCACAGAAAGAAGAGAAAGGAGGGGGATGATCTCACTGCACGCAATACCTTT 1008
AHSV1_AM883165      ACATTTGTTCACAGAAAGAAGAGAAAGGAGGGGGATGATCTCACTGCACGCAATACCTTT 1008
AHSV1_AY163329      ACATTTGTTCACAGAAAGAAGAGAAAGGAGGGGGATGATCTCACTGCACGCAATACCTTT 1008
AHSV1_FJ183365      ACATTTGTTCACAGAAAGAAGAGAAAGGAGGGGGATGATCTCACTGCACGCAATACCTTT 1008
AHSV2_AY163332      ACATTTGTTCATCGAAAGAAGAGAGAACGAGGCGATGATACCACAGCGCGTGACGTCTTC 1008
AHSV8_DQ868775      ACATTCGTACAC---AAGAAGAAAAAAGATGGTGAGGAGGAAACCGCACGACAGTTTTTT 1014
AHSV8_AY163333      ACATTCGTACAC---AAGAAGAAAAAAGATGGTGAGGAGGAAACCGCACGACAGTTTTTT 1014
                    ***** ** **    ******* * *    ** ** **    ** ** **  *    **

AHSV1_FJ011108      CGGCAGGCGCTGATTAAGAGTATGCCAACCATGAATTTCAAGAATCAAATGAAAATGAC- 1067
AHSV1_AM883165      CGGCAGGCGCTGATTAAGAGTATGCCAACCATGAATTTCAAGAATCAAATGAAAATGAC- 1067
AHSV1_AY163329      CGGCAGGCGCTGATTAAGAGTATGCCAACCATGAATTTCAAGAATCAAATGAAAATGAC- 1067
AHSV1_FJ183365      CGGCAGGCGCTGATTAAGAGTATGCCAACCATGAATTTCAAGAATCAAATGAAAATGAC- 1067
AHSV2_AY163332      AGAAATGCCTTAGTTGGAAGTATGCCTAAAATGGACTTCAAGAATCAAATGAAGATGGCC 1068
AHSV8_DQ868775      AAAAACAAGTGGATACAGGGGATGCCCAAGATGAATTTTGAAAGTGAGATGAAGGTATCT 1074
AHSV8_AY163333      AAAAACAAGTGGATACAGGGGATGCCCAAGATGAATTTTGAAAGTGAGATGAAGGTGTTT 1074
                        *       *     * ***** *  *** * **  * * * * *****  *

AHSV1_FJ011108      -GAGAGGGTGGGGAAATTATAC-ATTTTTCTCATATATTGATAGATTCAGTCGTATTTAT 1125
AHSV1_AM883165      -GAGAGGGTGGGGAAATTATAC-ATTTTTCTCATATATTGATAGATTCAGTCGTATTTAT 1125
AHSV1_AY163329      -GAGAGGGTGGGGAAATTATAC-ATTTTTCTCATATATTGATAGATTCAGTCGTATTTAT 1125
AHSV1_FJ183365      -GAGAGGGTGGGGAAAATATAC-ATTTTTCTCATATATTGATAGATTCAGTCGTATTTAT 1125
AHSV2_AY163332      AAAGAGGGTGGGGCAACTATACCGTTCTTTTCATACATTGATAGGTTTAGCCGGACTTAC 1128
AHSV8_DQ868775      CGCGGACCATGGGCTAACATTCAATTCTTCTGGAGCATTGATATGTTTAAAAGAAACAAT 1134
AHSV8_AY163333      CGCGGACCATGGGCTAACATTCAATTCTTCTGGAGCATTGATATGTTTAAAAGAAACAAT 1134
                       *      ***  *  ** *  ** ** *     *******  ** *   * *   *

AHSV1_FJ011108      AATATGAATATTGATCCGAATGGTAAGCTTTGGATTGAACATAAACAAACGGTGAGTGAG 1185
AHSV1_AM883165      AATATGAATATTGATCCGAATGGTAAGCTTTGGATTGAACATAAACAAACGGTGAGTGAG 1185
AHSV1_AY163329      AATATGAATATTGATCCGAATGGTAAGCTTTGGATTGAACATAAACAAACGGTGAGTGAG 1185
AHSV1_FJ183365      AATATGAATATTGATCCGAATGGTAAGCTTTGGATTGAACATAAACAAACGGTGAGTGAG 1185
AHSV2_AY163332      AAGATGAATATTGACCCGAATAAGGGTTTATGGAACGAACACAAACAAAAAGTGAAGAAA 1188
AHSV8_DQ868775      GGAGTGGATATAGATCCCAACGGCGAAAACTGGAAAAAATATAAGGCGGAAGTCCAAGAA 1194
AHSV8_AY163333      GGGGTGGATATAGATCCGAACGGCGAAAATTGGAAAAAATATAAGGCGGAAGTCCAAGAA 1194
                        ** **** ** ** **          ****   ** * **       **     *

AHSV1_FJ011108      CAGTTGAAAAAGAAACAAGAGGAGAACCGA---GCGCCTCTAACCGTTCAAATTGATGGG 1242
AHSV1_AM883165      CAGTTGAAAAAGAAACAAGAGGAGAACCGA---GCGCCTCTAACCGTTCAAATTGATGGG 1242
AHSV1_AY163329      CAGTTGAAAAAGAAACAAGAGGAGAACCGA---GCGCCTCTAACCGTTCAAATTGATGGG 1242
AHSV1_FJ183365      CAGTTGAAAAAGAAACAAGAGGAGAACCGA---GCGCCTCTAACCGTTCAAATTGATGGG 1242
AHSV2_AY163332      CAATTAGAAGAAAAACAGGAAGAGAATGGG---TCTCCCATGTCCGTTCAGATCGATGGG 1245
AHSV8_DQ868775      CGTTTGAATGAAGCGCAGAAGAAGAATCGAAATGTTCCTCATTTAATGCTTGTTGATGGA 1254
AHSV8_AY163333      CGTTTGAATGAAGCGCAGAAGAAGAATGGAGGTGTTCCTCATTTAATGCTTGTTGATGGA 1254
                    *  **  *  *    **  *  ****  *       **        * *   * *****

AHSV1_FJ011108      GTGCACATACGTACGGATGAAACCTATGGAACAGTAGATCATTGGGTTGAATGGGTCGTT 1302
AHSV1_AM883165      GTGCACATACGTACGGATGAAACCTATGGAACAGTAGATCATTGGGTTGAATGGGTCGTT 1302
AHSV1_AY163329      GTGCACATACGTACGGATGAAACCTATGGAACAGTAGATCATTGGGTTGAATGGGTCGTT 1302
AHSV1_FJ183365      GTGCACATACGTACGGATGAAACCTATGGAACAGTAGATCATTGGGTTGAATGGGTCGTT 1302
AHSV2_AY163332      GTTTATATCCGAACAGATGTGCCGTATGGAACGGTTGATCATTGGGTTGATTGGGTTGTT 1305
AHSV8_DQ868775      GTGAATATTATGACAGATAAAAAATATGGGACCGTTCAAAATTGGGTTGATTGGGTCGTG 1314
AHSV8_AY163333      GTGAATATTATGACAGATAAAAAATACGGGACCGTTCAAAATTGGGTTGATTGGGTCGTG 1314
                    **  * **    ** ***      ** ** ** **  *  ********** ***** **

AHSV1_FJ011108      GACACAATCATGCTTAGAGAGACTGAAAAAATGATTAAGGATTATCGGTTCAAAAAACTT 1362
AHSV1_AM883165      GACACAATCATGCTTAGAGAGACTGAAAAAATGATTAAGGATTATCGGTTCAAAAAACTT 1362
AHSV1_AY163329      GACACAATCATGCTTAGAGAGACTGAAAAAATGATTAAGGATTATCGGTTCAAAAAACTT 1362
AHSV1_FJ183365      GACACAATCATGCTTAGAGAGACTGAAAAAATGATTAAGGATTATCGGTTCAAAAAACTT 1362
AHSV2_AY163332      GACACAATCATGCTTAAGGAGACTGACAAAATGATAAAGGATTACGAATTTAAGAAATTA 1365
AHSV8_DQ868775      AATTATATCATGTTATCGCACGTGAAACGTTTAGTTAAGGATTATAAATTTAAAAGATTG 1374
AHSV8_AY163333      AATTATATCATGTTATCGCACGTGAAACGTTTAGTTAAGGATTATAAATTTAAAAAACTG 1374
                     *    ****** *     *     *     *  * ********    ** ** * * *

AHSV1_FJ011108      AAGCGTGAGGAGCTGATCTCTGGAATGAATAAATTAGAGGATGGCTTACGATGTATCGTG 1422
AHSV1_AM883165      AAGCGTGAGGAGCTGATCTCTGGAATGAATAAATTAGAGGATGGCTTACGATGTATCGTG 1422
AHSV1_AY163329      AAGCGTGAGGAGCTGATCTCTGGAATGAATAAATTAGAGGATGGCTTACGATGTATCGTG 1422
AHSV1_FJ183365      AAACGTGAGGAGCTGATCTCTGGAATGAATAAATTAGAGGATGGCTTACGATGTATCGTG 1422
AHSV2_AY163332      AAACGTGAAGAATTGATAGCTGGTATGAACAAGTTGGAGGATGGTTTGAGATGCATTGTT 1425
AHSV8_DQ868775      CAACCGGATAATTTGATGTCAGGCATGAATAAGCTTGTAGGTGCGTTGAGGTGTTACGCA 1434
AHSV8_AY163333      CAACCGGATAATTTGATGTCAGGCATGAATAAGCTTGTAGGTGCGTTGAGGTGTTACGCA 1434
                     * *  **  *  ****  * ** ***** **  * *  * **  **  * **    *

AHSV1_FJ011108      TATTGCTTAATACTTGCTCTATACGATTATTATGAAGGAGATATCGAGGGTTTTAAGAAG 1482
```

```
AHSV1_AM883165      TATTGCTTAATACTTGCTCTATACGATTATTATGAAGGAGATATCGAGGGTTTTAAGAAG 1482
AHSV1_AY163329      TATTGCTTAATACTTGCTCTATACGATTATTATGAAGGAGATATCGAGGGTTTTAAGAAG 1482
AHSV1_FJ183365      TATTGCTTAATACTTGCTCTATACGATTATTATGAAGGAGATATCGAGGGTTTTAAGAAG 1482
AHSV2_AY163332      TATTGCTTGATTTTAGCGTTATATGATTATTATGGGGCTGAGATTGAGGGATTCAAAAAG 1485
AHSV8_DQ868775      TATTGCTTAATCCTTGCGTTGTATGATCATTTCGGAGCGGAAATCGAAGGATTTAGGAAG 1494
AHSV8_AY163333      TATTGCCTAATCCTTGCGTTGTATGATCATTTCGGAGCGGAAATTGAAGGATTTAGGAAG 1494
                    ****** * **  * **  * ** *** ***  *  *  ** ** ** ** ** *  ***

AHSV1_FJ011108      GGGACTATTGCTTCGTCAATAGTTGAGACCGTTTCACAGATGTTTCCAAATTTTCGAAGC 1542
AHSV1_AM883165      GGGACTATTGCTTCGTCAATAGTTGAGACCGTTTCACAGATGTTTCCAAATTTTCGAAGC 1542
AHSV1_AY163329      GGGACTATTGCTTCGTCAATAGTTGAGACCGTTTCACAGATGTTTCCAAATTTTCGAAGC 1542
AHSV1_FJ183365      GGGACTATTGCTTCGTCAATAGTTGAGACCGTTTCACAGATGTTTCCAAATTTTCGAAGC 1542
AHSV2_AY163332      GGGACAAACGCTTCATCTATAGTTGAGACTGTATCACAAATGTTCCCAAACTTCCGTGGA 1545
AHSV8_DQ868775      GGGACTAACGCAGCTTCGATAGTTGAAACAGTTTCCCAGATGTTTCCAAATTTCAGAAAG 1554
AHSV8_AY163333      GGGACTAACGCAGCTTCGATAGTTGAAACAGTTTCCCAAATGTTTCCAAATTTCAGAAAG 1554
                    ***** *  **  * ** ******** ** ** ** ** ***** *****  **  *

AHSV1_FJ011108      GATATAATAGATAAATTCGGTATTTCTCTGAAAGTTAAAACTGAGGCCGAAGAATTGTTT 1602
AHSV1_AM883165      GATATAATAGATAAATTCGGTATTTCTCTGAAAGTTAAAACTGAGGCCGAAGAATTGTTT 1602
AHSV1_AY163329      GATATAATAGATAAATTCGGTATTTCTCTGAAAGTTAAAACTGAGGCCGAAGAATTGTTT 1602
AHSV1_FJ183365      GATATAATAGATAAATTCGGTATTTCTCTGAAAGTTAAAACTGAGGCCGAAGAATTGTTT 1602
AHSV2_AY163332      GATATCATCGACAAATTTGGCATACAGCTGAAGGTGAAAAGGGAAGCTGAGGAGTTGTTC 1605
AHSV8_DQ868775      GAAGTTTCGGAAACTTTTGGCATCGATCTCAAAACAAAAGAGATTAAGCACGAACTTTTC 1614
AHSV8_AY163333      GAGGTTTCGGAAACTTTTGGCATCGATCTCAAAACAAAAGAGATTAAGCACGAACTTTTC 1614
                    **  *    ** *  ** ** **    ** **    ***          * **  * **

AHSV1_FJ011108      CTACCCAAGAATATGAAGTCATCTATGAATGTCGGGGAAGAGAGAGGATACAAGTATAAG 1662
AHSV1_AM883165      CTACCCAAGAATATGAAGTCATCTATGAATGTCGGGGAAGAGAGAGGATACAAGTATAAG 1662
AHSV1_AY163329      CTACCCAAGAATATGAAGTCATCTATGAATGTCGGGGAAGAGAGAGGATACAAGTATAAG 1662
AHSV1_FJ183365      CTACCCAAGAATATGAAGTCATCTATGAATGTCGGGGAAGAGAGAGGATACAAGTATAAG 1662
AHSV2_AY163332      CTTCCGAAGGATATGGTATCATCTTTTCTAGAGGATGGCGAAGAGGGATATAAATATCAA 1665
AHSV8_DQ868775      AAAGCTCAAAATATGAATGTTAAAGCGGCTGATGTTGGAGATTACGGATACAAGTTTCAG 1674
AHSV8_AY163333      AAAGCTCAAAATATGAATGTTAAAGCGGCTGATGTTGGAGATTACGGATACAAGTTTCAG 1674
                        *  *  *****               *  *  *  **    ***** ** * * *

AHSV1_FJ011108      TTTGGGTGGAAGGATAATGAGGAGAGAGTGATGAGTGATTACGGGGAAATTTTGACTGAA 1722
AHSV1_AM883165      TTTGGGTGGAAGGATAATGAGGAGAGAGTGATGAGTGATTACGGGGAAATTTTGACTGAA 1722
AHSV1_AY163329      TTTGGGTGGAAGGATAATGAGGAGAGAGTGATGAGTGATTACGGGGAAATTTTGACTGAA 1722
AHSV1_FJ183365      TTTGGGTGGAAGGATAATGAGGAGAGAGTGATGAGTGATTACGGGGAAATTTTGACTGAA 1722
AHSV2_AY163332      TACGGTTGGAAAGATAATGAAGAATTAGTGGCAAGCGATTATGGTGAAATTTTGACTCAG 1725
AHSV8_DQ868775      TACGGGTGGACTCGAACAGCGGAGCAAGTAATGAGTGATTATGGAGAAATATTGACTGAA 1734
AHSV8_AY163333      TACGGGTGGACTCGAACAGCGGAGCAGGTAATGAGTGATTACGGAGAAATATTGACTGAA 1734
                    *  ** ****     *  *  **    **    ** ***** ** ***** ****** *

AHSV1_FJ011108      TCGGTGGAGATCCTATTTAAGAAGCTTCTTAAGGGAGAAAAGTGGAAGATTATCGTTGAT 1782
AHSV1_AM883165      TCGGTGGAGATCCTATTTAAGAAGCTTCTTAAGGGAGAAAAGTGGAAGATTATCGTTGAT 1782
AHSV1_AY163329      TCGGTGGAGATCCTATTTAAGAAGCTTCTTAAGGGAGAAAAGTGGAAGATTATCGTTGAT 1782
AHSV1_FJ183365      TCGGTGGAGATCCTATTTAAGAAGCTTCTTAAGGGAGAAAAGTGGAAGATTATCGTTGAT 1782
AHSV2_AY163332      TCAGTACAAATTCTGTTCGAAGGATTGATGAGAGGGGAGAAGTGGACTTCGATTATAGAT 1785
AHSV8_DQ868775      GAAATTGAAACGCTATATCAATCCATTTTAGCAGGCAAAGAATGGGAAAAGGTTTCTGAT 1794
AHSV8_AY163333      GAAATTGAAACGTTATATCAATCAATTTTAGCAGGCAAAGAATGGGGAAAGGTTTCTGAT 1794
                        *  * *   * *   *     *  *    **  *  * ***       *    ***

AHSV1_FJ011108      GATCCGCAAACTTACTTCGAAGATGACTTGTTCGTTGATCGGGCGAACAAGATTTTCTCT 1842
AHSV1_AM883165      GATCCGCAAACTTACTTCGAAGATGACTTGTTCGTTGATCGGGCGAACAAGATTTTCTCT 1842
AHSV1_AY163329      GATCCGCAAACTTACTTCGAAGATGACTTGTTCGTTGATCGGGCGAACAAGATTTTCTCT 1842
AHSV1_FJ183365      GATCCGCAAACTTACTTCGAAGATGACTTGTTCGTTGATCGGGCGAACAAGATTTTCTCT 1842
AHSV2_AY163332      GATCCTCAGTCCTACTTTGAGGATGATATATTTGCGGGAAAAGCTAATAGGATGTTTTTG 1845
AHSV8_DQ868775      GAAACGGATGTTTATTTTATCGATGATTTATTTTCCTCAACGCCGGACAAGGTATTCAGA 1854
AHSV8_AY163333      GAAACGGATGTTTATTTCATCGATGATTTATTTTCCTCAACGCCGGACAAGGTATTCAGA 1854
                    **  *  *    ** **    *****  * **           *  * * * * **

AHSV1_FJ011108      AGGGGTGGACAGACGGTGAATCAGCTGATAAGTATCAAGGTGAATGCGCAATCAAATAAC 1902
AHSV1_AM883165      AGGGGTGGACAGACGGTGAATCAGCTGATAAGTATCAAGGTGAATGCGCAATCAAATAAC 1902
AHSV1_AY163329      AGGGGTGGACAGACGGCGAATCAGCTGATAAGTATCAAGGTGAATGCGCAATCAAATAAC 1902
AHSV1_FJ183365      AGGGGTGGACAGACGGTGAATCAGCTGATAAGTATCAAGGTGAATGCGCAATCAAATAAC 1902
AHSV2_AY163332      AGAGGCGGAGAGACGGTTGAACGGCATGTGAAATTGAAGGTTAACGCTCAGACAGAGAAC 1905
AHSV8_DQ868775      CGTGTTGGAC------TAGATTCTCAAAATAATATCAAGATTGAGGGTAAAATGAATGA- 1907
AHSV8_AY163333      CGTGTTGGAC------TAGATTCTCAAAATAATATCAAGATTGAGGGTAAAATGAATGA- 1907
                     * *  ***          *    *     *   * *** *  * *   *     *  *

AHSV1_FJ011108      GTTGAGGGTACGACCTATTTTTCGAAAAGATTTGTTTCTTATTGGTTCAGAATAGAACAT 1962
AHSV1_AM883165      GTTGAGGGTACGACCTATTTTTCGAAAAGATTTGTTTCTTATTGGTTCAGAATAGAACAT 1962
AHSV1_AY163329      GTTGAGGGTACGACCTATTTTTCGAAAAGATTTGTTTCTTATTGGTTCAGAATAGAACAT 1962
AHSV1_FJ183365      GTTGAGGGTACGACCTATTTTTCGAAAAGATTTGTTTCTTATTGGTTCAGAATAGAACAT 1962
AHSV2_AY163332      GTTGAGGGCATCACATACTTTTCAAAAAGATTTGTATCTTATTGGTTCAGAATTGAACGC 1965
```

```
AHSV8_DQ868775      GTTGA-----CTACATACTTCTCAAAACGTTTTGTTACCTATTGGTATAAAATTACAAAG 1962
AHSV8_AY163333      GTTGA-----CTACATACTTCTCAAAACGTTTTGTTACCCATTGGTATAAAATTACAAGG 1962
                    *****       ** ** ** ** *** * *****  *  ******  * ***   *

AHSV1_FJ011108      TTTTCGATTACGACAGCAAAAAAGCGAACTGACATTCGAGATAAAAAGAC-TGAATATAA 2021
AHSV1_AM883165      TTTTCGATTACGACAGCAAAAAAGCGAACTGACATTCGAGATAAAAAGAC-TGAATATAA 2021
AHSV1_AY163329      TTTTCGATTACGACAGCAAAAAAGCGAACTGACATTCGAGATAAAAAGAC-TGAATATAA 2021
AHSV1_FJ183365      TTTTCGATTACGACAGCAAAAAAGCGAACTGACATTCGAGATAAAAAGAC-TGAATATAA 2021
AHSV2_AY163332      ACAACGCACGTAAAGGGAGGGGGAAGAGTAGATATTCGGGATCGAAAAAC-AGGGTACCA 2024
AHSV8_DQ868775      GTGGAGAAGAAAGATTTACTCATTGTGAATGATATCTACGATGAAAAAAC-GGAATATCA 2021
AHSV8_AY163333      GTGGAGAAGAAAGATTTACTCATTGTGAATGATATCTACGATGAAAAAACCGGAATATCA 2022
                         *           *            ** **    ***  *** **  *  **  *

AHSV1_FJ011108      CGAGTTTGACTT-CGAAGACTTCAAGCCGG-CATGTATTGGAGAATTGGGGATACACGCG 2079
AHSV1_AM883165      CGAGTTTGACTT-CGAAGACTTCAAGCCGG-CATGTATTGGAGAATTGGGGATACACGCG 2079
AHSV1_AY163329      CGAGTTTGACTT-CGAAGACTTCAAGCCGG-CATGTATTGGAGAATTGGGGATACACGCG 2079
AHSV1_FJ183365      CGAGTTTGACTT-CGAAGACTTCAAGCCGG-CATGTATTGGAGAATTGGGGATACACGCG 2079
AHSV2_AY163332      GCAGTTCGATGT-AGAAGATTTTAAACCTG-CAAGTGTAGGGGAACTTGGATTTCACGCG 2082
AHSV8_DQ868775      ACAGTTTGATCC-GGATGATTTCAAGCCAA-TGGTTATTGGAGAGATGGGTGTTCATGCT 2079
AHSV8_AY163333      GCAGTTTTATCCCGGATGATTTCAAGCCAAATGGTTATTGGAGAGATGGGTGTTCACGCT 2082
                      ****  *     ** ** ** ** **       * * ** **  * **  * ** **

AHSV1_FJ011108      TCGACATATATCTACCAGGATTTGTTGGTCGGGAAGAGCAGAGGGGAACGAGTGAAAGAC 2139
AHSV1_AM883165      TCGACATATATCTACCAGGATTTGTTGGTCGGGAAGAGCAGAGGGGAACGAGTGAAAGAC 2139
AHSV1_AY163329      TCGACATATATCTACCAGGATTTGTTGGTCGGGAAGAGCAGAGGGGAACGAGTGAAAGAC 2139
AHSV1_FJ183365      TCGACATATATCTACCAGGATTTGTTGGTCGGGAAGAGCAGAGGGGAACGAGTGAAAGAC 2139
AHSV2_AY163332      TCAACATATATTTATCAAGATTTACTTGTGGGAGCAAATAGAGGCGAGCGTGTGAAGGAC 2142
AHSV8_DQ868775      TCGACATATATATATCAAAACTTGATTTTAGGTAGAAATAGGGGTGAGCGGATTGTTGAT 2139
AHSV8_AY163333      TCAACATATATATATCAAAACTTGATTTTAGGTAGAAATAGGGGTGAGCGGATTGTTGAT 2142
                    ** ******** ** **  * **  *  * **    *  ** ** ** **  *    **

AHSV1_FJ011108      GCGAAGGAATTGGTGTGGATGGATCTTTCGCTGGCGAATTTTGGGTGTTCGCGCTGCTAT 2199
AHSV1_AM883165      GCGAAGGAATTGGTGTGGATGGATCTTTCGCTGGCGAATTTTGGGTGTTCGCGCTGCTAT 2199
AHSV1_AY163329      GCGAAGGAATTGGTGTGGATGGATCTTTCGCTGGCGAATTTTGGGTGTTCGCGCTGCTAT 2199
AHSV1_FJ183365      GCGAAGGAATTGGTGTGGATGGATCTTTCGCTGGCGAATTTTGGGTGTTCGCGCTGCTAT 2199
AHSV2_AY163332      GCGAAAGAGTTAGTGTGGATGGATTTATCTCTTACCAATTTCGGGTTTGTGCGAAGCTAC 2202
AHSV8_DQ868775      AGCAAGGAGATCGTGTGGTATGATTTGTCGTTGACCAATTTCGGCCTGGTGCGTTCGCAG 2199
AHSV8_AY163333      AGCAAAGAGATCGTGTGGTATGATTTGTCGTTGACCAATTTCGACCTGGTGCGTTCGCAG 2202
                       ** **  * ******   *** * **  *  * ***** *       ***     *

AHSV1_FJ011108      GATCGATGTTGGCCAGCTTCCTGCGTTGAAGCGGAGATCTCCTTGAGGTACTATTTAGTC 2259
AHSV1_AM883165      GATCGATGTTGGCCAGCTTCCTGCGTTGAAGCGGAGATCTCCTTGAGGTACTATTTAGTC 2259
AHSV1_AY163329      GATCGATGTTGGCCAGCTTCCTGCGTTGAAGCGGAGATCTCCTTGAGGTACTATTTAGTC 2259
AHSV1_FJ183365      GATCGATGTTGGCCAGCTTCCTGCGTTGAAGCGGAGATCTCCTTGAGGTACTATTTAGTC 2259
AHSV2_AY163332      AATAGATGTTGGATTGCGGCCTTTGTGGAGGCGGAGATTTCGCTCAGATTTTATCTCATA 2262
AHSV8_DQ868775      AATCAATGCTGGATTGGATCAATTTCAAATTTTGAGTTAAGTATGCGATATCACATCATA 2259
AHSV8_AY163333      AATCAATGTTGGATTGGATCAATTTCAAATTTTGAGTTAAGTATGCGATATCACATCATA 2262
                     **  *** ***   *   *        *    *** *     *  * *   *  *  *

AHSV1_FJ011108      ACATCTATTTTCGCTAGATACCTTAACCGTGAAGGA-TTGAGCTTTTCAAAGATTTTGAT 2318
AHSV1_AM883165      ACATCTATTTTCGCTAGATACCTTAACCGTGAAGGA-TTGAGCTTTTCAAAGATTTTGAT 2318
AHSV1_AY163329      ACATCTATTTTCGCTAGATACCTTAACCGTGAAGGA-TTGAGCTTTTCAAAGATTTTGAT 2318
AHSV1_FJ183365      ACATCTATTTTCGCTAGATACCTTAACCGTGAAGGA-TTGAGCTTTTCAAAGATTTTGAT 2318
AHSV2_AY163332      ACGTCGATCTTTTGTAGATATTTTACTGGCGATAGG-AAGAGTTTCGCTAAGATACTAGA 2321
AHSV8_DQ868775      ACCGAAATTTTCCAGAGGTATAGAGTGGATTCAGCACATAAGTCTTACCACGAAATTATC 2319
AHSV8_AY163333      ACCGAAATTTTCCAGAGGTATAGAGTGGATTCAGCACATAAGTCTTACCACGAAATTATC 2322
                    **    ** **    ** **                    **  *  * * * **   *

AHSV1_FJ011108      CTCTCTCAAAGATTTTTCGGATAGATTATGGTTTCCAACGTATAAACATTTTTATGTTGC 2378
AHSV1_AM883165      CTCTCTCAAAGATTTTTCGGATAGATTATGGTTTCCAACGTATAAACATTTTTATGTTGC 2378
AHSV1_AY163329      CTCTCTCAAAGATTTTTCGGATAGATTATGGTTTCCAACGTATAAACATTTTTATGTTGC 2378
AHSV1_FJ183365      CTCTCTCAAAGATTTTTCGGATAGATTATGGTTTCCAACGTATAAACATTTTTATGTTGC 2378
AHSV2_AY163332      TGGAGTCAAGTCATTGAAAGAAAGATTATGGTTCCCTACCTACAAACATTACTATGTTGC 2381
AHSV8_DQ868775      AGCGGACTGACTAAGAAAGACGTGATTCTT-TTCCCTAGTTATAAACATTATTATGTTAG 2378
AHSV8_AY163333      AGCGGACTGACTAAGAAAGACGTGATTCTT-TTCCCTAGTTATAAACATTATTATGTTCG 2381
                          *               **** *  ** ** *  ** *******  ******

AHSV1_FJ011108      AGTTGTACAAAAAGTGCTCCGCGATGATAGACGCTTAGATTATGTACTCTTTTGTTCTAG 2438
AHSV1_AM883165      AGTTGTACAAAAAGTGCTCCGCGATGATAGACGCTTAGATTATGTACTCTTTTGTTCTAG 2438
AHSV1_AY163329      AGTTGTACAAAAAGTGCTCCGCGATGATAGACGCTTAGATTATGTACTCTTTTGTTCTAG 2438
AHSV1_FJ183365      AGTTGTACAAAAAGTGCTCCGCGATGATAGACGCTTAGATTATGTACTCTTTTGTTCTAG 2438
AHSV2_AY163332      CGTCATTCAGAAGATTTACTCAGATGATAGGAATCTAGATAGGAATGAATTTTTGTAATAG 2441
AHSV8_DQ868775      AGTTATACAAGATGTATTTCAAGATTCGCAAAAGGTAGATGTTTTAGATTTCTGTTTGAG 2438
AHSV8_AY163333      AGTTATACAAGATGTATTTCAAGATTCGCAAAAGGTAGATGTTTTAGATTTCTGTTTGAG 2441
                     **  * **  *  *       ***          *****         ** ***   **
```

```
AHSV1_FJ011108      GGTCTCGGCAATCACAACCCGGCGTGCGACGTTAATGGAATTTAGTACCTTTAAACAGAT 2498
AHSV1_AM883165      GGTCTCGGCAATCACAACCCGGCGTGCGACGTTAATGGAATTTAGTACCTTTAAACAGAT 2498
AHSV1_AY163329      GGTCTCGGCAATCACAACCCGGCGTGCGACGTTAATGGAATTTAGTACCTTTAAACAGAT 2498
AHSV1_FJ183365      GGTCTCGGCAATCACAACCCGGCGTGCGACGTTAATGGAATTTAGTACCTTTAAACAGAT 2498
AHSV2_AY163332      AGTCATGAATATCATGACAAGACGGTCAGTACTCAATGAGTTTGAGAGGTTTAGAAGAGC 2501
AHSV8_DQ868775      GATTGCCAACCCAGAGACGCGCTTATCCACGCTGCTGAAGATTCAGGGCTTCAGAGCATG 2498
AHSV8_AY163333      GATTGCGAACCCTGAGACGCGCTTATCTACGCTGCTGAAGATTCAGGGTTTCAGAGCATG 2501
                      *            **  *     *     *     *  **      ** * *

AHSV1_FJ011108      GGTGGGATCAACACGTTTATTGGATACGCTATTCTTAAATTTTCTACTTTGGATCATTTT 2558
AHSV1_AM883165      GGTGGGATCAACACGTTTATTGGATACGCTATTCTTAAATTTTCTACTTTGGATCATTTT 2558
AHSV1_AY163329      GGTGGGATCAACACGTTTATTGGATACGCTATTCTTAAATTTTCTACTTTGGATCATTTT 2558
AHSV1_FJ183365      GGTGGGATCAACACGTTTATTGGATACGCTATTCTTAAATTTTCTACTTTGGATCATTTT 2558
AHSV2_AY163332      TATTGAGTCGCCAAAGCTGATTGACACTTTGTCGCTTAATTTTCTCCTTTGGATAATTTT 2561
AHSV8_DQ868775      TGTGGAATCTGAGTTCCTTCTCCCAACACTTCATCTGAATTTTTTGATTTGGCTGCTGAT 2558
AHSV8_AY163333      TGTGGAATCTGAGTTCCTTCTCCCAACACTTCACCTGAATTTTTTGATTTGGTTGCTGAT 2561
                      * *  **        *  *    **  *     * ****** *  ***** *  *  *

AHSV1_FJ011108      CGAACAGGAGAATATAGATGTTGATTTCGCAAATAAGTGGCATCCTCTATTAATTTCTAC 2618
AHSV1_AM883165      CGAACAGGAGAATATAGATGTTGATTTCGCAAATAAGTGGCATCCTCTATTAATTTCTAC 2618
AHSV1_AY163329      CGAACAGGAGAATATAGATGTTGATTTCGCAAATAAGTGGCATCCTCTATTAATTTCTAC 2618
AHSV1_FJ183365      CGAACAGGAGAATATAGATGTTGATTTCGCAAATAAGTGGCATCCTCTATTAATTTCTAC 2618
AHSV2_AY163332      CGAACAAGAGAACATAGATGTTAATTTTGCGGATAAGAGGCATCCACTATTAATATCAAC 2621
AHSV8_DQ868775      TGACATGGAAAATGGGGACATAAATTACTCGAAGAAAAGACTTCCTTTATTGATTTCTAC 2618
AHSV8_AY163333      TGACATGGAAAACGGGGACATAAATTACTCGAAGAAAAGGCTTCCTTTATTGATTTCTAC 2621
                     **    ** **    **  *  ***   *  * **  * * ***  **** ** ** **

AHSV1_FJ011108      AGAAAAGGGCTTGAGAGTTATTGCGGTTGATGTTTTTAATAGTTCACTTACGTTATCAAC 2678
AHSV1_AM883165      AGAAAAGGGCTTGAGAGTTATTGCGGTTGATGTTTTTAATAGTTCACTTACGTTATCAAC 2678
AHSV1_AY163329      AGAAAAGGGCTTGAGAGTTATTGCGGTTGATGTTTTTAATAGTTCACTTACGTTATCAAC 2678
AHSV1_FJ183365      AGAAAAGGGCTTGAGAGTTATTGCGGTTGATGTTTTTAATAGTTCACTTACGTTATCAAC 2678
AHSV2_AY163332      GACTAAAGGTTTGAGAGTAATCCCGATTGACGTTTTCAATAGTTCACTAGCTCTTTCTCC 2681
AHSV8_DQ868775      GACGAACGGTTTGAGGGTGATGGCGGTCGACGCATTCAATAACATGATTGCCATGTCTTA 2678
AHSV8_AY163333      GACGAAGGGTTTGAGGGTGATGGCGGTCGACGCATTCAATAACTTGATTGCCATGTCTTA 2681
                        ** ** ***** ** **  ** * ** *  ** ****      *  *  * **

AHSV1_FJ011108      GAGCGGATGGCTGCCATATTTAGAGCGGATTTGCTCTGAGTCCGCGATGGATCGAGCTCT 2738
AHSV1_AM883165      GAGCGGATGGCTGCCATATTTAGAGCGGATTTGCTCTGAGTCCGCGATGGATCGAGCTCT 2738
AHSV1_AY163329      GAGCGGATGGCTGCCATATTTAGAGCGGATTTGCTCTGAGTCCGCGATGGATCGAGCTCT 2738
AHSV1_FJ183365      GAGCGGATGGCTGCCATATTTAGAGCGGATTTGCTCTGAGTCCGCGATGGATCGAGCTCT 2738
AHSV2_AY163332      AAGTGGTTGGATCCCTTACGTTGAGAGGATATGTGCAGAGGCTAAGGAAAACCGTACGCT 2741
AHSV8_DQ868775      TAGCGGTTGGCTCCCGTATTTAGAGAGAATATGTCACGAAACAAAGCAGCGGACGAGACT 2738
AHSV8_AY163333      TAGCGGTTGGCTCCCGTATTTAGAGAGAATATGTCACGAAACAAAGCAGCGGACGAGACT 2741
                     ** ** *** * ** **  * *** * ** **    **  *   *           **

AHSV1_FJ011108      CACCGCTGACGAAATAAATCTTAAACGATGGTTTGTTGATTACTACATGGAGCTGAAGTT 2798
AHSV1_AM883165      CACCGCTGACGAAATAAATCTTAAACGATGGTTTGTTGATTACTACATGGAGCTGAAGTT 2798
AHSV1_AY163329      CACCGCTGACGAAATAAATCTTAAACGATGGTTTGTTGATTACTACATGGAGCTGAAGTT 2798
AHSV1_FJ183365      CACCGCTGACGAAATAAATCTTAAACGATGGTTTGTTGATTACTACATGGAGCTGAAGTT 2798
AHSV2_AY163332      GAGTTCCGATGAATTGAGAATTAAAACCTGGTTCGTAGAGTACTATCTAAATATAAACTT 2801
AHSV8_DQ868775      CAATGCTGATGAATTAAAATTAAAGAAGTGGTTTCTGAATTACGTTACGAAATACGAAGT 2798
AHSV8_AY163333      CAATGCTGATGAATTAAAATTAAAGAAGTGGTTTCTGAATTACGTTACGAAATACGAAGT 2801
                     *   * ** *** * *   * **    *****  *  * ***       *     *  *

AHSV1_FJ011108      GGAGAGACGAGCGGAACCTCGAATGAGTTTCAAGAGCGAGGCTTTGATCACGTGGATCGG 2858
AHSV1_AM883165      GGAGAGACGAGCGGAACCTCGAATGAGTTTCAAGAGCGAGGCTTTGATCACGTGGATCGG 2858
AHSV1_AY163329      GGAGAGACGAGCGGAACCTCGAATGAGTTTCAAGAGCGAGGCTTTGATCACGTGGATCGG 2858
AHSV1_FJ183365      GGAGAGACGAGCGGAGCCTCGAATGAGTTTCAAGAGCGAGGCTTTGATCACGTGGATCGG 2858
AHSV2_AY163332      AGAGAGGAGGGCGGAGCCTAGGATGAGTTTCAAGAGTGAAGCGCTGATCACGTGGATCGG 2861
AHSV8_DQ868775      TGAGAGAAGGGCGGAGCCGCGTATGAGTTTCAAAATGGAGGGCATAACAACGTGGATTGG 2858
AHSV8_AY163333      TGAAAGAAGGGCGGAGCCGCGTATGAGTTTCAAAATGGAGGGCATAACAACGTGGATTGG 2861
                     ** **  * ***** **  * *********** *  ** *   * *  ******** **

AHSV1_FJ011108      GTCAAATTGTGGAGGAGTGACCGATTATGTCGTACAACTTCTACCCGTTCGAAAGCCGAA 2918
AHSV1_AM883165      GTCAAATTGTGGAGGAGTGACCGATTATGTCGTACAACTTCTACCCGTTCGAAAGCCGAA 2918
AHSV1_AY163329      GTCAAATTGTGGAGGAGTGACCGATTATGTCGTACAACTTCTACCCGTTCGAAAGCCGAA 2918
AHSV1_FJ183365      GTCAAATTGTGGAGGAGTGACCGATTATGTCGTACAACTTCTACCCGTTCGAAAGCCGAA 2918
AHSV2_AY163332      ATCGAATTGTGGTGGAGTGACTGATTATGTGGTTCAGCTTTTGCCTGTTCGGAAACCGAA 2921
AHSV8_DQ868775      ATCAAACTGCGGTGGGGTTCAGGATTACATCTTACATTTGATACCATCCCGGAAACCGAA 2918
AHSV8_AY163333      ATCAAACTGCGGTGGGGTTCAGGATTACATCTTACATTTGATACCATCCCGGAAACCAAA 2921
                     ** ** ** ** ** **    *****  *  * **  *  * **    ** ** ** **

AHSV1_FJ011108      ACCGGGGTTATTGGTTGTCGTATATTCGGAGGATGGTGGGGAAAAATGGGCAGAGTGGGC 2978
AHSV1_AM883165      ACCGGGGTTATTGGTTGTCGTATATTCGGAGGATGGTGGGGAAAAATGGGCAGAGTGGGC 2978
AHSV1_AY163329      ACCGGGGTTATTGGTTCTCGTATATTCGGAGGATGGTGGGGAAAAATGGGCAGAGTGGGC 2978
AHSV1_FJ183365      ACCGGGGTTATTGGTTGTCGTATATTCGGAGGATGGTGGGGAAAAATGGGCAGAGTGGGC 2978
```

```
AHSV2_AY163332      ACCGGGCCTGCTAGTGGTTGTTTATTCGGAGGACGGGAGTGGGAAATGGGCAGAATGGGC 2981
AHSV8_DQ868775      GCCTGGATTATTATTTTTGATTTATACAGACGCAGGGGATGTAGATTGGGTAACACGGAT 2978
AHSV8_AY163333      ACCTGGATTATTATTTTTGATTTATACGGACGCAGGGGATGTAGATTGGGTAACACGGAT 2981
                     ** **  *  *  *  *  * *** * ** *  **    *   * **** *    **

AHSV1_FJ011108      TTTACGTGACTACCTCGAAATTGATGGTAGTTTGGGTTTAGTATTCATTACGCGGAAGGC 3038
AHSV1_AM883165      TTTACGTGACTACCTCGAAATTGATGGTAGTTTGGGTTTAGTATTCATTACGCGGAAGGC 3038
AHSV1_AY163329      TTTACGTGACTACCTCGAAATTGATGGTAGTTTGGGTTTAGTATTCATTACGCGGAAGGC 3038
AHSV1_FJ183365      TTTACGTGACTACCTCGAAATTGATGGTAGTTTGGGTTTAGTATTCATTACGCGGAAGGC 3038
AHSV2_AY163332      GCTACGCGATTTTTTAGACGTTGAAGGTAGCTTAGGATTAATTTTCATAACACGTAAAAC 3041
AHSV8_DQ868775      GCTTTACGATGTGTGTCGACTAGAGGGTAGCTTGGGCTTCATTTTAATCGACGACCGAGT 3038
AHSV8_AY163333      GCTTTACGATGTGTGTCGATTAGAGGGTAGCTTGGGCTTCATTTTAATCGACGATCGAGT 3041
                      *    **           * ** ***** ** ** **  * ** **

AHSV1_FJ011108      AGTAAAGAATAAGAGTAAACTTGGCGTACGCGATCTGAAAATCTATAATAGAGGGAGAGT 3098
AHSV1_AM883165      AGTAAAGAATAAGAGTAAACTTGGCGTACGCGATCTGAAAATCTATAATAGAGGGAGAGT 3098
AHSV1_AY163329      AGTAAAGAATAAGAGTAAACTTGGCGTACGCGATCTGAAAATCTATAATAGAGGGAGAGT 3098
AHSV1_FJ183365      AGTAAAGAATAAGAGTAAACTTGGCGTACGCGATCTGAAAATCTATAATAGAGGGAGAGT 3098
AHSV2_AY163332      TGTCAAGAATGGGAGCGCATTGGGAGTCCGAGATTTAAAAATCTACAATCGAGGGAGAGT 3101
AHSV8_DQ868775      TATGGTGAACAAAAGCCAATTGAGGGCACGGATCTTGAAGATTTATAACAGGGGAAAATT 3098
AHSV8_AY163333      TATGGTGAACAAAAGCCAATTGAGGGCACGGATCTTAAAGATTTATAACAGGGGAATATT 3101
                      *   ***    **   * *  * *  **     * ** ** ** **  * ** * * *

AHSV1_FJ011108      TGATAGGTTGATTTTAATTTCGAGCGGTGTTTATACTTTTGGAAATAAGTTTCTCTTCTC 3158
AHSV1_AM883165      TGATAGGTTGATTTTAATTTCGAGCGGTGTTTATACTTTTGGAAATAAGTTTCTCTTCTC 3158
AHSV1_AY163329      TGATAGGTTGATTTTAATTTCGAGCGGTGTTTATACTTTTGGAAATAAGTTTCTCTTCTC 3158
AHSV1_FJ183365      TGATAGGTTGATTTTAATTTCGAGCGGTGTTTATACTTTTGGAAATAAGTTTCTCTTCTC 3158
AHSV2_AY163332      AGATAGATTAGTTTTAATTTCGAGCGGCGTTTATACTTTTGGGAACAAATTTTTATTCTC 3161
AHSV8_DQ868775      AGATAAATTGATTTTGATTTCAGGGGGGAATTACACTTTCGGGAACAAATTCTTGCTCTC 3158
AHSV8_AY163333      AGATAAATTGATTTTGATTTCAGGGGGGAATTACACTTTCGGGAACAAATTCTTGCTCTC 3161
                     ****  **  **** *****  * **   *** ***** ** ** ** **  *  ****

AHSV1_FJ011108      AAAGTTATTGTCGAAGATAGAGTAACGGTGTGACAACCGTTCCATGCTGATCACCCTTAC 3218
AHSV1_AM883165      AAAGTTATTGTCGAAGATAGAGTAACGGTGTGACAACCGTTCCATGCTGATCACCCTTAC 3218
AHSV1_AY163329      AAAGTTATTGTCGAAGATAGAGTAACGGTGTGACAACCGTTCCATGCTGATCACCCTTAC 3218
AHSV1_FJ183365      AAAGTTATTGTCGAAGATAGAGTAACGGTGTGACAACCGTTCCATGCTGATCACCCTTAC 3218
AHSV2_AY163332      GAAACTACTATCCAAAATAGAGTAACGGCGTGACTGCCGTTCTATGCTGAATACACATAC 3221
AHSV8_DQ868775      AAAACTACTAGCCAAAACAGAGAAGTAGCGTGACTGCTACTC-ATGATGAATACACTTAC 3217
AHSV8_AY163333      AAAACTACTAGCCAAAACAGAGAAGTAGCGTGACTGCTACTC-ATGATGAATACACTTAC 3220
                     **  ** *  * ** * **** *   * *****  *   ** *** ***  ** * ***
```

Appendix E3

AHSV segment 2 full-length alignment of Clade C (Serotypes 4, 5, 6 and 9)

```
CLUSTAL 2.0.12 multiple sequence alignment(AHSV 100630 FL Seg2 C ST4,5,6,9)


AHSV9_DQ868776       GTTTAATTCACCATGGCGTTCGAGTTTGGAATACTTCAGACGGACAAAATTAGAGAGAAT 60
AHSV9_AF043926       GTTTAATTCACCATGGCGTTCGAGTTTGGAATACTTCAGACAGATAAAATTAGAGAGAAT 60
AHSV6_NC_005996      GTTAAATTCACCATGGCTTCCGAATTTGGCATTTTGATTTGTGATAAATTGAAGGAAAAT 60
AHSV6_AF021235       GTTAAATTCACCATGGCTTCCGAATTTGGCATTTTGATTTGTGATAAATTGAAGGAAAAT 60
AHSV6_DQ868774       GTTAAATTCACCATGGCTTCCGAATTTGGCATTTTGATTTGTGATAAATTAAAGGAAAAC 60
AHSV4_DQ868773       GTTTAATTCACCATGGCGTCCGAGTTTGGAATATTGATGACAAATGAAAAATTTGACCCA 60
AHSV4_EU046574       GTTTAATTCACCATGGCGCCCGAGTTTGGAATATTGATGACAAATGAAAAATTTGACCCA 60
AHSV4_D26570         GTTTAATTCACCATGGCGTCCGAGTTTGGAATATTGTTGACAGATGAAAAATTTGACCCG 60
AHSV5_AY163331       GTTTATTTCATCATGGCTTCAGAGTTTGGCGTTCTGTTGACCGATAAAGTTGAAGGCGAT 60
                     *** * **** ******    ** *****  *  *        *  **      *

AHSV9_DQ868776       ACACTCGAAAAAACAAATTGTGATGTGATTCTTACGAAAGAAAATAGAGTGCGGATGAAA 120
AHSV9_AF043926       ACACTTGAAAAGACAAACTGTGACGTGATTCTTACGAGAGAGAATAGAGTGCGAACGAGG 120
AHSV6_NC_005996      ACTTTAGAAAAAACGAATTGTGACGTTATTATTACGGGAGTGGGAAAAGTAGGTGTACAC 120
AHSV6_AF021235       ACTTTAGAAAAAACGAATTGTGACGTTATTATTACGGGAGTGGGAAAAGTAGGTGTACAC 120
AHSV6_DQ868774       ACCTTGGAAAAAACGAATTGTGACGTTATTATTACGGGAGTAGGAAAGGTGAGTGTACGC 120
AHSV4_DQ868773       AGCTTAGAGAAAACCATTTGCGATGTTATAGTTACGAAGAAGGGAAGAGTGAAGCATAAA 120
AHSV4_EU046574       AGCATAGAGAAAACCATTTGCGATGTTATAGTTACGAAGAAGGGAAGAGTGAAGCATAAA 120
AHSV4_D26570         AGTTTAGAGAAGACCATTTGCGATGTTATAGTTACGAAGAAGGGGAGAGTGAAACATAAA 120
AHSV5_AY163331       GCTTTAGAGAAAACGAATTGTGAAGTAATTCTTACACGAAGTGGTCGCGTACGGCGGAGG 120
                         * ** ** ** *  ** ** ** **  ****            **

AHSV9_DQ868776       GAGGTCGAAGGAGTGAAAGGATATTATTGGGAGGACACCGATCACAGGTTAGGTTTATGT 180
AHSV9_AF043926       GAAGTTGATGGAGTGAAAGGATATTACTGGGAAGATACCGATCACAGGTTGGGCTTATGT 180
AHSV6_NC_005996      GAAGAGGACGGTGTGTTAGGATATGAGTGGGAGGAGACTAACTATAGGTTAGGATTGTGC 180
AHSV6_AF021235       GAAGAGGACGGTGTGTTAGGATATGAGTGGGAGGAGACTAACTATAGGTTAGGATTGTGC 180
AHSV6_DQ868774       GAAGAAGACGGCATATTAGGTTACGAGTGGGAAGAGACTAATCATAGATTGGGATTGTGC 180
AHSV4_DQ868773       GAGGTGGATGGCGTATGTGGATACGAGTGGGATGAAACGAATCACCGATTCGGATTGTGT 180
AHSV4_EU046574       GAGGTGGATGGCGTATGTGGATACGAGTGGGATGAAACGAATCACCGATTCGGATTGTGT 180
AHSV4_D26570         GAGGTGGATGGCGTGTGTGGATACGAGTGGGATGAAACGAACCACCGATTTGGATTGTGT 180
AHSV5_AY163331       GAGGTTGACGGAGTTAAAGGATATGAATGGGAATTTACAGATCATCGATTAGGATTATGT 180
                     ** *  ** **  *    ** **  * *****    **  *  *  * ** ** ** **

AHSV9_DQ868776       GAGGTCGAACATACTGTGTCTGTGAGGGATTTTGTGTATAAACAAACGAAATGTGAAGGA 240
AHSV9_AF043926       GAAGTCGAACATACTGTGTCGGTGAGGGATTTTATGTACAAACAAACGAAATGTGAAGGG 240
AHSV6_NC_005996      GAAATAGAGAATACGATGTCAATCAGTGATTTTGTTTATAAGCAAATAAGATGTGAGGGA 240
AHSV6_AF021235       GAAATAGAGAATACGATGTCAATCAGTGATTTTGTTTATAAGCAAATAAGATGTGAGGGA 240
AHSV6_DQ868774       GAAATAGAAAATACGGTATCAATCAGTGATTTCGTCTATAAGCAAATAAGATGTGAAGGA 240
AHSV4_DQ868773       GAGGTGGAACACGACATGTCTATATCGGAATTTATGTACAATGAGATCAGATGTGAGGGG 240
AHSV4_EU046574       GAGGTGGAACACGACATGTCTATATCGGAATTTATGTACAATGAGATCAGATGTGAGGGG 240
AHSV4_D26570         GAGGTGGAACACGATATGTCAATATCGGAGTTTATGTACAATGAGATCAGATGTGAGGGG 240
AHSV5_AY163331       GAAATAGAGCATACAATGTCTATGGCGGATTTCTTTTATAATCAAATTAAGTGCGAGGGT 240
                     **  * **  *     * **  *    ** **  * ** **  * *  *  ** ** **

AHSV9_DQ868776       TCATATCCGGTTGTGCCTTTATACATGATTGATGCAATTAAATATGGACGAATGATTGAC 300
AHSV9_AF043926       TCATATCCGGTCGTGCCTTTATATATGATTGATGCAATTAAATATGGACGAATGATCGAT 300
AHSV6_NC_005996      GCATACCCCATTTTGCCGCACTATGTTACAGACGTCATTAAATATGGCATGGTAATTCAT 300
AHSV6_AF021235       GCATACCCCATTTTGCCGCACTATGTTACAGACGTCATTAAATATGGCATGGTAATTCAT 300
AHSV6_DQ868774       GCGTACCCGATTTTACCGCACTATGTTACGGACGTCATTAAATATGGGATGGTAATCGAT 300
AHSV4_DQ868773       GCATATCCAATTTTTCCGCGTTATATAATTGATACGTTAAAATACGAGAAATTTATTGAT 300
AHSV4_EU046574       GCATATCCAATTTTTCCGCGTTATATAATTGATACGTTAAAATACGAGAAATTTATTGAT 300
AHSV4_D26570         GCATATCCAATTTTTCCACGTTACATAATTGATACGTTGAAATACGAGAAATTTATTGAT 300
AHSV5_AY163331       GCATATCCGATATTTCCACATTATATTACCGACGTGCTAAAATATGGGAAAATGGTTGAT 300
                      * ** **  *  * **    **  * *  **     * ***** *      *  *  *

AHSV9_DQ868776       AGGAACGACCACCAAATTAGAGTAGACAAAGATGATAAAATTCTATCTAAAATACAAGTA 360
AHSV9_AF043926       AGGAATGACCTCCAAATTAGAGTAGACAAAGATGATAAAACTCTATTTAAGATACAAGTG 360
AHSV6_NC_005996      AGAAATGATCATCAGATCCGAGTTGACAGAGATGAAAAAAGTATTGGAAAAATCCAGATT 360
AHSV6_AF021235       AGAAATGATCATCAGATCCGAGTTGACAGAGATGAAAAAAGTATTGGAAAAATCCAGATT 360
AHSV6_DQ868774       AGAAACGATCATCAGATCCGAGTTGACAGAGATGAAAAAAGTATTGGAAAAATCCAGATT 360
AHSV4_DQ868773       AGGAATGACCATCAAATTAGAGTGGATAGAGATGATAACGAAATGAGGAAAATATTGATA 360
AHSV4_EU046574       AGGAATGACCATCAAATTAGAGTGGATAGAGATGATAACGAAATGAGGAAAATATTGATA 360
AHSV4_D26570         AGGAATGATCATCAGATTAGAGTGGACAGAGACGATAATGAAATGAGGAAAATATTGATA 360
AHSV5_AY163331       AGAAATGATCACCAAGTTAGAGTTGATAGGGATGTTAAAGAGCTAAGCAAAATATTGATA 360
                     ** ** ** *  **  *  **** ** *  ** *  **     *    ** **     *
```

```
AHSV9_DQ868776      CAGCCGTATTTAGGCGACGCTTATTTTTCGCCAGAGTATTACACTGCTACCTTCTTTAAA 420
AHSV9_AF043926      CAGCCGTACTTAGGTGATGCCTATTTTTCACCAGAGCATTACACCGCGACCTTCTTTAAA 420
AHSV6_NC_005996     CAGCCGTATTTTGGCGATATGTATTTCTCCCCCGAGTACTACCCGGCAACTTTTATTAAA 420
AHSV6_AF021235      CAGCCGTATTTTGGCGATATGTATTTCTCCCCCGAGTACTACCCGGCAACTTTTATTAAA 420
AHSV6_DQ868774      CAGCCGTATTTCGGCGATATGTATTTCTCCCCCGAGTATTACCCGGCAACTTTCGTTAAA 420
AHSV4_DQ868773      CAGCCGTATGCAGGTGAGATGTACTTTTCGCCGGAATGTTATCCGAGCGTTTTTCTTCGG 420
AHSV4_EU046574      CAGCCGTATGCAGGTGAGATGTACTTTTCGCCGGAATGTTATCCGAGCGTTTTTCTTCGG 420
AHSV4_D26570        CAGCCGTATGCGGGTGAGATGTATTTTTCGCCAGAATGTTATCCGAGCGTTTTCCTTCGG 420
AHSV5_AY163331      CAACCATACTTCGGTGAGGCGTACTTTTCACCAGAATTTTACACCTCAACTTTTTGAAG 420
                    ** ** **    ** **    ** ** ** ** **    **  *       **  *

AHSV9_DQ868776      AGAGAACCGCTGCCAATTCATGTGGATATGATTCGGGAT---TATATCGGAAAACGAAT- 476
AHSV9_AF043926      AGAGAACCGCTGCCTATTCATGTAGATACGATTCGAGAT---TACATTGGAAAACGGAT- 476
AHSV6_NC_005996     CGTGAGTCTTTACCAATCTCAGTAGATACGATCAGAGGT---TATATTGGAGCTAGAATG 477
AHSV6_AF021235      CGTGAGTCTTTACCAATCTCAGTAGATACGATCAGAGGT---TATATTGGAGCTAGAATG 477
AHSV6_DQ868774      CGTGAGCCTCTGCCAATCTCAGTAGATATGATCAGAGAT---TATATTGGAGCCAGAATG 477
AHSV4_DQ868773      AGGGAAGCGCGAAGTCAAAAGCTTGATCGGATTCGGAAT---TATATTGGAAAGAGAGTC 477
AHSV4_EU046574      AGGGAAGCGCGAAGTCAAAAGCTTGATCGGATTCGGAAT---TATATTGGAAAGAGAGTC 477
AHSV4_D26570        AGGGAGGCGCGAAGCCAAAAGCTTGATCGAATTCGGAAT---TACATTGGAAAAAGAGTC 477
AHSV5_AY163331      AGACAGGCG---ATTCAAATGAATGTTGAGATGCTGAGAGCGTTTGTACCAAAAAGGGTG 477
                     *  *  *               * *   **          *   *   *    *  *

AHSV9_DQ868776      TAATTATTTTGAGCGAGAATTAAGTGG--TGGGGTGCGAGATGCAAATTTAGAGATGATA 534
AHSV9_AF043926      TAATTATTTCGAGCGAGAGTTAGGTAG--TGGAGTACGAGATGCGAACTTAGAAATGATC 534
AHSV6_NC_005996     CGAGGGATTGAAGCTAGGGCTGGGCGAATTAGGGAGGGTGATGGAAACTTGTTAGAATGC 537
AHSV6_AF021235      CGAGGGATTGAAGCTAGGGCTGGGCGAATTAGGGAGGGTGATGGAAACTTGTTAGAATGC 537
AHSV6_DQ868774      CGAAAGATTGAAGCCAGGGCGGGACGAATTAAGGAGGGTGGTGGAAATTTGTTGGAGTGC 537
AHSV4_DQ868773      GAATTTTATGAAGAGGAGAGTAAGAGAAAAGCAATCCTTGATCAGAATAAGATGTCTAAG 537
AHSV4_EU046574      GAATTTTATGAAGAGGAGAGTAAGAGAAAAGCAATCCTTGATCAGAATAAGATGTCTAAG 537
AHSV4_D26570        GAATTTTTTGAAGAGGAGAGTGGGAGAAAGGCGATCCTTAATCAGAATAAGATGTCTAAG 537
AHSV5_AY163331      GCTTTTTATGAAGACGATATGAGGAGGGGCGGTACTATTAACGGGAATTGGATTGGAGCG 537
                            *  **                                 **

AHSV9_DQ868776      GTTGAGAAGTGGAAAGATAATACTTATAAAAGGATTGAAGGTGAGAAAACGACGATG--- 591
AHSV9_AF043926      GTTGGGAAGTGGAAGGATAATACCTATAAAAGAATTGAAGGTGAAAAAACGACGATG--- 591
AHSV6_NC_005996     GCGCGCAGATGGGAAAAAGCGGCGTATGAGAGGATTGAGAATGAAAAAGCGTTGCGG--- 594
AHSV6_AF021235      GCGCGCAGATGGGAAAAAGCGGCGTATGAGAGGATTGAGAATGAAAAAGCGTTGCGG--- 594
AHSV6_DQ868774      GCGCGCAGATGGGAAAAAGCGGCATATGAGAGAATTGAGAATGAAAGAGCATTACGG--- 594
AHSV4_DQ868773      GTTGAACAATGGAGAGATGCGGTTAATGAAAGGATTGTGAGTATCGAACCAAAGCGAGGT 597
AHSV4_EU046574      GTTGAACAATGGAGAGATGCGGTTAATGAAAGGATTGTGAGTATCGAACCAAAGCGAGGT 597
AHSV4_D26570        ATTGAGCAGTGGAGAGATGCGGTTAATGAAAGGATTGTAAGTGCCGAACCAAAGCGAGGT 597
AHSV5_AY163331      TTACAGGCGTGGAAGGAAAAAGCGGATTTGCAAATGTCGCGCGAGGGGAATAGTCAAACT 597
                            ***    *        **      **

AHSV9_DQ868776      ---TGCGTGAGACATGAACCAGACTCAGTGCTACAGATGTTGAAAAAGATGAGGTTTGGG 648
AHSV9_AF043926      ---TGCGTGAGGCATGAACCAGATTCGGTACTACAGATATTAAAAAAGATGAGGTTTGGA 648
AHSV6_NC_005996     ---TGCGTGGCACATGAAACAGATCCAACGTATCAAATTCTTAAAAAACAAAGATTTGGA 651
AHSV6_AF021235      ---TGCGTGGCACATGAAACAGATCCAACGTATCAAATTCTTAAAAAACAAAGATTTGGA 651
AHSV6_DQ868774      ---TGTGTGGTGCATGAAACAGATCCGACGTATCAAATTCTTAAAAAACTAAGATTTGGA 651
AHSV4_DQ868773      GAGTGCTATGATCACGGAACCGACATTATCTACCAATTCATAAAAAAGCTGAGATTTGGA 657
AHSV4_EU046574      GAGTGCTATGATCACGGAACCGACATTATCTACCAATTCATAAAAAAGCTGAGATTTGGA 657
AHSV4_D26570        CAATGCTATGATCATGGTACCGACATTATCTACCAATTCATAAAAAAGCTAAGATTCGGA 657
AHSV5_AY163331      AATTGCGTTGACCATAATGCGGATGTAATATATCAACACATGAAGAAGTTAAGATTTGGA 657
                       **       **     * **          **     * ** **    ** ** **

AHSV9_DQ868776      ATGTTATATCCAAACTACTATATGCTGAATACAGATTATATAGTTACTGAATCAAGTAAG 708
AHSV9_AF043926      ATGTTATATCCAAATTATTATATGTTGAATACAGGTTATATAGTTACTGAATCAAGTAAG 708
AHSV6_NC_005996     TTTGTCTATCCGCATTATTATGTTTTGAATACTAATTATAATCCAACAACGGTGACTAGA 711
AHSV6_AF021235      TTTGTCTATCCGCATTATTATGTTTTGAATACTAATTATAATCCAACAACGGTGACTAGA 711
AHSV6_DQ868774      TTCATTTATCCGCATTATTATGTCTTGAATACTGACTATAATCCAACAACTGTGACTAGA 711
AHSV4_DQ868773      ATGATGTACCCACACTATTATGTTTTGCCTAGTGATTACTGTATTGTACCAAATAAGGGG 717
AHSV4_EU046574      ATGATGTACCCACACTATTATGTTTTGCATAGTGATTACTGTATTGTACCAAATAAGGGG 717
AHSV4_D26570        ATGATGTACCCACATTATTATGTTCTGCATAGTGACTATTGTATTGTACCAAACAAAGGC 717
AHSV5_AY163331      TTACTGTATCCGCATTACTATATGCTCAATCCAGAATATACGGTTGAAGAAAAGAGCAAA 717
                     *  * ** **  * ** *** *  *   *      **              *

AHSV9_DQ868776      GAGGCGCCGTTAAATCGATGGTTAGTGAAGGAGAAAACAGTTGGGAAAGTTAAAGCGGCC 768
AHSV9_AF043926      GGGGCACCGTTGAATCGATGGTTGGTGAAAGAGAGAACAGTTGGAAAAGTCAAGGCGGCC 768
AHSV6_NC_005996     ACTTCGCGGATTAATGATTGGTTGCTAAAAGAAAAGACACAAGGAGTTGTGAAGACCGCT 771
AHSV6_AF021235      ACTTCGCGGATTAATGATTGGTTGCTAAAAGAAAAGACACAAGGAGTTGTGAAGACCGCT 771
AHSV6_DQ868774      ACTTCGCGGATTAATGATTGGTTGCTAAAAGAAAAGACACAAGGAGTTGTGAAGGCCGCT 771
AHSV4_DQ868773      GGAACTAGTATTGGATCATGGCATATAAGAAAACGTACTGAGGGTGATGCGAAAGTTTCT 777
AHSV4_EU046574      GGAACTAGTATTGGATCATGGCATATAAGAAAACGTACTGAGGGTGATGCGAAAGCTTCT 777
AHSV4_D26570        GGCACAAGTATCGGATCATGGCATATAAGAAAACGTACTGAAGGTGACGCGAAAGCTTCC 777
AHSV5_AY163331      GGAGGTTTGATAGCCAACTGGTTAGTGAAAGAGAAGGCGGCGGGACGTGCTGAGAATTCA 777
```

```
                          *      ***    * *   *     *    **    *   *     *

AHSV9_DQ868776       GAAGCTTTTGCGGGTAATTCGTTATTAAAAAGCTTGGCGAGCCGGATGGAGGACGAGGAG 828
AHSV9_AF043926       GAGGCCTTTGCGGGCAATTCGTTATTAAAAAACTTGGCAAGCCGGATGGAAGACGAAGAA 828
AHSV6_NC_005996      GAGGCGTTTTCCGACAACGCAGAGTTGAAGACTTTAGCGGAACGAATGGAAGAGGAGGAG 831
AHSV6_AF021235       GAGGCGTTTTCCGACAACGCAGAGTTGAAGACTTTAGCGGAACGAATGGAAGAGGAGGAG 831
AHSV6_DQ868774       GAGGCGTATTCCGATAACGCGGAGTTGAAAACTTTAGCGGAACGAATGGAGGAGGAGGAA 831
AHSV4_DQ868773       GCTATGTATTCTGGAAAAGGTCCACTGAATGACTTACGAGTTAAAATTGAGCGGGATGAT 837
AHSV4_EU046574       GCTATGTATTCTGGAAAAGGTCCACTGAATGACTTACGAGTTAAAATTGAGCGGGATGAT 837
AHSV4_D26570         GCCATGTATTCTGGAAAGGGTCCGCTGAATGACTTACGAGTTAAAATTGAGCGGGATGAT 837
AHSV5_AY163331       CCAATGTATTCGGGGGTCGGACCGCTAAATACATCGCGTGAGCGTATCGAGAGGGATGAG 837
                           * * * *           * **    *          ** **    ** **

AHSV9_DQ868776       TTGAGTCGAGAAATAATAATTGCAGTGATCAATTATGGTTCGAAATTTGGAACTAGATCT 888
AHSV9_AF043926       TTGAGTCGGGAAATAATAGTTGCGGTGATCAATTATGGTTCGAAGTTCGGGACTAGGTCC 888
AHSV6_NC_005996      CTGACTGAGGATATTATTCGAGCAGTGATCAGGTATGGAGCCAAATACGCTACGCGCTCG 891
AHSV6_AF021235       CTGACTGAGGATATTATTCGAGCAGTGATCAGGTATGGAGCCAAATACGCTACGCGCTCG 891
AHSV6_DQ868774       CTGACTGTGGATATCATTCGGGCGGTAATCAGGTATGGGGCCAAATATGCTACGCGCTCG 891
AHSV4_DQ868773       TTATCTCGAGAGACAATTATTCAGATCATTGAGTACGGTAAGAAATTTAATTCATCAGCA 897
AHSV4_EU046574       TTATCTCGAGAGACAATTATTCAGATCATTGAGTACGGTAAGAAATTTAATTCATCAGCA 897
AHSV4_D26570         TTATCTCGAGAGACGATTATTCAGATTATCGAATACGGTAAAAAATTTAATTCATCTTCA 897
AHSV5_AY163331       TTAGATGAAAAAGTTATTCAGGAAATCATTGCTTATGGATCCAAATTTAGCACCTACGCG 897
                      *   *    *    **        * **    ** **    ** *      *     *

AHSV9_DQ868776       GGAAAGAAGAAGGATTTGATGACTATT--GATAAGCTTGAAAAATATTGTGATTCGTTGA 946
AHSV9_AF043926       GGGAAGAAAAAAGATTTGATGACCATT--GATAAGCTTGAAAAATACTGTGAATCCTTAA 946
AHSV6_NC_005996      GGTATGCGAGAGGATACACTGTCACTC--CAGGAGTTGGATCGTTATTGCGATTCTCTAA 949
AHSV6_AF021235       GGTATGCGAGAGGATACACTGTCACTC--CAGGAGTTGGATCGTTATTGCGATTCTCTAA 949
AHSV6_DQ868774       GGTATGCGAGAGGATACACTGTCACTC--CAGGAGTTGGATCGTTATTGCGATTCCCTAA 949
AHSV4_DQ868773       GGTGATAAGCAGGGGAACATTTCAATT--GAAAAATTGGTAGAGTATTTTGATTTTTTGA 955
AHSV4_EU046574       GGTGATAAGCAGGGGAACATTTCAATT--GAAAAATTGGTAGAGTATTGTGATTTTTTGA 955
AHSV4_D26570         GGTGATAAGCAGGGGAATATTTCAGTT--GATAAATTGGTGGAGTATTGTGACTTCTTGA 955
AHSV5_AY163331       GGT-ACACGCACAGGAG-ATCTCACTTTGAATGAATTAGTAAAGTATTGCGAAAGTTTAA 955
                     **        *        *  *  *    *  *  * *     ** *  **     * *

AHSV9_DQ868776       CGACGTTCGTCCACAAAAAGAAGCGTGACGAAGGTGACGATGAAACAGCTAGGGCTATCA 1006
AHSV9_AF043926       CGACGTTTGTTCACAAAAAGAAGCGTGATGAAGGTGATGATGAAACAGCTAGGGCTATCA 1006
AHSV6_NC_005996      CAACTTTTGTTCATAAAAAGAAGAAGGATGAAGGTGATGATGAAACAGCACGTACGATAA 1009
AHSV6_AF021235       CAACTTTTGTTCATAAAAAGAAGAAGGATGAAGGTGATGATGAAACAGCACGTACGATAA 1009
AHSV6_DQ868774       CAACTTTTGTTCATAAAAAGAAGAAGGATGAAGGCGATGATGAAACAGCGCGTACGATAA 1009
AHSV4_DQ868773       CAACATTCGTTCATGCGAAGAAGAAAGAAGAGGGTGAGGATGATACTGCTCGACAGGAGA 1015
AHSV4_EU046574       CAACATTCGTTCATGCGAAGAAGAAAGAAGAGGGTGAGGATGATACTGCTCGACAGGAGA 1015
AHSV4_D26570         CAACATTTGTCCACGCGAAGAAGAAAGAAGAGGGTGAAGATGATACCACTCGACAGGAGA 1015
AHSV5_AY163331       CGACTTTTGTTCAT---AAGAAAAAGAAGGAGGGAGAGGATGAGACTGCAAGGGAGTTTT 1012
                     * ** ** ** **    *****     * ** ** ** ***** **  *  *

AHSV9_DQ868776       TTAGAAACCAATGGATTAAGGGGATGCCGAGTATGAATTTGAAAAAAGAAATGAAAGTTT 1066
AHSV9_AF043926       TTAGGAATCAATGGATTAAGGGAATGCCAAGCATGAATTTGAAAAAAGAAATGAAAGTTT 1066
AHSV6_NC_005996      TTAGAAATCAGTGGATTAAAGGGATGCCTCGAATGGATTTCAAAAAAGAGATGAAAATCA 1069
AHSV6_AF021235       TTAGAAATCAGTGGATTAAAGGGATGCCTCGAATGGATTTCAAAAAAGAGATGAAAATCA 1069
AHSV6_DQ868774       TTAGAAATCAGTGGATTAAGGGAATGCCACGAATGGATTTCAAAAAAGAGATGAAAATCA 1069
AHSV4_DQ868773       TAAGAAAAGCATGGGTTAAGGGGATGCCTTATATGGATTTCTCAAAACCGATGAAAATCA 1075
AHSV4_EU046574       TAAGAAAAGCATGGGTTAAGGGGATGCCTTATACGGATTTCTCAAAACCGATGAAAATCG 1075
AHSV4_D26570         TAAGAAAAGCATGGGTTAAGAGGATGCCTTATATGGATTTCTCAAAACCGATGAAAATAA 1075
AHSV5_AY163331       TCAAAAGTAAATGGATACAAGGTATGCCAAAGATGAACTTTGAAAATGAAATGATTATGT 1072
                     * *  *     *** *  *  * *****    * * * **   ***    ****   *

AHSV9_DQ868776       CGCGTGGTCCTATTCAAAATTGGTCGTTTTTCATGTCCCTAGAGATGTTTAAACGTAATA 1126
AHSV9_AF043926       CGCGTGGTCCTATTCAAAATTGGTCGTTTTTTATGTCCCTTGAGGTGTTTAAACGTAATA 1126
AHSV6_NC_005996      CTCGAGGTCCGATTGCGAACTGGTCGTTTTTTATGTCTATAGATGCTTTCAAAAGGAATA 1129
AHSV6_AF021235       CTCGAGGTCCGATTGCGAACTGGTCGTTTTTTATGTCTATAGATGCTTTCAAAAGGAATA 1129
AHSV6_DQ868774       CACGAGGCCCGATTGCGAACTGGTCGTTTTTTATGTCTATAGATGCATTTAAAAGAAACA 1129
AHSV4_DQ868773       CGCGTGGATTCAACAGAAATATGCTTTTCCTTGCGGCGCTCGATTCATTCAGAAAGAGGA 1135
AHSV4_EU046574       CGCGTGGATTCAACAGAAATATGCTTTTCTTTGCGGCGCTCGATTCATTCAGAAAGAGGA 1135
AHSV4_D26570         CGCGTCGGTTCAACAAGAATATGCTTTTCTTTGCGGCACTCGATTCATTCAGAAAGAGGA 1135
AHSV5_AY163331       CAAGAAAGTCATGGGCGAATACAAAATTCTTTTGGAGTATTGATATGTTCAAGAGAAATA 1132
                     *  *            **       **  *   *    * **    ** *     *  *

AHSV9_DQ868776       ACAAAGTTGATATTGATCCGAATCATGATACGTGGAAAAATCACGTTAAAGAGATCAGGG 1186
AHSV9_AF043926       ATAAAGTTGATATTGATCCAAATCATGATACATGGAAAAACCATGTCAAAGAAATCAGAG 1186
AHSV6_NC_005996      ATAAGGTTGATATTAATCCGAATCACCAGACGTGGAAGGATCACATTAAAGAAGTGACTG 1189
AHSV6_AF021235       ATAAGGTTGATATTAATCCGAATCACCAGACGTGGAAGGATCACATTAAAGAAGTGACTG 1189
AHSV6_DQ868774       ATAAGGTCGACATTAATCCGAACCACCAAACGTGGAAGGATCATATCAAAGAAGTTACTG 1189
AHSV4_DQ868773       ACGGTGTAGATGTTGATCCGAATAAGGGTAAGTGGAAAGAACATATAAAGGAGGTAACCG 1195
AHSV4_EU046574       ACGGTGTAGATGTTGATCCGAATAAGGGTAAGTGGAAAGAACATATAAAGGAGGTAACCG 1195
AHSV4_D26570         ACGGCGTAGACGTTGATCCAAATAAGAATAAGTGGAAAGAACATATAAAAGAGGTAACCG 1195
```

```
AHSV5_AY163331      ATGGCGTTGATATTGATCCAAACGGTAAGAATTGGAAAGATTACAAGAAAAAGGTACAAG 1192
                    *    ** **  ** **** **       *  *****  *  *    **  *  *    *

AHSV9_DQ868776      AGAGGATGCAGAAAGAACAGAGCGCGAATTCTAATTCACCC-TTAAAGATCC-AGGTTGA 1244
AHSV9_AF043926      AGAGGATGCAGAAAGAACAGAGCGCGAATTCCAACTTACCCCTTAAAGATCCCAAGTTGA 1246
AHSV6_NC_005996     ATCAAATGAATCGTGCGCAACAAGGCAACAATAATAAGCCT-CTAAAGGTTC-AAATCGA 1247
AHSV6_AF021235      ATCAAATGAATCGTGCGCAACAAGGCAACAATAATAAGCCT-CTAAAGGTTC-AAATCGA 1247
AHSV6_DQ868774      ATCAAATGAATCGTGCGCAGCAAGGCAACAATAATAAACCT-CTAAAGATTC-AGATTGA 1247
AHSV4_DQ868773      AAAAATTGAAGAAAGCGCTAACCGAAAATGGAGGACAACCATGCCAAGTGTC--GATCGA 1253
AHSV4_EU046574      AAAAATTGAAGAAAGCGCAAACCGAAAATGGAGGACAACCATGCCAAGTGTC--GATCGA 1253
AHSV4_D26570        AAAGATTAAAGAAAGCGCAAAACGAAAATGGAGGACAGCCATGCCAAGTGTC--GATCGA 1253
AHSV5_AY163331      AGCAGTTGGATGAGGCGCAAAAGAAGAACAATAACGAACCGTATAAAGTAAT--GGTTGA 1250
                    *     *  *    *  *        **          **     ***       * **

AHSV9_DQ868776      TGGGGTCAGTTTATCAACCGGTGAATTCTACG-GTACGGTTGAACATTGGATAGATTGGG 1303
AHSV9_AF043926      TGGCGTCAGCTTATCTACAAGTGAATTCTACGCGCACGGTCGAACATTGGATAGATTGGG 1306
AHSV6_NC_005996     TGGTGTTAGCATACTCACGAGTGAAAAATATG-GTACCGTTGGTCATTGGGTCGATTGGG 1306
AHSV6_AF021235      TGGTGTTAGCATACTCACGAGTGAAAAATATG-GTACCGTTGGTCATTGGGTCGATTGGG 1306
AHSV6_DQ868774      TGGAGTTAGCATACTCACGAATGAAAAGTATG-GTACCGTTGGTCATTGGGTTGATTGGG 1306
AHSV4_DQ868773      TGGAGTAAACGTCTTGACTAACGTAGATTACG-GTACGGTTAATCATTGGATAGATTGGG 1312
AHSV4_EU046574      TGGAGTAAACGTCTTGACTAACGTAGATTACG-GTACGGTTAATCATTGGATAGATTGGG 1312
AHSV4_D26570        TGGGGTAAACATCTTAACTAACGTGGATTATG-GAACGGTTAATCATTGGATCGATTGGG 1312
AHSV5_AY163331      TGGGGTTAACATCATGACGAATAAGAAGTACG-GATCCGTTGAAAACTGGGTCGATTGGG 1309
                    *** ** *   *    **          ** * *  * **     * *** * *******

AHSV9_DQ868776      TTGTTGATTTAATTATGTTAGCACAGGTGAAACGATTAATCAAGGAGTACAAGTTTGTAA 1363
AHSV9_AF043926      TTGTTGATTTAATTATGTTAGCACAGGTTAAACGATTAATTAAGGAGTACAAGTTTATAA 1366
AHSV6_NC_005996     TTGTTGATTTGATTATGTTGGCGCAGGTGAAAATGTTAATAAAAGAATATAAGTTTAAAA 1366
AHSV6_AF021235      TTGTTGATTTGATTATGTTGGCGCAGGTGAAAATGTTAATAAAAGAATATAAGTTTAAAA 1366
AHSV6_DQ868774      TTGTTGACTTAATTATGTTAGCGCAGGTGAAGATGTTAATAAAAGAATATAAGTTTAAAA 1366
AHSV4_DQ868773      TAACAGATATAATTATGGTTGTACAAACTAAACGTTTGGTGAAAGAGTATGCATTTAAAA 1372
AHSV4_EU046574      TAACAGATATAATTATGGTTGTACAAACTAAACGTTTGGTGAAAGAGTATGCATTTAAAA 1372
AHSV4_D26570        TAACAGATATGATTATGGTCGTACAGACTAAACGATTAGTAAAAGAGTATGCGTTTAAAA 1372
AHSV5_AY163331      TTGTAAATTATATTATGTTATCGCACGTCAAAAGGCTGGTTAAGGACTATAAATTTAAGA 1369
                    *     *    ****** *    **    **     *  * ** ** **    ***   *

AHSV9_DQ868776      GATTGGAAACCTCGAACTTAATGGCGGGAATGAATAAATTAGTTGGAGCCTTGCGCTGCT 1423
AHSV9_AF043926      GATTAGAGACTACGAGCTTAATGGCAGGAATGAATAAACTAGTCGGAGCTTTACGTTGCT 1426
AHSV6_NC_005996     GATTAAATAGCCAAAATTTGATGTCGGGTATGAACAAACTGGTTGGTGCGCTGAGATGTT 1426
AHSV6_AF021235      GATTAAATAGCCAAAATTTGATGTCGGGTATGAACAAACTGGTTGGTGCGCTGAGATGTT 1426
AHSV6_DQ868774      GATTGAATAGCCAAAATTTGATGTCGGGTATGAATAAACTGGTCGGTGCACTGAGATGTT 1426
AHSV4_DQ868773      AACTAAAGAGCGAAAACTTACTTGCTGGAATGAATAGTTTAGTTGGGGTATTAAGATGTT 1432
AHSV4_EU046574      AACTAAAGAGCGAAAACTTACTTGCTGGAATGAATAGTTTAGTTGGGGTATTAAGATGTT 1432
AHSV4_D26570        AACTGAAGAGCGAAAACCTACTTGCCGGAATGAATGGTTTAGTTGGGATATTAAGATGTT 1432
AHSV5_AY163331      GGCTCAAGCCGGATAATTTGATGTCCGGGATGAATAAGCTAGTCGGCGCACTAAGATGTT 1429
                       *  *       *   *  *  * ** *****     * ** **     *  * ** *

AHSV9_DQ868776      ACGCCTATTGCTTGATCTTAGCTCTCTATGATTTTTATGGCGCAGATATTGAAGGTTTTG 1483
AHSV9_AF043926      ATGCCTATTGCTTGATTCTGGCTCTCTATGATTTCTATGGTGCGGATATCGAAGGTTTTG 1486
AHSV6_NC_005996     ATGCTTACTGCTTGATTCTTGCTTTATATGACTATTATGGTCAAGATATTGAGGGCTTCA 1486
AHSV6_AF021235      ATGCTTACTGCTTGATTCTTGCTTTATATGACTATTATGGTCAAGATATTGAGGGCTTCA 1486
AHSV6_DQ868774      ATGCTTACTGCTTGATTCTCGCTTTGTATGACTATTATGGTCAAGATATCGAGGGCTTCA 1486
AHSV4_DQ868773      ATATGTATTGCTTAGCTTTAGCGATCTATGATTTTTATGAAGGGACTATTGATGGTTTTA 1492
AHSV4_EU046574      ATATGTATTGCTTAGCTTTAGCGATCTATGATTTTTATGAAGGGACTATTGATGGTTTTA 1492
AHSV4_D26570        ATATGTATTGTTTAGCTTTAGCGATTTATGATTTTTATGAAGGAATTATTGATGGTTTTA 1492
AHSV5_AY163331      ATGCGTATTGTTTGATACTCGCGTTATATGATTATTTCGGGGAGGATATCGAAGGGTTTA 1489
                    *    ** ** **     * **  * ***** *  *  *       *** ** ** **

AHSV9_DQ868776      AGAAGGGTTCGAACTCATCCGCGATTGTGGAGACGGTTGTACAGATGTTCCCGAACTTCA 1543
AHSV9_AF043926      AAAAGGGTTCAAACTCTTCCGCGATAGTAGAGACGGTTGTACAGATGTTCCCGAACTTCA 1546
AHSV6_NC_005996     AGAAGGGATCAAATTCGTCTGCGATATTAGAAACGGTTATTCAGATGTTTCCGAATTTTA 1546
AHSV6_AF021235      AGAAGGGATCAAATTCGTCTGCGATATTAGAAACGGTTATTCAGATGTTTCCGAATTTTA 1546
AHSV6_DQ868774      AGAAGGGATCAAATTCTTCCGCGATATTAGAGACGGTTATTCAAATGTTTCCGAATTTTA 1546
AHSV4_DQ868773      AGAAAGGCTCGAATGCTTCCGCTATCATTGAAACTGTCGCGCAGATGTTTCCGGACTTTC 1552
AHSV4_EU046574      AGAAAGGCTCGAATGCTTCCGCTATCATTGAAACTGTCGCGCAGATGTTTCCGGACTTTC 1552
AHSV4_D26570        AGAAAGGTTCAAACGCTTCCGCTATCATTGAAACCGTCGCGCAGATGTTTCCAGACTTTC 1552
AHSV5_AY163331      AGAAAGGAACGAACGCGGCTTCAATTGTAGAAACAGTGTCCCAAATGTTCCCGCAGTTTA 1549
                    * ** **  * **  *  *  * **  * ** ** **    ** ***** **  * **

AHSV9_DQ868776      AGCAGGAGATTCAAGCTAATTTTGGTATAAATCTAAATATCAAGGATAAAAAA-CAGGCG 1602
AHSV9_AF043926      AGCAGGAGATTCAAGCTAATTTCGGTATAAATTTAAATATCAAAGATAAGAAG-CAAGTG 1605
AHSV6_NC_005996     AACAGGAAATTCAAGCTAATTTCGGAATAAATTTGAATATTAAAGACAAAAAAACAATCG 1606
AHSV6_AF021235      AACAGGAAATTCAAGCTAATTTCGGAATAAATTTGAATATTAAAGACAAAAAAACAATCG 1606
AHSV6_DQ868774      AACAGGAAATTCAAGCTAATTTCGGGATAAATTTGAACATTAAAGATAAAAAA-CAATCG 1605
AHSV4_DQ868773      GCAGAGAGCTTGTCGAAAAATTCGGTATAGATTTAAGGATGAAGGAAATCACG-CGTGAG 1611
AHSV4_EU046574      GCAGAGAACTTGTCGAAAAATTCGGTATAGATTTAAGGATGAAGGAAATCACG-CGTGAG 1611
```

```
AHSV4_D26570         GTAGAGAGCTCGTTGAAAAGTTCGGTATAGATCTAAGGATGAAGGAAATCACG-CGTGAG 1611
AHSV5_AY163331       GGAAAGAAGTTTCAGAGACCTTTGGAATCACTCTGAATACAAAAGACGTCAAA-TATGAG 1608
                          **  *    *  *  ** ** **   * * *  *  ** **    *       *

AHSV9_DQ868776       TTGTTCGTCAGGATGGATATGGATTCAGAGTTTAGTGAAGATGAGCAGAAGGGATATATG 1662
AHSV9_AF043926       TTGTTCGTCAGGATGGATATGGGTTCTGAGTTTAGTGAGGATGAGCAGAAAGGATATATG 1665
AHSV6_NC_005996      CTATTCGTCGAGCGA-CGATGCATTCGGACTTCTCATCGAATGAAGAGTACGGATATAAA 1665
AHSV6_AF021235       CTATTCGTCGAGCGA-CGATGCATTCGGACTTCTCATCGAATGAAGAGTACGGATATAAA 1665
AHSV6_DQ868774       TTATTCGTTGAGCGAACGATGCATTCGGATTTCTCATCAAATGAAGAGTACGGATATAAA 1665
AHSV4_DQ868773       TTGTTTGTTGGTAAGAGCATGACGTCAAAATTTATGGAGGAAGGTGAATATGGATATAAG 1671
AHSV4_EU046574       TTGTTTGTTGGTAAGAGCATGACGTCAAAATTTATGGAGGAAGGTGAATATGGATATAAG 1671
AHSV4_D26570         TTGTTTGTCGGTAAGAGCATGACGTCAAAATTTATGGAAGAAGGTGAATATGGATATAAG 1671
AHSV5_AY163331       TTGTTTATCGCTAGAGACATGAGTGCGAAAGAGGCTCAGTTCGGTGAGGTTGGGTACAAA 1668
                      * **  *          ***    *  *            *   *    ** ** *

AHSV9_DQ868776       TTTGAGTATGGATGGGCGAAGAGAGAAGAGCAAATATGGTCAAATTATGGTGACATATTA 1722
AHSV9_AF043926       TTTGAGTACGGATGGGCGAAAAGGGAAGAGCGAATATGGACGAATTACGGTGACATATTA 1725
AHSV6_NC_005996      TTTGTATTTGGATGGGCGGCAAGAGGTGAAGAAGTGTTGAGTAATTATGGAGATGTTCTC 1725
AHSV6_AF021235       TTTGTATTTGGATGGGCGGCAAGAGGTGAAGAAGTGTTGAGTAATTATGGAGATGTTCTC 1725
AHSV6_DQ868774       TTTGTATTTGGGTGGGCGGCAAGAGGTGAAGAAGTGTTGAGTAATTATGGAGATATTCTC 1725
AHSV4_DQ868773       TTCGCCTATGGATGGCGTAGGGATGGCTTCGCGGTGATGGAAGATTACGGAGAAATTTTG 1731
AHSV4_EU046574       TTCGCCTATGGATGGCGTAGGGATGGCTTCGCGGTGATGGAAGATTACGGAGAAATTTTG 1731
AHSV4_D26570         TTCACCTATGGGTGGCGTAGGGATGGCTTCGCGGTGATGGAAGATTACGGAGAGATTTTG 1731
AHSV5_AY163331       TTCCAGTATGGGTGGAGAAAAACGGATCAAAAAGTCATGAGCGATTACGCTGACATTTTG 1728
                     **    *  ** ***         *         *   *    **** *  **  *  *

AHSV9_DQ868776       ACTGACTTGGTTGAACAGCTTTATAAGAGCATTATGAATCATGAGGAGTGGGAGAAAATC 1782
AHSV9_AF043926       ACTGATTTGGTCGAACAGCTTTATAAGAGCATTTTGGATCATGAGGAATGGGAGAAAATC 1785
AHSV6_NC_005996      TCAGATGAGGTTGAAGAATTATTCACGAAACTTAGGAAGAAAGAGCATTGGGATAAGGTT 1785
AHSV6_AF021235       TCAGATGAGGTTGAAGAATTATTCACGAAACTTAGGAAGAAAGAGCATTGGGATAAGGTT 1785
AHSV6_DQ868774       TCAGATGAGGTTGAAGAATTATTCACAAAACTTAGGAAGAAAGAGCATTGGGATAAGGTT 1785
AHSV4_DQ868773       ACAGAAAAAGTGGAGGACCTATATAAGGGTGTACTTTTAGGACGAAAGTGGGAGGATGAG 1791
AHSV4_EU046574       ACAGAAAAAGTGGAGGACCTATATAAGGGTGTACTTTTAGGACGAAAGTGGGAGGATGAG 1791
AHSV4_D26570         ACAGAGAAAGTGGAGGATTTATATAAGAGTGTACTTTTAGAGCGAAAGTGGGAAGATGAG 1791
AHSV5_AY163331       AGCGAAAAGGTTGAAGCATTATATCAAGCACTACTTTCTGGAAGGAAGTGGAGCGATATA 1788
                        **    ** **     * *         *             * ***    *

AHSV9_DQ868776       GTTGATGACCCAGAAAAGTATTTCTATGATGATCTTTTTAACGCATCACCAGAGACGGCT 1842
AHSV9_AF043926       GTTGATGATCCTGAGAGGTATTTCTATGATGAGCTTTTTAACGCATCACCAGAGACAGTT 1845
AHSV6_NC_005996      GTGGAAGATCCAGAATCTTATTTCATAGATGAGCTTTATCAAAAGAATCCGGCGGAAGTG 1845
AHSV6_AF021235       GTGGAAGATCCAGAATCTTATTTCATAGATGAGCTTTATCAAAAGAATCCGGCGGAAGTG 1845
AHSV6_DQ868774       GTGGAAGATCCAGAGTCCTATTTCGTAGATGAGCTTTATCAAAAGAATCCAGCGGAAGTA 1845
AHSV4_DQ868773       GTTGATGATCCAGAGAGTTATTTTTATGATGATCTTTATACTAATGAGCCCCACAGAGTG 1851
AHSV4_EU046574       GTTGATGATCCAGAGAGTTATTTTTATGATGATCTTTATACTAATGAGCCCCACAGAGTG 1851
AHSV4_D26570         GTCGATGATCCAGAGAGCTATTTCTATGATGATCTTTATACCAATGAGCCCCACAGAGTA 1851
AHSV5_AY163331       GCTGATGATACGGAAGAGTATTTTATAGATGATTTGTACGTTAATAAGCCAGATAGGGTC 1848
                     *  ** **  * **    *****    *****  * *          **       *

AHSV9_DQ868776       TTTATTAGCAAAGGTTATGATCCTGACAATAATATCGTTATTGAGGGAAAGGTAGGTCAA 1902
AHSV9_AF043926       TTTATTAGCAAAGGTTATGACCTTGACAATAATATCGTAATTGAGGGAAAGGTAGGTCAA 1905
AHSV6_NC_005996      TTTTATAGCGCAGGCTATGATACAGATCAAAATGTGGTAATCGATGGGAAAATGACAGAG 1905
AHSV6_AF021235       TTTTATAGCGCAGGCTATGATACAGATCAAAATGTGGTAATCGATGGGAAAATGACAGAG 1905
AHSV6_DQ868774       TTTTTTAGTGCAGGTTATGATACAGATCAAAATGTGGTAATCGATGGAAAAATGACAGAG 1905
AHSV4_DQ868773       TTTCTAAGCGCAGGAAAGGATGTGGATAATAATATCACGCTTCGATCGATTTCGCAGGCG 1911
AHSV4_EU046574       TTTCTAAGCGCAGGAAAGGATGTGGATAATAATATCACGCTTCGATCGATTTCGCAGGCG 1911
AHSV4_D26570         TTTCTAAGCGCAGGAAAGGATGTGGACAATAATATTACACTTCGATCGATTTCGCAGGCG 1911
AHSV5_AY163331       TTTGAGAGAGCTGGGTTAGATCCGGAGAGACACATCAAGGTTAAAGGTGTGATGAATGAG 1908
                     ***   **    **    **    **     *  *     *

AHSV9_DQ868776       GATGTTACTTATTTTTCGAAACGGTTTGTATCATATTGGTATCGAGTTCGACAGGTTCAG 1962
AHSV9_AF043926       GATGTCACCTATTTTTCGAAACGGTTTGTATCATATTGGTATCGAGTTCGACAGGTTCAA 1965
AHSV6_NC_005996      GGAGTCACGTACTTCTCTAAAAGATTTGTTTCGTATTGGTATCGTGTTGAGAAAAT---A 1962
AHSV6_AF021235       GGAGTCACGTACTTCTCTAAAAGATTTGTTTCGTATTGGTATCGTGTTGAGAAAAT---A 1962
AHSV6_DQ868774       GGGGTCACGTACTTCTCTAAAAGATTCGTATCGTACTGGTATCGTGTTGAGAAAAT---A 1962
AHSV4_DQ868773       GAAACCACGTATCTATCGAAACGTTTCGTATCATATTGGTATAGAATATCACAAGTTGAA 1971
AHSV4_EU046574       GAAACCACGTATCTATCGAAGCGTTTCGTATCATATTGGTATAGAATATCACAAGTTGAA 1971
AHSV4_D26570         GAGACTACGTATTTGTCGAAACGTTTCGTATCGTATTGGTATAGAATATCGCAAATTGAA 1971
AHSV5_AY163331       CTGACGACGTACTTCTCAAAACGTTTCATTTCTTATTGGTATAAAATAACTAAGGTTGAA 1968
                           ** **  * ** **  * **  * ** ** ******    *     *  *

AHSV9_DQ868776       ACCTCAAA---GGGTGCTGAGAGG---AGATCGATTGAGGATGTCAAA---TATAGGGAG 2013
AHSV9_AF043926       ACCTCAAA---GGGTATTGAGAGG---AGGTCGATTGAGGATGTCAAA---TATAGGGAG 2016
AHSV6_NC_005996      ACAACGAA---GCACCTTGAGTTT---TTAACTGAAGAGAATCGAAAA---GTCGCGCAG 2013
AHSV6_AF021235       ACAACGAA---GCACCTTGAGTTT---TTAACTGAAGAGAATCGAAAA---GTCGCGCAG 2013
AHSV6_DQ868774       ACAACGAA---GCATCTCGAGTTT---TTAAATGAAGAGGGTCGAAAA---GTTGCGCAA 2013
AHSV4_DQ868773       GTAACGAAGGCGCGTAATGAAGTTCTGGACATGAATGAGAAACAGAAGCCGTATTTTGAA 2031
```

```
AHSV4_EU046574       GTAACGAAGGCGCGTAATGAAGTTCTGGACATGAATGAGAAACAGAAGCCGTATTTTGAA 2031
AHSV4_D26570         GTGACAAAGGCGCGTAATGAGGTTCCGGATATGAATGAGAAACAGAAGCCGTATTTTGAA 2031
AHSV5_AY163331       GCAAGGAATCTATTGACTTTAACT---GATATAGGGGGGGATGCAAAAAAGTATACACAG 2025
                           **                            * *      **          *

AHSV9_DQ868776       TTTGATATAGAAAGTTTTAAGCCTTACGCGATTGGTGAGATCGGTATTCACGCATCAACT 2073
AHSV9_AF043926       TTTGATATAGAAAGTTTTAAGCCTTACGCTATTGGCGAGATCGGTATTCACGCGTCAACT 2076
AHSV6_NC_005996      TTTGATTTTGAGGATTATAAACCGATGGCTATTGGAGAGATGGGGATTCATGCGTCGACA 2073
AHSV6_AF021235       TTTGATTTTGAGGATTATAAACCGATGGCTATTGGAGAGATGGGGATTCATGCGTCGACA 2073
AHSV6_DQ868774       TTTGATTTCGAGGATTATAAACCGATGGCTATTGGAGAGATGGGGATTCATGCATCGACA 2073
AHSV4_DQ868773       TTTGAATATGATGATTTCAAACCCTGTTCAATTGGAGAGTTGGGGATCCATGCATCCACA 2091
AHSV4_EU046574       TTTGAATATGATGATTTCAAACCCTGTTCAATTGGAGAGTTGGGGATCCATGCATCCACA 2091
AHSV4_D26570         TTTGAGTATGACGATTTTAAGCCTTGCTCGATTGGAGAGTTGGGGATCCATGCATCGACA 2091
AHSV5_AY163331       TTTGATCCTGATGATTTTAAACCAATGGCTGTGGCTGAGCTGGGAGCACACGCGTCGACG 2085
                     *****    **   **  ** **     *  * *  *** * **    ** ** ** **

AHSV9_DQ868776       TACAAATATCTGGATCTATTAGCGGGGCGTAATCGCGGAGAGAAAGTGAAGGATTCGCAA 2133
AHSV9_AF043926       TACAAGTATCAGGATTTATTAGCGGGGCGTAATCGCGGAGAAAAAGTGAAGGACTCGCAA 2136
AHSV6_NC_005996      TATAAGTATGAGTCGTTGCTCCTTGGGAAAAATAGAGGGCAAAAAGTGAATGATTCCATC 2133
AHSV6_AF021235       TATAAGTATGAGTCGTTGCTCCTTGGGAAAAATAGAGGGCAAAAAGTGAATGATTCCATC 2133
AHSV6_DQ868774       TATAAGTATGAGTCGTTGCTTCTTGGAAAGAATAGAGGGCAAAAAGTGAAAGACTCCATT 2133
AHSV4_DQ868773       TATATATATCAGAACCTACTGGTCGGACGTAATAGAGGTGAGGAAATACTTGATTCGAAA 2151
AHSV4_EU046574       TATATATATCAGAACCTACTGGTCGGACGTAATAGAGGTGAGGAAATACTTGATTCGAAA 2151
AHSV4_D26570         TACATATATCAGAACCTCCTCGTTGGACGTAATAGGGGCGAGGAGATACTTGATTCGAAG 2151
AHSV5_AY163331       TATGTTTATCAGAATTTGATTTTAGGGAGGAACAGAGGCGAGAAAATTGGTGATGCGAAG 2145
                     **    ***  *    *  *    **    **  * **  *  *  *    **  *

AHSV9_DQ868776       GCGCTCGTGTGG-TATGATTTCGCTTTAACTAACTACACGCTAGTGCGACCACAAGATAG 2192
AHSV9_AF043926       GCGCTCGTGTGG-TATGATCTTGCTTTGACTAATTACACACTAGTGCGGCCACAAGATAG 2195
AHSV6_NC_005996      GCTCT-GTGTAACTACGATCTTGCACTTACGAATTTCGGGGTTTCGAGGCGTCAGGACTG 2192
AHSV6_AF021235       GCTCT-GTGTAACTACGATCTTGCACTTACGAATTTCGGGGTTTCGAGGCGTCAGGACTG 2192
AHSV6_DQ868774       GCTTT-GTGTAACTATGATCTTGCACTTACGAACTTCGAAGTCTCGAGGCGTCAGGATTG 2192
AHSV4_DQ868773       GAGCTCGTCTGG-ATGGATATGTCACTTTTAAATTTTGGAGCGGTCAGATCTCACGATAG 2210
AHSV4_EU046574       GAGCTCGTCTGG-ATGGATATGTCACTTTTAAATTTTGGAGCGGTCAGATCTCACGATAG 2210
AHSV4_D26570         GAGCTTGTCTGG-ATGGATATGTCGCTATTAAATTTTGGAGCGGTCAGACCTCACGATAG 2210
AHSV5_AY163331       GAGATCGTTTGG-TATGATTTATCTTTGACTAATTTTGGATGTTCTAGATCGTTAGATTC 2204
                     *   * ** *      *** *  *  *    ** *           *       **

AHSV9_DQ868776       ATGTTGGATAATGTCGTGTACTGATTGTGAATACACTTTGAGATTTGCAACGATCACTAT 2252
AHSV9_AF043926       ATGTTGGATAATGTCGTGTACTGATTCTGAATACACTTTGAGATTCGCGATGATCACTAT 2255
AHSV6_NC_005996      TTGCTGGATCTCATCGTGTAGTGCCATTGAGCTTTCGATGAGAGCCAACATCATTATCGC 2252
AHSV6_AF021235       TTGCTGGATCTCATCGTGTAGTGCCATTGAGCTTTCGATGAGAGCCAACATCATTATCGC 2252
AHSV6_DQ868774       CTGCTGGATCTCATCGTGTAGCGCCATTGAGCTTTCGATGAGAGCCAACATCACTATCGC 2252
AHSV4_DQ868773       GTGCTGGATCTCCTCAAGCGTCGCGATTGAGGTGAATTTACGTCATGCACTAATAGTTAG 2270
AHSV4_EU046574       GTGCTGGATCTCCTCAAGCGTCGCGATTGAGGTGAATTTACGTCATGCACTAATAGTTAG 2270
AHSV4_D26570         GTGTTGGATTTCTTCAAGCGTCGCGATTGAGGTAAATCTACGTCACGCACTGATAGTTAG 2270
AHSV5_AY163331       TTGTTGGGTGGGGTCAGTTGCTAGATCTGAGCTGAATTTGCGGTTCCACCTTATATCCGC 2264
                      ** *** *    **           ***        *  *         *

AHSV9_DQ868776       GATATTCGAACGTTTATCTGAGGAAGCTGATCTTTC----TTATCATGATATCTTATTGA 2308
AHSV9_AF043926       GATATTCGAGCGCTTATCTGAGGAGACTGATCTTTC----TTACCATGATATTTTATTGA 2311
AHSV6_NC_005996      TATTTTTAGGAGAATCGAAGACAAGAGATATGAGAA----TTTCGCGAAAATATTATCCG 2308
AHSV6_AF021235       TATTTTTAGGAGAATCGAAGACAAGAGATATGAGAA----TTTCGCGAAAATATTATCCG 2308
AHSV6_DQ868774       AATTTTTAGGAGAATCGAAGACAGAAGATATGAGAG----TTTCGCGAAAATACTATCCG 2308
AHSV4_DQ868773       GATTTTTTCACGCT-TTGACATGATGTCGGAAAGAGAAACGTTTTCAACCATTTTAGAAA 2329
AHSV4_EU046574       GATTTTTTCACGCT-TTGACATGATGTCGGAAAGAGAAACGTTTTCAACCATTTTAGAAA 2329
AHSV4_D26570         GATTTTTTCACGCT-TTGACATGATGTCGGAGAGAGAAGCGTATTCAATGATTTTGGAAA 2329
AHSV5_AY163331       AATATTTGAACGATATCAGCATGATGCACGACGGAG---CTCCTTTTATGAAATTATCTT 2321
                      ** **     *       *                              *   *

AHSV9_DQ868776       AGGTCCGCGAATATCCGATCCA------ATCATTCGCTTCGTATAAACATTTCTATGTTC 2362
AHSV9_AF043926       GGGTTCGCGAATATCCGATACA------ATCATTCGCTTCATACAAACATTTCTATGTTC 2365
AHSV6_NC_005996      GACTCACACAGCAGCAAGACCT------ATATTTCCCTACGTATAAGCATTATTATCTGT 2362
AHSV6_AF021235       GACTCACACAGCAGCAAGACCT------ATATTTCCCTACGTATAAGCATTATTATCTGT 2362
AHSV6_DQ868774       GACTTTCGCAGCAGCAAGACTT------ATACTTTCCTACGTATAAGCATTATTATCTGT 2362
AHSV4_DQ868773       AAGTCATGGAGGATGTGAAAGAGTTGAGATTTTTCCCGACATATCGTCATTATTATTTGG 2389
AHSV4_EU046574       AAGTCATGGAGGATGTGAAAGAGTTGAGATTTTTCCCGACATATCGTCATTATTATTTGG 2389
AHSV4_D26570         AAGTCATGGAGGATGTGAAGGAGCTGAGATTTTTCCCAACATATCGCCATTATTATTTGG 2389
AHSV5_AY163331       CGATC-TGCCCTCTAAGAAAGA---GAGGATCTTCCCGAGTTACAAACATTATTACGTCG 2377
                        *                           **  *    **    ****  **  *

AHSV9_DQ868776       GCGTCTTGCAGCACGTTTTTAGAGATAACCAAGAAATCGACGTATTAGAGTTCTGTACTA 2422
AHSV9_AF043926       GCGTATTACAGCACGTTTTTAGAGACTACCAAGAGATCGATGTATTAGAGTTCTGTACTA 2425
AHSV6_NC_005996      TTGTGTTACAAAAGGTATTACGAGATGAGAGGAGGATAGATCTAAATAGAATATGCACCG 2422
AHSV6_AF021235       TTGTGTTACAAAAGGTATTACGAGATGAGAGGAGGATAGATCTAAATAGAATATGCACCG 2422
AHSV6_DQ868774       TTGTATTACAAAAGGTGTTACGAGATGAGAGGAGGATAGATCAGAATAGAATGTGCACAG 2422
```

```
AHSV4_DQ868773       AAACTCTCCAACGTGTCTTTAACGATGAGAGACGCTTAGAAGTTGATGACTTTTATATGA 2449
AHSV4_EU046574       AAACTCTCCAACGTGTCTTTAACGATGAGAGACGCTTAGAAGTTGATGACTTTTATATGA 2449
AHSV4_D26570         AAACTCTCCAACGTGTCTTTAACGATGAGAGACGTTTGGAGGTTGATGACTTTTATATGA 2449
AHSV5_AY163331       CTTTGCTACAGAATATCTTTAATGATACTCAACGATTAGAGGTAATGGACTATTGCGAGA 2437
                           * **     * **    **           * **             *

AHSV9_DQ868776       GGATGCTCGATCCGAGGACACGTGAAGCGGGGTTAAATAAGTTCTCAAGGTTTAGACAAT 2482
AHSV9_AF043926       GGATGCTCGATCCGAGGACACGTGAGTCGGGGCTAAACAAGTTTTCGAGATTCAAACAAT 2485
AHSV6_NC_005996      AGTTGTTTGATACACAGAGGCGAAGAGGTATTCTCCTTTCGTTTACCGCGTTGAGATTTT 2482
AHSV6_AF021235       AGTTGTTTGATACACAGAGGCGAAGAGGTATTCTCCTTTCGTTTACCGCGTTGAGATTTT 2482
AHSV6_DQ868774       AGCTGTTTGATATACAGAGGCGAAGAGGTATCCTCCTTTCGTTTACCACGTTGAGATTTT 2482
AHSV4_DQ868773       GGTTATATGATGTGCAGACAAGGGAGCAGGCACTAAATACTTTCACGGATTTTCACAGGT 2509
AHSV4_EU046574       GGTTATATGATGTGCAGACAAGGGAGCGGGCACTAAATACTTTCACGGATTTTCACAGGT 2509
AHSV4_D26570         AGTTATATAATGTGCAAACAAGGGAGCAGGCACTAAATACTTTCACGGACTTTCAAAGGT 2509
AHSV5_AY163331       GACTGATGAATCCGGAAACGAGGATGTCAGCCCTCCTATCACTTCAGGGGTTCAGAAACT 2497
                        *     **      *   *          *       *       **       *

AHSV9_DQ868776       GGAGAGAATCGGAATTCTTGATAGATGCTCTTAAAATGAATTTCCTTTTGTGGGTGGTCT 2542
AHSV9_AF043926       GGAGAGAATCGGAATTCTTGATAGATGCTCTTAAGATGAATTTTCTCCTGTGGGTAGTTT 2545
AHSV6_NC_005996      GGAATGATTCAGAATTTTTGGGTGATGCGTTAATGATGAATTTTCTACATAGGGTGGTTT 2542
AHSV6_AF021235       GGAATGATTCAGAATTTTTGGGTGATGCGTTAATGATGAATTTTCTACATAGGGTGGTTT 2542
AHSV6_DQ868774       GGAACGATTCGGAGTTTCTAGGTGATACGTTAATGATGAATTTTCTACTATGGGTGGTTT 2542
AHSV4_DQ868773       GTGTTGAGTCGGAACTGCTCTTACCGACACTTAAACTTAACTTTCTGCTGTGGATTGTTT 2569
AHSV4_EU046574       GTGTTGAGTCGGAACTGCTCTTACCGACACTTAAACTTAACTTTCTGCTGTGGATTGTTT 2569
AHSV4_D26570         GTGTTCAGTCAGAATTGCTCTTACCAACGCTTAAGCTCAATTTTTTGTTGTGGATCGTTT 2569
AHSV5_AY163331       GTGTCGAGTCGGAGTTCGTGGCCCCAACGTTGAAGATGAATGCACTTCTTTGGGTTTTAG 2557
                     *     * ** **  *  *        *  * *   * **     *     ** *  *

AHSV9_DQ868776       TCGAACTGGAAAATATAGATGTTGATTATAGTAAGAAAAGGCATCCTTTACTAATATCTA 2602
AHSV9_AF043926       TTGAACTGGAGAATATAGACGTTGATTATAGCAAGAAGAGGCACCCTTTGCTGATATCTA 2605
AHSV6_NC_005996      TCGAGATGGAAAACGTCGATGTGGATTATGGGAAGAAGTGGCATCCGCTACTAGTATCGT 2602
AHSV6_AF021235       TCGAGATGGAAAACGTCGATGTGGATTATGGGAAGAAGTGGCATCCGCTACTAGTATCGT 2602
AHSV6_DQ868774       TTGAGATGGAAAACATCGATGTGGATTATGGGAAAAAGTGGCATCCGCTGCTAGTATCGT 2602
AHSV4_DQ868773       TTGAAATGGAAAATGTTGAAGTGAACGCGGCGTACAAGCGTCATCCGCTTTTAATCTCAA 2629
AHSV4_EU046574       TTGAAATGGAAAATGTTGAAGTGAACGCGGCGTACAAGCGTCATCCGCTTTTAATCTCAA 2629
AHSV4_D26570         TTGAGATGGAAAATGTTGAAGTGAATGCAGCGGACAAGCGTCATCCGCTTTTAATTTCAA 2629
AHSV5_AY163331       CGGATATGGAGAATATTGATATAAACTACTCGAACAAGCGGATGCCGCTGTTGTTATCAA 2617
                       **  **** **  * **  *  *        * **  *    **  *  *  * **

AHSV9_DQ868776       CCGACAAAGGGTTAAGAGTAGTCTCAGTTGATCTTTTTAATTCTATGCTTAGCGTTTCCC 2662
AHSV9_AF043926       CTGACAAAGGATTAAGAGTAGTTCCAGTTGATCTTTTCAATTCTATGCTTAGTGTTTCTT 2665
AHSV6_NC_005996      CAGAGAAGGGGCTTAGAGTGATCGCGGTTGATGTTTTTAACTCAATGATGGGAGTGTCGA 2662
AHSV6_AF021235       CAGAGAAGGGGCTTAGAGTGATCGCGGTTGATGTTTTTAACTCAATGATGGGAGTGTCGA 2662
AHSV6_DQ868774       CAGAAAAGGGGCTTAGAGTGATTGCGGTTGACGTTTTTAATTCAATGATGGGAGTATCAA 2662
AHSV4_DQ868773       CTGCCAAAGGGTTAAGGGTTATCGGCGTTGATATTTTCAACTCACAGCTTTCGATATCAA 2689
AHSV4_EU046574       CTGCCAAAGGGTTAAGGGTTATCGGCGTTGATATTTTCAACTCACAGCTTTCGATATCAA 2689
AHSV4_D26570         CTGCCAAAGGATTAGGGGTTATTGGCGTTGACATTTTCAACTCGCAGCTTTCGATATCAA 2689
AHSV5_AY163331       CTGAGAAGGGCCTACGTGTGATTTCTATTGATATGTTTAACGGAATGCTGGGTGTTTCTT 2677
                     * *  ** **  *  * **  *     ****  * ** **      * *     * **

AHSV9_DQ868776       TGAGTGGGTGGATCCCATATGTTGAAAGAGTGTGTGAACGCTCGGAAGCTAAAAGAAGAT 2722
AHSV9_AF043926       CGAGCGGGTGGATTCCATATGTTGAAAGAGTGTGTGAGCGTTCGGAGATTAAAAGGAGAT 2725
AHSV6_NC_005996      CAAGTGGCTGGCTTCCTTATGTTGAACGCATTTGTTCCGAGTCTGATATGCGCAGGCGAT 2722
AHSV6_AF021235       CAAGTGGCTGGCTTCCTTATGTTGAACGCATTTGTTCCGAGTCTGATATGCGCAGGCGAT 2722
AHSV6_DQ868774       CGAGTGGTTGGCTTCCTTATGTTGAACGCATCTGTTCTGAGTCCGATATGCGCAGACGAC 2722
AHSV4_DQ868773       TGAGCGGATGGATTCCGTATGTCGAACGGATGTGCGCGGAGAGTAAAGTTCAAACAAAAT 2749
AHSV4_EU046574       TGAGCGGATGGATTCCGTATGTCGAACGGATGTGCGCGGAGAGTAAAGTTCAAACAAAAT 2749
AHSV4_D26570         TGAGCGGGTGGATTCCGTACGTCGAAAGGATGTGCGCGGAGAGTAAAGTTCAAACAAAAT 2749
AHSV5_AY163331       ATAGCGGCTGGATCCCATACTTAGAGAGGATCTGCAGTGAAGTAAATCTACAGAGACGCT 2737
                       ** ** *** * ** **  * **  *  * **          *       *

AHSV9_DQ868776       TGAATGCGGATGAATTGAAACTAAAGAACTGGTTTATTGCGTATTATGTCACTT-TGCCT 2781
AHSV9_AF043926       TGAATGCAGATGAATTGAAATTAAAGAACTGGTTCATTGCGTATTATATCACTT-TGCCC 2784
AHSV6_NC_005996      TGAATGCAGATGAACTAGAGTTAAAACGGTGGTTCTTTGACTACTATGCGACAT-TACCG 2781
AHSV6_AF021235       TGAATGCAGATGAACTAGAGTTAAAACGGTGGTTCTTTGACTACTATGCGACAT-TACCG 2781
AHSV6_DQ868774       TGAATGCGGATGAATTAGAGTTGAAGCGCTGGTTCTTTGATTATTACGCGACAT-TATTG 2781
AHSV4_DQ868773       TGACGGCTGATGAGCTGAAATTGAAGAGGTGGTTCATCTCATATTATACGACGT-TGAAA 2808
AHSV4_EU046574       TGACGGCTGATGAGCTGAAATTGAAGAGGTGGTTCATCTCATATTATACGACGT-TGAAA 2808
AHSV4_D26570         TGACGGCCGATGAACTAAAGTTGAAGAGGTGGTTTATTTCATATTATACGACGT-TGAAG 2808
AHSV5_AY163331       TAAGAGCGGATGAGCTAAAATTGAGGAAGTGGTTTATCAGCTACTACGCTACCTATGAAG 2797
                     * *  ** *****  *  *  * *     *****  *    ** **    ** * *

AHSV9_DQ868776       CTGTTAAGGCGTGCGGAACCAAGGATGAGCTTTAAGTATGAGGGAATTACAACGTGGATT 2841
AHSV9_AF043926       TTGTTAAGGCGTGCGGAACCGAGGATGAGCTTTAAGTATGAAGGAATTACAACTTGGATT 2844
AHSV6_NC_005996      CTCGAAAGGAGAGGAGAGCCTCGGTTGAGCTTTAAGTATGAAGGATTGACCACGTGGATT 2841
AHSV6_AF021235       CTCGAAAGGAGAGGAGAGCCTCGGTTGAGCTTTAAGTATGAAGGATTGACCACGTGGATT 2841
```

```
AHSV6_DQ868774       CTTGAAAGGAGGGGGGAGCCTCGGTTGAGCTTCAAGTATGAAGGATTGACCACGTGGATT 2841
AHSV4_DQ868773       TTGGACCGCAGAGCGGAGCCACGTATGAGTTTCAAATTTGAGGGGTTGAGTACATGGATC 2868
AHSV4_EU046574       TTGGACCGCAGAGCGGAGCCACGTATGAGTTTCAAATTTGAGGGGTTGAGTACATGGATC 2868
AHSV4_D26570         TTGGACCGCAGAGCGGAGCCACGTATGAGTTTCAAATTCGAAGGGTTAAGTACATGGATC 2868
AHSV5_AY163331       TTGAGAGAC-GTGCTGAGCCAAGAATGAGTTTTAAAATGGAGGGAATCTCCACCTGGATT 2856
                      *        * *  ** **  *  **** ** **    ** **  *    ** *****

AHSV9_DQ868776       GGTTCAAATTGCGGGGGGGTACGAGACTATCTGATTCAGATGCTCCCAGCAAGAAAACCG 2901
AHSV9_AF043926       GGTTCAAACTGTGGTGGGGTACGAGATTATCTAATTCAAATGCTCCCAGCGAGGAAACCG 2904
AHSV6_NC_005996      GGCTCAAATTGTGGAGGGGTGCGGGATTACGTTGTGCAATTGCTTCCTATGCGCAAATCA 2901
AHSV6_AF021235       GGCTCAAATTGTGGAGGGGTGCGGGATTACGTTGTGCAATTGCTTCCTATGCGCAAATCA 2901
AHSV6_DQ868774       GGCTCAAATTGTGGAGGAGTGCGCGATTACGTTGTACAATTGCTTCCCATGCGTAAACCA 2901
AHSV4_DQ868773       GGTTCGAACTGCGGAGGTGTTAGGGATTACGTAATACAGATGCTTCCTACCAGAAAACCT 2928
AHSV4_EU046574       GGTTCGAACTGCGGAGGTGTTAGGGATTACGTAATACAGATGCTTCCTACCAGAAAACCT 2928
AHSV4_D26570         GGTTCGAACTGCGGAGGTGTTAGGGATTACGTGATACAGATGCTTCCTACCAGAAAACCG 2928
AHSV5_AY163331       GGTTCAAACTGTGGGGGCGTCCAAGATTACGTGTTACATTTGATTCCTTCACGAAAACCA 2916
                     ** ** ** ** ** ** **    ** **  *  * **  ** * **     * *** *

AHSV9_DQ868776       AAACCGGGCGTTTTAATCTTAGCTCATGGTGCGGAGATTAACGTAGCGTGGTTGAACCAT 2961
AHSV9_AF043926       AAGCCAGGCGTTTTAATTTTAGCTTATGGCGCGGAGACTAACGTAGCGTGGTTGAACCAT 2964
AHSV6_NC_005996      AAGCCAGGGCTTCTCTGCATCGCTTACGGTGATGACGTCAATGTACAGTGGGTTGAACAT 2961
AHSV6_AF021235       AAGCCAGGGCTTCTCTGCATCGCTTACGGTGATGACGTCAATGTACAGTGGGTTGAACAT 2961
AHSV6_DQ868774       AAGCCAGGGCTTCTTTGCATCGCTTATGGCGATGACGTCAATGTACAGTGGGTTGAACAT 2961
AHSV4_DQ868773       AAACCGGGAGCTTTGATGGTGGTATACGCGCGGGATTCGAGAATCGAGTGGATCGAAGCA 2988
AHSV4_EU046574       AAACCGGGAGCTTTGATGGTGGTATACGCGCGGGATTCGAGAATCGAGTGGATCGAAGCA 2988
AHSV4_D26570         AAACCGGGAGCCTTGATGGTAGCGTACGCGCGGGATTCGAGAATTGAATGGATCGAGGCG 2988
AHSV5_AY163331       AAGCCTGGACTTCTTTTTCTGATATATGCGGATGATGGTGACGTTGACTGGGTAGCGAAC 2976
                     ** ** **     *     *     * *     **        *    *** *

AHSV9_DQ868776       GCGCTACGTGATATACTTTCGCTAG-AGGGATCGTTAGGGATAATTATTGTGAGTGACGG 3020
AHSV9_AF043926       GCGCTACGTGATATACTTTCGCTAG-AGGGGTCGTTAGGGATGATTATTATCAGTGATGG 3023
AHSV6_NC_005996      GAGTTAAGAGATTTTTTGATGCATG-AGGGCTCACTCGGCTTAGTGGTAATTAGCGGAAA 3020
AHSV6_AF021235       GAGTTAAGAGATTTTTTGATGCATG-AGGGCTCACTCGGCTTAGTGGTAATTAGCGGAAA 3020
AHSV6_DQ868774       GAGTTAAGGGATTTTTTGACACATG-AGGGCTCGCTCGGCTTAGTGGTAATTAGCGGGAA 3020
AHSV4_DQ868773       GAGCTATCACA-GTGGCTGCAAATGGAAGGTTCGCTTGGTTTGATCCTCGTTCATGATTC 3047
AHSV4_EU046574       GAGCTATCACA-GTGGCTGCAAATGGAAGGTTCGCTTGGTTTGATCCTCGTTCATGATTC 3047
AHSV4_D26570         GAGCTATCACA-GTGGCTGCAAATGGAGGGTTCGCTCGGATTGATTCTCGTTCATGATTC 3047
AHSV5_AY163331       ATGCTATCAGATGTGATTG-GTTCGGAGGGTAGTTTAGGATTCATCTTTATTAATGATCG 3035
                       * **    *  *          * * **     * **  *  *  *  *    *

AHSV9_DQ868776       CTCAGTGGTGAATAAGAGCAAGCTCCGCGTAAGGGATATGAAGATATATAATAGGTGGGA 3080
AHSV9_AF043926       CTCGGTGGTGAATAAAAGCAAGCTCCGTGTGAGAGATATGAAGATATATAATAGGGGAGA 3083
AHSV6_NC_005996      GATGTTAGTTAATAAAAGTAAATTAAGGGTAAGGAACTTGAAAATTTACAATCGCGGTAC 3080
AHSV6_AF021235       GATGTTAGTTAATAAAAGTAAATTAAGGGTAAGGAACTTGAAAATTTACAATCGCGGTAC 3080
AHSV6_DQ868774       GATGTTAGTTAATAAAAGTAAGTTGAGGGTAAGGAACTTGAAAATTTATAATCGCGGTAC 3080
AHSV4_DQ868773       AGGTATAATAAATAAGAGCGTATTGAGAGCGAGAACTCTGAAAATTTACAATAGGGGTTC 3107
AHSV4_EU046574       AGGTATAATAAATAAGAGCGTATTGAGAGCGAGAACTCTGAAAATTTACAATAGGGGTTC 3107
AHSV4_D26570         CGGTATAATAAATAAAAGTGTATTGAGAGCGAGAACTCTGAAAATTTACAATAGAGGTTC 3107
AHSV5_AY163331       CACCTTCGTTAATAAGAGCCAGTTGAAAGTTAGAACTTTGAAGATATATAATCGAGGTAT 3095
                          *  * ***** **     *    *  **     **** ** ** *** *  *

AHSV9_DQ868776       GGTGGACAGATTAATTTTGATTTCGAGTGGCGATTACACATTTGGGAATAAATATCTCTT 3140
AHSV9_AF043926       AGTAGACAGATTAATTTTGATTTCAAGTGGGGATTACACATTTGGGAACAAATATCTCTT 3143
AHSV6_NC_005996      GCTTGATTCTTTATTCTTGATTTCGGGTGGCAACTATACATTTGGAAATAAGTTCCTATT 3140
AHSV6_AF021235       GCTTGATTCTTTATTCTTGATTTCGGGTGGCAACTATACATTTGGAAATAAGTTCCTATT 3140
AHSV6_DQ868774       GCTTGATTCTTTGTTCTTGATTTCGGGGGGCAGCTATACATTTGGAAATAAGTTCCTATT 3140
AHSV4_DQ868773       GATGGATACTTTAATTCTAATTTCGAGTGGAGTTTACACTTTCGGAAATAAATTCTTGTT 3167
AHSV4_EU046574       GATGGATACTTTAATTCTAATTTCGAGTGGAGTTTACACTTTCGGAAATAAATTCTTGTT 3167
AHSV4_D26570         GATGGACACTTTAATTCTGATCTCGAGTGGAGTCTATACCTTTGGAAATAAATTCTTGTT 3167
AHSV5_AY163331       GTTGGATAGGTTAATACTAATATCTGGAGGAAATTATACTTTTGGGAATAAGTTTTTATT 3155
                       * **    **  *  * ** **  * **    ** ** ** ** ** ** *   * **

AHSV9_DQ868776       ATCGAAACTAATGGCCAAGATCGAACAGTAGCGTGACTGCTACTCCATGTGAATACACTT 3200
AHSV9_AF043926       ATCGAAATTAATGGCTAAGATTGAACAGTAGCGTGACTGCTACTCCATGTGAATACACTT 3203
AHSV6_NC_005996      ATCGAAGCTGATGGCAAAAGCTGAATAGCGGAGTGACTTCCGCTCATGGTGATTCAACTT 3200
AHSV6_AF021235       ATCGAAGCTGATGGCAAAAGCTGAATAGCGGAGTGACTTCCGCTCATGGTGATTCAACTT 3200
AHSV6_DQ868774       ATCGAAGCTGATGGCAAAAGCCGAATAGCGGAGTGACTTCCGCTCATGGTGATTCAACTT 3200
AHSV4_DQ868773       GTCGAAGTTACTCGCAAAAACAGAATAGCAACGTGACTGTTGCTCCATGTGAATACACAT 3227
AHSV4_EU046574       GTCGAAGTTACTCGCAAAAACGGAATAGCAACGTGACTGTTGCTCCATGTGAATACACAT 3227
AHSV4_D26570         GTCGAAGTTACTCGCAAAGACGGAATAGCAACGTGACTGTTGCTCCATGTGAATACACAT 3227
AHSV5_AY163331       ATCAAAATTACTCGCCAAGACAGAAAAGTAGCGTGACTGCTACTCCAGATGAATACACTT 3215
                      ** **  *  * ** **    *** **    ******    ***    *** *  ** *

AHSV9_DQ868776       AC- 3202
AHSV9_AF043926       AC- 3205
AHSV6_NC_005996      ACC 3203
```

```
AHSV6_AF021235       ACC 3203
AHSV6_DQ868774       ACC 3203
AHSV4_DQ868773       AC- 3229
AHSV4_EU046574       AC- 3229
AHSV4_D26570         AC- 3229
AHSV5_AY163331       AC- 3217
                     **
```